

M-62-65-2
OCTOBER 1965

FINAL REPORT

**PCM TELEMETRY DATA
COMPRESSION STUDY, PHASE I**
(15 SEPTEMBER 1964 TO 15 AUGUST 1965)

by
W. R. BECHTOLD
J. E. MEDLIN
D. R. WEBER

Contract No. NAS 5-9729

Prepared by
LOCKHEED MISSILES & SPACE COMPANY
Sunnyvale, California
for
GODDARD SPACE FLIGHT CENTER
Greenbelt, Maryland

FOREWORD

This report describes a Lockheed Missiles & Space Company study of PCM Telemetry Data Compression. The work was performed for the National Aeronautics and Space Administration under Contract No. NAS 5-9729 during the period between 15 September 1964 and 15 August 1965.

The authors wish to thank GSFC scientists Gerald J. Hogg and Thomas Lynch for their significant contributions throughout the investigation, Dr. Jay W. Schwartz for his valuable assistance on the evaluation of bit plane encoding; and the GSFC S-3 and S-6 Satellite experimenters for their explanations of the data and the tolerance accuracy requirements. We also wish to thank LMSC programmers James L. Hunts, Gerald W. O'Shaughnessy, and Charles P. Giallanza for their work in developing the computer programs.

SUMMARY

Data compression reduces the amount of bandwidth and/ or time necessary for transmitting information between two points. This study, using S-6 (Explorer XVII) satellite PCM data, evaluated various methods in which this reduction can be achieved and determined the most effective techniques.

The following steps were taken:

- 1) Literature search
- 2) Compression model selection
- 3) Compression model and buffer simulation
- 4) Time and channel identification study
- 5) Proposal of optimum compression models

LITERATURE SEARCH

The initial step was a search of international literature on data compression. A list of over 30 different methods was compiled; each was critically examined to determine its probable merits.

COMPRESSION MODEL SELECTION

The second step was an elimination process to reduce the number of models found during the literature search to a small group containing those showing the greatest promise of high performance. Six data compression models were placed in this group for subsequent testing. These included five polynomial sample selectors and one bit plane encoding technique.

COMPRESSION MODEL AND BUFFER SIMULATION

The next step, constituting the bulk of the work, was divided into two parts, (1) a compression model simulation analysis, and (2) an adaptive buffer queuing control study.

Compression Model Simulation Analysis

Using an IBM 7094 digital computer, simulation analyses were made of the compression models chosen in the second step. S-6 data waveforms used in this simulation were selected to match particular data classes specified by GSFC. The results of these tests showed that a particular type of first-order polynomial interpolator achieved the highest performance in reducing the bandwidth of the S-6 telemetry data. This interpolator is capable of fitting straight lines to the sampled data waveform by adjusting their end-points with four degrees of freedom.

Another part of the simulation analysis investigated the effects of precompression filtering and adaptive techniques on compression efficiency, and on reconstructed data fidelity. The results of this investigation indicated that both adaptive and nonadaptive precompression filtering may effectively enhance data compressor performance. This portion of the study, however, was too brief to be conclusive.

Adaptive Buffer Queuing Control Study

In this study, simulation tests were performed to determine the type of queuing control, if any, that would be needed to curtail or eliminate data loss from buffer overflow in an S-6 satellite telemetry data compressor. The most important result of this study was that, because of the data stationarity, adaptive queuing control would not be required for the S-6 data, as long as the buffer readout rate exceeded the average readin rate by a factor of at least $1/0.98$. However, to guard against the possibility of an abnormally low readout rate setting, a control system which monitored queue length was found to be necessary.

TIME AND CHANNEL IDENTIFICATION STUDY

Relative efficiencies of several methods of time and channel coding were investigated. It was found that the transmission of a minor frame channel identification word with each data sample was the most efficient coding technique for S-6 data among those studied. With this method at least one data/channel word in each minor frame must be transmitted in order to maintain a time reference and to identify subcommutated sensors.

PROPOSAL OF OPTIMUM COMPRESSION MODELS

The final step consisted of a tradeoff analysis of the six compression models tested. The models which demonstrated the highest overall performance are proposed for compressing S-6 and similar data.

The spread in compression model performance resulting from the tradeoff analysis was surprisingly low. The first-order, four-degree-of-freedom interpolator mentioned above is proposed for the groundbased data compression applications, and, because this model is relatively complex, a simpler, though less effective, first-order interpolator is proposed for space applications. Queuing control, time and channel coding, and reconstruction methods are proposed for both applications.

As the study progressed, it became apparent that the effectiveness of existing compression techniques on S-6 data was not as high as had been experienced previously at LMSC on other data. A typical example of the overall bandwidth compression ratios obtained on the S-6 data is 3.3:1. A number of methods for improving the compression are proposed, including partial data processing before transmission (signal reduction), and methods to take advantage of the periodicity which exists in many of the S-6 data waveforms. It is estimated that with the proper application of these techniques, bandwidth compression ratios exceeding 10:1 can be achieved on S-6 data. Recommendations for future study therefore include investigations of these data compression techniques.

CONTENTS

Section		Page
	FOREWORD	iii
	SUMMARY	v
	ILLUSTRATIONS	xi
	TABLES	xvi
1	INTRODUCTION	1-1
	1.1 Purpose	1-1
	1.2 Scope	1-1
	1.3 Project	1-2
	1.4 Background	1-4
2	CATAGORIES OF DATA COMPRESSION	2-1
	2.1 General	2-1
	2.2 Signal Reduction	2-1
	2.3 Adaptive Sampling	2-2
	2.4 Redundancy Reduction	2-3
	2.5 Encoding	2-4
3	SELECTION AND EVALUATION OF COMPRESSION MODELS	3-1
	3.1 Model Selection	3-3
	3.2 Data Selection	3-6
	3.3 Nonadaptive Compression	3-8
	3.4 Nonadaptive Filtering	3-15
	3.5 Adaptive Compression (Single Channel)	3-20
4	QUEUING CONTROL EVALUATION	4-1
	4.1 Simulated Compression System	4-2
	4.2 Data Selection	4-3
	4.3 Experiments, Organization	4-3
	4.4 Experiments, Procedure	4-4
	4.5 Results and Conclusions	4-11

Section		Page
5	CHANNEL AND TIME CODING	5-1
	5.1 Channel Identification	5-1
	5.2 Relative Time Coding	5-2
	5.3 Absolute Time Coding	5-7
6	FINAL ANALYSIS	6-1
	6.1 Bandwidth Compression Ratios	6-1
	6.2 Compression Models and Data Classes	6-5
	6.3 Adaptive Aperture and Filtering Techniques	6-7
	6.4 Compression Model Trade-Off Analysis	6-12
	6.5 Compression Ratio Analysis	6-20
7	CONCLUSIONS AND RECOMMENDATIONS	7-1
	7.1 Proposed Data Compression Models	7-1
	7.2 Ground Data Compression System Concept	7-3
	7.3 Future State of the Art	7-4
	7.4 Recommendations For Future Work	7-6
8	NEW TECHNOLOGY	8-1
	8.1 Adaptive Reference Pattern Selector	8-1
	8.2 Short Term Frequency Component Selector	8-2
	8.3 Peak Rms Error Selector	8-2
Appendix		
I	CRITIQUE OF KNOWN MODELS	I-1
	I.1 Signal Reduction	I-1
	I.2 Adaptive Sampling	I-1
	I.3 Redundancy Reduction	I-5
	I.4 Encoding	I-24
II	S-6 SENSOR ASSIGNMENTS	II-1
III	BIT PLANE ENCODING AND DATA ENTROPY CALCULATION	III-1
	III.1 Bit Plane Encoding	III-1
	III.2 Entropy Calculations	III-5
	III.3 Reconstruction Considerations and Error Calculations	III-6

Appendix		Page
IV	SIMULATED MULTISENSOR DATA COMPRESSOR	IV-1
	IV.1 DECOM	IV-1
	IV.2 COMPRESS	IV-1
	IV.3 RECON	IV-3
	IV.4 K-PLOT	IV-3
	IV.5 Queuing Control Subroutines	IV-3
	IV.6 Compressor Simulation Output	IV-4
V	BIBLIOGRAPHY	V-1
VI	GLOSSARY	VI-1

ILLUSTRATIONS

Figure		Page
2-1	Classification of Data Compression Models	2-7
2-2	Functional Organization of Adaptive Telemetry	2-8
2-3	Adaptive Multiplexer Block Diagram	2-9
3-1	Data Classes	3-25
3-2	Raw Data, Sensor 9	3-26
3-3	Raw Data, Sensor 10	3-33
3-4	Raw Data Data, Sensor 11	3-39
3-5	Class 1 Original and Reconstructed Data (ZOI)	3-46
3-6	Class 2 Original and Reconstructed Data (ZOI)	3-47
3-7	Class 3 Original and Reconstructed Data (ZOI)	3-49
3-8	Class 5 Original and Reconstructed Data (ZOI)	3-51
3-9	Class 1 Original and Reconstructed Data (FOIDIS)	3-52
3-10	Class 2 Original and Reconstructed Data (FOIDIS)	3-53
3-11	Class 3 Original and Reconstructed Data (FOIDIS)	3-55
3-12	Class 5 Original and Reconstructed Data (FOIDIS)	3-57
3-13	Class 1 Short-Term Compression Ratio (FOIDIS)	3-58
3-14	Class 2 Short-Term Compression Ratio (FOIDIS)	3-59
3-15	Class 3 Short-Term Compression Ratio (FOIDIS)	3-61
3-16	Class 5 Short-Term Compression Ratio (FOIDIS)	3-63
3-17	Digitally Filtered Data	3-64
3-18	Precompression Filtering (Sensor 9)	3-68
3-19	Precompression Filtering (Sensor 10)	3-69
3-20	Precompression Filtering (Sensor 11)	3-70
3-21	Original and Reconstructed Data Using Nonadaptive Precompression Filtering	3-71

Figure		Page
3-22	Single Channel Data Compressor With Adaptive Aperture	3-75
3-23	Adaptive Aperture Control Function	3-76
3-24	Original and Reconstructed Data Using Adaptive Aperture	3-77
3-25	Single Channel Data Compressor With Adaptive Precompression Filtering	3-81
3-26	Adaptive Precompression Filtering Control Function	3-81
3-27	Original and Reconstructed Data Using Adaptive Precompression Filtering	3-82
4-1	Queue Length vs Time, Runs S6-03 and S6-04	4-28
4-2	Queue Length and Buffer Input Arrival Rate vs Time, Runs S6-05 and S6-06	4-31
4-3	Buffer Input Arrival Rate Histogram, Run S6-07	4-34
4-4	Histogram of Time Intervals Between Buffer Input Arrivals, Run S6-07	4-35
4-5	Queue Length Histogram, Run S6-07	4-36
4-6	Queue Length and Buffer Input Arrival Rate vs Time, Run S6-07	4-37
4-7	Queue Length and Buffer Input Arrival Rate vs Time, Run S6-08	4-41
4-8	Queue Length and Buffer Input Arrival Rate vs Time, Run S6-09	4-45
4-9a	Sensor 9 Original Data, Reconstructed Data, and Error vs Time, Run S6-08	4-50
4-9b	Sensor 9 Tolerance vs Time, Run S6-08	4-51
4-10a	Sensor 9 Original Data, Reconstructed Data, and Error vs Time, Run S6-09	4-56
4-10b	Sensor 9 Tolerance vs Time, Run S6-09	4-57
4-11	Sensor 9 Original Data, Reconstructed Data, and Error vs Time, Run S6-07	
4-12	Sensor 9 Error Histogram, Run S6-08	4-65
4-13	Sensor 9 Error Histogram, Run S6-09	4-66
4-14	Sensor 9 Error Histogram, Run S6-07	4-67
4-15a	Sensor 11 Original Data, Reconstructed Data, and Error vs Time, Run S6-08	4-68

Figure		Page
4-15b	Sensor 11 Tolerance vs Time, Run S6-08	4-69
4-16a	Sensor 11 Original Data, Reconstructed Data, and Error vs Time, Run S6-09	4-76
4-16b	Sensor 11 Tolerance vs Time, Run S6-09	4-77
4-17	Sensor 11 Original Data, Reconstructed Data, and Error vs Time, Run S6-07	4-84
4-18	Sensor 11 Error Histogram, Run S6-08	4-88
4-19	Sensor 11 Error Histogram, Run S6-09	4-89
4-20	Sensor 11 Error Histogram, Run S6-07	4-90
4-21	Comparative Rms Errors, Test Groups 2 and 3	4-91
4-22	Queue Length and Buffer Input Arrival Rate vs Time, Run S6-10	4-92
4-23a	Sensor 9 Original Data, Reconstructed Data, and Error vs Time, Run S6-10	4-96
4-23b	Sensor 9 Tolerance vs Time, Run S6-10	4-97
4-24	Sensor 9 Error Histogram, Run S6-10	4-102
4-25a	Sensor 11 Original Data, Reconstructed Data, and Error vs Time, Run S6-10	4-104
4-25b	Sensor 11 Tolerance vs Time, Run S6-10	4-105
4-26	Sensor 11 Error Histogram, Run S6-10	4-112
4-27	Queue Length and Buffer Input Arrival Rate vs Time, Run S6-12	4-113
4-28a	Sensor 9 Original Data, Reconstructed Data, and Error vs Time, Run S6-12	4-118
4-28b	Sensor 9 Tolerance vs Time, Run S6-12	4-119
4-29a	Sensor 11 Original Data, Reconstructed Data, and Error vs Time, Run S6-12	4-124
4-29b	Sensor 11 Tolerance vs Time, Run S6-12	4-125
4-30	Queue Length vs Time, Run S6-11	4-128
4-31	Sensor 9 Original Data, Reconstructed Data, and Error vs Time, Run S6-11	4-130
4-32	Sensor 11 Original Data, Reconstructed Data, and Error vs Time, Run S6-11	4-133
4-33	Comparison of Average Compression Ratios With and Without Sync Losses	4-135

Figure		Page
4-34	Queue Length and Buffer Input Arrival Rate vs Time, Runs S6-16 and S6-17	4-136
4-35	Queue Length Histogram, Run S6-16	4-140
4-36	Buffer Input Arrival Rate Histogram, Runs S6-14, S6-15, S6-16, and S6-17	4-141
4-37	Histogram of Time Intervals Between Buffer Input Arrivals, Runs S6-14, S6-15, S6-16, and S6-17	4-142
4-38	Queue Length and Buffer Input Arrival Rate vs Time, Run S6-18	4-143
4-39	Queue Length and Buffer Input Arrival Rate vs Time, Run S6-19	4-147
4-40a	Sensor 9 Original Data, Reconstructed Data, and Error vs Time, Run S6-18	4-152
4-40b	Sensor 9 Tolerance vs Time, Run S6-18	4-153
4-41a	Sensor 9 Original Data, Reconstructed Data, and Error vs Time, Run S6-19	4-156
4-41b	Sensor 9 Tolerance vs Time, Run S6-19	4-157
4-42	Sensor 9 Original Data, Reconstructed Data, and Error vs Time, Run S6-07	4-160
4-43	Sensor 9 Error Histogram, Run S6-18	4-162
4-44	Sensor 9 Error Histogram, Run S6-19	4-163
4-45	Sensor 9 Error Histogram, Run S6-07	4-164
4-46a	Sensor 11 Original Data, Reconstructed Data, and Error vs Time, Run S6-18	4-166
4-46b	Sensor 11 Tolerance vs Time, Run S6-18	4-167
4-47a	Sensor 11 Original Data, Reconstructed Data, and Error vs Time, Run S6-19	4-168
4-47b	Sensor 11 Tolerance vs Time, Run S6-19	4-169
4-48	Sensor 11 Original Data, Reconstructed Data, and Error vs Time, Run S6-07	4-170
4-49	Sensor 11 Histogram, Run S6-18	4-171
4-50	Sensor 11 Error Histogram, Run S6-19	4-172
4-51	Sensor 11 Error Histogram, Run S6-07	4-173
4-52	Comparative R.ms Errors, Test Group 4	4-174

Figure		Page
5-1	Conversion Characteristics from Sample Compression Ratio to Bandwidth Compression Ratio for S-3 Satellite Telemetry Multiplexing Format	5-10
5-2	Conversion Characteristics from Sample Compression Ratio to Bandwidth Compression Ratio for S-6 Satellite Telemetry Multiplexing Format	5-11
5-3	S-6 Telemetry Frame Format, Showing Use of Short Frame in Time and Channel Coding	5-12
5-4	Conversion Characteristics from Sample Compression Ratio to Bandwidth Compression Ratio for S-49 Satellite Telemetry Multiplexing Format	5-13
6-1	Comparative Bandwidth Compression Ratios, Averaged Between Tolerance Values of 2 and 4 Data Units	6-24
6-2	Bandwidth Compression Efficiencies of Bit Plane Encoding and Redundancy Reduction Selectors, Sensor 9	6-25
6-3	Bandwidth Compression Efficiencies of Bit Plane Encoding and Redundancy Reduction Selectors, Sensor 11	6-26
6-4	Comparison of Bandwidth Compression Ratios, FOIDIS, Tolerance = 4 Data Units	6-27
6-5	Compression Model Performance Factors	6-28
6-6	Summary of Bandwidth Compression Ratios for Other Telemetry Data	6-29
7-1	Proposed Spaceborne Data Compressor for S-6 Data	7-9
7-2	Proposed Ground-Based Data Compressor for S-6 Data	7-10
7-3	Block Diagram, Generalized Ground Data Compression System	7-11
7-4	Block Diagram, Future Adaptive Telemetry System	7-12
I-1	Cumulative Difference, Zero Order Predictor, Floating Aperture	I-6
I-2	Zero Order Polynomial Interpolator, Computed Sample Transmitted	I-18
I-3	First Order Interpolator Redundancy Reduction	I-21
III-1	Coding Format	III-2
IV-1	Generalized Simulation Program Block Diagram	IV-2
IV-2	Typical Control Curves for Compression Ratio Monitoring Queuing Control Control System	IV-5
IV-3	Typical Control Curves for Queue Length Monitoring Queuing Control System	IV-6

TABLES

Table		Page
3-1	Sensor Numbers and Data Classes	3-7
3-2	Compression Characteristics, Sensors 9, 10, and 11	3-9
3-3	Compression Ratios vs Data Classes	3-11
3-4	Redundancy Reduction and Bit Plane Coding Results	3-14
3-5	Compression Ratio and Rms Error Summary, Filtered Data	3-18
3-6	Adaptive Aperture Compression Summary	3-22
3-7	Adaptive Filtering Compression Summary	3-24
4-1	Assigned Tolerance Values for Buffer Queuing Control Study	4-5
4-2	Compressor Run Summary, Test Group 1	4-6
4-3	Compressor Run Summary, Test Group 2	4-7
4-4	Compressor Run Summary, Test Group 3	4-8
4-5	Compressor Run Summary, Test Group 4	4-10
4-6	Combined Results by Individual Sensor – Test Groups 2 and 3	4-16
4-7	Compression of Average Compression Ratios With and Without Sync Losses, FOIDIS Compression Model	4-22
4-8	Combined Results by Individual Sensor – Test Group 4	4-25
4-9	Compressor Run Summary	4-175
6-1	Bandwidth Compression Ratios From Single Sensor Experiments (Section 3)	6-2
6-2	Bandwidth Compression Ratios From Multi-Sensor Experiments (Section 4)	6-4
6-3	Bandwidth Compression Ratios vs Data Classes	6-6
6-4	Compression Model Performance Factors	6-18
I-1	Compression Model Listing	I-2
II-1	S-6 Sensor Designations	II-1
III-1	Code Words and Code Groups	III-3

Figure		Page
5-1	Conversion Characteristics from Sample Compression Ratio to Bandwidth Compression Ratio for S-3 Satellite Telemetry Multiplexing Format	5-10
5-2	Conversion Characteristics from Sample Compression Ratio to Bandwidth Compression Ratio for S-6 Satellite Telemetry Multiplexing Format	5-11
5-3	S-6 Telemetry Frame Format, Showing Use of Short Frame in Time and Channel Coding	5-12
5-4	Conversion Characteristics from Sample Compression Ratio to Bandwidth Compression Ratio for S-49 Satellite Telemetry Multiplexing Format	5-13
6-1	Comparative Bandwidth Compression Ratios, Averaged Between Tolerance Values of 2 and 4 Data Units	6-24
6-2	Bandwidth Compression Efficiencies of Bit Plane Encoding and Redundancy Reduction Selectors, Sensor 9	6-25
6-3	Bandwidth Compression Efficiencies of Bit Plane Encoding and Redundancy Reduction Selectors, Sensor 11	6-26
6-4	Comparison of Bandwidth Compression Ratios, FOIDIS, Tolerance = 4 Data Units	6-27
6-5	Compression Model Performance Factors	6-28
6-6	Summary of Bandwidth Compression Ratios for Other Telemetry Data	6-29
7-1	Proposed Spaceborne Data Compressor for S-6 Data	7-9
7-2	Proposed Ground-Based Data Compressor for S-6 Data	7-10
7-3	Block Diagram, Generalized Ground Data Compression System	7-11
7-4	Block Diagram, Future Adaptive Telemetry System	7-12
I-1	Cumulative Difference, Zero Order Predictor, Floating Aperture	I-6
I-2	Zero Order Polynomial Interpolator, Computed Sample Transmitted	I-18
I-3	First Order Interpolator Redundancy Reduction	I-21
III-1	Coding Format	III-2
IV-1	Generalized Simulation Program Block Diagram	IV-2
IV-2	Typical Control Curves for Compression Ratio Monitoring Queuing Control System	IV-5
IV-3	Typical Control Curves for Queue Length Monitoring Queuing Control System	IV-6

TABLES

Table		Page
3-1	Sensor Numbers and Data Classes	3-7
3-2	Compression Characteristics, Sensors 9, 10, and 11	3-9
3-3	Compression Ratios vs Data Classes	3-11
3-4	Redundancy Reduction and Bit Plane Coding Results	3-14
3-5	Compression Ratio and Rms Error Summary, Filtered Data	3-18
3-6	Adaptive Aperture Compression Summary	3-22
3-7	Adaptive Filtering Compression Summary	3-24
4-1	Assigned Tolerance Values for Buffer Queuing Control Study	4-5
4-2	Compressor Run Summary, Test Group 1	4-6
4-3	Compressor Run Summary, Test Group 2	4-7
4-4	Compressor Run Summary, Test Group 3	4-8
4-5	Compressor Run Summary, Test Group 4	4-10
4-6	Combined Results by Individual Sensor – Test Groups 2 and 3	4-16
4-7	Compression of Average Compression Ratios With and Without Sync Losses, FOIDIS Compression Model	4-22
4-8	Combined Results by Individual Sensor – Test Group 4	4-25
4-9	Compressor Run Summary	4-175
6-1	Bandwidth Compression Ratios From Single Sensor Experiments (Section 3)	6-2
6-2	Bandwidth Compression Ratios From Multi-Sensor Experiments (Section 4)	6-4
6-3	Bandwidth Compression Ratios vs Data Classes	6-6
6-4	Compression Model Performance Factors	6-18
I-1	Compression Model Listing	I-2
II-1	S-6 Sensor Designations	II-1
III-1	Code Words and Code Groups	III-3

Section 1
INTRODUCTION

Section 1
INTRODUCTION

Data compression provides an answer to a major problem that currently faces the field of information technology: the increasing volume of scientific and engineering data being telemetered and processed.

Telemetry, an absolute necessity to the development of missiles and spacecraft, is a wasteful user of the radio-frequency spectrum. There are vehicles operating now that must use several r-f links to transmit all of the data they obtain. As space experiments and vehicles get more complex, the dilemma becomes more serious and more widespread: masses of data virtually saturate ground networks and tax their ability for vital real-time data handling, preflight checkout time and costs increase, demands on data-processing time and facilities exceed practical limits, data-storage archives overflow.

1.1 PURPOSE

The purpose of this study was to investigate and select optimum techniques for compressing satellite telemetry data and to devise methods for re-establishing the original time base after compression. Also, the knowledge and art of data compression were to be extended and new concepts and techniques developed. (Goddard Space Flight Center (GSFC) S-6, Explorer XVII, satellite data were used in all experiments.)

1.2 SCOPE

This report has eight sections and six appendices. Section 1 introduces the problem, the project, and the report. The various categories of data compression, such as signal reduction, adaptive sampling, redundancy reduction and encoding are defined in Section 2. Appendix I discusses the more than 30 compression techniques found during the study; Section 3 selects and evaluates those that are most promising.

Section 4 evaluates buffer queuing control and Section 5 describes methods of channel identification and time base reconstruction. Section 6 presents the final analysis. Conclusions and recommendations are given in Section 7, and concepts and techniques developed late in the study are summarized in Section 8. As a general rule, figures are placed at the ends of the sections, rather than within the text.

Appendix I describes and criticizes the compression models found during the data-compression literature search and existing in-house. Appendix II is a table of the identification numbers assigned to the S-6 data sensors. The techniques used in the report for encoding bit planes and calculating entropy are described in Appendix III. Reconstruction and error magnitudes are also discussed. Appendix IV describes the four computer programs developed to simulate a multisensor data compressor. Appendix V lists more than 200 references found in the literature search. Appendix VI presents a glossary to define several terms either unique to this study or not in general usage.

1.3 PROJECT

The project consisted of six tasks: simulation, search, selection, control, identification, and liaison.

1.3.1 Task I - Compression Model Simulation Analysis

Task I involved a computer simulation and evaluation of various data compression models applied to the S-6 data. A special computer program was developed to demultiplex and sort selected data channels. Redundancy reduction and encoding models were evaluated and compression ratios were obtained for candidate compression models for the various classes of data identified by GSFC.

1.3.2 Task II - Literature Search

Task II involved an extensive search of international literature to identify all announced data compression models. The models were compared primarily on

compression ratio and the most promising models were evaluated in the Task I computer simulation work. In addition to the literature search, LMSC provided monthly summaries of the LMSC Independent Development and Independent Research activities conducted through the study. As a conclusion to the literature search and Task I, LMSC was required to predict the probable future of data compression.

1.3.3 Task III - Selection of Optimum Models

Task III determined the optimum data compression model based on the following minimum criteria:

- Compression ratio
- Influence of noise in the raw telemetry data
- Data resolution and accuracy considering peaks and rms error
- Ease of data reconstruction
- Effectiveness with adaptive techniques

1.3.4 Task IV - Adaptive Buffer Queuing Control

This task involved the development and investigation of adaptive buffer queuing control techniques for minimizing data loss due to buffer overflow while keeping data fidelity degradation to a minimum. Three new computer programs were developed for this work, one for demultiplexing, one for compression, and one for reconstruction.

1.3.5 Task V - Time and Channel Identification

This task developed ways for coding compressed data to make the reconstructed time base equivalent to conventional PCM, found methods to identify channels, and determined the influence of time and channel coding on overall compression ratios.

1.3.6 Task VI - Computer Programs

This task consisted of sending to GSFC FORTRAN statements of computer programs developed during the study.

1.4 BACKGROUND

Over the last 20 years, Lockheed has developed numerous bandwidth reduction devices for aircraft, missile, and satellite programs. In 1961, LMSC became actively engaged in redundancy reduction as a means for alleviating the data explosion problem referred to above. Since then, LMSC has written and published more than 50 reports and papers on data compression and has developed seven operational compression systems.

Early computer simulations confirmed that required bandwidth and/or transmission time could be reduced substantially by using a zero order predictor. Later studies explored the effectiveness of other predictor and interpolator compression models and theoretical studies were made of buffer queue behavior and compression efficiency. Nonstationarity of telemetry data, however, caused discrepancies between the theoretical and empirical results. The Wiener predictor and other polynomial predictors were investigated under the LMSC Independent Research Program using stationary artificial data. Due to internal funding limitations, these studies were not completed.

The interpolator was refined by studies conducted under the LMSC Independent Development Program. Several interpolators were found which consistently provided higher compression ratios than the early zero order predictor. Recent work has been devoted to improving overall compression efficiency by means of adaptive aperture and adaptive filtering techniques. A rather extensive set of software programs have been developed for compression and reconstruction of telemetry and video data.

Section 2

CATEGORIES OF DATA COMPRESSION

Section 2 CATEGORIES OF DATA COMPRESSION

This section categorizes, defines and gives examples of the basic techniques of data compression. Categories are signal reduction, adaptive sampling, redundancy reduction, and encoding.

2.1 GENERAL

Data compression is a technique for reducing the amount of bandwidth necessary for transmission of a given amount of information in a given amount of time, or, for reducing the amount of time necessary for the transmission of a given amount of information in a given bandwidth. This must be accomplished without sacrificing the information requirements of the user. Four basic categories of data handling come under this definition: signal reduction, adaptive sampling, redundancy reduction and encoding. Figure 2-1 shows a schematic classification of data compression models by category. It is shown later in this report that two or more categories can be combined for improved data-compression efficiency. Figure 2-2 shows an adaptive telemetry system example that combines all four.

2.2 SIGNAL REDUCTION

Signal reduction is a technique for reducing the bandwidth required for transmission of data by means of an irreversible transformation. Although the term "entropy reduction" (References 24 and 192) has been used to identify this category of data compression, this report prefers the term "signal reduction" to avoid a dual definition of entropy. If a signal reduction process does reduce entropy, it is considered to be unintentional. Signal conditioning devices producing reductions in information bandwidth are included in this category.

Signal reduction represents the oldest and most widely used form of data compression. Spectrum analyzers, rectifier-filters, phase comparators, etc., are typical examples of the virtually unlimited number of different techniques which have been used or could be devised. It is generally considered good design practice to use a signal reduction process wherever practical since, in many applications, it will reduce vehicle power, size and weight requirements. In most circumstances, inclusion of signal reduction is complimentary to other forms of data compression. Since the information desired from each sensor may be different, signal reduction devices are usually tailored to each data source.

2.3 ADAPTIVE SAMPLING

Adaptive sampling is a technique for adjusting the sampling rate of a given sensor to correspond to its information rate. In this manner, the total sample rate of all sensors is adjusted to conform with the channel capacity (Reference 217) of the data link. As in signal reduction, the definition of information for each source can be different, requiring different criteria for measuring information rates. Since the overall objective of adaptive sampling is to improve communication efficiency by minimizing the channel capacity requirements, this report recognizes this class of data management as a category of data compression. Adaptive sampling is a reversible process since it is possible to reconstruct the original signal waveform within the error requirements stipulated by the user (and the information rate analyzer).

Figure 2-1 divides adaptive sampling into two categories, telemetry format variation by ground station control, and self-adaptive sampling. The former is straightforward; an example of the latter is shown in Figure 2-3. Note that a separate analyzer is needed for each sensor corresponding to the information required by each user. The sampling frequency of each gate is assumed to be related to the short-duration frequency components of the desired information, and the relative priority of the sensor. To measure or determine the instantaneous frequency spectrum of a source, a finite period of time is required. Considerable error due to aliasing can result if an abrupt change in data activity occurs unless a delay is placed between the sensor and the multiplexer gate to store the data until corrective action (such as changing sampling frequency) can be taken.

The system shown in Figure 2-3 is somewhat inflexible because the multiplexer output sample rate is constant. Since all sampling must be synchronized to the speed of the multiplexer, a nonvarying output rate restricts the sampling times and maximum sampling rate of a sensor. This inflexibility could be overcome by (1) using variable analog delays for each sensor in place of the constant delays shown in Figure 2-3, (2) using a variable-speed multiplexer, or (3) using a combination of (1) and (2). In the second technique, a queuing buffer must be placed between the multiplexer and the transmitter so that the variable-rate data samples emerging from the multiplexer can be transmitted at a constant rate.

2.4 REDUNDANCY REDUCTION

Redundancy reduction is a technique for eliminating data samples that can be implied by examination of preceding or succeeding samples, or by comparison with arbitrary reference patterns. The basic difference between adaptive sampling and redundancy reduction is that in adaptive sampling, the sampling rate of the original data waveform is varied, while in redundancy reduction the waveform is initially sampled at a constant rate and nonessential samples eliminated later.

The concept of redundancy reduction is designed to overcome many of the problems inherent in adaptive sampling. Since it is possible for redundancy reduction to achieve results similar to adaptive sampling the former has at times been classified as a form of adaptive sampling. As in the case of adaptive sampling, the significant sample rate is assigned in accordance with the information rate of each sensor. In this sense redundancy reduction is also adaptive. This category is also reversible.

Shannon (Reference 217) has defined redundancy as "that fraction of a message or datum which is unnecessary and hence repetitive in the sense that if it were missing the message would still be essentially complete, or at least could be completed". Redundancy exists whenever the sampling frequency of a multiplexer exceeds the frequency required to describe the input function in accordance with the user accuracy requirements.

The choice of reference patterns used to detect redundancy is virtually unlimited. Polynomials, exponentials, and sine waves are good examples of reference patterns by which real data can often be approximated. Arbitrary cyclic patterns such as the periodic components of an electrocardiogram or a commercial television picture, for instance, can be used as references to detect redundancy data from a given sensor. The process of redundancy reduction can be achieved by means of "prediction" from a priori knowledge of previous samples, or by a posteriori "interpolation" from future samples.

2.4.1 Error Characteristics

For redundancy reduction to achieve reasonable compression efficiencies, it is often necessary to introduce certain errors. These errors are caused from filtering and/or thresholding within the redundancy reduction process and do result in slight reductions in the source entropies. Why then, are not adaptive sampling and redundancy reduction processes classified as subsets to signal reduction? Unlike signal reduction, adaptive sampling and redundancy reduction are designed such that the original source waveforms can be reconstructed with a guaranteed fidelity. However, since errors are introduced during these compression processes, this goal cannot be achieved absolutely. It must be recognized that it is impossible to design any instrumentation or data acquisition system which does not have error. The design objectives of adaptive sampling and redundancy reduction are identical to the design objectives of any instrumentation system; i. e., to supply the data within the accuracy requirements of the user.

2.5 ENCODING

Encoding is a technique for transforming a given message into a corresponding sequence of code words. As in the cases of adaptive sampling and redundancy reduction, an effective coding technique requires sequential message words to exhibit a high average correlation. Consequently, to achieve the desired coding it is desirable to know the source statistics. If statistics are stationary and are known a priori, a nonadaptive encoding procedure can be specified. In many cases, however, the statistics are not well known to the experimenter, and/or the statistics of the measurement source may be

nonstationary. Under these conditions a nonadaptive encoding procedure can result in a bandwidth expansion instead of a bandwidth reduction. To circumvent this problem, adaptive encoding techniques can be devised whereby the code assignments are based upon the most recent statistic measured by the encoder itself. Encoding is generally a reversible process.

2.5.1 Classification

It is possible to classify encoding as a redundancy reduction process. Similarly, redundancy reduction can also be classified as an encoding process. In most cases the differences between redundancy reduction and adaptive encoding are small. In fact it is possible to select examples in which no differences exist between these two categories. The primary difference pertains to the form of redundancy which is to be removed and other system considerations, such as time delay, response to major changes in stationarity, and the message structure (format) of the transmitted information.

In nonadaptive encoding the estimated amplitude probability distribution of the message sequence or run length probabilities are often used as a basis for coding, i. e., short code words are assigned to message words having the largest probability of occurrence and long code words are assigned to message words which infrequently occur. Thus, a measure of redundancy is assumed to be the frequency of occurrence of each set of data values. On the other hand, the redundancy reduction category achieves compression based on the assumption that the data amplitude will remain the same, or nearly the same, for long durations, or that the data sequence will continue to change at a prescribed rate.

2.5.1.1 Data Stationarity. The operations involved in redundancy reduction are not influenced by abrupt changes in data statistics. On the other hand, many forms of adaptive encoding are organized so that rules for encoding change in accordance with measured statistics. The measurement of a new set of statistics following a major change in data characteristics requires considerable time and can result in low compression efficiency during the measurement period. For this reason, certain forms

of adaptive encoding are restricted to quasi-stationary classes of data (Reference 24).

2.5.1.2 Transmission Formats. The production of code words of varying length for varying input message words is characteristic of nonadaptive encoding. In the case of adaptive encoding, output code words are also variable in length, but for certain models the number of bits in the output code words may be less than the number of bits in the input messages. Redundancy reduction, on the other hand, maintains a constant length for each transmitted code word, the number of transmitted code words always being less than or equal to the number of input message words. The constant word length characteristic has been imposed to minimize the problems of time and channel identification and word synchronization.

Because of the above differences, encoding and redundancy reduction have been classified as separate data compression categories in this report. The possibility of cascading redundancy reduction and encoding are discussed in later sections.

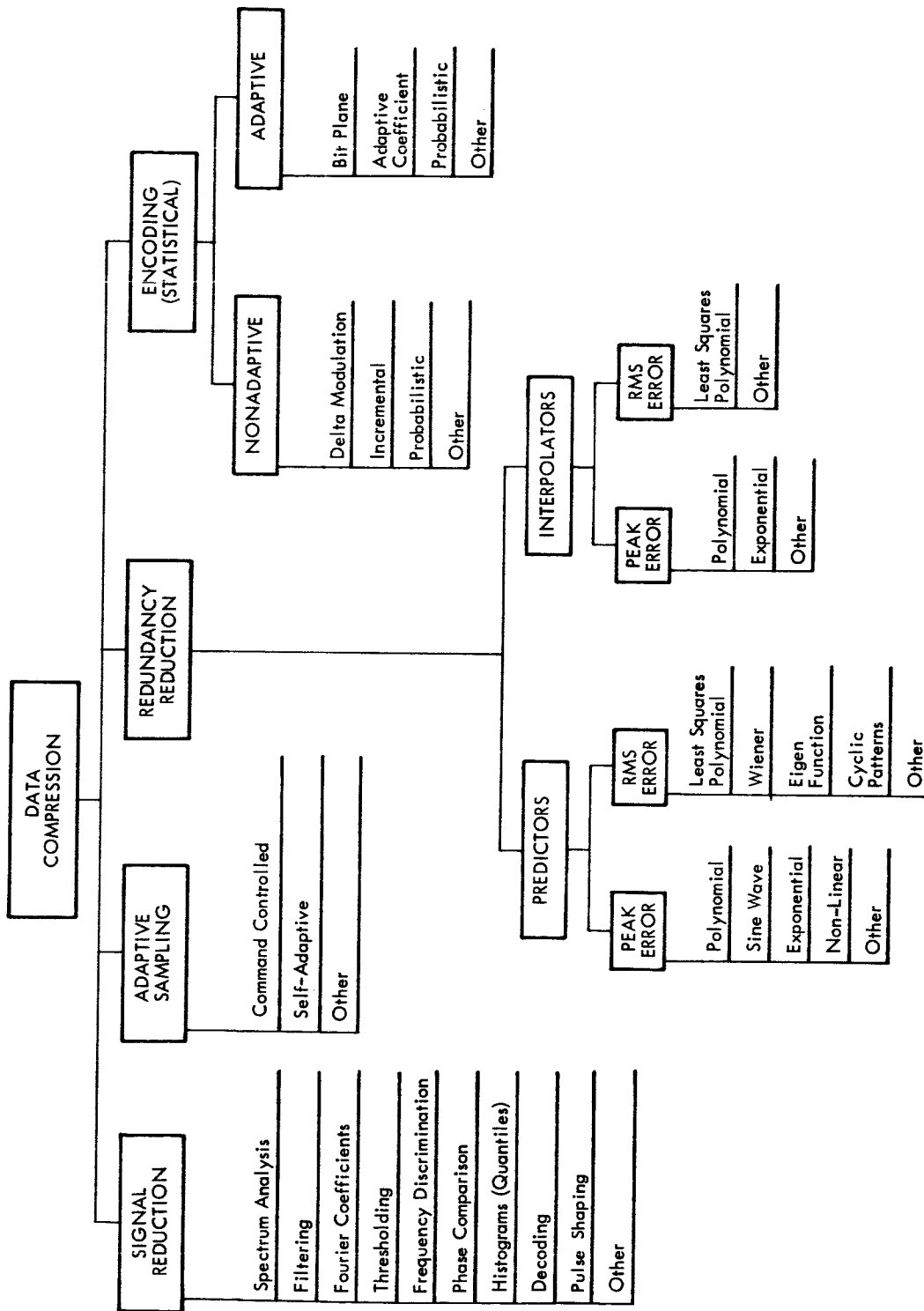
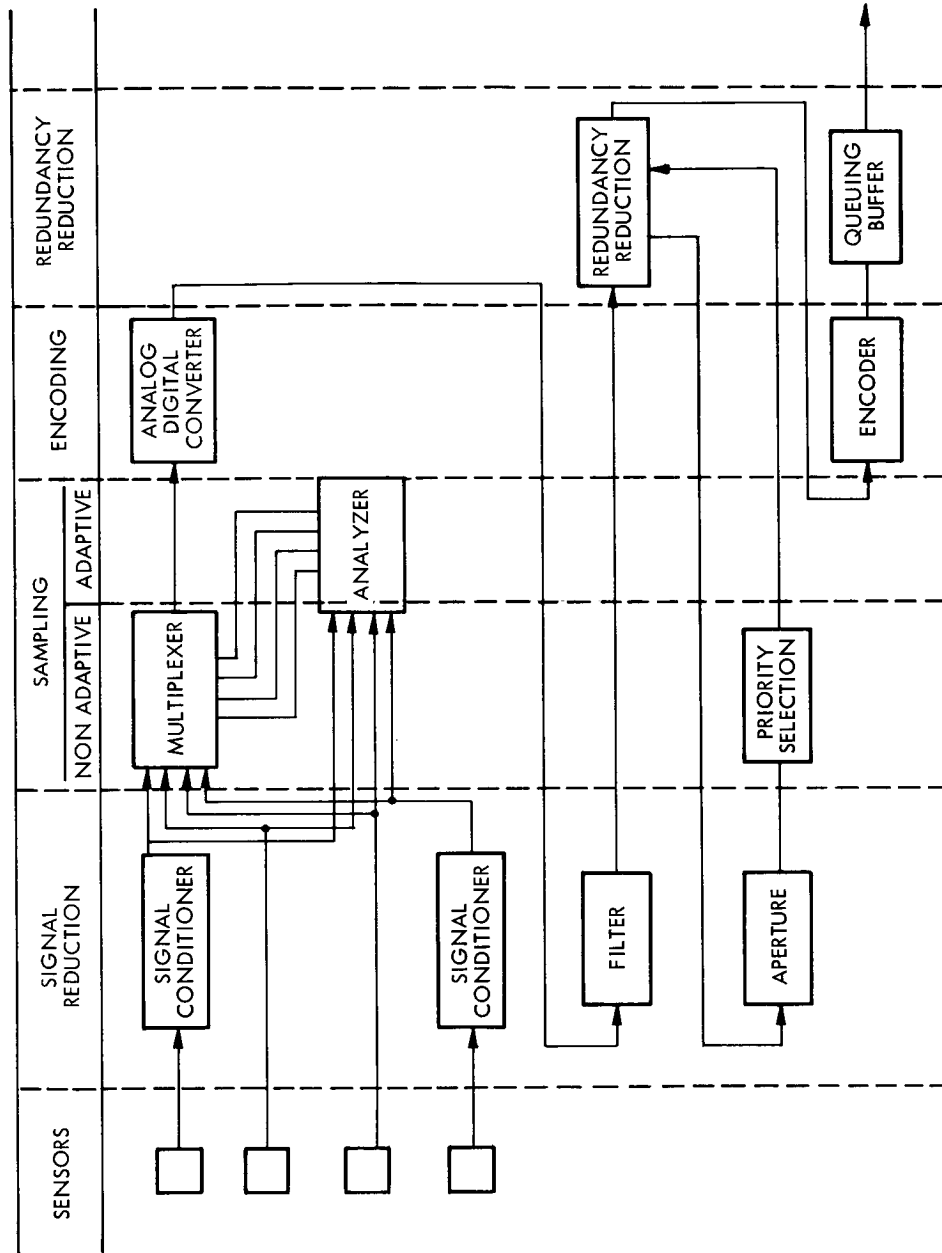


Fig. 2-1 Classification of Data Compression Models



NOTE: Adaptive Controls not shown

Fig. 2-2 Functional Organization of Adaptive Telemetry

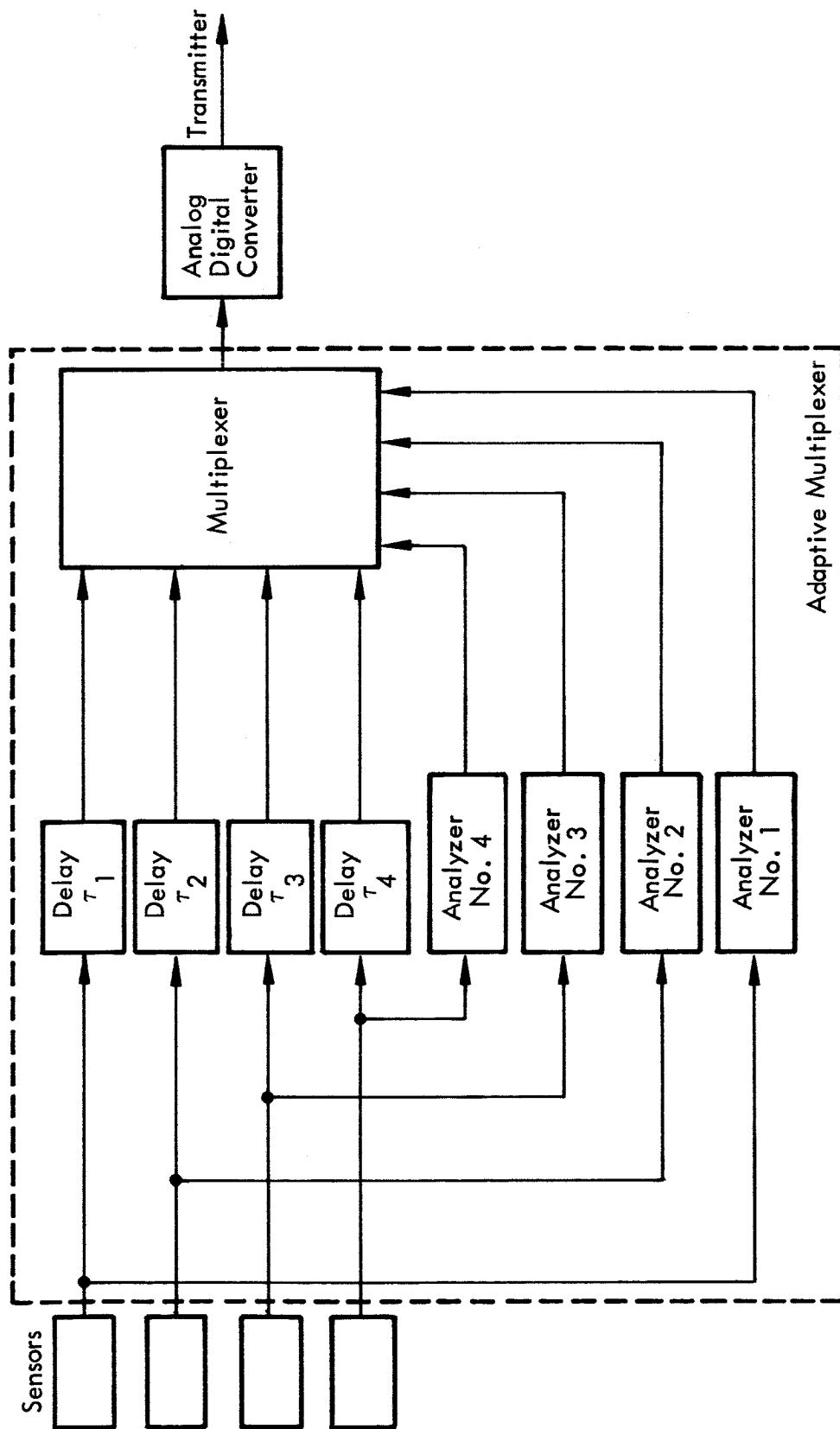


Fig. 2-3 Adaptive Multiplexer Block Diagram

Section 3

SELECTION AND EVALUATION
OF COMPRESSION MODELS

Section 3

SELECTION AND EVALUATION OF COMPRESSION MODELS

Over 30 data compression techniques exist for evaluation by this report either as a result of in-house projects or the literature search. This section selects, compares, and evaluates the more promising ones in the context of nonadaptive and adaptive compression. It also discusses nonadaptive and adaptive filtering.

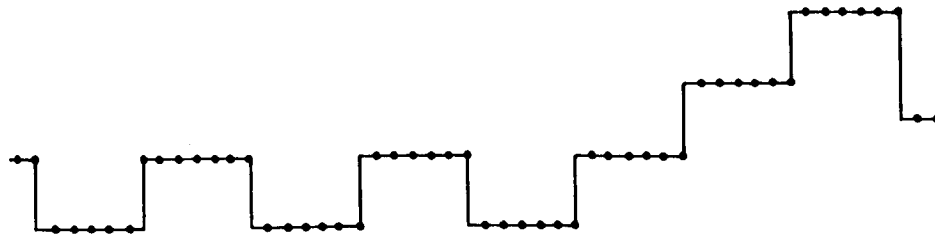
A basic objective of this study was to investigate the correlation of data compression models with classes of data specimens. Since previous data classification techniques using information such as data spectral and statistical properties have had limited success, this study took a more straightforward approach.

First of all, five data classes were postulated, each having data with a characteristic waveshape:

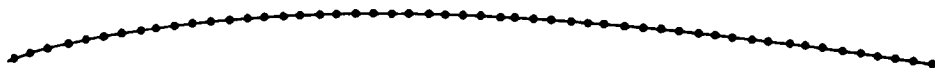
- Class 1, Squarewaves and Step Transients
- Class 2, Constant or Slowly Drifting Amplitudes
- Class 3, Exponential Transients
- Class 4, Sawtooth Waveforms
- Class 5, Waveforms not Included in Classes 1 through 4

Examples are given in Figure 3-1.

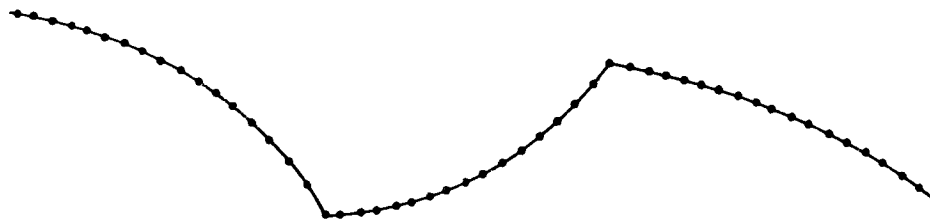
Next, it was conjectured that in most instances, all specimens of data falling into a given class would be most efficiently compressed by only one compressor configuration and the compressor performance would be predictable. Experiments were then made to see if this were true. Since a telemetry system usually conveys many different classes of multiplexed data from the same vehicle, it is desirable in the interest of simplicity to use one compression model for all classes. Experiments were made to find if this is possible.



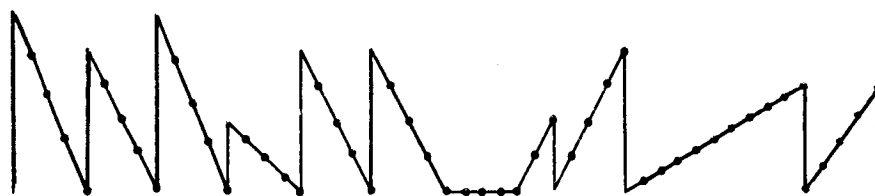
Data Class 1 – Squarewaves and step-like transients



Data Class 2 – Constant or slowly drifting amplitudes



Data Class 3 – Exponential transients



Data Class 4 – Sawtooth waveforms



Data Class 5 – Waveforms not included in Classes 1-4

Fig. 3-1 Data Classes

3.1 MODEL SELECTION

To understand the reasoning behind the selection, it is first necessary to have a general understanding of redundancy reduction methods and techniques. (A detailed discussion of each technique is given in Appendix I.)

3.1.1 Redundancy Reduction Techniques

Redundancy reduction techniques can be divided into polynomial and nonpolynomial techniques. The polynomial techniques can be further divided into subclasses according to the order of the polynomial used in approximating data, zero order and first order, for instance. Also, both polynomial and nonpolynomial compression techniques can be further divided into two categories, prediction and interpolation.

3.1.1.1 Prediction. Prediction of the magnitude of future data samples requires some knowledge of the data history. The history used can be in terms of statistics or repetitive patterns in data acquired during previous flights or experiments. This history can also be obtained from data samples recently generated by the particular sensor in question. The manner in which these histories are used to predict a time function is limited only by the practical considerations of hardware simplicity and prediction efficiency. Such factors as noise, frequency response, errors and data significance must be considered when selecting a prediction model. A prediction is a guess, and, to be effective, requires that the characteristics of data remain relatively constant from one time interval to the next. If data is varying in a random fashion as if perturbed by high frequency noise, redundancy-reduction efficiency of a predictor is generally low for reasonable system accuracies. By examining the behavior of a predictor applied to real data, one can see that a greater number of redundant samples can be eliminated if both future and past data samples are used to eliminate redundant samples. If the decision concerning the redundancy of a data sample can be deferred until subsequent data values are known, there is a greater likelihood that the sample in question can be classified as redundant.

3.1.1.2 Interpolation. The process of eliminating redundant data samples by after the fact, a posteriori, polynomial curve fitting is termed interpolation. Like the predictor, the interpolator can be applied to sinewaves and exponentials as well as polynomials.

3.1.2 Choice of Compression Models

The first step in the selection process was to critically examine each compression model found during the literature search. (Each is detailed in Appendix I and listed in Table I-1.) The next step was to reduce these models to a manageable number, consisting only of those which the examiners considered to be the most promising. The rationale used in this selection process is presented in the following paragraphs.

For ease of comparison the compression models were grouped into the following classes and subclasses (see Table I-1):

- Adaptive sampling
- Redundancy reduction
 - Zero and first order polynomial predictors and interpolators
 - Higher order polynomial predictors and interpolators
 - All other predictors and interpolators
- Encoding

The first class considered was adaptive sampling. The associative data compressor, (designated as Model No. 1 in Table I-1) and transient event recorder, Model 3, were rejected because their applications were too limited. Adaptive (format) telemetry, Model 2, was rejected because man is an essential part of its feedback link. Self-adaptive telemetry, Model 4, was eliminated mainly because of the difficulties anticipated in implementing satisfactory analog delays.

The second class considered was that containing zero and first order polynomial predictors and interpolators. The floating aperture, cumulative difference, zero order predictor (ZOP), Model 7, was selected primarily because of its past performance and ease of implementation and was selected over the other zero-order, polynomial predictors, Models 5, 6, and 8, because of its superior compression efficiency and error characteristics. Of the zero and first order polynomial interpolators constrained by peak error, the computed sample transmitted, zero order interpolator (ZOI), Model 21, and the computed sample transmitted, four degree of freedom, first

order interpolator (FOI4DG), Model 23, were selected because they are both optimum compression models. The last redundant sample transmitted, zero order interpolator, Model 22, was rejected because its performance was found to be inferior to that of the ZOI selector. Because of their demonstrated insensitivity to low level sensor noise and their high compression efficiency, the disjointed line segment first order interpolator (FOIDIS), Model 25, and the offset-out-of-tolerance (direction indicated) first order interpolator (FOIOOT), Model 27, were also chosen. The direction-indicated version of the latter selector was chosen over the last-slope version, Model 26, because of its higher compression efficiency. The first order predictors, Models 9-14, and the joined line segment, first order interpolator, Model 24, were rejected due to their tendency to oscillate in the presence of low level sensor noise. The last data sample transmitted, first order interpolator, Model 28, was rejected due to its incompatibility with adaptive aperture techniques. The least squares polynomial interpolator, Model 20, was not chosen because of its extreme complexity. The higher-order polynomial predictors, such as the second-order predictor, Model 15, were not used due to their susceptibility to low-level noise.

Compression models using more classical methods of prediction and interpolation, i. e., the Wiener predictor, Model 16, the adaptive nonlinear predictor, Model 17, and the finite difference interpolator, Model 19, were rejected primarily because they are relatively unable to deal with nonstationary input data, exhibit relatively low compression ratios, are susceptible to low-level sensor noise, and may be difficult to implement. The exponential predictor, Model 18, the exponential interpolator, Model 29, and the adaptive reference pattern interpolator, Model 30, were all developed late in the study and could not be evaluated. They do, however, show promise in compressing data from Class 3 and, perhaps, data from other classes as well.

From the encoding techniques, bit plane encoding, Model 35, was selected because it had shown promise as being competitive to redundancy reduction in compression efficiency, reconstructed data fidelity, and simplicity. Delta modulation, Model 31, was rejected because of its relatively low anticipated compression efficiency. Difference modulation, Model 32, was not chosen because it is susceptible to cumulative error. Probabilistic encoding techniques, Models 33 and 34, were eliminated primarily because of their variable word length characteristic.

This elimination process left the following six compression models:

- Model 7: Zero Order Predictor (floating aperture), ZOP
- Model 21: Zero Order Interpolator (computed sample transmitted), ZOI
- Model 23: First Order Interpolator (four degree of freedom), FOI4DG
- Model 25: First Order Interpolator (dis-joined-line segment), FOIDIS
- Model 27: First Order Interpolator (offset-out-of-tolerance), FOIOOT
- Model 35: Bit Plane Encoding

3.2 DATA SELECTION

The first major step in the experimental procedure was to select portions of Goddard S-6 Satellite data to be used in the single channel compression model evaluation. The tape chosen by Goddard experimenters was Goddard Buffer Tape No. 59 because it contained relatively few periods of word sync loss. Tape begin time is 10 days, 23 hours, 35 minutes, 17.913 seconds. The tape was decommutated and a standard single channel T-3 format tape written from it so that existing Lockheed computer programs could be used without modification. Each data word on the original tape contained nine bits. The resulting amplitude range of 0-511 was left undisturbed for all sensors.

A representative selection of sensors was made from the decommutated tape and portions were plotted using the 4020 plotter. The resulting plots were inspected visually and portions of three sensors selected as containing data representing four of the five data classes. The sensors, their sampling rates, the time periods relative to the beginning of the tape, and the data classes represented are shown in Table 3-1. Plots are given in Figures 3-2, 3-3 and 3-4. More detailed information concerning these sensors may be found in Appendix II.

Table 3-1
SENSOR NUMBERS AND DATA CLASSES

Sensor	Sampling Rate Samp/sec.	Time Period, sec.		Data Classes Represented
		Begin	End	
9	60	104	136	1, 3
10	20	72	168	1, 2, 3
11	60	104	136	1, 2, 5

None of the plotted data was felt to be sufficiently representative of Class 4 to warrant study. A small portion of Sensor 23, S-3 Goddard Buffer Tape No. 606 was found to contain data belonging to Class 4, but was not of sufficient extent to be used. Conclusions concerning the compression of Class 4 data will therefore be made on the basis of judgment and previous experience, and not on the experimental results of this study.

3.3 NONADAPTIVE COMPRESSION

The data compression models listed at the end of Paragraph 3.1.2 may be used either with or without the aid of adaptive aperture and adaptive filtering techniques. This paragraph examines the performance of the chosen compression models without the incorporation of these techniques. Single-channel experiments concerning their use are discussed in Paragraph 3.5.

3.3.1 Predictors and Interpolators

3.3.1.1 Experiment: Comparison of Predictor and Interpolator Efficiencies. In order to gain a rough idea of relative compression efficiencies, a number of compression simulations were made on the entire chosen portions of Sensors 9, 10 and 11, using the first five selectors listed above with several different peak error constraints (tolerances). The compression ratios¹ obtained and the rms errors between original and reconstructed data are summarized in Table 3-2.

Results. A comparison of the zero order selector results summarized in Table 3-2 indicate that for a given peak error constraint, the zero order interpolator produced significantly higher compression ratios than did the zero order predictor and that for a given peak error constraint, the use of the zero order predictor resulted in an rms error that was significantly less than the zero order interpolator. Although rms error is presumably a measure of reconstructed data quality, it appears that the reconstructed data resulting from the use of both the zero order predictor and interpolator are visually equivalent, in spite of the differences in rms errors.

¹ The compression ratios, as calculated, are equal to the ratio of input data points to compressed output line segments. Conversion to bandwidth compression ratios will be discussed in Section 5.

Table 3-2
 COMPRESSION CHARACTERISTICS, SENSORS 9, 10 AND 11

Table 2
 COMPRESSION CHARACTERISTICS, SENSORS 9, 10 and 11

SENSOR	TOLERANCE	COMPRESSION RATIO/RMS ERROR				
		ZOP	ZOI	FOIDIS	FOIOOT	FOI4DG
9	1	-	2.13/.410	4.95/.613	-	-
	2	2.61/.612	5.09/.884	8.84/.921	5.69/.948	9.75/.932
	3	-	6.79/1.21	11.31/1.31	-	-
	4	5.66/1.41	8.65/1.67	13.54/1.67	9.05/1.69	15.42/1.64
10	1	-	-	-	-	-
	2	3.42/.524	6.42/.898	10.76/.917	7.29/.994	11.99/.953
	3	-	-	-	-	-
	4	7.16/1.15	9.75/1.52	15.30/1.69	9.71/1.89	16.31/1.64
11	1	-	-	-	-	-
	2	2.73/.546	6.00/.929	11.50/.950	7.60/1.01	13.54/.992
	3	-	7.08/1.10	14.21/1.19	-	-
	4	6.32/1.14	7.90/1.38	15.14/1.43	10.26/1.68	17.45/1.37

NOTE: RMS error expressed in terms of data units

A rough comparison of the first order selector results summarized in Table 3-2 indicates that for a given peak error constraint, the four degree of freedom interpolator produced significantly higher compression ratios than did other interpolators. Also, for a given peak error constraint, there appears to be no consistent advantage in terms of rms error to be gained by using any one of the various interpolators.

It should be noted at this point that comparisons on a compression ratio basis between zero order and first order selectors are of little significance. A truly meaningful comparison between selectors must be made in terms of bit or bandwidth compression

ratios. Since the determination of these bandwidth compression ratios requires a discussion of coding and addressing, calculation of bit compression ratios will be deferred until Section 5.

3.3.1.2 Experiment: Comparison of Interpolator Efficiencies On Data Classes. The next step in the experimental procedure was to gain some idea as to the relative compression efficiency of zero order and first order interpolators on the various defined classes of data. With this objective in mind, several computer compression simulations were made on the available classes of data, using the zero order and first order interpolators, with equivalent peak error constraints of three units. Plots of representative original and reconstructed data are shown in Figures 3-5 through 3-12. The original data is shown displaced upward and the reconstructed data displaced downward. In each instance, short term compression ratios² were calculated as a function of time as a means of selector comparison. Plots of the log of short term compression ratios versus time for examples of four data classes are shown in Figures 3-13 through 3-16. Due to a plotting program idiosyncrasy, for those time intervals during which there were no compressed output points, the associated log short term compression ratio is plotted as zero rather than the correct infinite value. A summary of overall compression ratios obtained using ZOI and FOIDIS on the various data classes is given in Table 3-3.

Results. For several classes of data, more than one data specimen was evaluated. In these cases, the maximum and minimum compression ratios obtained for a given tolerance differed by as much as several hundred percent. An example of this variation is seen in the case of compression of two examples of Class 1 data by FOIDIS in Table 3-3. The first example yielded a compression ratio of 10.04 while the second example yielded a compression ratio of 4.42.

² Short term compression ratio is calculated at regular intervals and is equal to the ratio of the count of input points for the preceding interval of time to the count of compressed output line segments for the preceding interval of time.

Table 3-3
 COMPRESSION RATIOS VS DATA CLASSES

CLASS	EXAMPLE	SENSOR	TIME SEGMENT, SEC	ZOI	FOIDIS
1	a	9	104-116.5		10.04
	b	10	87-120	5.079	4.42
2	a	11	104-120.5	4.90	5.62
3	a	9	116.5-133		5.70
	b	10	79-87	5.64	5.50
	c	10	120-142	5.56	4.43
5	a	11	130.5-136	2.78	6.44

Note: Tolerance is two data units in all cases

This spread can perhaps be explained by considering the proposed data classification technique in some detail. The classification of a given data specimen must be made on the basis of the tolerance to be used in compression as well as the waveform's general shape. For very small tolerances, almost any data specimen appears noisy and must be included in Class 5. Similarly, for very large tolerances, almost any data specimen looks well behaved and can be included in Classes 1 or 2. The most significant feature of the S-6 data used in this portion of the study was the wild points due to bit drop out. It was not possible to choose a tolerance large enough to disregard these wild points without throwing away desired data information. Moreover, upper bounds on permissible tolerances had been fixed by conferences with the experimenters. For this reason, compression ratios were affected strongly by the presence or absence of these wild points, as well as the actual sensor waveform between wild points.

It should be mentioned that, of those sensors which were plotted, very few parameters, other than housekeeping parameters, appeared to fall entirely into any one data class other than Class 5. Although many sensors appeared to progress regularly through a consistent series of data classes, very few parameters remained characteristic of only one data class, other than Class 5, for an appreciable amount of time.

3.3.2 Bit Plane Encoding

Having applied several predictors and interpolators to the chosen specimens of data, the next step was to compare the results with bit plane encoding.

Bit plane encoding, while a data compression technique, is in a different category than the five predictors and interpolators of Paragraph 3.3. These predictors and interpolators are essentially devices which perform operations on raw data while bit plane encoding can be applied to compressed data as well as raw data. (In this study, bit plane coding was applied only to raw data which was in either straight binary or cyclic Gray coded form.) It is reasonable to expect that coding techniques such as bit plane encoding, when effectively applied to compressed data resulting from an initial application of redundancy reducing techniques such as ZOI or FOIDIS, would allow the conversion factor between bit and word compression ratios to approach one.

One bit plane encoding technique has been described by Schwartz in Reference 214 and another technique described by EMR in Reference 59. The former was adopted, in part, for this experiment. The experimental results given by Schwartz, however, were relative to a bit plane encoding technique which retained only statistical data information and did not allow data reconstruction. It is difficult at best to make a meaningful comparison between a bit plane encoding technique not allowing reconstruction and the previously described predictors and interpolators, all of which allow reconstruction. For this reason, Schwartz's technique was expanded to allow data reconstruction within an arbitrary peak error. The actual bit plane encoding algorithm used is described in Appendix III.

3.3.2.1 Experiment: Bit Plane Encoding. Those portions of Sensors 9 and 11 data between 104 and 136 seconds were coded both in straight binary and cyclic Gray coded form. For each form, entropy calculations were made using both a zero order and a first order Markov source model. These entropy figures were then used to calculate corresponding theoretical upper bounds on the obtainable compression ratios, consistent with the given data source models. See Paragraph III.2. Bit plane encoding was then applied to both the straight binary and Gray coded data. A summary of bit plane encoding compression results, entropy calculations, and previously obtained results is given in Table 3-4.

Most compression models yield word compression ratios not translatable into bit compression ratios unless predicated upon a specific system and coding configuration. A nominal conversion factor has been determined for ZOI and FOIDIS, however, equating bit compression ratio with $9/13$ word compression ratio in the case of the floating aperture zero order interpolator (ZOI), and equating bit compression ratio with $9/22$ word compression ratio in the case of the disjointed line segment first order interpolator (FOIDIS)³.

Results. For the data specimens used in this experiment, both the binary and Gray coded versions of bit plane encoding were more effective than either ZOI or FOIDIS when a tolerance of 0.5 was used, and the Gray coded version exceeded both redundancy reduction selectors for a tolerance of 1.5. Although the behavior of bit plane encoding compression ratios with larger tolerances should be investigated, the results of this experiment indicate that the compression efficiency of bit plane encoding exceeds that of ZOI and FOIDIS for the tolerances chosen. It is possible that the total number of bits in the compressed output of ZOI could be reduced as much as 40 percent by employing finer quantization (see References 91 and 109), but it is also possible that the performance of bit plane encoding could be increased by employing more efficient coding techniques.

³ Conversion factor for ZOI assumes nine bits/data magnitude and four bits/channel and frame ID. Conversion factor for FOIDIS assumes eighteen bits/data magnitude, and four bits/channel and frame ID. Additional sync bits, etc., have been disregarded in each case. This is roughly compatible with the Goddard S-6 multiplexing format. More complete explanations for these conversion factors are presented in Paragraph 6.1.

Table 3-4

REDUNDANCY REDUCTION AND BIT PLANE CODING RESULTS

SENSOR	TOLER- ANCE	COMPRESSION RATIOS							
		ZOI	FOIDIS	BINARY			GRAY		
				BIT PLANE CODING	UPPER BOUND USING H ₀	UPPER BOUND USING H ₁	BIT PLANE CODING	UPPER BOUND USING H ₀	UPPER BOUND USING H ₁
9	1/2	.864	1.07	1.759	2.115	2.507	2.281	2.195	2.788
	3/2	2.49	2.82	2.269	2.728	3.413	3.117	2.756	3.738
11	1/2	1.10	1.22	2.588	3.120	3.490	3.752	3.373	3.929
	3/2	3.66	3.15	2.831	4.280	5.087	4.213	4.528	5.703

Notes: All figures are bit compression ratios (ZOI and FOIDIS converted from word compression ratios). H₀ bound and H₁ bound are based on entropies of first order and second order Markov data source models, respectively. Time segment for both sensors was 104 to 136 sec.

For the data specimens used in this experiment, the rms error between the original and the reconstructed data was somewhat less than one-half the tolerance used in compression, using ZOI and FOIDS. Although the rms error due to bit plane coding was not determined empirically, a good theoretical approximation is: $\text{tol} = 0.5$, $\text{rms error} = 0.5$; $\text{tol} = 1.5$, $\text{rms error} = 1.12$. This approximation is discussed in Paragraph III. 3. These theoretical projections indicate that rms error incurred in bit plane encoding is expected to be somewhat greater than one-half tolerance. Final conclusions regarding the relative fidelity of reconstructed data obtained from compression by a polynomial interpolator and by equivalent bit plane encoding must await further experimentation, however.

3.4 NONADAPTIVE FILTERING

In general, there are at least two possible benefits to be realized by compressing data which has been digitally filtered: higher compression ratios and greater reconstructed data fidelity. Reconstructed data resulting from compression of filtered data may be more representative of desired data information than reconstructed data resulting from compression of unfiltered data. This fact is supported by results in Reference 244 describing the compression of artificial data with and without additive low-level noise. It was assumed that the original S-6 analog data was sampled at a rate sufficiently high to reduce aliasing of both information and noise to a negligible level. It was also assumed that this sampling rate was higher than the Nyquist rate dictated by the information bandwidth and that digital filtering or smoothing could be used to attenuate any high frequency noise which was present while passing desired information unattenuated for compression. Two nonadaptive digital filtering techniques were applied to selected portions of the S-6 data:

- Simple Averaging
- Exponential

3.4.1 Simple Averaging Filter

Simple averaging filtering consists of replacing each unfiltered data sample by an ordinary average of the given sample and a number of its unfiltered neighbors. If

x_n and \hat{x}_n are the unfiltered and filtered n^{th} data points, respectively, and if $(2N + 1)$ samples are to be included in the average, then

$$\hat{x}_n = \frac{1}{(2N + 1)} \sum_{i=-N}^N x_{n+i}$$

This digital filtering operation is a low pass filtering operation, the degree of low pass filtering increasing with an increasing number of points included in the average.

3.4.2 Exponential Filter

Exponential filtering consists of replacing each unfiltered data sample with a weighted average of the present data sample and all previous data samples so that the weighting of previous samples decreases geometrically into the past. This may be done in a recursive manner as follows. If x_n and \hat{x}_n are the unfiltered and filtered n^{th} data points, respectively, and if a and b are two constants chosen by the user so that $a + b = 1$, then

$$\hat{x}_n = a x_n + b \hat{x}_{n-1}$$

This exponential filter behaves like a sampled R-C filter with equivalent time constant $\tau = -1/\ln b$. Reference 155 shows it to be essentially a low pass filter, the degree of low pass filtering increasing with increasing b .

3.4.3 Experiment Organization

The chosen portions of Sensors 9, 10 and 11 were initially filtered with the simple averaging filter using three then five data points. The same portions of data were then filtered with the exponential filter using equivalent time constants of one, two, three and five data sample periods. In each case, filtered data tapes were written for future processing. Filtered data was plotted by the SC4020 plotter for each filtering technique. These plots were inspected visually and a subjective selection was made of those degrees of filtering which appeared to best filter out unwanted noise while passing desired data information. For the data used in this study, it was decided

that the simple averaging filter incorporating three data samples in the average and the exponential filter with a time constant of one sample period were optimum.

An important part of the filtering experiments was the filtering of wild points caused by transmission noise. (These points were caused by noise in the r-f link and were not present in the vehicle.) In many instances, these points were as much as one-half of full scale removed from immediately adjacent sample points. The effect of filtering a wild point by either digital filtering technique was to produce a transient waveform of reduced amplitude compared to the original wild point, and lasting over many sample periods. In the case of the averaging filter, the transient is flat-topped and lasts over as many sample periods as samples included in the average. In the case of the exponential filter, the transient is a decaying exponential with a time constant equal to the time constant of the particular filter used. Examples of filtered wild points and resulting transients are shown in Figure 3-17.

3.4.3.1 Experiment: Effects of Precompression Filtering. The portions of Sensors 9, 10 and 11 which had been filtered with the two optimum filters were compressed with several apertures by ZOI and FOIDIS to determine the effect of precompression filtering on their compression efficiencies. In each instance, the resulting reconstructed data was statistically compared with the unfiltered original data and rms errors and error distributions were calculated. This experiment is summarized in Table 3-5 and Figures 3-18 through 3-20. Examples of compressed and reconstructed data are shown in Figure 3-21, where original, uncompressed data is shown displaced upwards, while the filtered, compressed and reconstructed data is shown displaced downwards.

Results. In almost every instance, the effect of both precompression filtering techniques was to significantly raise the compression ratios obtained by using either ZOI or FOIDIS on unfiltered data. In the case of Sensor 10, however, the compression of exponentially filtered data resulted in lower compression ratios than the compression of unfiltered data.

Table 3-5

COMPRESSION RATIO AND RMS ERROR SUMMARY, FILTERED DATA

SENSOR	UNFILTERED DATA		EXPONENTIALLY FILTERED DATA		AVERAGE FILTERED DATA		SELECTOR	TOLERANCE
	\bar{N}	RMS ERROR	\bar{N}	RMS ERROR	\bar{N}	RMS ERROR		
9	5.09	.884	5.54	9.238	6.61	14.923	ZOI	2
	8.65	1.672	9.19	9.399	10.50	15.004	ZOI	4
	8.84	.922	9.86	9.260	11.62	14.920	FOIDIS	2
	13.54	1.665	15.13	9.450	17.25	15.024	FOIDIS	4
10	6.42	.898	6.25	13.636	7.59	22.678	ZOI	2
	9.75	1.517	8.69	13.716	10.05	22.766	ZOI	4
	10.76	.917	10.15	13.646	12.32	22.676	FOIDIS	2
	15.30	1.695	13.72	13.715	15.60	22.731	FOIDIS	4
11	6.00	.929	7.77	6.973	10.12	12.926	ZOI	2
	7.90	1.382	10.15	7.107	12.41	12.993	ZOI	4
	11.50	.950	14.63	6.999	17.62	12.924	FOIDIS	2
	15.19	1.434	18.10	7.144	21.28	13.004	FOIDIS	4

NOTE: \bar{N} = (No. data samples in/No. line segments out)

Rms error is in terms of data units

The cause of lower compression ratios when exponential precompression filtering was used on data from Sensor 10 could be the relatively high density of wild points contained in data from this sensor. Because of the high density of wild points in the original data, a significant fraction of the filtered data consisted of transients resulting directly from the filtering operation. The transients resulting from use of the simple averaging filter were flat-topped and easily compressed by both the zero and first order interpolator. In the case of the exponential filter, however, the transients were exponential in shape, and were not easily compressible by either the zero or first order interpolators. Therefore, the explanation for lowering of compression ratios when using exponential filtering is that exponential transients are relatively difficult to compress as compared with flat-topped transients resulting from averaging filtering.

It appears as if a significant improvement in the compression ratios obtained from compression of filtered data could be realized if some method were employed for rejecting wild points prior to filtering, especially in the case of the exponential filter. Prefiltering techniques, similar to those of adaptive sampling and redundancy reduction, might be used to reject these wild points.

In each case, the rms error between the original data and reconstructed data having used precompression filtering was a significant fraction of full-scale data. (See Table 3-5.) In addition, this rms error appears to be quite insensitive to the tolerance used in compression operation. This implies that the overwhelming portion of rms error was due to the filtering operation and not the compression operation. Moreover, it appears from inspection of the filtered data that the majority of rms error incurred during filtering was in the vicinity of wild points and the resulting transients and not in other sections of the data. This contention is supported by the following facts:

- In the case of reconstruction of compressed raw data, all sensors have roughly equivalent rms errors for a given tolerance.
- In the case of reconstruction of compressed data using precompression filtering, the rms error for Sensor 10 is significantly larger than for Sensors 9 and 11 for a given tolerance.
- Sensor 10 contains significantly more wild points than either Sensors 9 or 11.
- Visual inspection of the reconstructed waveforms makes it clear that errors of the magnitude of the rms errors in Table 3-5 are incurred only in the vicinity of wild points.

Based on these four points it appears that rms error is more a measure of wild point severity than a measure of reconstructed data fidelity and information loss due to compression in the case of precompression filtering and compression of Goddard S-6 data.

3.5 ADAPTIVE COMPRESSION (SINGLE CHANNEL)

In fixed-parameter compression, system parameters are based on probabilistic, a priori knowledge of the data to be processed. Fixed-parameter compression systems, however, often give unsatisfactory results because a priori knowledge of data is limited, probabilistic considerations often fail to make allowances for interesting data trends that are statistically unlikely, and most data specimens have wide variations in data activity.

An adaptive system which adjusts itself as some function of data activity and system status may give more uniformly satisfactory results in spite of data nonstationarities by producing uniform-quality reconstructed data that is more independent of changing data activity, and by alleviating buffer overflow due to surges in data activity.

The two single channel adaptive compressor configurations which were used in this study are the adaptive aperture compressor and the fixed aperture compressor having adaptive precompression filtering.

3.5.1 Adaptive Aperture Compressor

The adaptive aperture data compressor adjusts the tolerance used during compression by a function of measured system parameters. Three such system parameters or control variables were used: short term compression ratio, present line segment run length, and exponentially filtered present line segment run length. Short term compression ratio is a quantity which is calculated at the end of successive, equal time intervals, and is equal to the ratio of the number of samples processed to the number of significant samples occurring during that time interval. Present line segment run length is a quantity which is equal to the number of samples processed since the last significant sample. Exponentially weighted line segment run length is a quantity which is equal to a weighted sum of the present line segment run length and all previous run lengths, with weighting decreasing geometrically into the past. The system configuration that was simulated for this study is shown in Figure 3-22 and the functional form of the control logic or tolerance control function used with each control variable is shown in Figure 3-23.

3.5.1.1 Experiment: Simulation. For each control variable, simulations were made using both the zero and first order interpolators on portions of Sensors 9, 10 and 11. A summary of the experiments and results which were obtained is given in Table 3-6, with the convention used in Table 3-6 being the same as in Figure 3-23. Plots containing original data and reconstructed data from the simulations are in Figure 3-24.

Results. For a given data specimen, selector, and compression ratio, the rms error between original and reconstructed data was somewhat higher with adaptive aperture compression than with nonadaptive compression. Visually, the reconstructed data resulting from both fixed and adaptive aperture compression appear to be of equal fidelity. A heuristic argument for the apparent paradox of different rms errors but equal fidelity can be made as follows. In the case of adaptive aperture compression, relatively large errors are allowed during periods of high data activity and these large errors do tend to contribute to a relatively large overall rms error. In the case of fixed aperture compression, relatively small errors are maintained at all times resulting in relatively small rms error. During periods of high data activity, however, relatively large errors can be visually tolerated with no subjective degradation in fidelity. For this reason, it is possible to obtain different rms errors consistent with apparently equal fidelity. It might also be possible that the human eye is simply unable to detect any subjective difference in picture fidelity when rms errors differ by a maximum of only fifty percent.

In most instances, for a given data specimen, selector, and buffer readout rate, the use of adaptive aperture compression techniques resulted in a lower maximum single channel buffer queue length than the use of fixed aperture compression techniques.

It was not possible to use tolerance control functions which permitted sufficient variations in aperture to reject wild points in Sensor 9, 10 and 11 data, because they were as much as one-half of full scale removed from adjacent data points. A tolerance control function that would have permitted these points to remain within tolerance would have overly degraded reconstructed data fidelity and information content. It appears that overall system effectiveness, measured in terms of compression ratios and reconstructed data fidelity, would have been greatly increased if precompression wild point rejection had been included in the simulated compression system.

Table 3-6
ADAPTIVE APERTURE COMPRESSION SUMMARY

SENSOR	SELECTOR	CONTROL VARIABLE	A	B	C	D	ρ	BUFFER READOUT RATE	COMPR RATIO	RMS ERROR	MAX QUEUE
9	ZOI	STCR	6	1	3	10	1.07	8.6	6.53	2.08	44
		PRL	6	1	.05	.166	.818	8.6	8.54	2.30	22
		PRL (f)	6	1	.05	.166	.869	8.6	8.03	2.17	23
		FIXED, TOL = 3	-	-	-	-	1.03	8.6	6.79	1.21	-
9	FOIDIS	STCR	6	1	3	10	.755	6.8	11.70	2.02	24
		PRL	6	1	.05	.166	.900	6.8	9.80	1.60	13
		PRL (f)	6	1	.05	.166	.961	6.8	9.17	1.54	14
		FIXED, TOL = 3	-	-	-	-	.806	6.8	10.93	1.26	28
10	ZOI	STCR	6	1	3	10	1.65	1.54	7.90	1.77	26
		PRL	6	1	.15	.5	1.49	1.54	8.73	1.98	25
		PRL (f)	6	1	.15	.5	1.77	1.54	7.34	1.52	28
		FIXED, TOL = 3	-	-	-	-	1.53	1.54	8.47	1.12	86
10	FOIDIS	STCR	6	1	3	20	.859	1.54	15.67	1.77	25
		PRL	6	1	.15	1	1.05	1.54	12.36	1.54	25
		PRL (f)	6	1	.15	1	1.04	1.54	12.75	1.45	24
		FIXED, TOL = 3	-	-	-	-	1.01	1.54	12.84	1.11	28
11	ZOI	STCR	6	1	3	20	.945	8.45	7.51	1.63	76
		PRL	6	1	.05	.333	.970	8.45	7.32	1.88	69
		PRL (f)	6	1	.05	.333	1.08	8.45	6.55	1.66	76
		FIXED, TOL = 3	-	-	-	-	5.50	1.54	7.08	1.10	131
11	FOIDIS	STCR	6	1	3	10	.862	4.47	15.54	1.55	23
		PRL	6	1	.05	.166	1.03	4.47	12.92	1.59	30
		PRL (f)	6	1	.05	.166	1.04	4.47	12.84	1.53	27
		FIXED, TOL = 3	-	-	-	-	.945	4.47	14.21	1.19	29

Control Variables:

STCR = Short term compression ratio
PRL = Present (line segment) run length
PRL (f) = Exponentially filtered PRL

ρ = (average input rate/output rate)_{buffer}

RMS error is in terms of data units

A, B, C, D, E, F, and G are used according to convention of Fig. 3-23

In general, average compression ratios were not significantly changed by the use of adaptive aperture instead of fixed aperture compression.

3.5.2 Adaptive Precompression Filtering

Compression with adaptive precompression filtering involves adaptively filtering data prior to compression by varying the filter bandwidth according to some function of measured system parameters. (The system parameter used for this study was the present line segment run length.)

The precompression filtering technique employed was a variation of the simple averaging filter. This technique consisted of averaging a block of N data samples and producing one filtered output sample for the entire block. The number of data samples, N , included in a given block of samples to be averaged was variable and was adaptively controlled by the filter control function in order to vary the degree of filtering. The system configuration that was simulated is shown in Figure 3-25. The control logic, or filter control function, is shown in Figure 3-26.

3.5.2.1 Experiment: Simulation. Compression simulations were made using only the zero order interpolator because of time limitations. Although the adaptive precompression filtering experiments were conducted using only a single selector, a single tolerance, and a single type of filter control function, the results obtained were sufficiently promising to warrant further study. A summary of the results obtained is given in Table 3-7. Plots containing original data and reconstructed data are in Figure 3-27. In these plots, missing data points were linearly interpolated producing reconstructed data similar in appearance to that resulting from first order compression.

Results. The use of adaptive precompression filtering improved compression ratios by a factor of two or three relative to compression of raw data. The use of adaptive precompression filtering also greatly increased the rms error between original and reconstructed data. As in the case of nonadaptive precompression filtering, it is felt that this increased rms error was attributable to the high density of wild points in the data and the resulting transients after filtering, and not degradation of data information because of filtering.

Table 3-7
ADAPTIVE FILTERING COMPRESSION SUMMARY

SENSOR	SELECTOR	CONTROL VARIABLE	A	B	C	D	E	F	G	ρ	BUFFER READOUT RATE	COMPR RATIO	RMS ERROR	MAX QUEUE
9	ZOI	PRL	7	5	3	1	.05	.15	.25	-	6.8	14.84	17.23	7
		FIXED, TOL = 3	-	-	-	-	-	-	-	-	8.6	6.79	1.21	-
10	ZOI	PRL	7	5	3	1	.15	.45	.75	-	1.54	10.92	20.19	30
		FIXED, TOL = 3	-	-	-	-	-	-	-	2.30	1.54	8.47	1.12	86
11	ZOI	PRL	7	5	3	1	.05	.15	.25	-	4.47	17.42	13.01	24
		FIXED, TOL = 3	-	-	-	-	-	-	-	2.75	1.54	7.08	1.10	131

Note: In each case using precompression filtering, tol = 2
PRL = present (line segment) run length

RMS error is in terms of data units
A, B, C, D, E, F, and G are used according to convention of Fig. 3-26

In most instances, the reconstructed data appeared to be more representative of actual data trends and less susceptible to noise than the reconstructed data resulting from compression of raw data. This is especially noticeable in the vicinity of 121 and 129 seconds in the case of Sensor 9 (Figure 3-27) where the data is quite noisy. The actual data information trend is easily discernable, however. Fixed-aperture compression techniques (with and without fixed precompression filtering) and adaptive aperture compression techniques were relatively ineffective in compressing these portions of data and yielded both poor compression ratios and poor reconstructed data. (See Figures 3-7, 3-11, 3-21, and 3-24.) However, compression of this data with adaptive precompression filtering was quite effective, yielding both high compression ratios and reconstructed data which is believed to better represent actual data information trends.

Compression with adaptive precompression filtering, although quite effective in compressing noisy data, appears to be quite susceptible to wild points. Both compression ratios and reconstructed data quality were adversely affected by these wild points. (See, for example, Figure 3-27, pages 3-83 and 3-85 .) It appears as if overall system effectiveness would have been improved if prefiltering wild point rejection had been included in the simulated system.

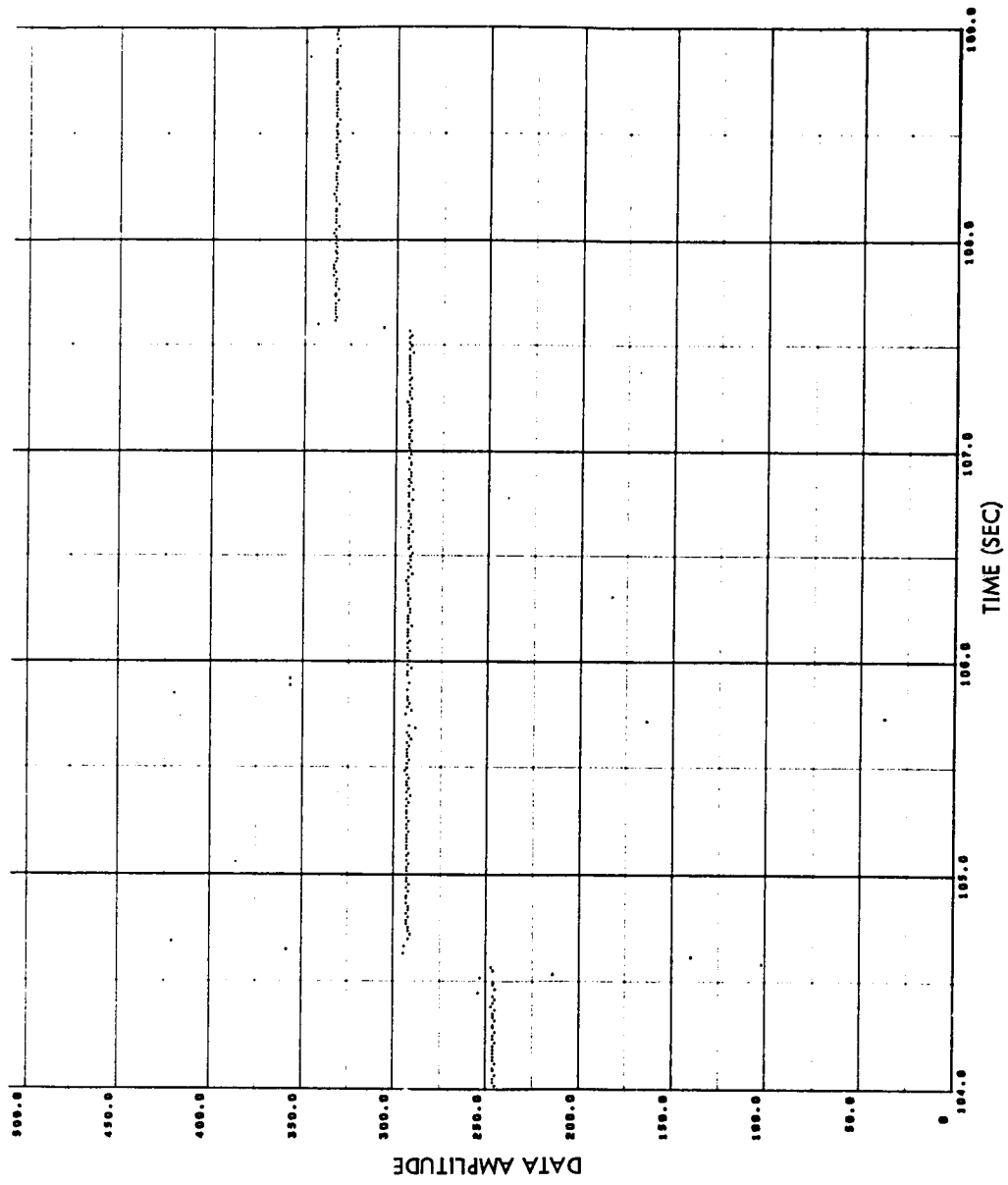


Fig. 3-2 Raw Data, Sensor 9

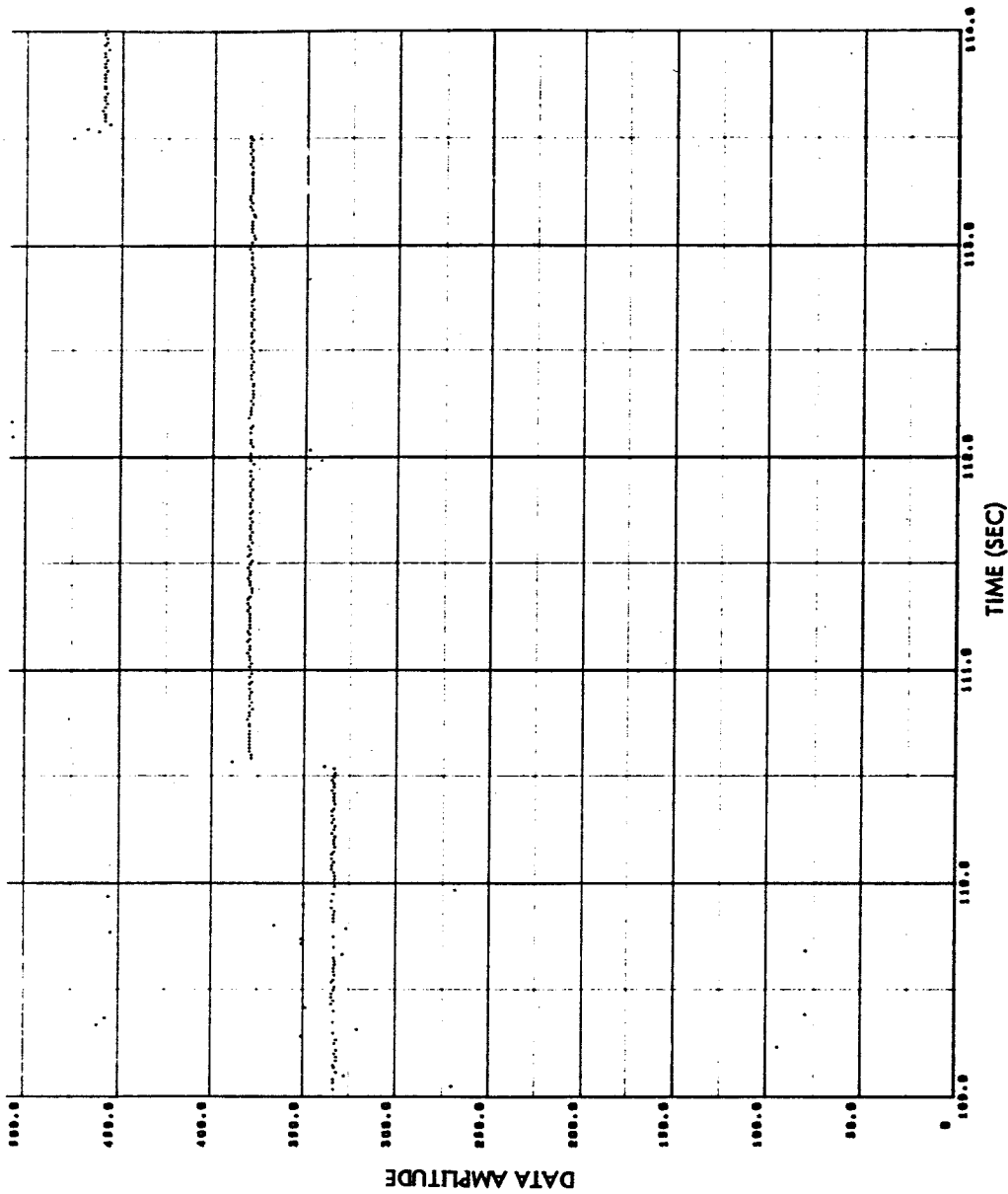


Fig. 3-2 (Cont'd) Raw Data, Sensor 9

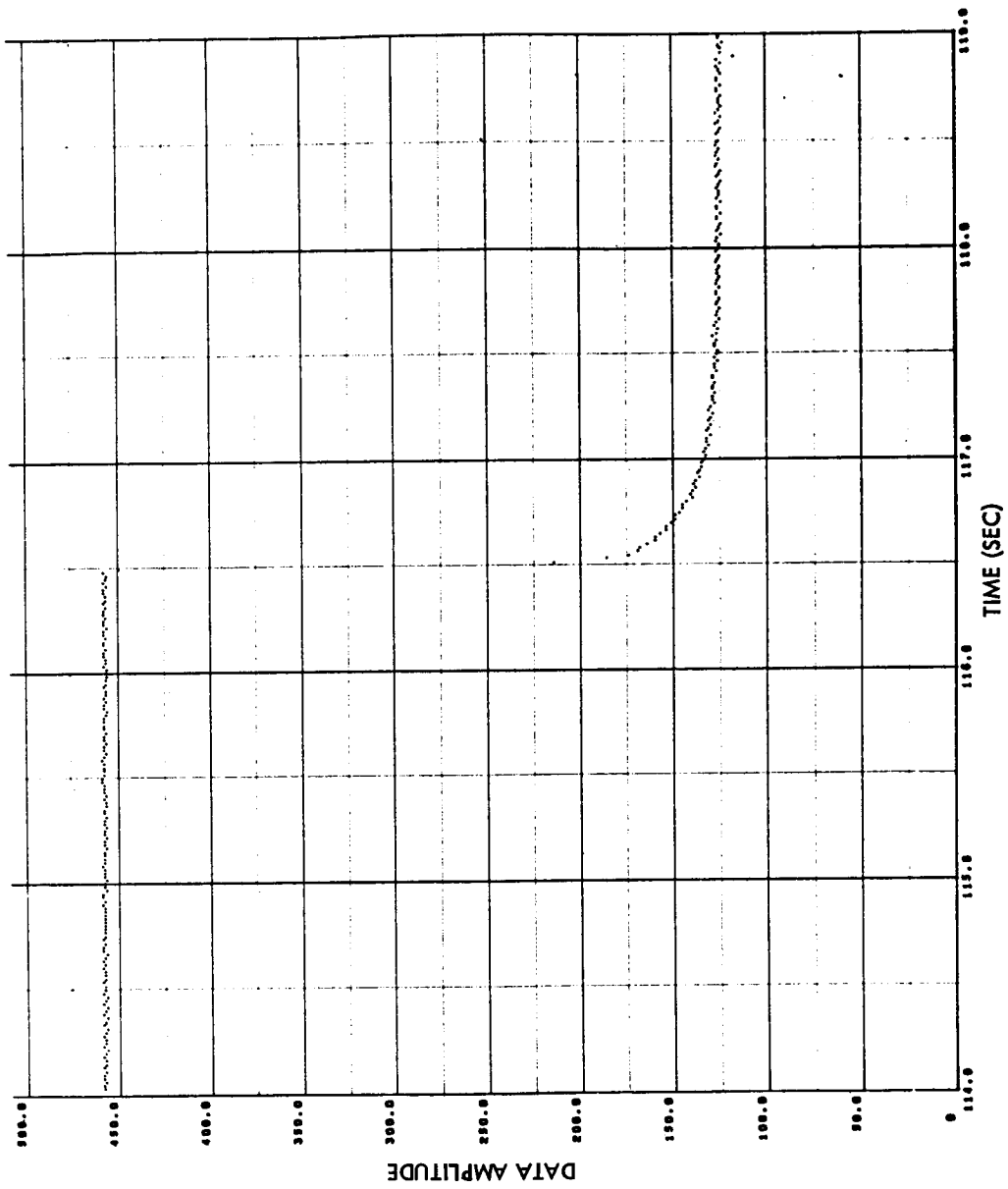


Fig. 3-2 (Cont'd) Raw Data, Sensor 9

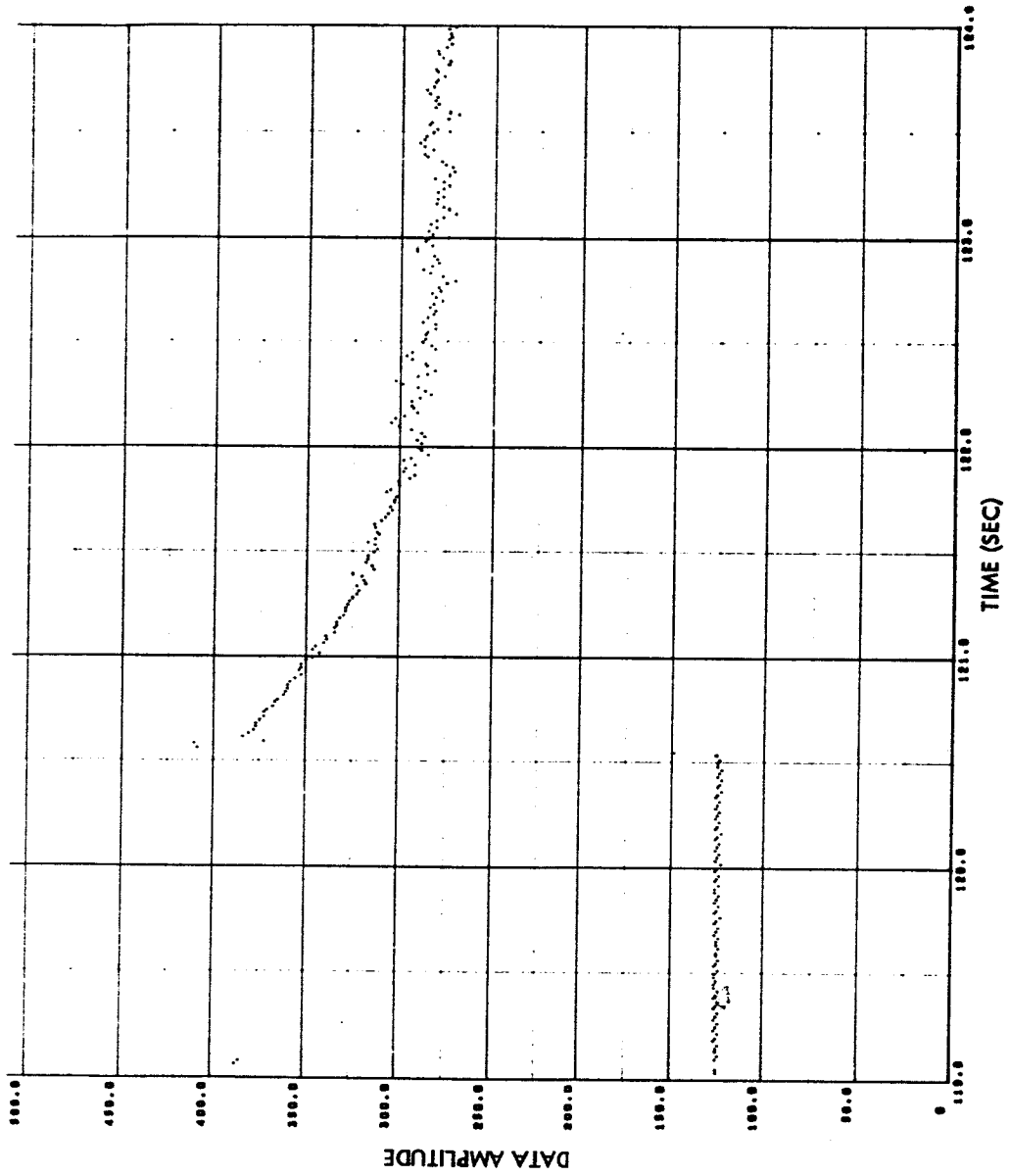


Fig. 3-2 (Cont'd) Raw Data, Sensor 9

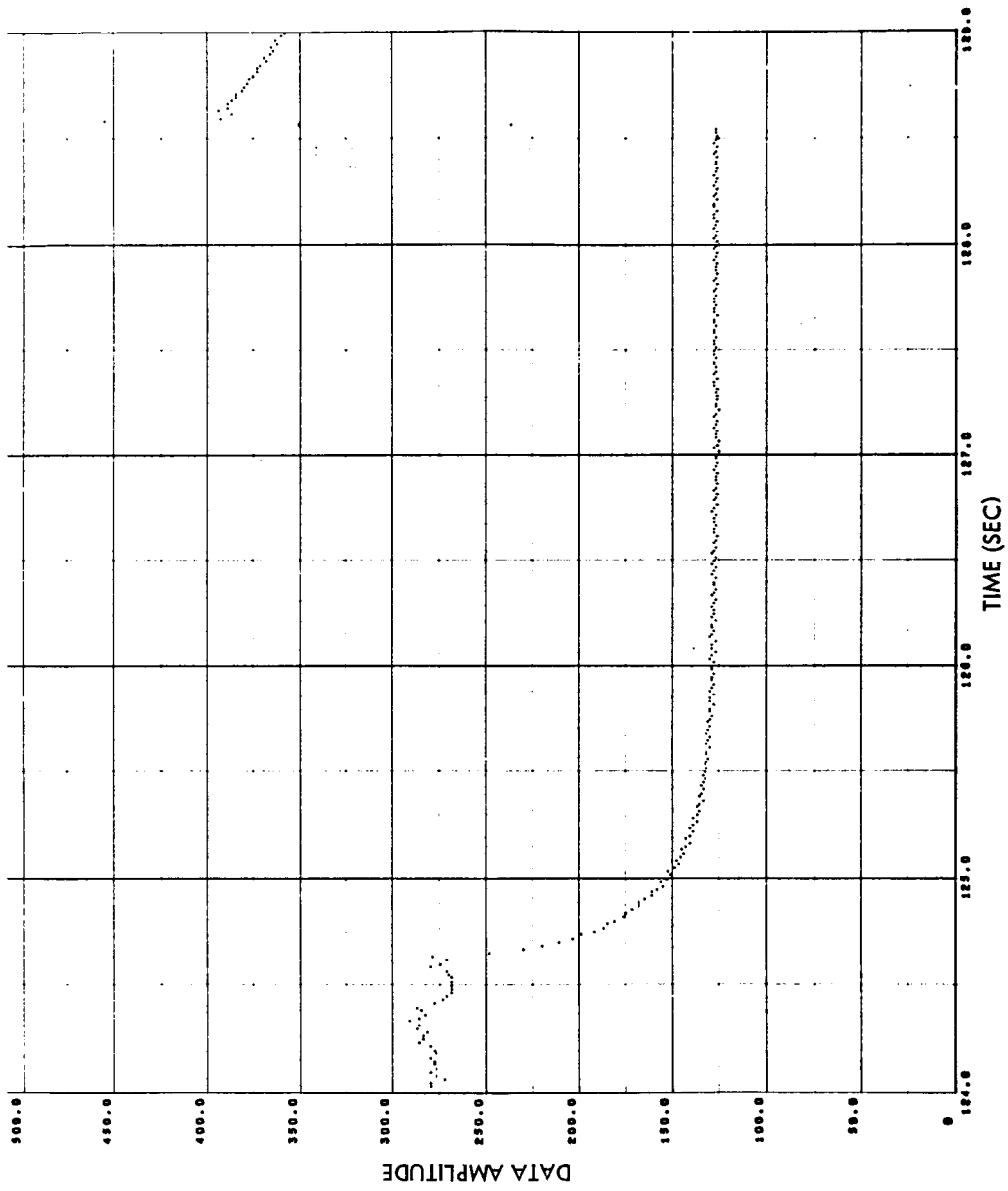


Fig. 3-2 (Cont'd) Raw Data, Sensor 9

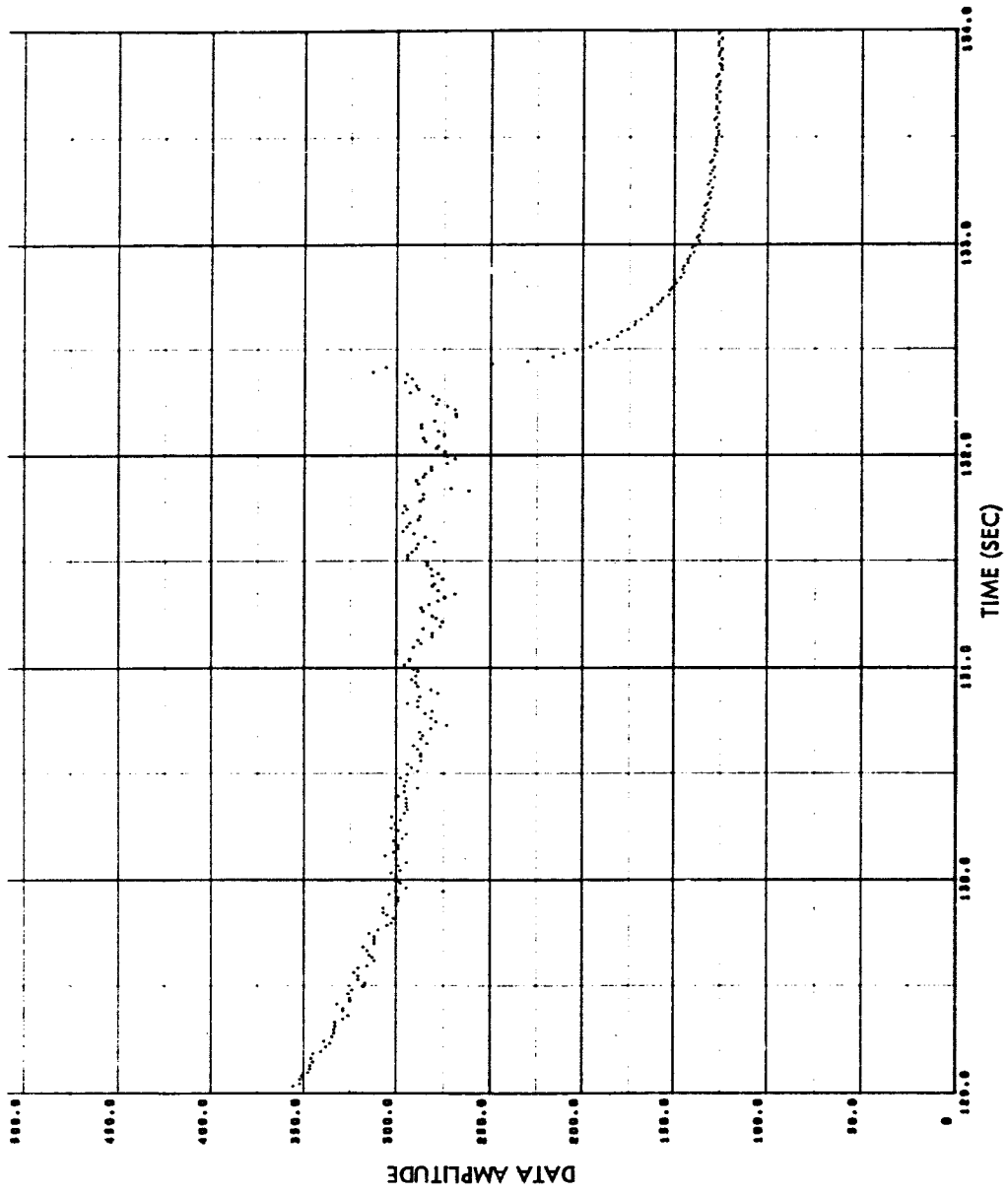


Fig. 3-2 (Cont'd) Raw Data, Sensor 9

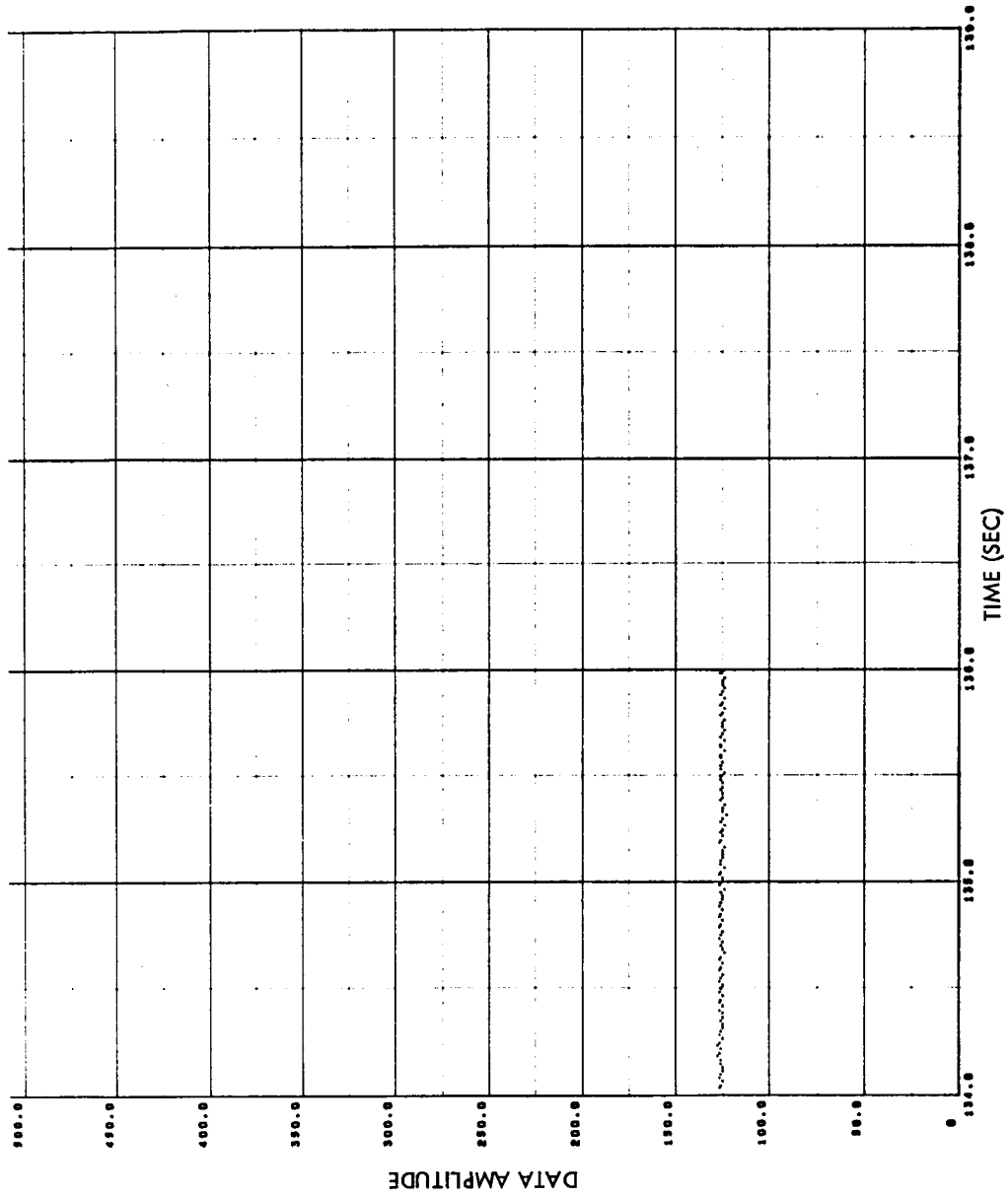


Fig. 3-2 (Cont'd) Raw Data, Sensor 9

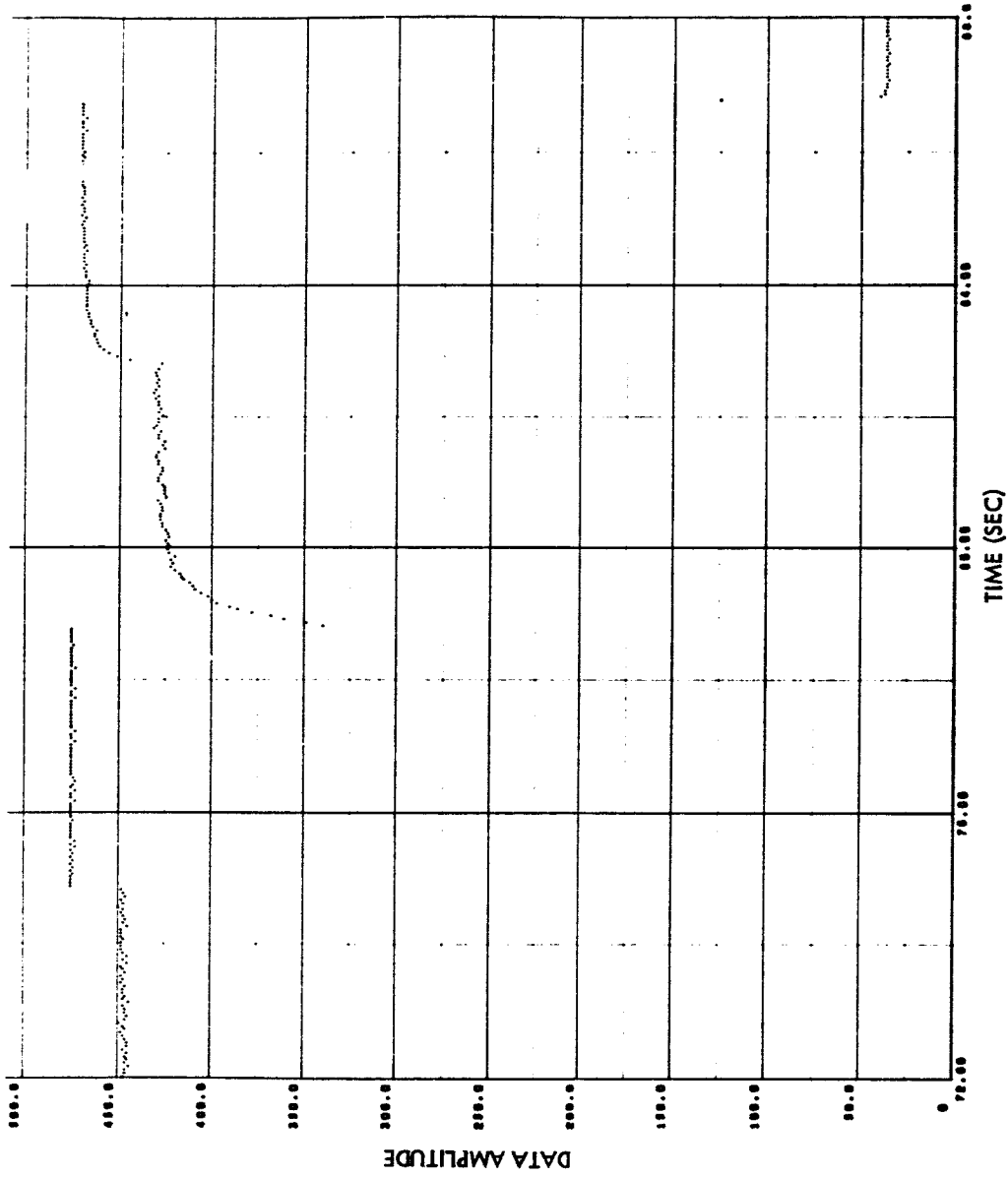


Fig. 3-3 Raw Data, Sensor 10

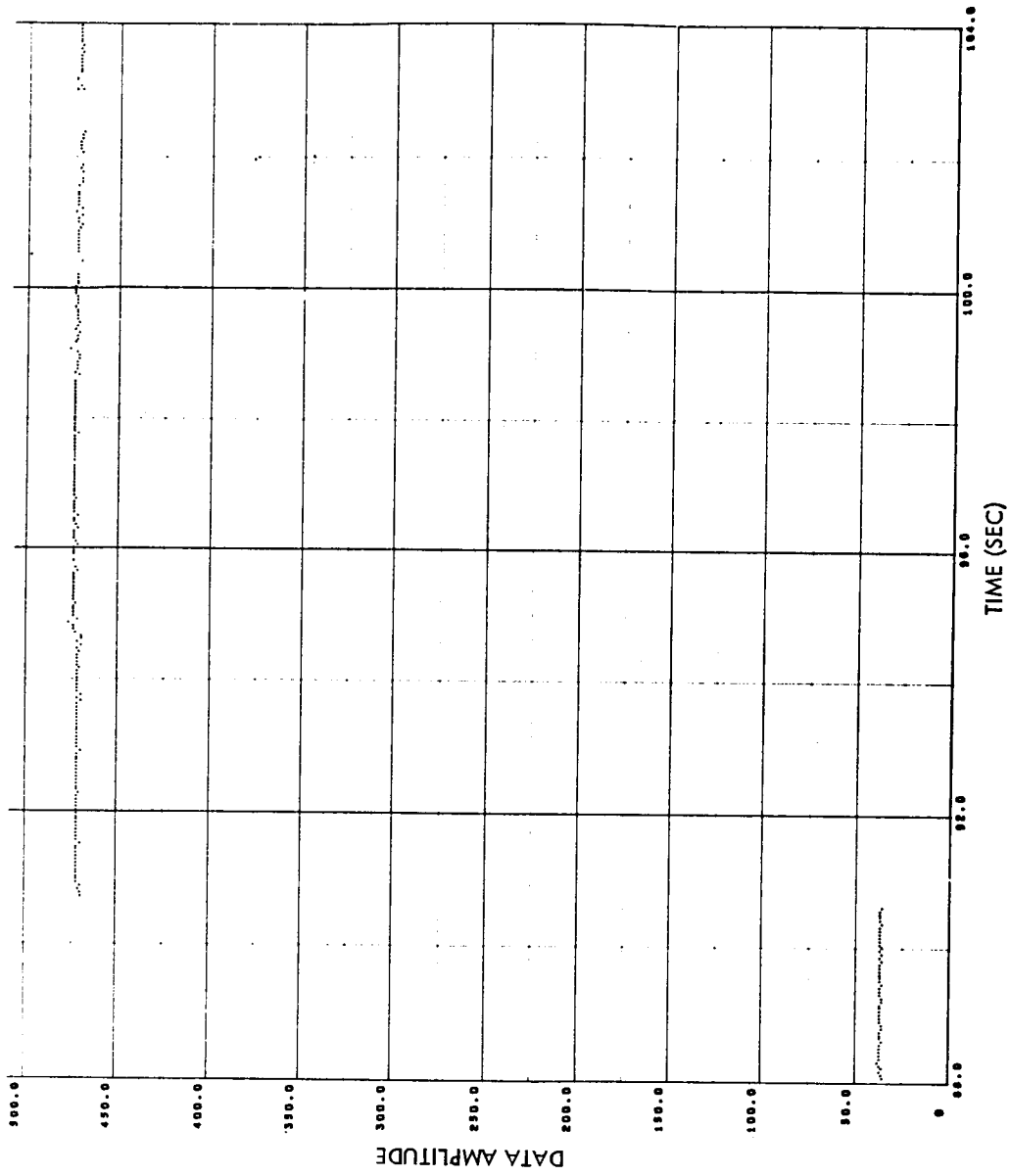


Fig. 3-3 (Cont'd) Raw Data, Sensor I0

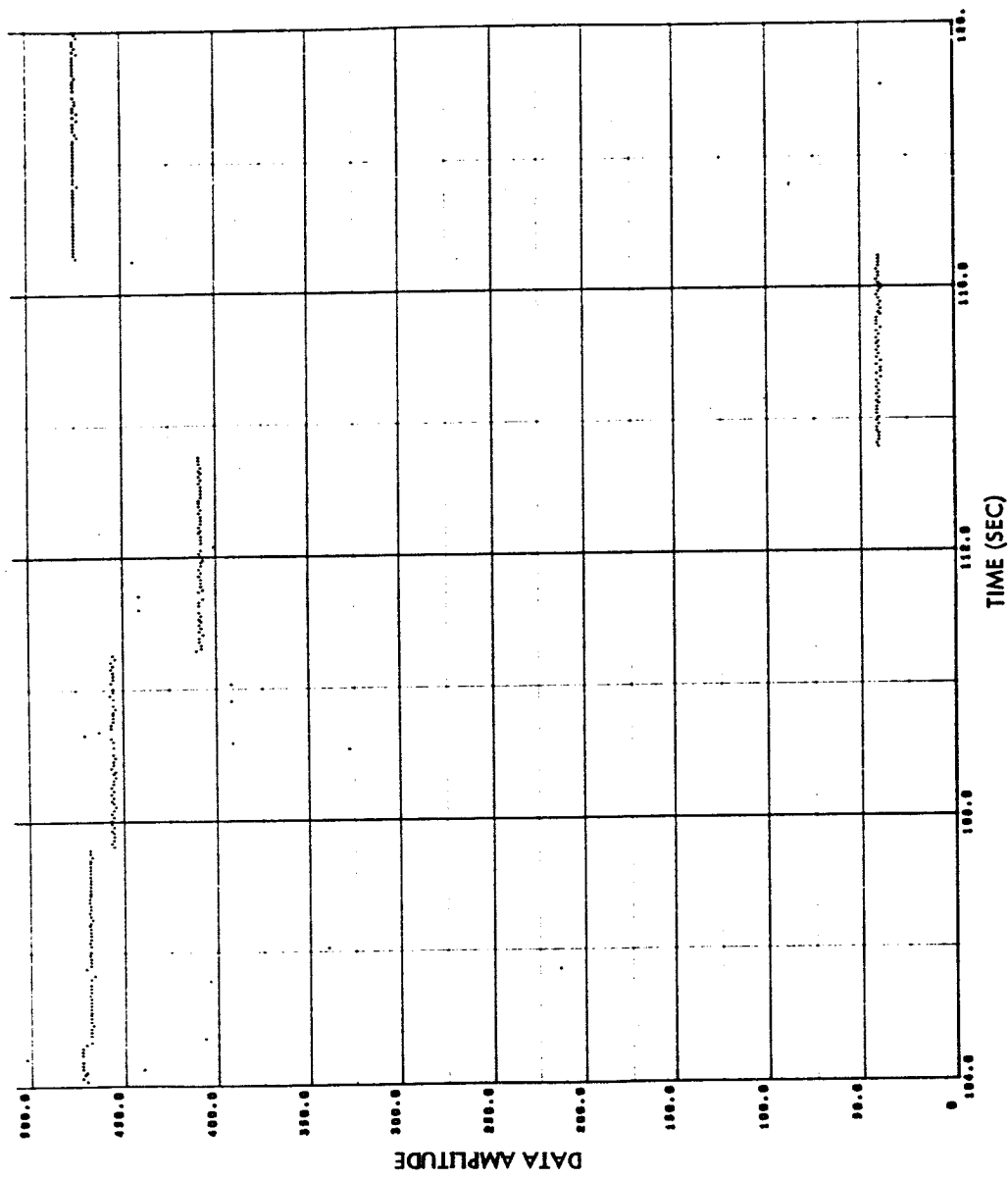


Fig. 3-3 (Cont'd) Raw Data, Sensor 10

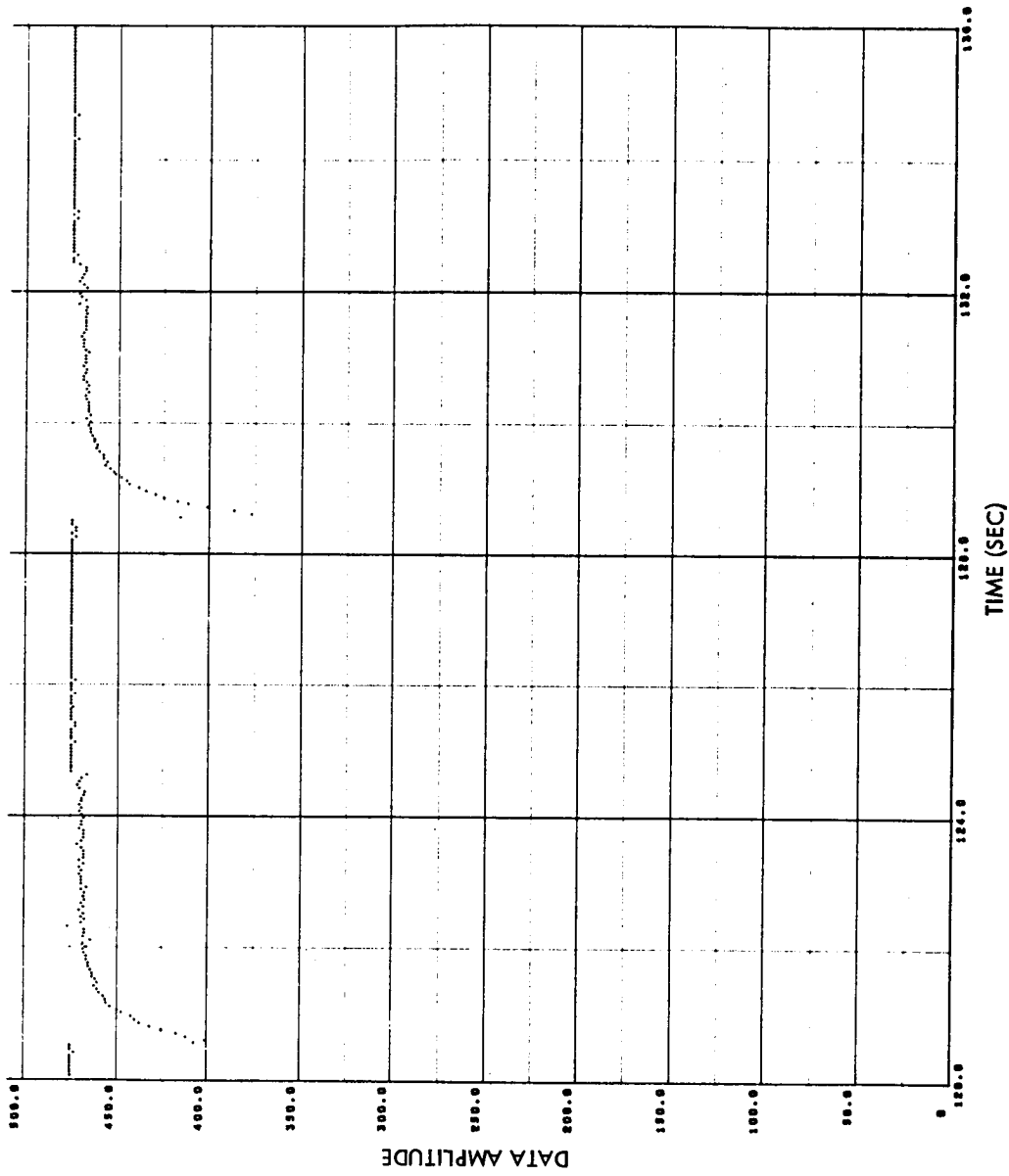


Fig. 3-3 (Cont'd) Raw Data, Sensor 10

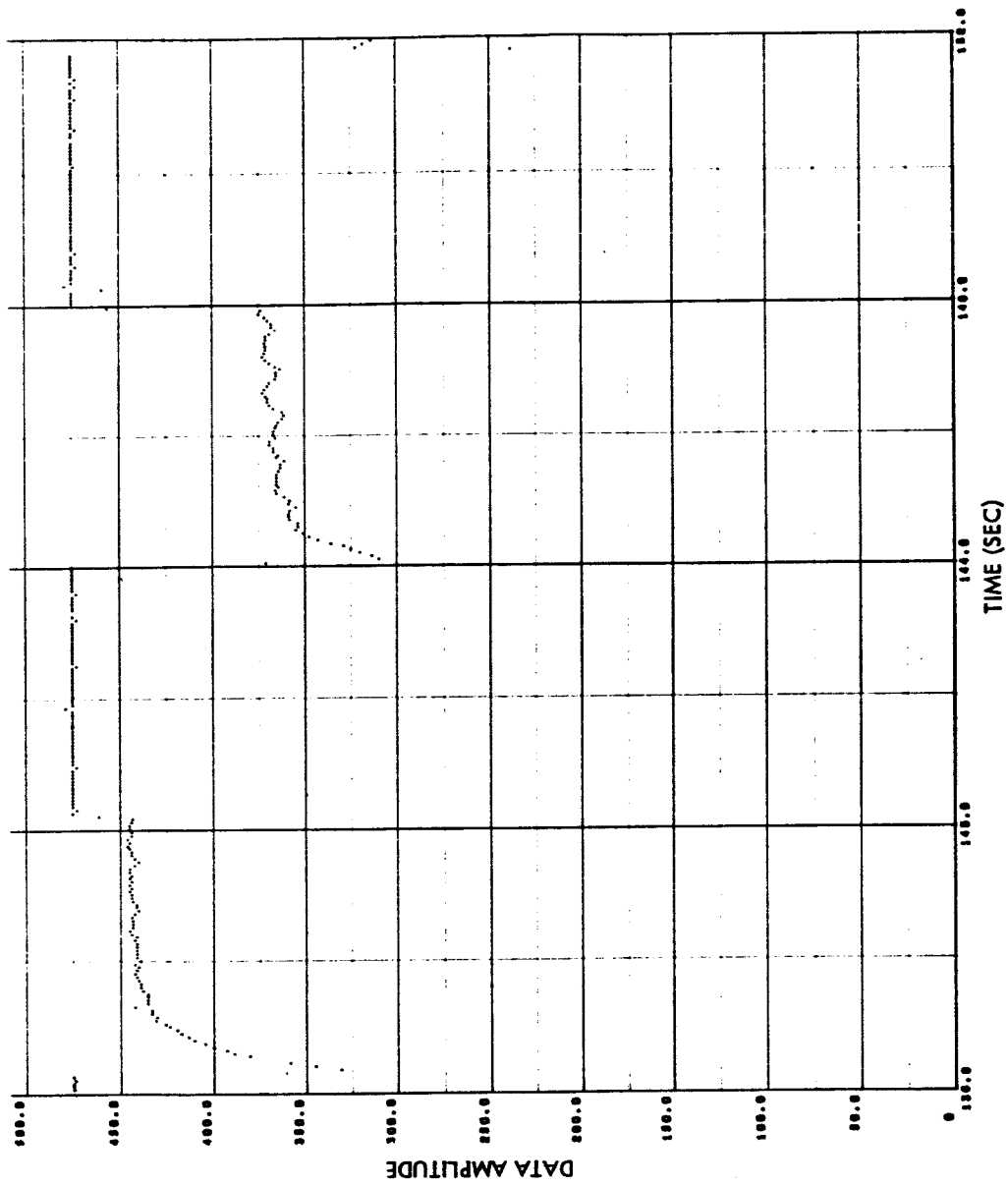


Fig. 3-3 (Cont'd) Raw Data, Sensor 10

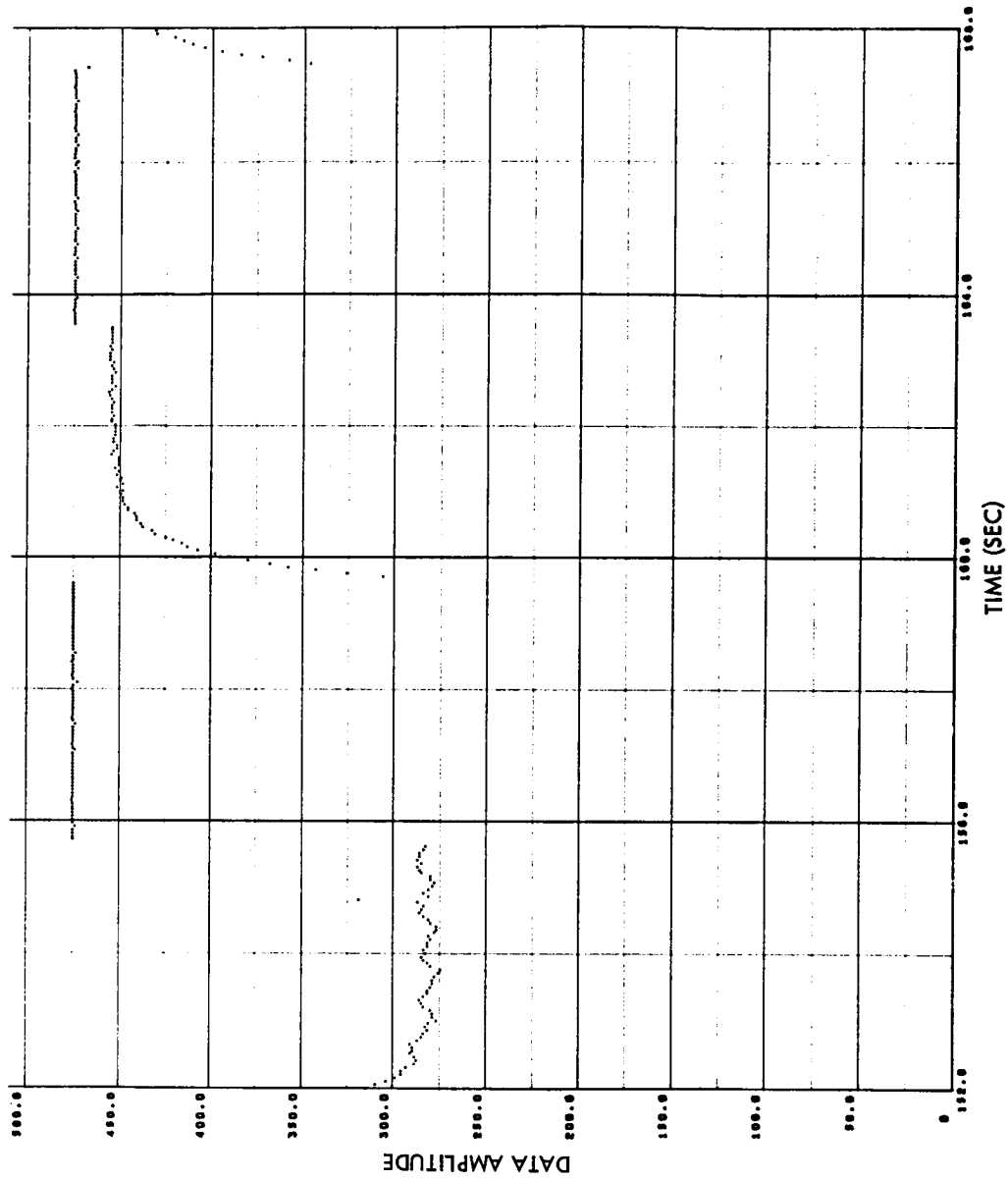


Fig. 3-3 (Cont'd) Raw Data, Sensor 10

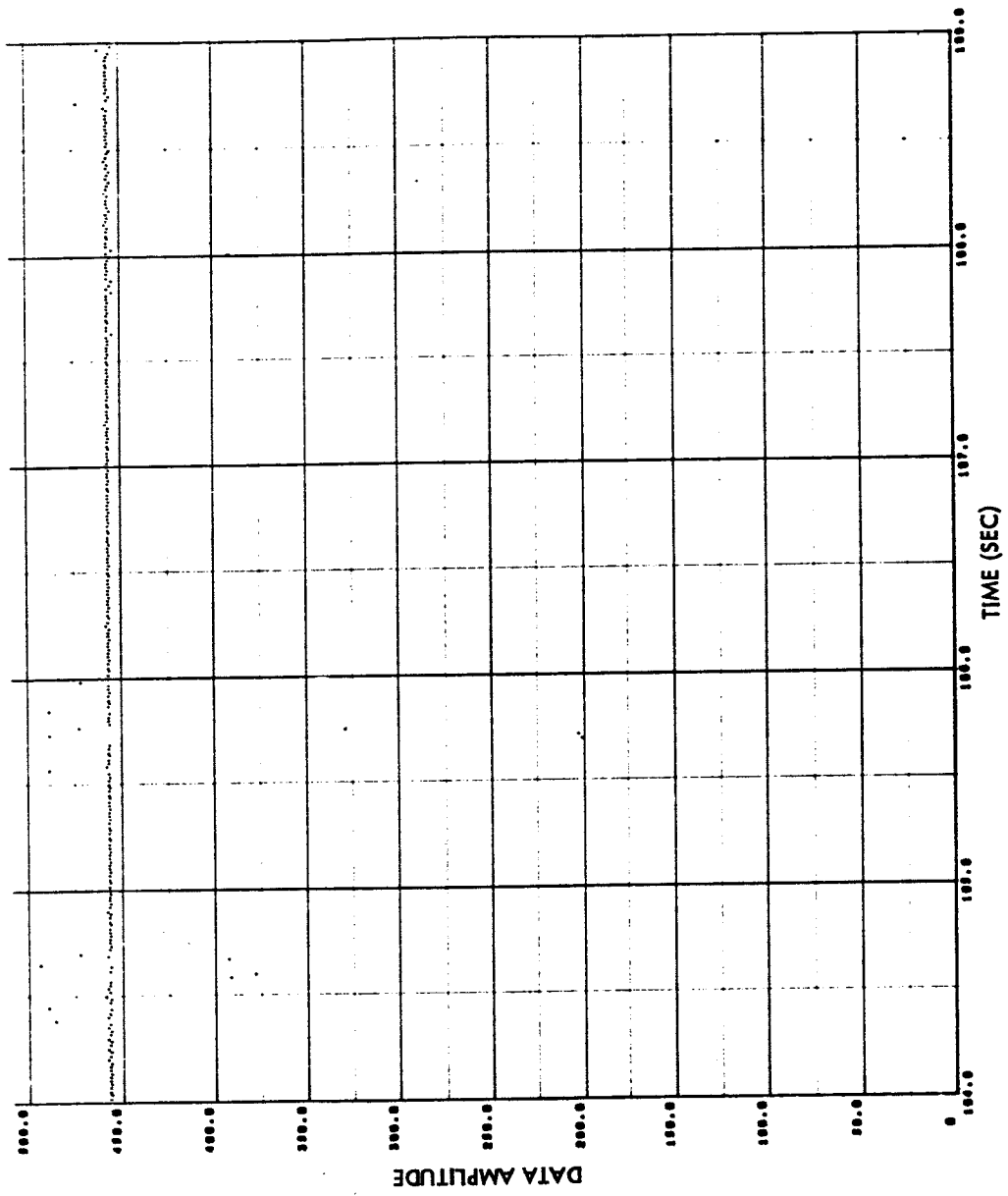


Fig. 3-4 Raw Data, Sensor II

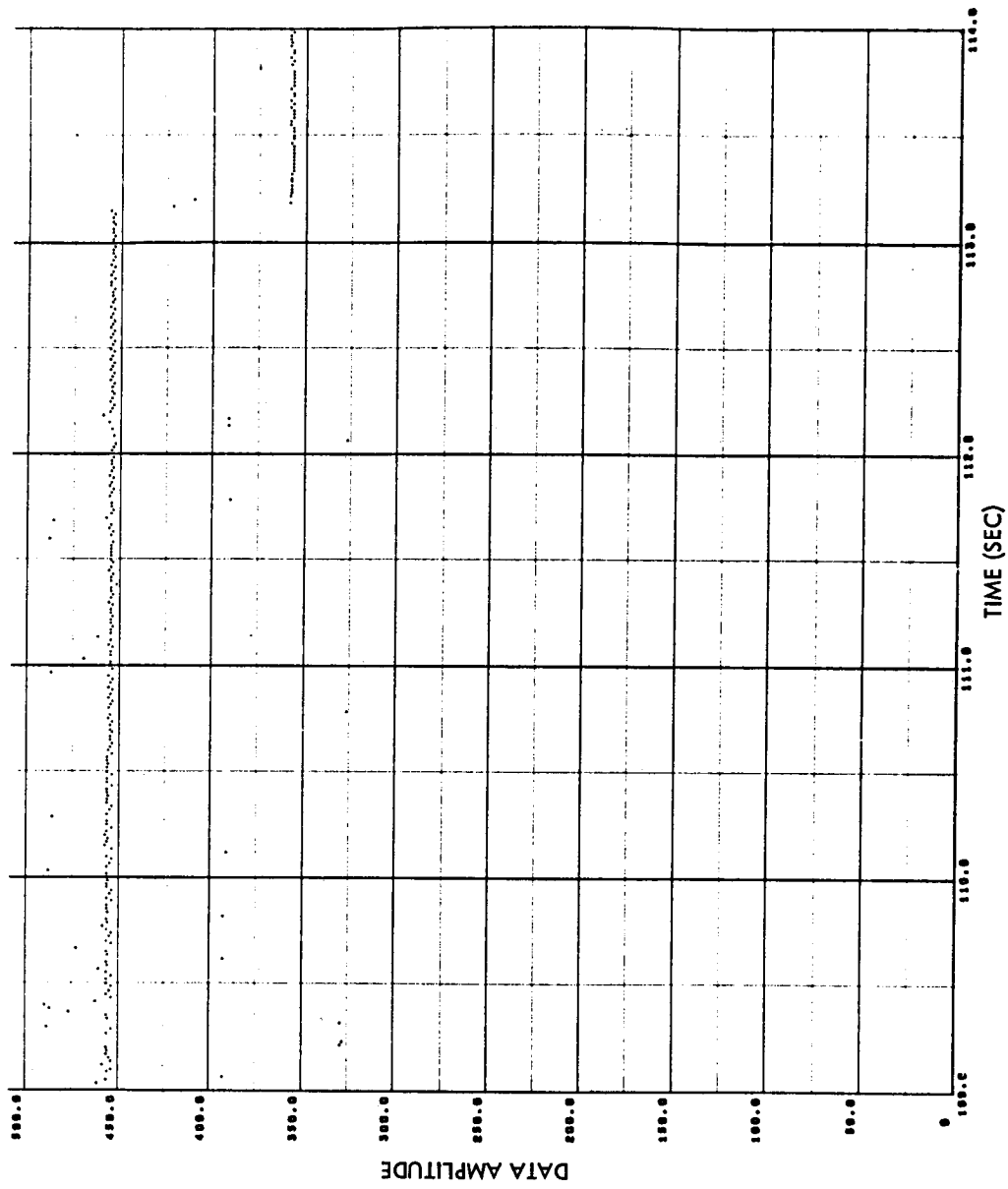


Fig. 3-4 (Cont'd) Raw Data, Sensor II

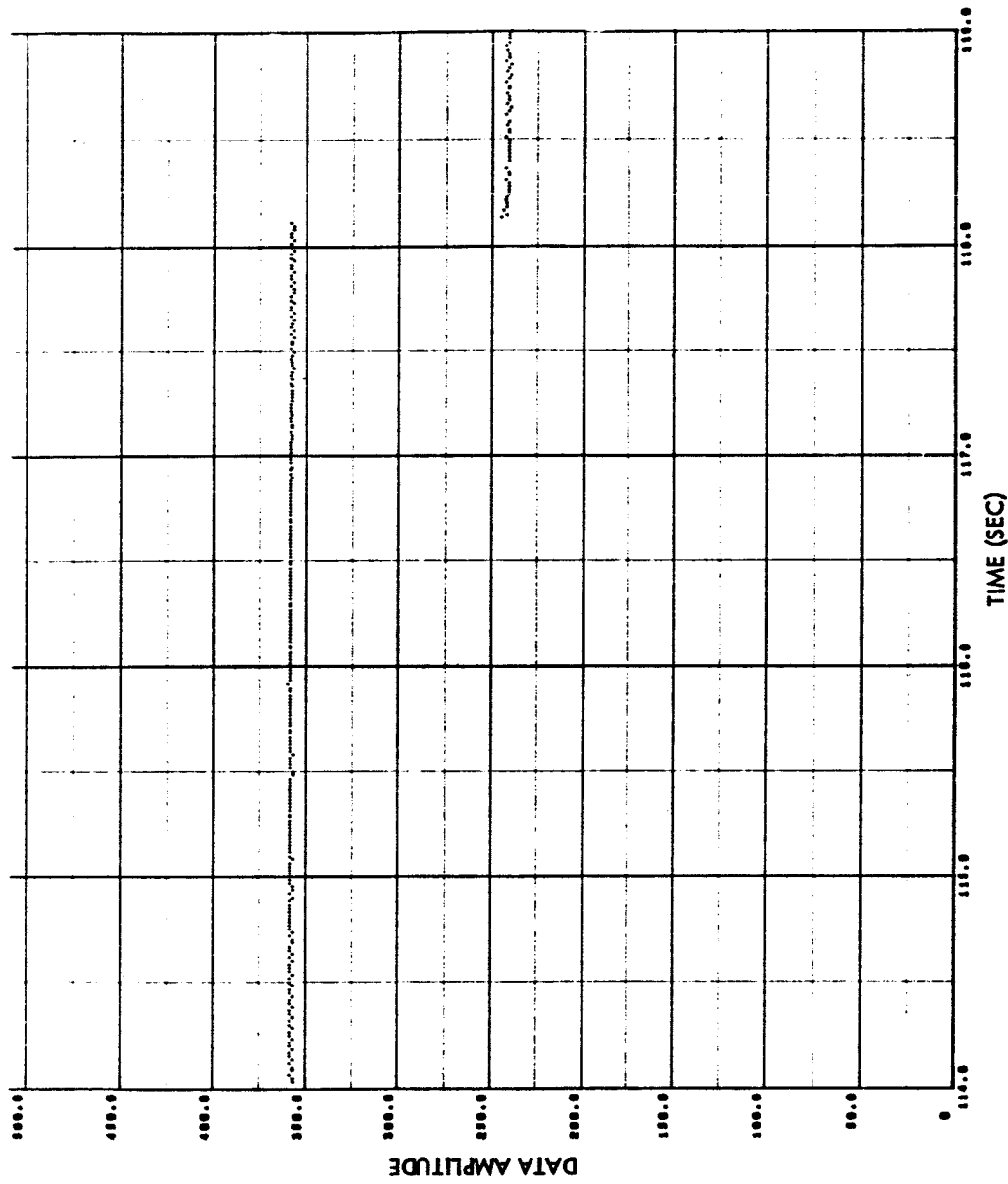


Fig. 3-4 (Cont'd) Raw Data, Sensor II

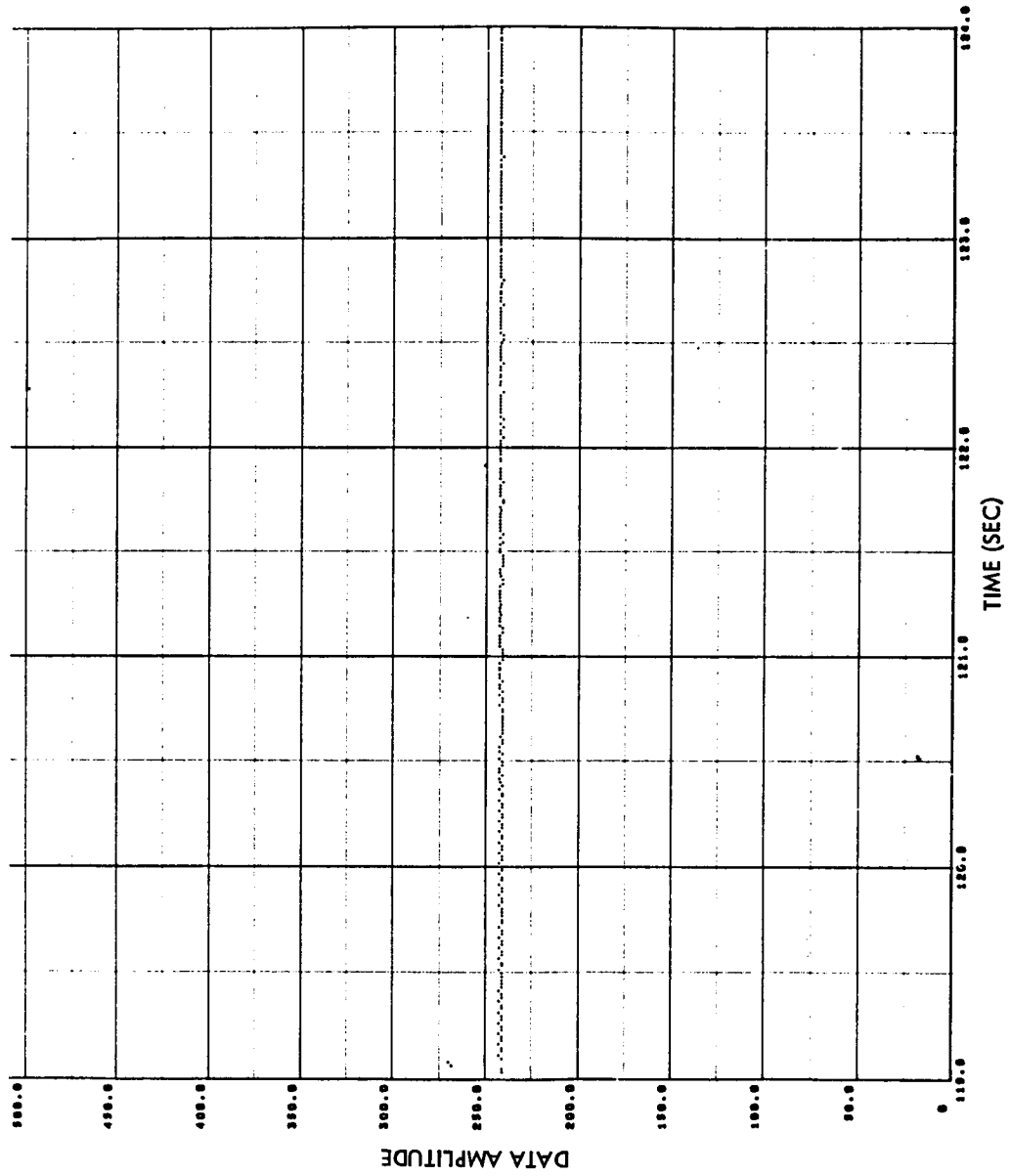


Fig. 3-4 (Cont'd) Raw Data, Sensor II

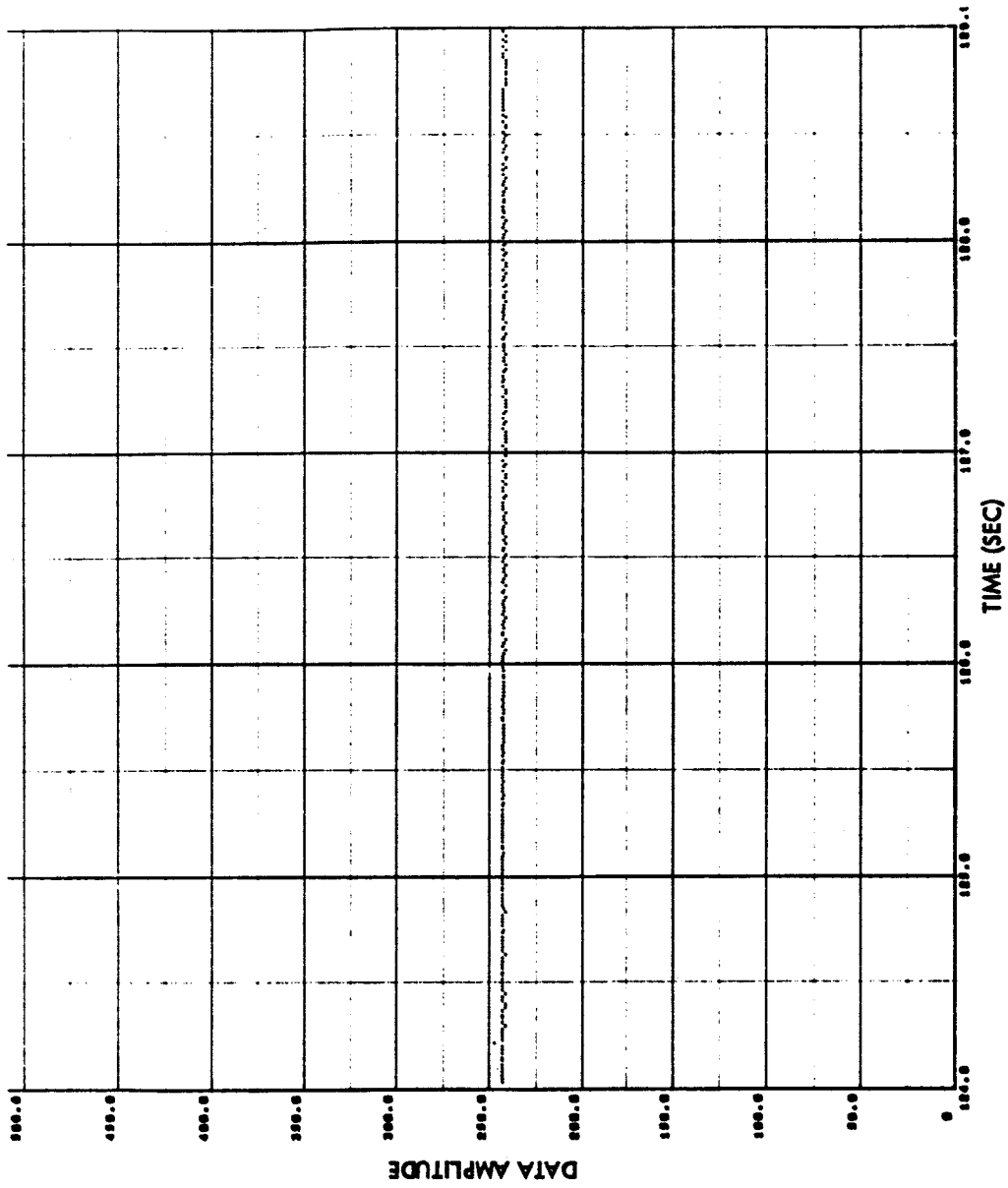


Fig. 3-4 (Cont'd) Raw Data, Sensor II

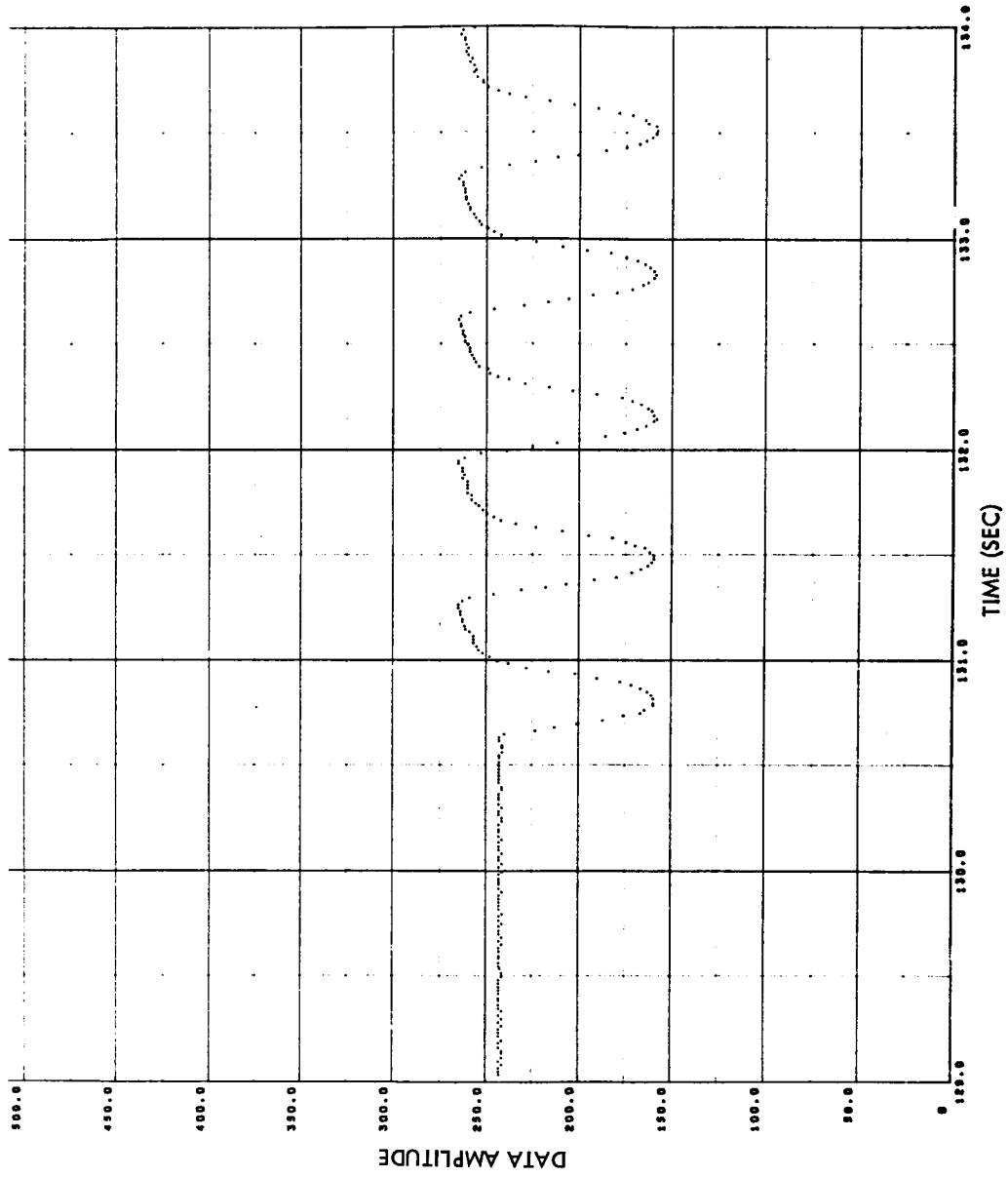


Fig. 3-4 (Cont'd) Raw Data, Sensor II

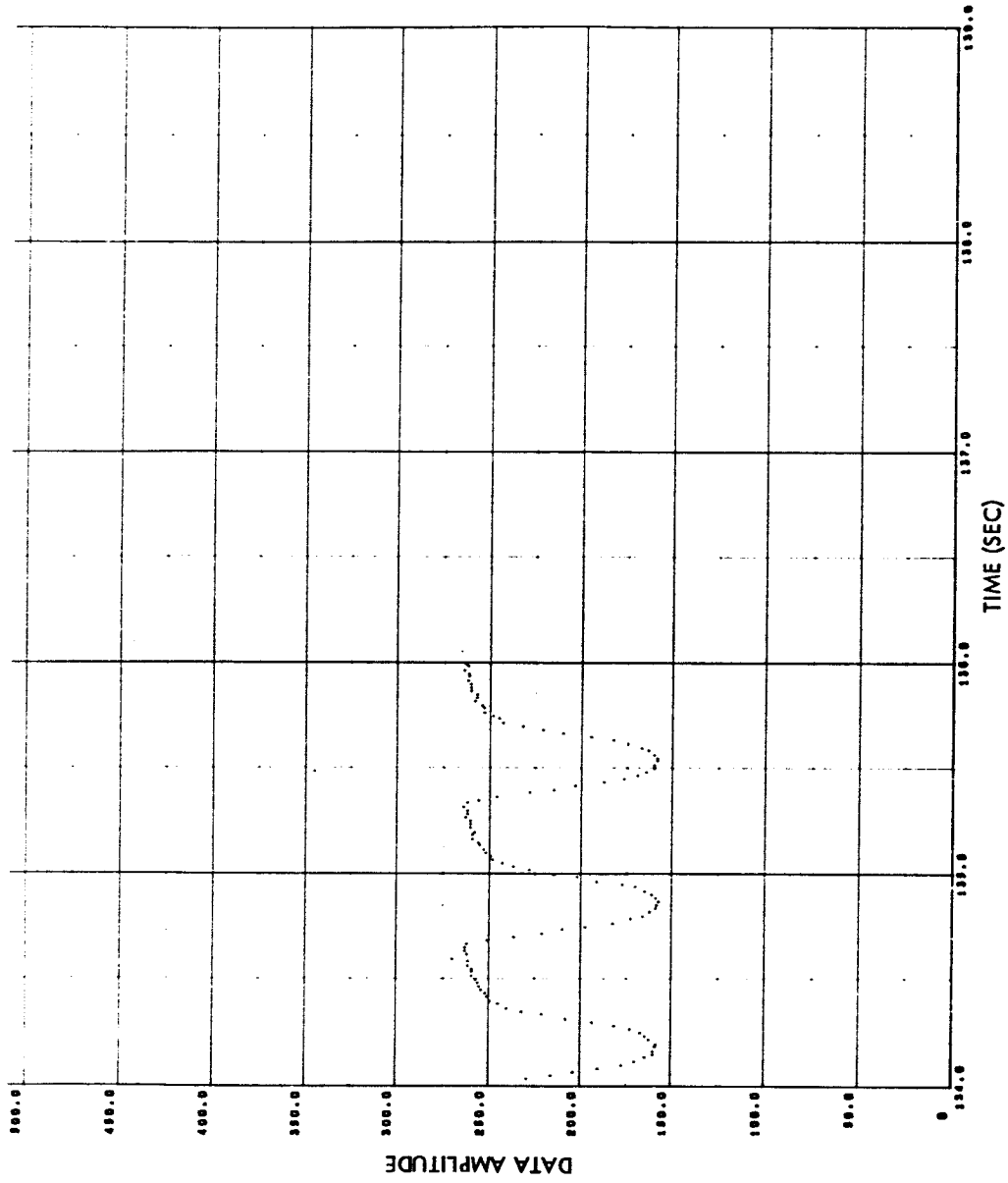
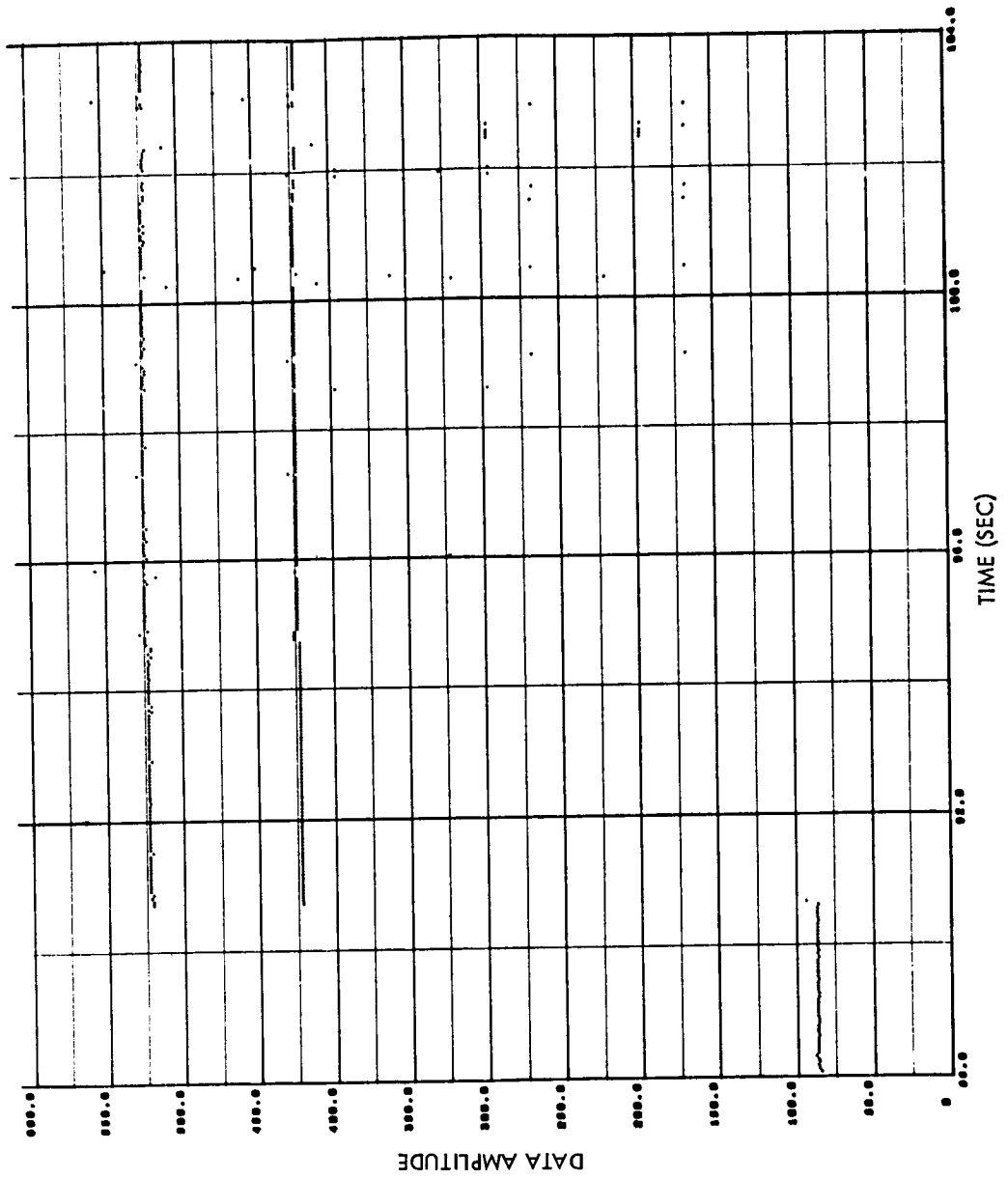
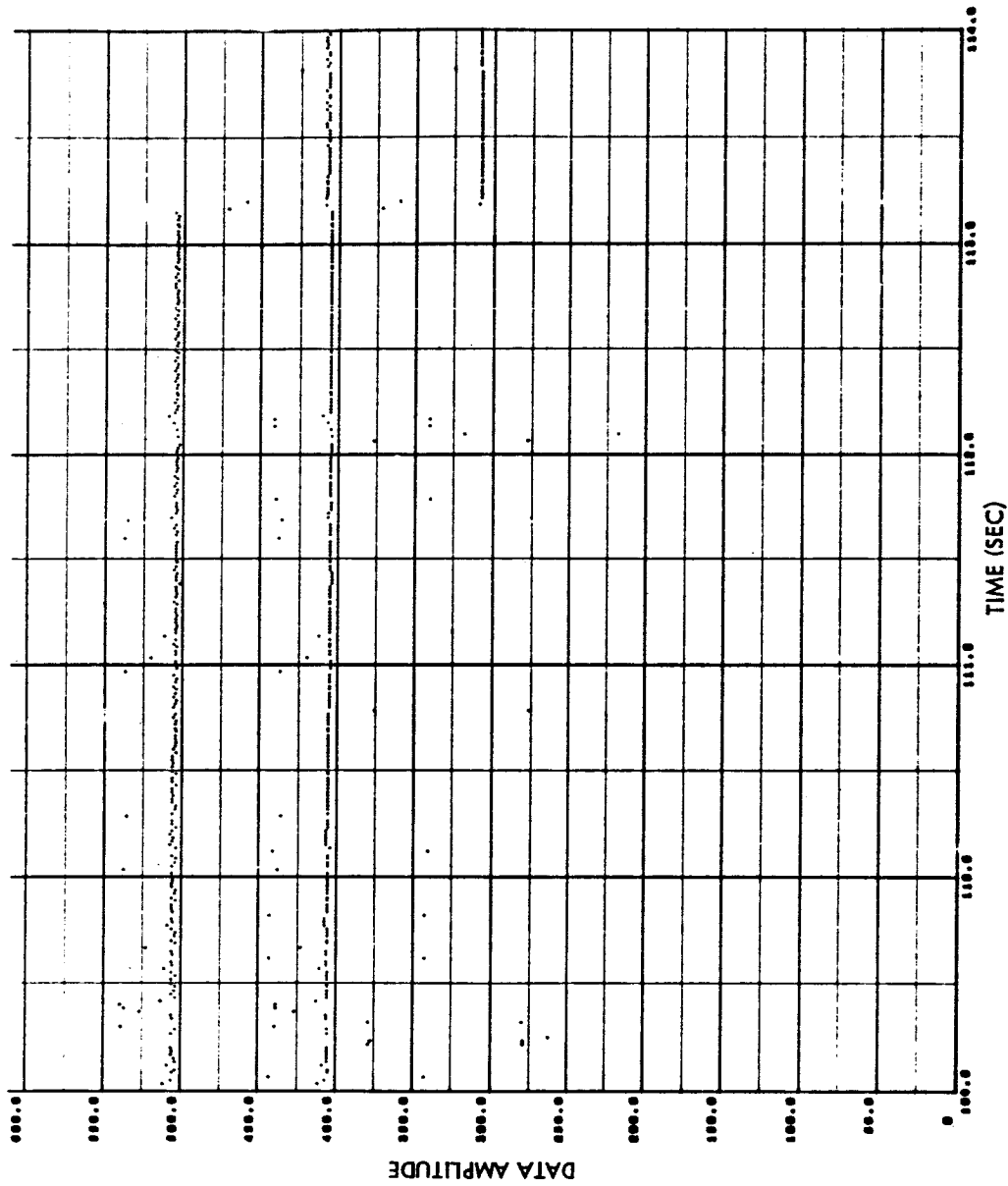


Fig. 3-4 (Cont'd) Raw Data, Sensor II



SENSOR 10
 DATA CLASS 1
 EXAMPLE B
 ZOI
 TOL=2
 N = 5.08

Fig. 3-5 Class 1 Original and Reconstructed Data (ZOI)



SENSOR 11
 DATA CLASS 2
 ZOI
 TOL = 2
 N = 4.90

Fig. 3-6 Class 2 Original and Reconstructed Data (ZOI)

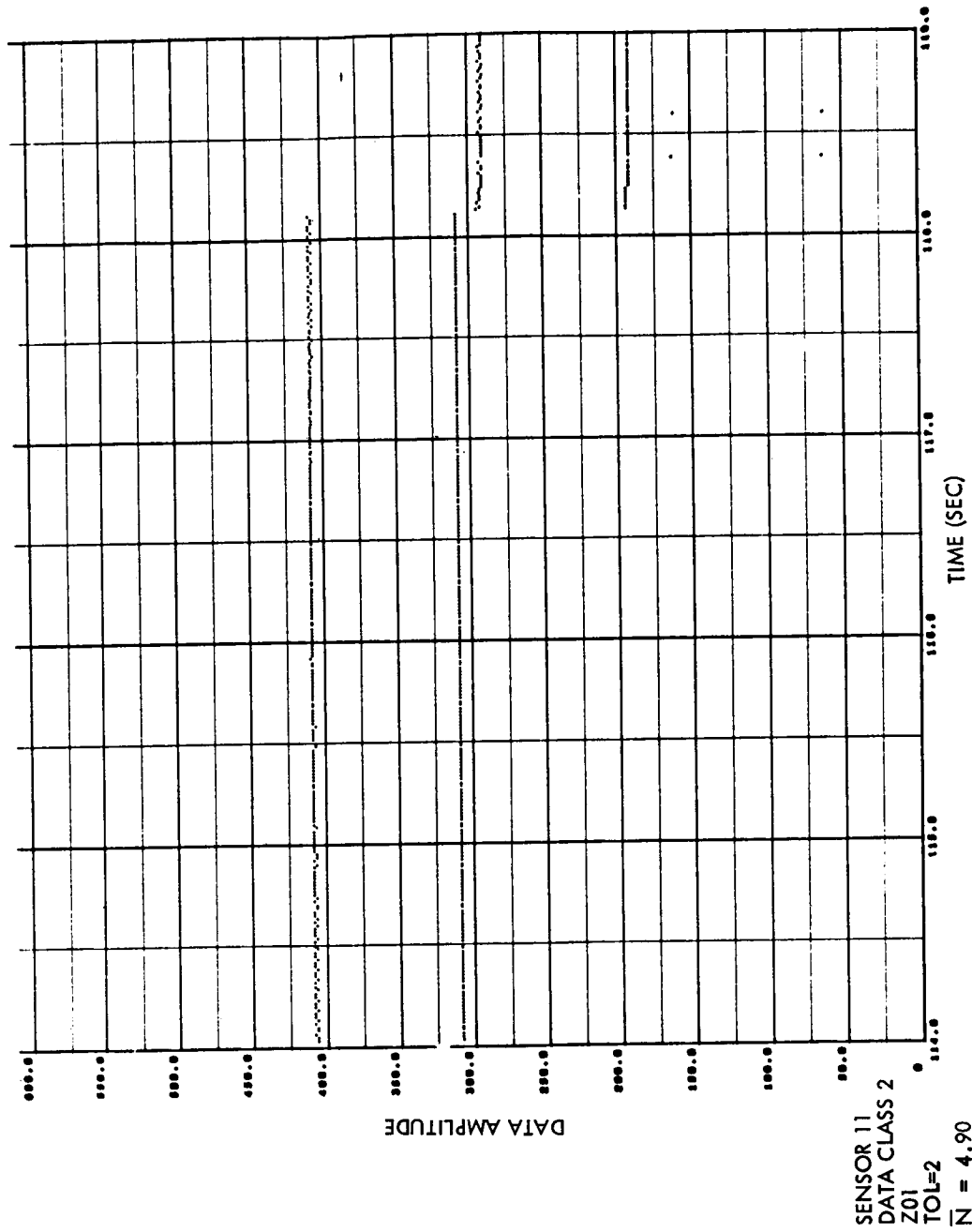
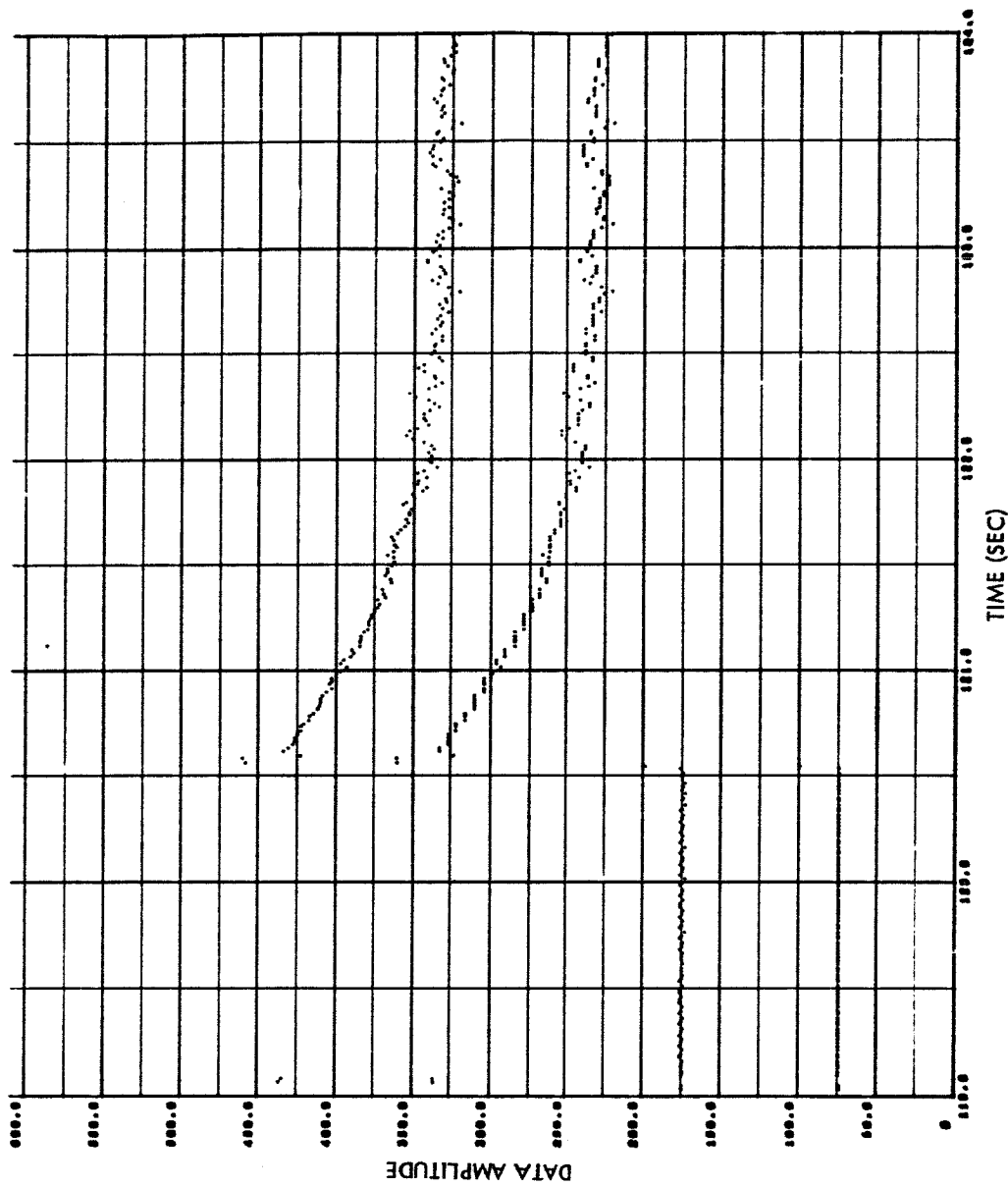
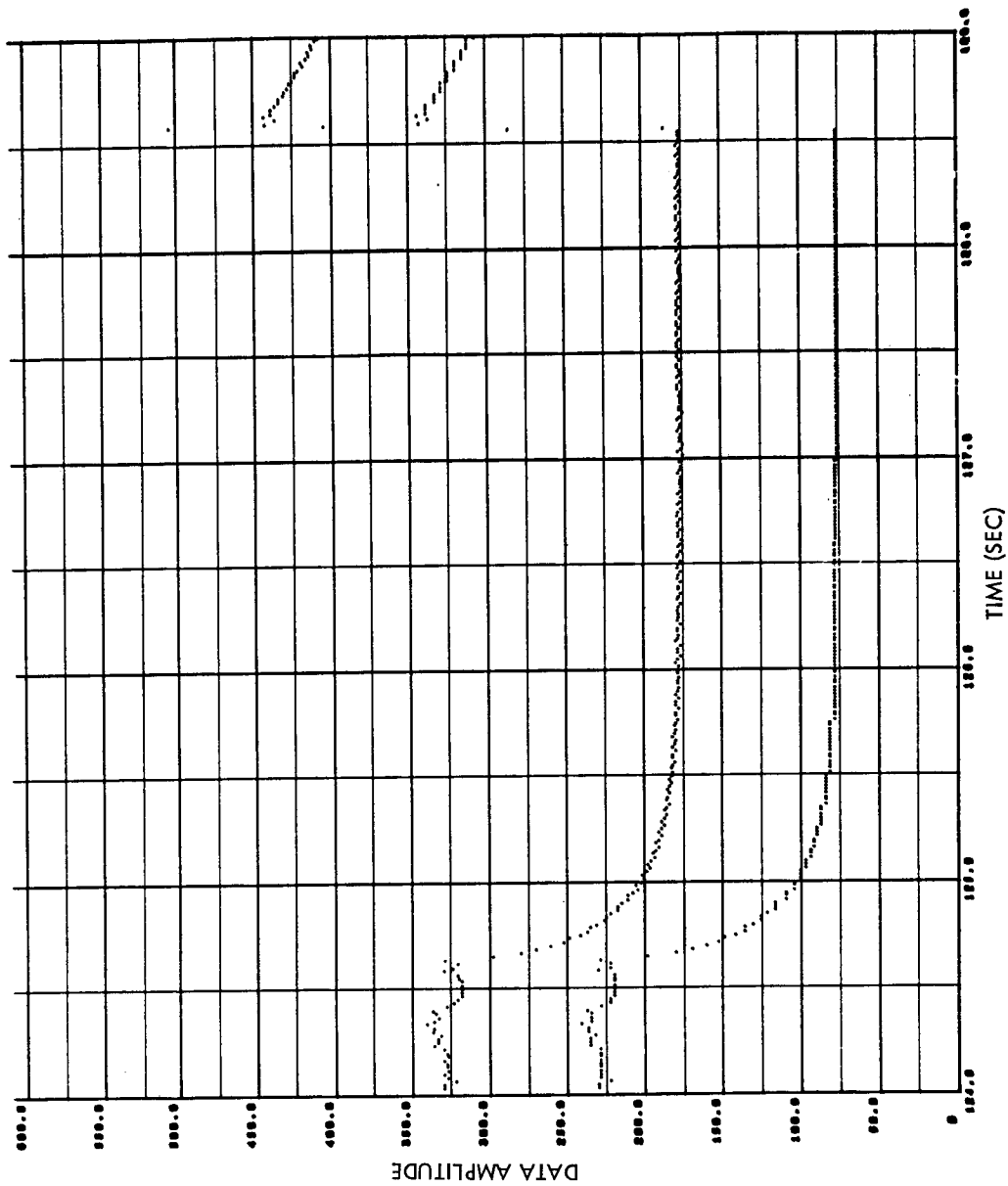


Fig. 3-6 (Cont'd) Class 2 Original and Reconstructed Data (Z01)



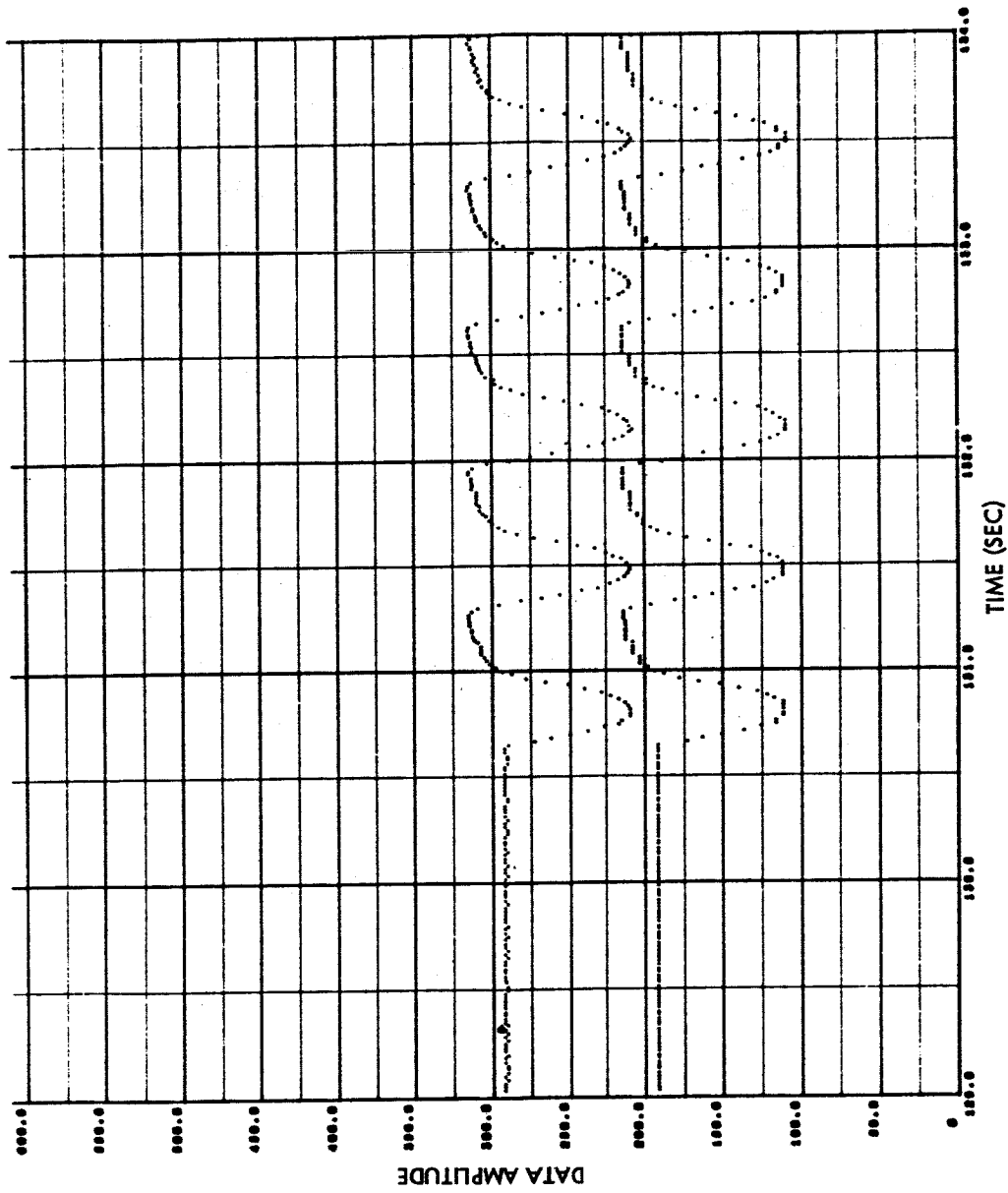
SENSOR 9
 DATA CLASS 3
 EXAMPLE A
 ZOI
 TOL=2

Fig. 3-7 Class 3 Original and Reconstructed Data (ZOI)



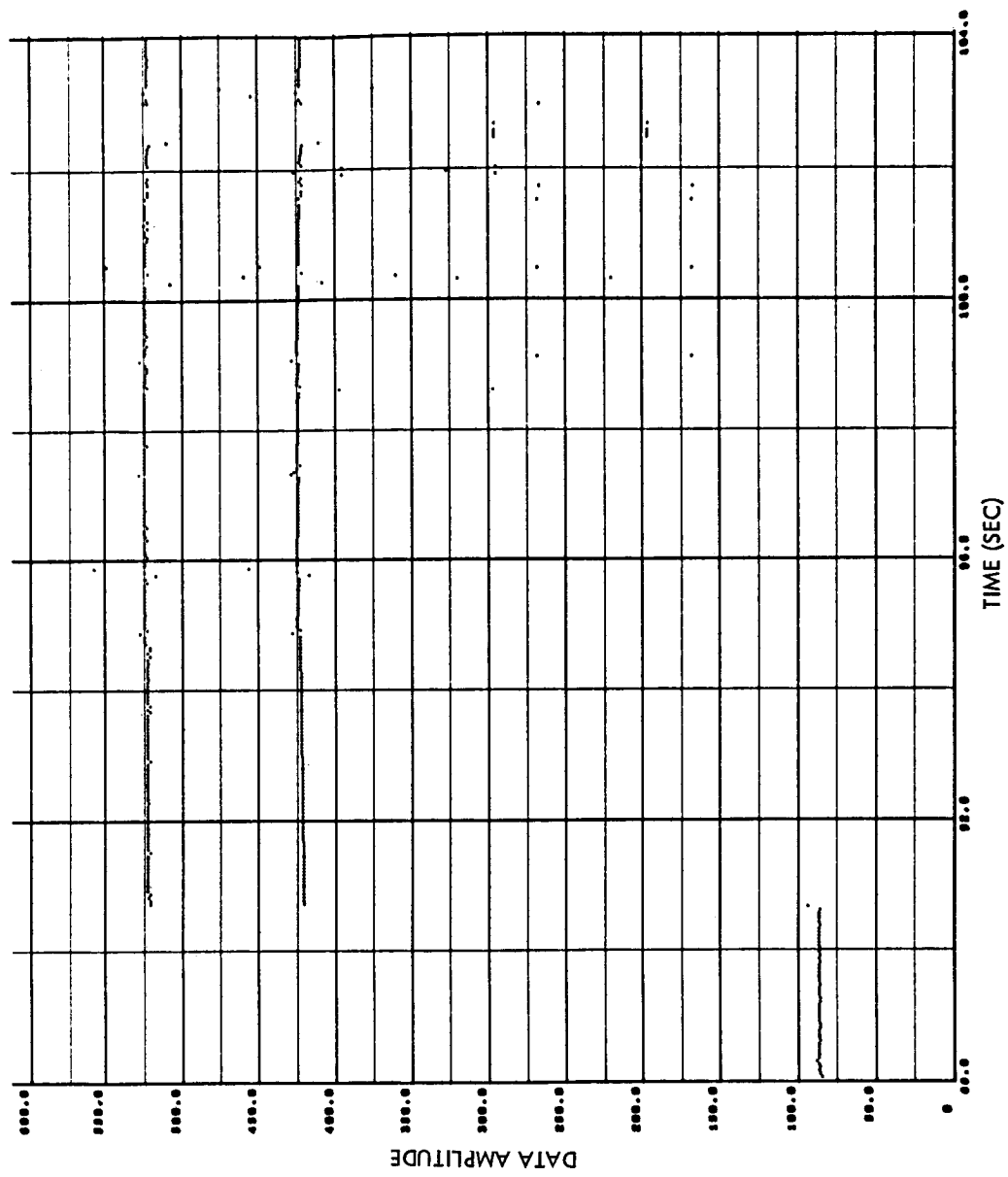
SENSOR 9
 DATA CLASS 3
 EXAMPLE A
 ZOI
 TOI=2

Fig. 3-7 (Cont'd) Class 3 Original and Reconstructed Data (ZOI)



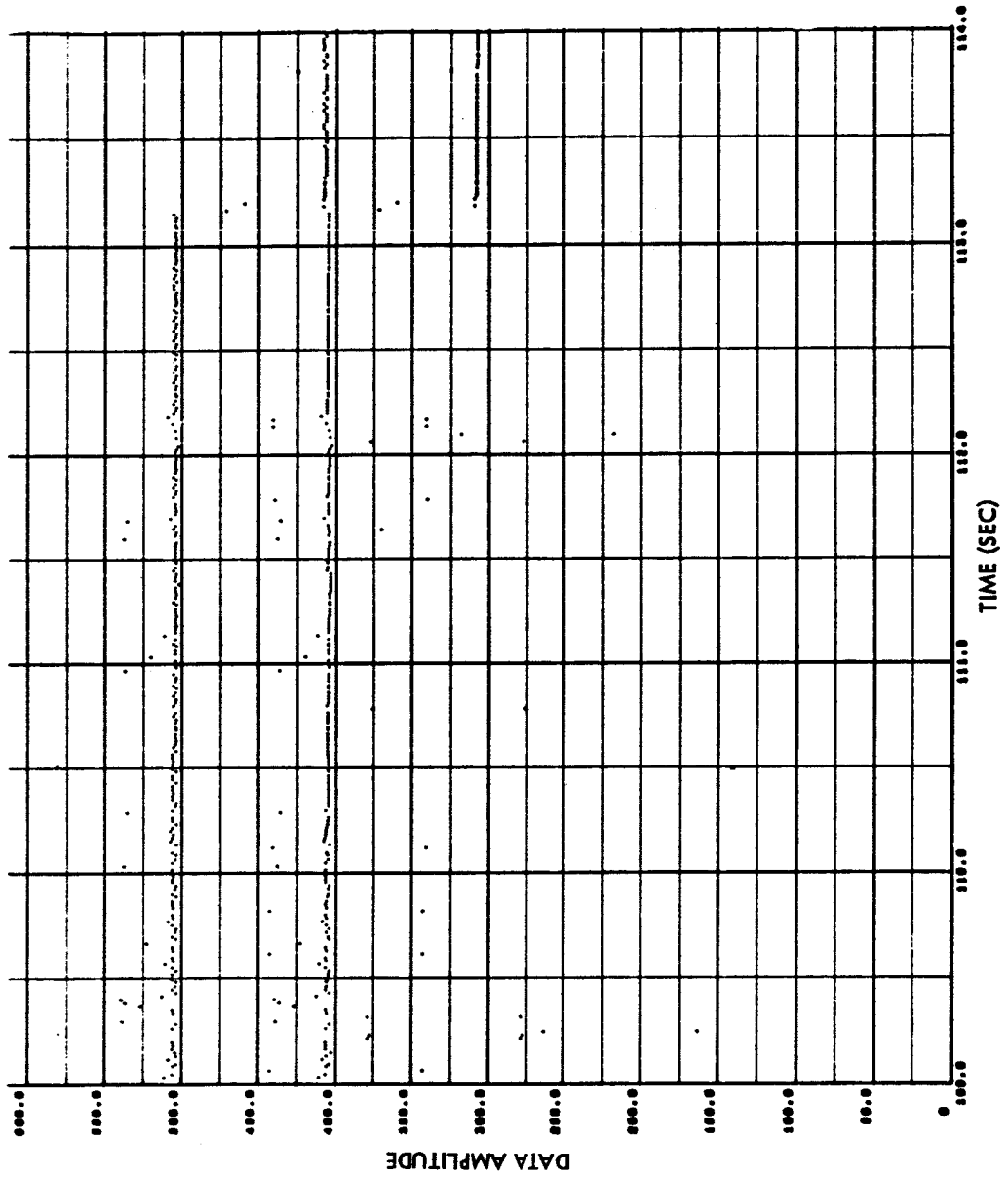
SENSOR 11
 DATA CLASS 5
 ZOI
 TOL = 2
 N = 2.78

Fig. 3-8 Class 5 Original and Reconstructed Data (ZOI)



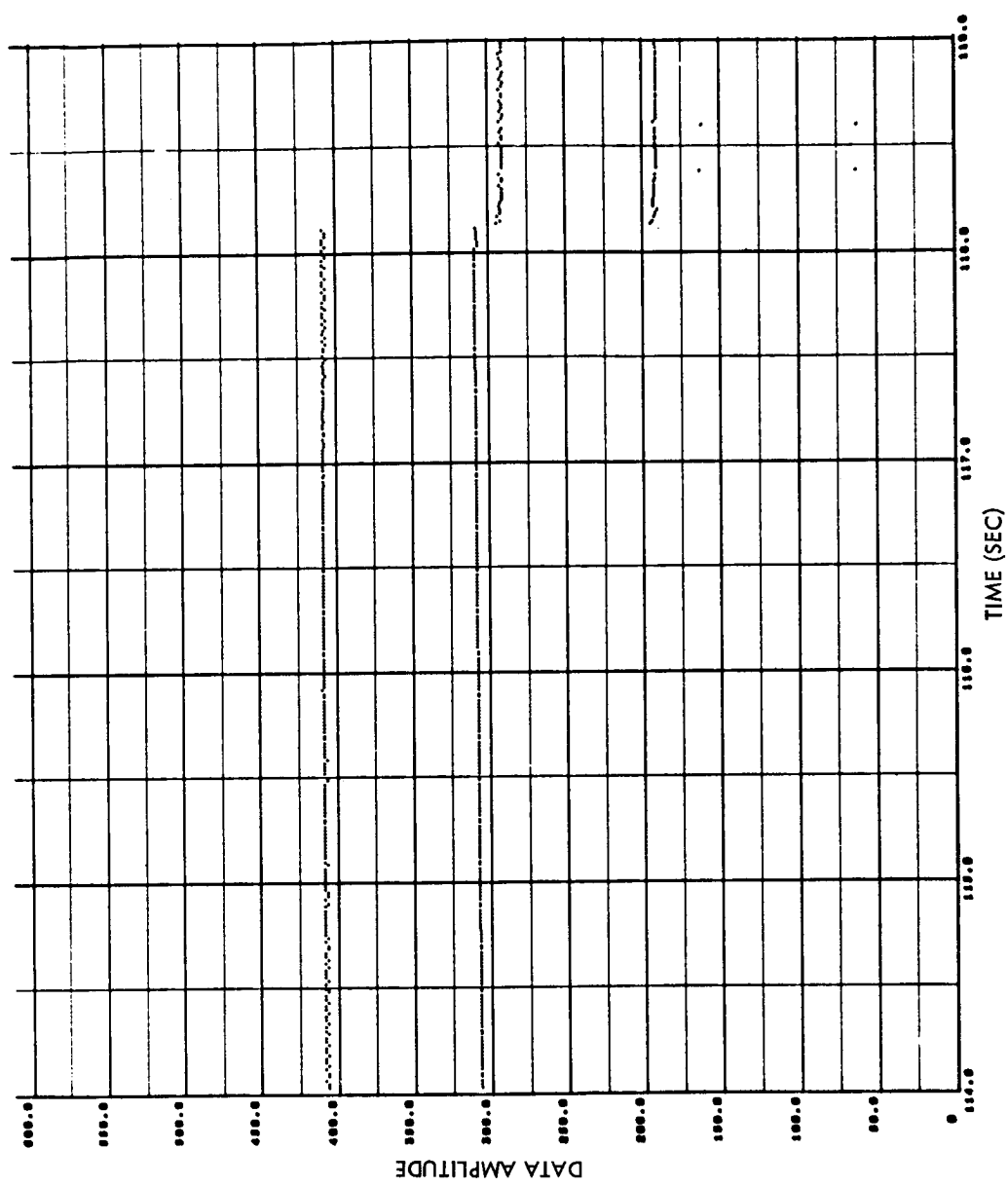
SENSOR 10
 DATA CLASS 1
 EXAMPLE B
 FOIDIS
 TOL= 2
 N = 4.42

Fig. 3-9 Class 1 Original and Reconstructed Data (FOIDIS)



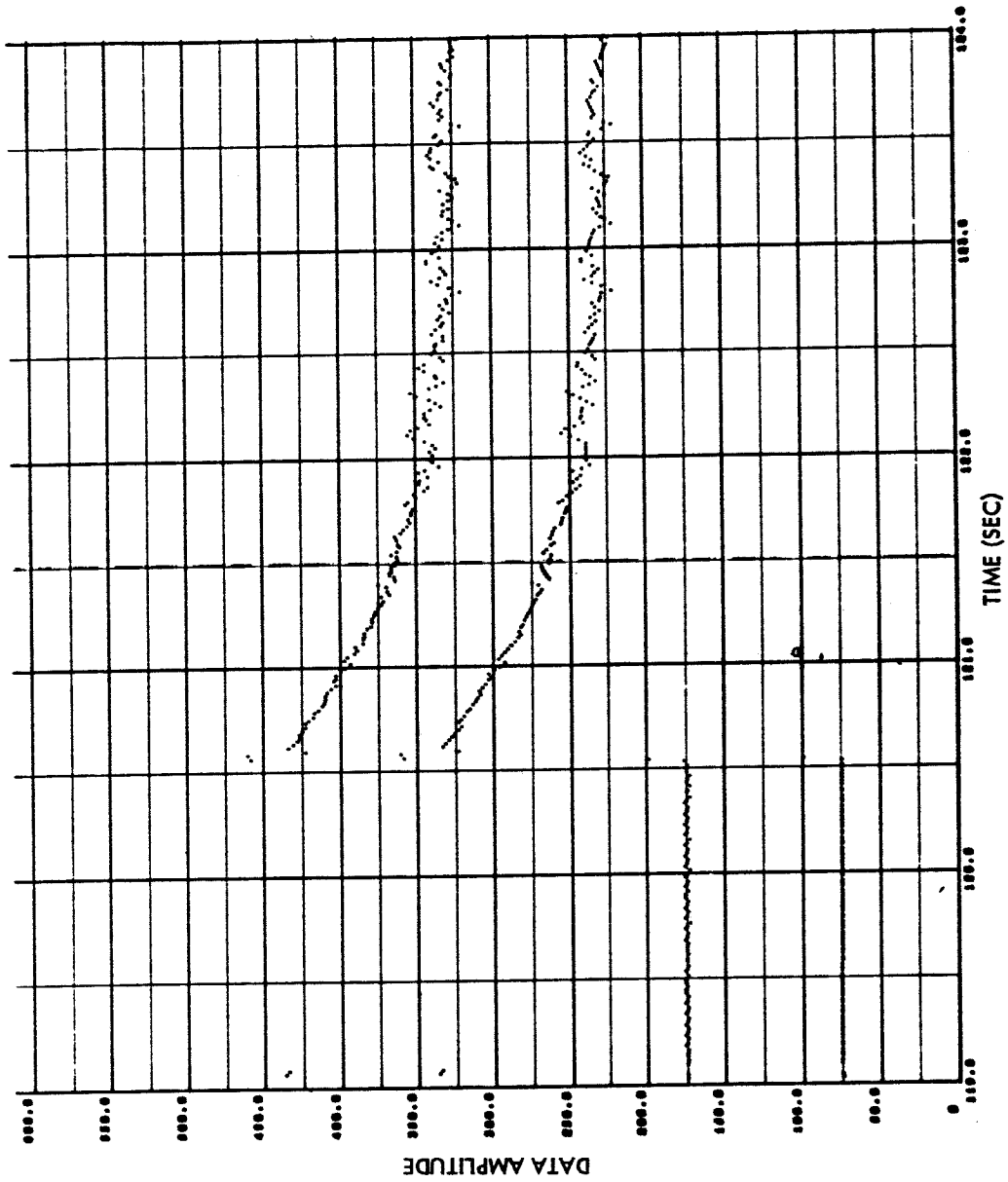
SENSOR 11
 DATA CLASS 2
 FOIDIS
 TOL = 2
 N = 5.62

Fig. 3-10 Class 2 Original and Reconstructed Data (FOIDIS)



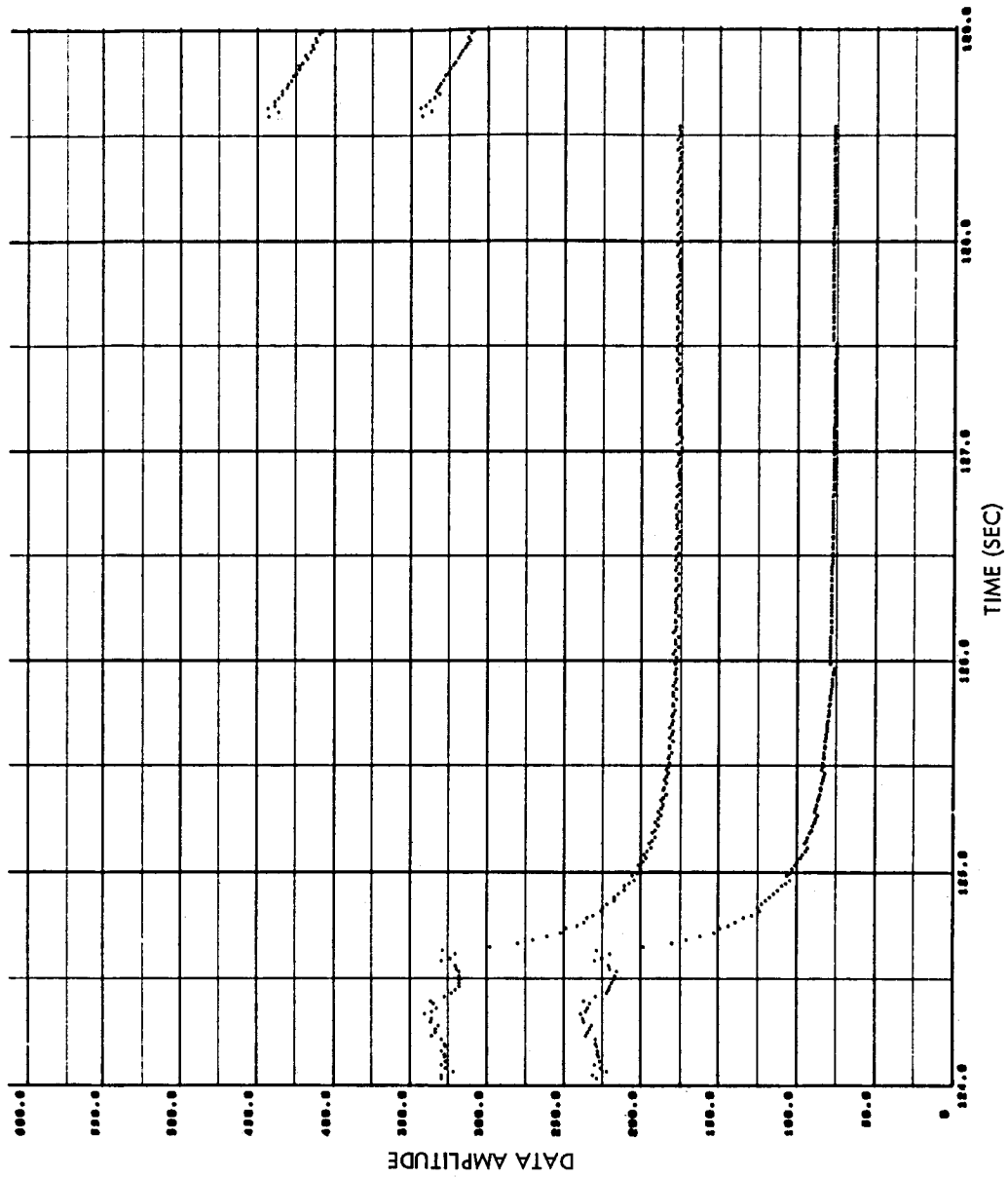
SENSOR 11
 DATA CLASS 2
 FOIDIS
 TOLF=2
 $\bar{N} = 5.62$

Fig. 3-10 (Cont'd) Class 2 Original and Reconstructed Data (FOIDIS)



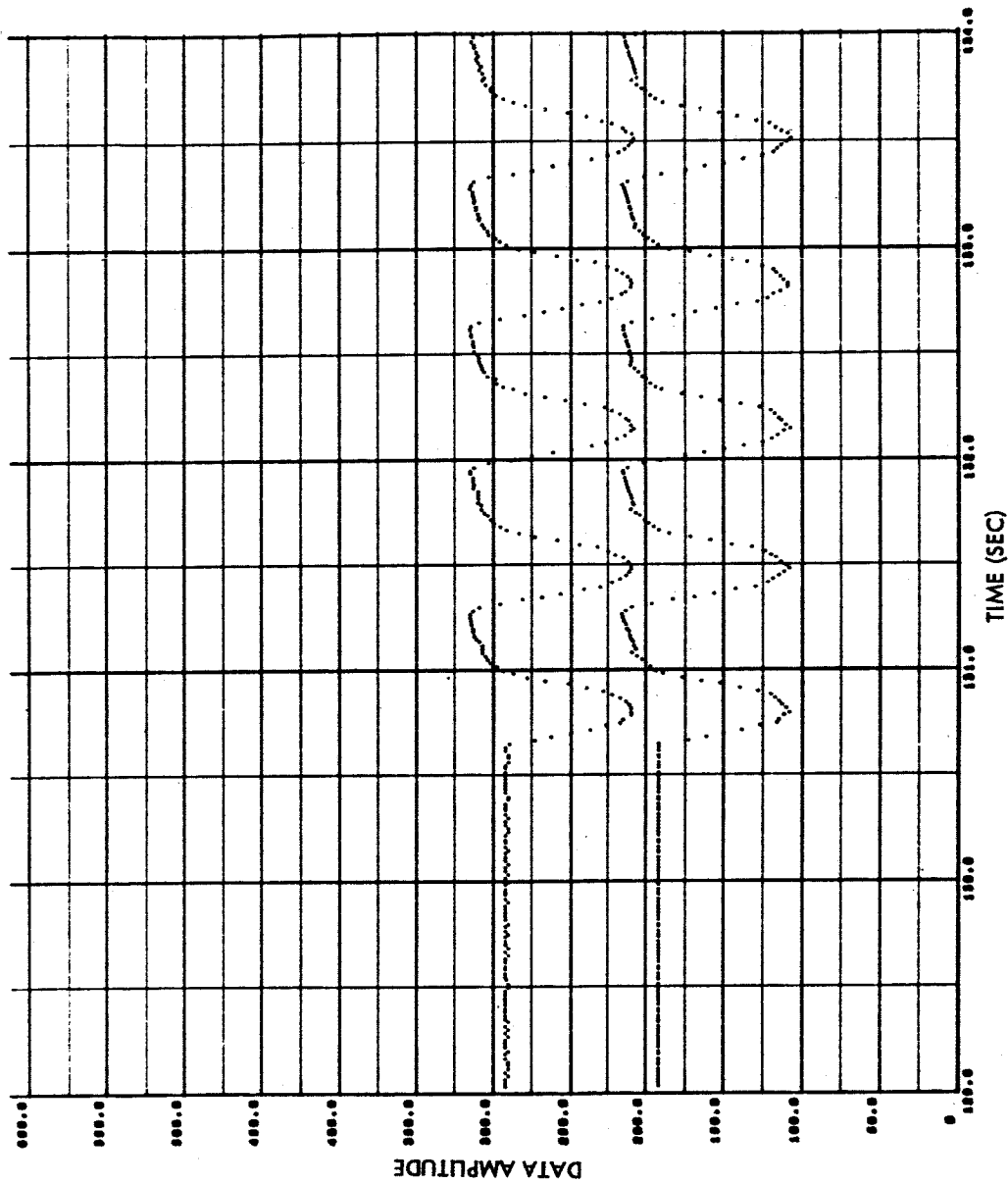
SENSOR 9
 DATA CLASS 3
 EXAMPLE A
 FOIDIS
 TOL = 2
 N = 5.70

Fig. 3-11 Class 3 Original and Reconstructed Data (FOIDIS)



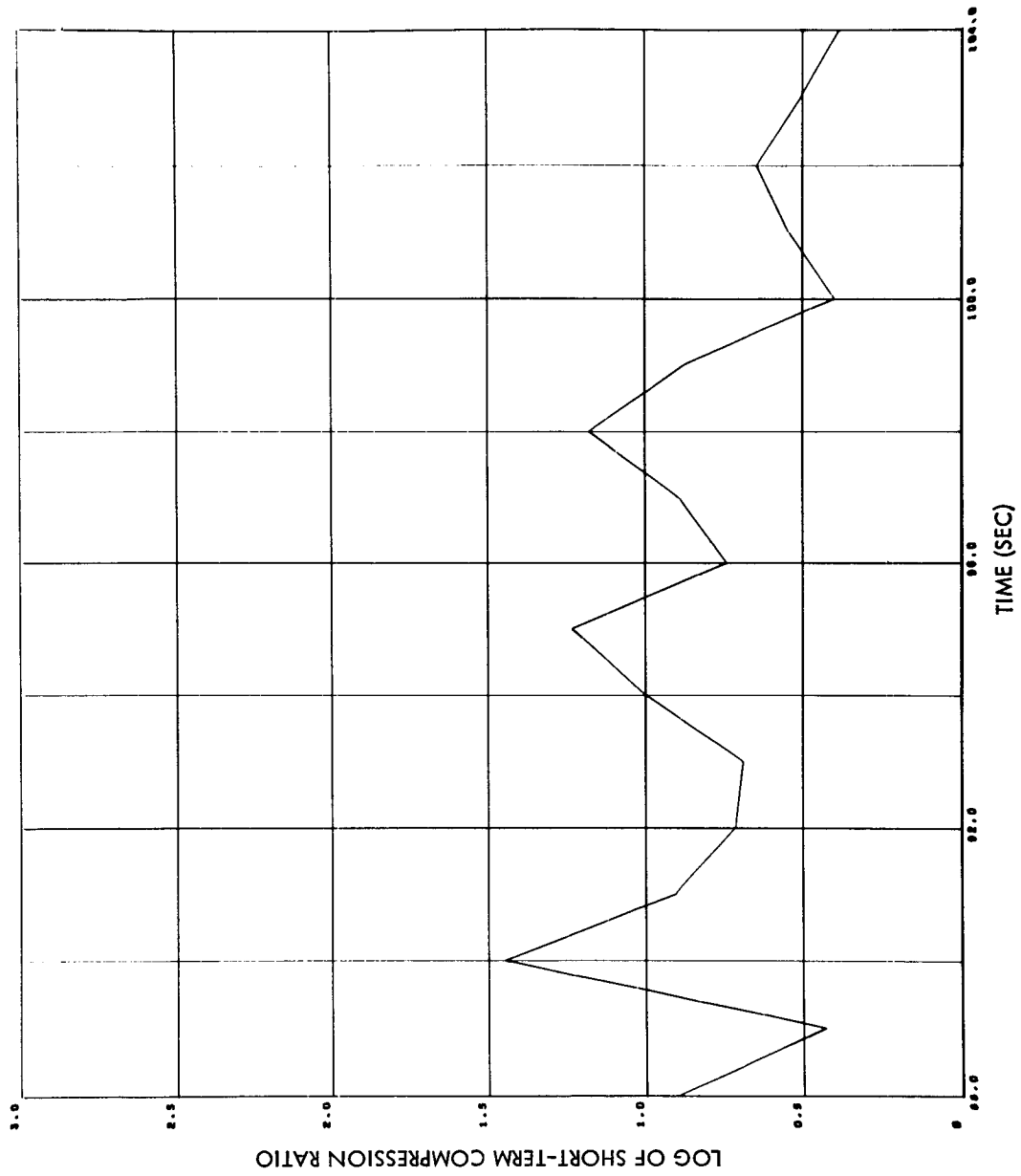
SENSOR 9
 DATA CLASS 3
 EXAMPLE A
 FOIDIS
 TOL=2
 $\bar{N} = 5.70$

Fig. 3-11 (Cont'd) Class 3 Original and Reconstructed Data (FOIDIS)



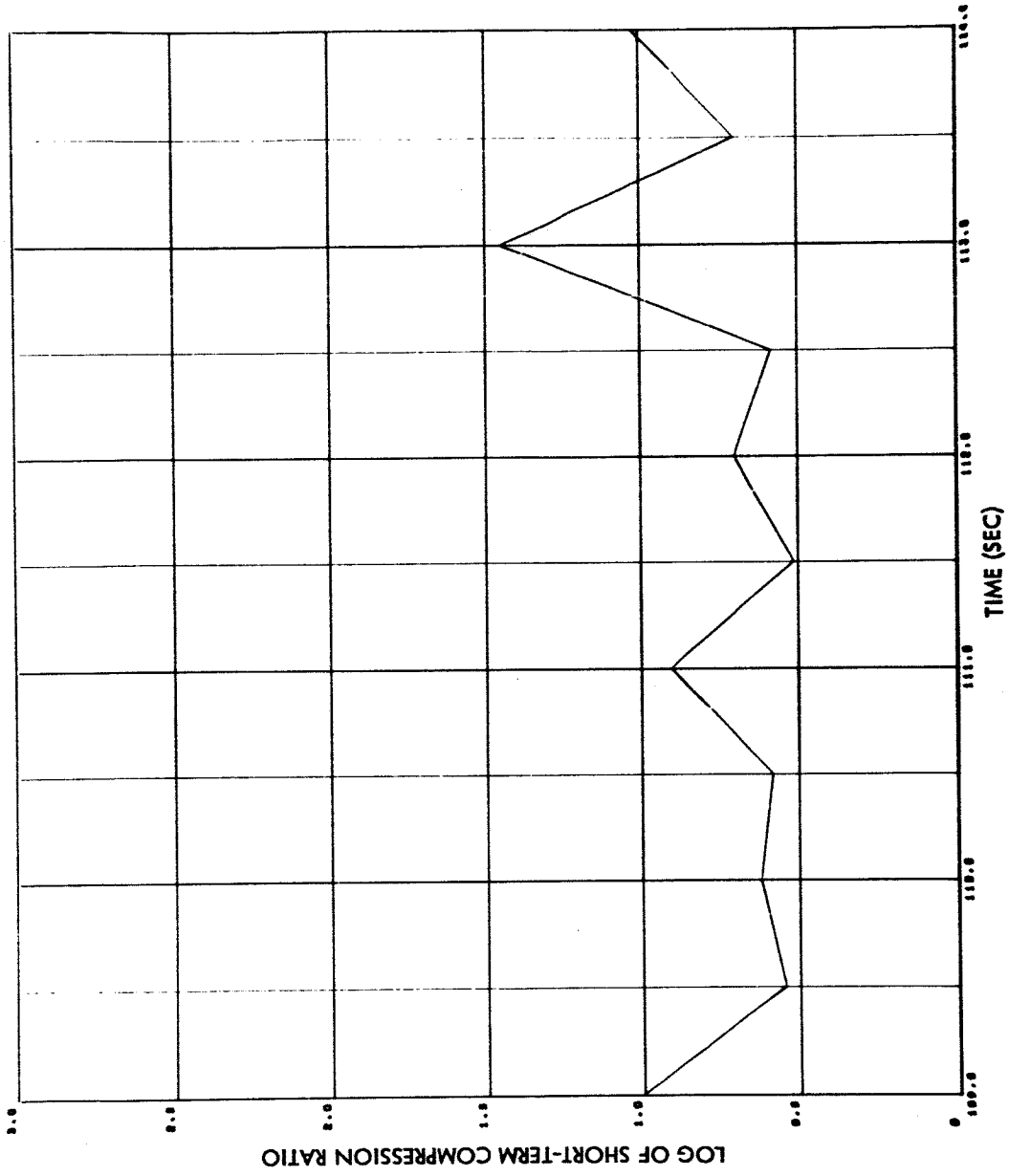
SENSOR 11
 DATA CLASS 5
 FOIDIS
 TOL = 2
 N = 6.44

Fig. 3-12 Class 5 Original and Reconstructed Data (FOIDIS)



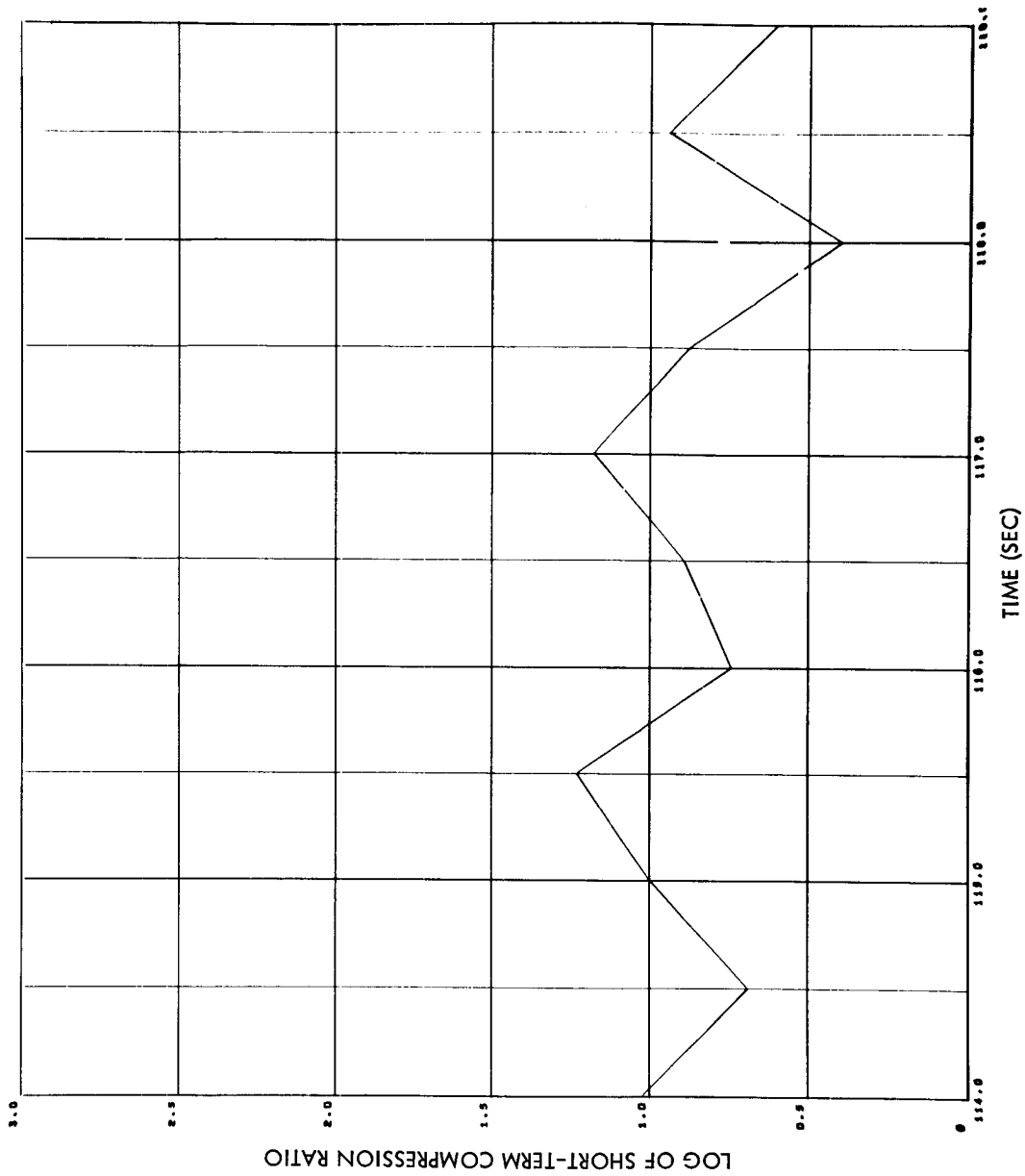
SENSOR 10
 DATA CLASS 1
 EXAMPLE B
 FOIDIS
 TOL=3
 N=4.42

Fig. 3-13 Class 1 Short-Term Compression Ratio (FOIDIS)



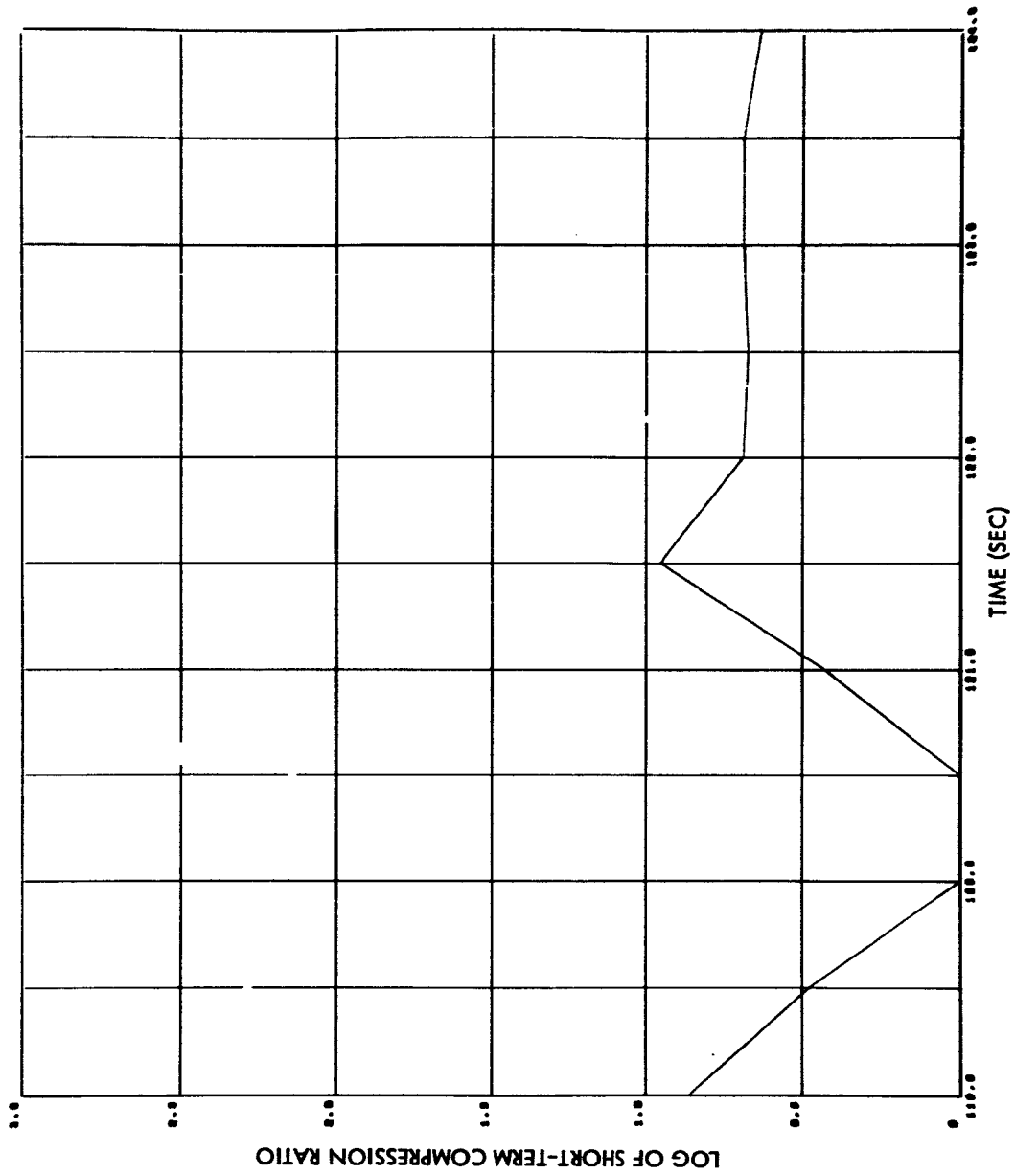
SENSOR 11
 DATA CLASS 2
 FOIDIS
 TOL=3
 N=5.62

Fig. 3-14 Class 2 Short-Term Compression Ratio (FOIDIS)



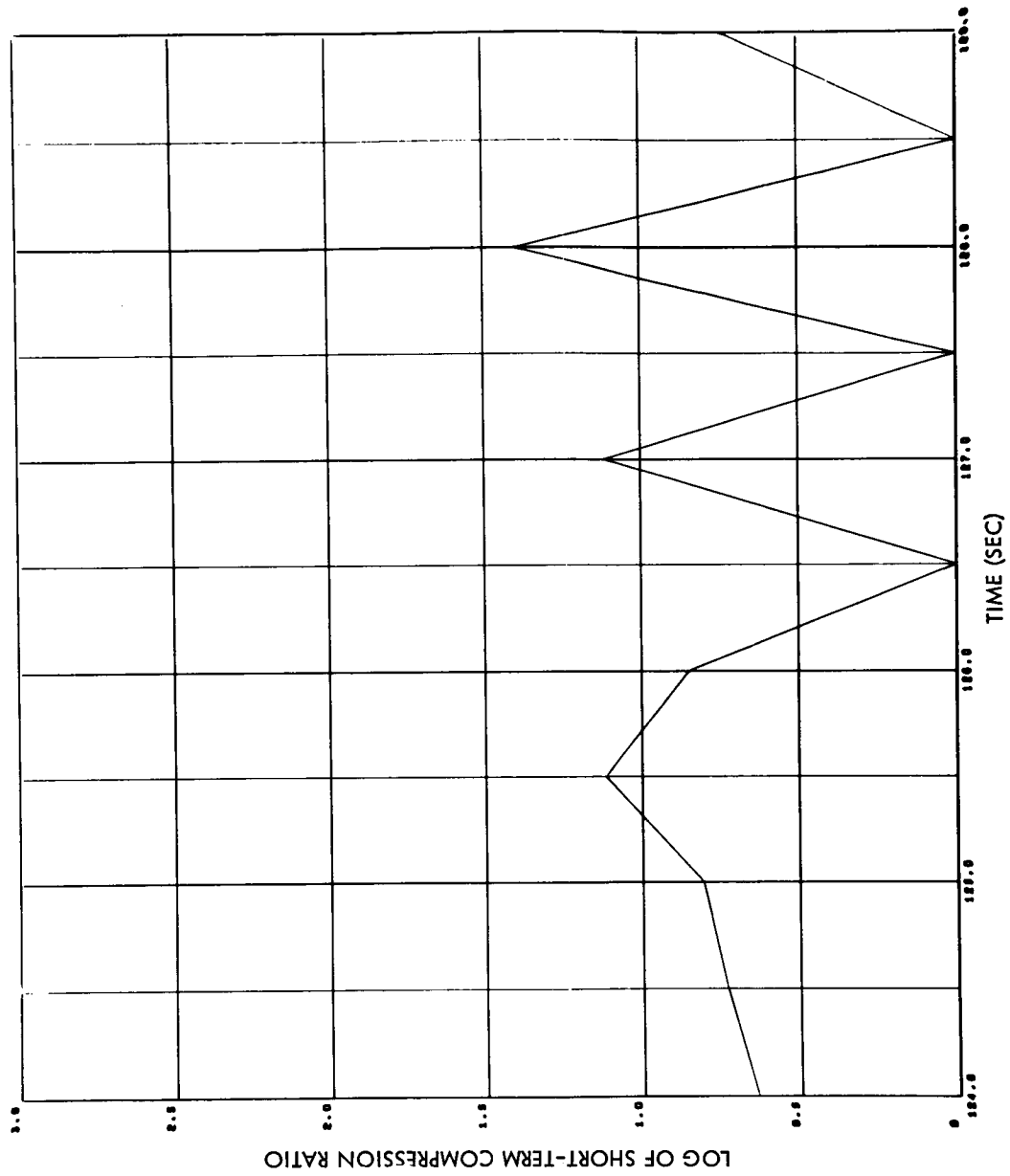
SENSOR 11
 DATA CLASS 2
 TOL=3
 $\bar{N}=5.62$

Fig. 3-14 (Cont'd) Class 2 Short-Term Compression Ratio (FOIDIS)



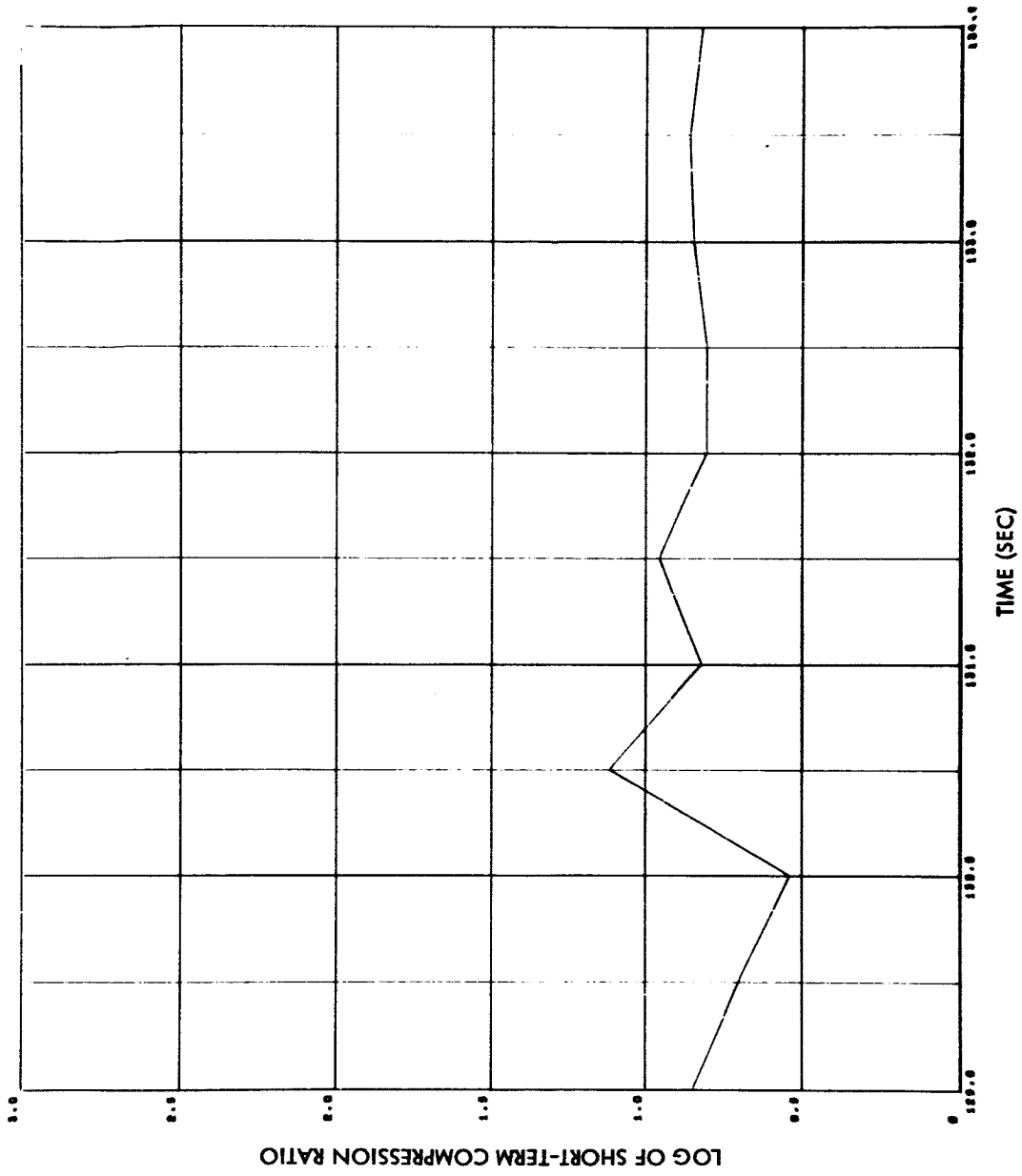
SENSOR
 DATA CLASS 3
 EXAMPLE A
 FOIDIS
 TOL=3
 N=5.70

Fig. 3-15 Class 3 Short-Term Compression Ratio (FOIDIS)



SENSOR 9
 DATA CLASS 3
 EXAMPLE A
 FOIDIS
 TOL = 3
 N = 5.70

Fig. 3-15 (Cont'd) Class 3 Short-Term Compression Ratio (FOIDIS)



SENSOR 11
 DATA CLASS 5
 FOIDIS
 TOL=3
 N=6.44

Fig. 3-16 Class 5 Short-Term Compression Ratio (FOIDIS)

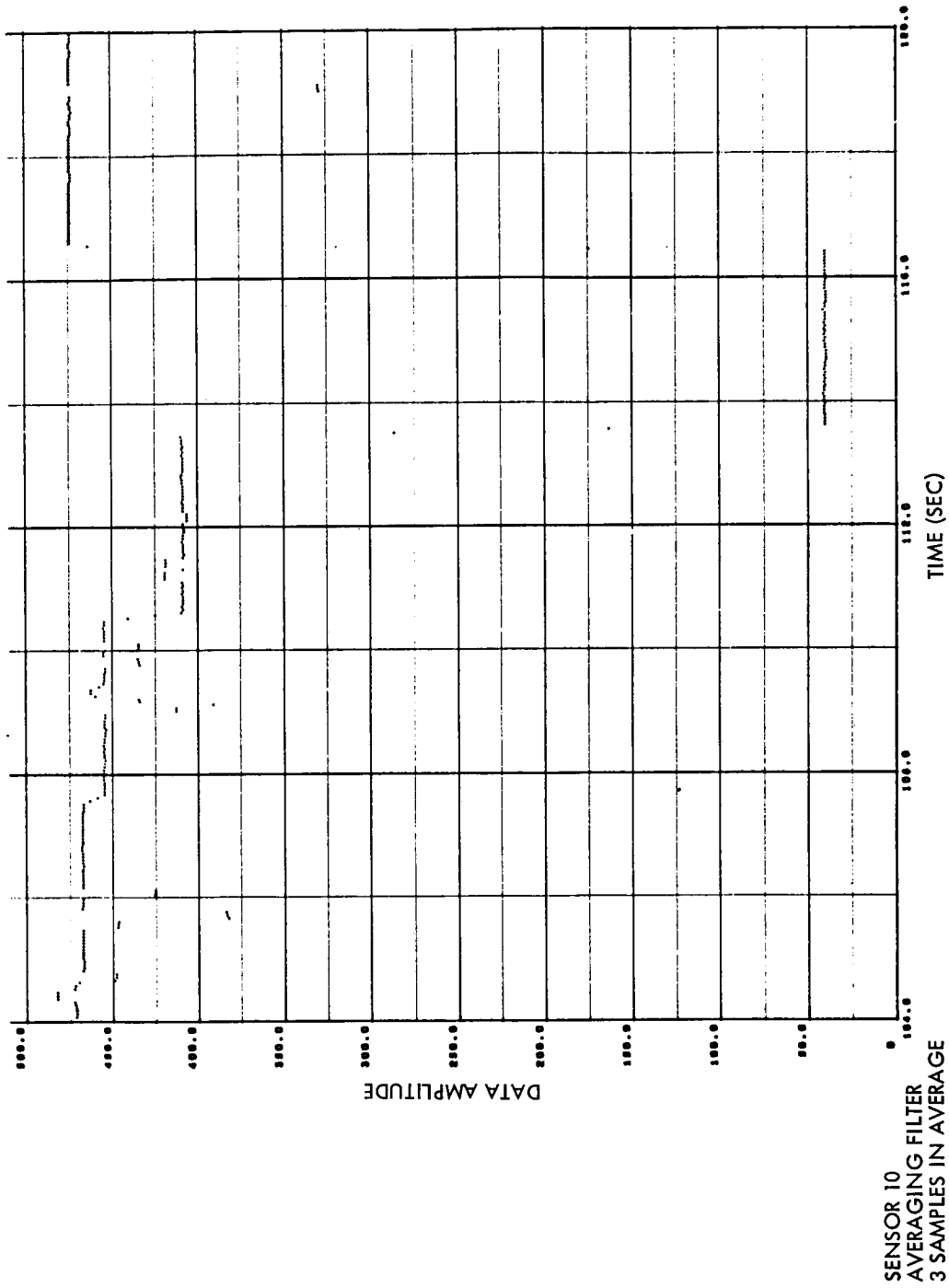


Fig. 3-17 Digitally Filtered Data

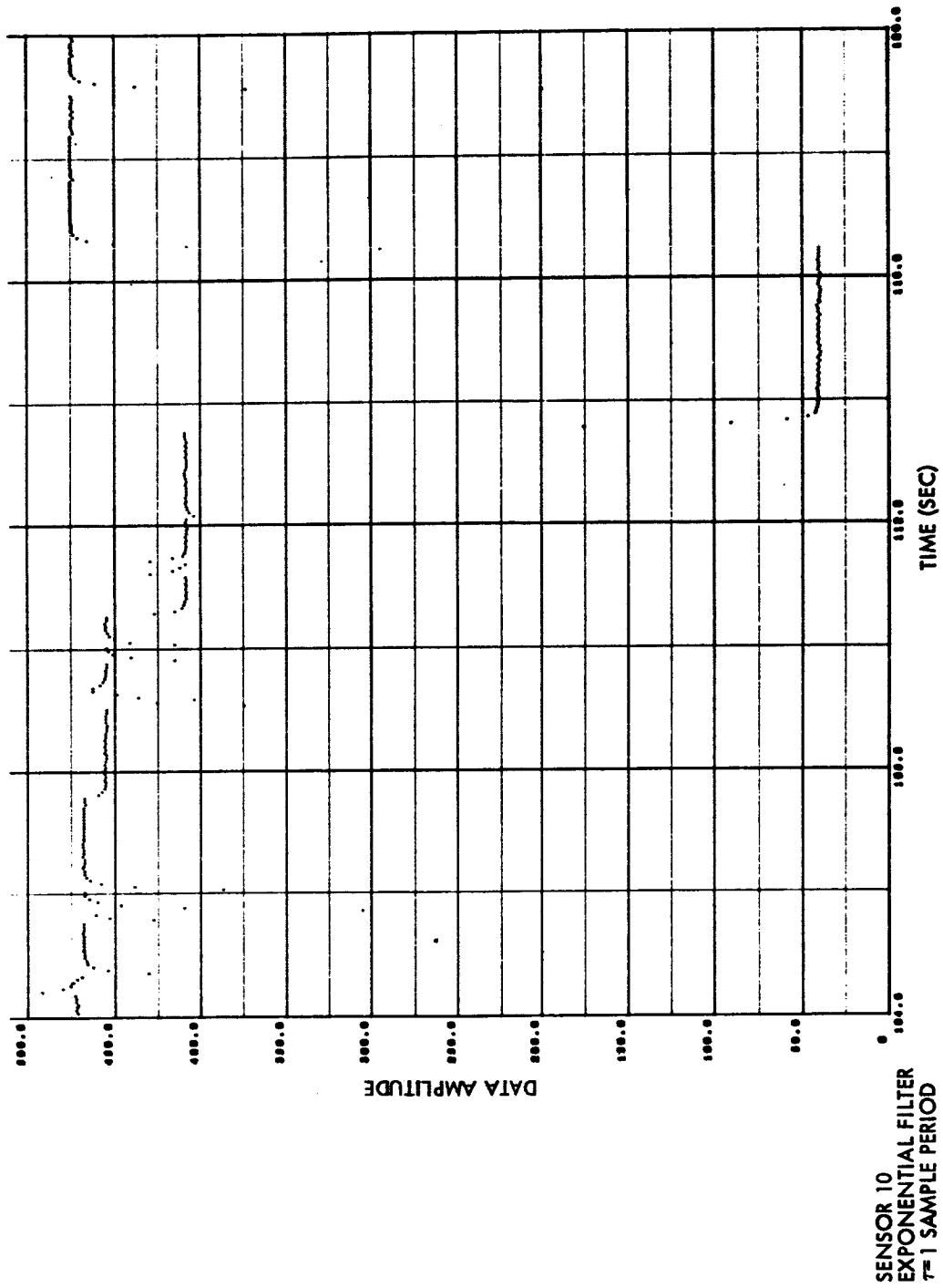


Fig. 3-17 (Cont'd) Digitally Filtered Data

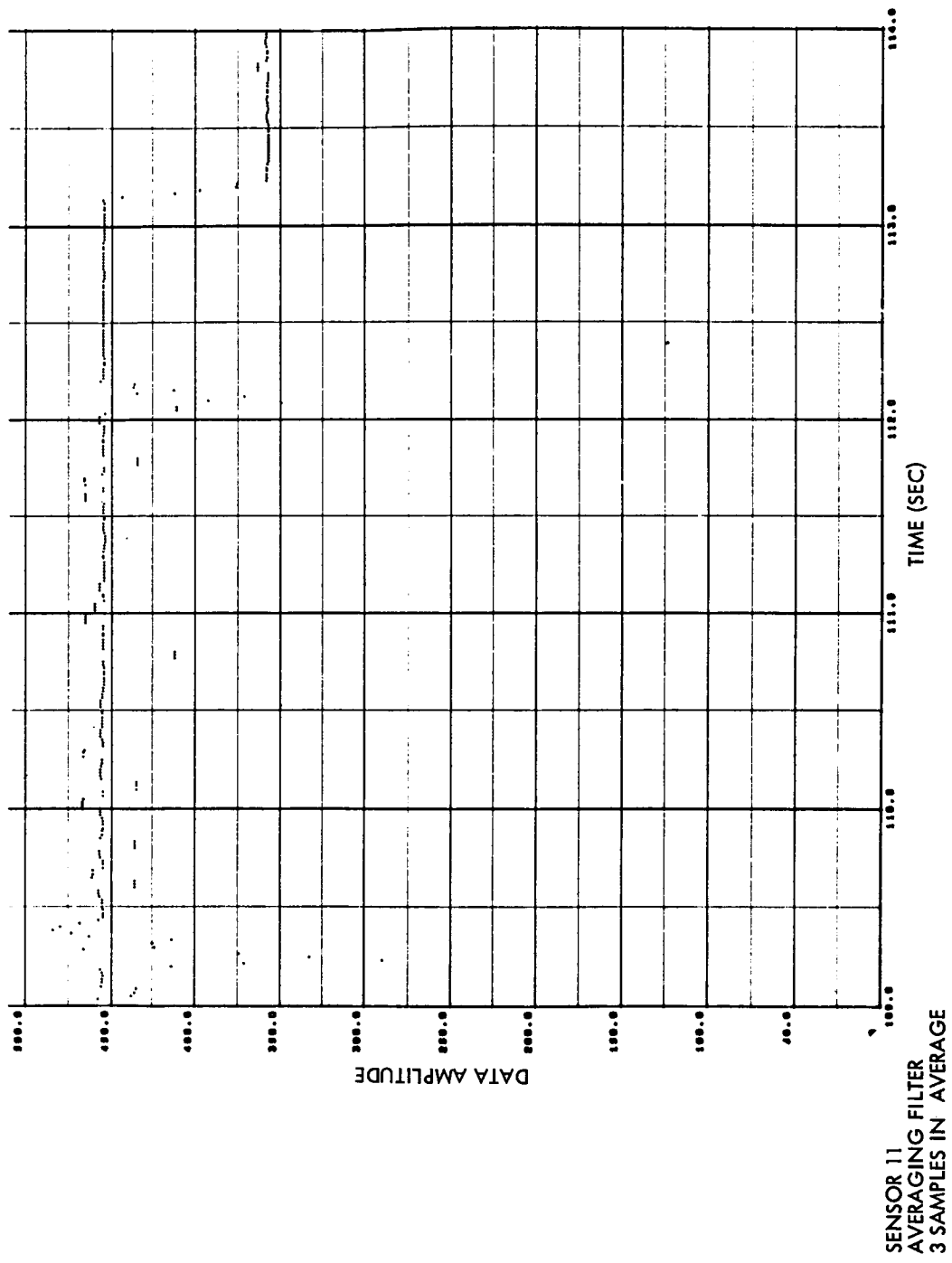


Fig. 3-17 (Cont'd) Digitally Filtered Data

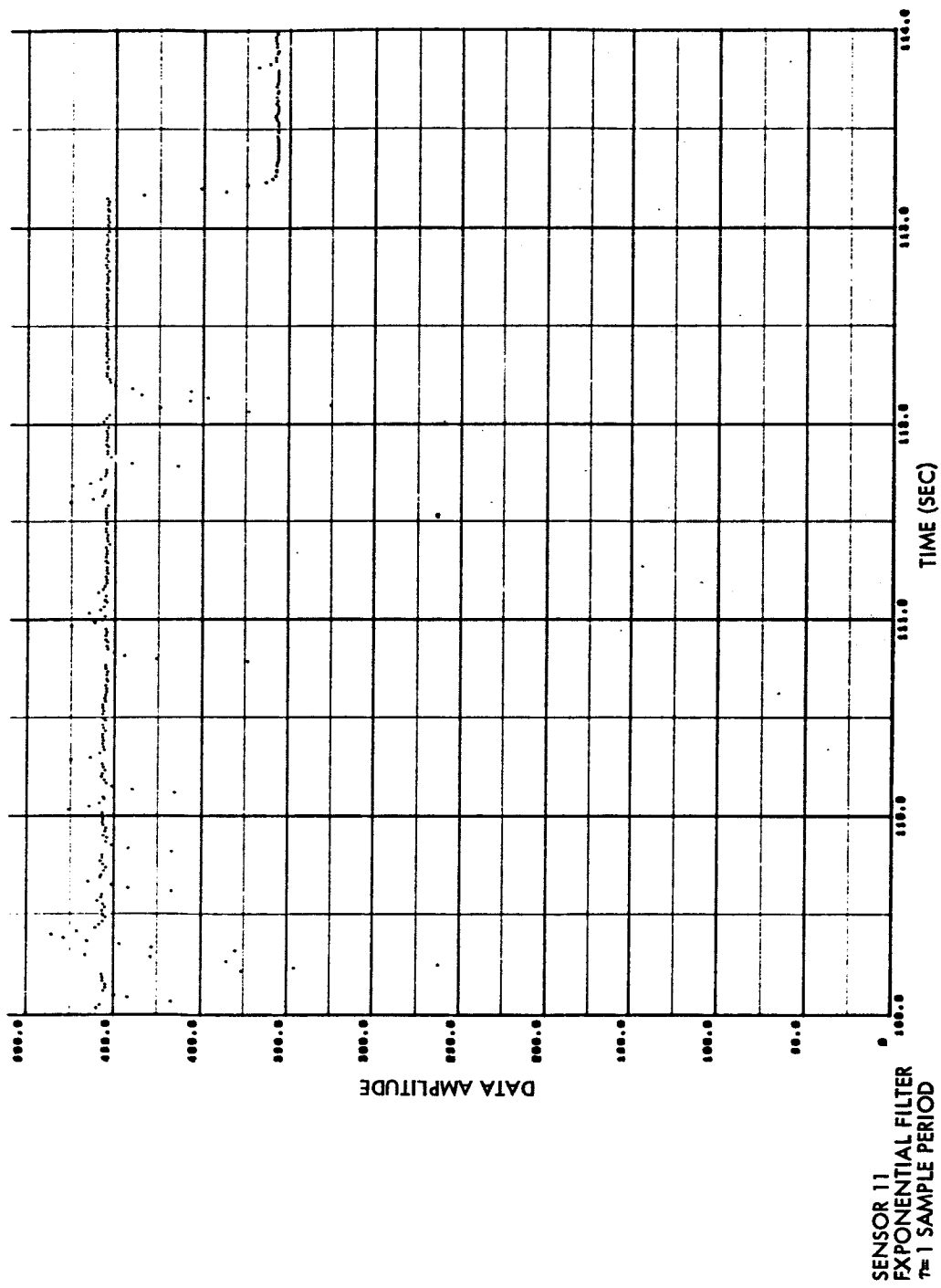


Fig. 3-17 (Cont'd) Digitally Filtered Data

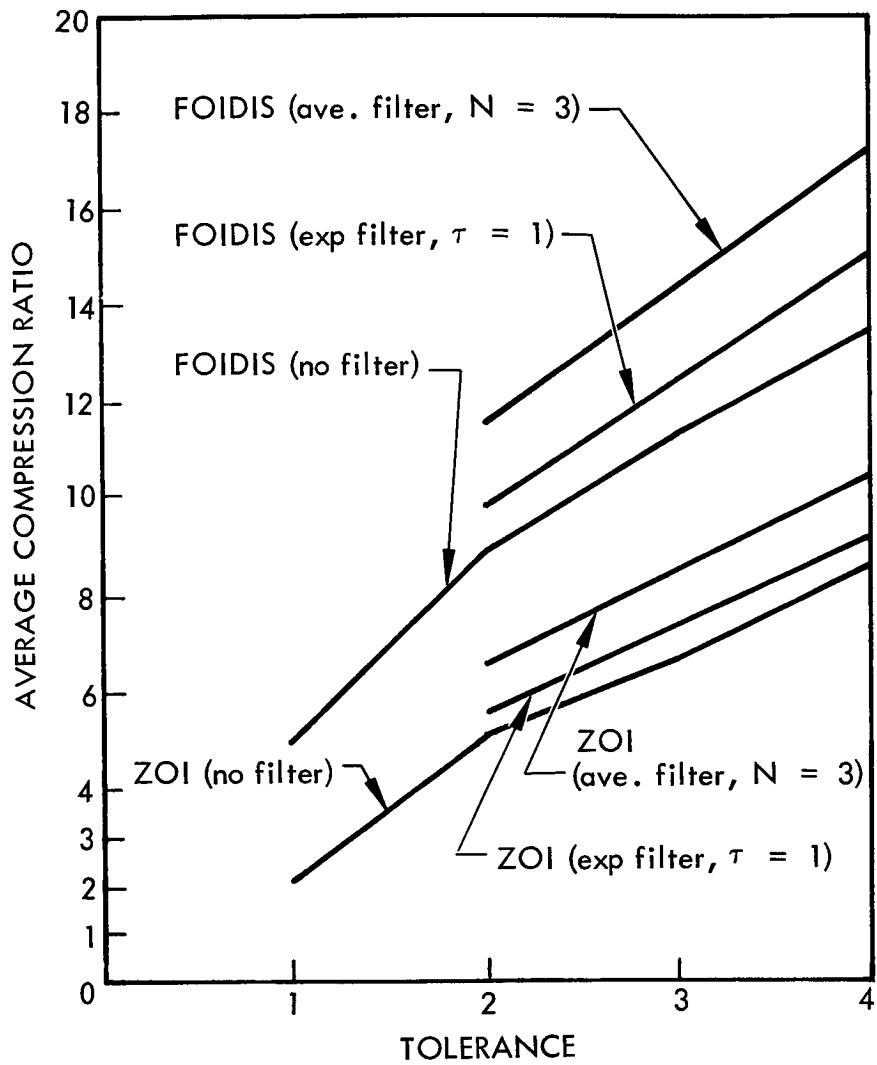


Fig. 3-18 Precompression Filtering (Sensor 9)

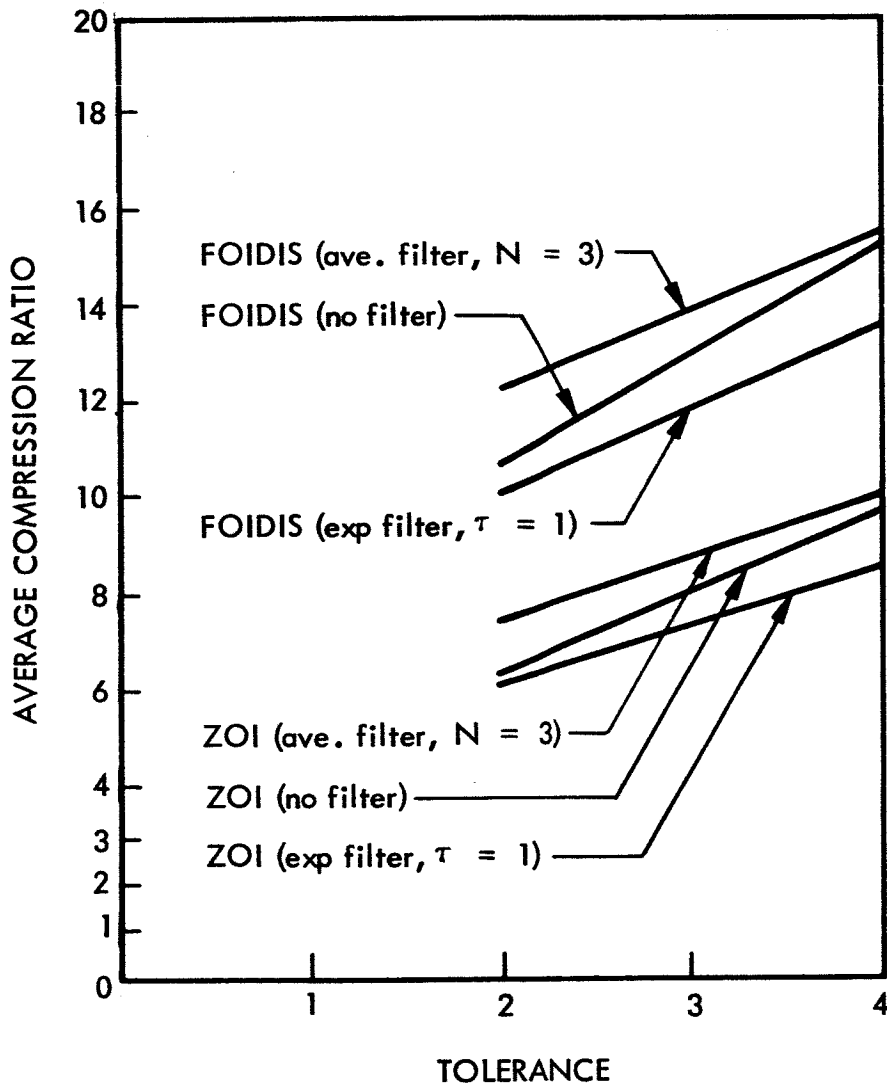


Fig. 3-19 Precompression Filtering (Sensor 10)

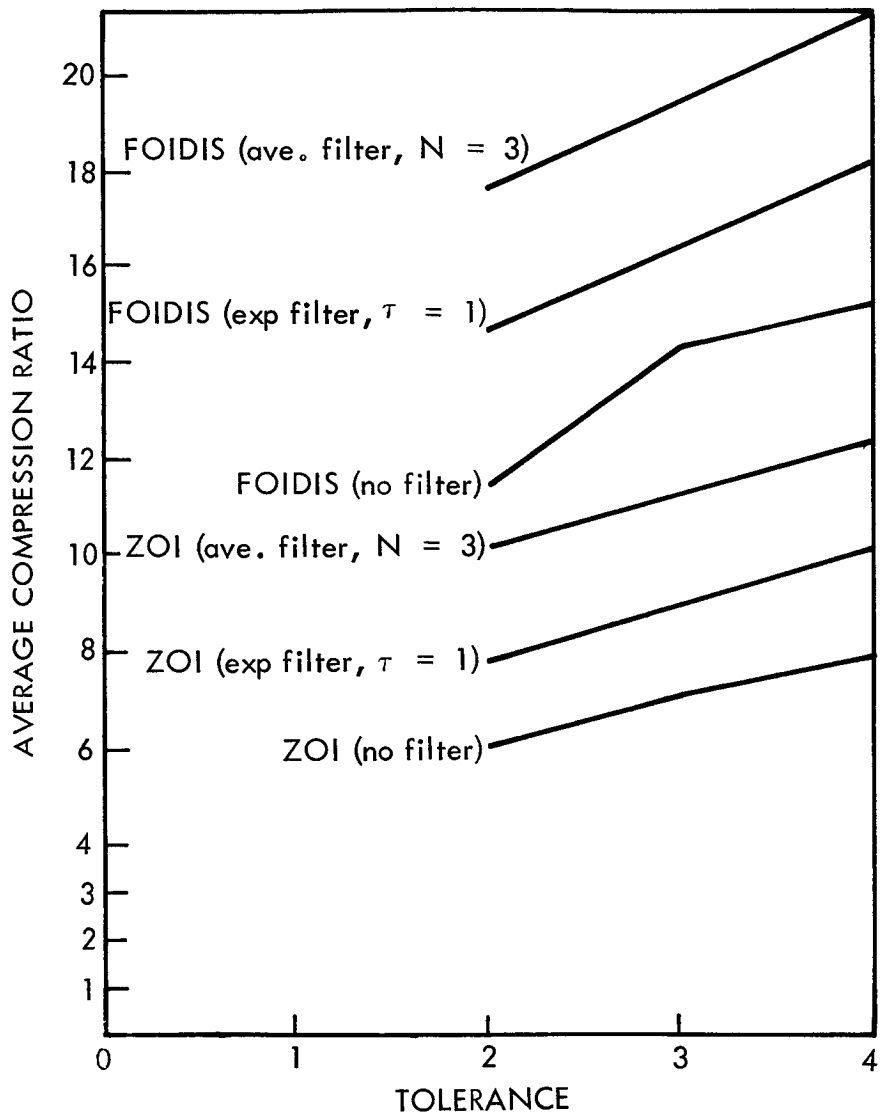
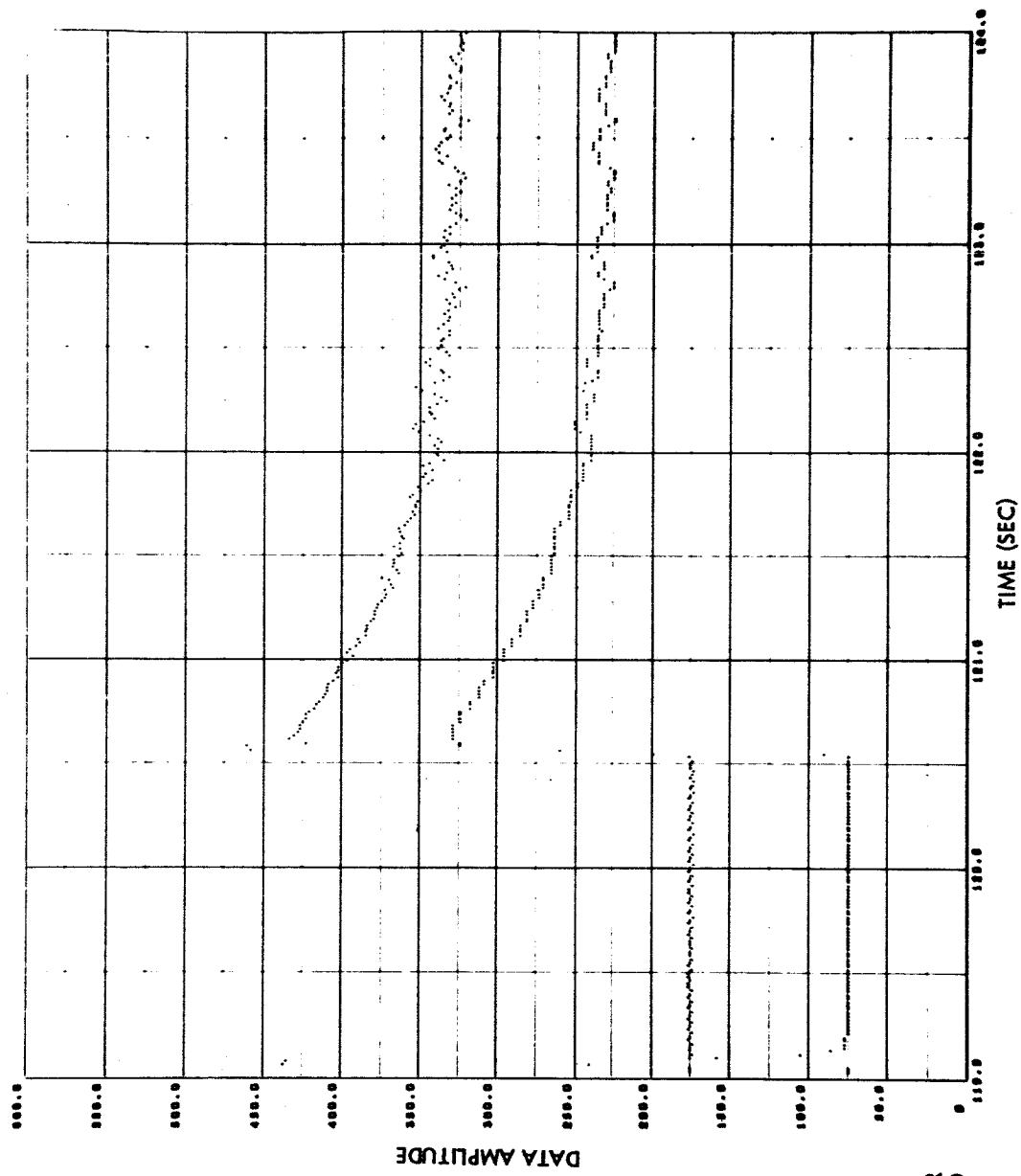


Fig. 3-20 Precompression Filtering (Sensor 11)



SENSOR 9
 EXPONENTIAL FILTER
 =1 SAMPLE PERIOD
 ZOI
 TOL = 2

Fig. 3-21 Original and Reconstructed Data Using
 Nonadaptive Precompression Filtering

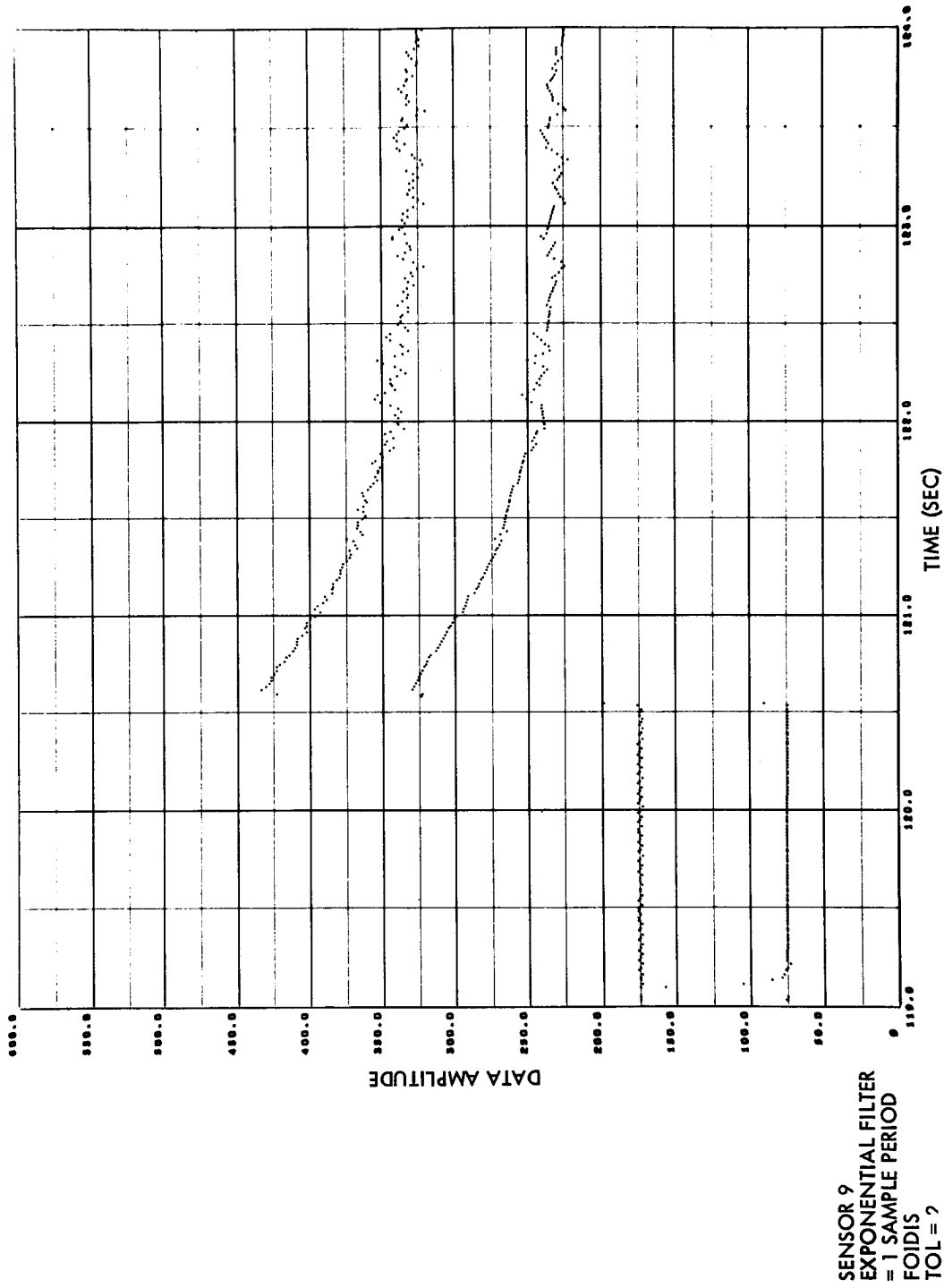


Fig. 3-21 (Cont'd) Original and Reconstructed Data
Using Nonadaptive Precompression Filtering

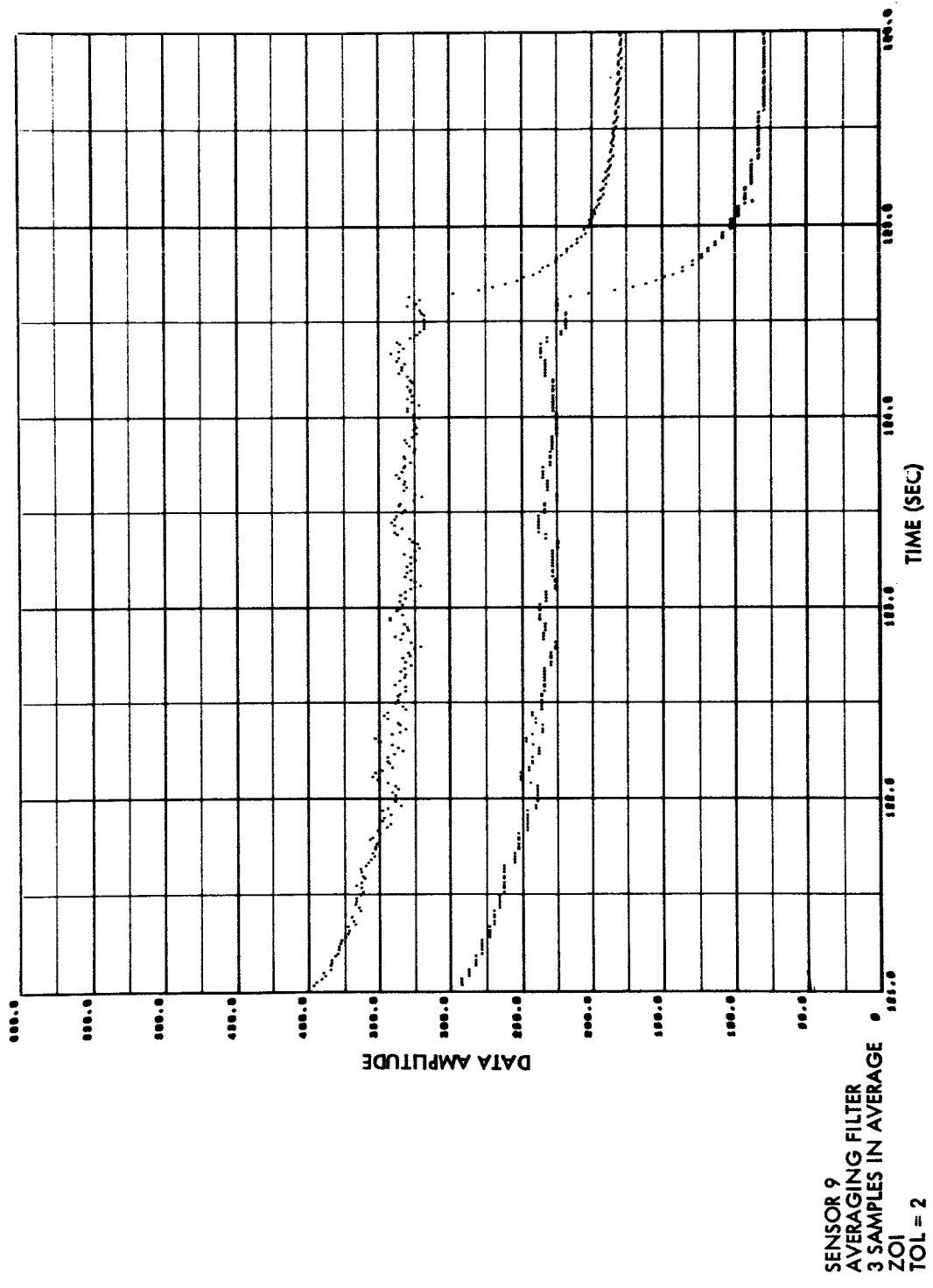


Fig. 3-21 (Cont'd) Original and Reconstructed Data
Using Nonadaptive Precompression Filtering

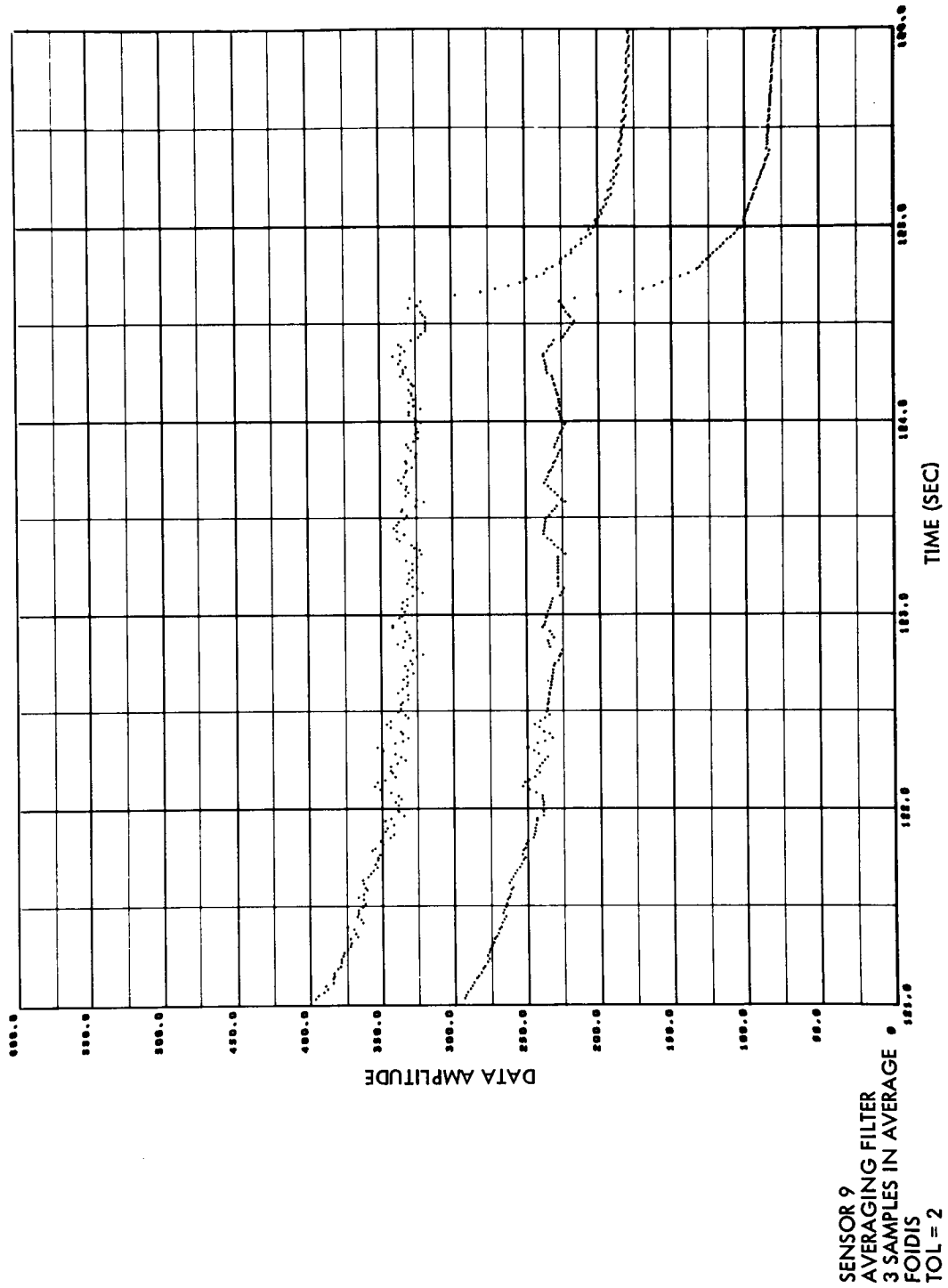


Fig. 3-21 (Cont'd) Original and Reconstructed Data Using Nonadaptive Precompression Filtering

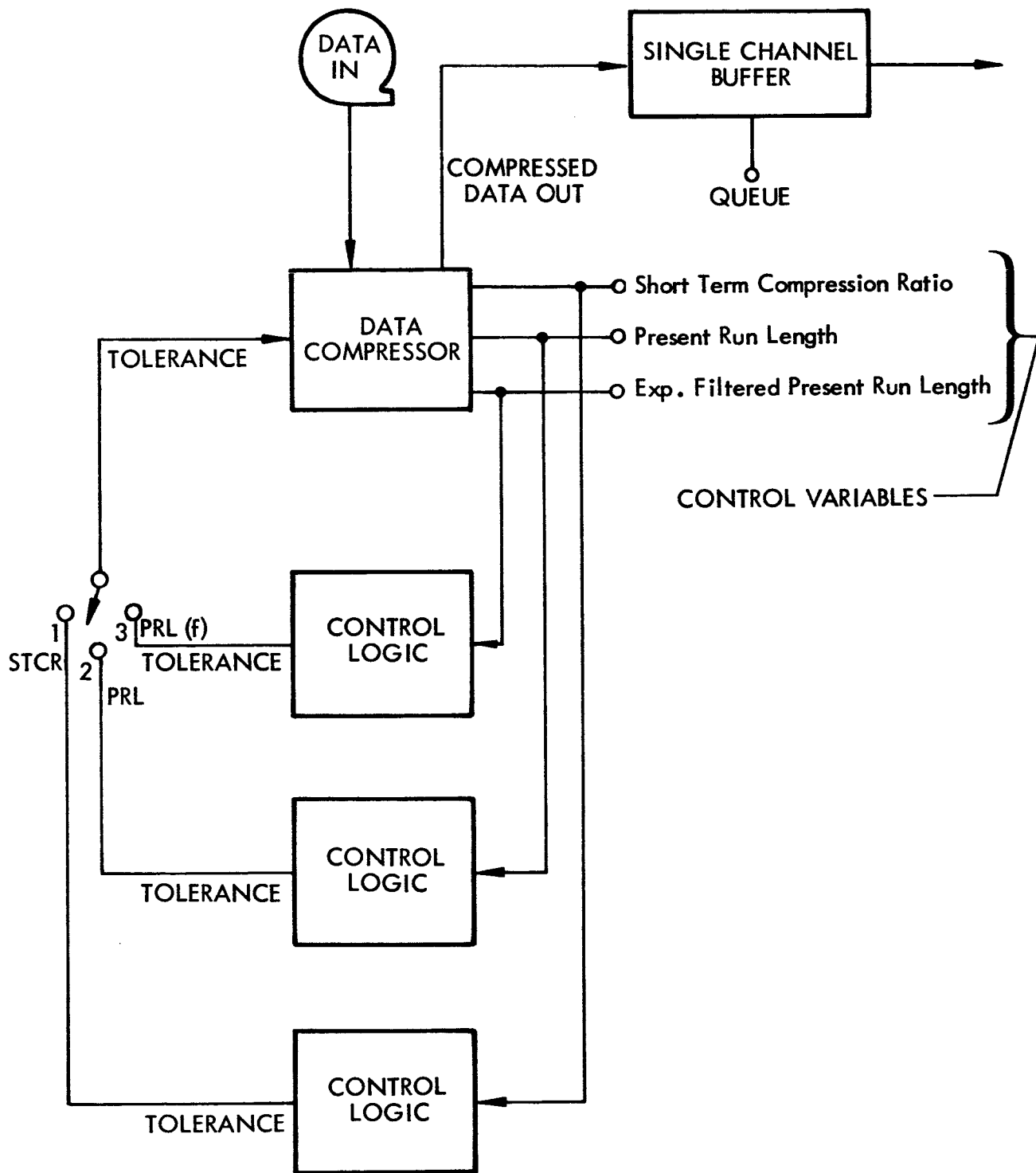


Fig. 3-22 Single Channel Data Compressor With Adaptive Aperture

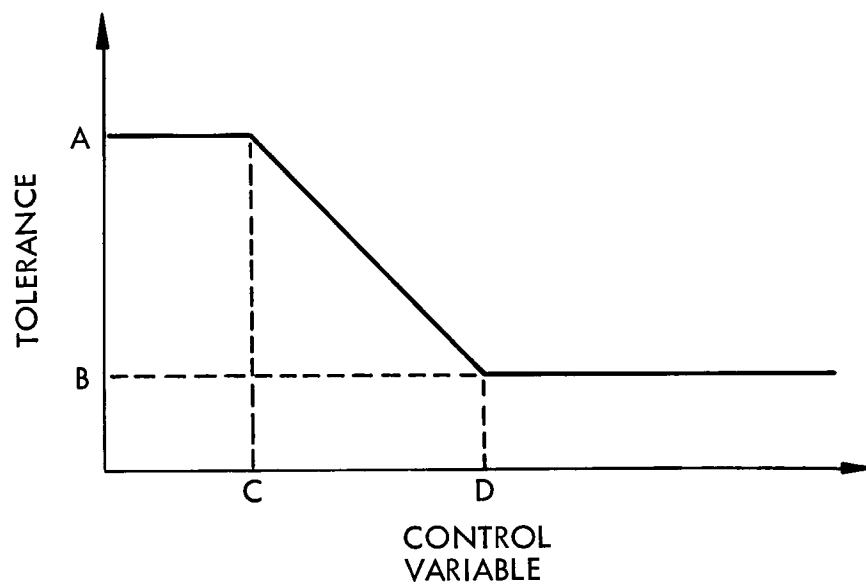


Fig. 3-23 Adaptive Aperture Control Function

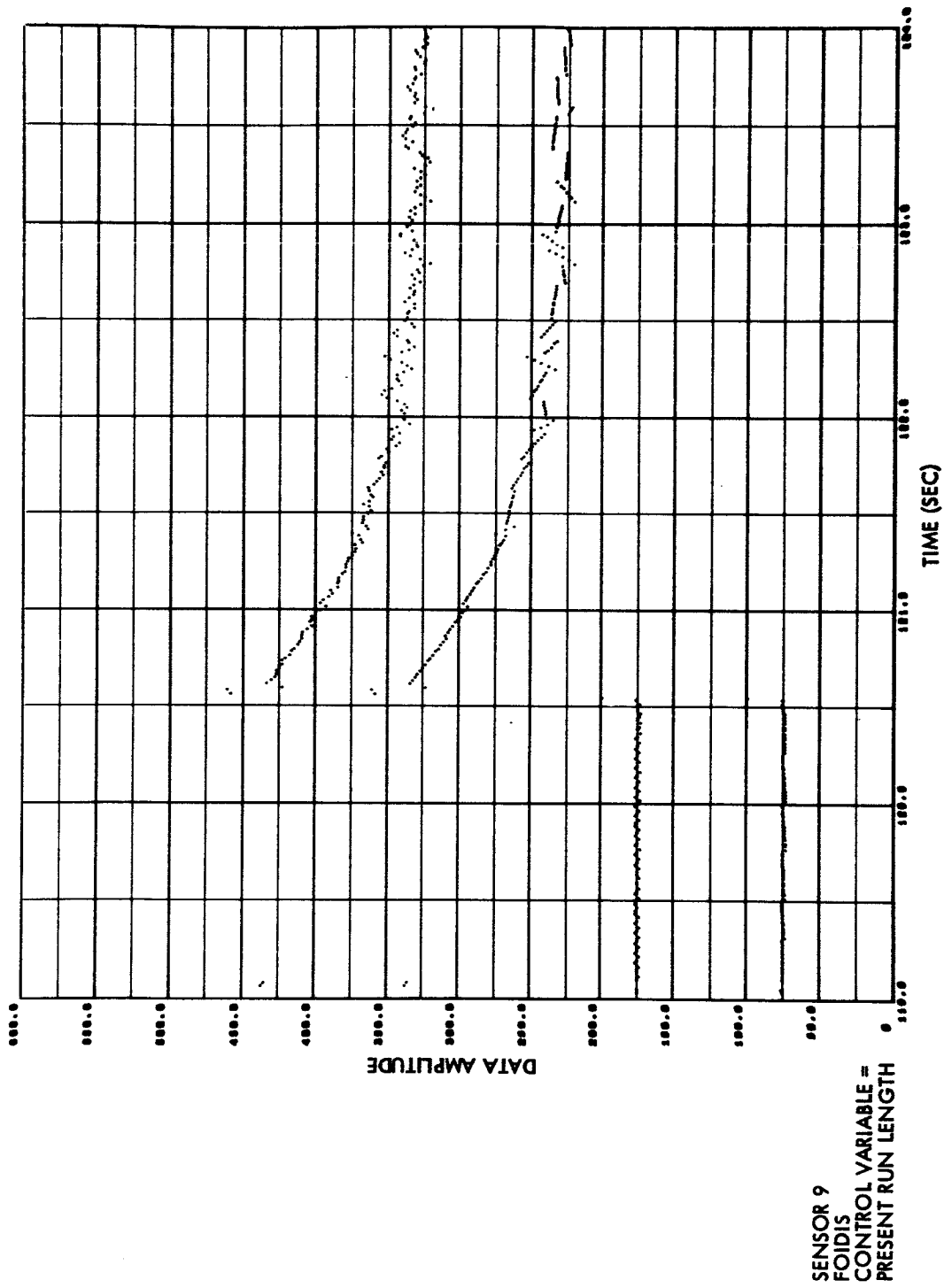


Fig. 3-24 Original and Reconstructed Data Using Adaptive Aperture

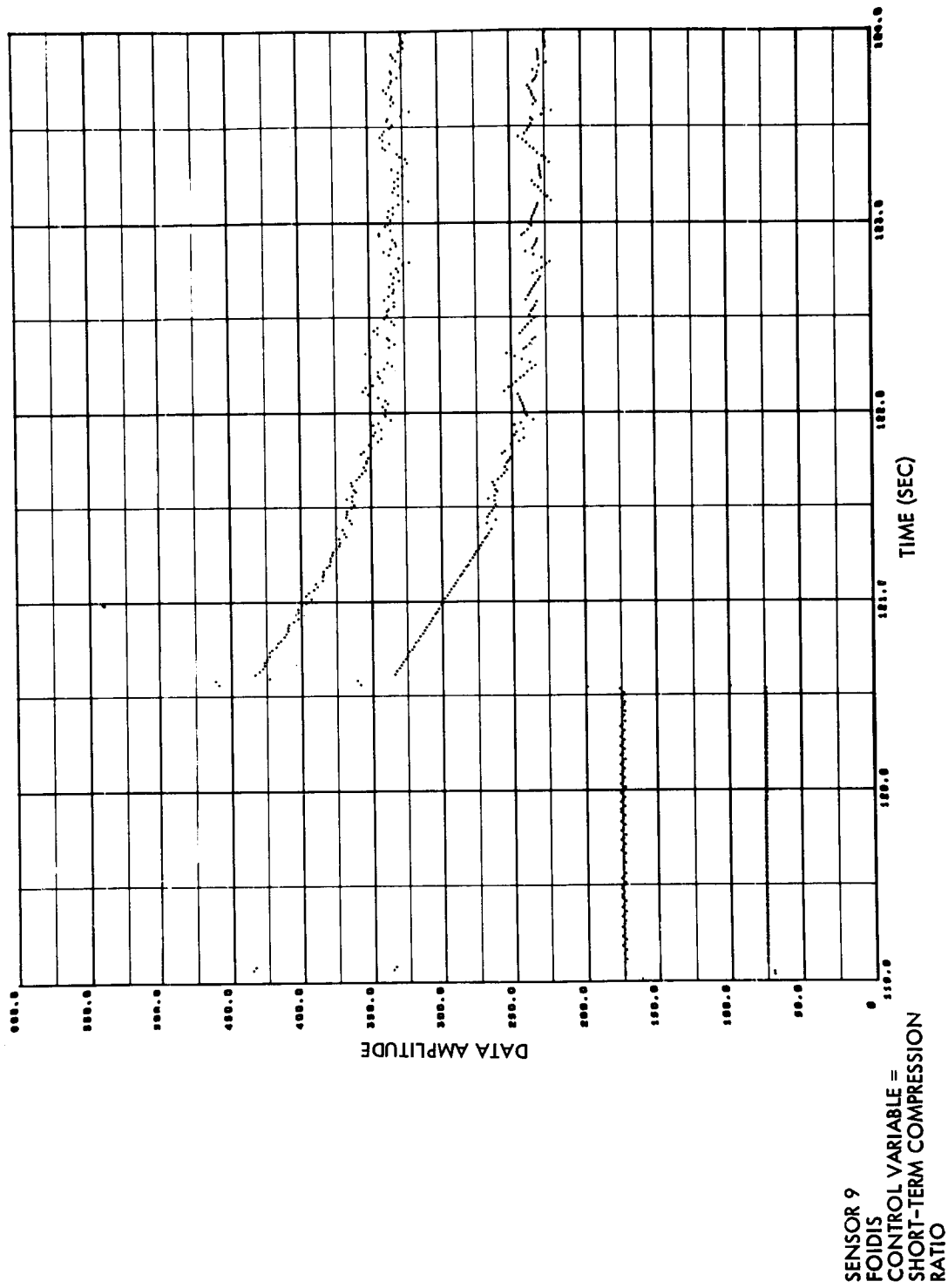


Fig. 3-24 (Cont'd) Original and Reconstructed Data Using Adaptive Aperture

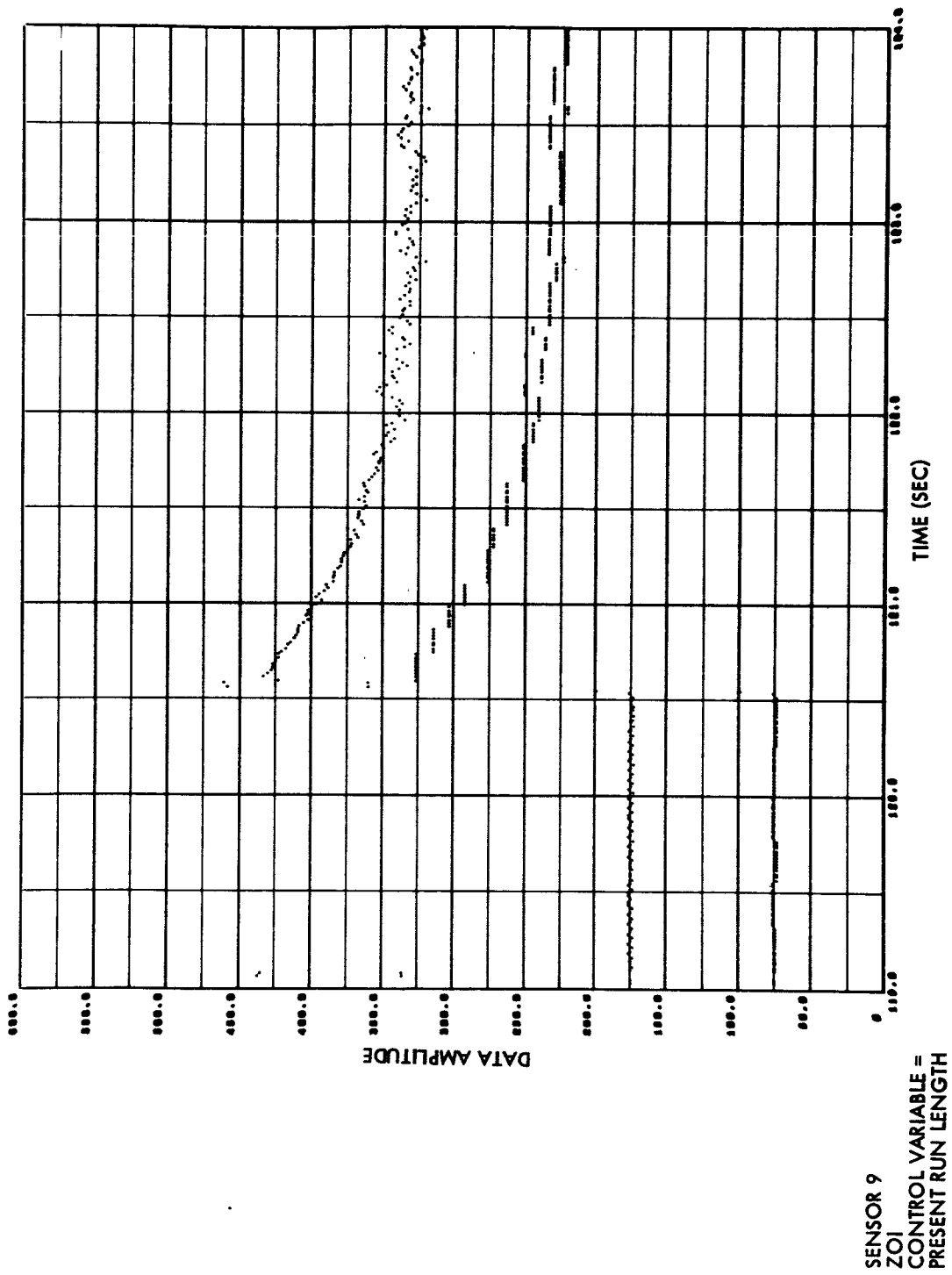


Fig. 3-24 (Cont'd) Original and Reconstructed Data Using Adaptive Aperture

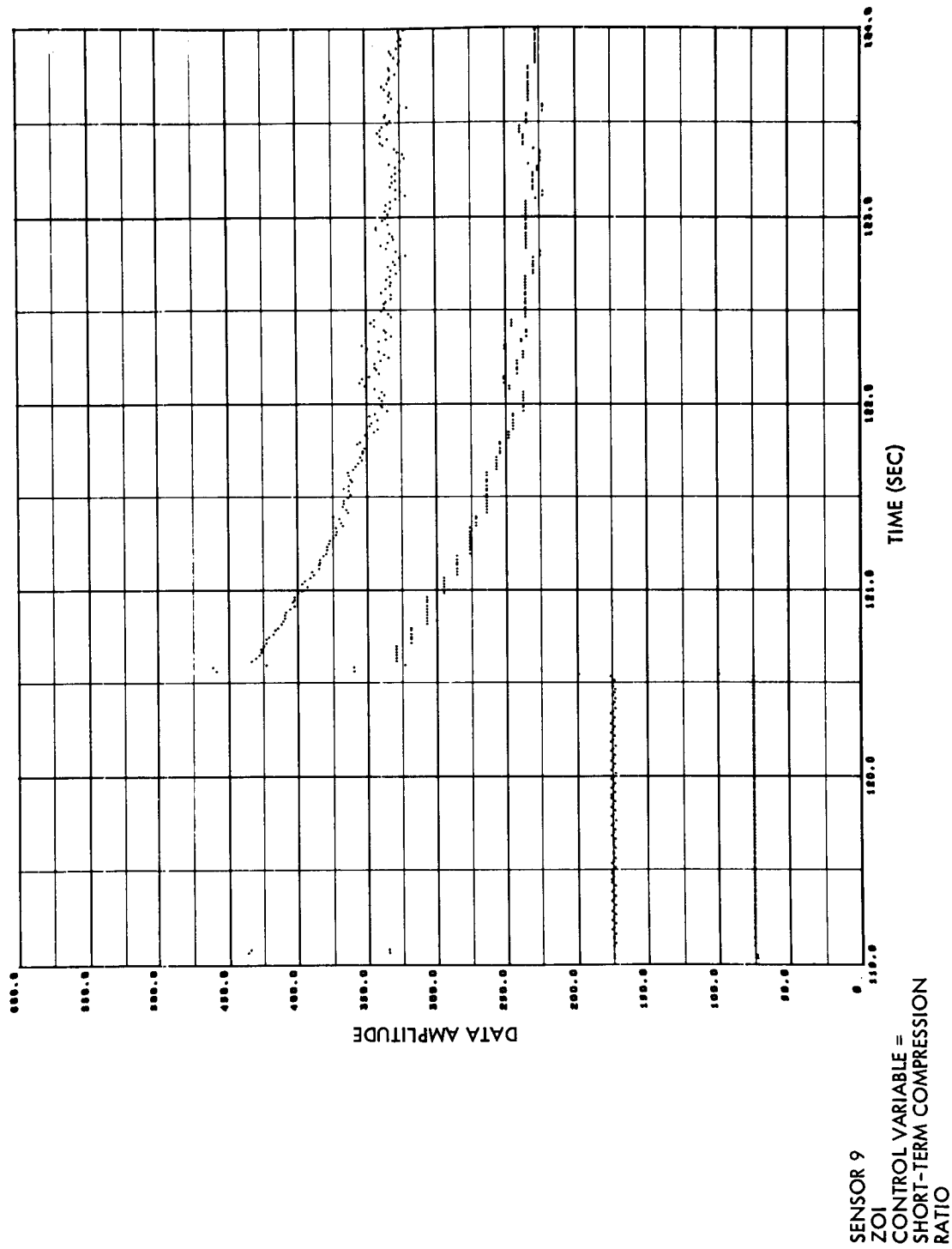


Fig. 3-24 (Cont'd) Original and Reconstructed Data Using Adaptive Aperture

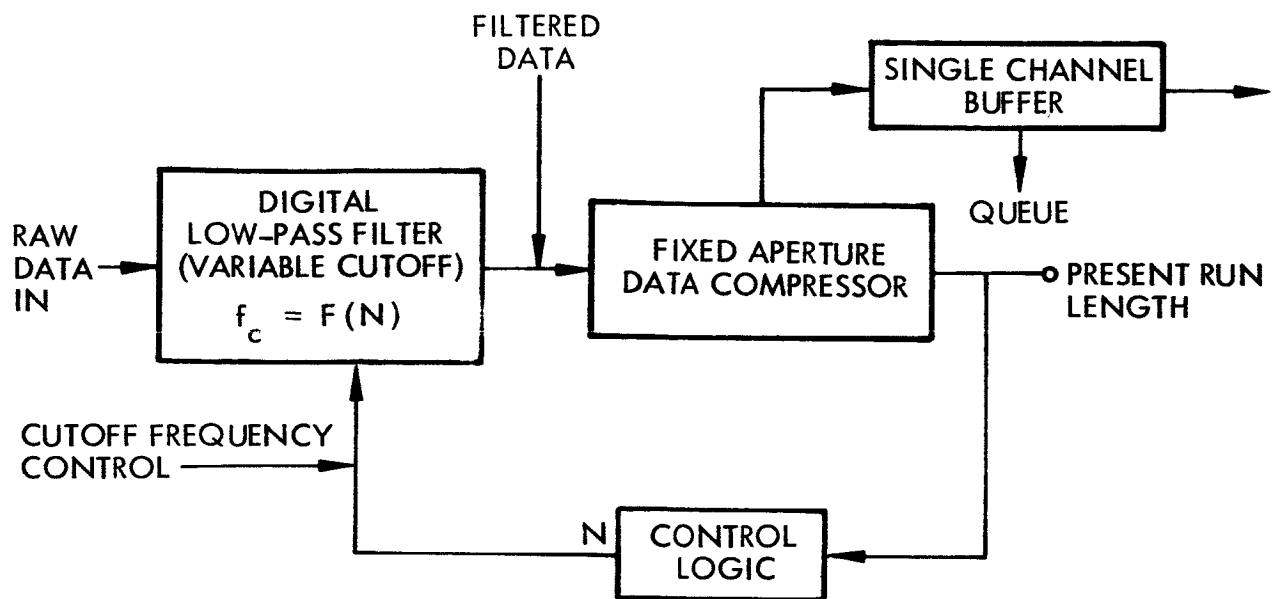


Fig. 3-25 Single Channel Data Compressor With Adaptive Precompression Filtering

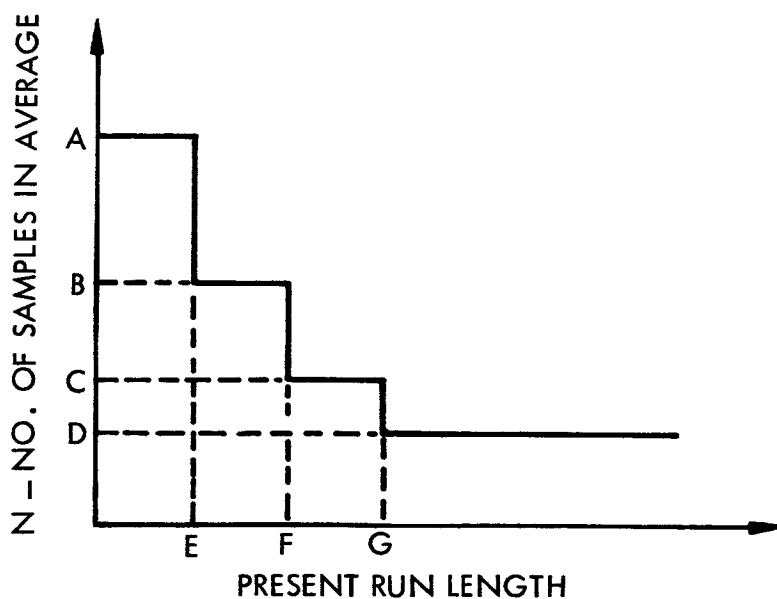


Fig. 3-26 Adaptive Precompression Filtering Control Function

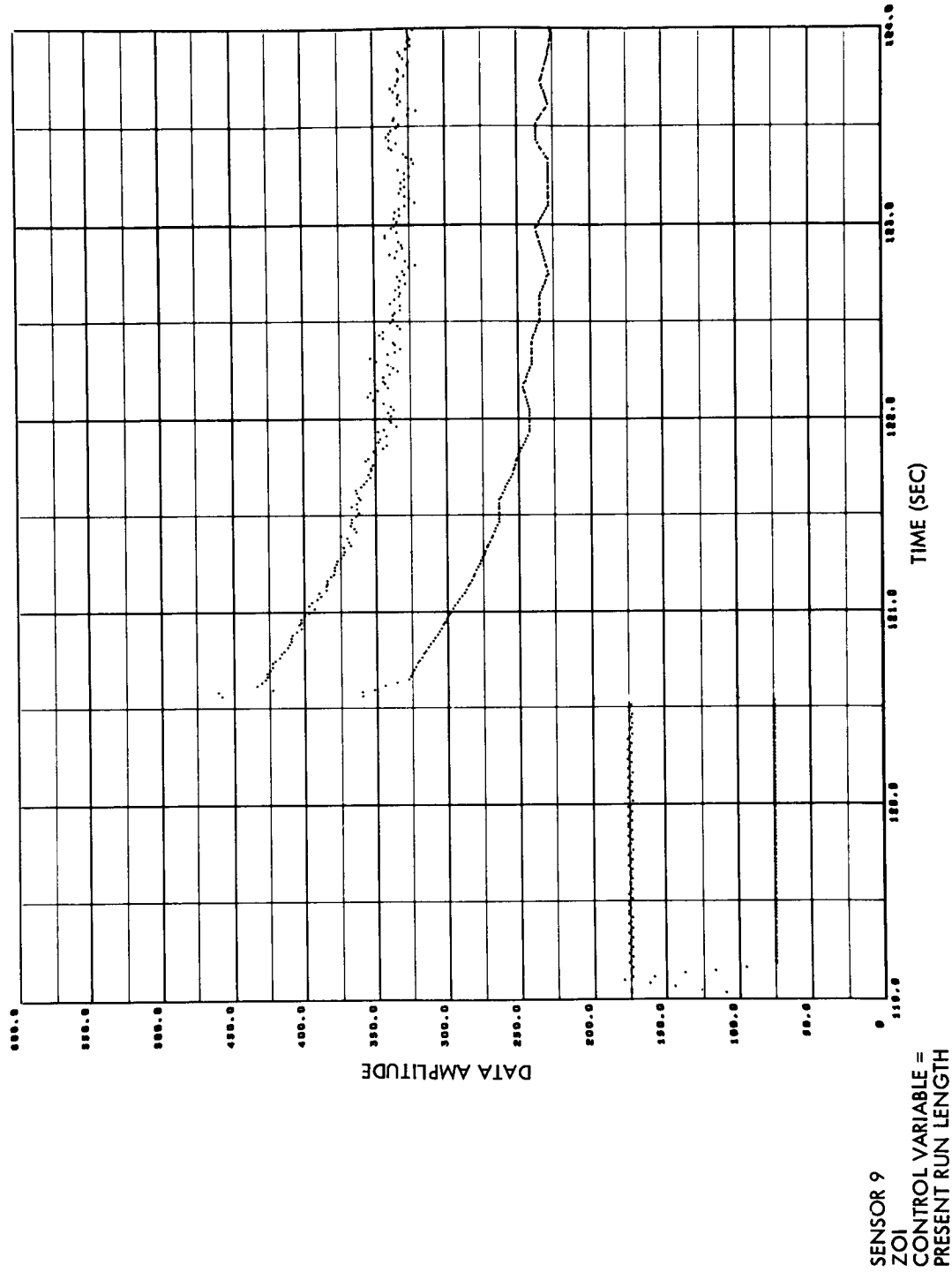


Fig. 3-27 Original and Reconstructed Data Using Adaptive Precompression Filtering

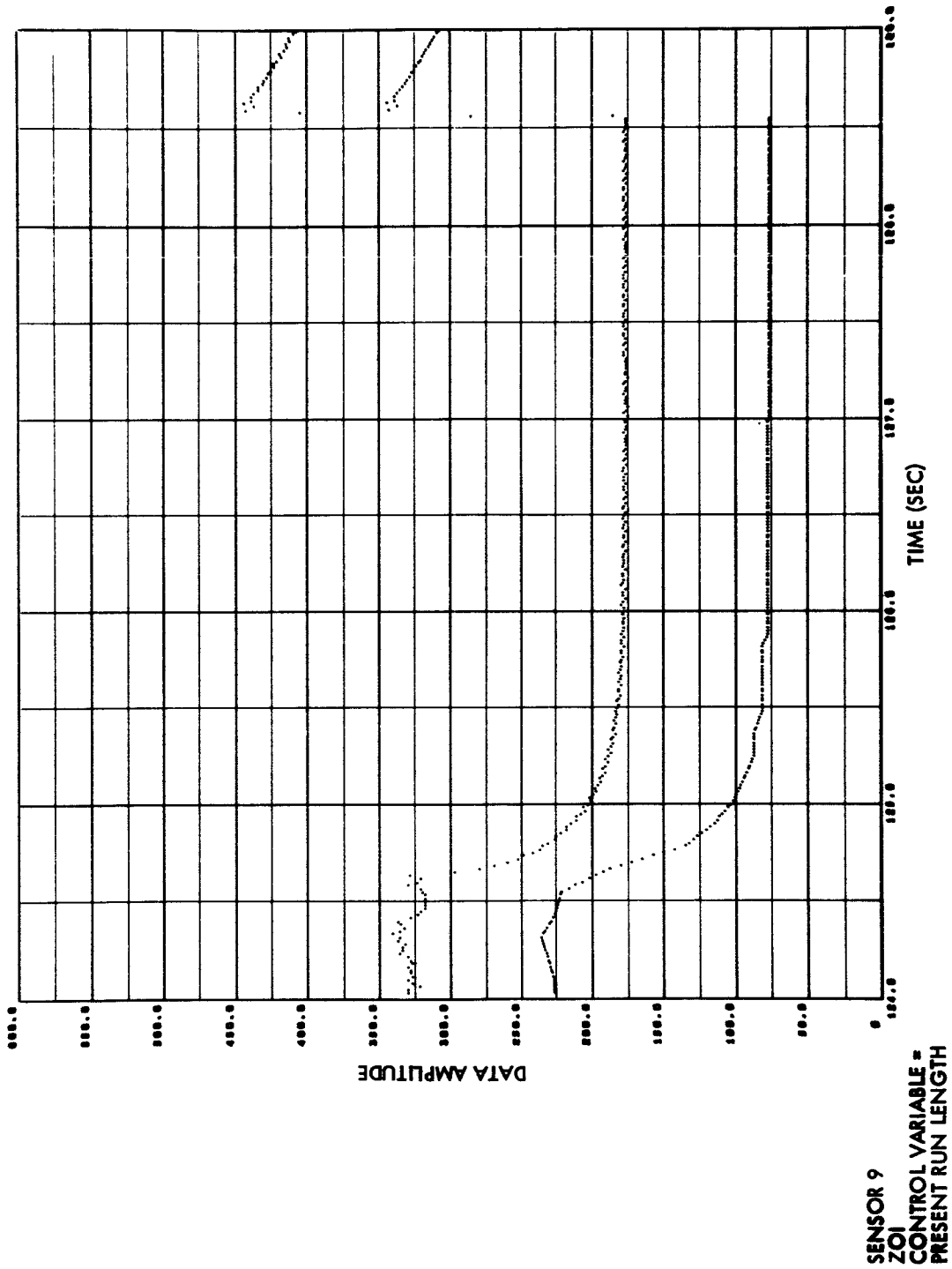


Fig. 3-27 (Cont'd) Original and Reconstructed Data Using Adaptive Precompression Filtering

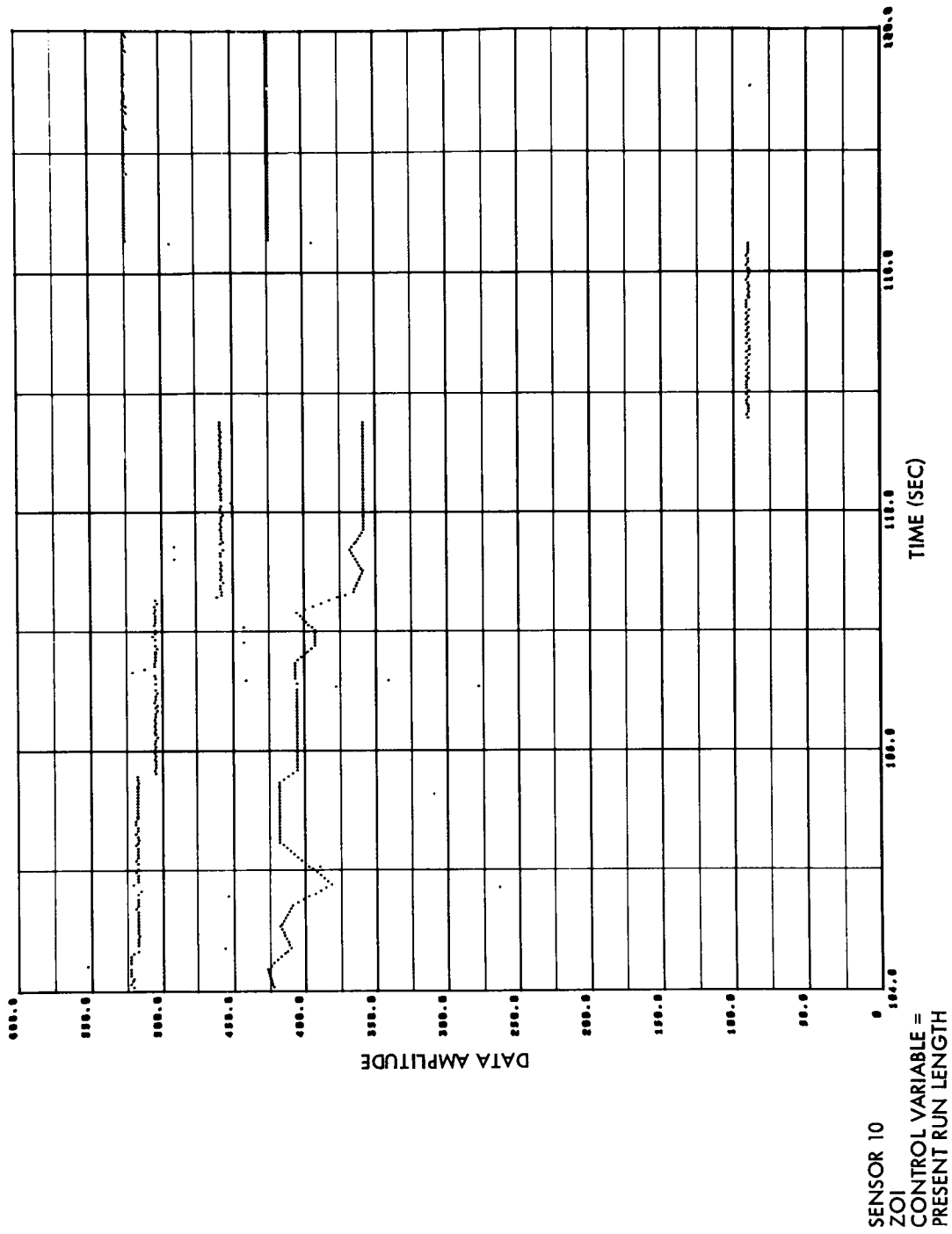


Fig. 3-27 (Cont'd) Original and Reconstructed Data
Using Adaptive Precompression Filtering

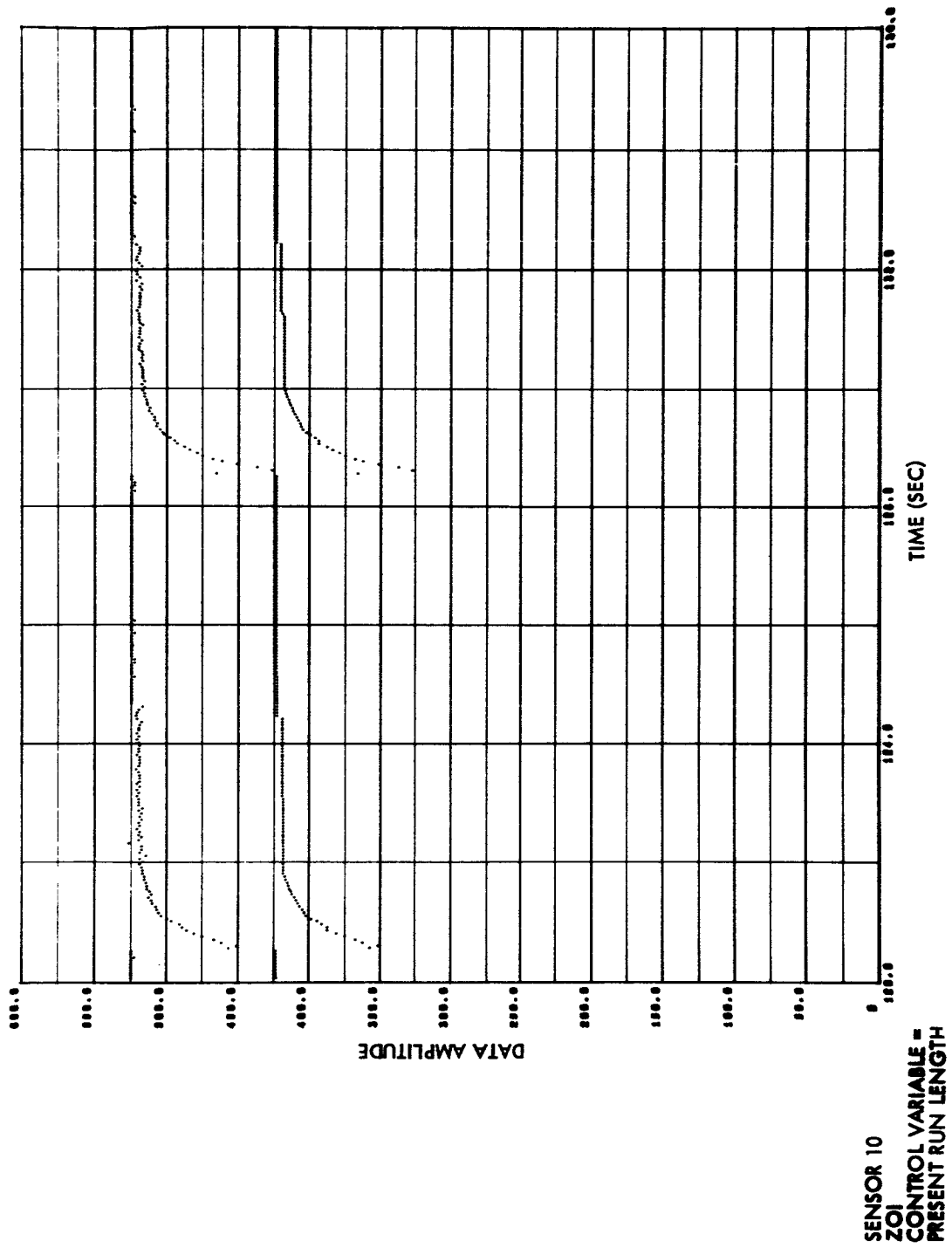


Fig. 3-27 (Cont'd) Original and Reconstructed Data
Using Adaptive Precompression Filtering

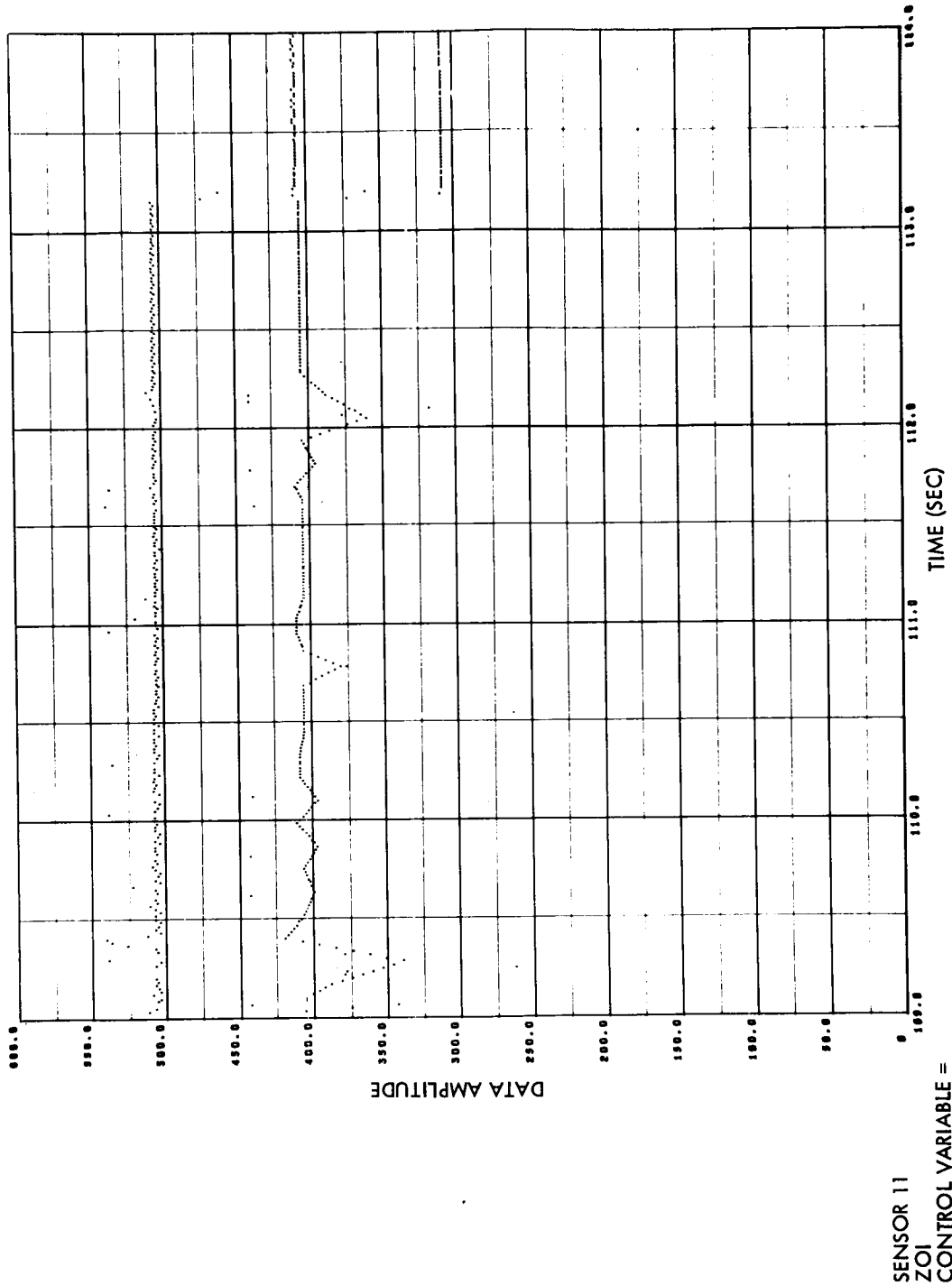


Fig. 3-27 (Cont'd) Original and Reconstructed Data
Using Adaptive Precompression Filtering

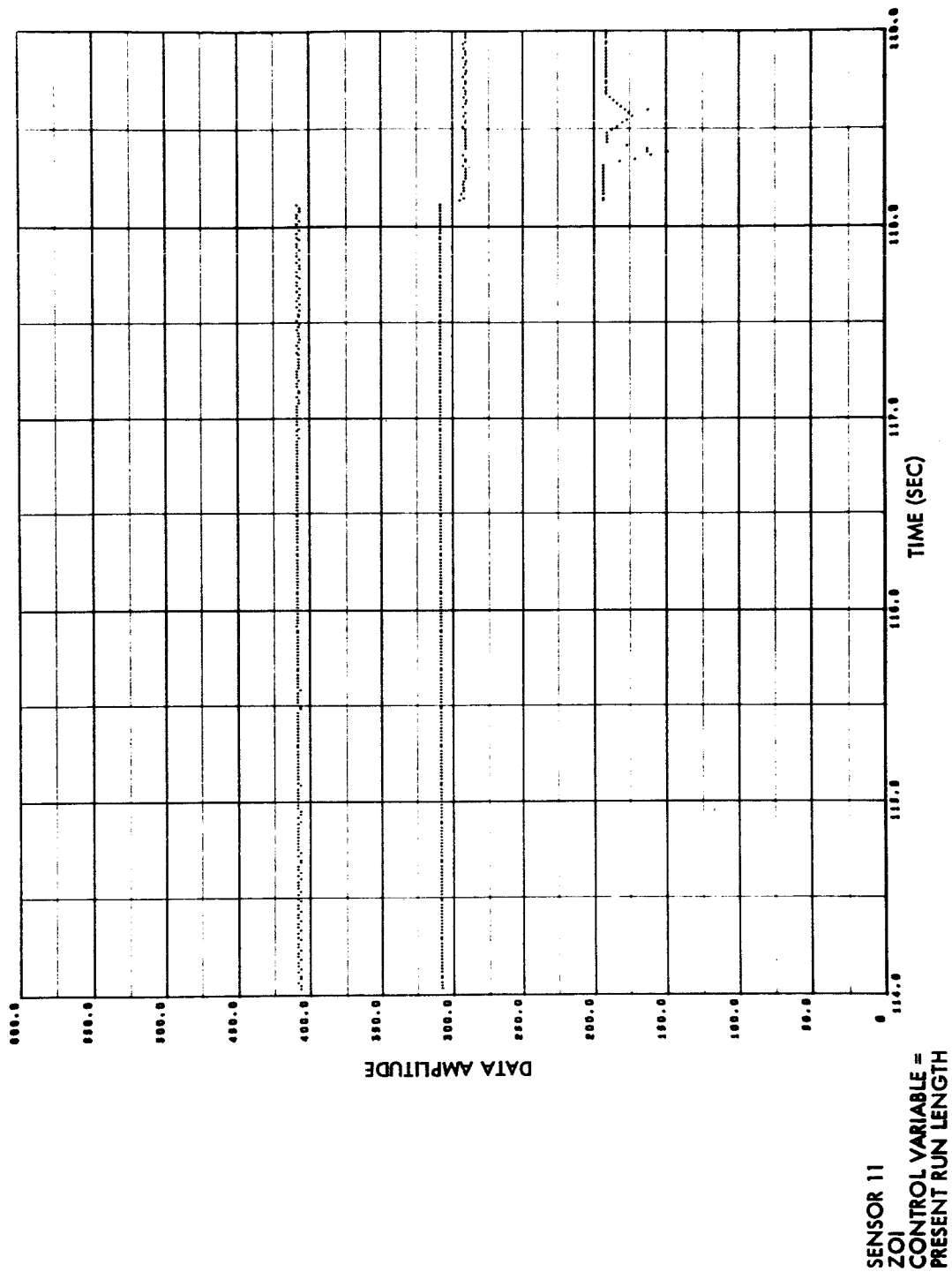


Fig. 3-27 (Cont'd) Original and Reconstructed Data
Using Adaptive Precompression Filtering

Section 4

QUEUING CONTROL EVALUATION

Section 4

QUEUING CONTROL EVALUATION

Buffer queuing control prevents data-sample loss due to buffer overflow. This buffer, placed at the outputs of redundancy reduction data compressors to temporarily store aperiodic data, overflows when its capacity is exceeded. Queuing control, however, transforms this overflow into controlled data-degradation, thus minimizing its effect on overall data quality.

A variety of system configurations can be used to control queue length. Most are basically similar, operating by monitoring a variable associated with queue length and using this information to control some parameter that affects buffer input rate. By controlling this parameter, the queuing control is able to reduce buffer input rate when the queue length starts to become excessive. This reduction follows a mathematical relationship existing between the monitored variable and the controlled parameter.

A variable closely associated with queue length is the retained sample input rate to the buffer. This sample retention rate can be controlled in several ways. The more common are by

- Varying the size of the aperture (called adaptive aperture)
- Varying the input sample rate before sample selector operation
- Passing the data through a low-pass digital filter prior to selector operation and varying the filter bandwidth
- Eliminating all data from low-priority sensors
- Using combinations of the above

Except for the work of Simpson (References 219 and 220), very little work had been done on investigating the relative effectiveness of different system configurations and feedback parameters prior to this study. This study helps fill that gap. Using Goddard Space Flight Center experimental data, this study examines queue behavior in a data compressor output buffer and investigates feedback systems and parameters for this data.

Multiplexed PCM telemetry data received from the Explorer XVII (S-6) satellite on 10 April 1963 was chosen for this study. An IBM 7094 digital computer program was used to compress the data and simulate the output buffer and its feedback queuing control. Post-compression reconstruction of data from selected sensors was made to evaluate queuing control effectiveness on the basis of reconstructed data fidelity.

4.1 SIMULATED COMPRESSION SYSTEM

Because the computer-simulated compression system was to be used as a research tool, design emphasis was placed on operating flexibility rather than maximum efficiency. As a result, the programmed system provides a choice of four sample selectors, six queuing control system configurations and can operate on multiplexed telemetry data having up to 150 sensors.

The computer simulation program did not provide for removal of multiplexer frames having excessive synchronization error. Hence, the simulated data compressor had to operate on a data tape containing frequent noisy periods of varying length and separation. During these periods, an excessive number of wild sample points appeared on all channels. This operating condition could prevail to some degree in the ground-based application of data compression since it may not be possible to remove, before compression, all frames having excessive sync error. However, in a spaceborne application, a data compressor would never have to contend with wild points caused by excessive transmission noise. It was therefore profitable to examine the operation of the simulated data compressor under both conditions, those in which excessive losses prevail, and those in which the data are free of error from noise. Fortunately a period of noise-free data sufficiently long to obtain a good statistical sample was available in the S-6 data.

4.2 DATA SELECTION

The nominal overall sample rate of the S-6 data was 900 samples per second, and, since one minor frame consisted of 45 channels, the minor frame rate was 20 frames per second. Three of the channels (17, 31 and 33) were submultiplexed with 16 positions each. Therefore 16 minor frames comprised one main frame. Each data word consisted of 9 bits. Most of the sensors were cross-strapped onto more than one channel; the data amplitude range of 0 to 511 counts was left undisturbed. Assigned sensor identification numbers, and their corresponding channel numbers, are given in Appendix II.

4.3 EXPERIMENTS, ORGANIZATION

Experiments were made to determine whether a queuing control system would be needed with the S-6 data, and if so, under what conditions and of what configuration and parameters. To do this, the following generalized test procedure was adopted:

- A nominal tolerance value was assigned to each data sensor, after consultation with GSFC experimenters.
- A sample selector was chosen from the group of four which were programmed and a representative specimen of S-6 telemetry data selected.
- Using the assigned tolerance values, an initial run was made without buffer simulation. This run determined the combined average compression ratio and, as a result, the average buffer readin rate.
- A number of buffer simulation runs were made without queuing control, using different ratios of average buffer readin rate to readout rate (designated $\bar{\rho}$), and an infinite-capacity buffer.

- Runs were then made with queuing control to establish the most desirable control system and its parameters. Criteria used were queue behavior and the quality of the reconstructed data judged on the basis of rms error and subjective evaluation of waveforms from selected sensors.

4.4 EXPERIMENTS, PROCEDURE

Tolerance values were assigned to the 57 sensors that provided the S-6 data. See Table 4-1. These are hereafter referred to as standard values of tolerance. Nineteen data compressor simulation runs were then made. These runs were divided into four test groups according to the portion of data selected for processing from the 240-second total. These groups are

- Exploratory Runs on Data Having Wild Points
- Exploratory Run on 200-Second Center Portion
- Queuing Control Runs on Data Having Wild Points
- Runs on Data Having No Wild Points

4.4.1 Test Group 1: Exploratory Runs on Data Having Wild Points

Using an arbitrarily selected 50,400-sample section of data (the 92 to 148 second portion), six computer runs were made to determine which sample selector should be used on subsequent runs and to study the queue behavior with different values of $\bar{\rho}$. See Table 4-2¹. Only the interpolators were tested in these runs because past experience has shown that the interpolators generally obtain a higher compression ratio than do the predictors. Also, available computer time was limited. The first order

¹ In order that the reader may conveniently use this information as a cross-reference while examining the computer output plots, Tables 4-2, 4-3, 4-4 and 4-5 are consolidated into a single table and placed on a fold-out page immediately following the illustrations in this section.

Table 4-1

ASSIGNED TOLERANCE VALUES FOR BUFFER QUEUING CONTROL STUDY

SENSOR	TOLERANCE, COUNTS	REMARKS	SENSOR	TOLERANCE, COUNTS	REMARKS
1	.01	Digital	31	16	Digital
2	4		32	4	
3	16		33	4	
4	4		34	8	
5	4		35	128	
6	4	36	128		
7	4	37	.01		
8	.01	38	8		
9	4	39	8		
10	4	40	32		
11	4	41	32		
12	4	42	32		
13	4	43	32		
14	4	44	16		
15	32	45	16		
16	32	46	32		
17	4	47	32		
18	4	48	8		
19	4	49	8		
20	4	50	4		
21	8	51	4		
22	4	52	4		
23	4	53	4		
24	32	54	8		
25	32	55	4		
26	4	56	4		
27	4	57	511	Spare	
28	16				
29	16				
30	16				

Table 4-2
 COMPRESSOR RUN SUMMARY, TEST GROUP 1
 (92 to 148 seconds)

RUN NUMBER	SELECTOR	$\bar{\rho}$	M	QUEUING CONTROL SYSTEM	REMARKS
S6-01	ZOI	—	—	NONE	NO BUFFER SIMULATION
S6-02	FOIDIS	—	—	NONE	NO BUFFER SIMULATION
S6-03	ZOI	0.95	261	NONE	
S6-04	FOIDIS	0.95	273	NONE	
S6-05	FOIDIS	0.90	288	NONE	
S6-06	FOIDIS	1.10	236	NONE	

Explanation of Symbols

- $\bar{\rho}$: Ratio of average buffer sample readin rate to readout rate
- M: Buffer readout rate, in samples per sec
- ZOI: Zero order interpolator, floating aperture
- FOIDIS: First order interpolator, disjoined line segment

interpolator, disjoined, selector was chosen for all runs subsequent to this test group because during these initial tests it exhibited a maximum queue higher than that obtained with the zero order interpolator and a worst case situation was desired.

Sample compression ratios given in this section for the first order interpolator, disjoined, selector are defined differently in this section than in the others. In this section it is defined in terms of two data samples per line segment, elsewhere in the report in terms of one sample per line segment. Thus, to compare the compression ratios given in this section with those in other sections, the values in this section must be doubled. In the final analysis, the important value is the bit, or bandwidth compression ratio, computed after address and time bits are included with the sample amplitude bits. It is this value on which selector comparisons are based later in the report.

4.2.2 Test Group 2: Exploratory Run on 200-Second Center Portion

The second test group consisted of one run, summarized in Table 4-3, that covered all but the first and last 20 seconds of the 240-second data file. This 180,000 sample run, made without queuing control, was done primarily to delineate from relatively

Table 4-3
COMPRESSOR RUN SUMMARY, TEST GROUP 2
(20 to 220 seconds)

RUN NUMBER	SELECTOR	$\bar{\rho}$	M	QUEUING CONTROL SYSTEM	REMARKS
S6-07	FOIDIS	0.91	288	NONE	NONE

Explanation of Symbols

$\bar{\rho}$: Ratio of average buffer sample readin rate to readout rate

M: Buffer readout rate, in samples per sec

FOIDIS: First order interpolator, disjointed line segment

quiet periods the periods of high data activity (caused mainly by excessive wild points) during which the queue tended to build up.

4.4.3 Test Group 3: Queuing Control Runs on Data Having Wild Points

The third test group, shown in Table 4-4 and consisting of five runs, concentrated on the most active 31,500-sample section of the data file. The compression-ratio-monitoring continuous queuing control system was used on the first two runs, S6-08 and S6-09. These runs differed only in the number of line segments used to compute the monitored average run length. The control curve, see Figure IV-2, was established by designating a point and a slope for each sensor. The point coordinates were (1) the standard tolerance value for that sensor, and (2) the value of average run length, recalculated after each data sample and averaged over the entire run. The slope was arbitrarily selected as -3 for most sensors; the minimum tolerance value was set to 0.01 counts. The runs used an infinite-capacity buffer.

Table 4-4

COMPRESSOR RUN SUMMARY, TEST GROUP 3
(180 to 215 seconds)

RUN NUMBER	SELECTOR	$\bar{\rho}$.	M	QUEUING CONTROL SYSTEM	REMARKS
S6-08	FOIDIS	0.97	288	CRC	$\beta_1 = -3$, $J_R = 3$ for all sensors
S6-09	FOIDIS	1.01	288	CRC	$\beta_1 = -3$, $J_R = 11$ for all sensors
S6-10	FOIDIS	0.98	288	QLC	Parameters chosen to correspond as closely as possible with S6-08
S6-11	FOIDIS	*	288	See Remarks	QLC used to simulate sample loss caused by buffer overflow, without queuing control
S6-12	FOIDIS	0.89	288	QLC	Control began at queue = 20; full-scale tolerance at queue = 100, for all sensors

*The true value of $\bar{\rho}$ was not determined for run S6-11.

Explanation of Symbols:

- $\bar{\rho}$: Ratio of average buffer sample readin rate to readout rate
- M: Buffer readout rate in samples per sec
- FOIDIS: First order interpolator, disjointed line segment
- CRC: Compression ratio monitoring, continuous (linear) control
- QLC: Queue length monitoring, continuous (linear) control
- β_1 : Slope of queuing control curve
- J_R : The number of most recent line segments, including current run, over which average run length is computed

The third run, S6-10, used the queue-length-monitoring continuous queuing control system and an infinite-capacity buffer. The control parameters for this run were chosen to correspond as closely as possible with Run S6-08. This was done by maintaining the standard tolerance values for all sensors when the queue was below 40 samples and determining the slope of the linear control curve above 40 samples by establishing a special point on the curve. See Figure IV-3. The coordinates of this point were (1) the maximum tolerance reached by each sensor in Run S6-08 and (2) the maximum queue reached in S6-08. Therefore, if the queue in S6-10 exceeded that obtained in S6-08, the maximum tolerances must also be exceeded for all sensors.

The fourth run, S6-11, was made to determine the effect on the data waveforms if a buffer of reasonable capacity were allowed to overflow without any control during the periods of excessive noise that caused the queue buildups. A buffer capacity of 100 was used.

The last run of the group, S6-12, was made to determine how large the tolerances had to become in order to maintain the queue at a value below 100 under conditions of excessive noise. The control parameters were chosen so that the tolerance reached full scale when the queue reached 100. Below a queue of 20, the standard tolerance values were used for all sensors. A buffer capacity larger than 100 was used on this run.

4.4.4 Test Group 4: Runs on Data Having No Wild Points

Test Group 4 concentrated on a 29,700-sample section of data having no wild points. This group, summarized in Table 4-5, was run to examine the queue behavior of data unaffected by transmission errors. This examination is necessary for obtaining a complete picture of spaceborne data compressor operation, for example, or of a ground based compressor operating on data from which wild points have been removed.

The first five of the seven runs in this group were made to determine the queue behavior with several different values of $\bar{\rho}$. No queuing control was used. The last two runs, S6-18 and S6-19, were made to compare the performance of the compression

Table 4-5
 COMPRESSOR RUN SUMMARY, TEST GROUP 4
 (62 to 95 seconds)

RUN NUMBER	SELECTOR	$\bar{\rho}$	M	QUEUING CONTROL SYSTEM	REMARKS
S6-13	FOIDIS	-	-	NONE	No buffer simulation
S6-14	FOIDIS	0.91	244	NONE	
S6-15	FOIDIS	0.95	233	NONE	
S6-16	FOIDIS	0.98	226	NONE	
S6-17	FOIDIS	1.50	148	NONE	
S6-18	FOIDIS	1.50	148	CRC	
S6-19	FOIDIS	1.04	148	QLC	

Explanation of symbols:

- $\bar{\rho}$: Ratio of average buffer sample readin rate to readout rate
- M: Buffer readout rate in samples per sec
- FOIDIS: First order interpolator, disjointed line segment
- CRC: Compression ratio monitoring, continuous (linear) control
- QLC: Queue length monitoring, continuous (linear) control
- β_1 : Slope of queuing control curve
- J_R : The number of most recent line segments, including current run, over which average run length is computed

ratio monitoring queuing control system with the queue length monitoring system under the special operating condition that arises when the buffer readout sample rate is set so low that $\bar{\rho}$ exceeds unity and causes a continuous queue buildup in the absence of queuing control. An infinite-capacity buffer was used. The control lines for S6-18 were established in the same manner as for S6-08 and S6-09 but a different value of J_R was used. The control lines for S6-19 were set so that the tolerance began to increase from the standard value for each sensor when the same queue reached 20, attained a value of twice the standard at a queue of 75, and thereafter continued to increase linearly with increasing queue.

4.5 RESULTS AND CONCLUSIONS

To keep the volume of the report within reasonable limits, data waveforms are given for only two of the seven minor-frame sensors for which reconstructed waveforms were obtained. Tables of rms error and compression ratio are given for all seven. The two sensors to be studied in relative detail are Sensor 9 (mass spectrometer #1 log amplifier output) and 11 (Redhead gauge #1).

4.5.1 Test Group 1: Exploratory Runs on Data Having Wild Points

4.5.1.1 Experiment 1: Comparison of Queue Behavior for Different Sample Selectors (Runs S6-03 and S6-04). This experiment compared the behavior of the buffer queue associated with two different sample selectors operating on the same section of S-6 data. The 92-148 second data period was chosen. Selectors tested were the zero-order interpolator and the first order interpolator, disjointed. An infinite-capacity buffer was used having a $\bar{\rho}$ of 0.95.

Results. Time histories of queue length in the output buffer are shown in Figure 4-1 for the 92 to 116 second portion of the two 56-second runs. Figure 4-1 shows an approximate maximum queue of 885 samples for the zero order interpolator, 1500 samples for the first order interpolator, disjointed. Because each sample represents a different number of bits for each selector, these maximum values of queue length must be converted to bits before they can be compared. For the case of the zero

order interpolator, assume that six bits are required per sample for address and time information. Thus each sample in the buffer represents 15 bits. With the first order interpolator, disjoined, the six address and time bits are required only for each line segment; hence, three address bits are required on a per sample basis and each sample in the buffer represents only 12 bits. The maximum queue for the zero order interpolator is therefore $885 \times 15 = 13,300$ bits, and the maximum queue for the first order interpolator, disjoined, is $1500 \times 12 = 18,000$ bits. Because it was considered desirable to study queuing behavior and control under worst-case conditions, the first order interpolator, disjoined, was used on all subsequent runs. (The break in the queue length curves near 103 seconds is due to an irregularity at this point in the TAD tape. The cause of this irregularity was subsequently removed from the S-6 DECOM program.)

In an effort to save graph space, a point was plotted on all queue length time histories at time intervals corresponding to nine input samples to the data compressor, or 0.01 seconds.

4.5.1.2 Experiment 2: Queue Behavior as a Function of $\bar{\rho}$ (Runs S6-04, S6-05 and S6-06). This experiment studied queue behavior with the first order interpolator, disjoined, as the ratio of average buffer sample readin rate to readout rate, $\bar{\rho}$, was varied. Values for $\bar{\rho}$ of 0.90, 0.95, and 1.10 over the period of 92-148 seconds were used by setting the buffer readout rates at values shown in Table 4-2.

Results. Time histories of queue length are shown in Figure 4-2 during the 92 to 116 second portion of the 56-second runs. A time history of the buffer input sample rate is also shown. Only the queue length curves for $\rho = 0.90$ and 1.10 are shown in this figure; the queue length time history for $\bar{\rho} = 0.95$ is shown for the first order interpolator, disjoined, in Figure 4-1. Note that the maximum queue lengths reached in an infinite-capacity buffer were approximately 1260 for $\bar{\rho} = 0.90$, 1500 for $\bar{\rho} = 0.95$, and 2160 for $\bar{\rho} = 1.10$. Because $\bar{\rho}$ exceeds unity in the last run, the total number of samples entering the buffer exceeded the total number of removal attempts, and the buffer could not be empty at the end of the run. In Run S6-06, the buffer does not empty after $t = 125$ seconds, and at the end of the run the queue length is approximately 1320.

Periods of excessive noise are indicated by the relatively high average buffer input rates shown between 95 and 114 seconds on the input rate time history of Figure 4-2. The time history of the buffer input sample rate was obtained by calculating the average input sample rate over a time interval corresponding to 45 data compressor input samples, or 0.05 seconds, at the end of each interval and plotting these values on the graph at the ends of the appropriate time intervals and joining them with straight lines. All buffer input rate time histories shown in this report were obtained in this manner.

4.5.2 Test Group 2: Exploratory Run on 200-Second Center Portion

4.5.2.1 Experiment 3: Queue and Buffer Input Statistics (Run S6-07). This experiment obtained statistics of buffer input and queue length over a large statistical sample to give maximum strength to the test results. An infinite-capacity buffer was used in this experiment.

Results. A histogram of the buffer input arrival rate over the 200-second period is shown in Figure 4-3. This histogram was constructed by dividing the available range of input sample rates into increments of 20 samples per second and counting the points on the input sample rate time history plot that fell in each increment. (All buffer input arrival rate histograms shown in the report were constructed in this manner.) A histogram of the time intervals between buffer input arrivals is shown in Figure 4-4. The width of the time interval increment is equal to one data compressor input sample period, 0.001111 second. The queue length histogram is shown in Figure 4-5. This histogram was constructed by dividing the range of queue length into increments of 10 samples, and counting the number of points on the queue length time history plot which fell into each increment.

Note that the buffer input arrival rate histogram has a rough Poisson shape and the histogram of time intervals between buffer input arrivals has a rough exponential shape. If the input statistics were purely Poisson, the queue length histogram would be exponential (Reference 175). Figure 4-5 shows that the histogram is relatively flat out to the maximum queue of approximately 1800. This characteristic is

probably due to the periods of excessive noise which occur sporadically during the course of the run and which cause a number of very high queue buildups, similar to the one shown in Figures 4- 1 and 4-2 . The exponential portion of this histogram, if one does in fact exist, is probably in its first line which covers the increment from 0 to 9 samples.

4.5.3 Test Group 3: Queuing Control Runs on Data Having Many Wild Points

The 35-second 180 to 215 second portion of the 200-second run was used for this test group. It was picked because it contained the highest value of queue reached throughout the entire 200-second run. See Figure 4-5 .

4.5.3.1 Experiment 4: Comparison of Long-Term and Short-Term Run Length Averages (Runs S6-08 and S6-09). An important parameter in the compression ratio monitoring queuing control system is J_R which is defined as the number of most recent line segments, including the current segment, over which the monitored average run length is computed for each sensor. In this experiment, a relatively short-term average run length ($J_R = 3$ for all sensors) was compared with a relatively long term average run length ($J_R = 11$ for all sensors). All other control parameters were the same for each computer run. The experiment tested the performance of the control system using both values of J_R in terms of maximum queue length attained in an infinite-capacity buffer, and reconstructed data fidelity. It also determined the efficiency with which the maximum queue is reduced under noisy conditions when relatively strong feedback, which materially reduces the fidelity of the data, is used. In this case, $\beta_1 = 0$ for sensors 1, 8, 37 and 57 and -3 for all others.

Results. Queue length and input rate time histories are shown in Figure 4- 6 for a portion of the run without queuing control. The buffer readout rate of 288 samples per second corresponds to $\bar{\rho} = 0.91$ over the period of 20 - 220 seconds. As shown in the input rate time history, the periods of excessive noise are between 181 and 192 seconds and between 206 and 210 seconds.

Queue length and input rate time histories are shown on the same data section in Figures 4-7 and 4-8. In both cases the buffer readout rate is 288 samples per second and the queuing control is by compression ratio monitoring. In Figure 4-7 $J_R = 3$; in Figure 4-8 $J_R = 11$. It can be seen from Figures 4-6, 4-7 and 4-8 that the information of compression ratio monitoring queuing control reduces the maximum queue from approximately 1800 without queuing control to 685 for $J_R = 3$ and to 825 for $J_R = 11$.

Time histories of the original and reconstructed Sensor 9 data and the reconstructed data error taken from a portion of Run S6-08 ($J_R = 3$) are shown in Figure 4-9a. Figure 4-9b. shows the corresponding time history of the tolerance. Sensor 9 data and tolerance time histories are shown for a portion of Run S6-09 ($J_R = 11$) in Figures 4-10a and 4-10b, respectively. For comparison, Figure 4-11 shows the same portion of the Sensor 9 reconstructed waveform from Run S6-07 for a standard tolerance of 4 counts and no queuing control. Error histograms are shown for S6-08, S6-09, and the case without queuing control in Figures 4-12, 4-13 and 4-14, respectively.

Time histories of the original and reconstructed Sensor 11 data and the reconstructed data error taken from a portion of Run S6-08 are shown in Figure 4-15a. Figure 4-15b shows the corresponding time history of the tolerance. Sensor 11 data and tolerance time histories are shown for a portion of Run S6-09 in Figures 4-16a and 4-16b, respectively. For comparison, Figure 4-17 shows the same portion of the Sensor 11 reconstructed waveform from Run S6-07 for a standard tolerance of 4 counts and no queuing control. Error histograms are shown for S6-08, S6-09, and the case without queuing control in Figures 4-18, 4-19 and 4-20, respectively.

The rms errors and average compression ratios obtained for Sensors 9 and 11, as well as for five other minor frame sensors, are shown in Table 4-6. A comparison of rms errors obtained for the seven minor frame sensors in Runs S6-08 ($J_R = 3$) and S6-09 ($J_R = 11$) can easily be made from the bar graph in Figure 4-21.

Table 4-6

COMBINED RESULTS BY INDIVIDUAL SENSOR-TEST GROUPS 2 AND 3

SENSOR	RUN	QUEUING CONTROL SYSTEM	J _R	MAXIMUM TOLERANCE COUNTS	RMS ERROR, COUNTS	ERROR MEAS INTERVAL SEC	N̄**	N̄ MEAS INTERVAL SEC
2	S6-07	NONE	-	4.0	1.25	200-212	1.76	20-220
	S6-08	CRC	3	7.4	1.54	205-210	1.65	180-215
	S6-09	CRC	11	7.7	1.46	205-210	1.64	180-215
	S6-10	QLC	-	7.6	1.66	205-210	1.70	180-215
	S6-11	Ovfl. sim.	-	-	99.61	205-210	*	180-215
	S6-12	QLC	-	185.5	37.18	205-210	1.91	180-215
3	S6-07	NONE	-	16.0	6.40	180-215	3.44	20-220
	S6-08	CRC	3	27.4	7.44	185-210	3.33	180-215
	S6-09	CRC	11	25.8	7.07	185-210	3.33	180-215
	S6-10	QLC	-	28.1	8.36	185-210	3.46	180-215
	S6-11	Ovfl. sim.	-	-	52.82	185-210	*	180-215
	S6-12	QLC	-	193.2	23.20	185-210	3.92	180-215
6	S6-07	NONE	-	4.0	1.98	180-215	4.31	20-220
	S6-08	CRC	3	15.6	2.78	194-210	3.51	180-215
	S6-09	CRC	11	16.2	3.03	194-210	3.52	180-215
	S6-10	QLC	-	16.3	3.57	194-210	3.76	180-215
	S6-11	Ovfl. sim.	-	-	39.74	194-210	*	180-215
	S6-12	QLC	-	179.3	19.44	194-210	4.46	180-215
7	S6-07	NONE	-	4.0	1.39	180-215	2.29	20-220
	S6-08	CRC	3	9.3	2.11	194-210	2.03	180-215
	S6-09	CRC	11	9.7	1.71	194-210	2.03	180-215
	S6-10	QLC	-	9.7	1.76	194-210	2.07	180-215
	S6-11	Ovfl. sim.	-	-	59.23	194-210	*	180-215
	S6-12	QLC	-	185.5	19.78	194-210	2.31	180-215
9	S6-07	NONE	-	4.0	1.78	180-215	6.72	20-220
	S6-08	CRC	3	39.1	7.65	194-210	7.07	180-215
	S6-09	CRC	11	33.7	5.61	194-210	6.71	180-215
	S6-10	QLC	-	41.4	4.82	194-210	6.98	180-215
	S6-11	Ovfl. sim.	-	-	56.08	194-210	*	180-215
	S6-12	QLC	-	179.3	18.83	194-210	6.16	180-215
10	S6-07	NONE	-	4.0	1.56	180-215	6.81	20-220
	S6-08	CRC	3	29.8	6.64	180-215	5.98	180-215
	S6-09	CRC	11	26.9	4.77	180-215	5.60	180-215
	S6-10	QLC	-	31.4	6.55	180-215	6.31	180-215
	S6-11	Ovfl. sim.	-	-	36.76	180-215	*	180-215
	S6-12	QLC	-	166.8	17.15	180-215	6.93	180-215
11	S6-07	NONE	-	4.0	2.06	180-215	3.51	20-220
	S6-08	CRC	3	20.3	5.21	194-210	3.58	180-215
	S6-09	CRC	11	16.9	3.88	194-210	3.29	180-215
	S6-10	QLC	-	21.3	4.25	194-210	3.18	180-215
	S6-11	Ovfl. sim.	-	-	43.19	194-210	*	180-215
	S6-12	QLC	-	179.3	18.92	194-210	3.34	180-215

*The true values of N̄ were not determined for run S6-11

**N̄ = Maximum average compression ratio

These results indicate that while the smaller value of J_R yields a lower maximum queue (685 for $J_R = 3$, against 825 for $J_R = 11$), almost without exception the reconstructed data fidelity is worse with the smaller J_R . This decrease in fidelity is manifested in the higher rms error for all but one of the sensors, obtained from Run S6-08, compared with Run S6-09. This can also be seen by comparing corresponding data time histories for $J_R = 3$ and $J_R = 11$. Thus, under noisy conditions and all other control parameters equal, the lower value of J_R yielded more severe queuing control which resulted in a smaller maximum queue. The cost was a generally lower reconstructed data fidelity.

It should be noted that even when relatively strong feedback is used, the control system using compression ratio monitoring did not reduce the queue in either run to what would be considered a reasonable value, e. g., under 200. Hence, it can be tentatively concluded that such a buffer control system cannot cope with the S-6 data under conditions of severe transmission noise.

4.5.3.2 Experiment 5: Comparison of Queue Length and Average Run Length as Monitored Parameters (Runs S6-08, S6-10). This experiment compared the performance of the queue length monitoring control system with that of the compression ratio monitoring system under severe noise conditions. The control parameters were chosen for the run using queue length monitoring (S6-10) in the manner discussed in the previous section so that a direct comparison could be made between the two monitoring methods.

Results. Queue length and input rate time histories are shown for Run S6-10 in Figure 4-22. The buffer readout rate was again set to 288 samples per second for this run. It is seen from Figure 4-22 that the maximum queue is approximately 730, which is slightly higher than in S6-08 where the maximum queue was 685. Therefore, the maximum values of tolerance for all sensors were higher for Run S6-10 than in Run S6-08. The maximum tolerances, shown for seven of the sensors in Table 4-6, bears this out.

Time histories of the original and reconstructed data and of the reconstructed data error for Run S6-10 are shown for Sensor 9 in Figure 4-23a. Figure 4-23b shows the corresponding time history of the tolerance and Figure 4-24 the error histogram. Data time histories for Sensor 11 are shown in Figure 4-25a. Figure 4-25b shows the corresponding tolerance time history and Figure 4-26 the error histogram. Rms errors and individual-sensor average compression ratios are shown for seven sensors in Table 4-6 .

Comparing Figure 4-23a with Figure 4-9a for Sensor 9 and Figure 4-25a with Figure 4-15a for Sensor 11, it can be seen that during the periods when the buffer is nearly empty the data fidelity is better with the queue length monitoring system. However, the errors are higher in S6-10 than in S6-08 when the queue is near its maximum value. In the case of the compression ratio monitoring system, the tolerance varies so rapidly with time, even with relatively high values of J_R , that the data fidelity appears to be fairly constant. Because the tolerance varies with the queue, in the case of the queue length monitoring system, it is easy to discern slow variations in data fidelity. From the standpoint of rms error, Table 4-6 and Figure 4-21 show a slight edge in favor of the queue length monitoring system, even though the maximum tolerance was higher on S6-10 for all sensors.

4.5.3.3 Experiment 6: Performance of Queue Length Monitoring Control System With Heavy Feedback (Run S6-12). Experiment 6 determined the extent of the degradation in reconstructed data fidelity when the feedback parameters of the queue length monitoring control system were set to limit the maximum queue to a value less than 100 under high noise conditions. As pointed out in the previous section, the control line slopes, β_2 , were chosen so that the tolerances for all sensors reached full scale at a queue of 100.

Results. Queue length and input rate time histories are shown for this compressor run in Figure 4-27 . The buffer readout rate was again set to 288 samples per second. Figure 4-27 shows that the queue was maintained below 100; its maximum value was approximately 49. The maximum values of tolerance, shown in Table 4-6, reached the vicinity of 200 counts in order to hold the queue to that value. The input rate

time history, shown in Figure 4-27 , indicates a leveling-off of the peaks of buffer input activity during high noise periods.

Time histories of the original and reconstructed data and of the reconstructed data error for Run S6-12 are shown for Sensor 9 in Figure 4-28a and the corresponding time history of the tolerance in Figure 4-28b. Data time histories for Sensor 11 are shown in Figure 4-29a; the corresponding tolerance time history is shown in Figure 4-29b. Rms errors and individual-sensor average compression ratios are given for seven sensors in Table 4-6.

The queue length time history, Figure 4-27 , demonstrates that except for the extremely noisy periods of 181 to 192 seconds, 206 to 210 seconds and two other intervals of less than one-second duration, the queue remained below 20. During these quiet periods, the reconstructed data fidelity was maximum because the tolerance was at its minimum value. For the most part, excessive data degradation occurred during the periods of excessive noise, as shown by the data time histories for Sensors 9 and 11 in Figures 4-28a and 4-29a. The degradation of the reconstructed data which occurred during these periods only added to the degradation caused by noise already present in the original data. In many cases, the data received during these periods are probably of little use to the data analyst anyway because of the large number of wild points.

4.5.3.4 Experiment 7: Simulation of Buffer Overflow Without Queuing Control (Run S6-11). The results of Experiment 6 suggest that a good way to cope with the problem of transmission noise in a ground station data compressor may be to ignore it and let a buffer of reasonable capacity overflow without queuing control. If the buffer readout rate were set high enough that the buffer did not overflow during the quiet (no noise) periods, then the only time the reconstructed data would be degraded beyond the prescribed amount would be during the periods of excessive noise. This experiment simulated these conditions so that the reconstructed data would be observed.

Buffer overflow was simulated by using the queue length monitoring, continuous queuing control system. A buffer capacity of 100 samples was simulated and the

tolerance was set to its standard value below a queue of 101. The slope of the control line, which began at a queue of 100 for all sensors, was set to 511 for each sensor so that when the queue reached 101, the tolerance exceeded full scale. Thus the maximum queue was maintained at approximately 100. (One hundred was not maintained because the first-order interpolator, disjoined, selector sent two samples to the buffer at each out-of-tolerance instance.) All samples lost due to buffer overflow were reconstructed on straight lines joining the transmitted samples.

Results. The queue length time history is shown for this run in Figure 4-30. The buffer readout rate was again set to 288 samples per second. Time histories of the original and reconstructed data and of the reconstructed data error for Run S6-11 are shown for Sensor 9 in Figure 4-31 and data time histories for Sensor 11 in Figure 4-32.

An examination of data time histories in Figures 4-31 and 4-32 shows that only during the periods of sync loss were the data degraded beyond the standard amount. During the short intervals between 206 and 210 seconds when sync was momentarily restored, the queue dropped below 100 allowing those portions of the waveform to be reconstructed at the standard accuracy. This was of course not true in the case of Experiment 6 (Run S6-12).

4.5.4 Test Group 4: Study of Data Having No Wild Points

As pointed out in Paragraph 4.4.4, it was necessary to investigate the queue behavior of data unaffected by transmission errors in order to perform a complete study of the S-6 data. An examination of the results of Run S6-07 revealed a section of data between 62 and 95 seconds, a relatively large statistical sample (29,700 data samples), which was virtually free of noisy data.

4.5.4.1 Experiment 8: Comparison of Average Compression Ratios Without Wild Points to Total Average Compression Ratios (Runs S6-07, S6-13). This experiment determined the degree by which the presence of wild points caused by transmission noise degraded the compression ratios obtained by the first order interpolator, disjoined, selector.

Results. Average compression ratios by individual sensor are shown for Runs S6-07 and S6-13 in Table 4-7 and in Figure 4-33. The period between 20 and 200 seconds included a number of randomly spaced variable-length intervals of high noise. Run S6-07 covered this section and Run S6-13 covered a 33-second section of noise free data. The standard values of tolerance shown in Table 4-1 were used on both runs. The average compression ratio of the data without wild points increased on all but six sensors, and the combined average compression ratio increased from 3.44 to 4.06.

4.5.4.2 Experiment 9: Queue Behavior as a Function of $\bar{\rho}$ (Runs S6-14, S6-15, S6-16, S6-17). This experiment observed the queue behavior as the ratio of average buffer sample readin rate to readout rate, $\bar{\rho}$, was varied on noise free data. Values for $\bar{\rho}$ of 0.91, 0.95, 0.98 and 1.50 over the period of 62 to 95 seconds were used by setting the buffer readout rates to the values shown in Table 4-5. An infinite-capacity buffer was used in all runs.

Results. Time histories of queue length and buffer input rate are shown in Figure 4-34 for $\bar{\rho} = 0.98$ (S6-16) and for $\bar{\rho} = 1.50$ (S6-17). Note that when the buffer readout rate exceeds the average readin rate, $\bar{\rho} < 1$, the queue length is nominal. The maximum queue varies from 28 for $\bar{\rho} = 0.91$ to 56 for $\bar{\rho} = 0.98$. This shows that even for a $\bar{\rho}$ as high as 0.98, a buffer of reasonable capacity, 100-200 samples, can, without any form of queuing control, easily handle noise free S-6 data compressed by the first-order interpolator, disjoined, selector. However, if the readout rate from the buffer is set so low that $\bar{\rho}$ exceeds unity, the queue will of course continue to build up indefinitely. An example of this is Run S6-17, during which the queue built up to approximately 2430 at the end of the 33-second run. From this it appears that some form of queuing control should be used to insure against buffer overflow in the event the transmission rate is too low.

The queue length histogram for $\bar{\rho} = 0.98$ is shown in Figure 4-35, a histogram of buffer input arrival rates in Figure 4-36, and a histogram of the time intervals between buffer input arrivals in Figure 4-37. Comparing Figure 4-36 with Figure 4-3, it is clear that the number of instances of high input rate is greatly reduced in the

Table 4-7

COMPARISON OF AVERAGE COMPRESSION RATIOS
WITH & WITHOUT LOSSES, FOIDIS COMPRESSION MODEL

SENSOR	CHANNEL AND POSITION NUMBERS	AVE COMP RATIO WITH SYNC LOSS (S6-07)	AVE COMP RATIO WITHOUT SYNC LOSS (S6-13)	SENSOR	CHANNEL AND POSITION NUMBERS	AVE COMP RATIO WITH SYNC LOSS (S6-07)	AVE COMP RATIO WITHOUT SYNC LOSS (S6-13)
1	1	5.51	6.80	29	31, pp 2	6.38	41.00
2	2, 7, 12, 18, 23, 28, 34, 39, 44	1.76	1.87	30	31, pp 3	16.20	41.00
				31	31, pp 4	11.86	41.00
				32	31, pp 5	12.95	41.00
3	16, 40	3.44	4.33	33	31, pp 6	6.81	41.00
4	3, 19, 35	12.07	396.00	34	31, pp 7	6.49	42.00
5	4, 20, 36	10.20	36.00	35	31, pp 8	48.20	42.00
6	5, 21, 37	4.31	5.06	36	31, pp 9	36.00	42.00
7	6, 22, 38	2.29	2.22	37	31, pp10	1.01	1.02
8	8, 32	2.92	3.50	38	31, pp11	6.12	41.00
9	9, 25, 41	6.72	17.85	39	31, pp12	5.00	41.00
10	24	6.81	15.35	40	31, pp13	11.13	41.00
11	10, 26, 42	3.51	3.82	41	31, pp14	13.21	41.00
12	11, 27, 43	3.77	4.05	42	33, pp15	10.12	41.00
13	13, 29, 45	6.28	10.82	43	33, pp 0	16.20	41.00
14	30	5.65	3.86	44	33, pp 1	6.81	41.00
15	14	16.72	660.00	45	33, pp 2	9.22	41.00
16	15	23.93	660.00	46	33, pp 3	14.29	41.00
17	17, pp 15, 6*	1.00	1.01	47	33, pp 4	9.96	41.00
18	17, pp 0, 7	1.00	1.00	48	33, pp 5	10.70	41.00
19	17, pp 1, 8	1.00	1.00	49	33, pp 6	8.69	41.00
20	17, pp 2, 9	1.31	1.63	50	33, pp 7	7.23	42.00
21	17, pp 3, 10	1.59	1.93	51	33, pp 8	16.07	42.00
22	17, pp 4, 11	6.02	82.00	52	33, pp 9	10.08	42.00
23	17, pp 5, 12	1.00	1.01	53	33, pp10	13.16	42.00
24	17, pp 13	8.26	41.00	54	33, pp11	6.78	41.00
25	17, pp 14	13.21	41.00	55	33, pp12	5.67	41.00
26	31, pp 15	7.23	41.00	56	33, pp13	6.24	41.00
27	31, pp 0	6.94	41.00	57	33, pp14	251.00	41.00
28	31, pp 1	6.15	41.00				
Combined (all sensors)						3.44	4.06

*Sensors 17 through 23 were erroneously thought to to be cross-strapped as shown. Since only one minor frame channel in 45 was involved, the resulting abnormally-low compression ratios obtained for these sensors did not materially affect the overall outcome of the experiment.

noise free data. In addition, the queue length histogram, Figure 4-35, resembles an exponential decay which is characteristic of Poisson input statistics. (It will be recalled that the queue length histogram for the 200-second run shown in Figure 4-5 did not.)

4.5.4.3 Experiment 10: Comparison of Queue Length and Compression Ratio Monitoring Under Conditions of Low Buffer Readout Rate (Runs S6-18, S6-19). This experiment, involving a buffer readout rate set so low that, without queuing control, $\bar{\rho}$ would exceed unity, compared the performance of a queuing control system which monitors average run length with one which monitors the queue length. Run S6-18 used the compression ratio monitoring, continuous queuing control system; Run S6-19 used the queue length monitoring, continuous queuing control system. All control parameters for Run S6-18 were essentially the same as in Runs S6-08 and S6-09 except J_R equalled 7 in Run S6-18.

Results. Time histories of queue length and buffer input rate for Run S6-18, compression ratio monitoring, are shown in Figure 4-38. A comparison of Figure 4-38 with Figure 4-34 indicates that the compression ratio monitoring system in its current form was completely ineffective in coping with an excessively-low readout rate situation. The queue buildup with this form of queuing control, Figure 4-38, was essentially the same as the buildup without control, Figure 4-34. Queue length and buffer input rate time histories for Run S6-19 (queue length monitoring) are presented in Figure 4-39. This figure shows that the queue built up during the first four or five seconds of the run, but leveled off to an average value of about 150. The maximum value of queue during the entire run was approximately 186.

If the queue length is monitored and used to control aperture width, the average queue length will reach an equilibrium value. Although this value was 150 in this experiment, it will in general depend on the starting points and slopes of the feedback curves and on the buffer readout rate. On the other hand, if compression ratio is monitored and used to control aperture width, no queue length equilibrium point will ever be reached and eventual buffer overflow is sure to result.

Figure 4-40a shows time histories of the original and reconstructed Sensor 9 data and of the reconstructed data error taken from a portion of Run S6-18 (compression ratio monitoring); Figure 4-40b, the corresponding time history of the tolerance; Figures 4-41a and 4-41b, Sensor 9 data and tolerance time histories for a portion of Run S6-19 (queue length monitoring), respectively; Figure 4-42, the same portion of the Sensor 9 reconstructed waveform for the standard tolerance of 4 counts without queuing control from Run S6-07; and Figures 4-43, 4-44, and 4-45, error histograms for S6-18, S6-19, and the case without queuing control, respectively.

Time histories of the original and reconstructed Sensor 11 data and of the reconstructed data error taken from a portion of Run S6-18 are shown in Figure 4-46a. Figure 4-46b shows the corresponding time history of the tolerance. Sensor 11 data and tolerance time histories are shown for a portion of Run S6-19 in Figures 4-47a and 4-47b. For comparison, the same portion of the Sensor 11 reconstructed waveform is shown in Figure 4-48 for the standard tolerance of 4 counts without queuing control from Run S6-07. Error histograms are shown for S6-18, S6-19 and the case without queuing control in Figures 4-49, 4-50 and 4-51, respectively. Rms errors and individual-sensor average compression ratios are given for seven sensors in Table 4-8. Figure 4-52 gives a comparison of the rms errors obtained for these sensors in Runs S6-07 (no queuing control), S6-18 (compression ratio monitoring control system), and S6-19 (queue length monitoring control system).

Figures 4-40a through 4-45 for Sensor 9 and Figures 4-46a through 4-51 for Sensor 11 show that the fidelity of the reconstructed data which results with the queue length monitoring system is worse than the data fidelity with the compression ratio monitoring system. In fact, a comparison of Figures 4-46a and 4-48 shows no appreciable fidelity degradation of the Sensor 11 waveform of the compression ratio monitoring system over the waveform of no queuing control. (Some degradation in the Sensor 9 waveform is noticeable when Figures 4-40a and 4-42 are compared.) An examination of the rms errors for the seven sensors shown in Table 4-8 and in Figure 4-52 also indicates an appreciable degradation of the reconstructed data for most of the sensors with the queue length monitoring queuing control system under conditions of excessively low buffer readout rate.

Table 4-8

COMBINED RESULTS BY INDIVIDUAL SENSOR - TEST GROUP 4

SENSOR RUN		QUEUING CONTROL SYSTEM	J _R	MAX TOL, COUNTS	RMS ERROR, COUNTS	ERROR MEAS. INTERVAL, SEC	\bar{N}^*	\bar{N} MEAS INTERVAL, SEC
2	S6-07	NONE	-	4.0	1.31	85-90	1.76	20-220
	S6-13	NONE	-	4.0	-	-	1.87	62-95
	S6-18	CRC	7	7.9	1.30	85-90	1.86	62-95
	S6-19	QLC	-	16.1	5.57	85-90	2.54	62-95
3	S6-07	NONE	-	16.0	6.66	62-95	3.44	20-220
	S6-13	NONE	-	16.0	-	-	4.33	62-95
	S6-18	CRC	7	28.1	7.28	67-92	4.33	62-95
	S6-19	QLC	-	63.7	25.14	67-92	6.14	62-95
6	S6-07	NONE	-	4.0	2.25	62-95	4.31	20-220
	S6-13	NONE	-	4.0	-	-	5.06	62-95
	S6-18	CRC	7	16.6	2.04	74-90	5.09	62-95
	S6-19	QLC	-	15.9	8.60	74-90	12.94	62-95
7	S6-07	NONE	-	4.0	1.57	62-95	2.29	20-220
	S6-13	NONE	-	4.0	-	-	2.22	62-95
	S6-18	CRC	7	8.8	1.84	74-90	2.24	62-95
	S6-19	QLC	-	15.9	6.37	74-90	3.14	62-95
9	S6-07	NONE	-	4.0	1.82	62-95	6.72	20-220
	S6-13	NONE	-	4.0	-	-	17.85	62-95
	S6-18	CRC	7	54.6	3.24	74-90	17.23	62-95
	S6-19	QLC	-	16.0	5.93	74-90	36.02	62-95
10	S6-07	NONE	-	4.0	1.73	62-95	6.81	20-220
	S6-13	NONE	-	4.0	-	-	15.35	62-95
	S6-18	CRC	7	40.5	5.26	62-95	12.94	62-95
	S6-19	QLC	-	16.0	4.60	62-95	20.00	62-95
11	S6-07	NONE	-	4.0	2.26	62-95	3.51	20-220
	S6-13	NONE	-	4.0	-	-	3.82	62-95
	S6-18	CRC	7	13.4	2.40	74-90	3.84	62-95
	S6-19	QLC	-	16.0	7.95	74-90	6.06	62-95

* \bar{N} = Maximum average compression ratio

4.5.5 Conclusions

4.5.5.1 Use Queuing Control With Queue Length Monitoring on S-6 Data. The results of these experiments indicate that, as long as the S-6 satellite telemetry data are free of wild points and other causes of prolonged digital error, and the transmission sample rate is sufficiently high, the data activity is so constant that the need for any form of queuing control does not exist. However, in order to insure against the possibility that the buffer readout rate will be set lower than the average readin rate to the buffer, it is desirable to use queuing control with queue length monitoring only. Because this control would only be used as a backup in the event $\bar{\rho}$ exceeds unity and the queue did not exceed 56 even for a $\bar{\rho}$ of 0.98, the aperture should not begin to increase until the queue reaches about 60. The relative slopes of the control lines for each sensor will of course depend partly on sensor priority, but on the average the slopes will be determined by the buffer capacity and the maximum anticipated value of $\bar{\rho}$ without queuing control. The control line slopes used in Experiment 10, which doubled the aperture on all sensors when the queue increased from 20 to 75, resulted in an average queue of about 150 when the buffer readout rate was reduced to 148 samples per second. Thus, enlarging the apertures by a factor of about two and one-half reduced the average buffer readin rate by one-third. A buffer with a capacity of at least 186 would have been required with the parameter values chosen in Run S6-19. However, an increase in the slopes of the control curves would cause the apertures to be increased by the above factor at a lower value of queue if control still began at 20 samples and require a smaller buffer to cope with the chosen reduction in buffer readout rate.

4.5.5.2 Rerun S6-19. It may be profitable to rerun S6-19 a number of times with different values of readout rate and control curve slopes in order to obtain a family of curves relating average and maximum queue lengths and readout rates, and to determine the effect of control curve slope on reconstructed data fidelity.

4.5.5.3 Compression Ratio Monitoring Systems Not Required. Because of the constancy of the S-6 data activity without noise, there is no need to consider compression ratio monitoring systems, even in conjunction with queue length monitoring, for the

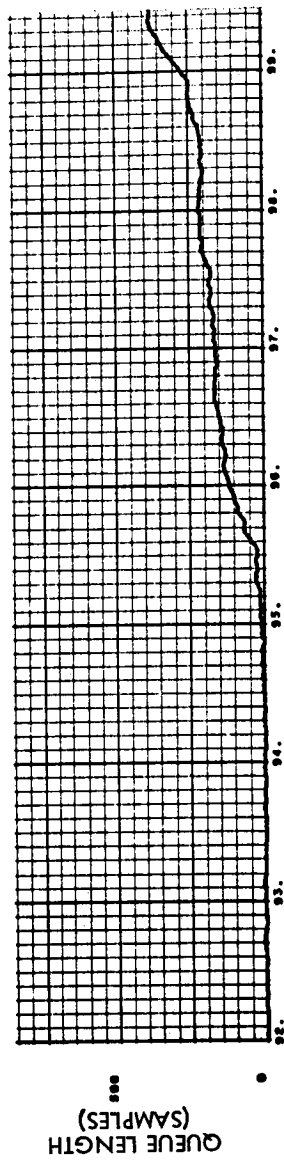
purpose of controlling the queue. If for some other reason, however, compression ratio monitoring in its present form is found desirable, then a combination system should be considered for data such as the S-6.

4.5.5.4 Allow Ground Station Data Compressor Buffer Overflow During High Noise.

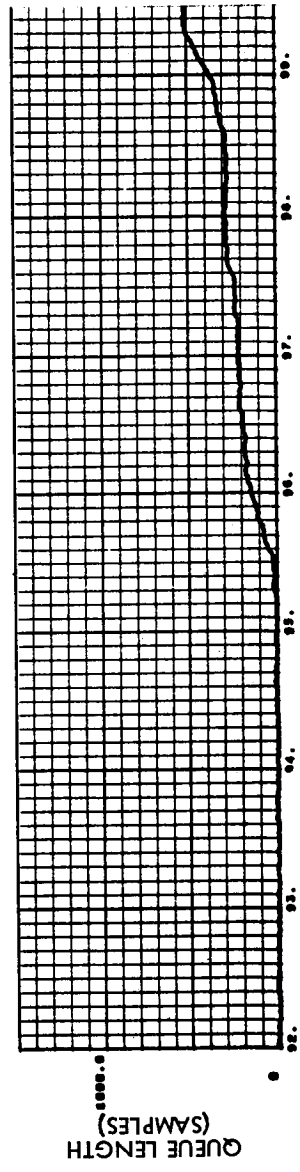
It was found that one good way to cope with the problem of noise in a ground station data compressor is merely to allow the buffer to overflow during periods of excessive sync loss. The data samples lost during these periods will usually be of little value to the data analyst anyway. Another way to cope with noise would be to employ some method of wild point rejection on the pre-compressed telemetry data.

4.5.5.5 Queue Length Monitoring Systems Are Self-Adjusting. It can be concluded that queue length monitoring systems are self-adjusting; i. e. , if the readout rate is set too low, the aperture will be automatically adjusted to match this rate. The compression ratio monitoring system, in its present form, clearly is not self-adjusting. It is believed, however, that this system could be made self-adjusting by, for example, using the integral of the error signal to control the aperture, rather than the error signal itself. The merits of this and other self-adjusting systems, compared with the queue length monitoring system, should be determined by further investigation.

4.5.5.6 Buffer Underflow Must Accompany Normal System Operation. In order for normal conditions, those yielding maximum data fidelity, to prevail with the queuing control system configuration recommended above, the queue would be so small that control would not be in effect. However, in order for this to occur, $\bar{\rho}$ must be less than one. This means buffer underflow will be present, and on some attempts to remove a sample from the buffer for transmission, the buffer will be empty and no sample will be read out. The resulting voids in transmission can of course be filled with some predetermined code word, or with redundant data samples from selected sensors to avoid the problems of bit synchronization if all zeros or ones were transmitted.



TIME (SEC)
RUN S6-03



TIME (SEC)
RUN S6-04

Fig. 4-1 Queue Length vs Time, Runs S6-03 and S6-04

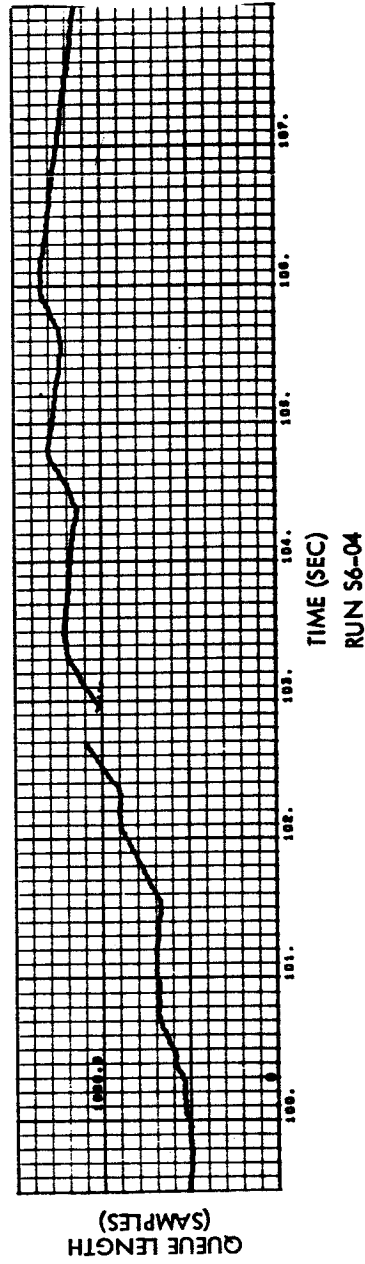
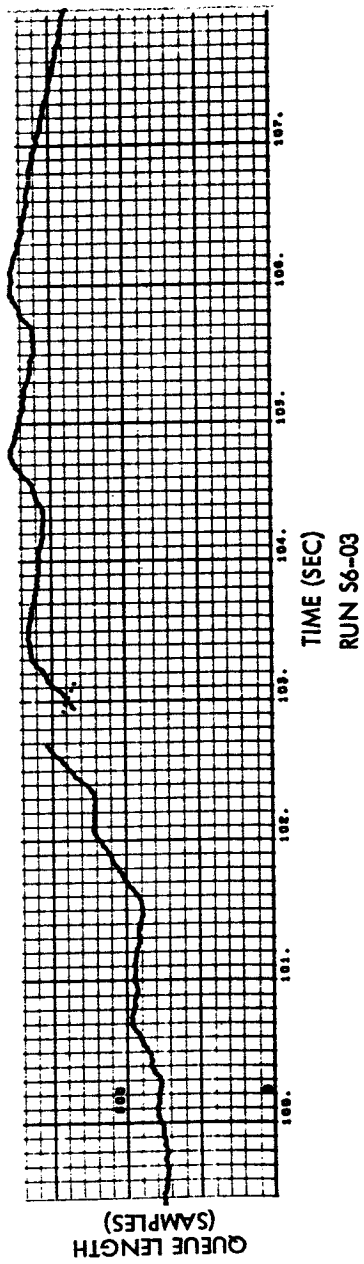
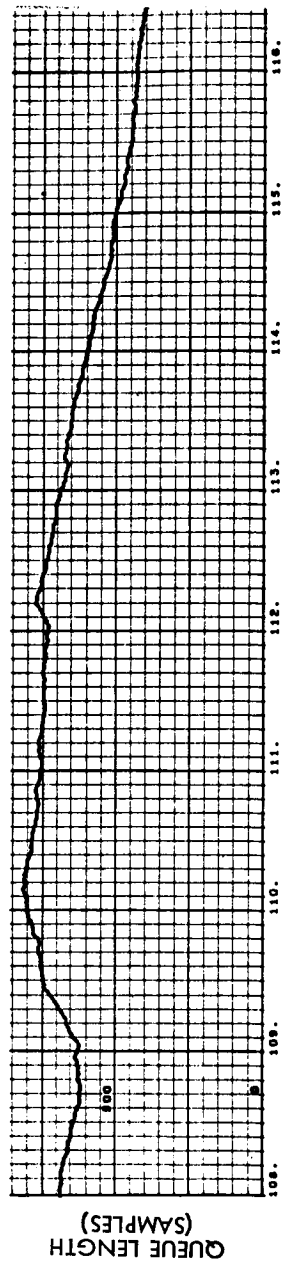
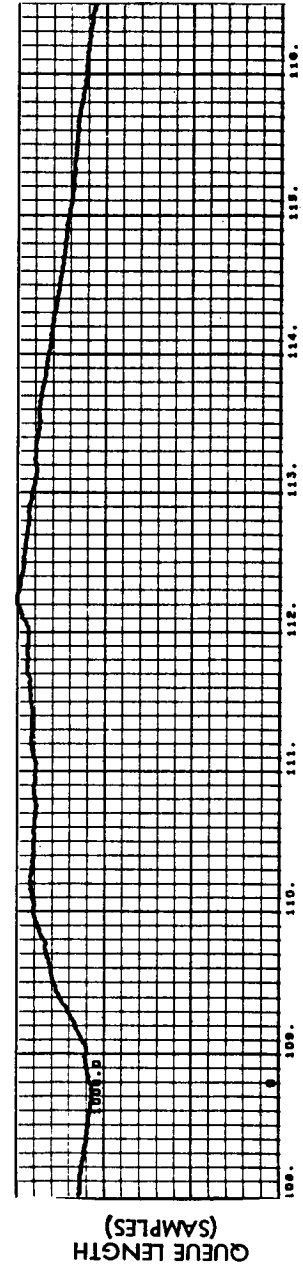


Fig. 4-1 (Cont'd) Queue Length vs Time, Runs S6-03 and S6-04

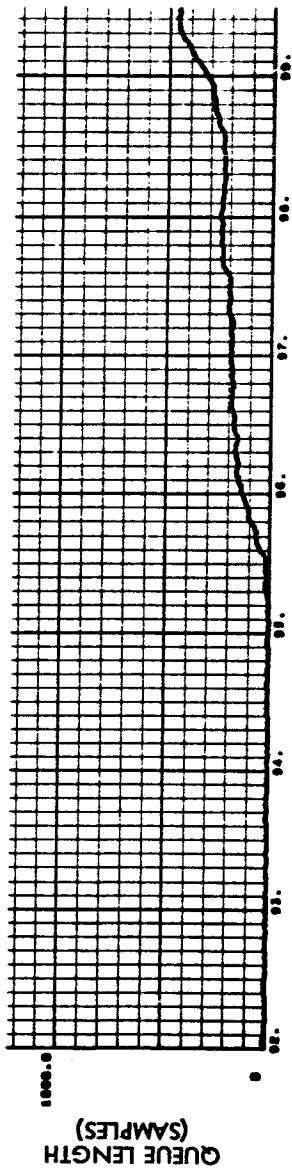


TIME (SEC)
RUN S6-03

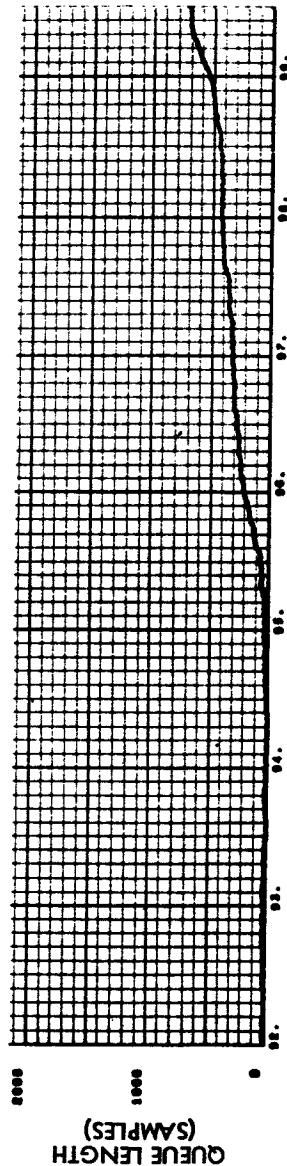


TIME (SEC)
RUN S6-04

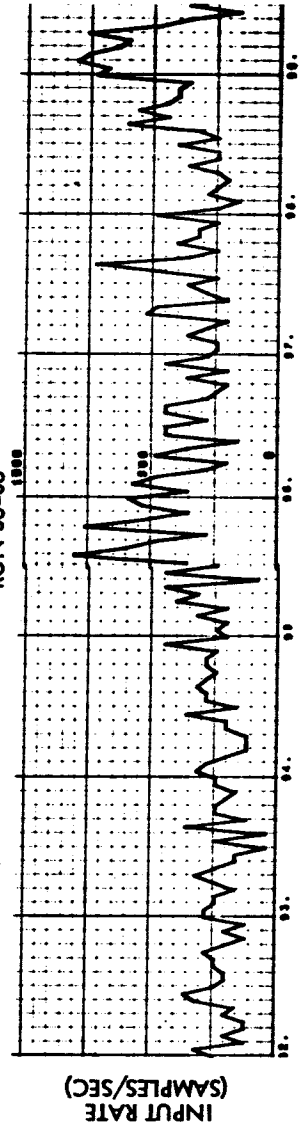
Fig. 4-1 (Cont'd) Queue Length vs Time, Runs S6-03 and S6-04



TIME (SEC)
RUN S6-05

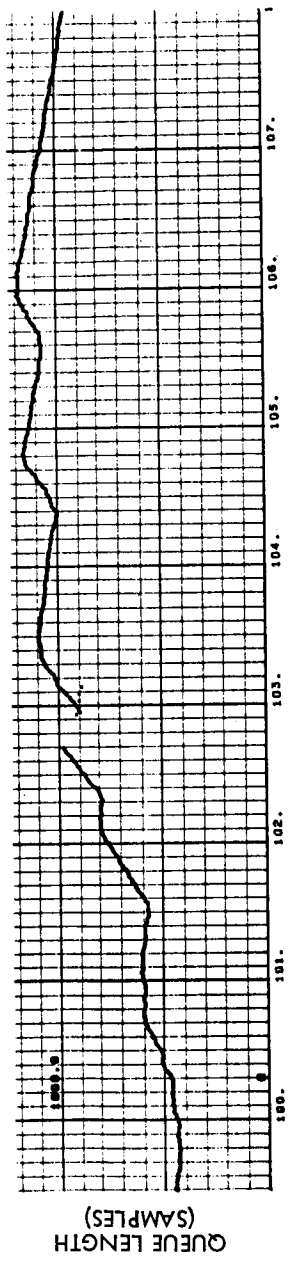


TIME (SEC)
RUN S6-06

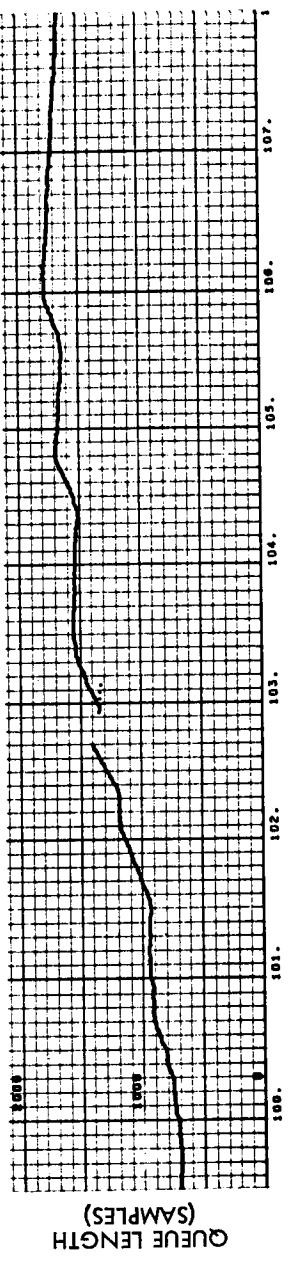


TIME (SEC)
BOTH RUNS

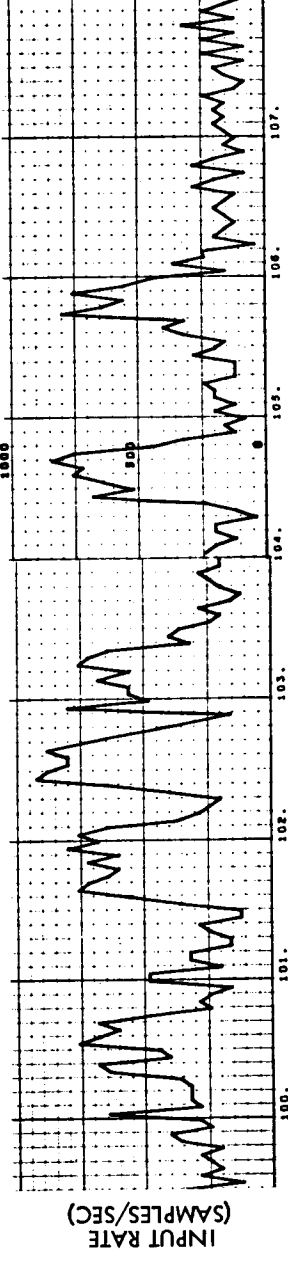
Fig. 4-2 Queue Length and Buffer Input Arrival Rate vs Time, Runs S6-05 and S6-06



TIME (SEC)
RUN S6-05



TIME (SEC)
RUN S6-06



TIME (SEC)
BOTH RUNS

Fig. 4-2 (Cont'd) Queue Length and Buffer Input Arrival Rate vs Time, Runs S6-05 and S6-06

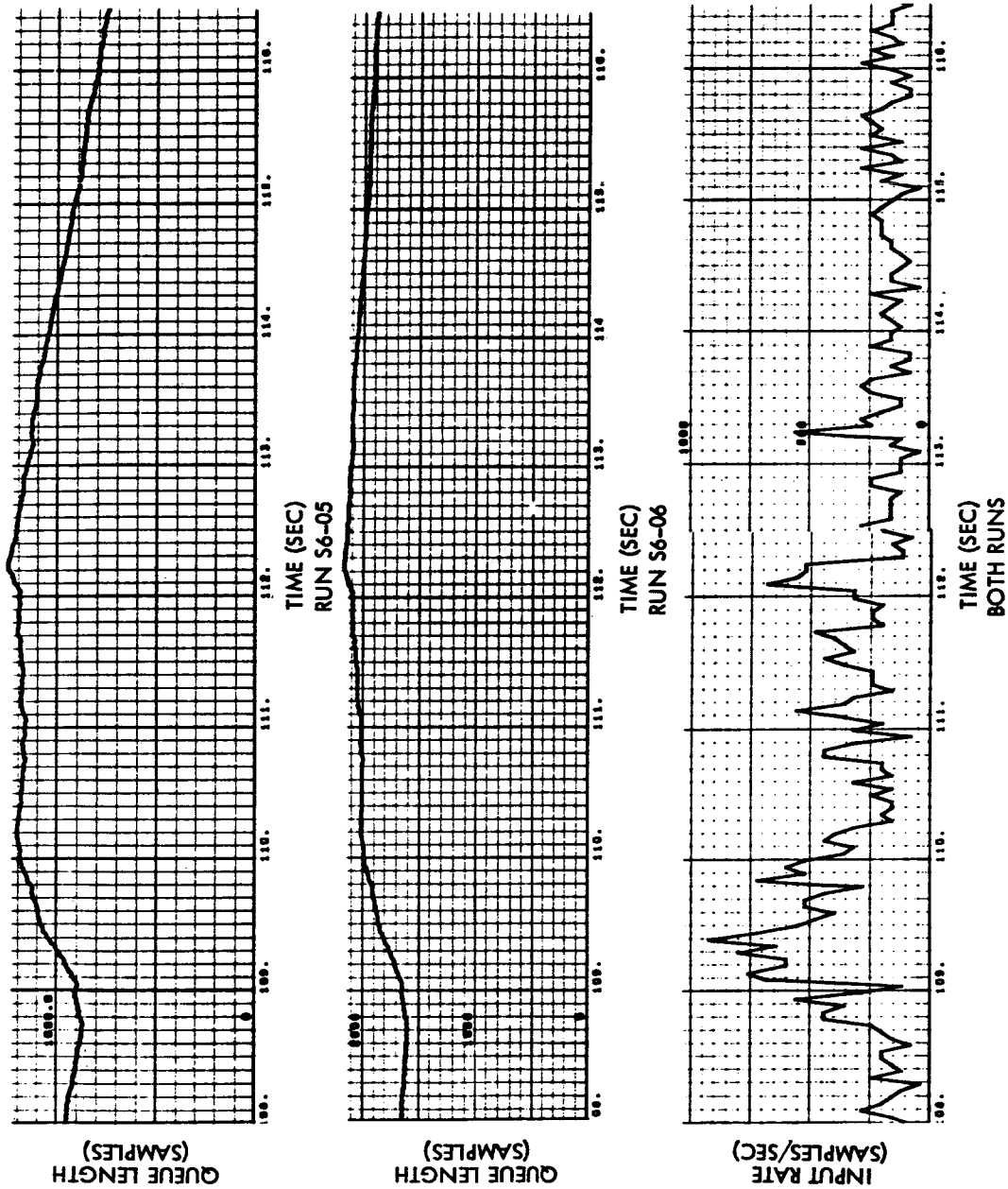


Fig. 4-2 (Cont'd) Queue Length and Buffer Input Arrival Rate vs Time, Runs S6-05 and S6-06

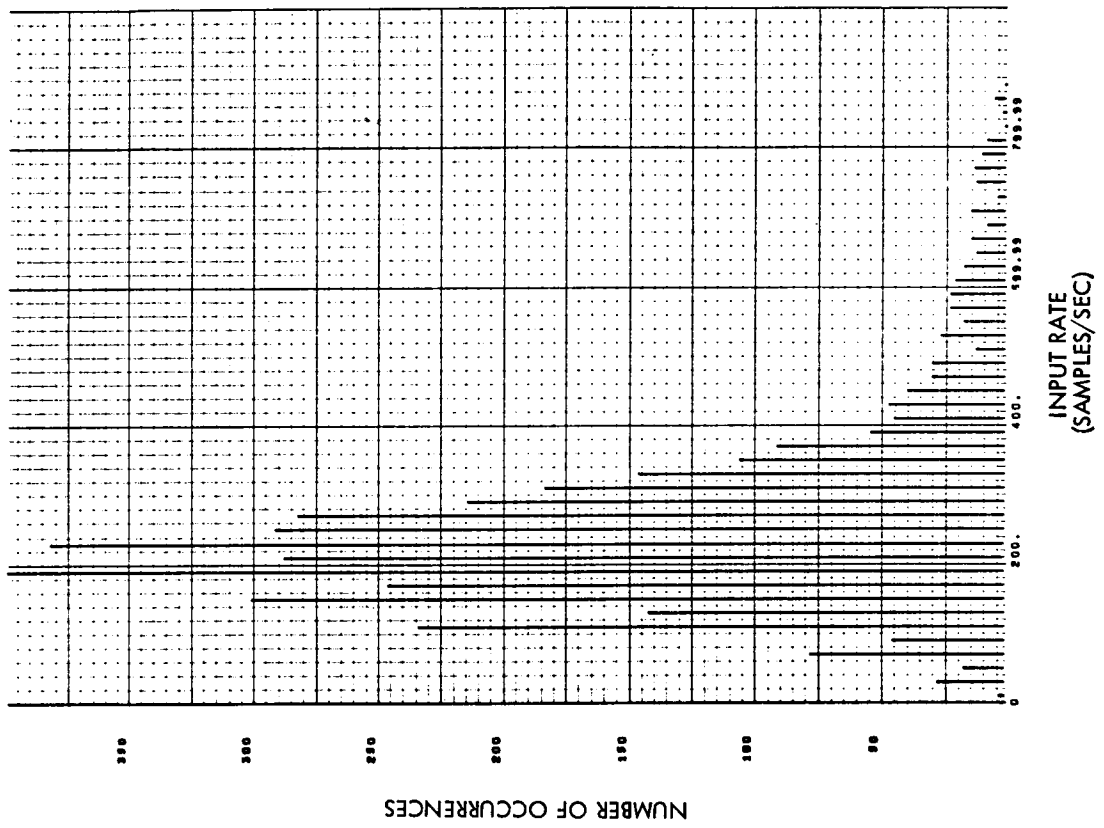


Fig. 4-3 Buffer Input Arrival Rate Histogram, Run S6-07

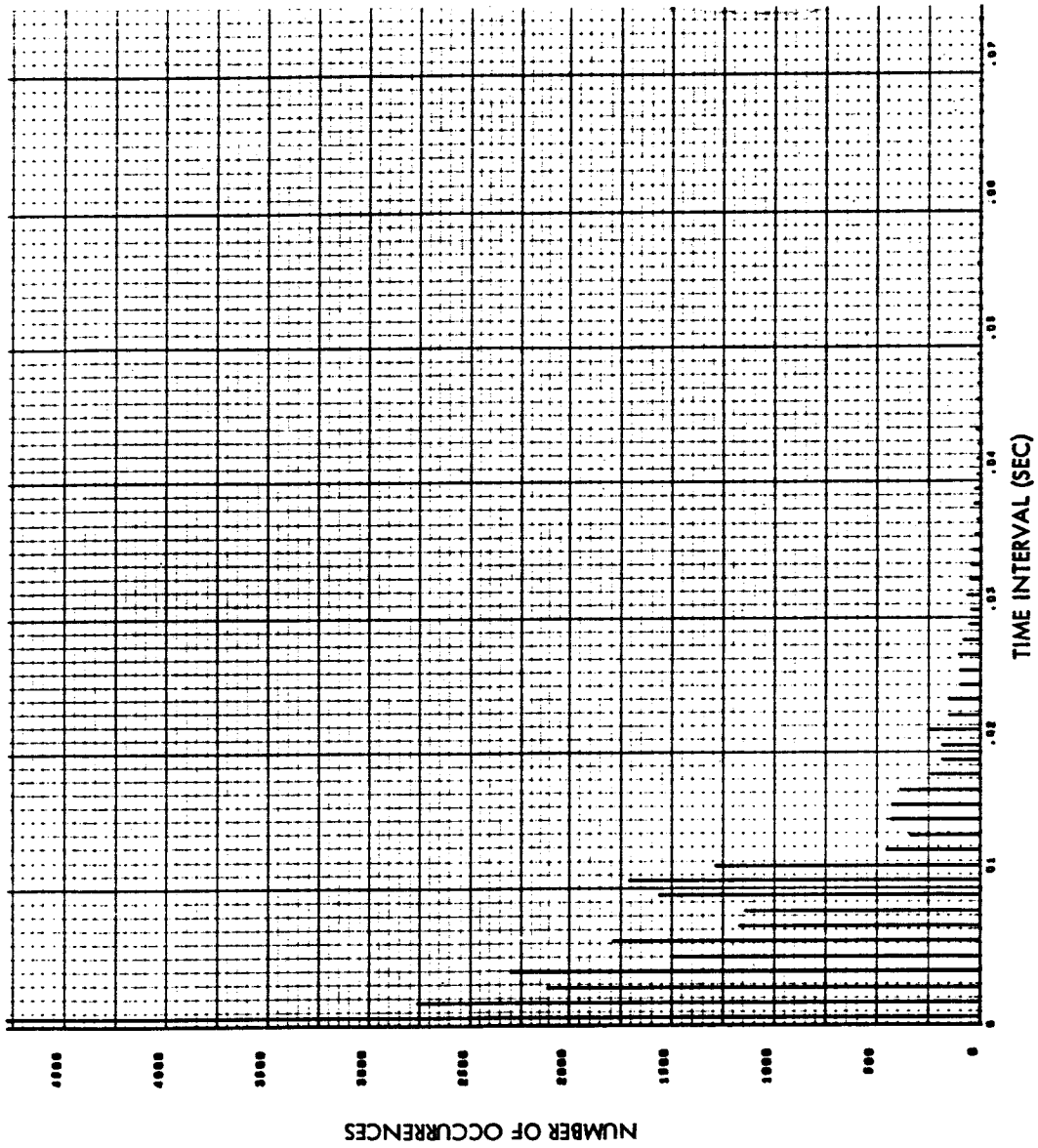


Fig. 4-4 Histogram of Time Intervals Between Buffer Input Arrivals, Run S6-07

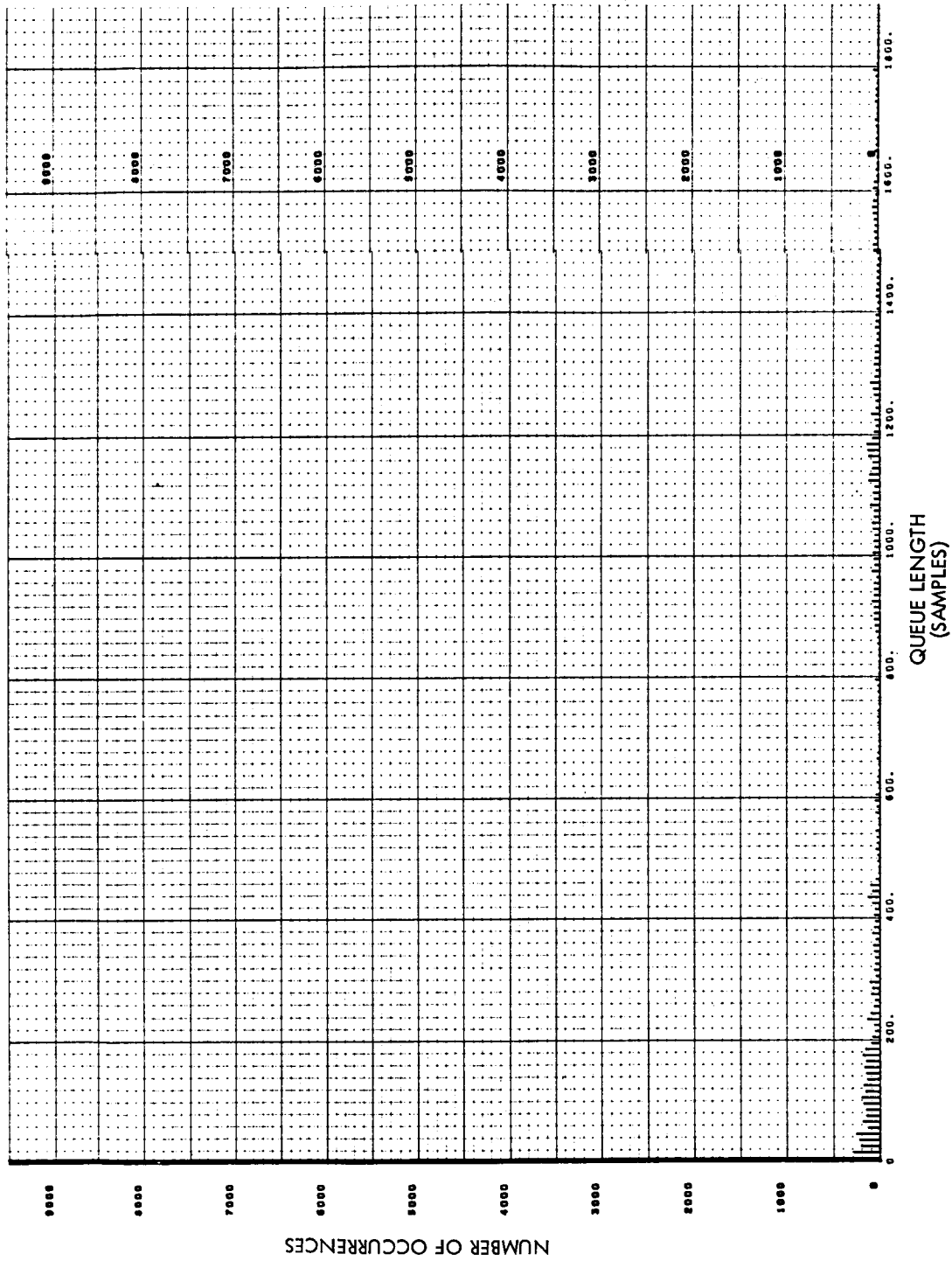


Fig. 4-5 Queue Length Histogram, Run S6-07

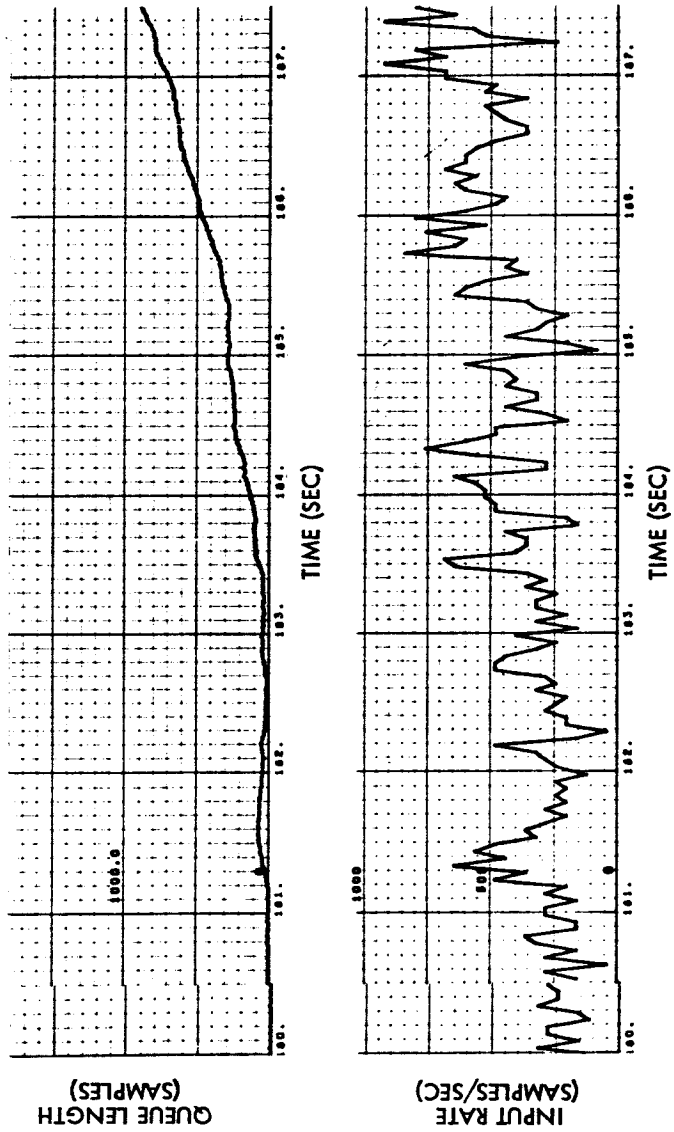


Fig. 4-6 Queue Length and Buffer Input Arrival Rate vs Time, Run S6-07

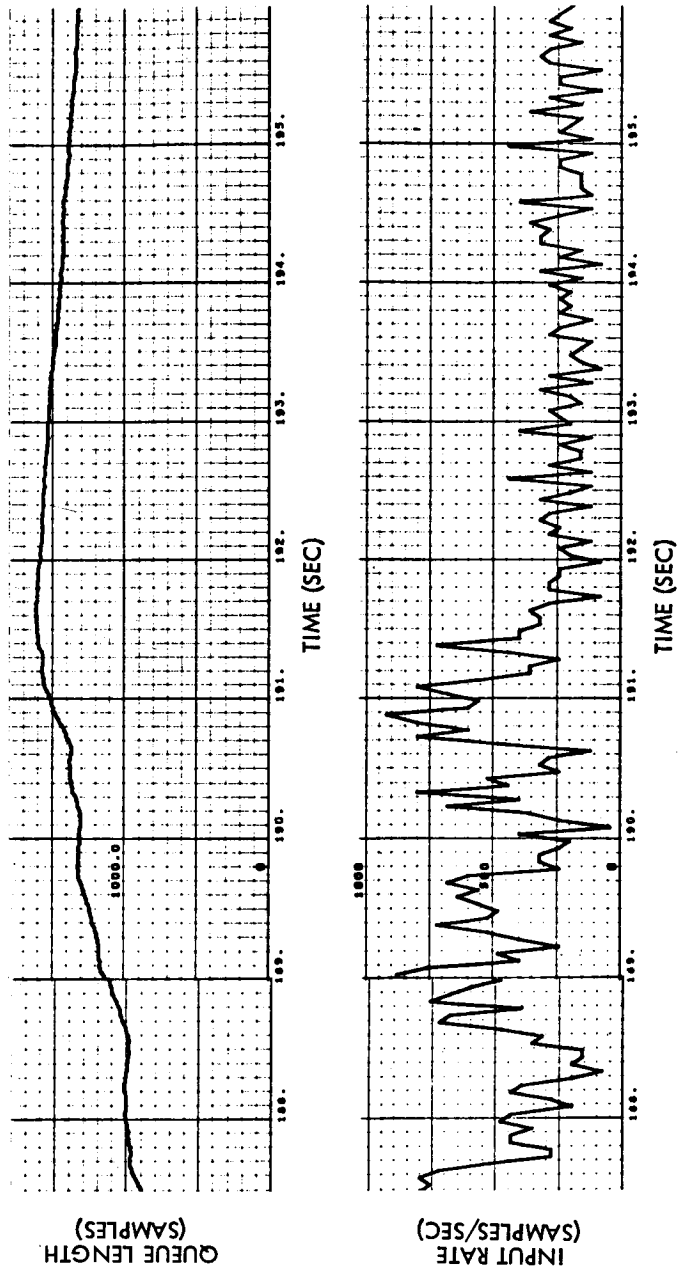


Fig. 4-6 (Cont'd) Queue Length and Buffer Input Arrival Rate vs Time, Run S6-07

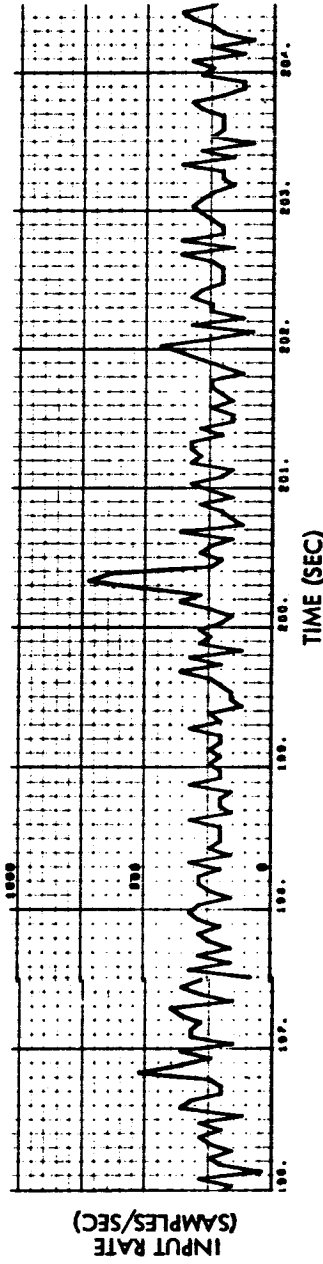
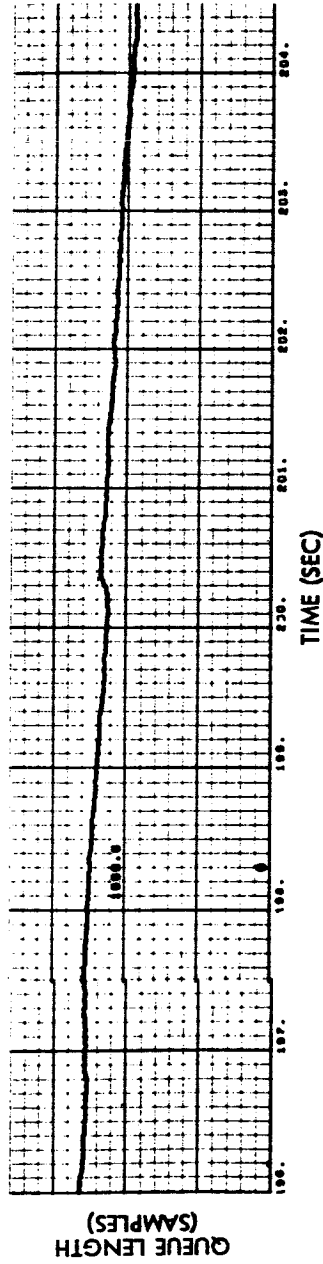


Fig. 4-6 (Cont'd) Queue Length and Buffer Input Arrival Rate vs Time, Run S6-07

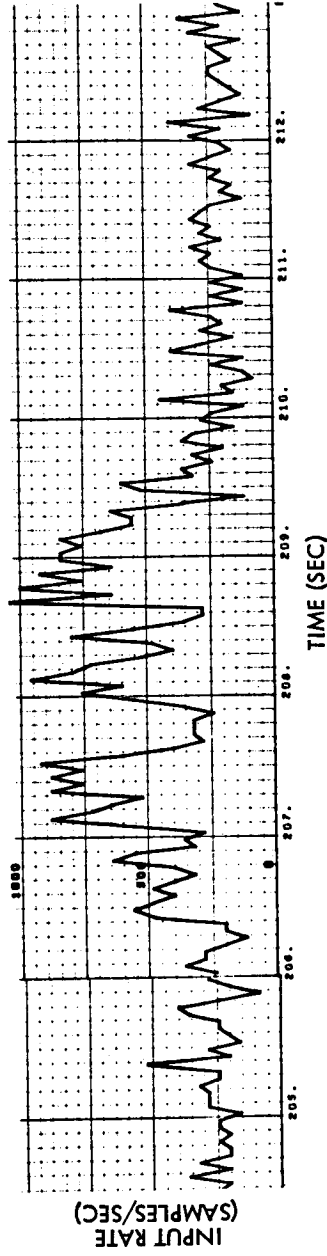
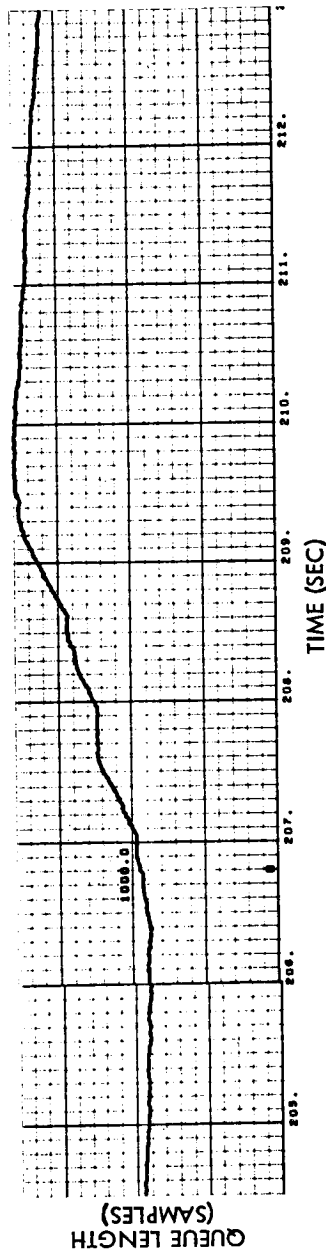


Fig. 4-6 (Cont'd) Queue Length and Buffer Input Arrival Rate vs Time, Run S6-07

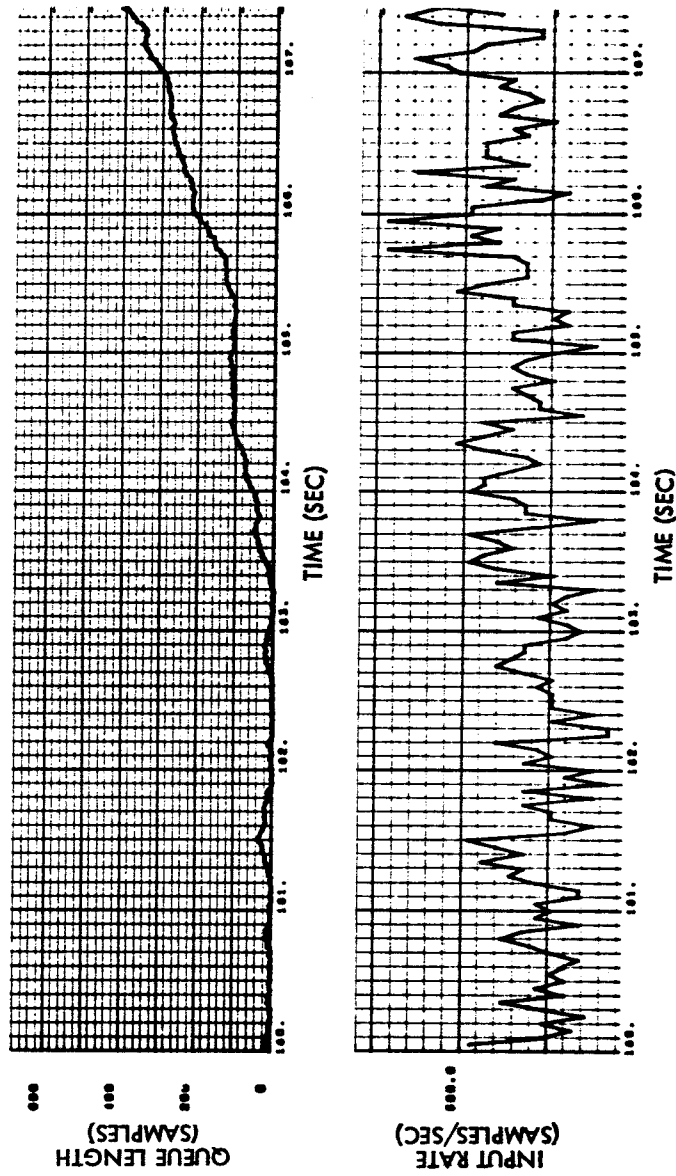


Fig. 4-7 Queue Length and Buffer Input Arrival
Rate vs Time, Run S6-08

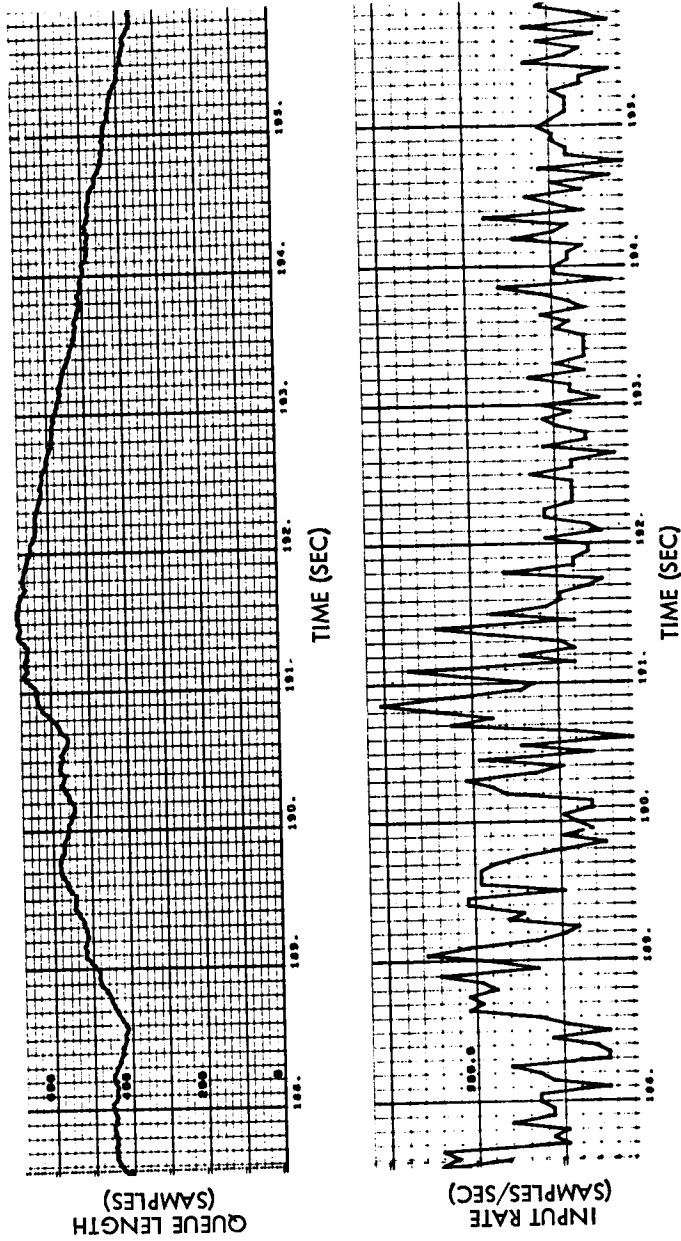


Fig. 4-7 (Cont'd) Queue Length and Buffer Input Arrival Rate vs Time, Run S6-08

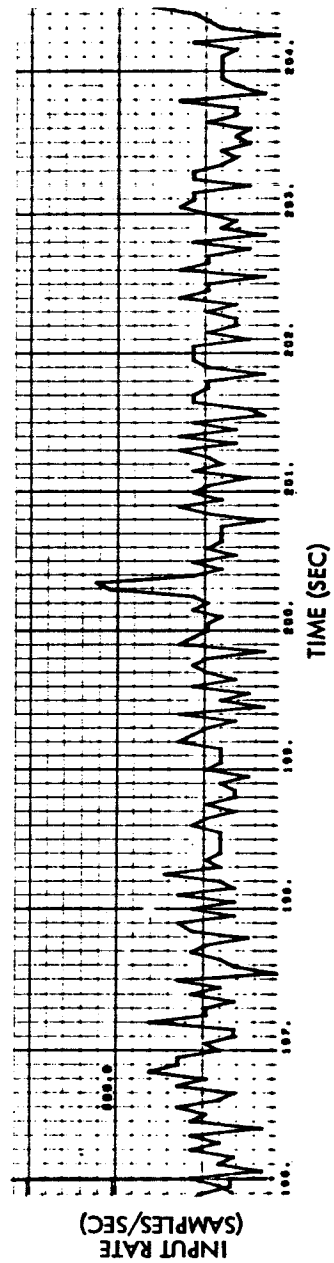
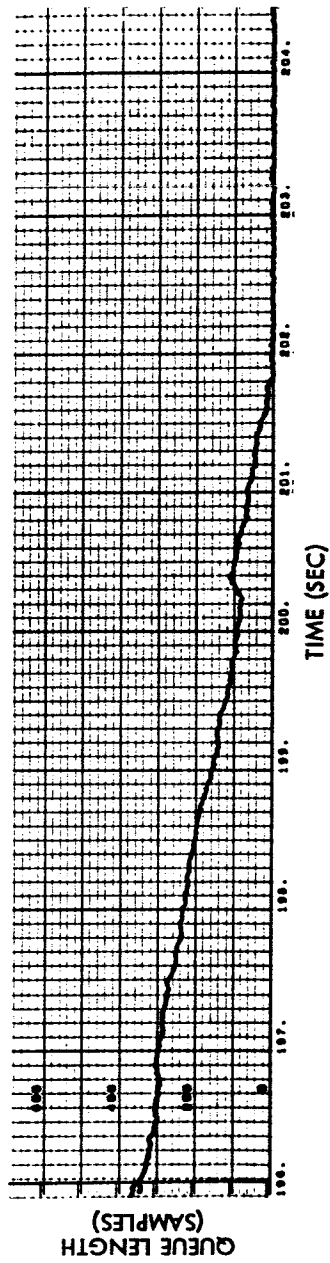


Fig. 4-7 (Cont'd) Queue Length and Buffer Input Arrival Rate vs Time, Run S6-08

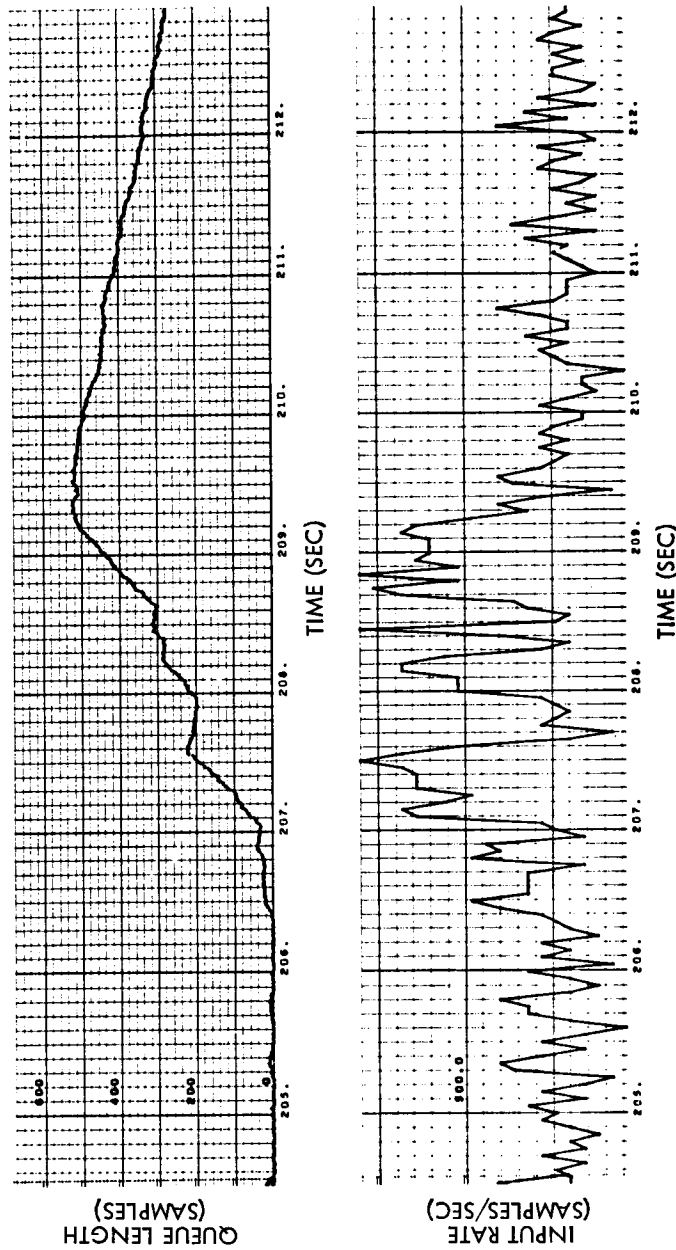


Fig. 4-7 (Cont'd) Queue Length and Buffer Input Arrival Rate vs Time, Run S6-08

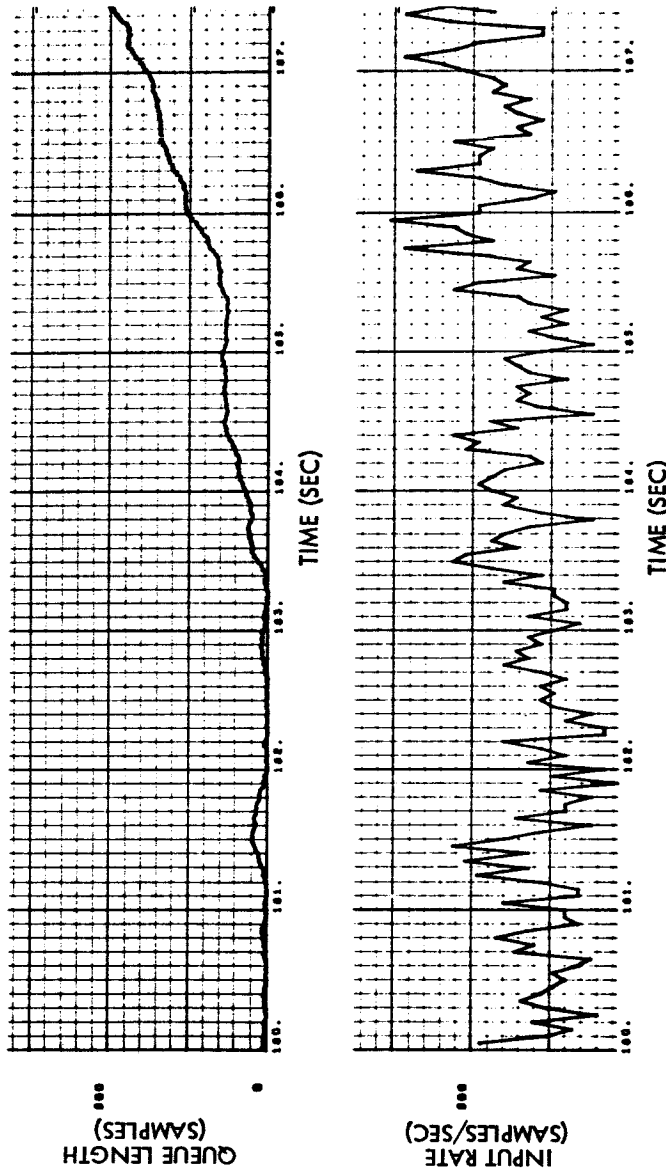


Fig. 4-8 Queue Length and Buffer Input Arrival Rate vs Time, Run S6-09

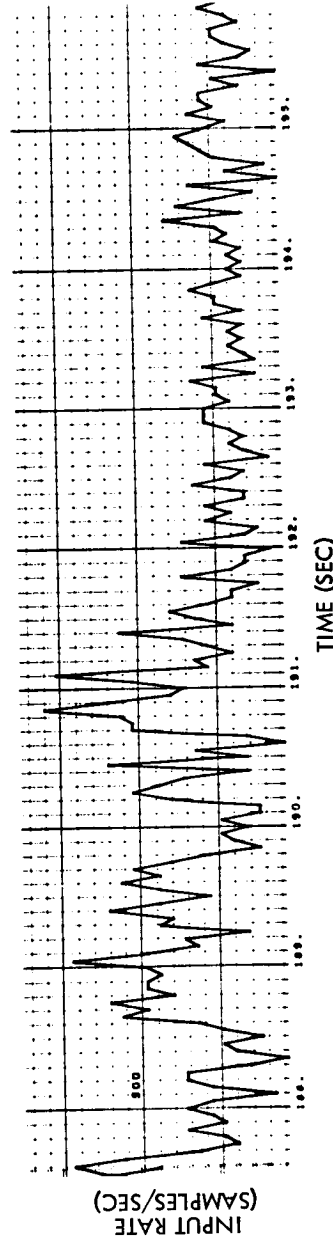
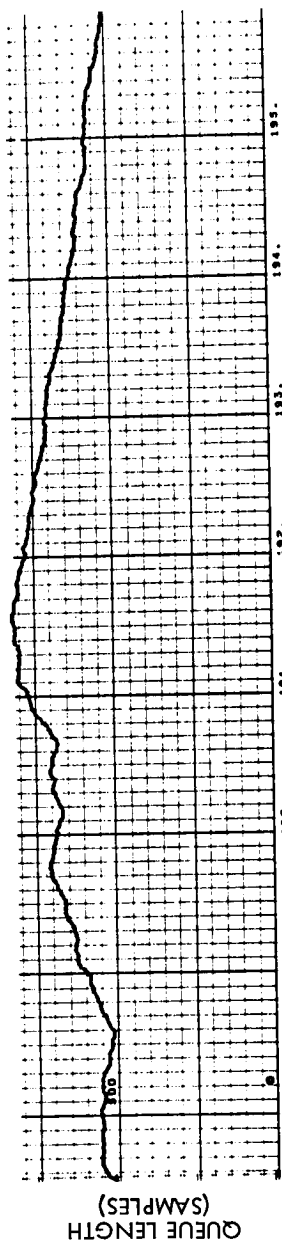


Fig. 4-8 (Cont'd) Queue Length and Buffer Input Arrival Rate vs Time, Run S6-09

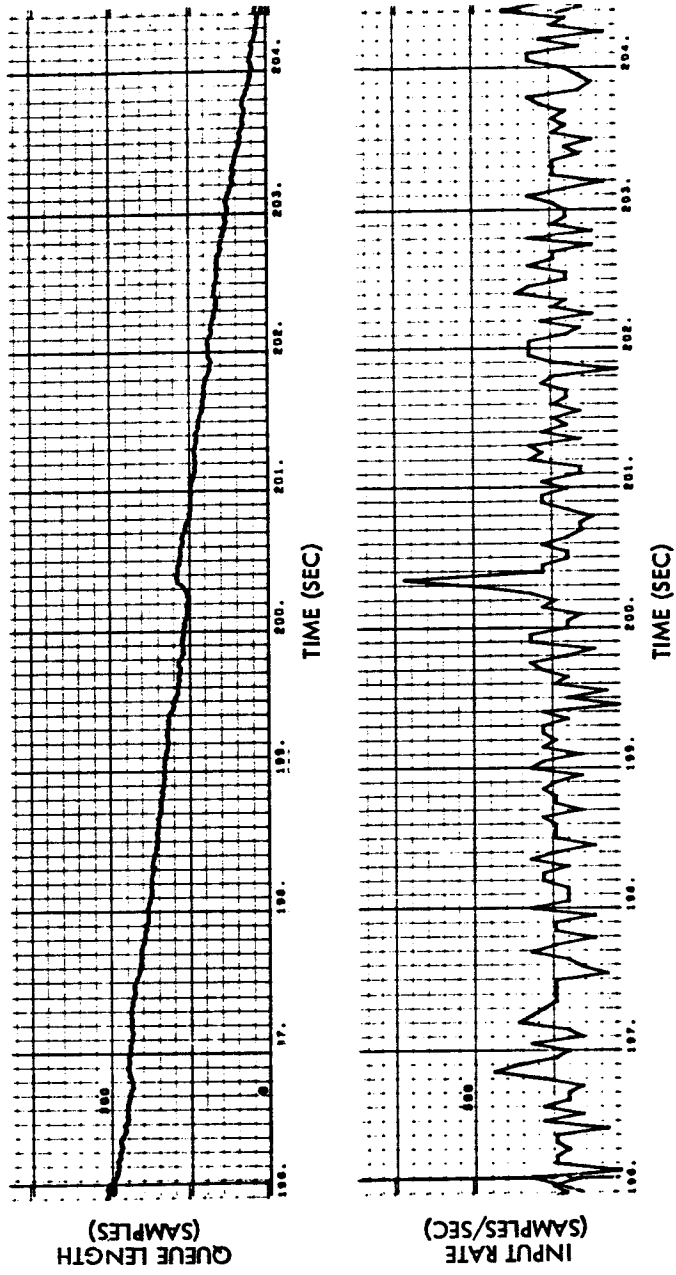


Fig. 4-8 (Cont'd) Queue Length and Buffer Input Arrival Rate vs Time, Run S6-09

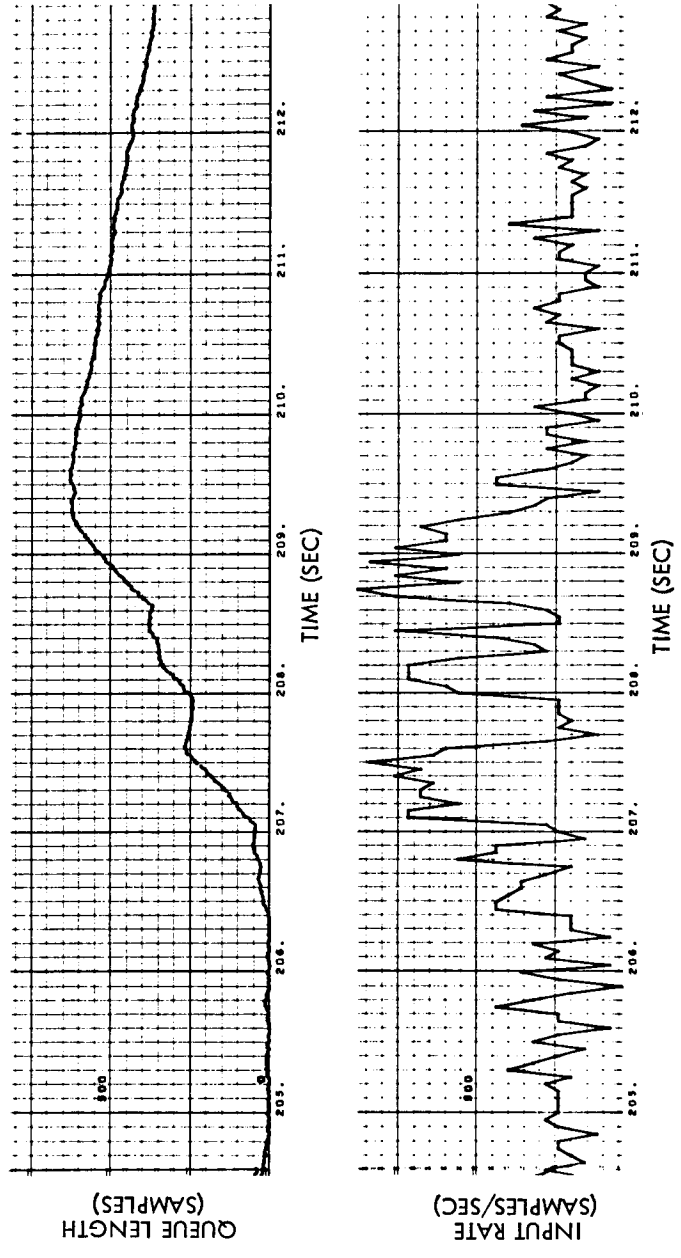


Fig. 4-8 (Cont'd) Queue Length and Buffer Input Arrival Rate vs Time, Run S6-09

(This page intentionally left blank.)

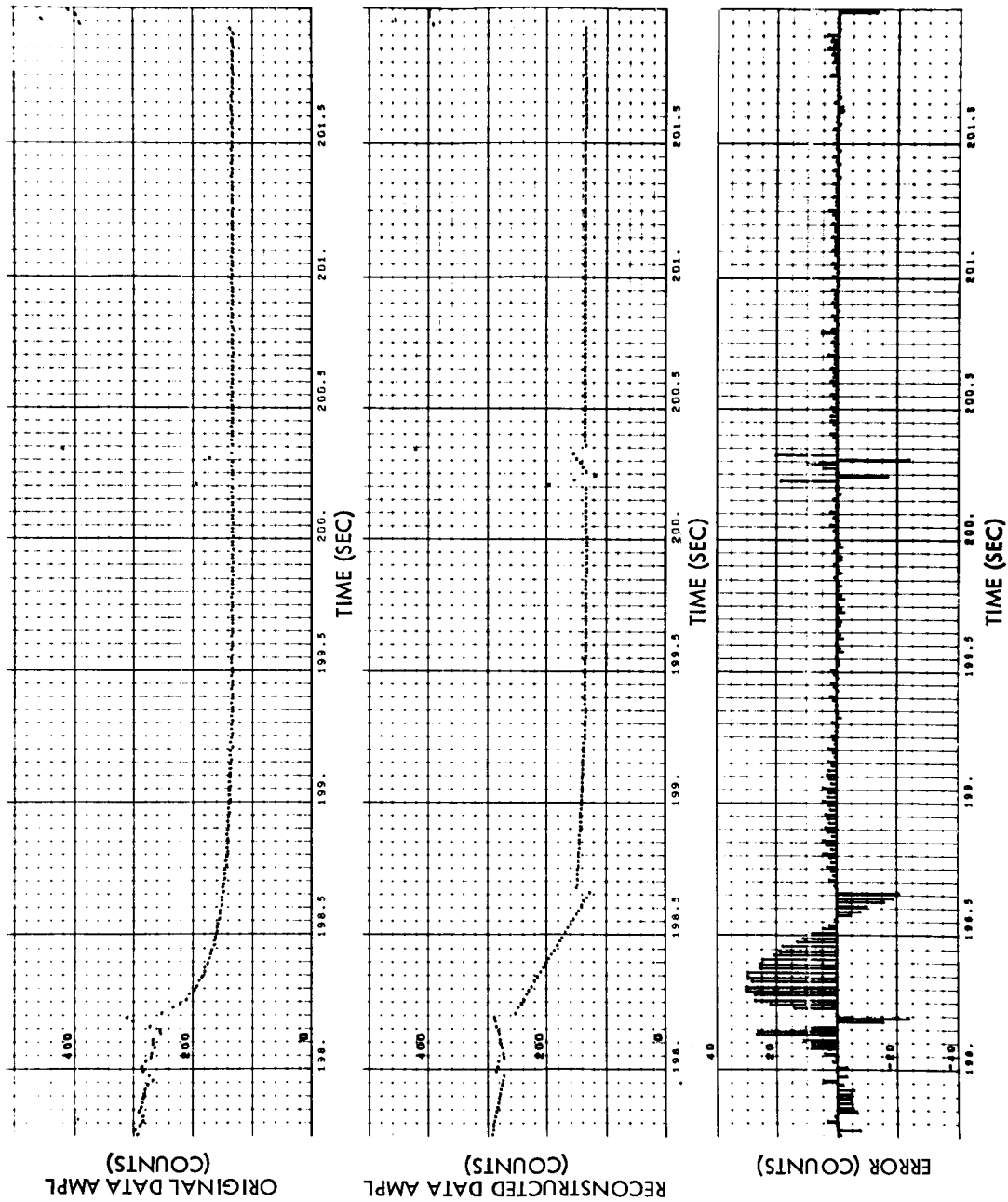


Fig. 4-9a Sensor 9 Original Data, Reconstructed Data, and Error vs Time, Run S6-08

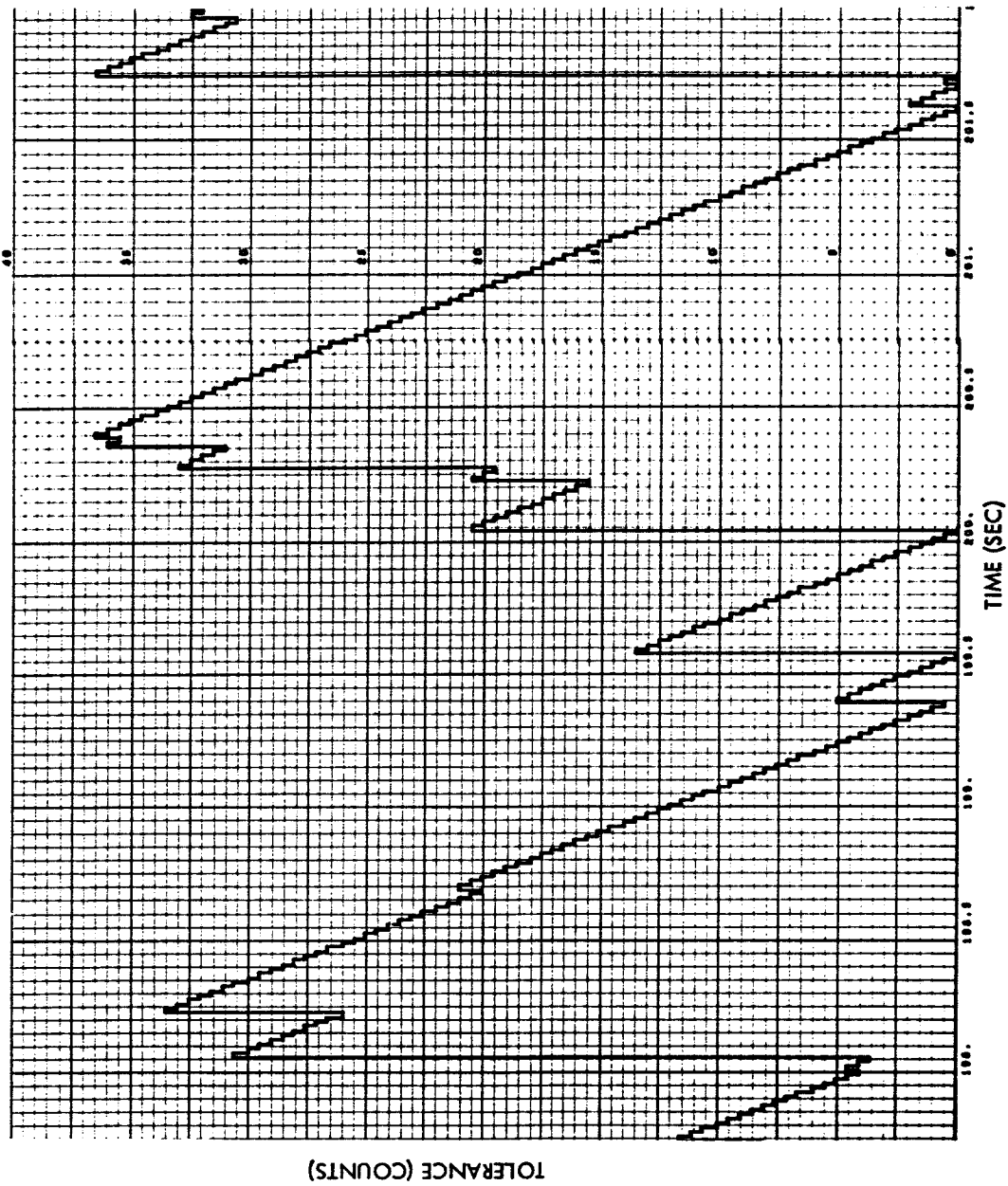


Fig. 4-9b Sensor 9 Tolerance vs Time, Run S6-08

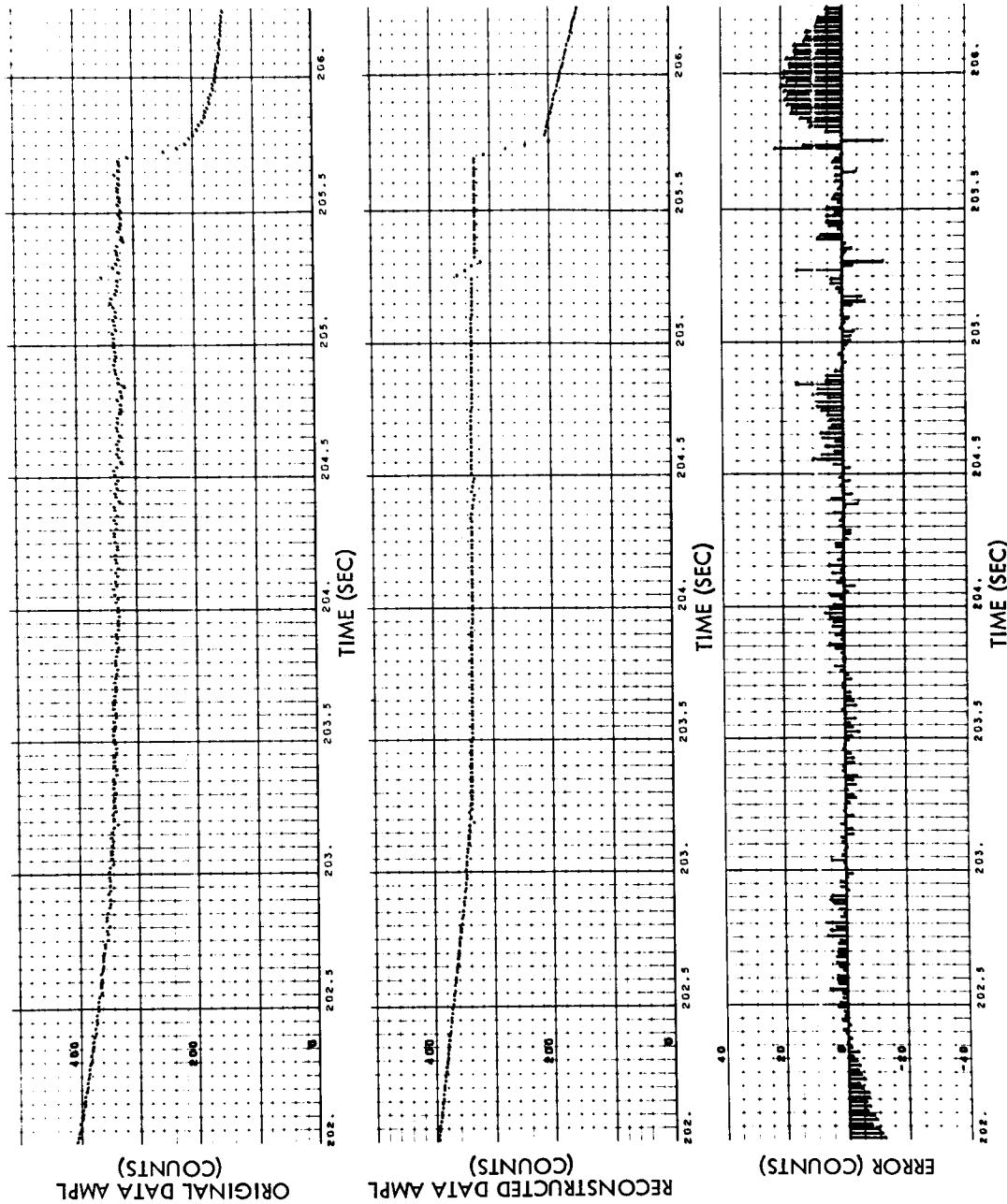


Fig. 4-9a (Cont'd) Sensor 9 Original Data, Reconstructed Data, and Error vs Time, Run S6-08

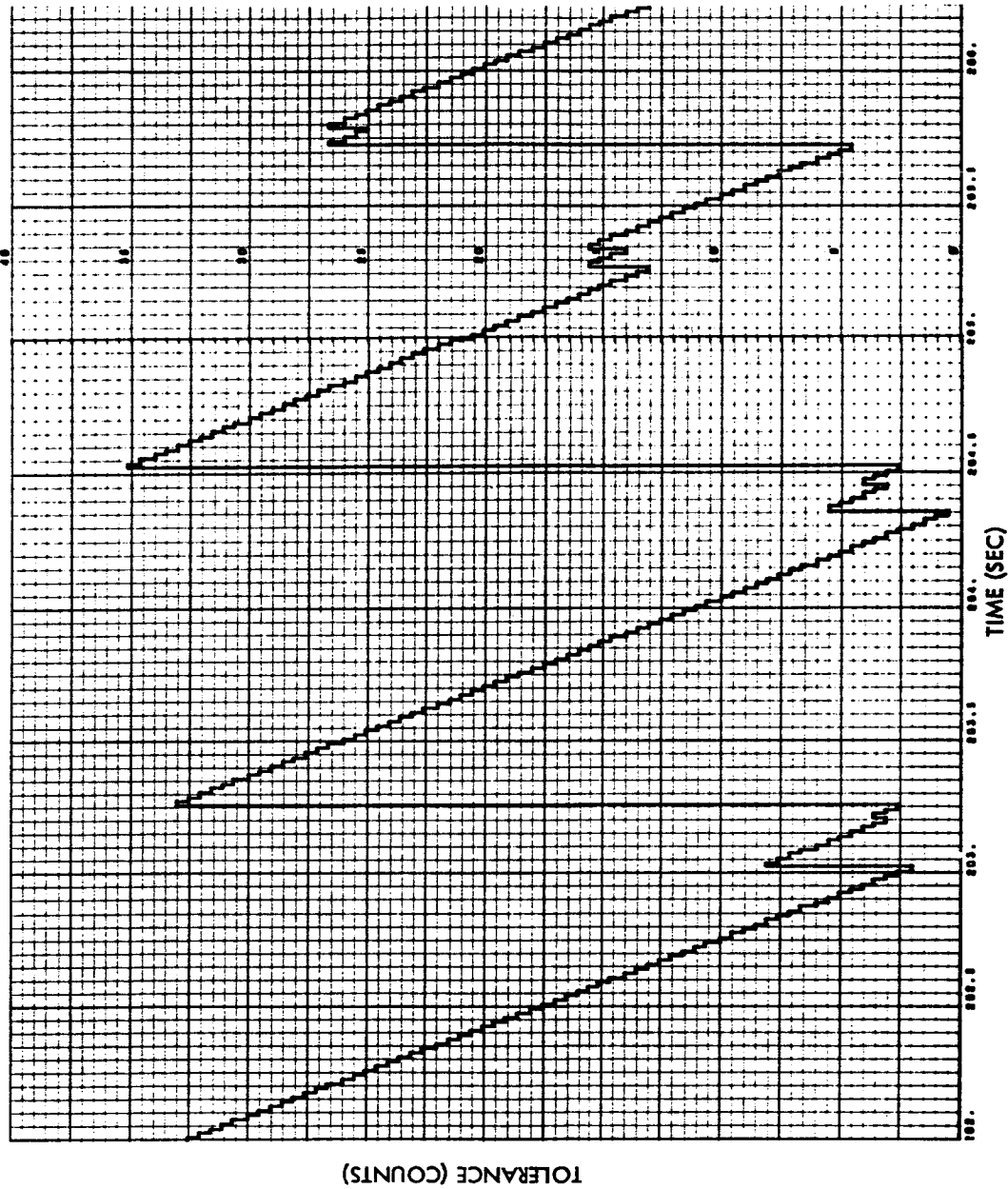


Fig. 4-9b (Cont'd) Sensor 9 Tolerance vs Time, Run S6-08

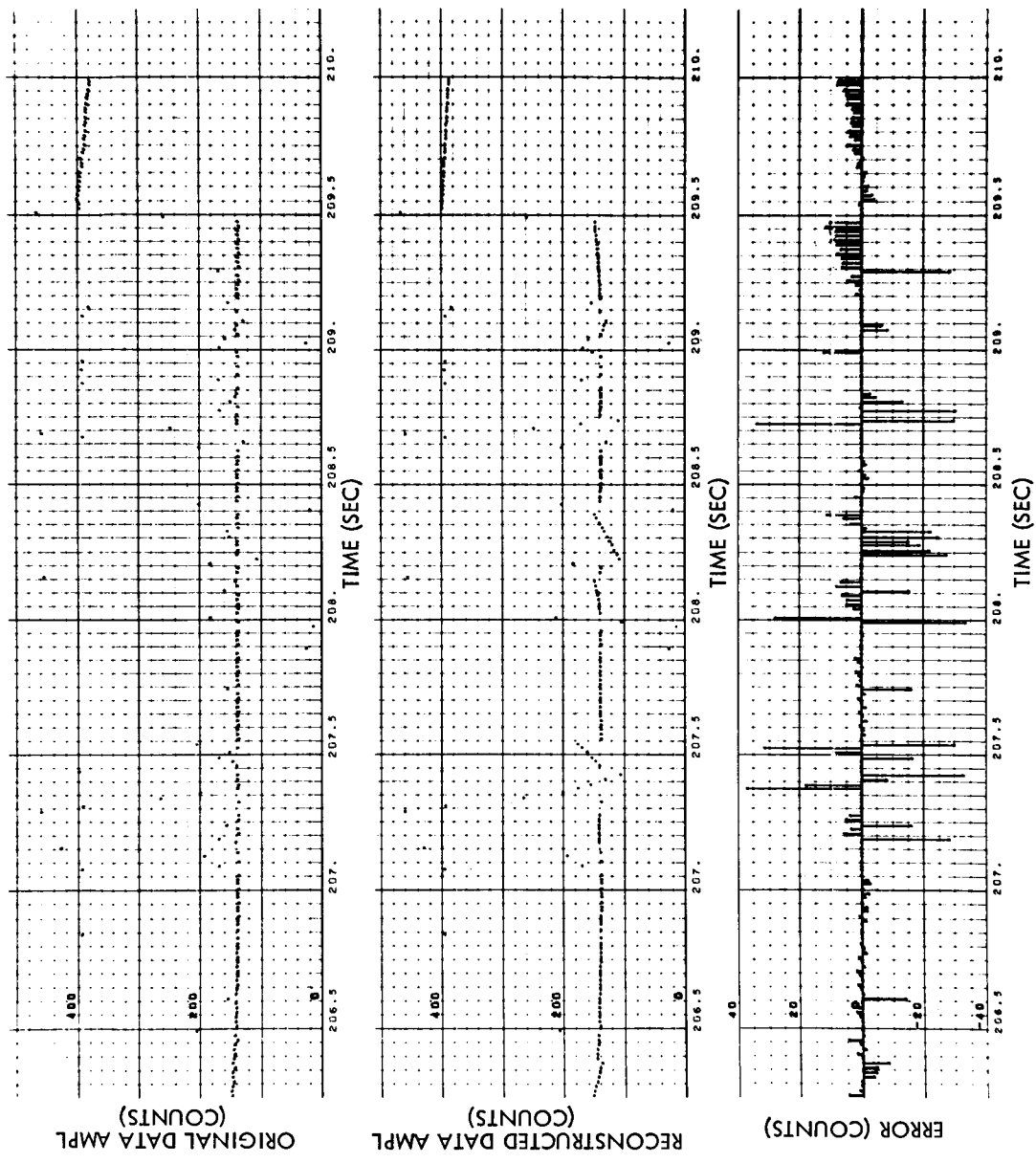


Fig. 4-9a (Cont'd) Sensor 9 Original Data, Reconstructed Data, and Error vs Time, Run S6-08

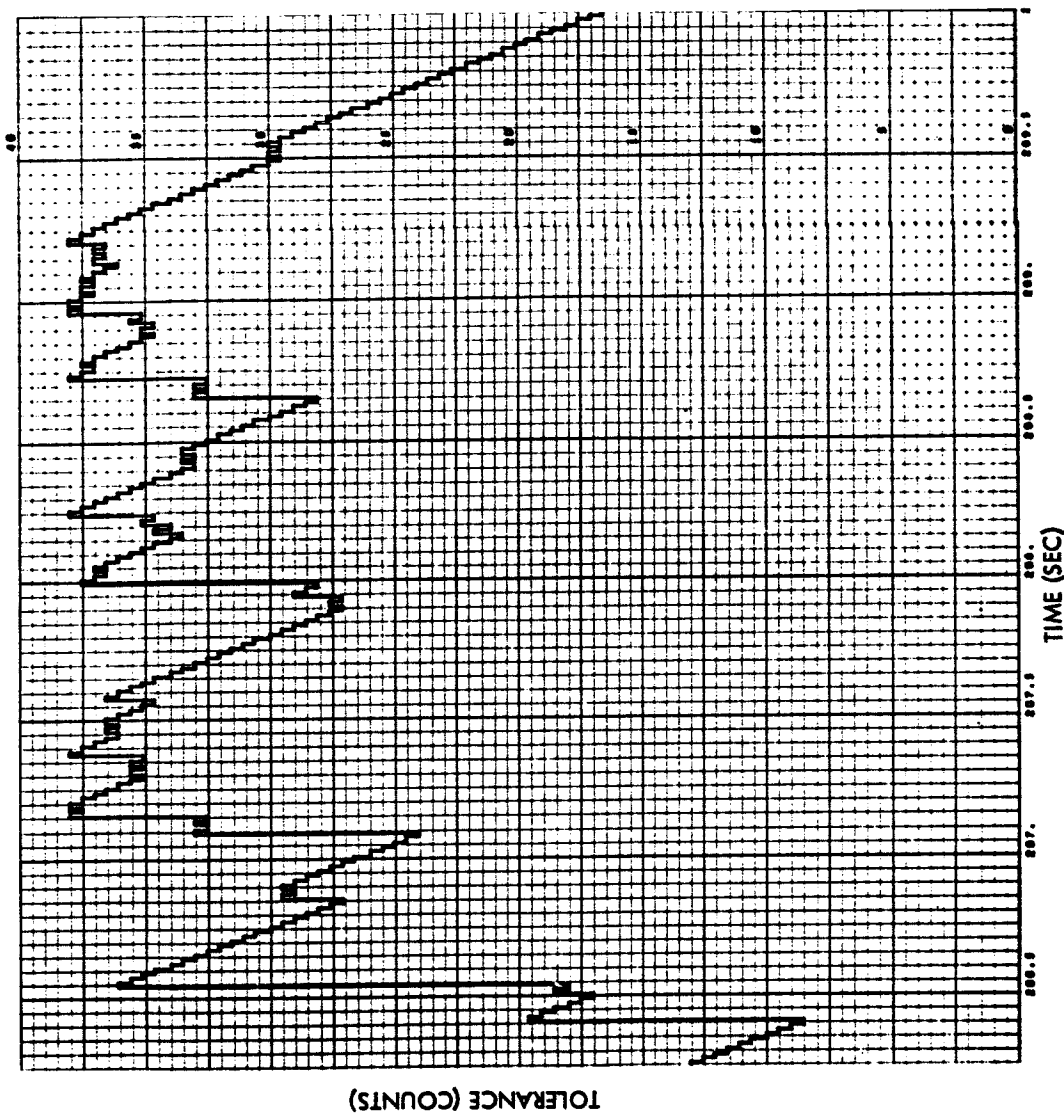


Fig. 4-9b (Cont'd) Sensor 9 Tolerance vs Time, Run S6-08

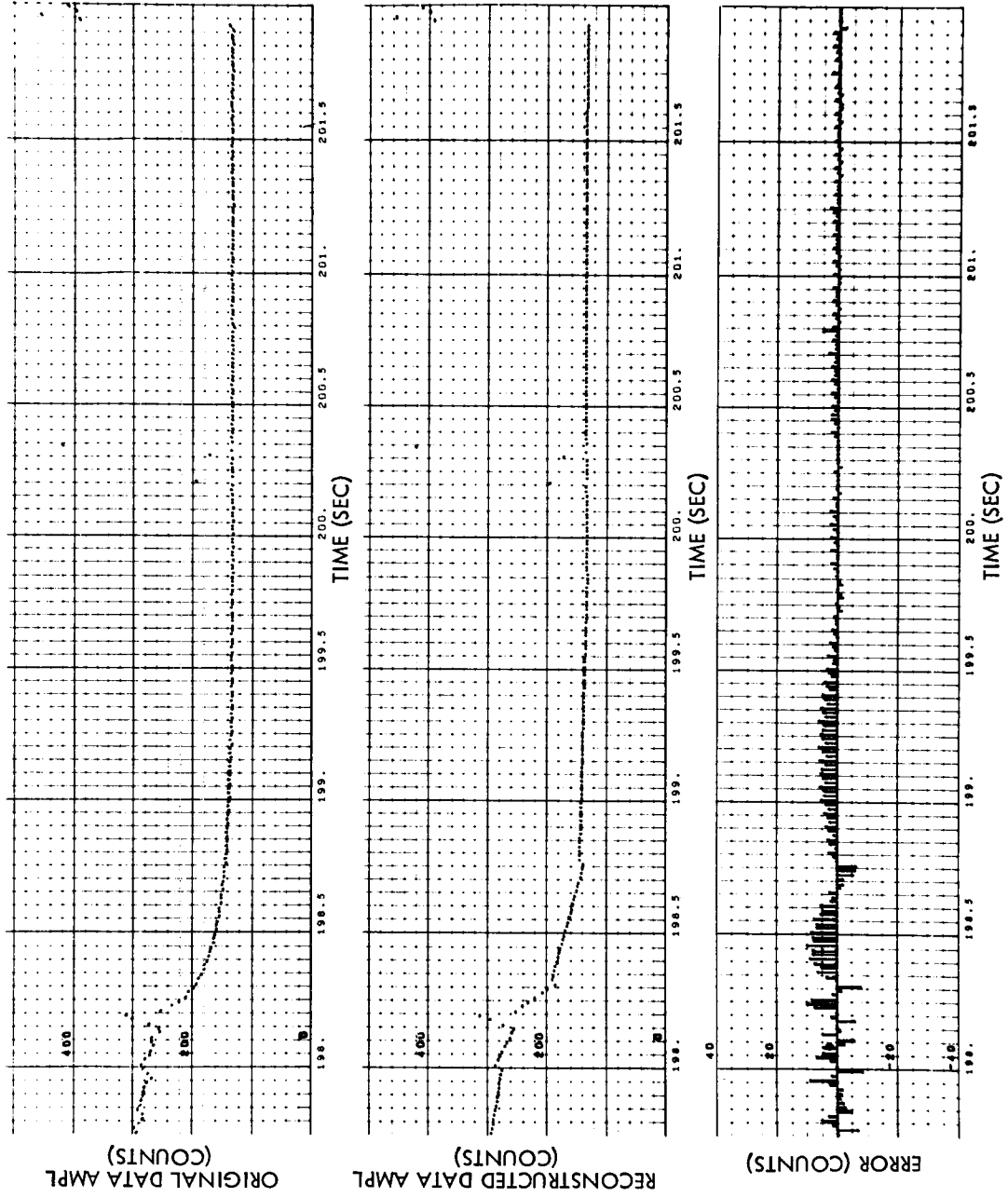


Fig. 4-10a Sensor 9 Original Data, Reconstructed Data, and Error vs Time, Run S6-09

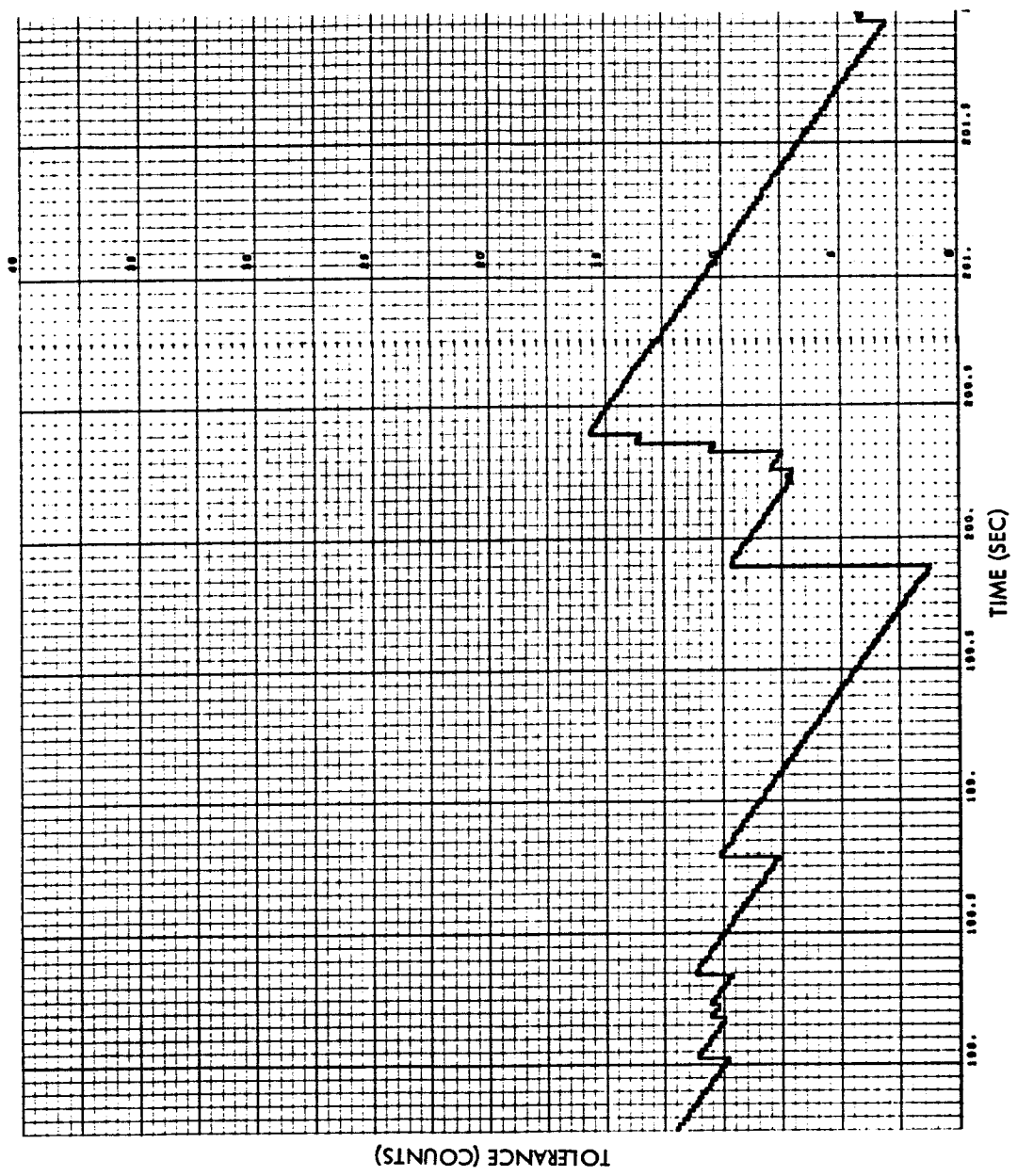


Fig. 4-10b Sensor 9 Tolerance vs Time, Run S6-09

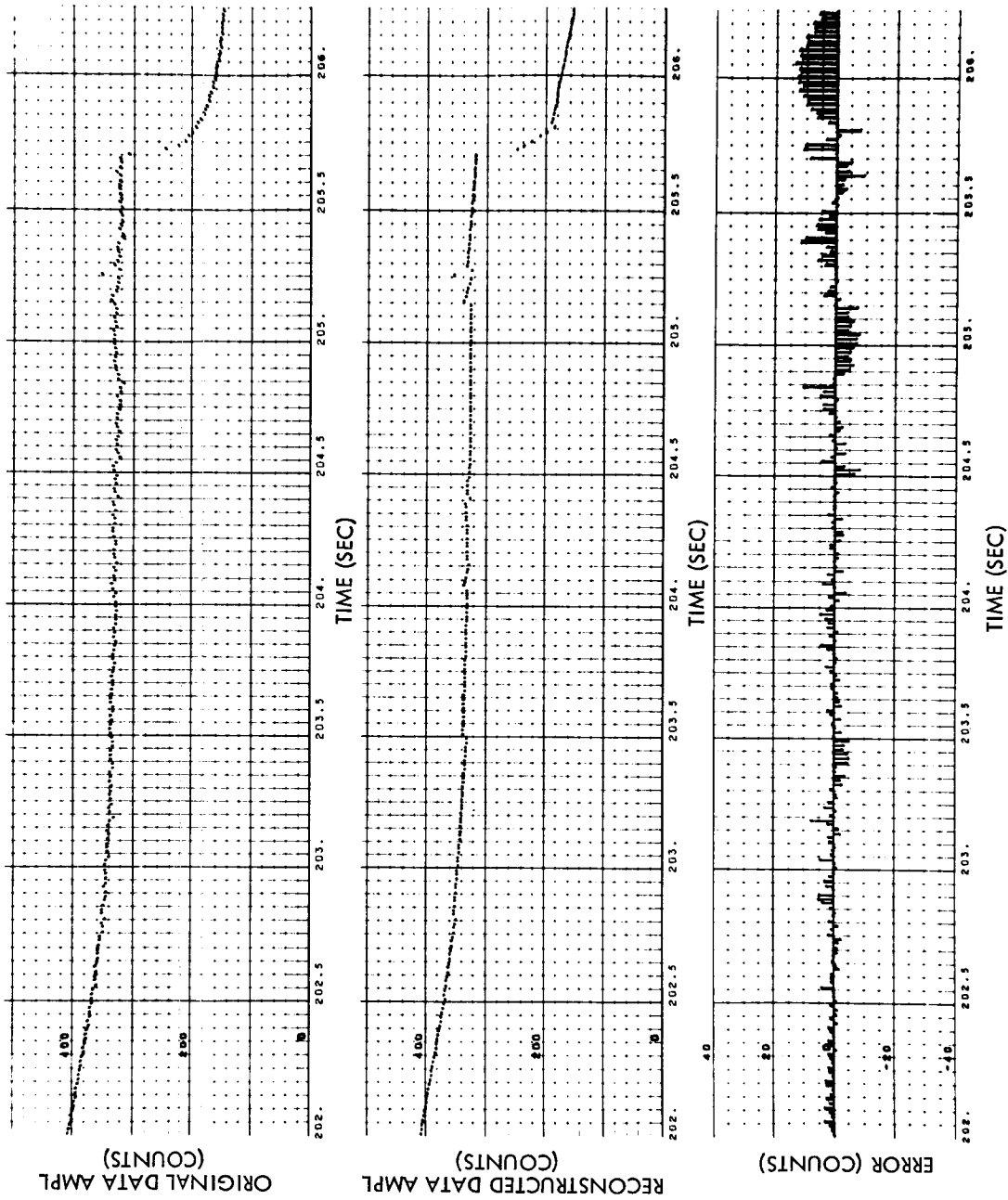


Fig. 4-10a (Cont'd) Sensor 9 Original Data, Reconstructed Data,
and Error vs Time, Run S6-09

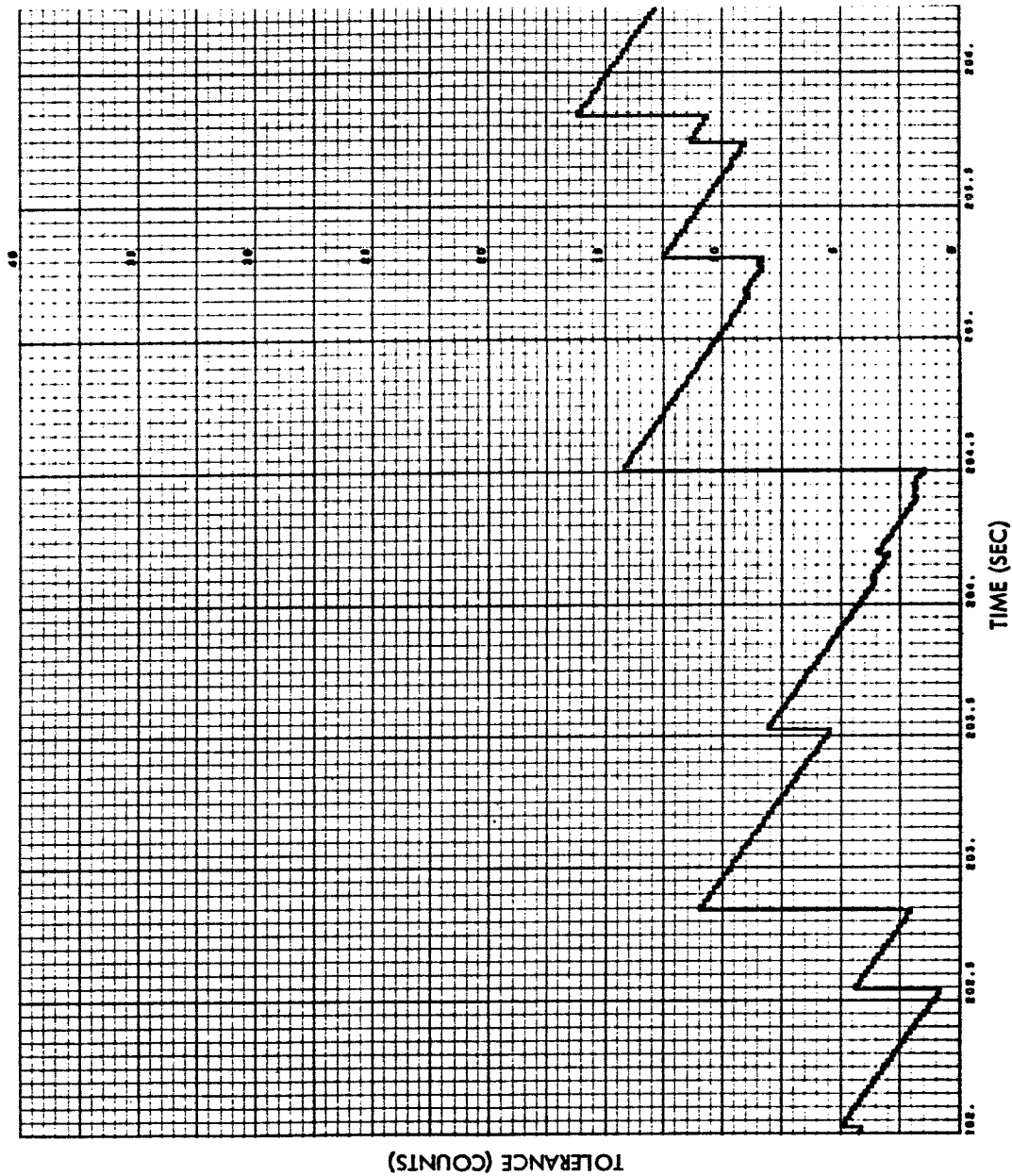


Fig. 4-10b (Cont'd) Sensor 9 Tolerance vs Time, Run S6-09



Fig. 4-10a (Cont'd) Sensor 9 Original Data, Reconstructed Data, and Error vs Time, Run S6-09

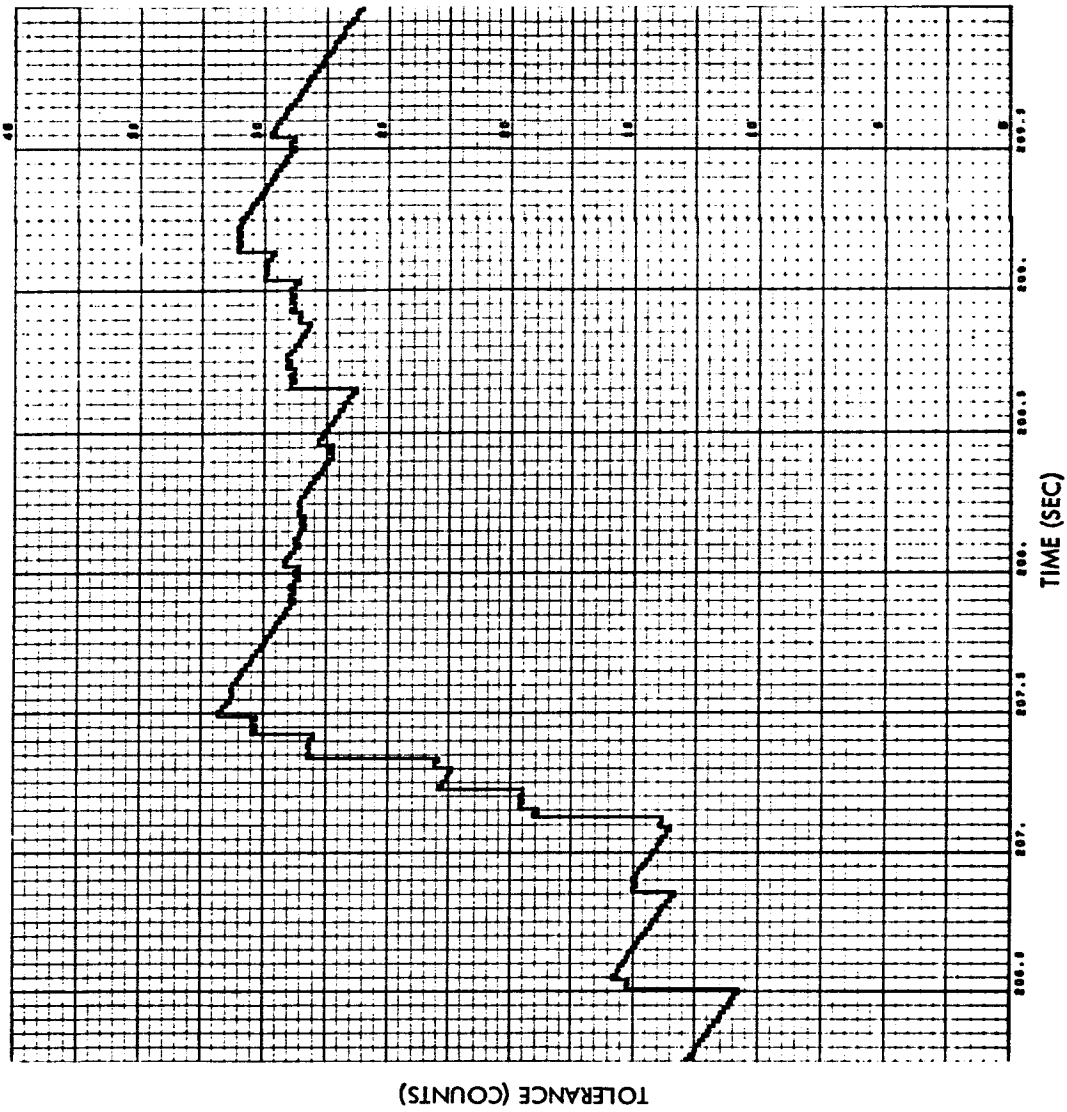


Fig. 4-10b (Cont'd) Sensor 9 Tolerance vs Time, Run S6-09

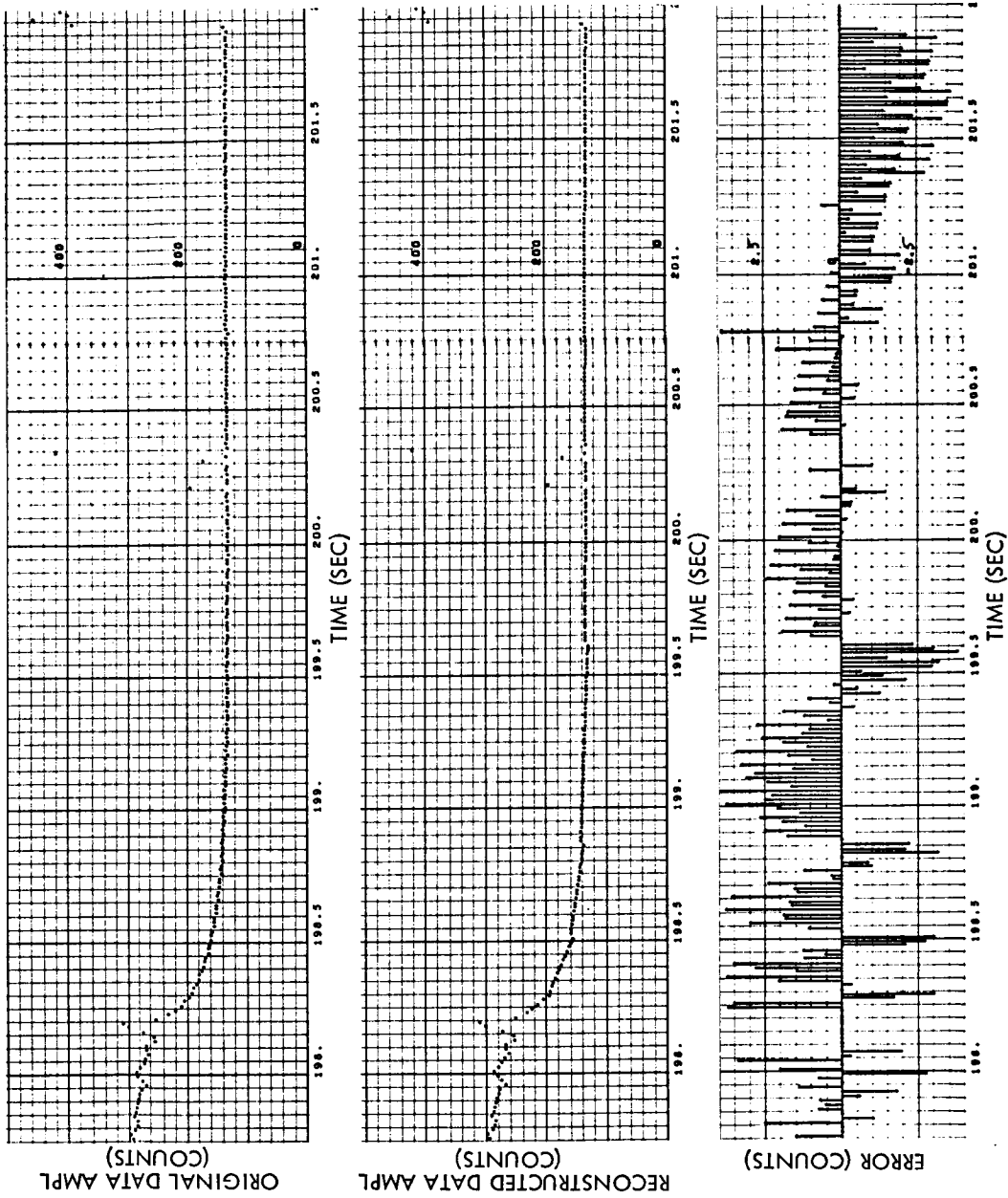


Fig. 4-11 Sensor 9 Original Data, Reconstructed Data, and Error vs Time, Run S6-07

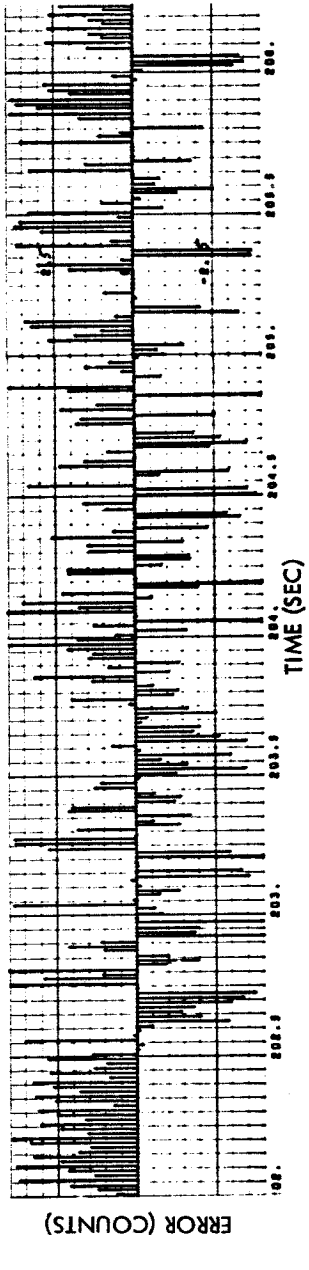
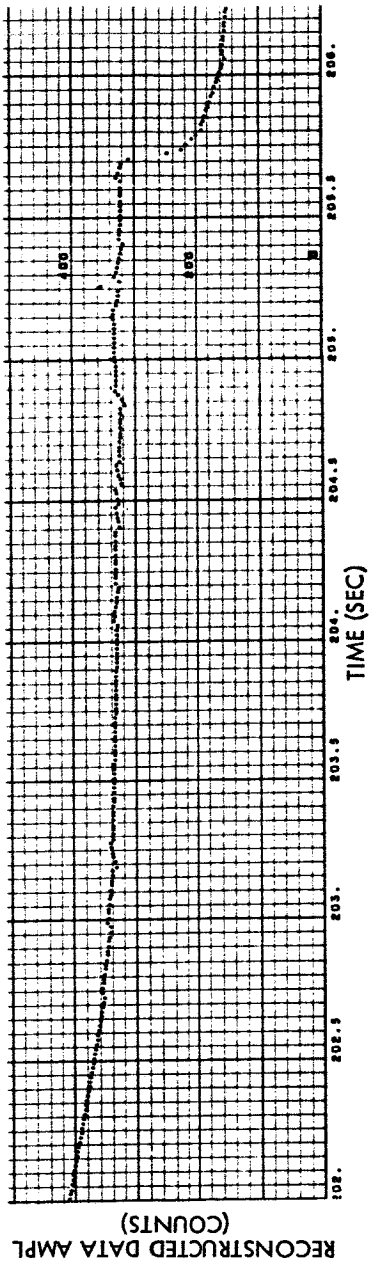
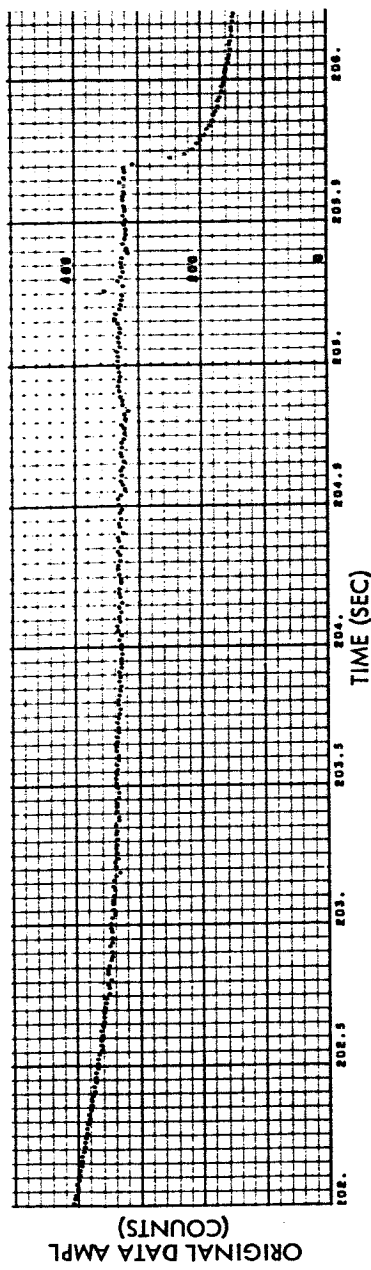


Fig. 4-11 (Cont'd) Sensor 9 Original Data, Reconstructed Data, and Error vs Time, Run S6-07

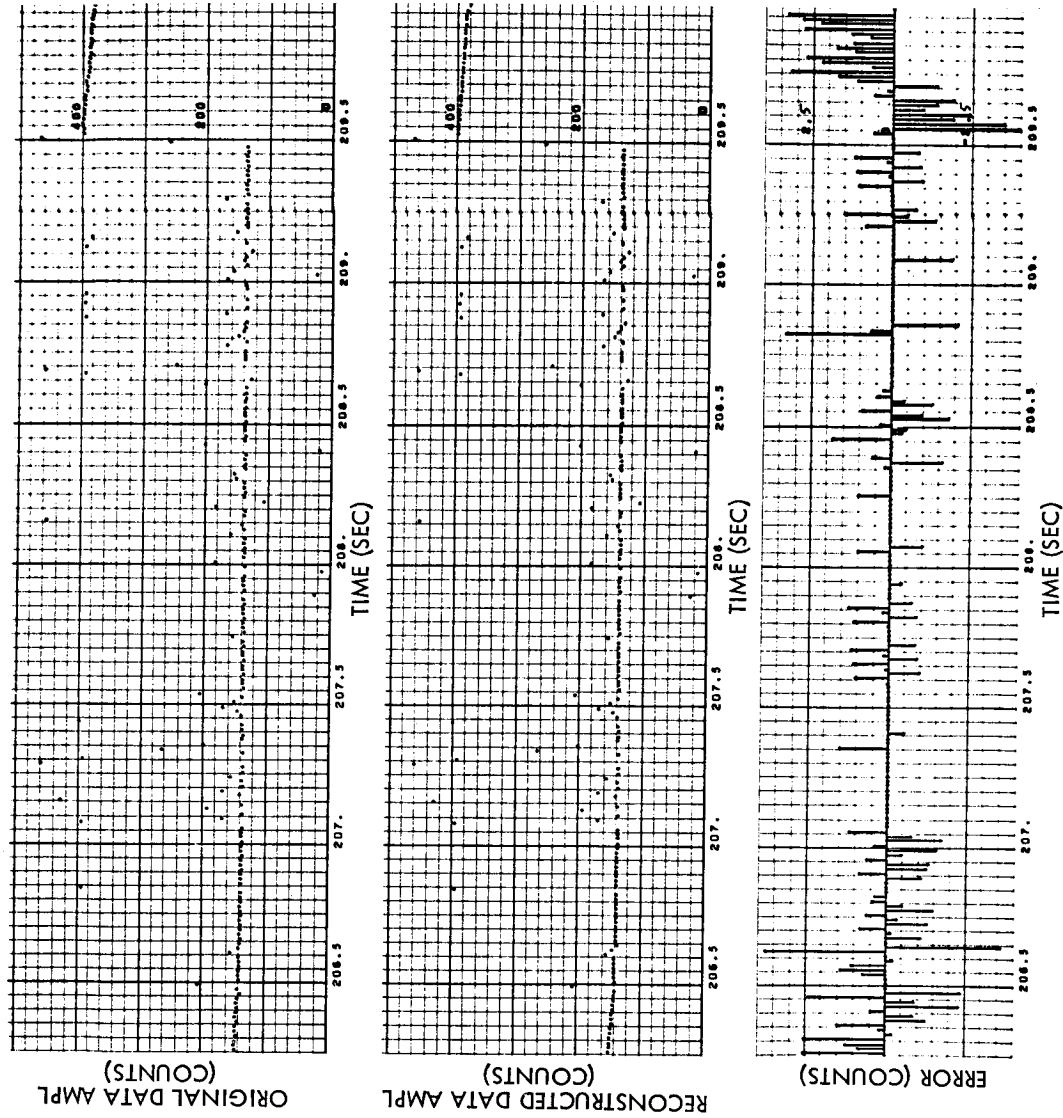


Fig. 4-11 (Cont'd) Sensor 9 Original Data, Reconstructed Data, and Error vs Time, Run S6-07

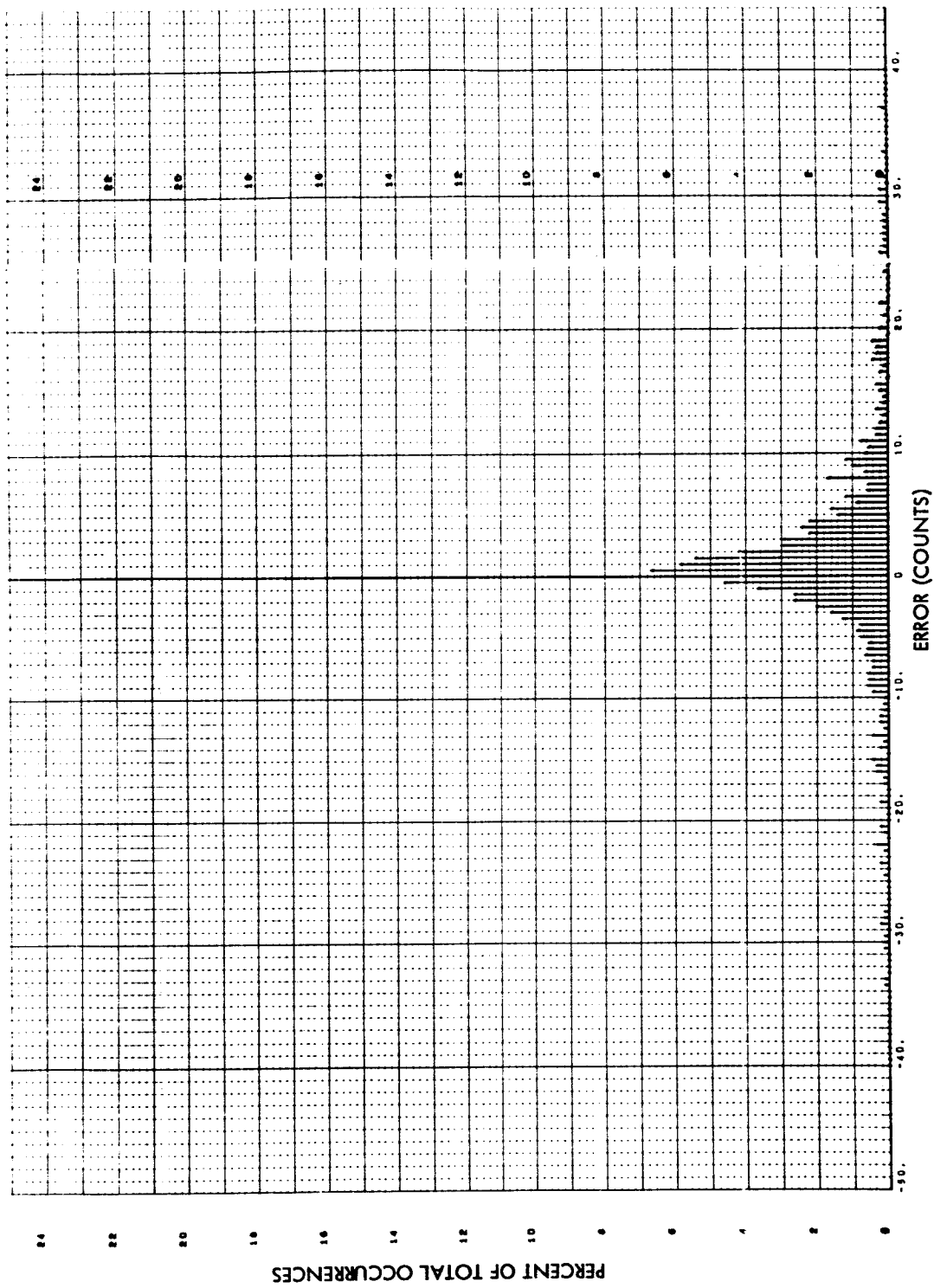


Fig. 4-12 Sensor 9 Error Histogram, Run S6-08

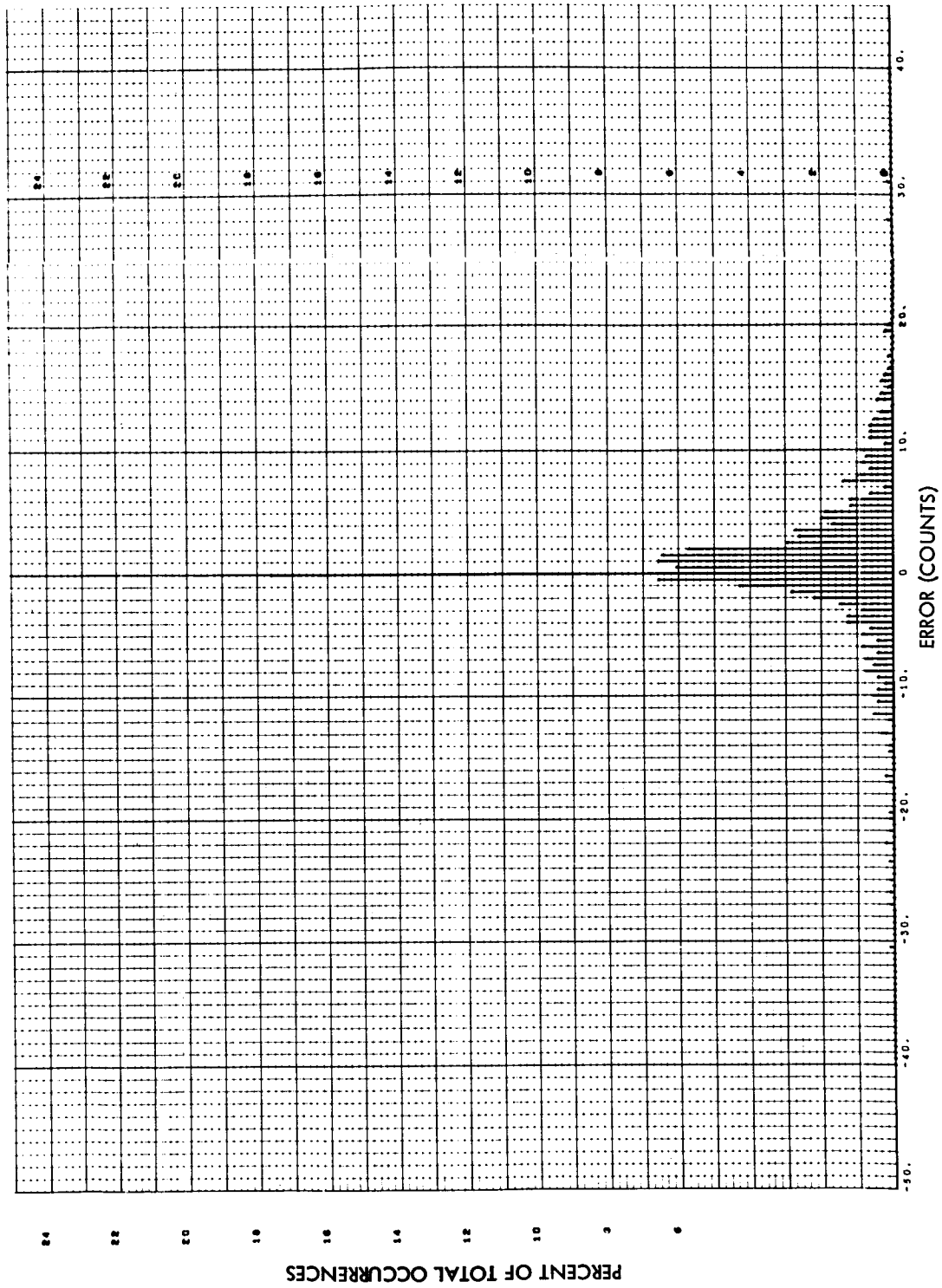


Fig. 4-13 Sensor 9 Error Histogram, Run S6-09

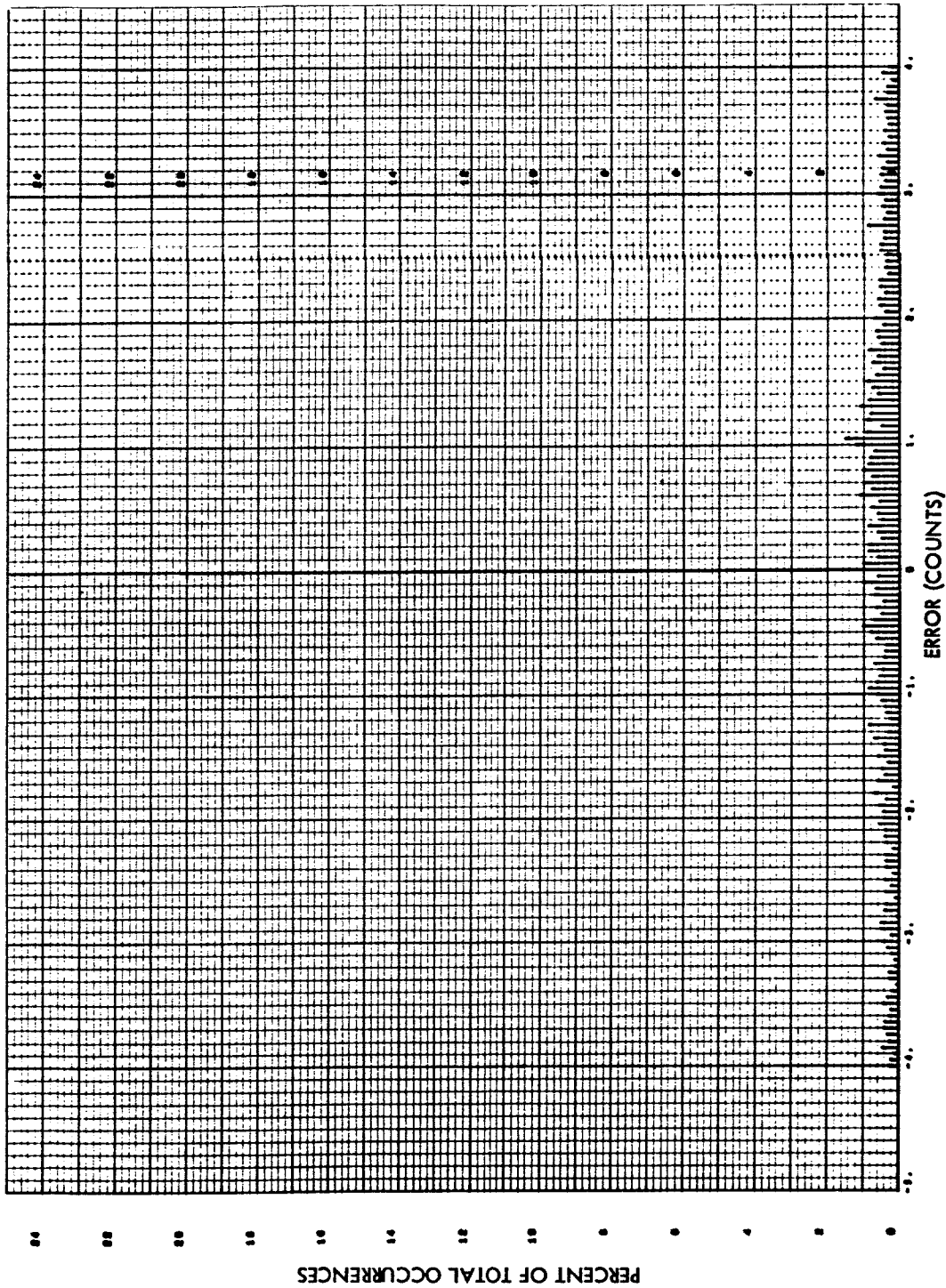


Fig. 4-14 Sensor 9 Error Histogram, Run S6-07

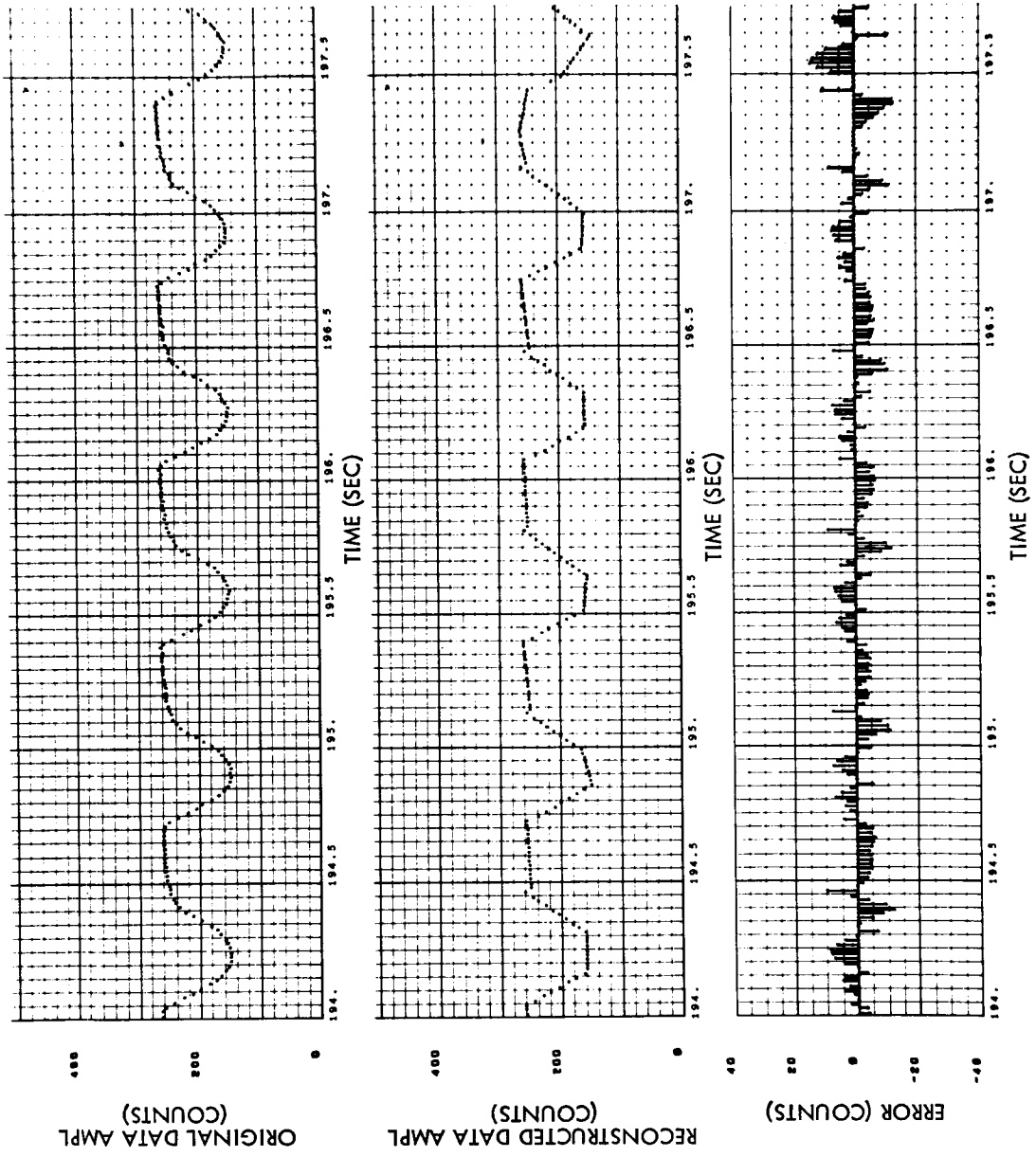


Fig. 4-15a Sensor 11 Original Data, Reconstructed Data, and Error vs Time, Run S6-08

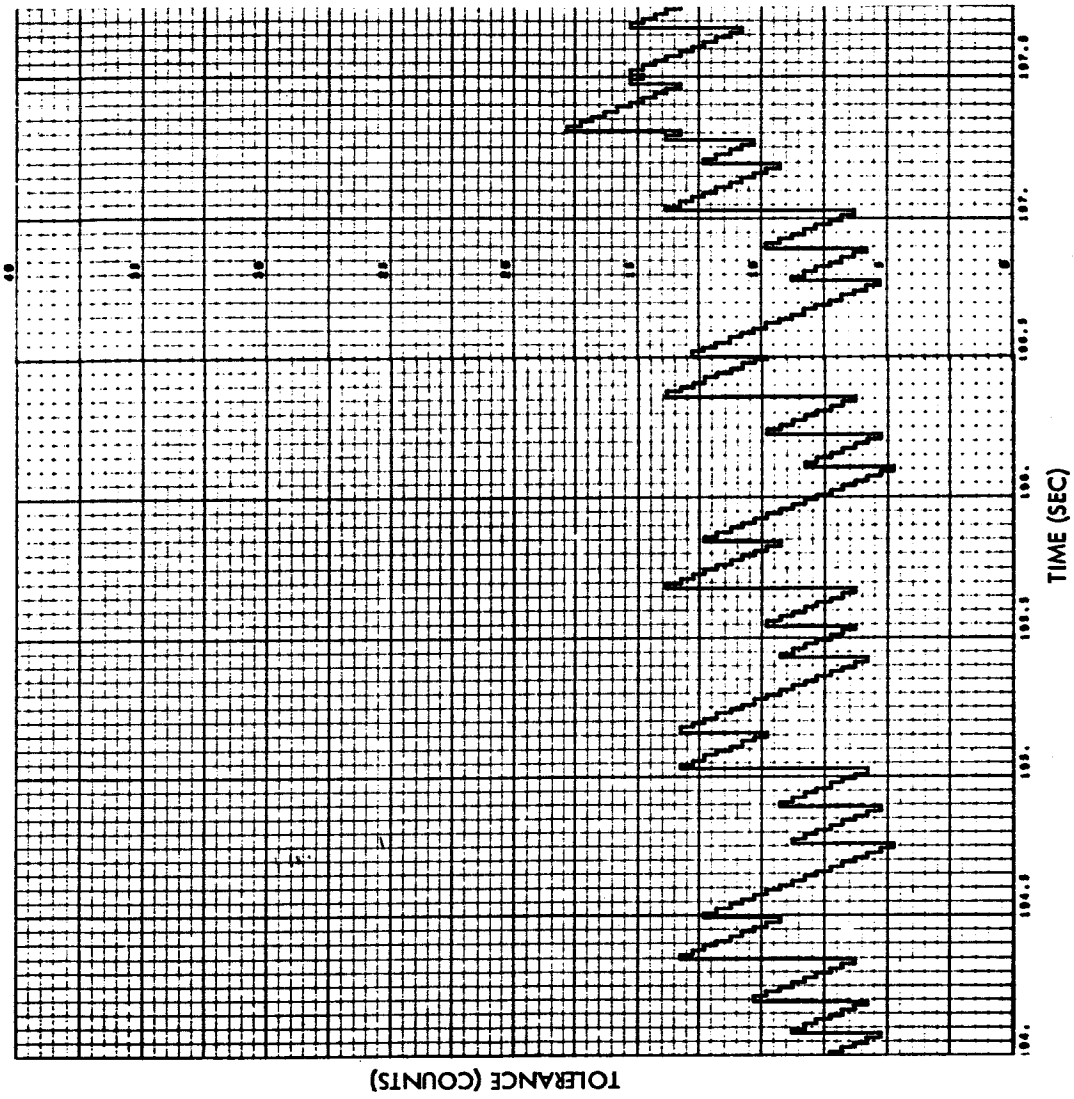


Fig. 4-15b Sensor 11 Tolerance vs Time, Run S6-08

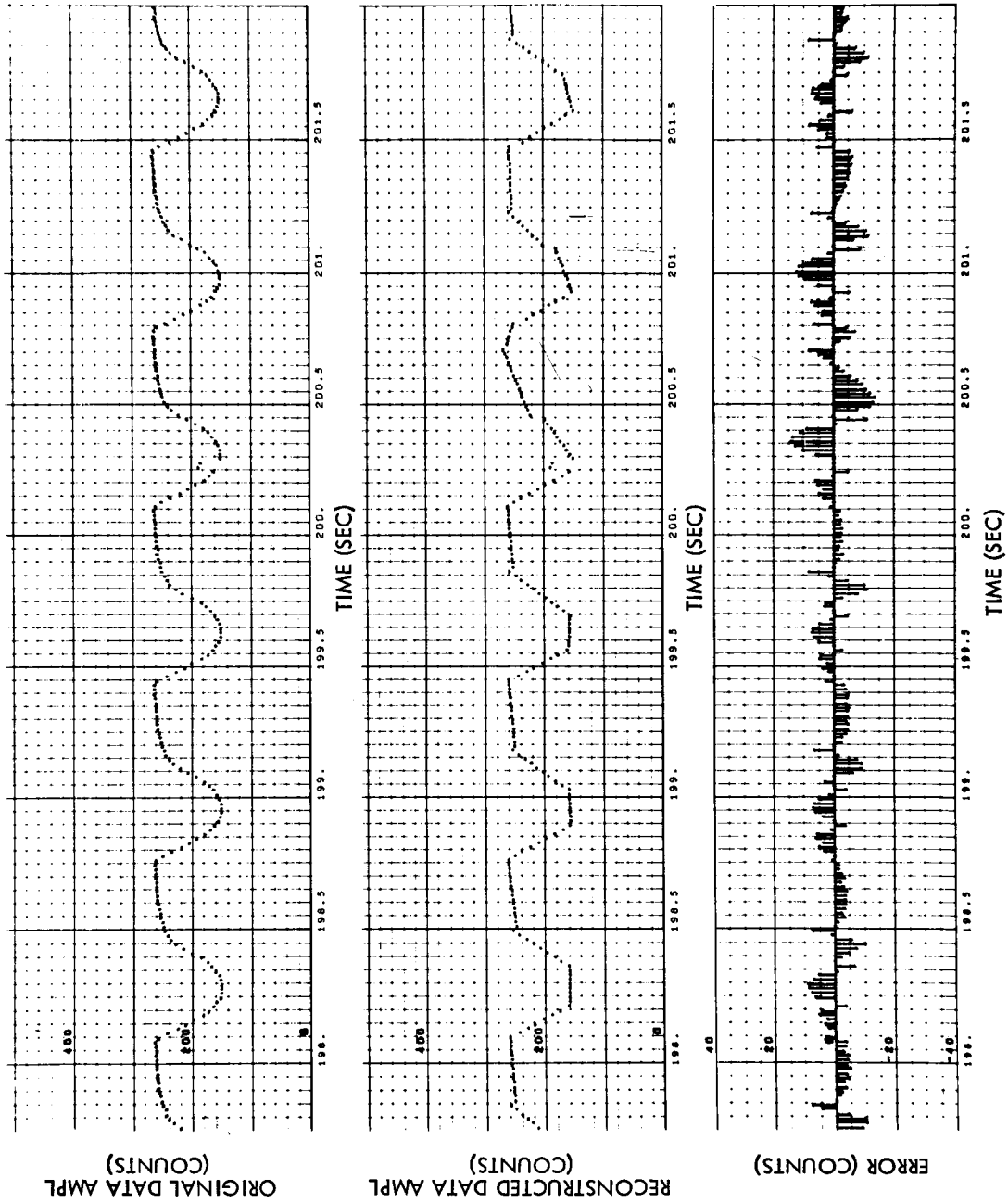


Fig. 4-15a (Cont'd) Sensor 11 Original Data, Reconstructed Data, and Error vs Time, Run S6-08

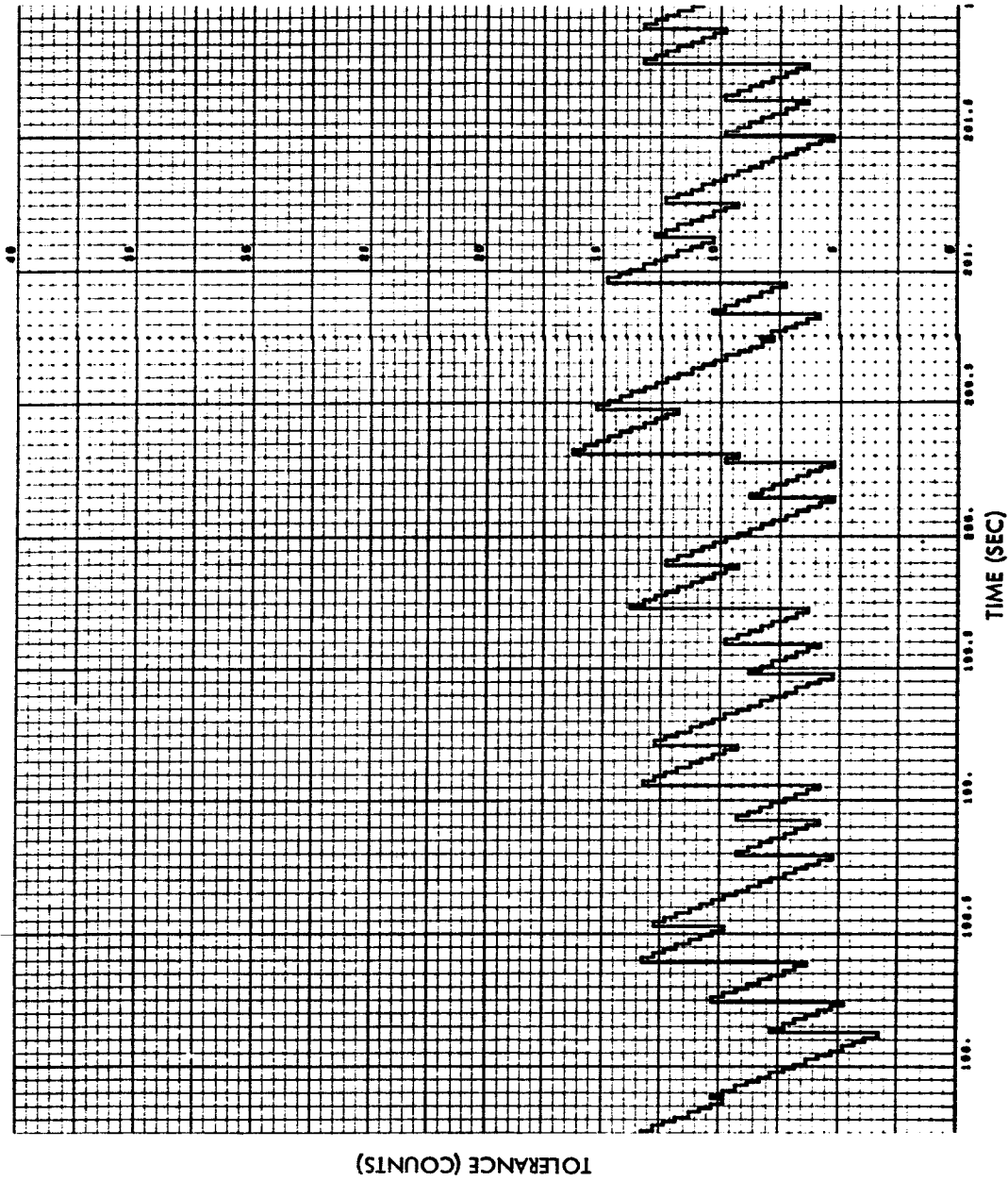


Fig. 4-15b (Cont'd) Sensor 11 Tolerance vs Time, Run S6-08

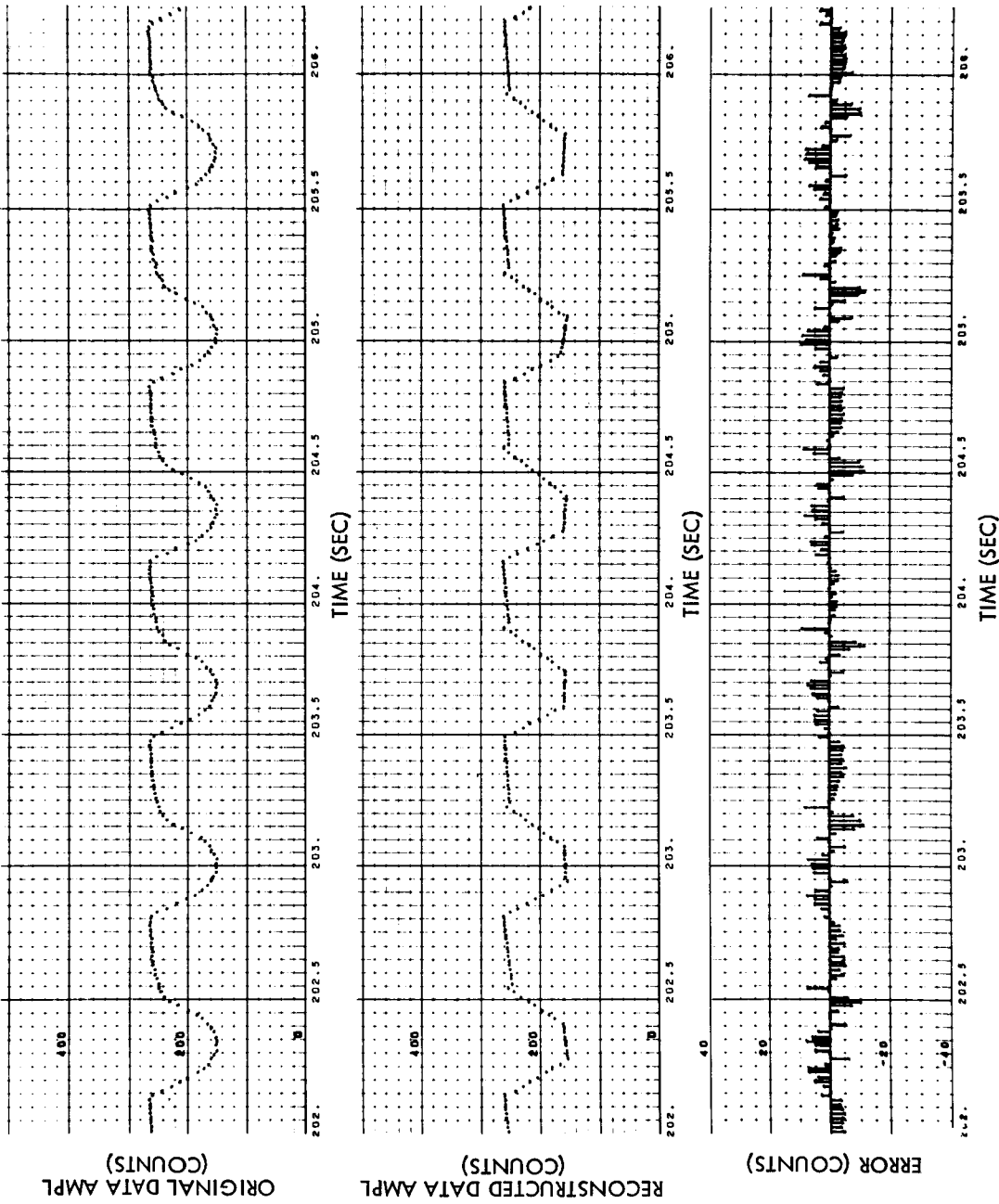


Fig. 4-15a (Cont'd) Sensor 11 Original Data, Reconstructed Data, and Error vs Time, Run S6-08

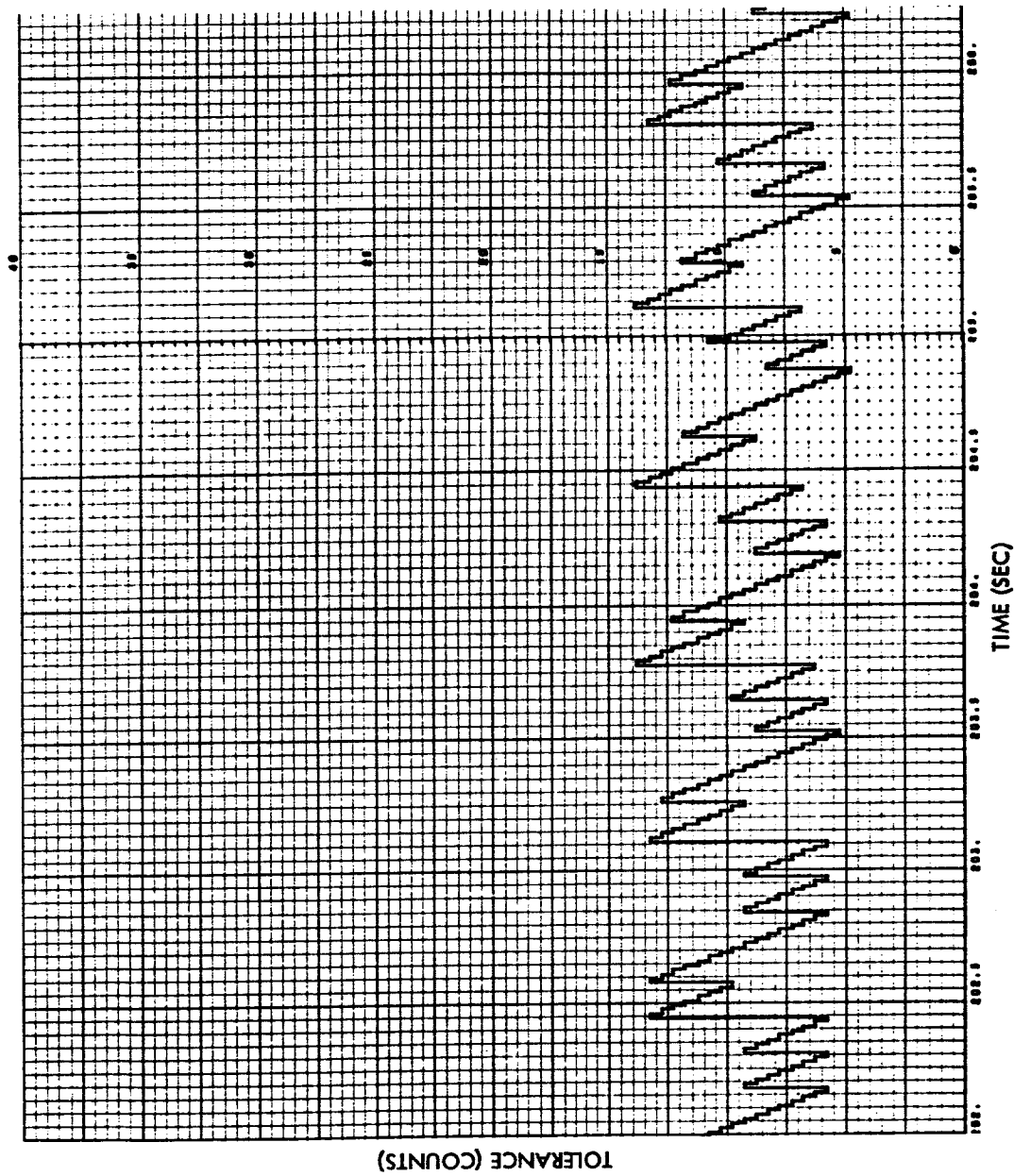


Fig. 4-15b (Cont'd) Sensor 11 Tolerance vs Time, Run S6-08

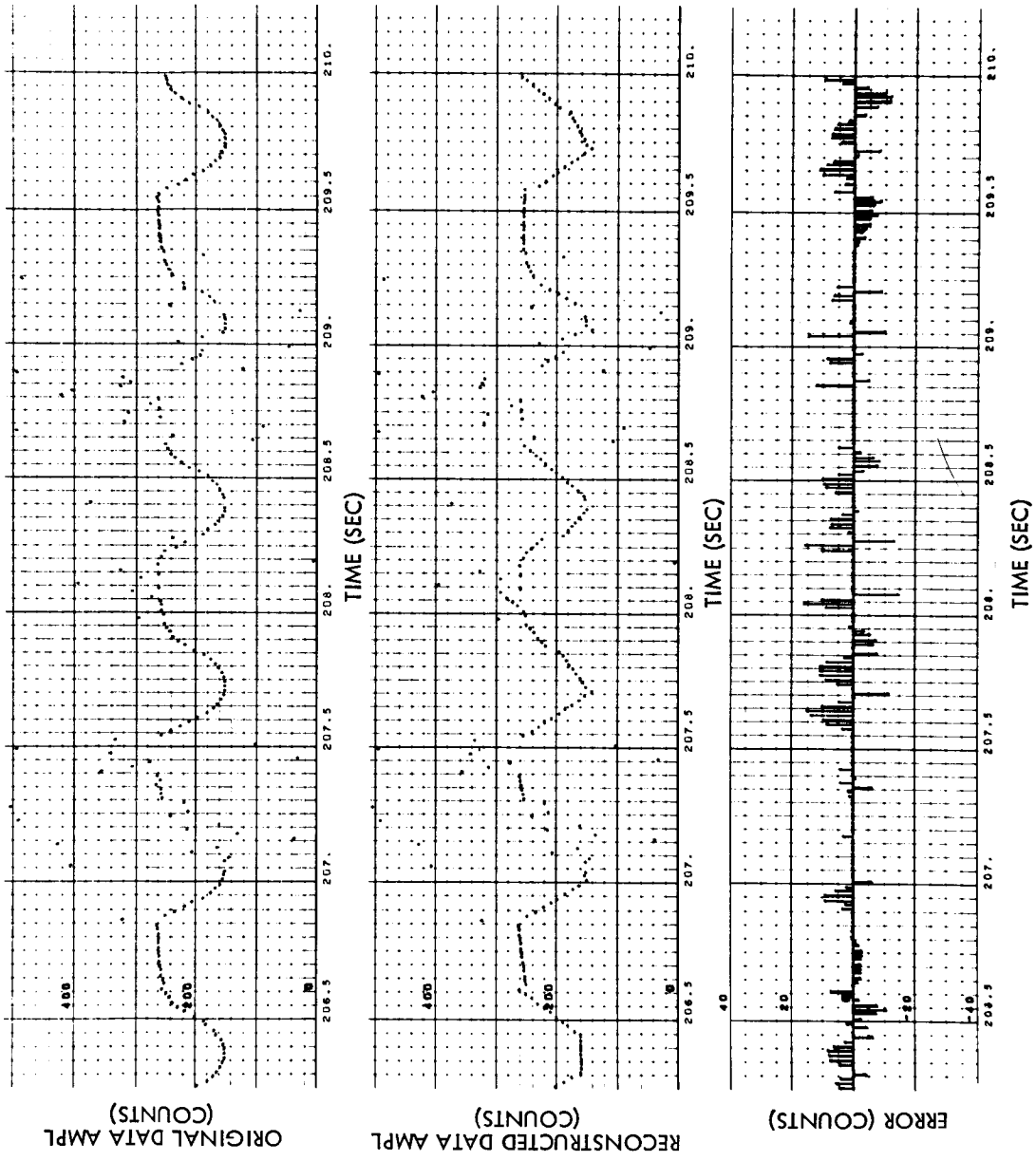


Fig. 4-15a (Cont'd) Sensor 11 Original Data, Reconstructed Data, and Error vs Time, Run S6-08

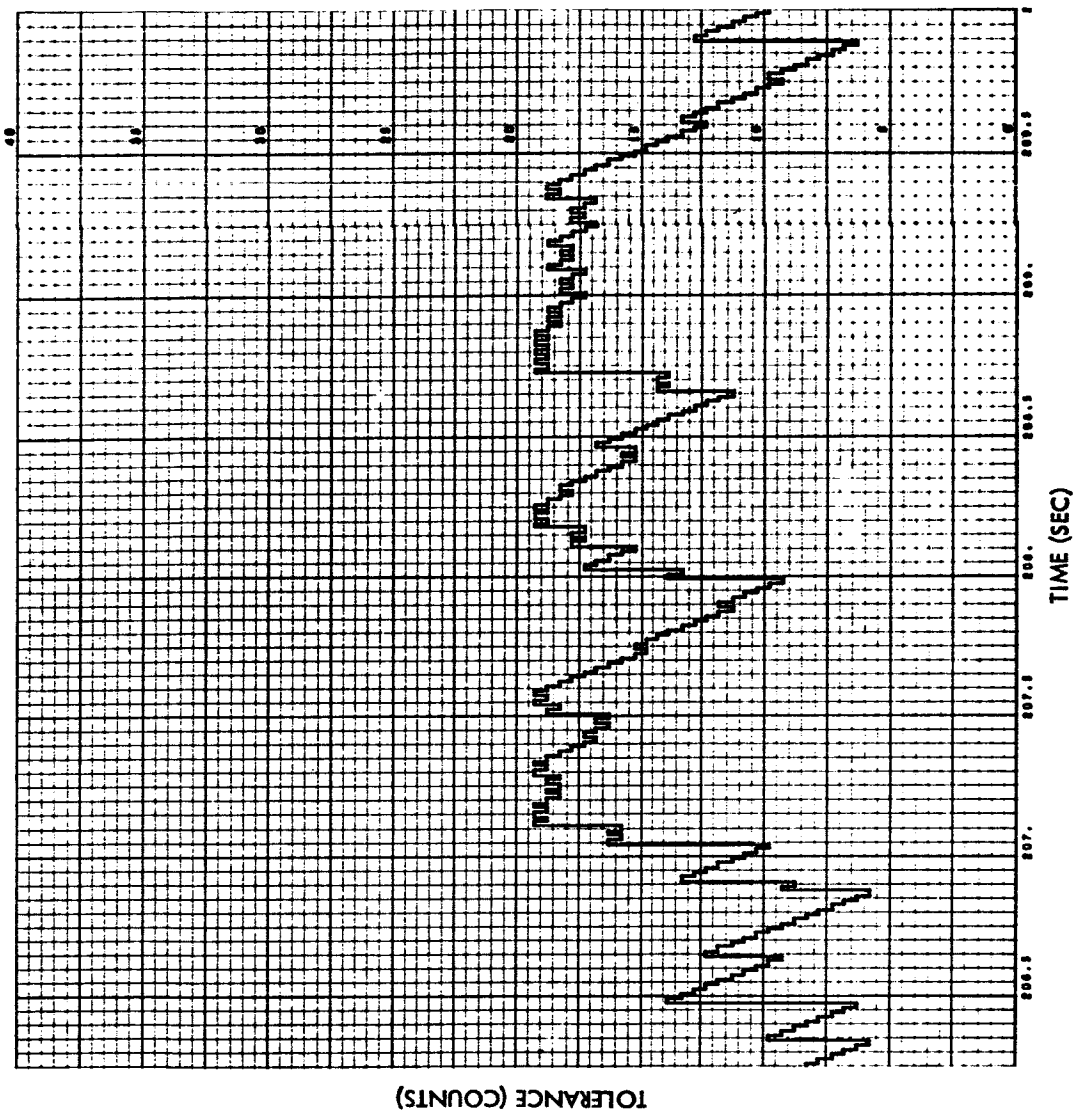


Fig. 4-15b (Cont'd) Sensor 11 Tolerance vs Time, Run S6-08

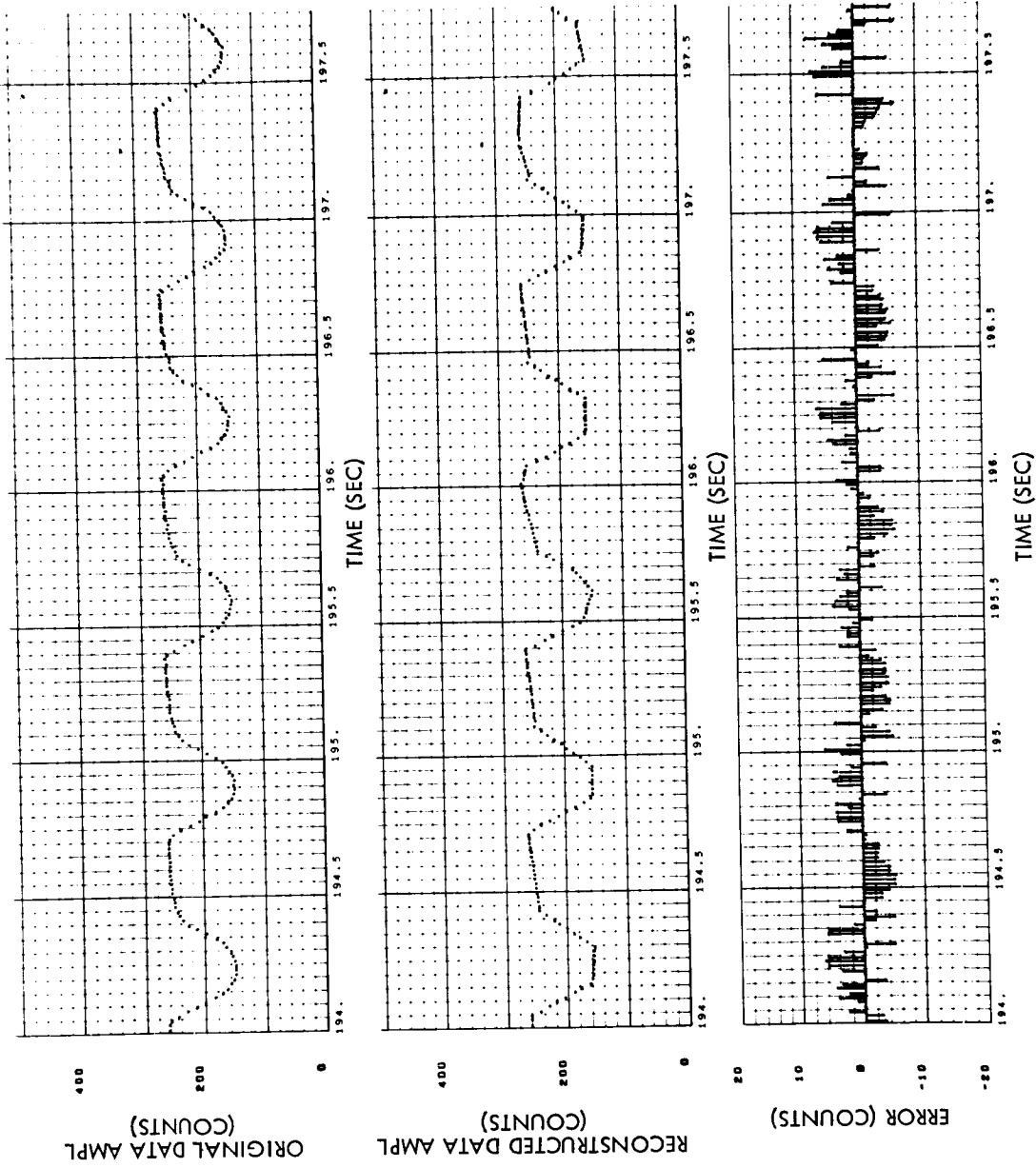


Fig. 4-16a Sensor 11 Original Data, Reconstructed Data, and Error vs Time, Run S6-09

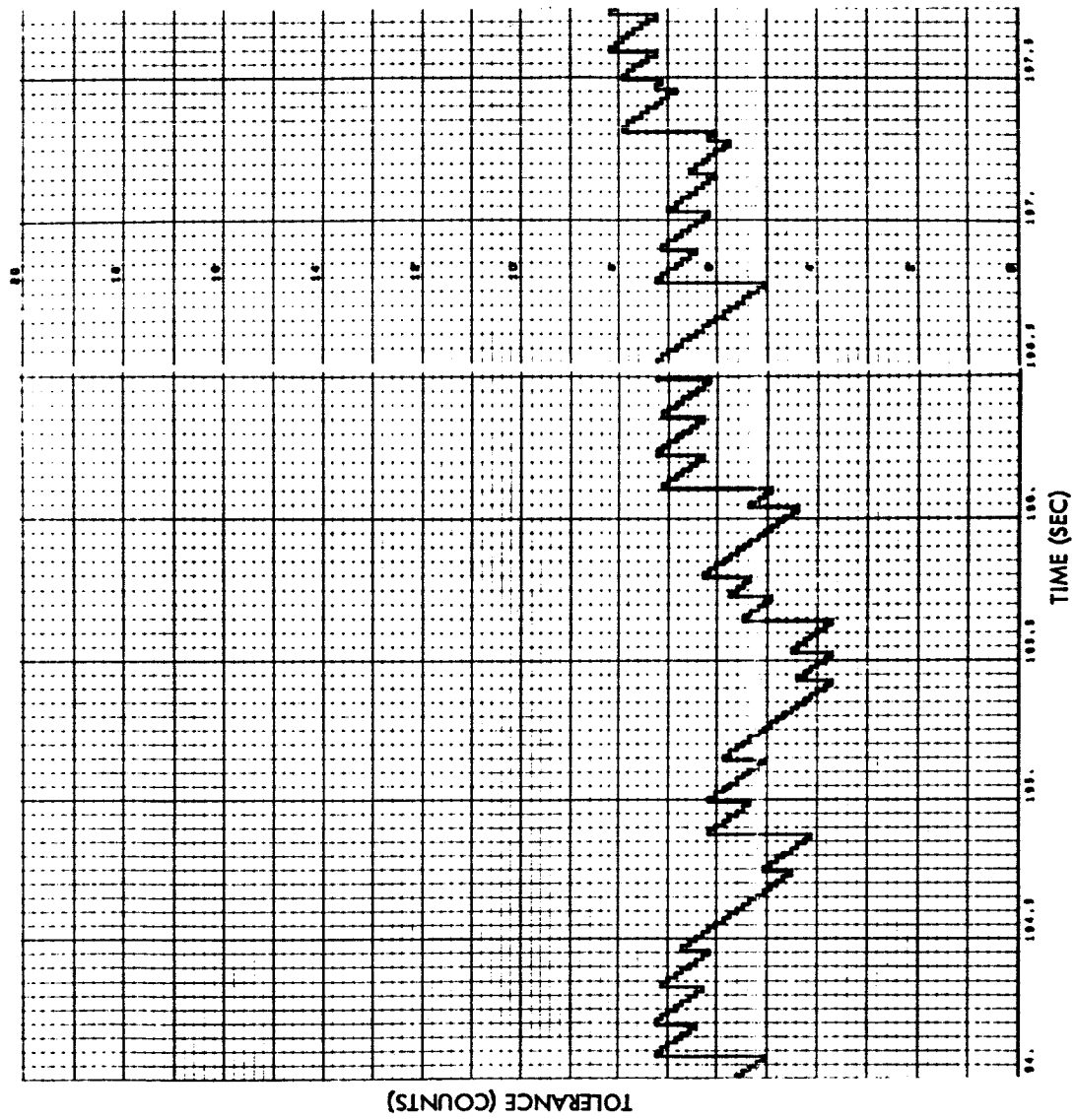


Fig. 4-16b Sensor 11 Tolerance vs Time, Run S6-09

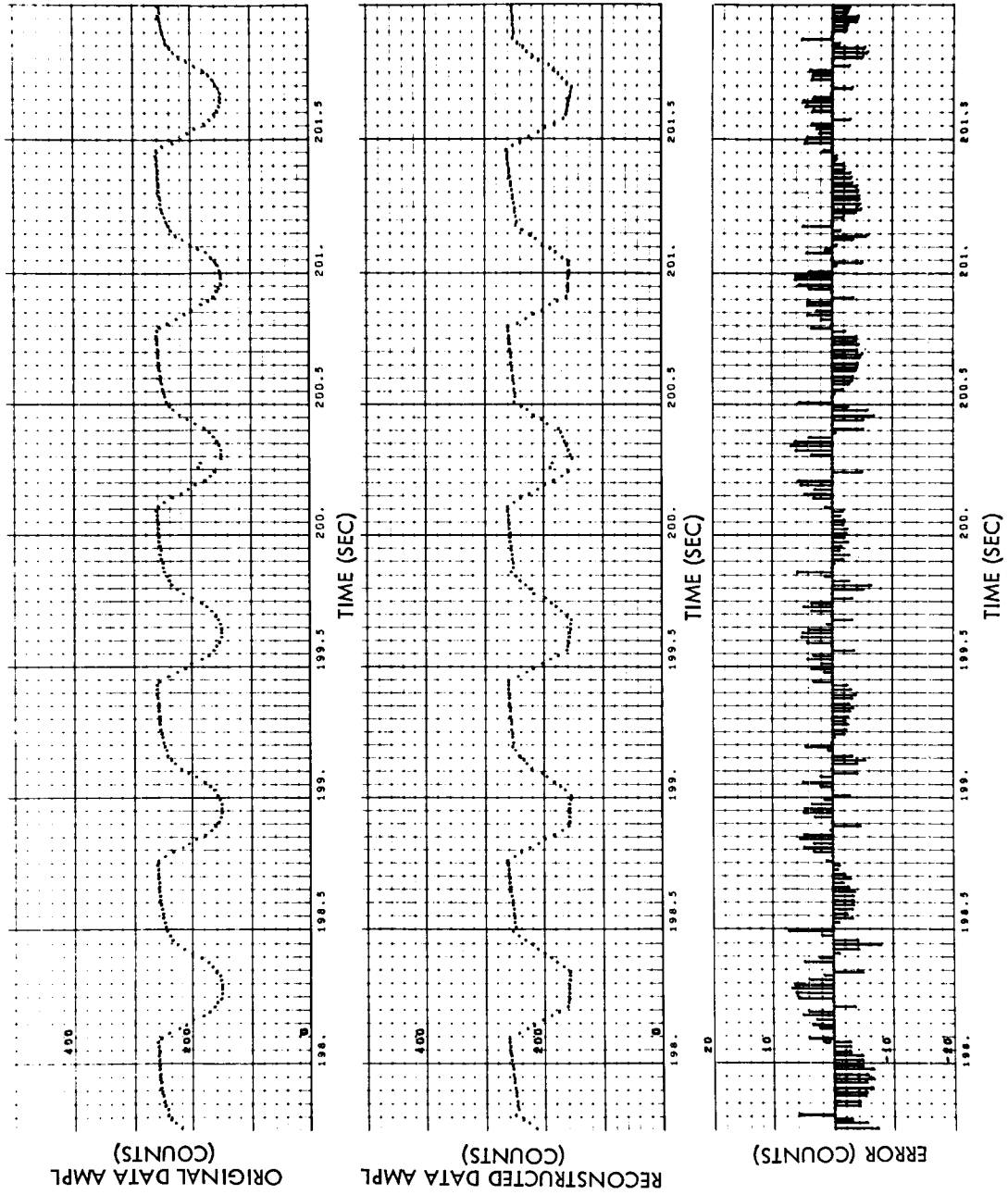


Fig. 4-16a (Cont'd) Sensor 11 Original Data, Reconstructed Data, and Error vs Time, Run S6-09

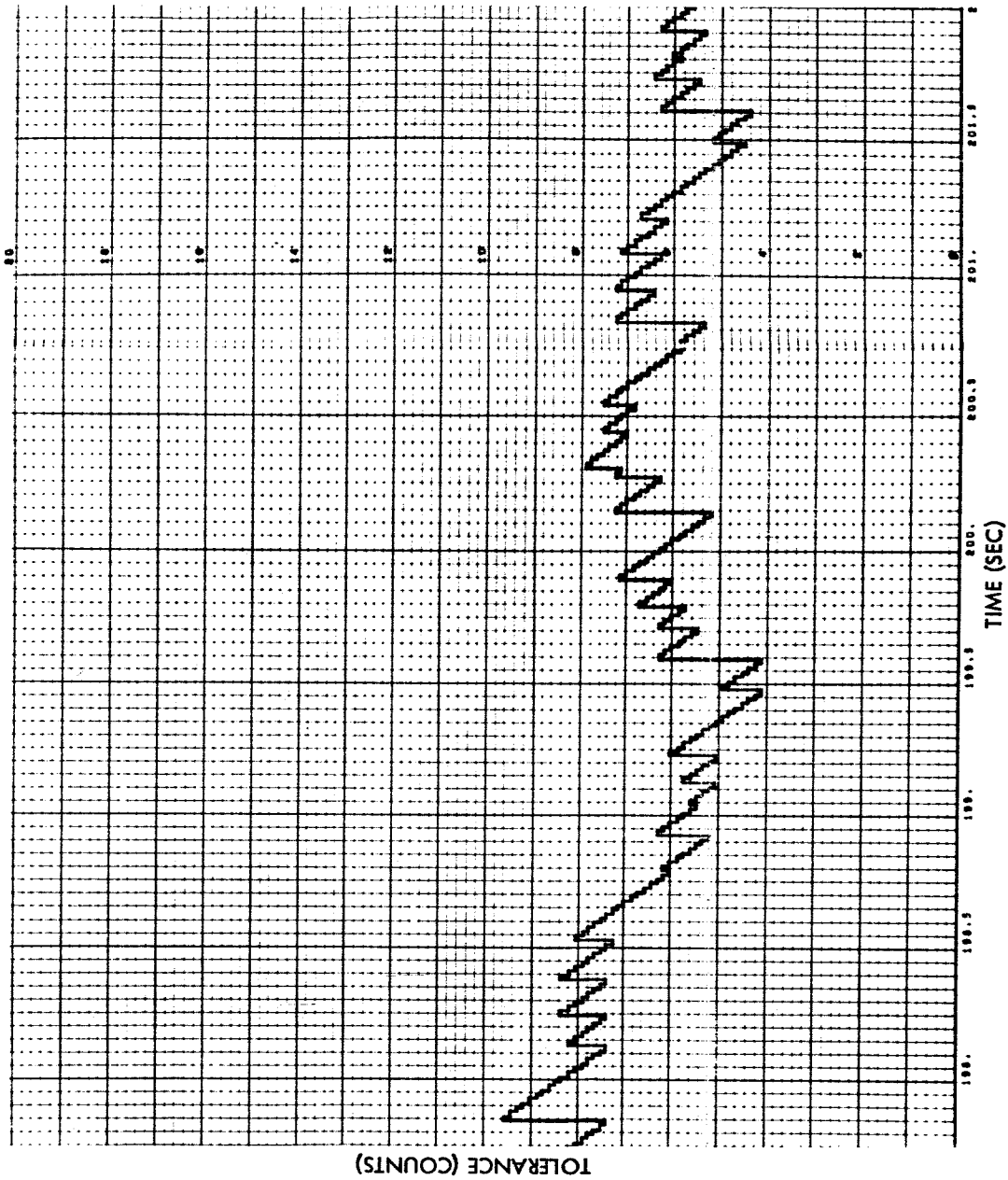


Fig. 4-16b (Cont'd) Sensor 11 Tolerance vs Time, Run S6-09

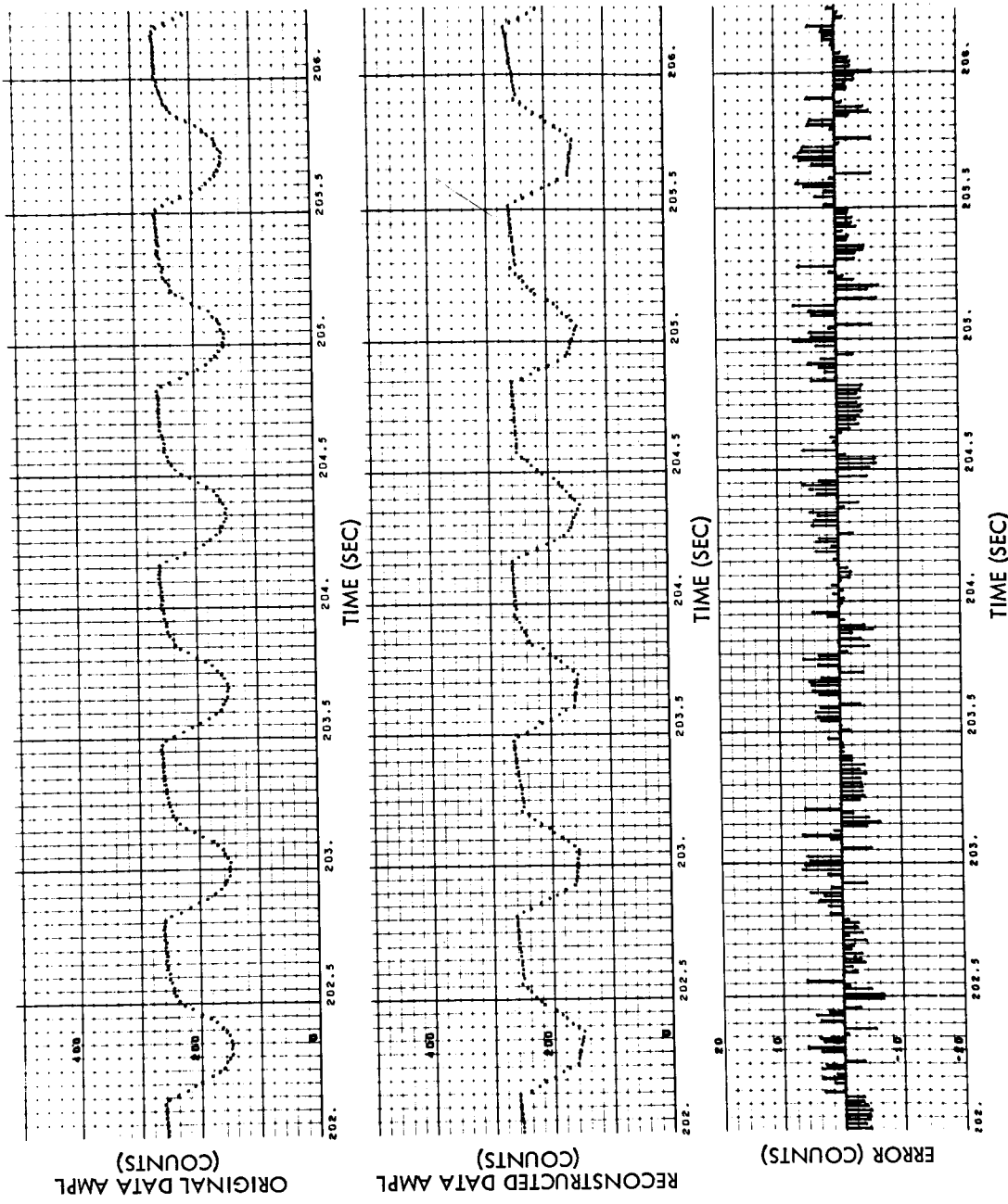


Fig. 4-16a (Cont'd) Sensor 11 Original Data, Reconstructed Data, and Error vs Time, Run S6-09

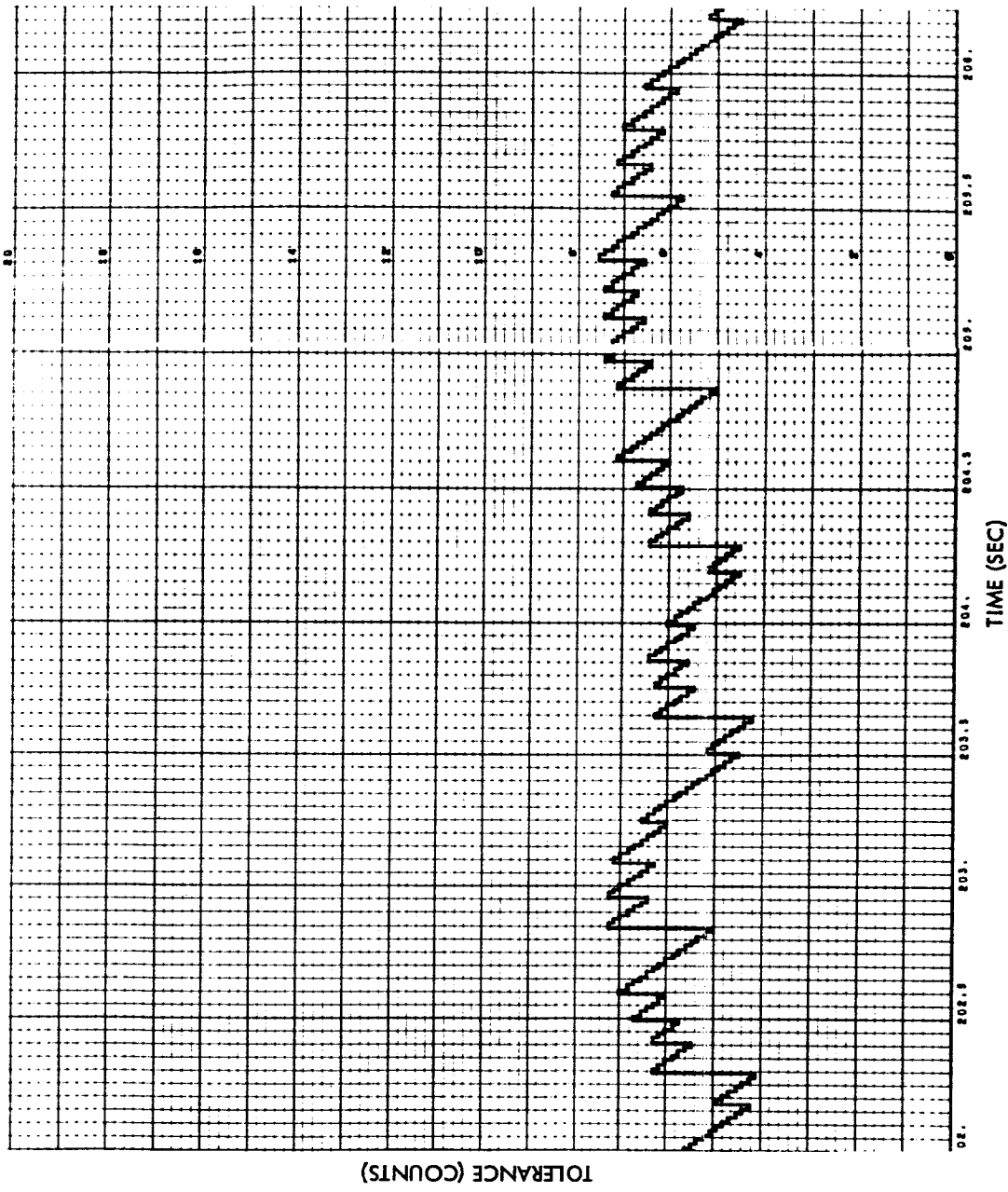


Fig. 4-16b (Cont'd) Sensor 11 Tolerance vs Time, Run S6-09

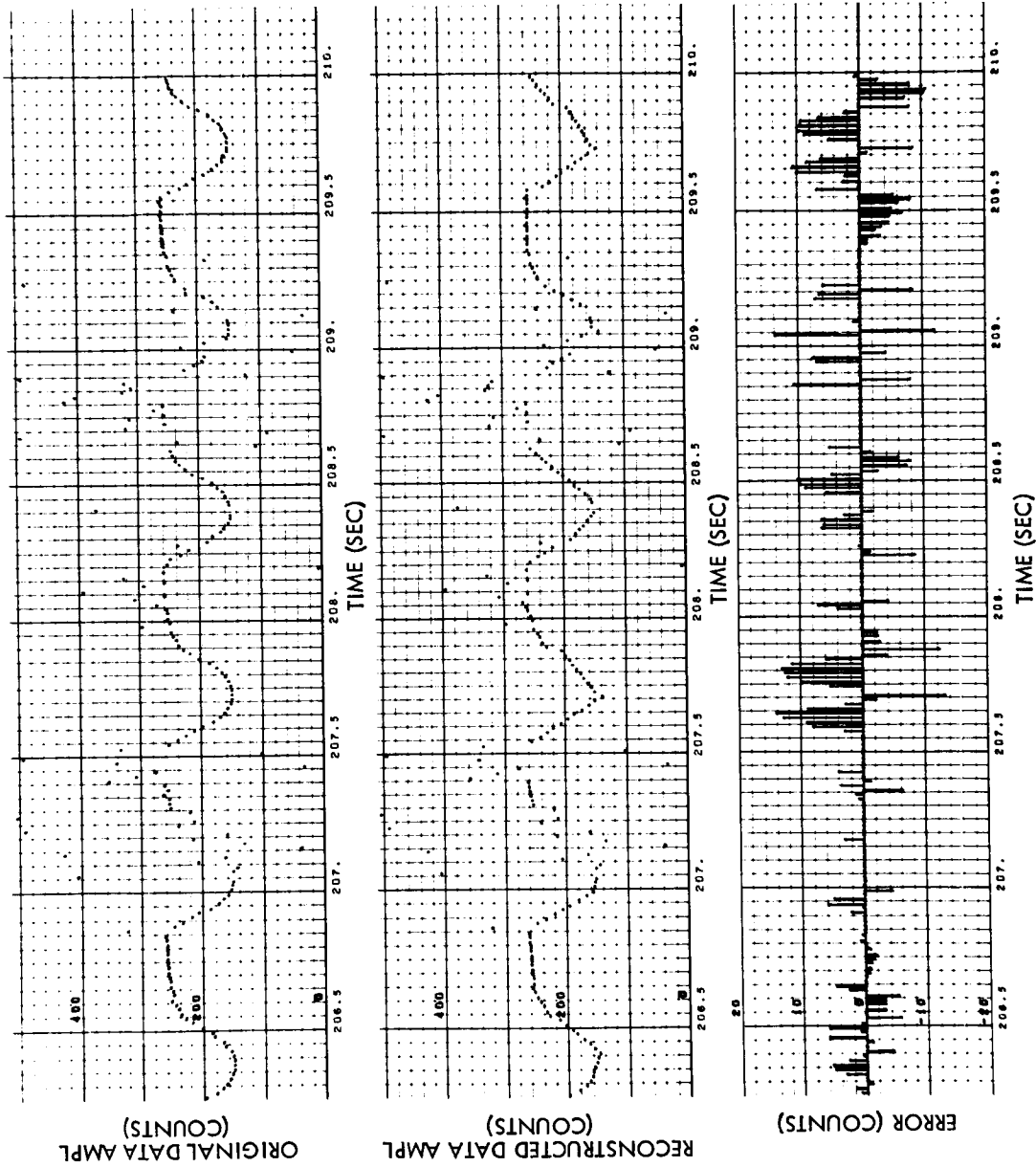


Fig. 4-16a (Cont'd) Sensor 11 Original Data, Reconstructed Data, and Error vs Time, Run S6-09

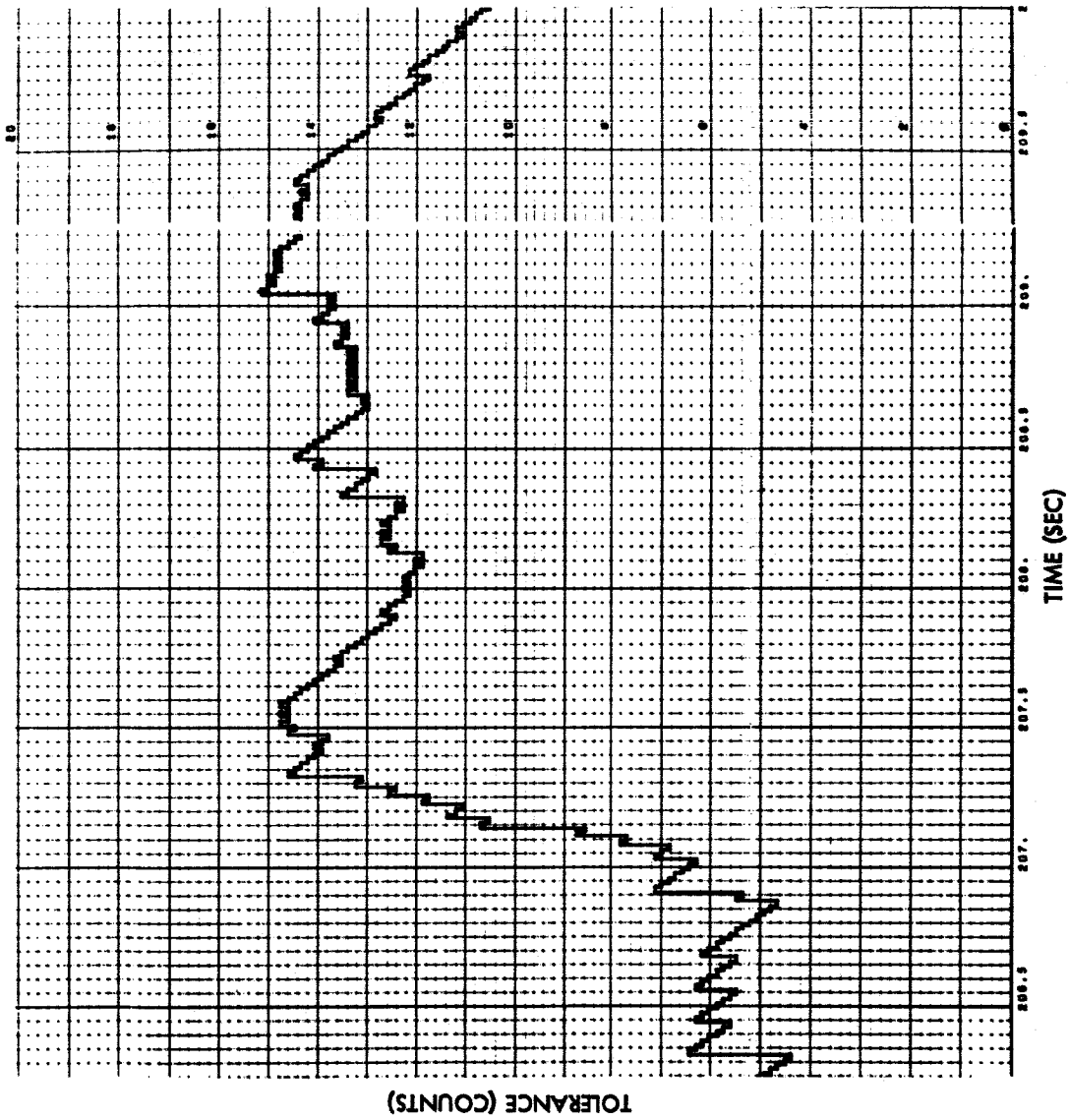


Fig. 4-16b (Cont'd) Sensor 11 Tolerance vs Time, Run S6-09

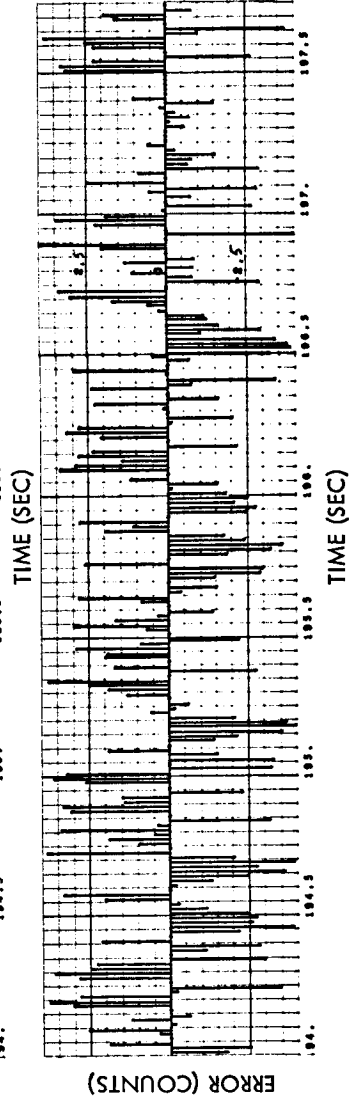
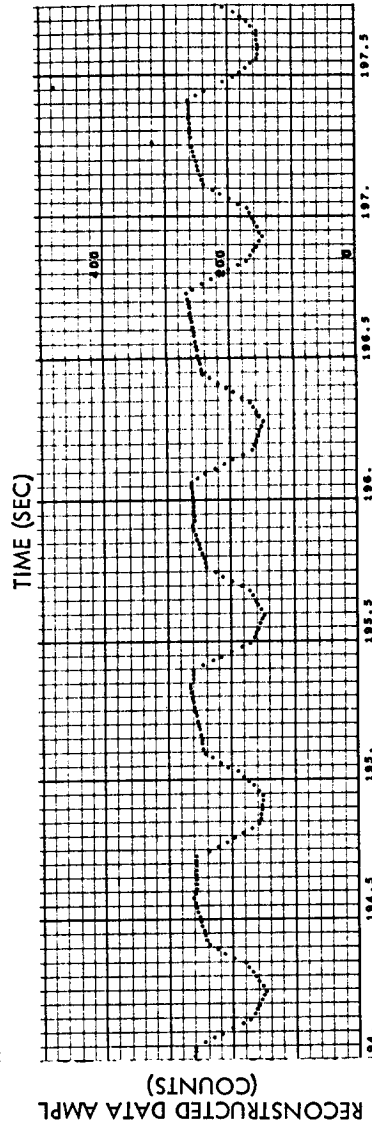
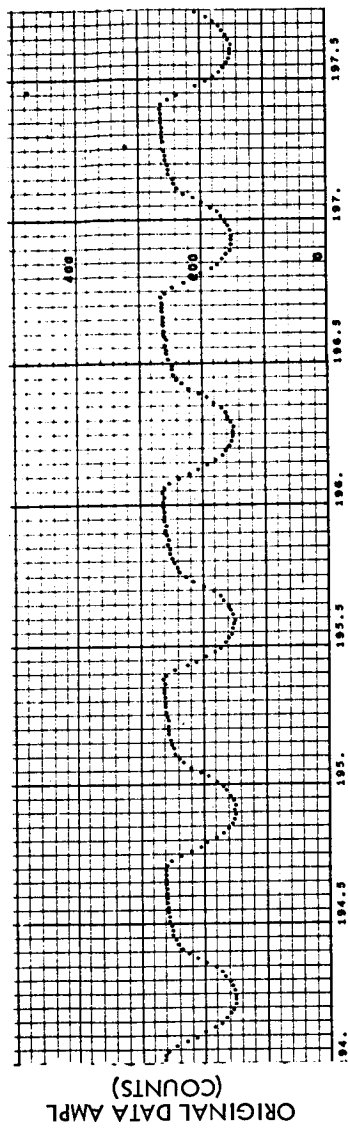


Fig. 4-17 Sensor 11 Original Data, Reconstructed Data, and Error vs Time, Run S6-07

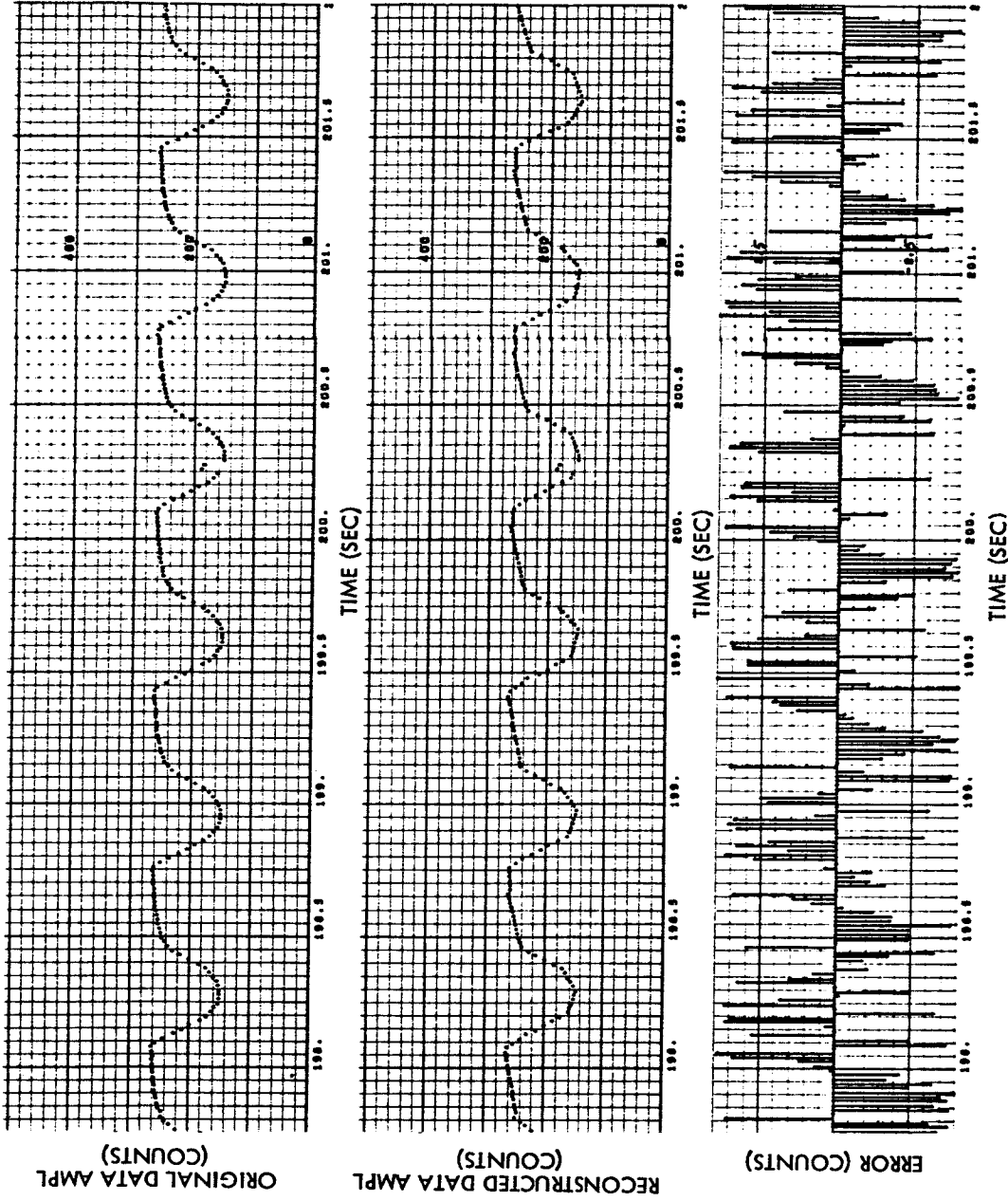


Fig. 4-17 (Cont'd) Sensor 11 Original Data, Reconstructed Data, and Error vs Time, Run S6-07

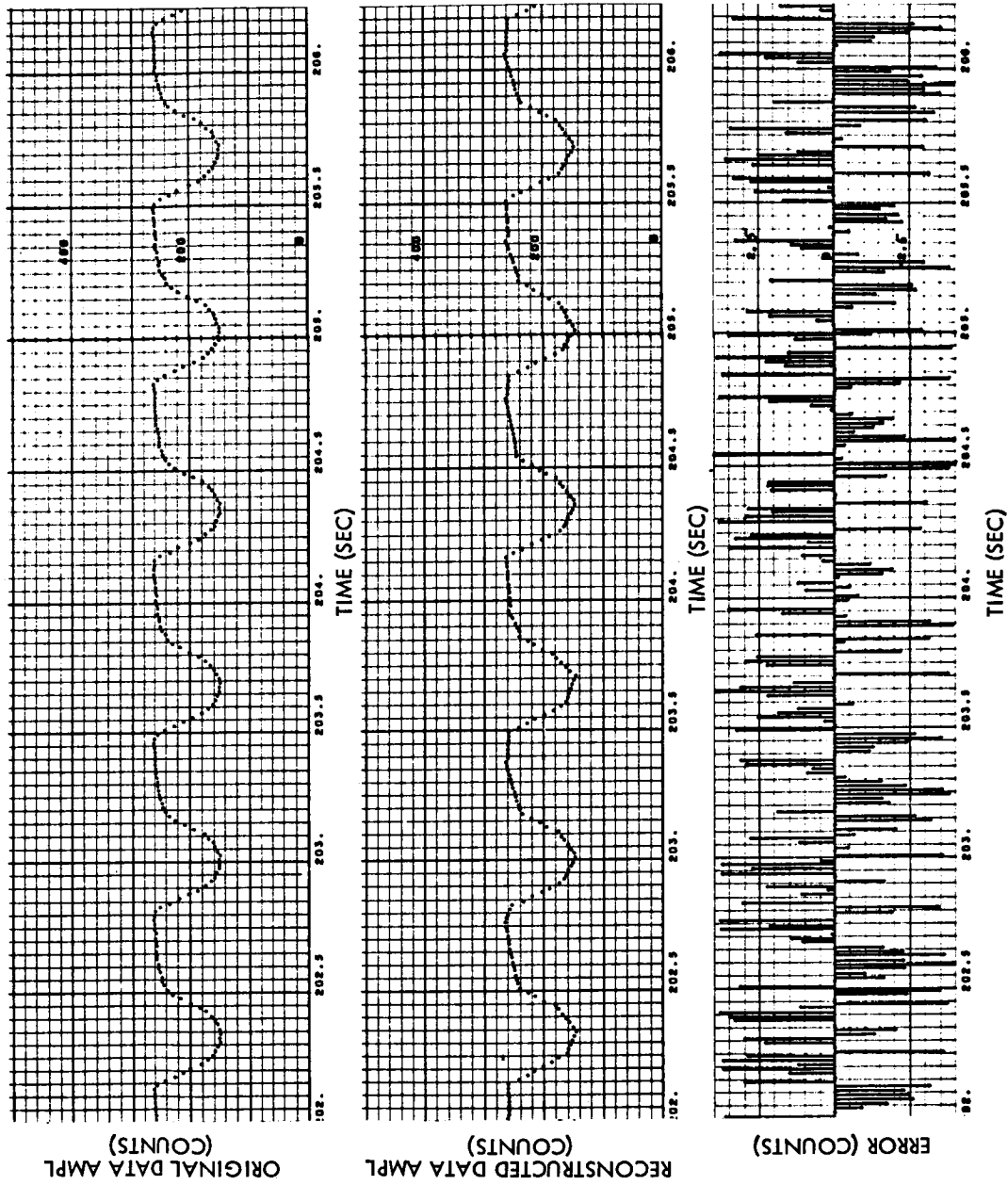


Fig. 4-17 (Cont'd) Sensor 11 Original Data, Reconstructed Data, and Error vs Time, Run S6-07

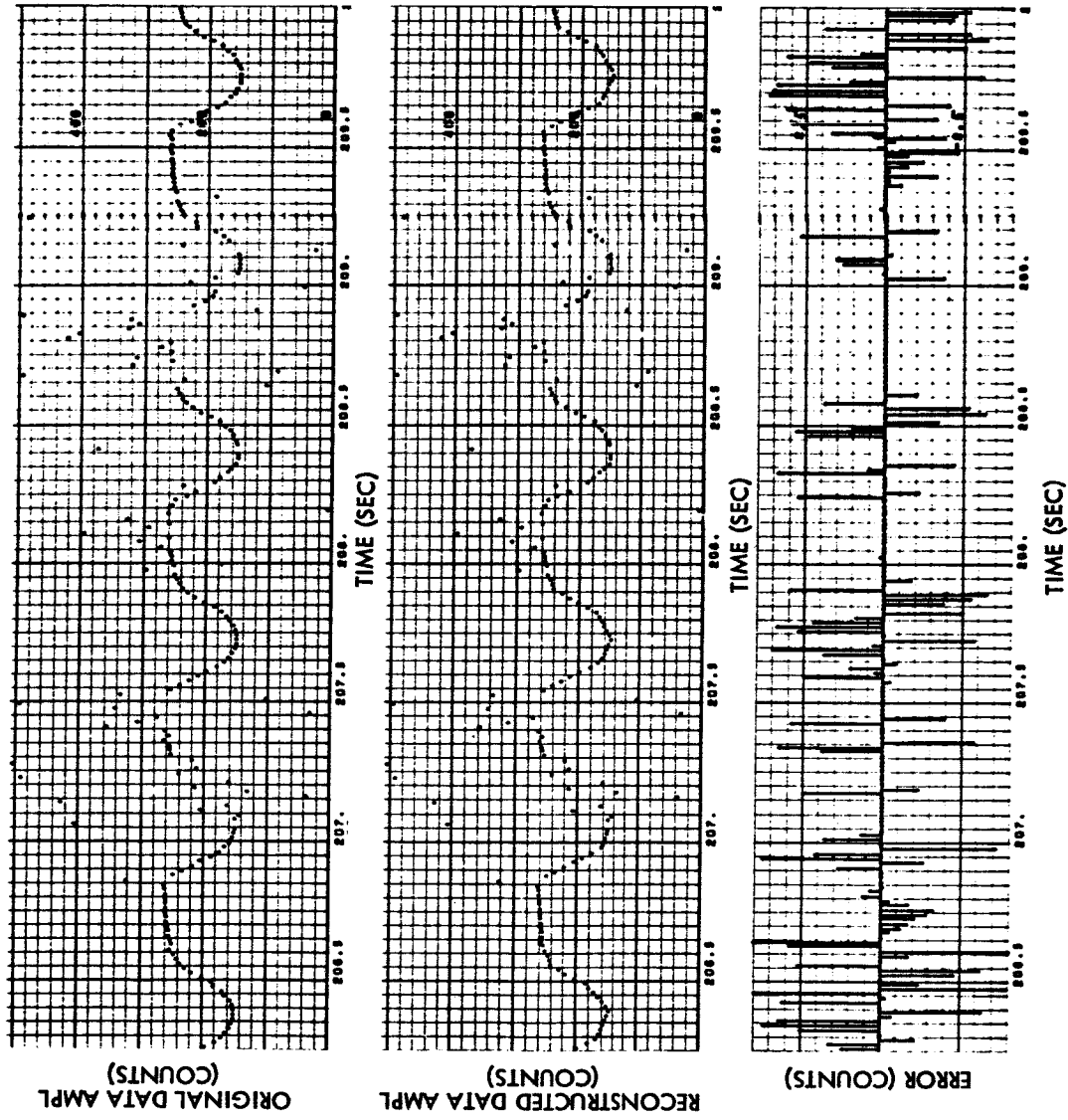


Fig. 4-17 (Cont'd) Sensor 11 Original Data, Reconstructed Data, and Error vs Time, Run S6-07

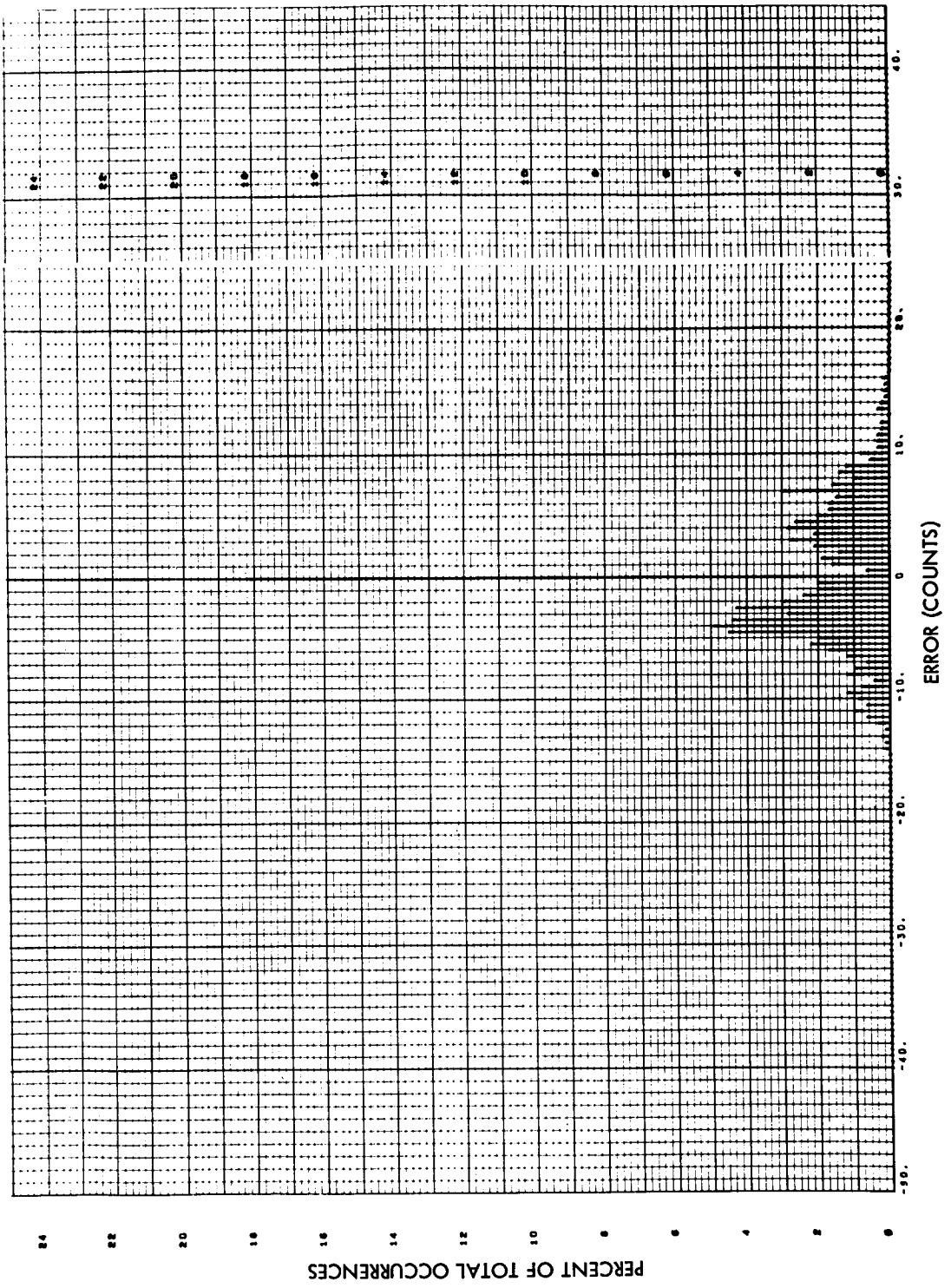


Fig. 4-18 Sensor 11 Error Histogram, Run S6-08

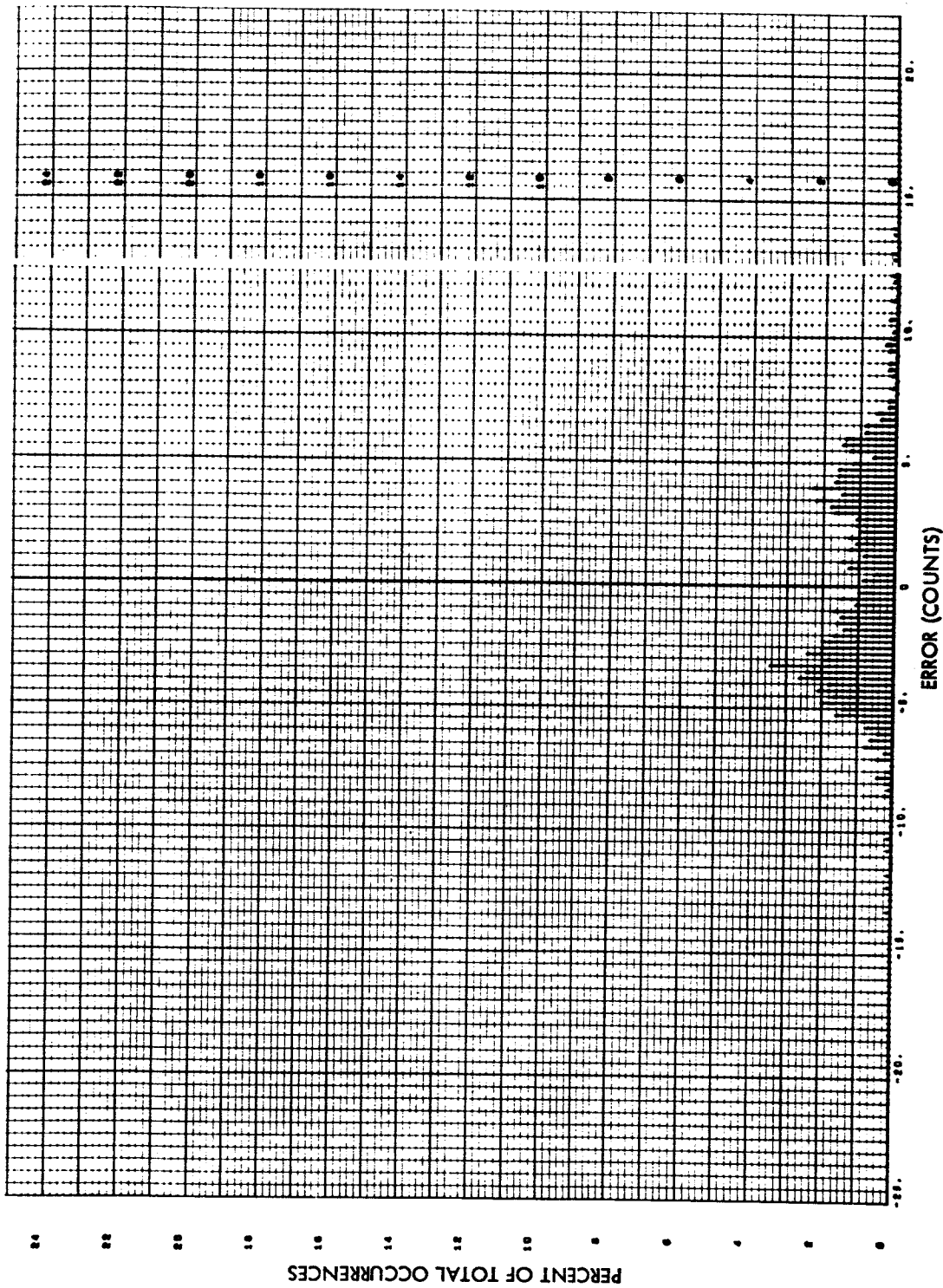


Fig. 4-19 Sensor 11 Error Histogram, Run S6-09

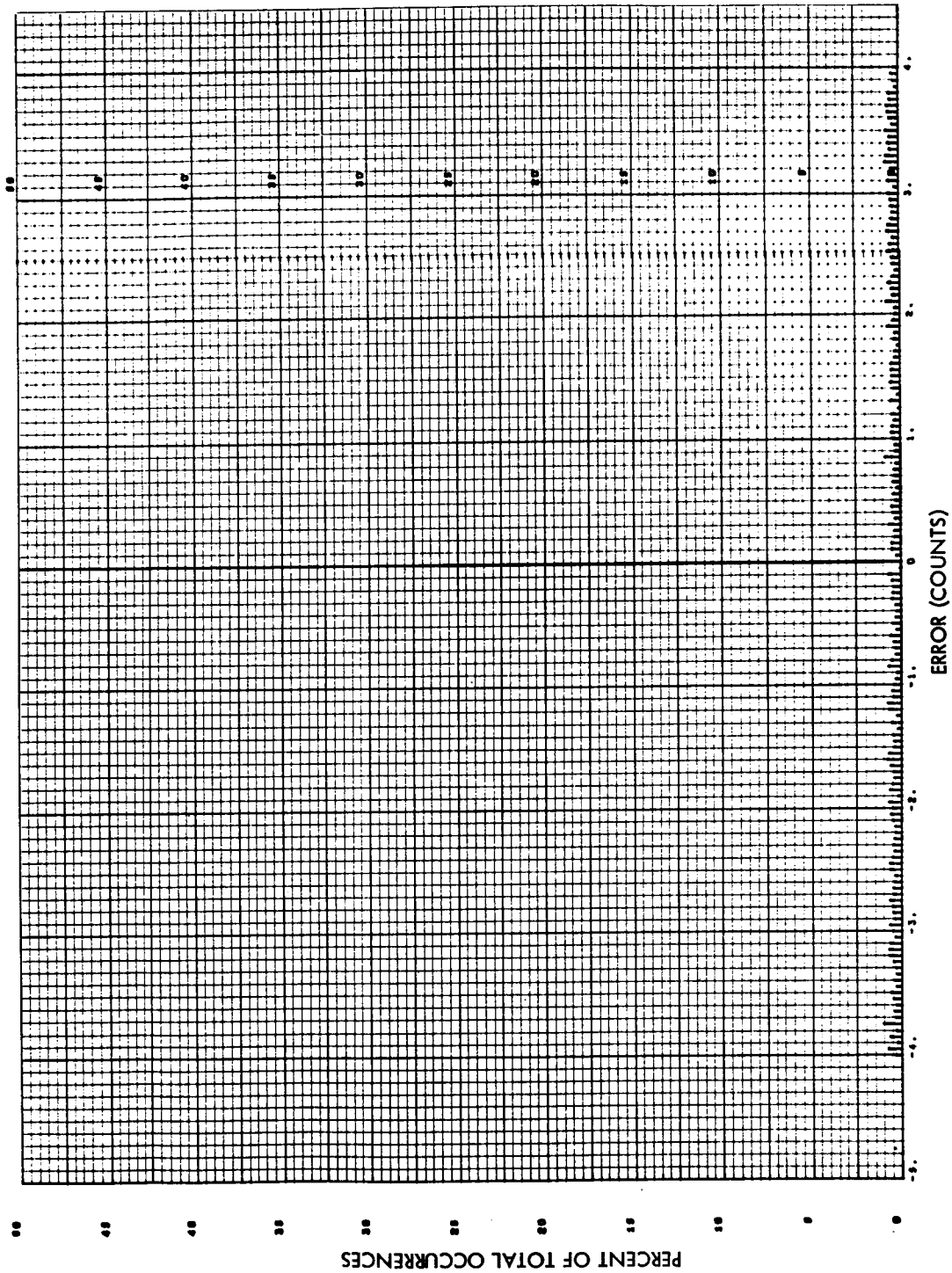
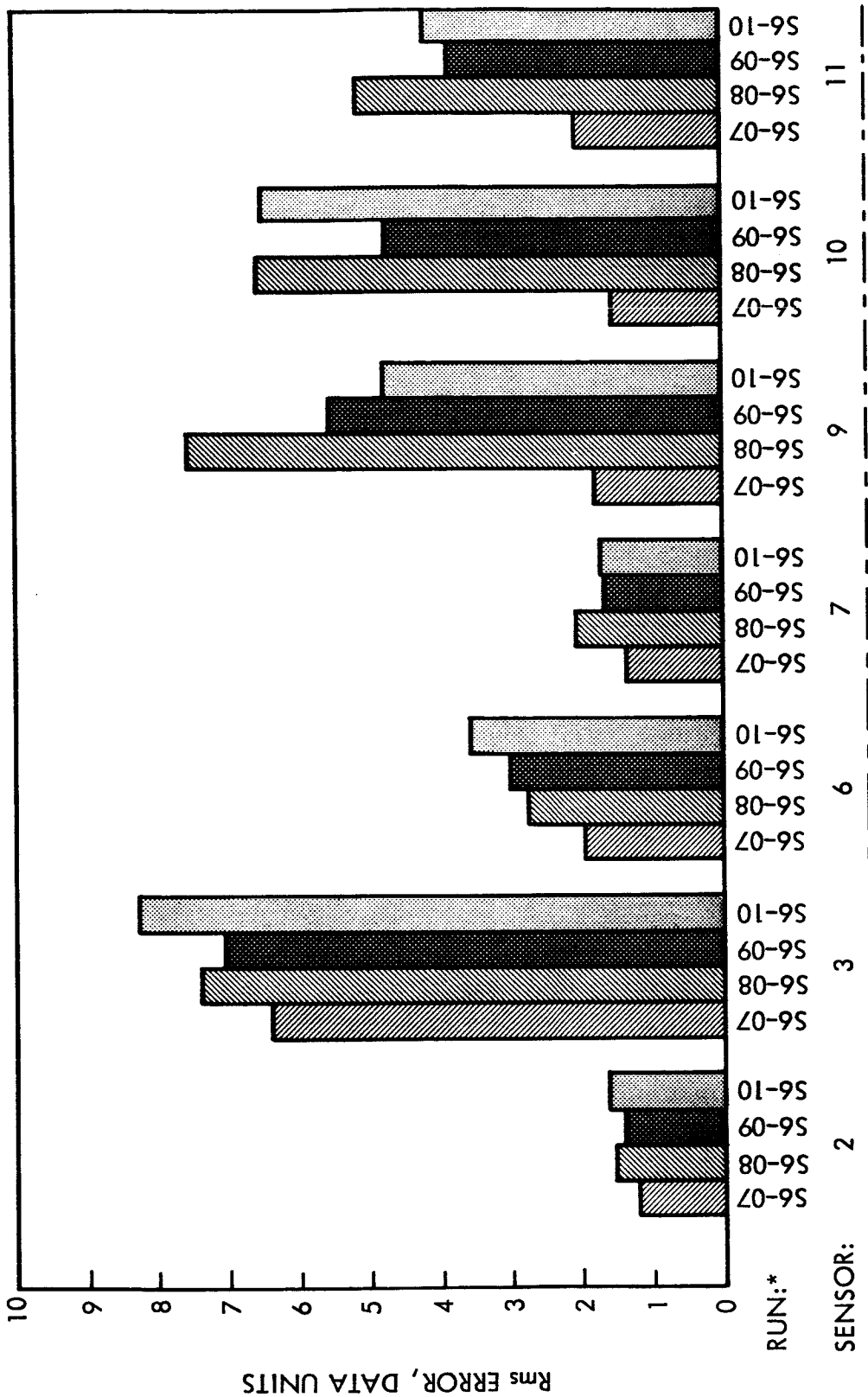


Fig. 4-20 Sensor 11 Error Histogram, Run S6-07



*S6-07: No queuing control
 S6-08: Compression ratio monitoring, continuous queuing control; JR = 3
 S6-09: Compression ratio monitoring, continuous queuing control; JR = 11
 S6-10: Queue length monitoring, continuous queuing control

Figure 4-21 Comparative Rms Errors, Test Groups 2 and 3

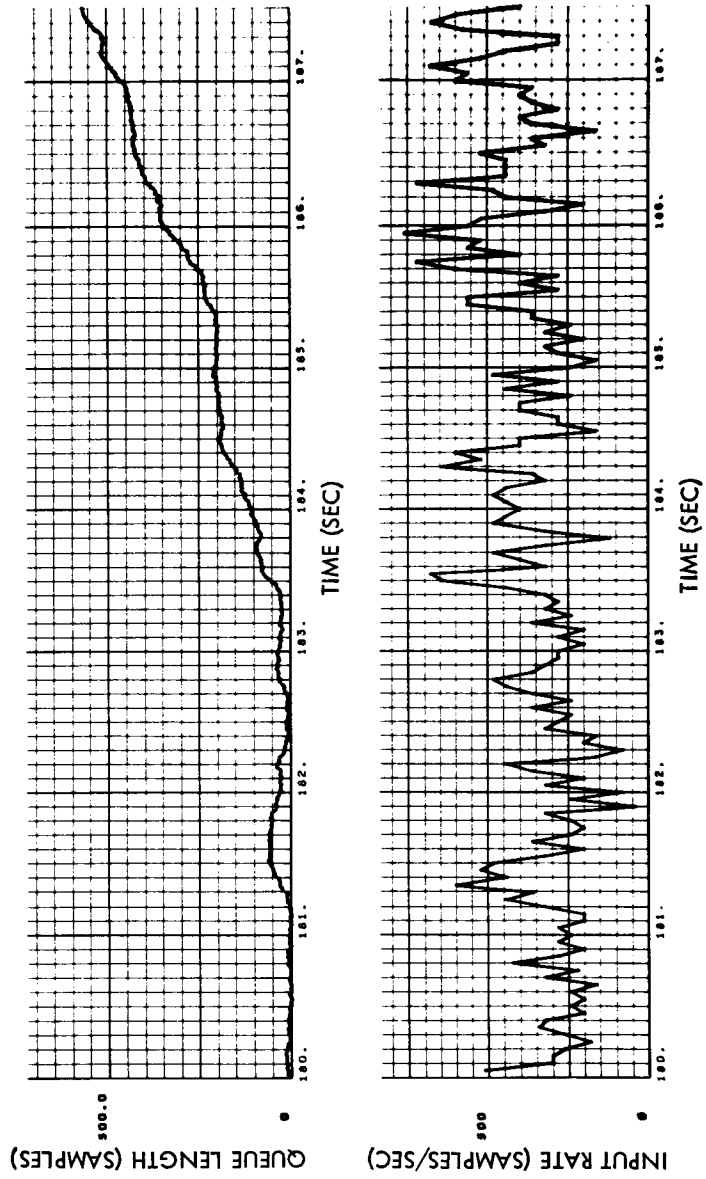


Fig. 4-22 Queue Length and Buffer Input
Arrival Rate vs Time, Run S6-10

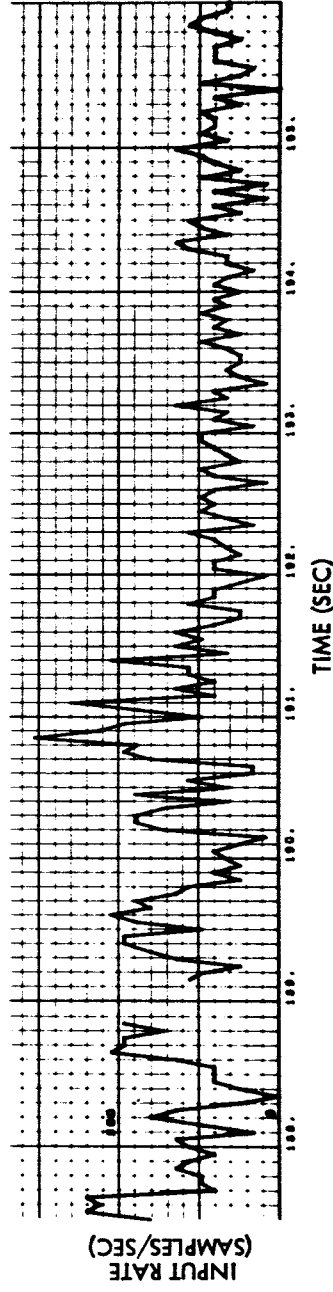
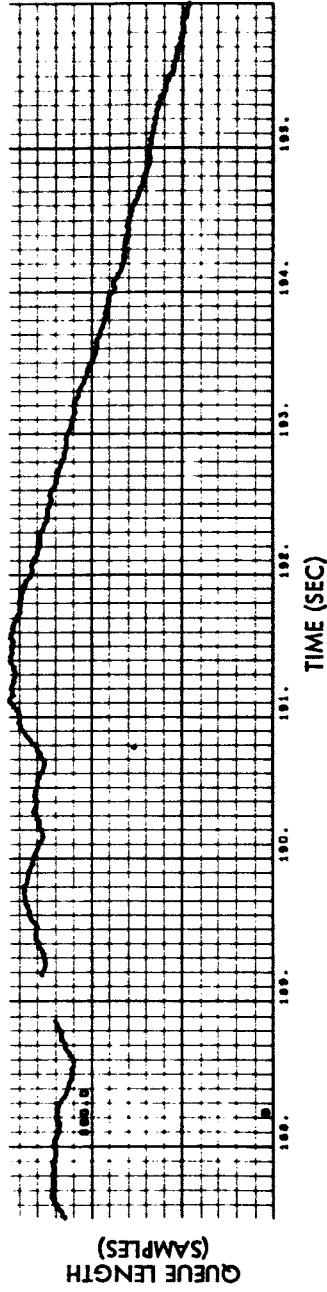


Fig. 4-22 (Cont'd) Queue Length and Buffer Input
Arrival Rate vs Time, Run S6-10

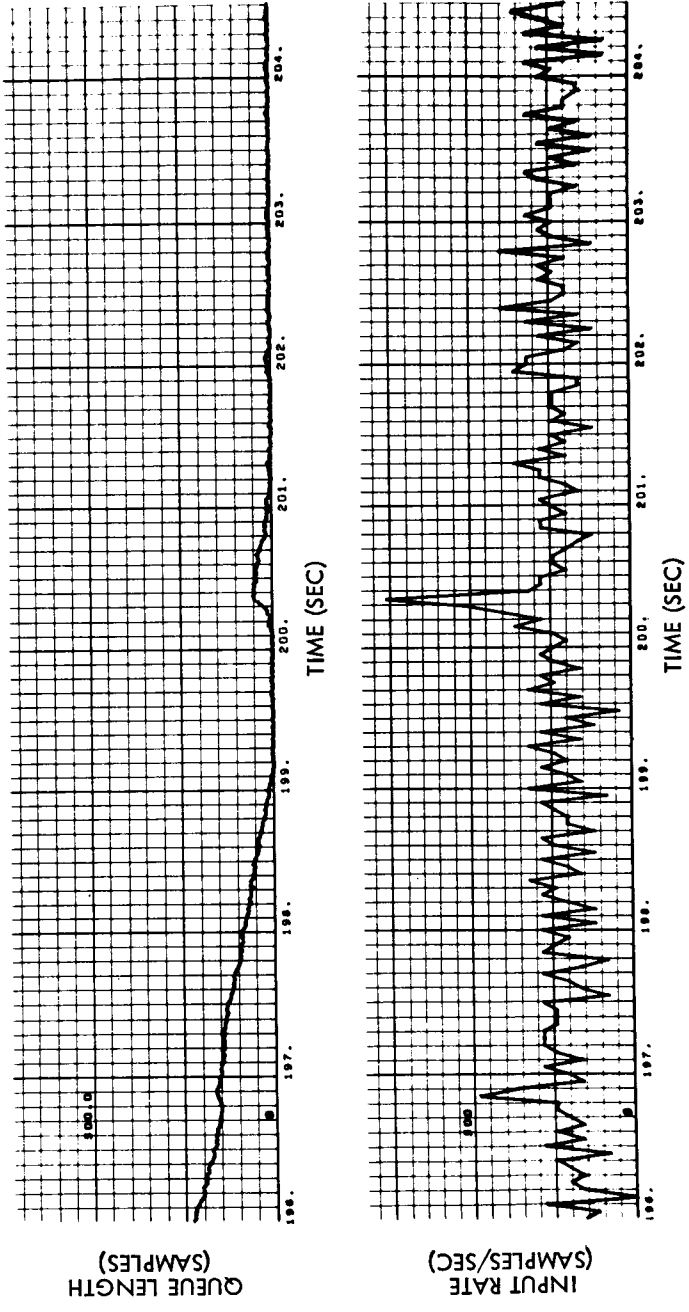


Fig. 4-22 (Cont'd) Queue Length and Buffer Input
Arrival Rate vs Time, Run S6-10

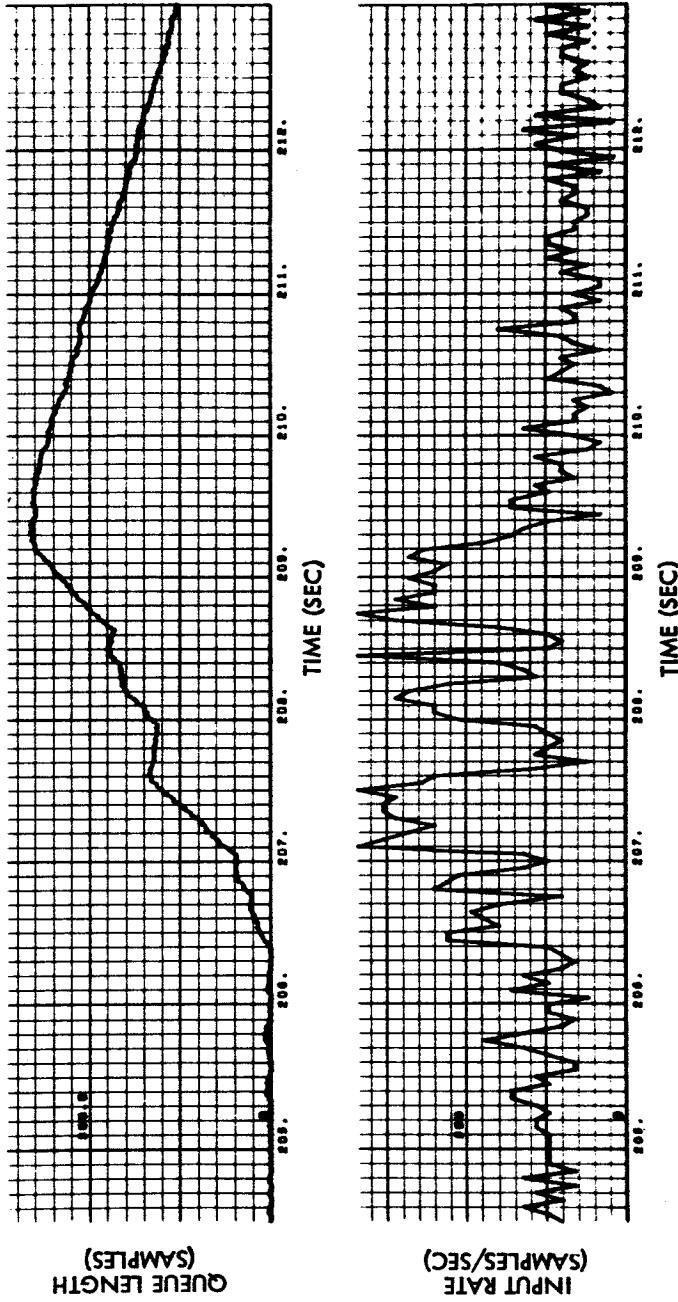


Fig. 4-22 (Cont'd) Queue Length and Buffer Input
Arrival Rate vs Time, Run S6-10

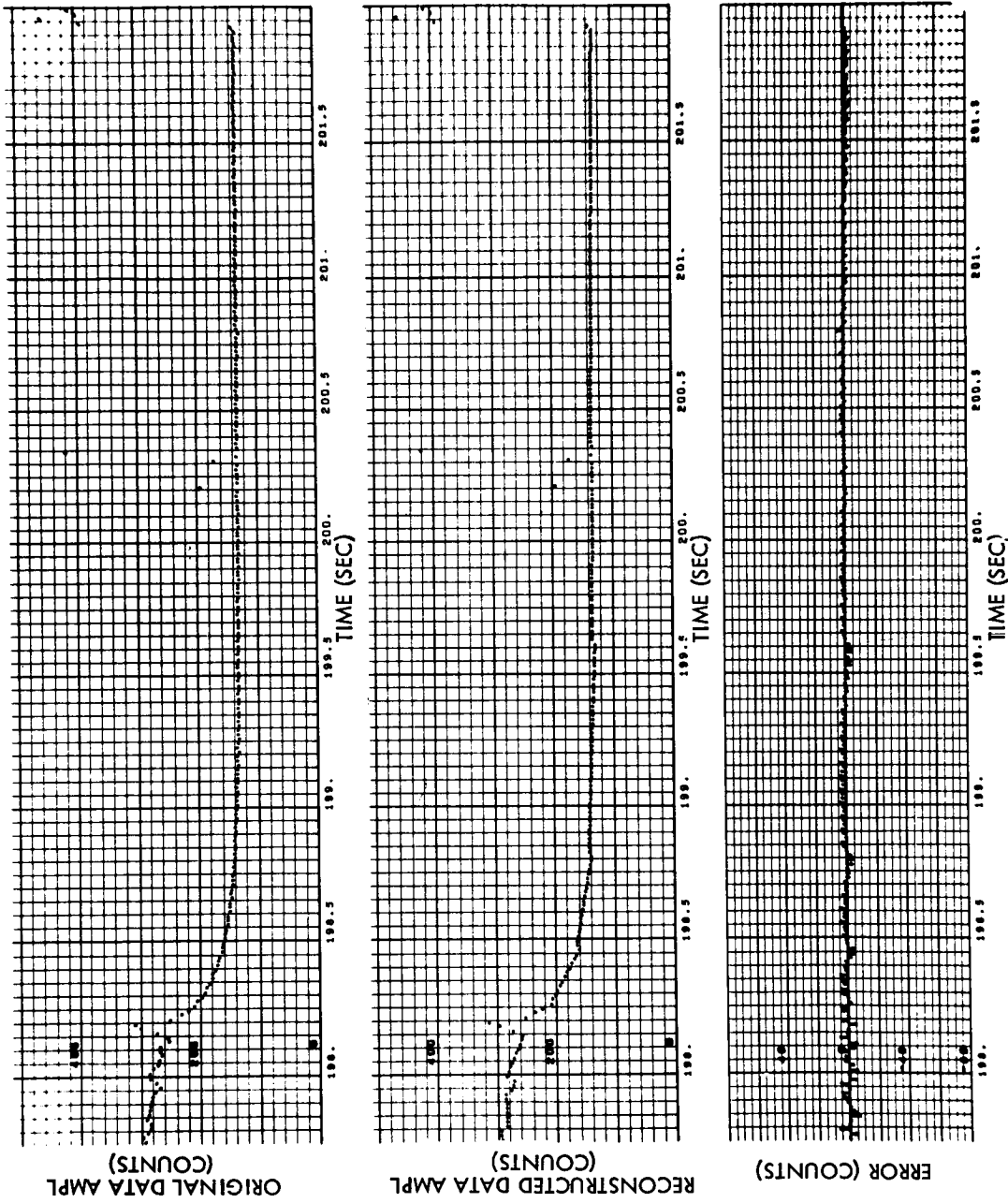


Fig. 4-23a Sensor 9 Original Data, Reconstructed Data, and Error vs Time, Run S6-10

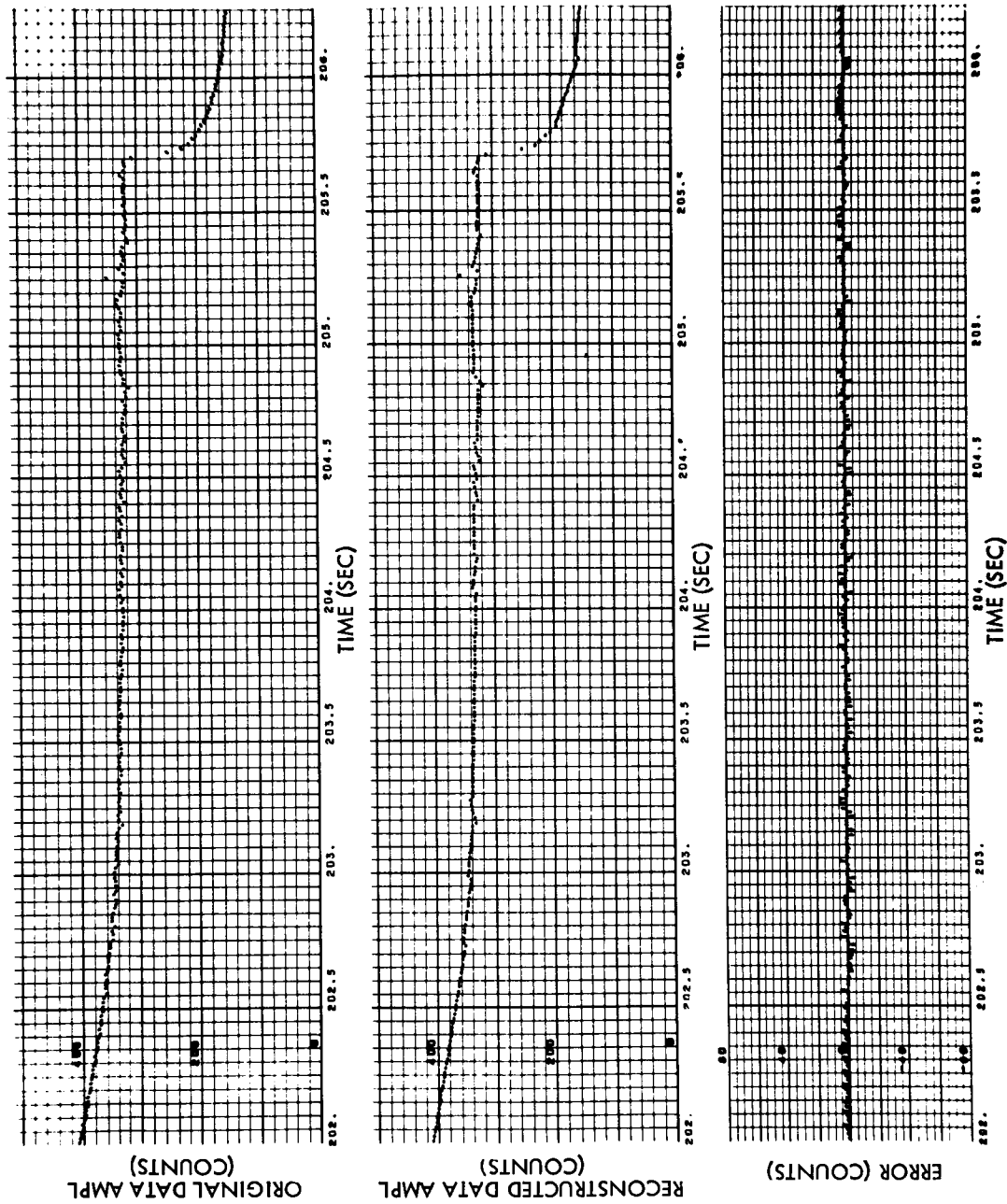


Fig. 4-23a (Cont'd) Sensor 9 Original Data, Reconstructed Data, and Error vs Time, Run S6-10

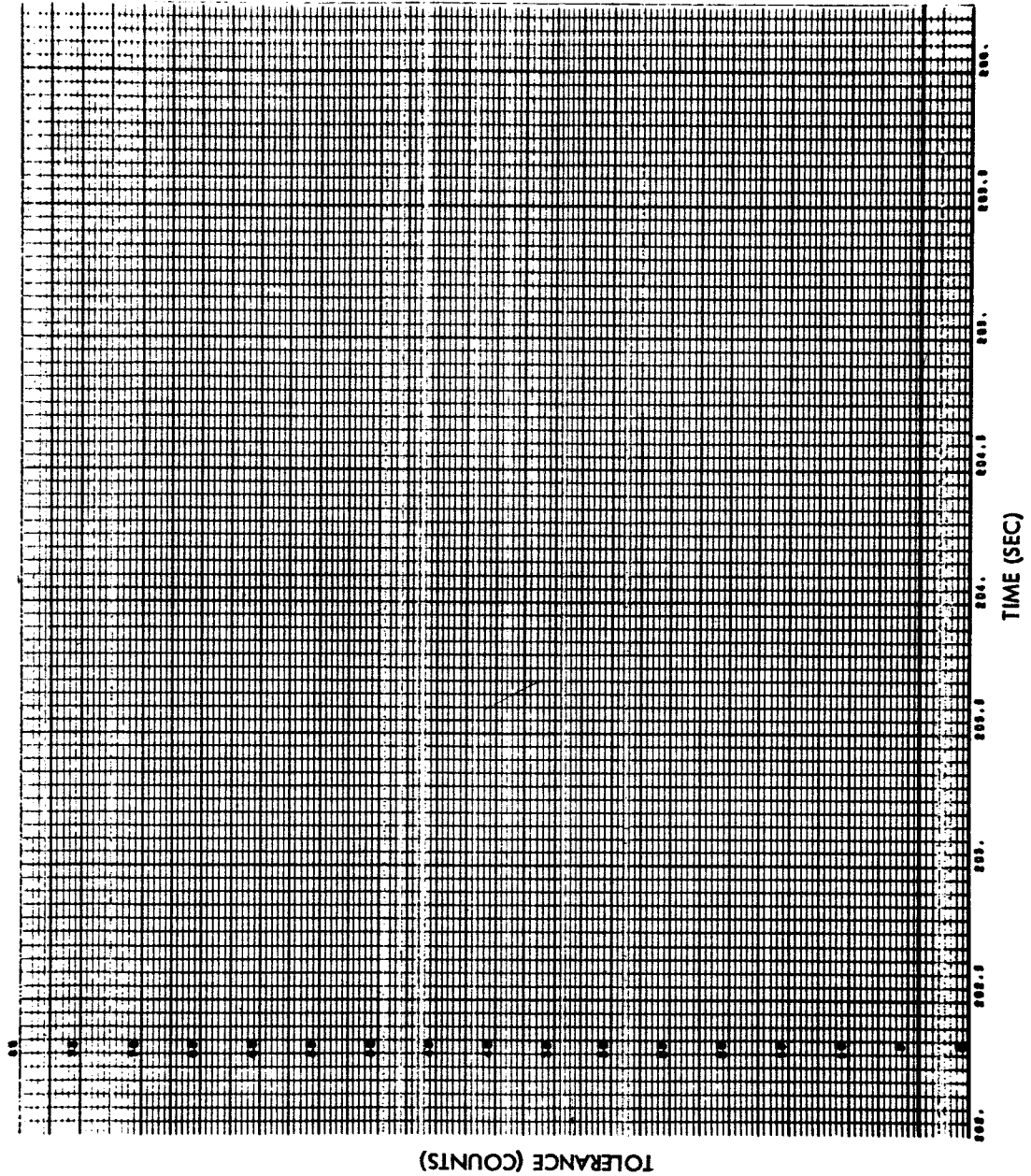


Fig. 4-23b (Cont'd) Sensor 9 Tolerance vs Time, Run S6-10

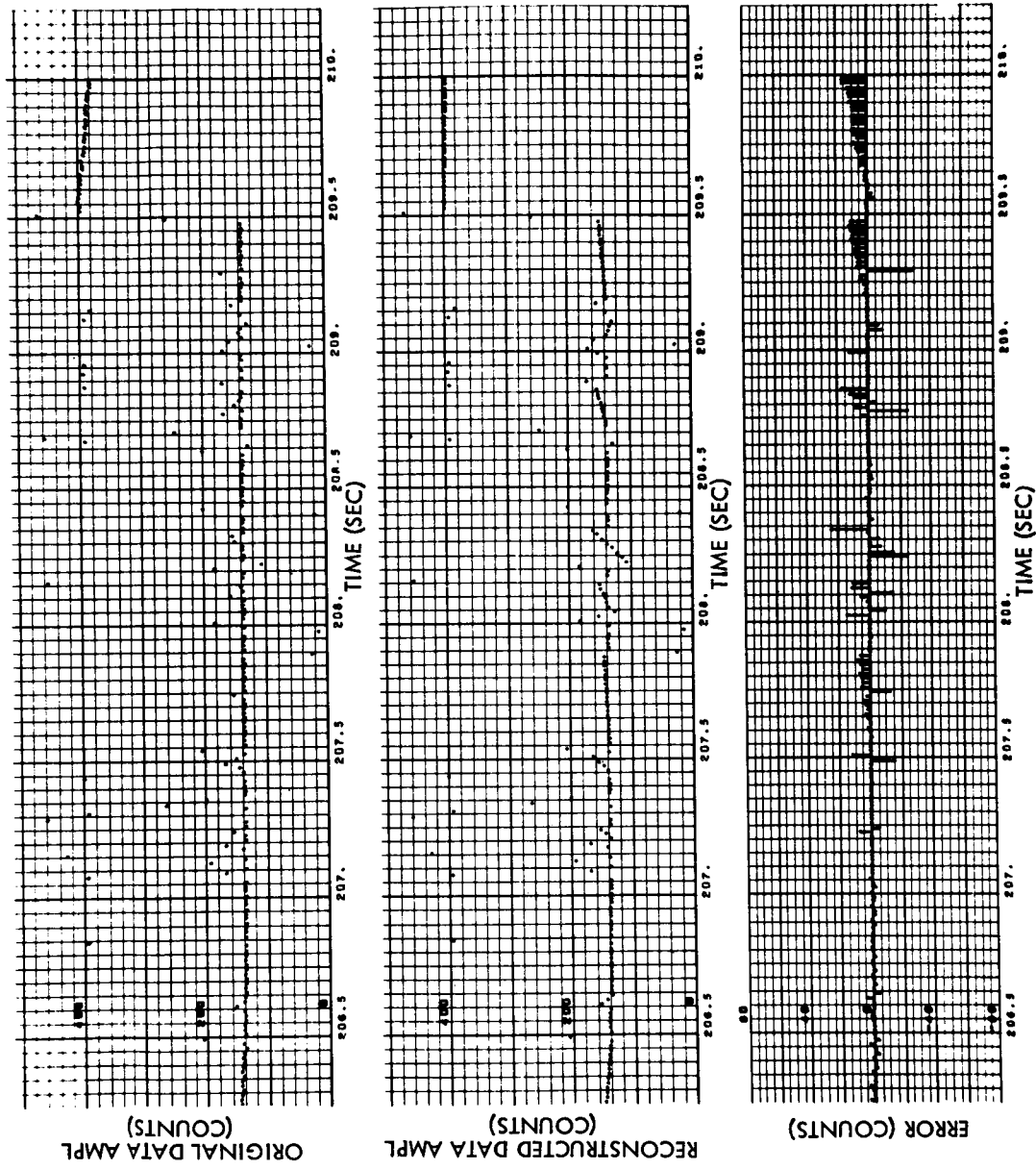


Fig. 4-23a (Cont'd) Sensor 9 Original Data, Reconstructed Data, and Error vs Time, Run S6-10

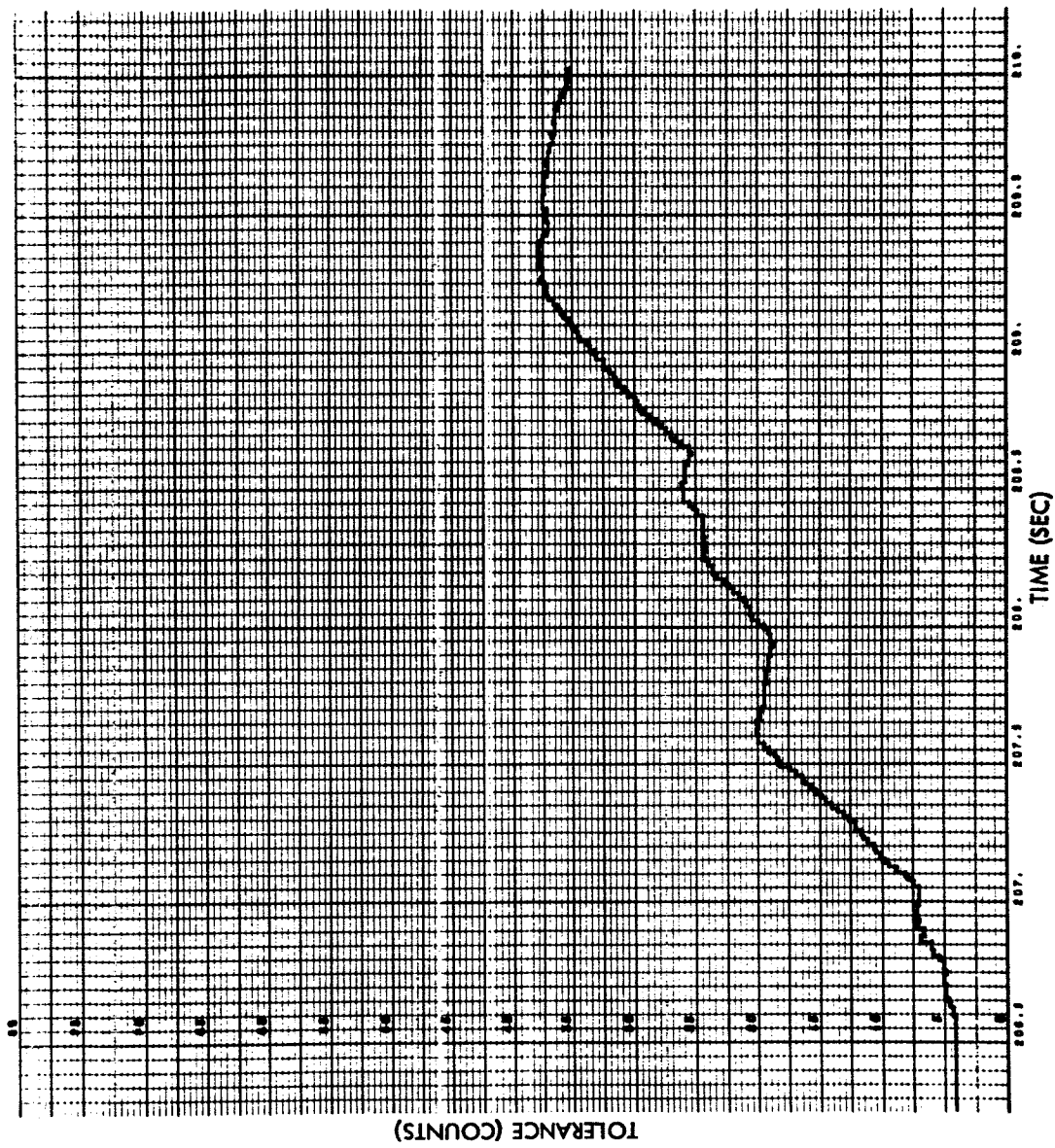


Fig. 4-23b (Cont'd) Sensor 9 Tolerance vs Time, Run S6-10

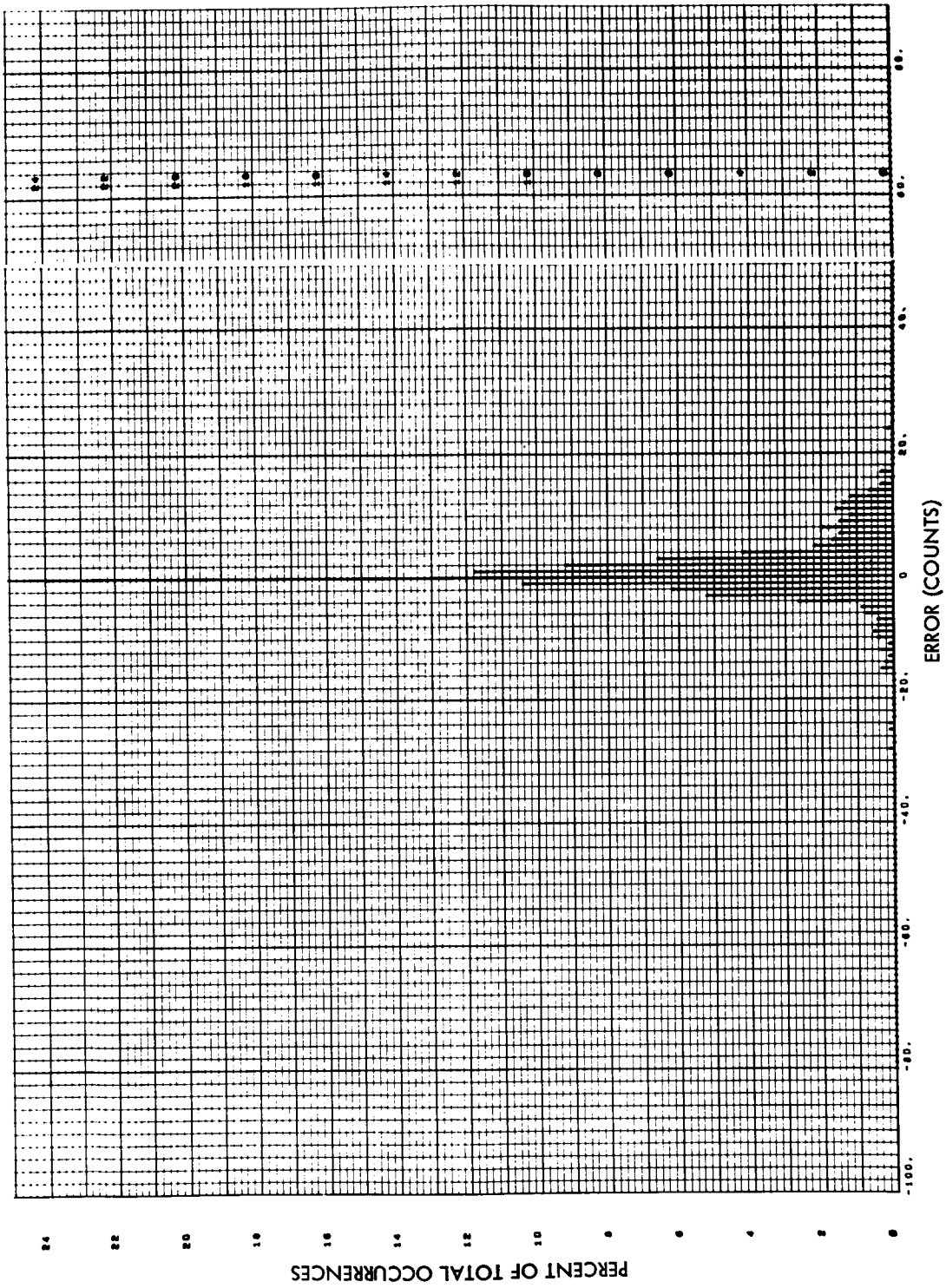


Fig. 4-24 Sensor 9 Error Histogram, Run S6-10

(This page intentionally left blank.)

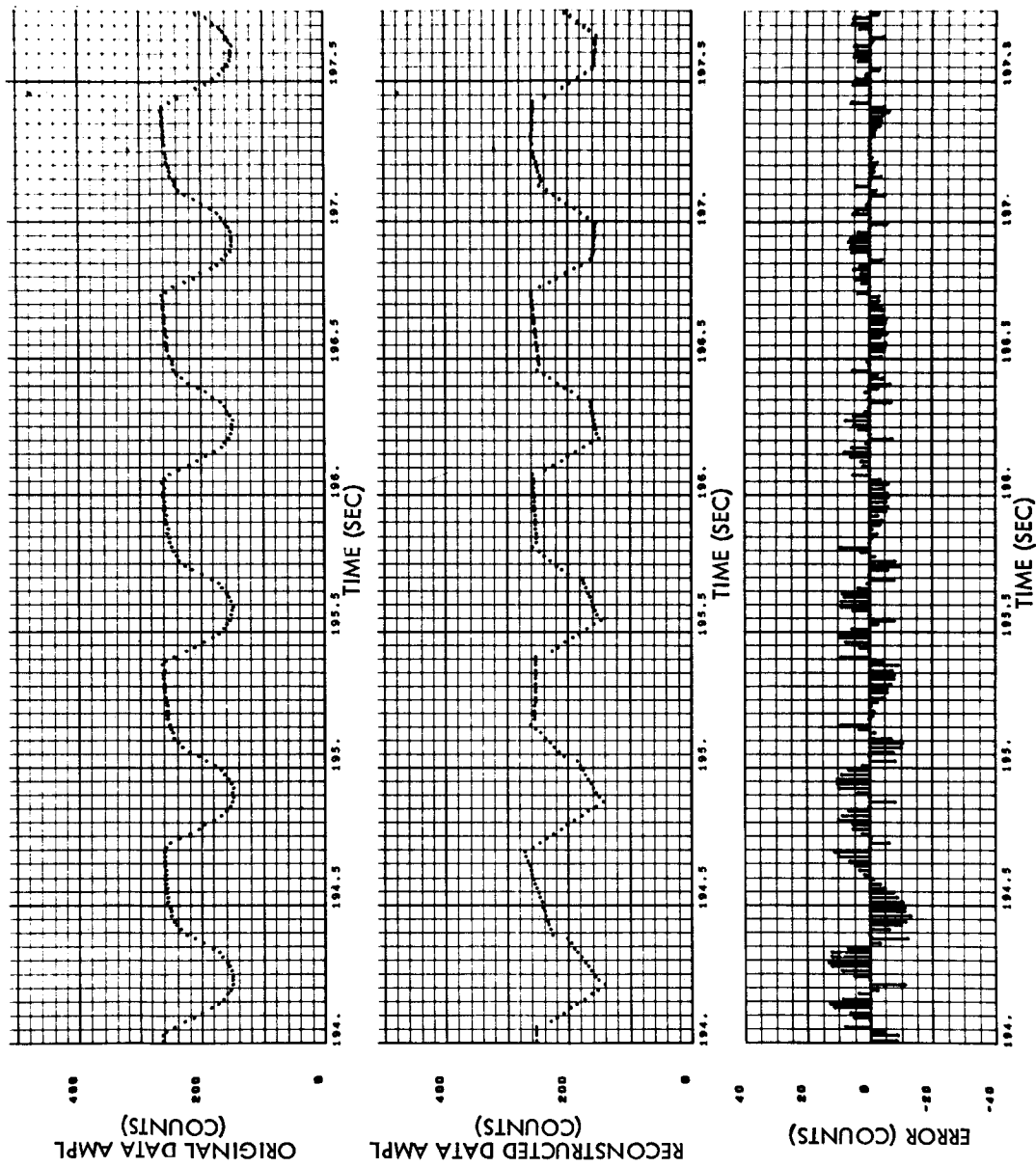


Fig. 4-25a Sensor 11 Original Data, Reconstructed Data, and Error vs Time, Run S6-10

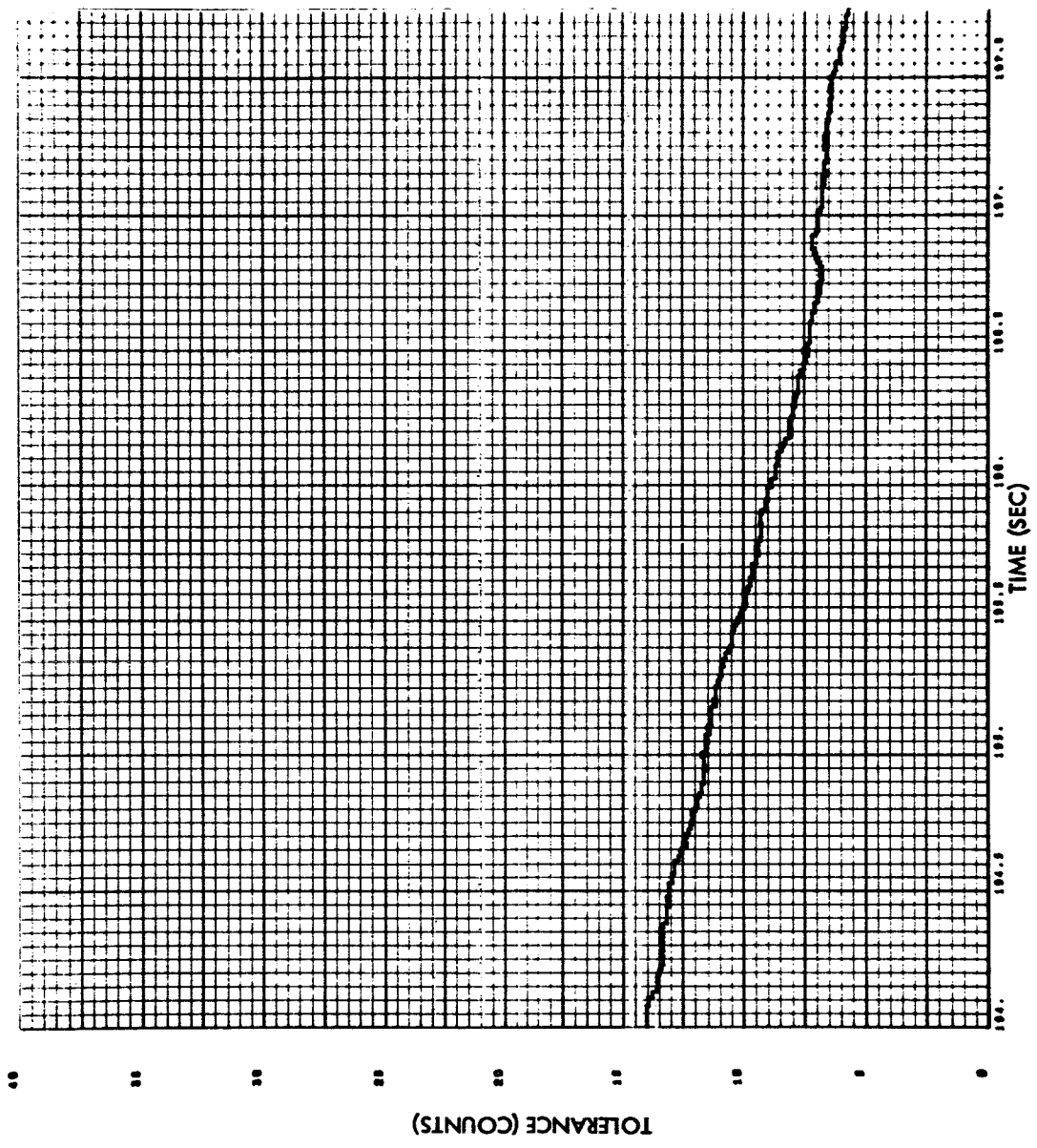


Fig. 4-25b Sensor 11 Tolerance vs Time, Run S6-10

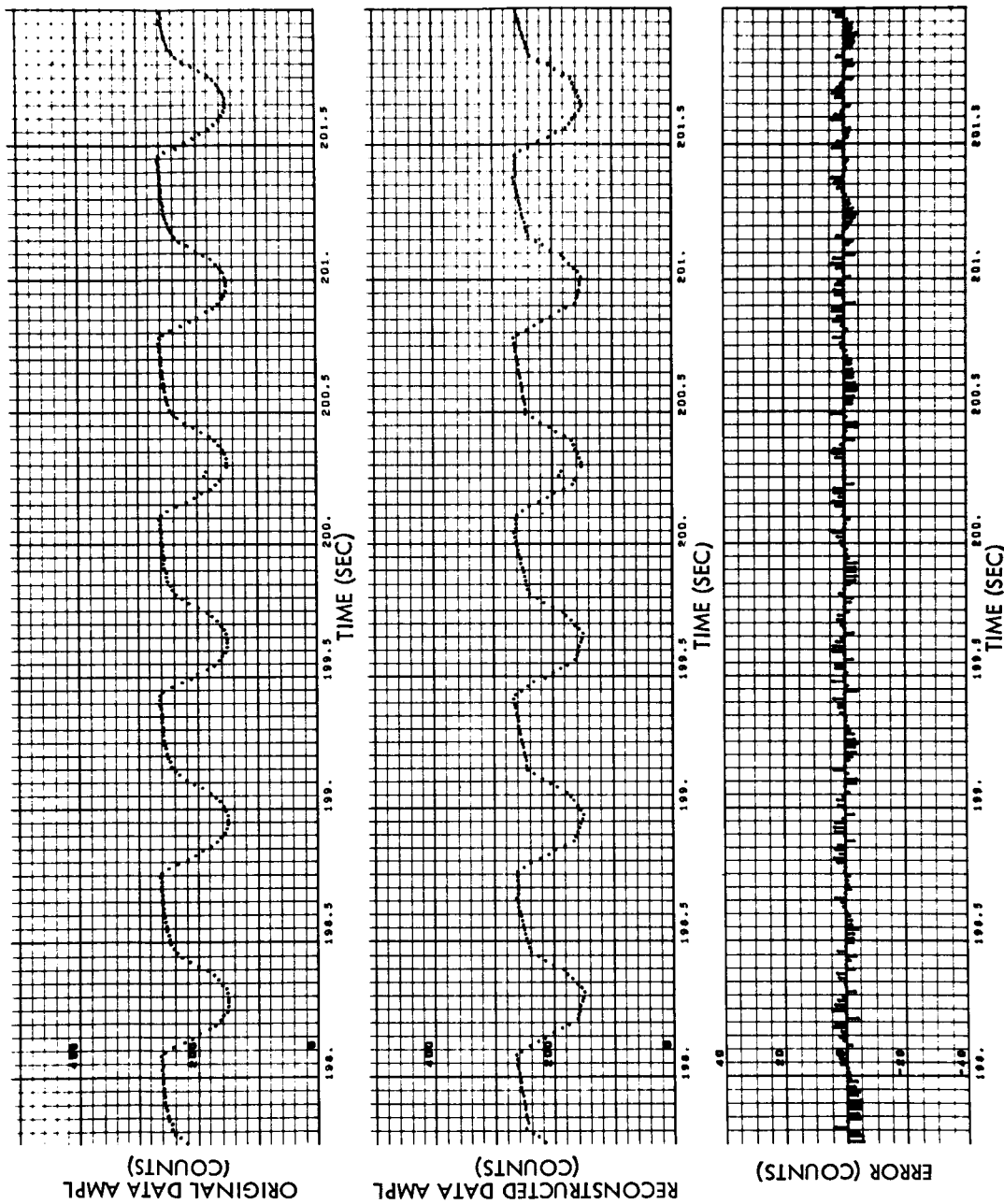


Fig. 4-25a (Cont'd) Sensor 11 Original Data, Reconstructed Data, and Error vs Time, Run S6-10

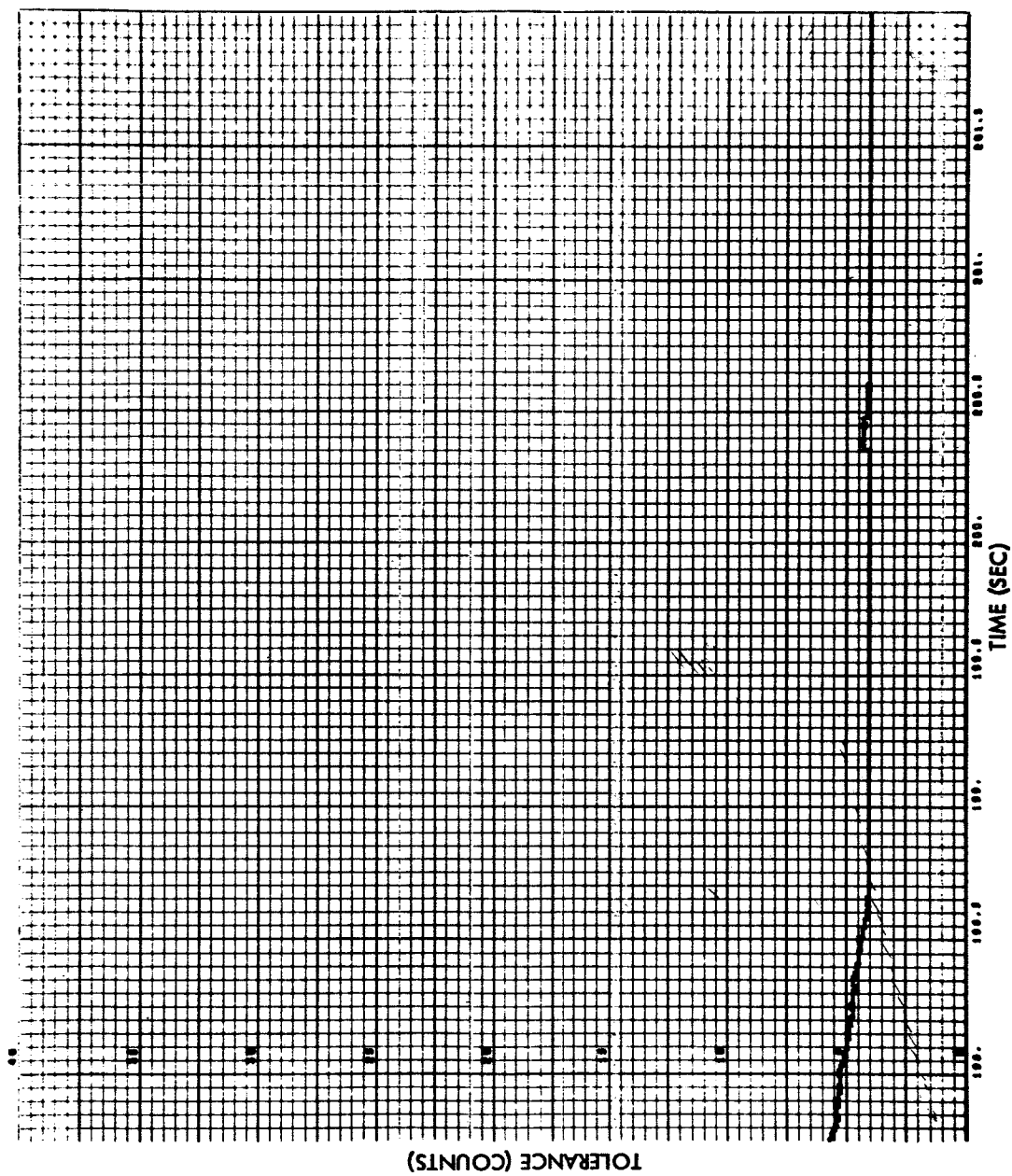


Fig. 4-25b (Cont'd) Sensor 11 Tolerance vs Time, Run S6-10

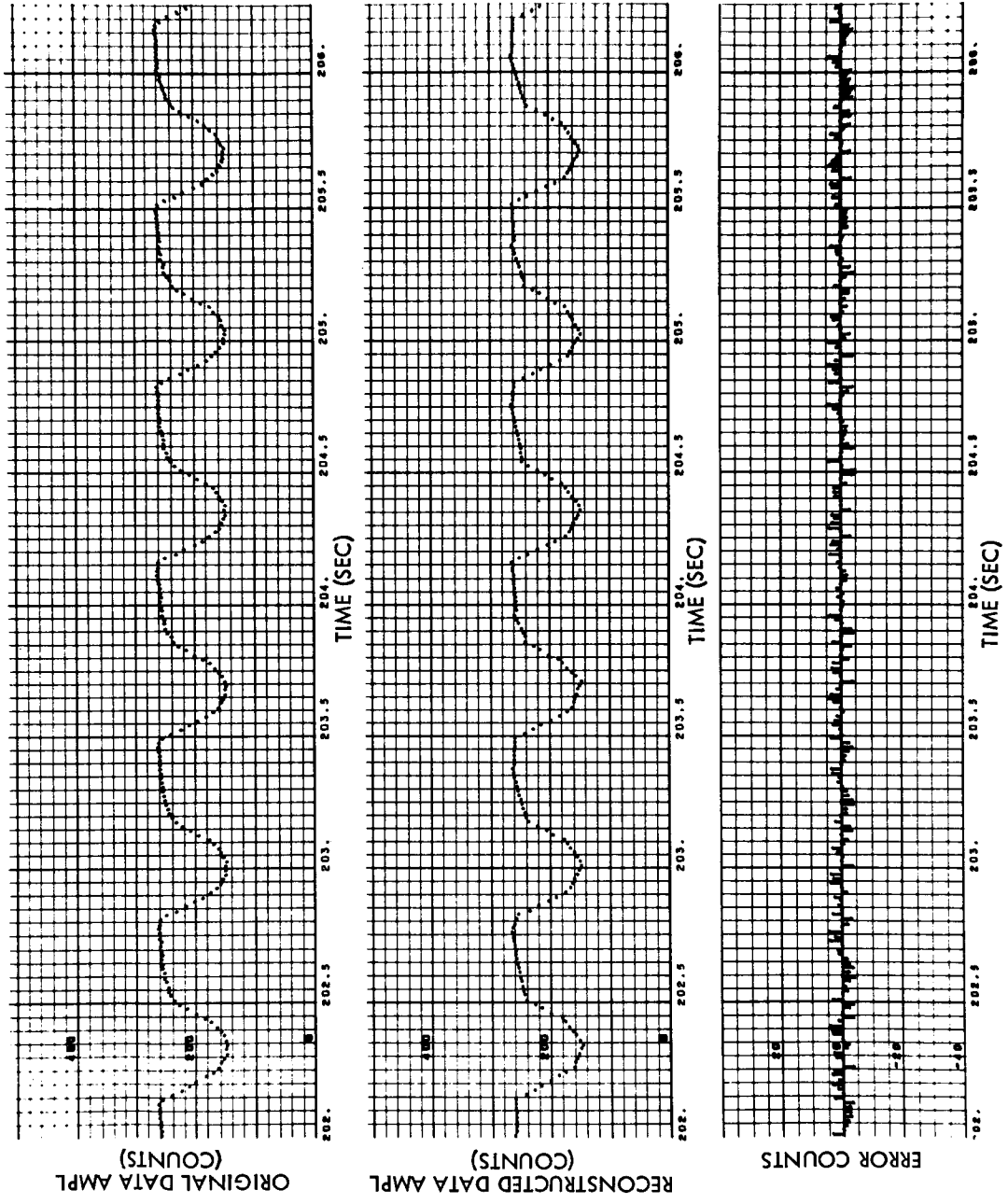


Fig. 4-25a (Cont'd) Sensor 11 Original Data, Reconstructed Data, and Error vs Time, Run S6-10

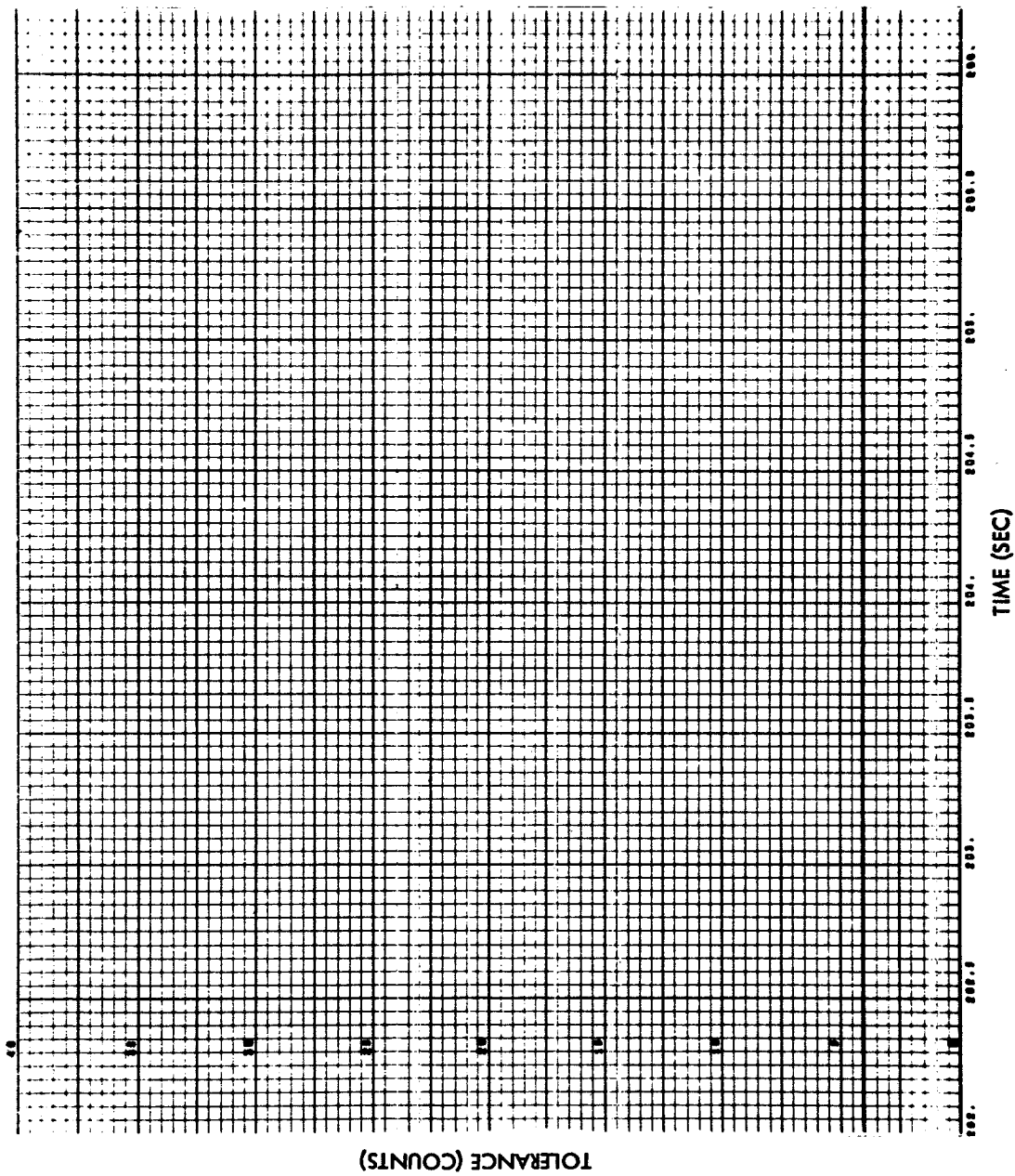


Fig. 4-25b (Cont'd) Sensor 11 Tolerance vs Time, Run S6-10

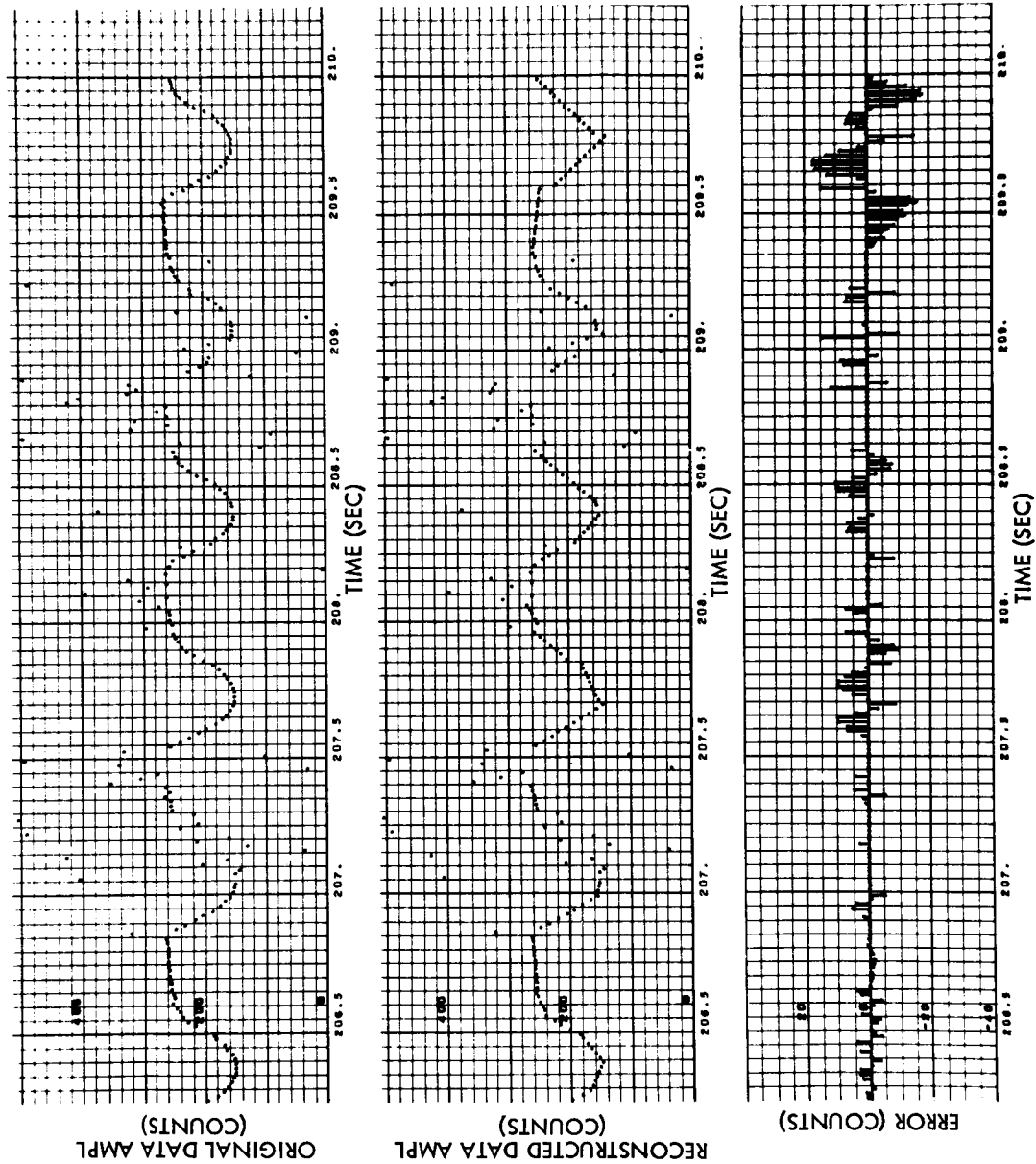


Fig. 4-25a (Cont'd) Sensor 11 Original Data, Reconstructed Data, and Error vs Time, Run S6-10

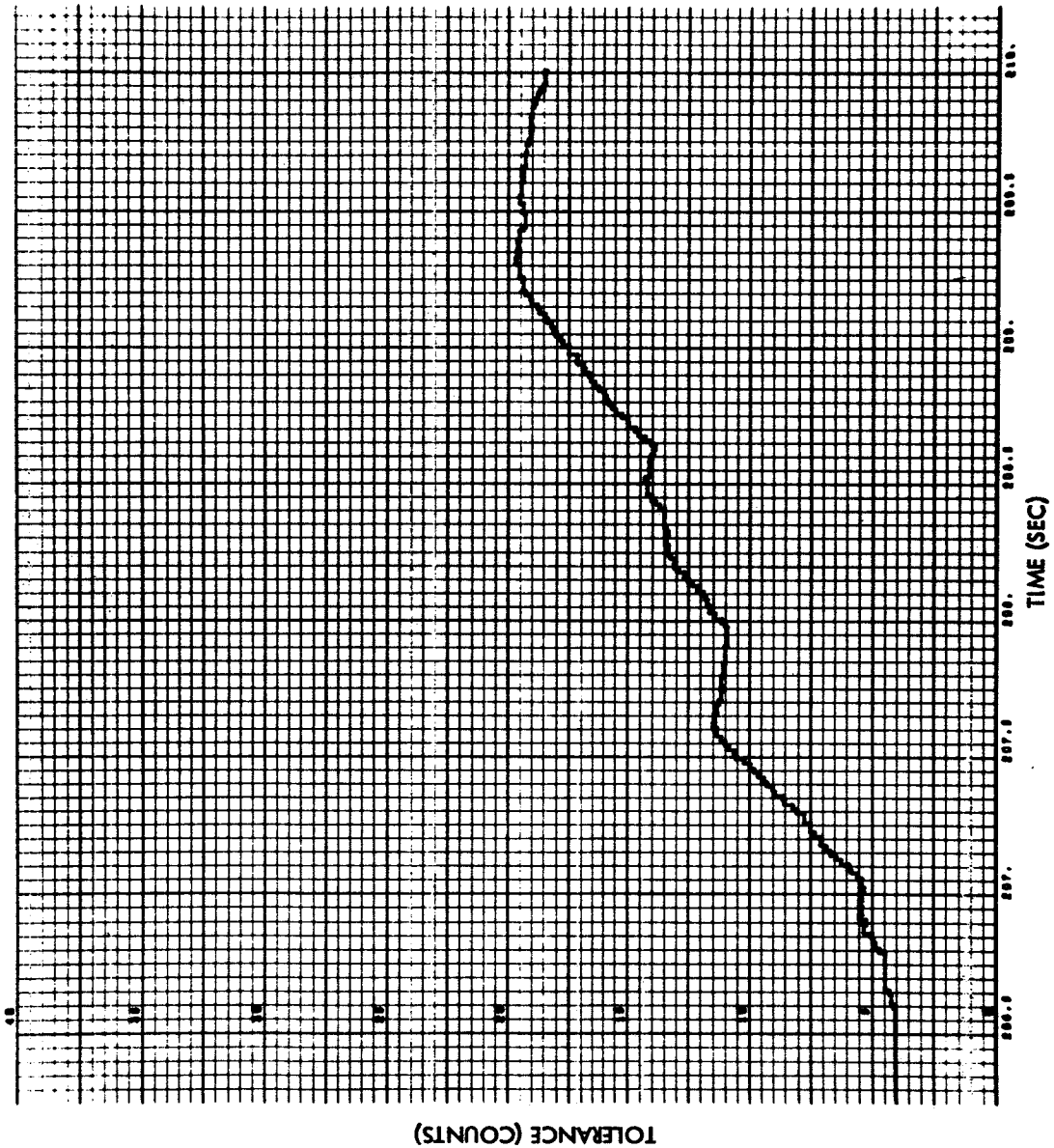


Fig. 4-25b (Cont'd) Sensor 11 Tolerance vs Time, Run S6-10

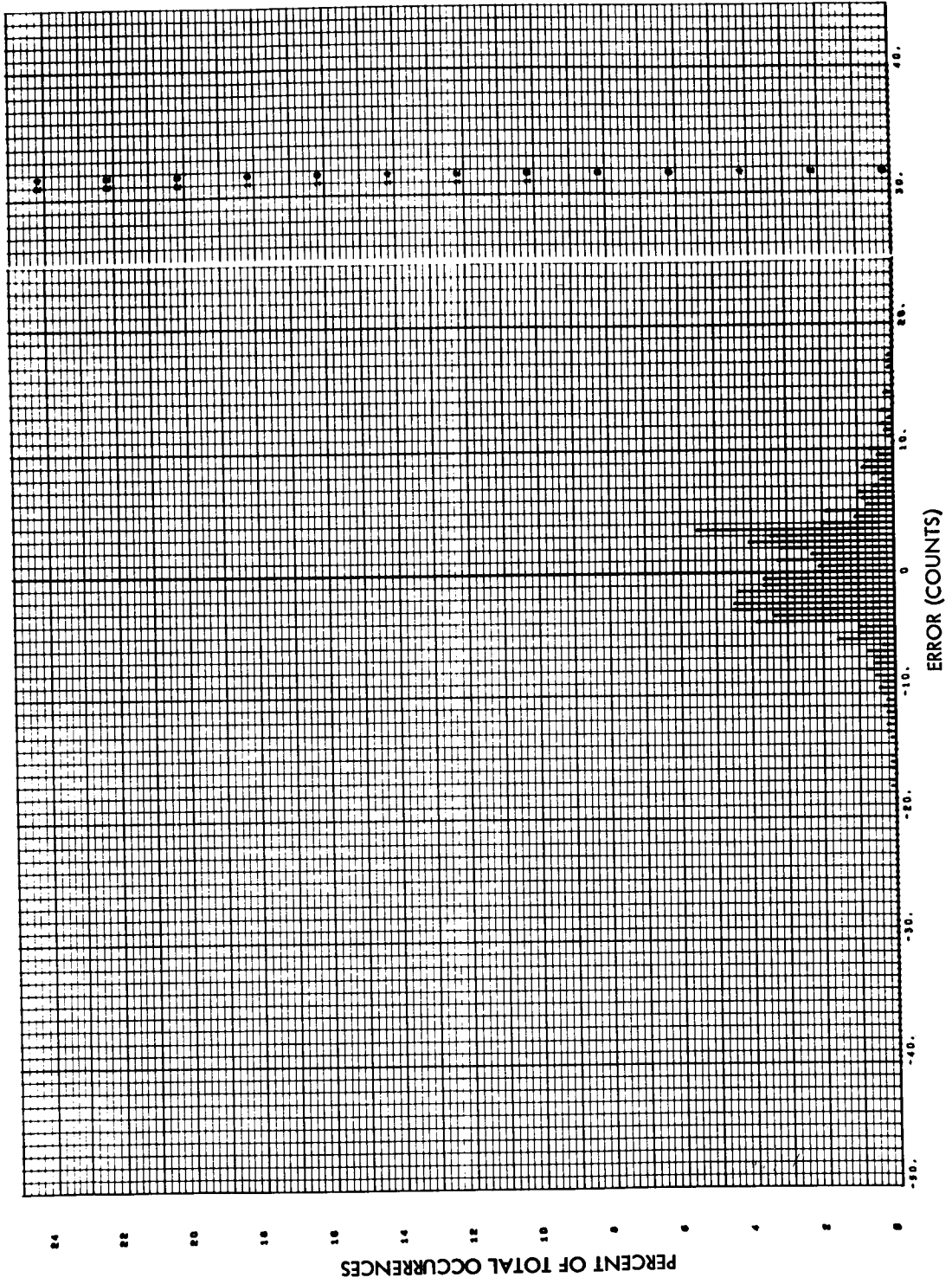


Fig. 4-26 Sensor 11 Error Histogram, Run S6-10

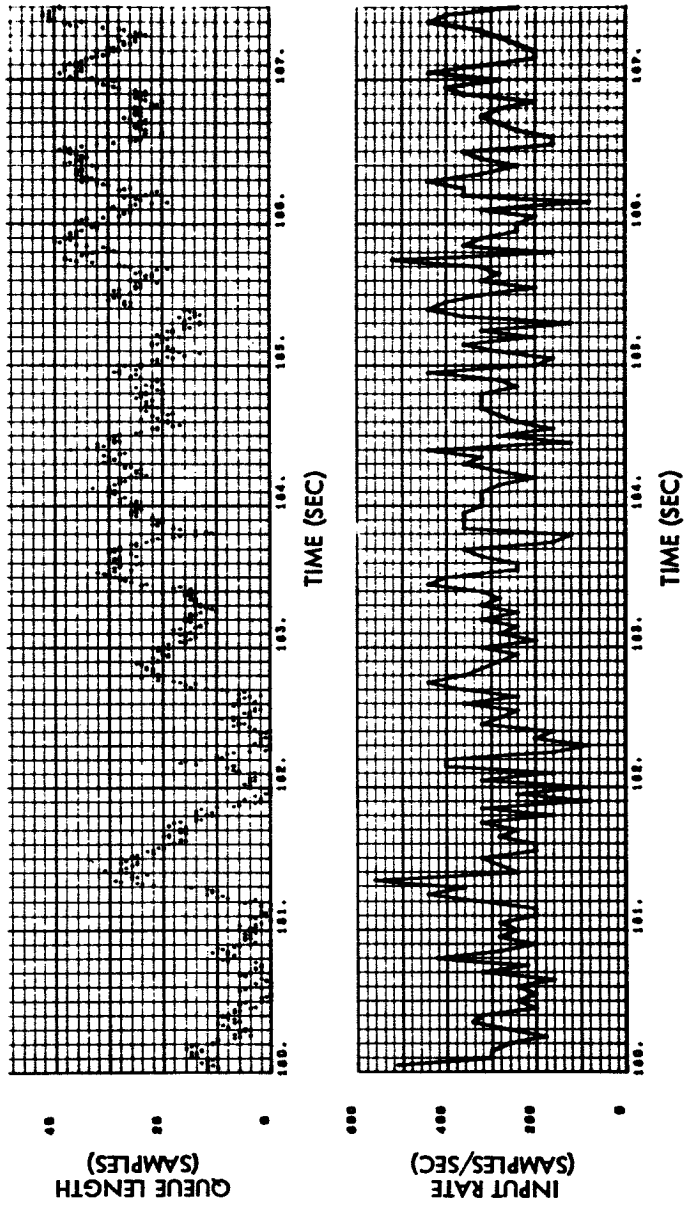
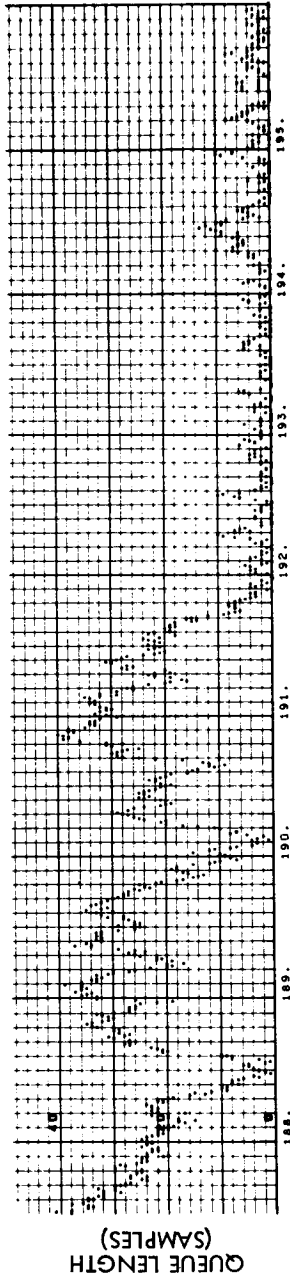
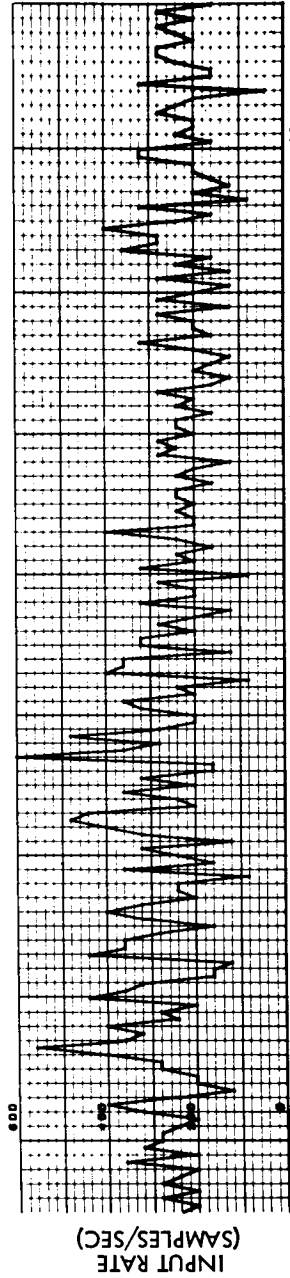


Fig. 4-27 Queue Length and Buffer Input Arrival Rate vs Time, Run S6-12



TIME (SEC)



TIME (SEC)

Fig. 4-27 (Cont'd) Queue Length and Buffer Input Arrival Rate vs Time, Run S6-12

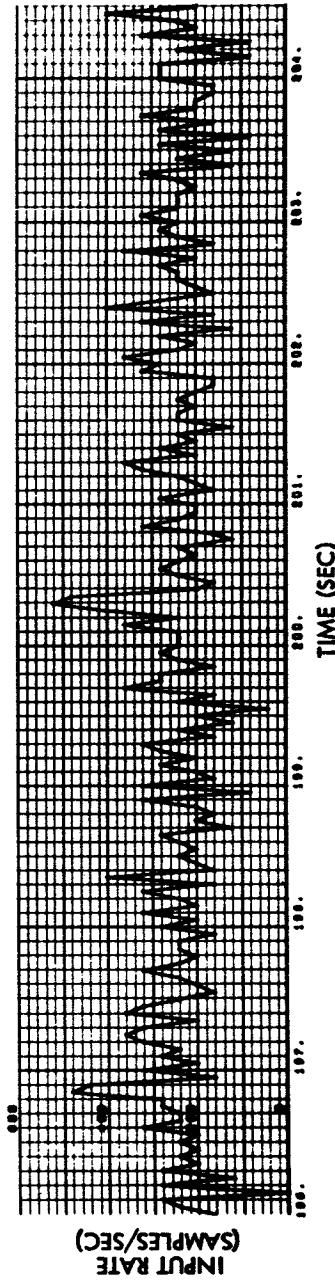
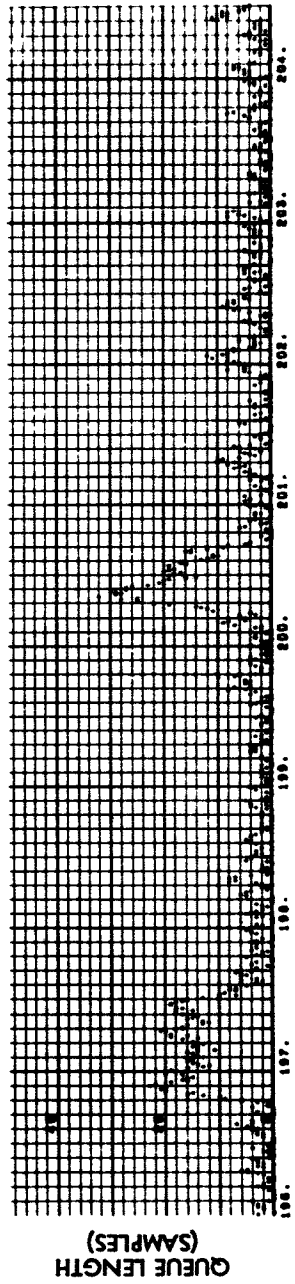


Fig. 4-27 (Cont'd) Queue Length and Buffer Input Arrival Rate vs Time, Run S6-12

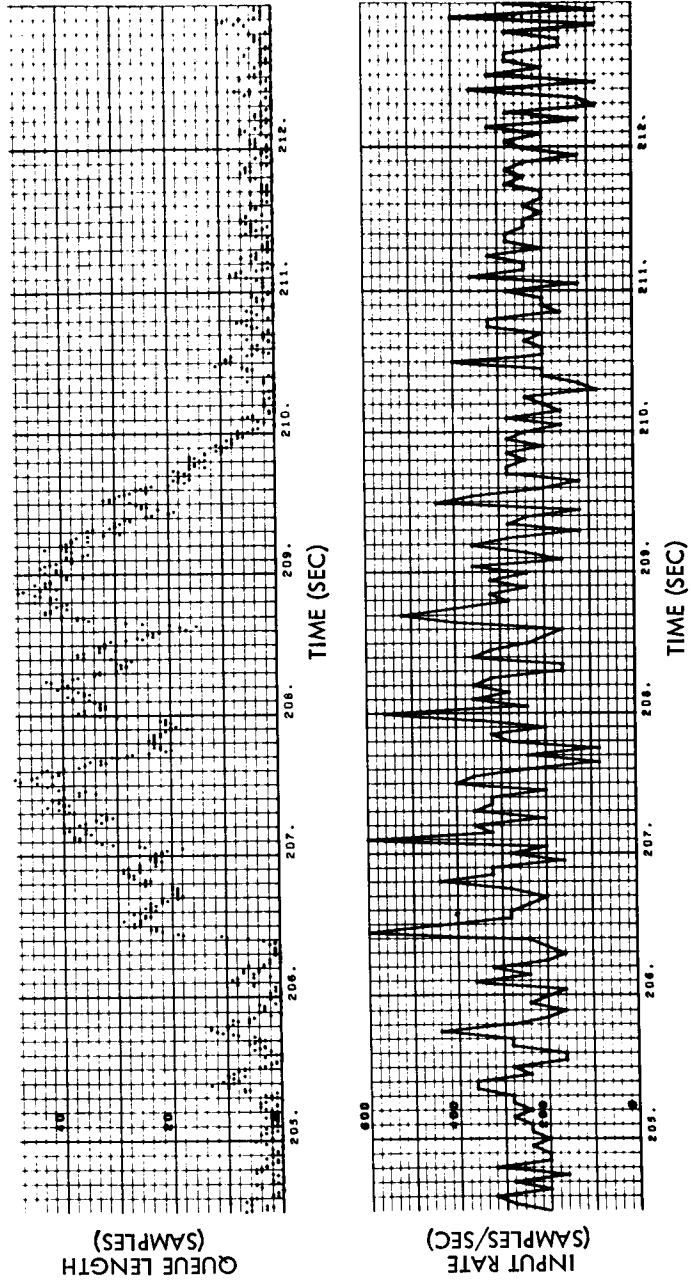


Fig. 4-27 (Cont'd) Queue Length and Buffer Input Arrival Rate vs Time, Run S6-12

(This page intentionally left blank.)

4-117

LOCKHEED MISSILES & SPACE COMPANY

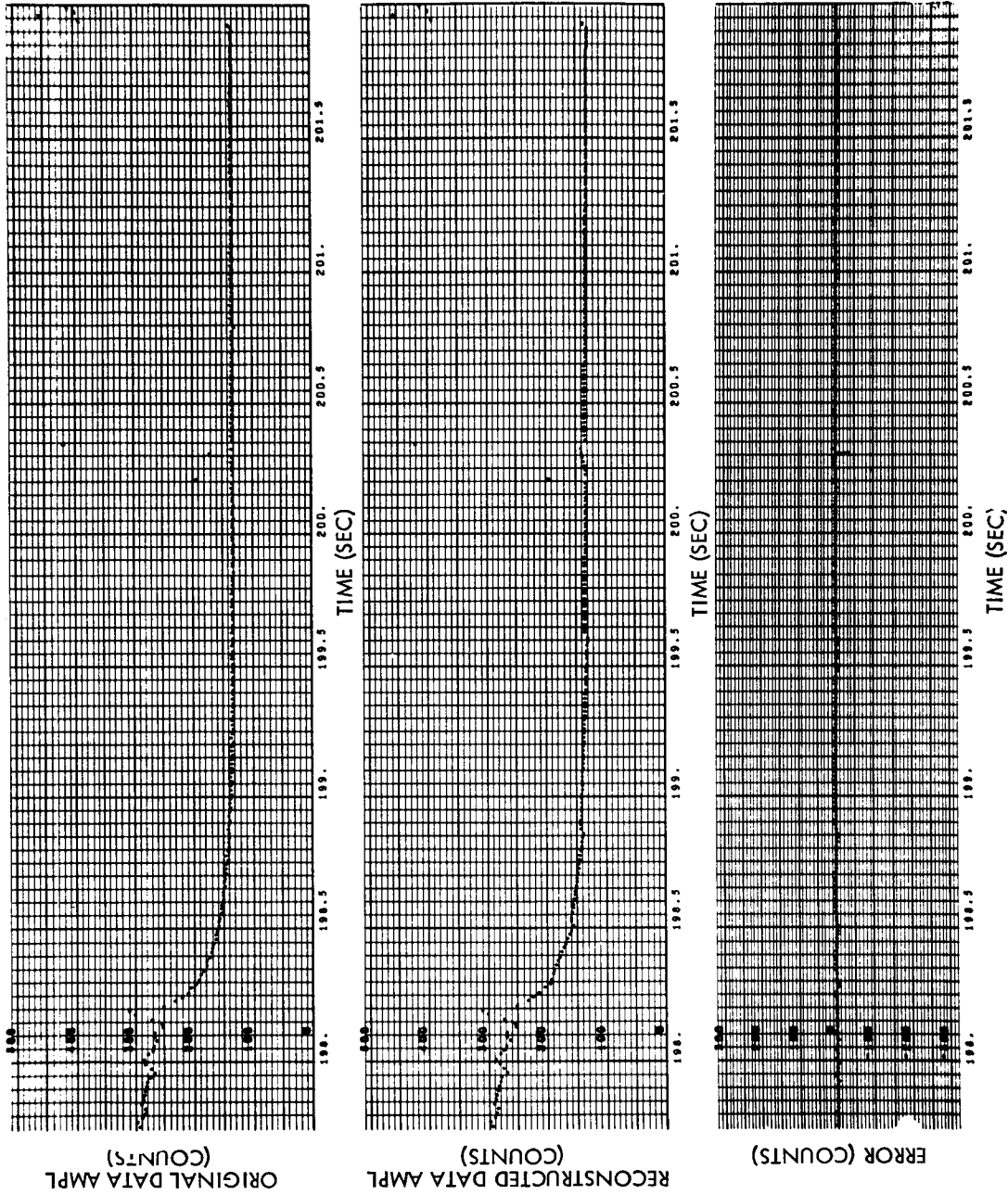


Fig. 4-28a Sensor 9 Original Data, Reconstructed Data, and Error vs Time, Run S6-12

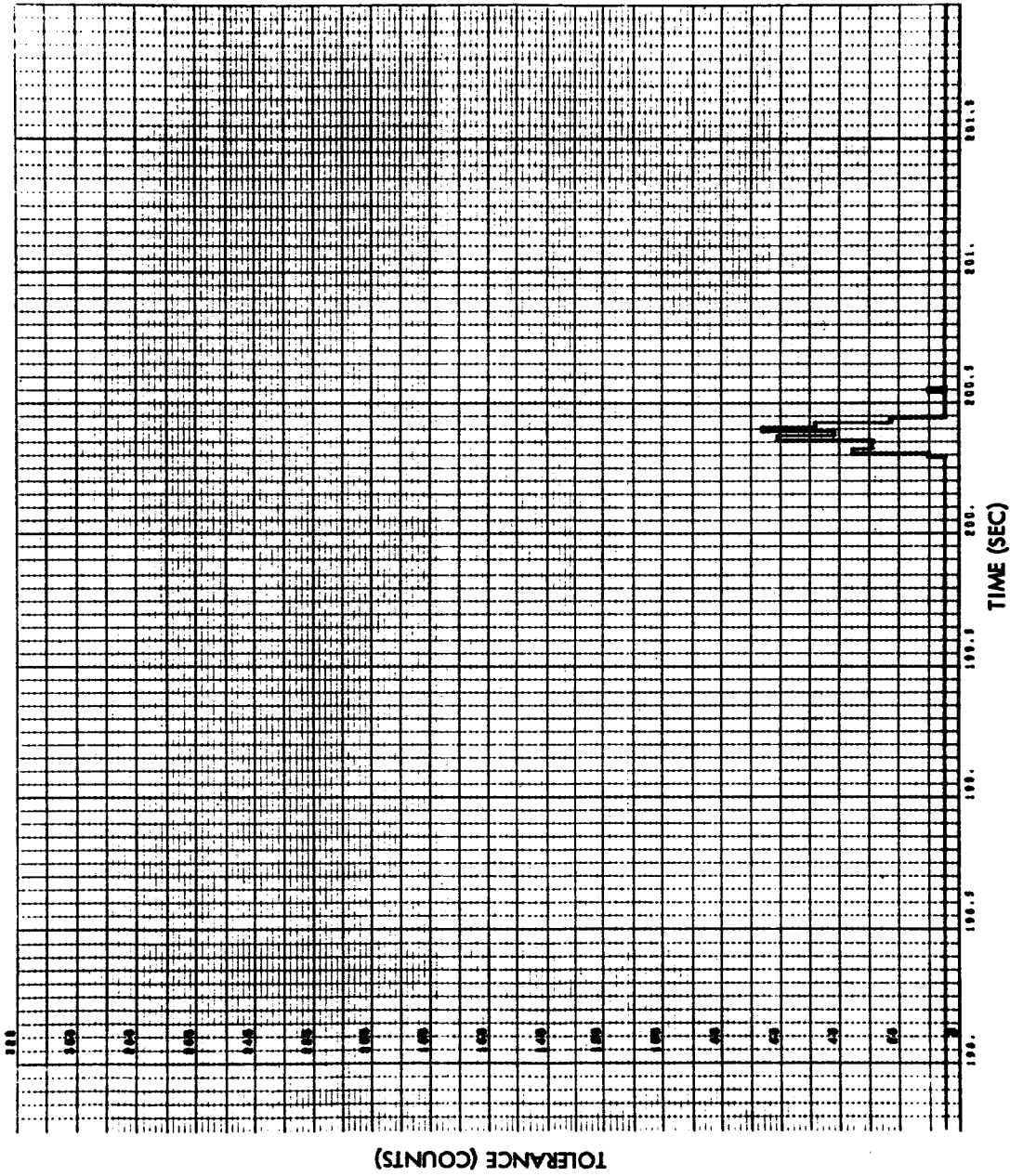


Fig. 4-28b Sensor 9 Tolerance vs Time, Run S6-12

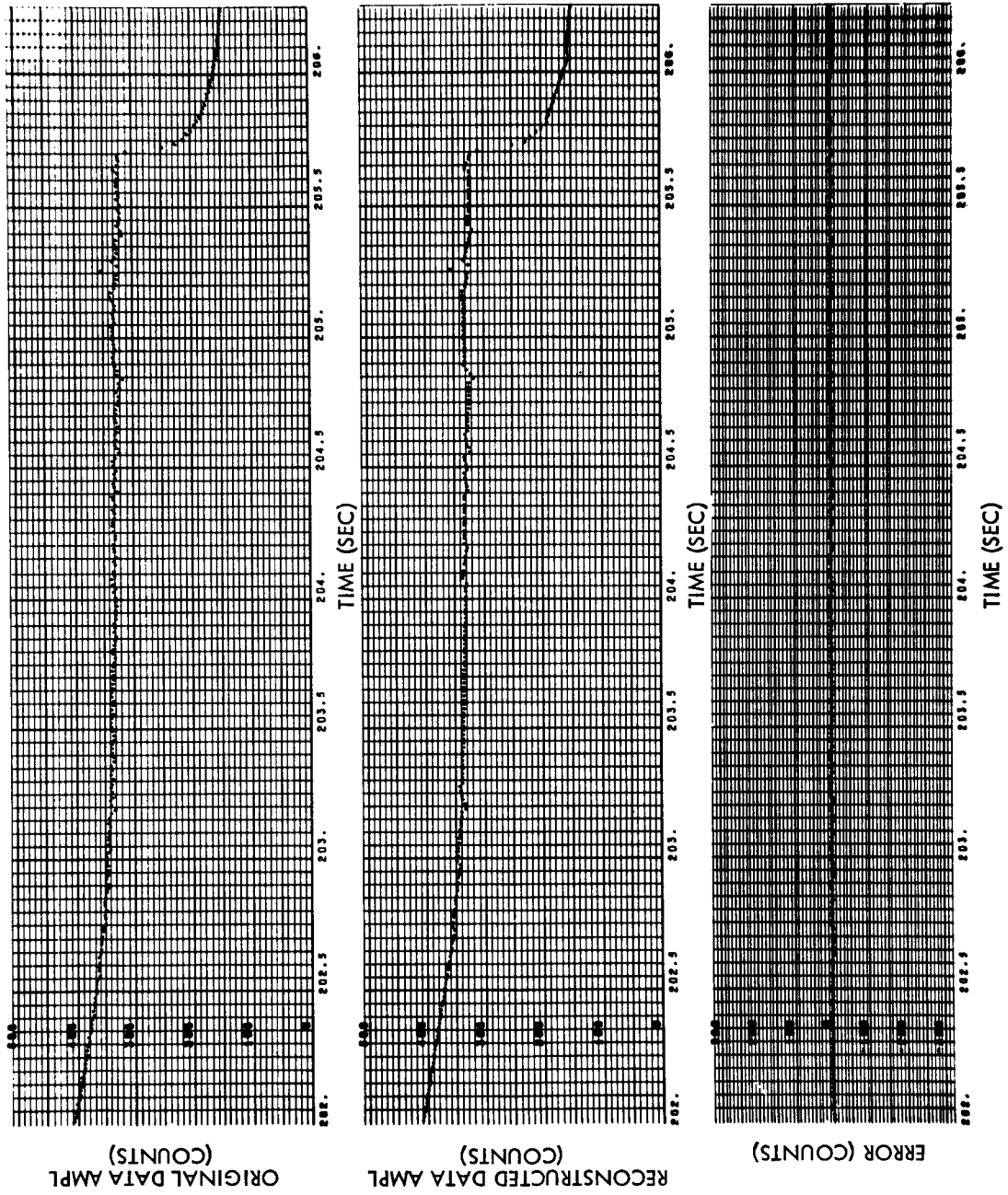


Fig. 4-28a (Cont'd) Sensor 9 Original Data, Reconstructed Data, and Error vs Time, Run S6-12

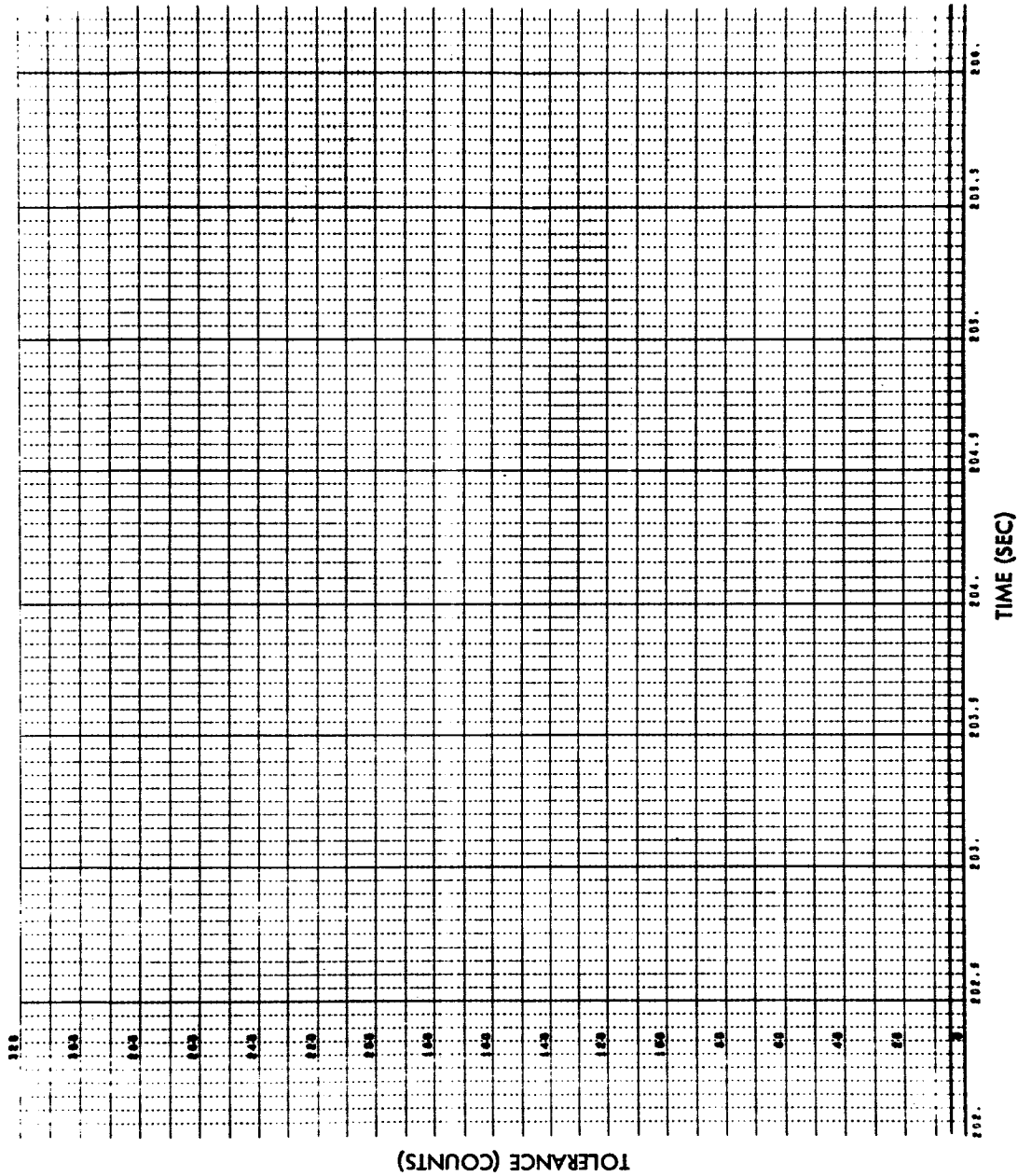


Fig. 4-28b (Cont'd) Sensor 9 Tolerance vs Time, Run S6-12

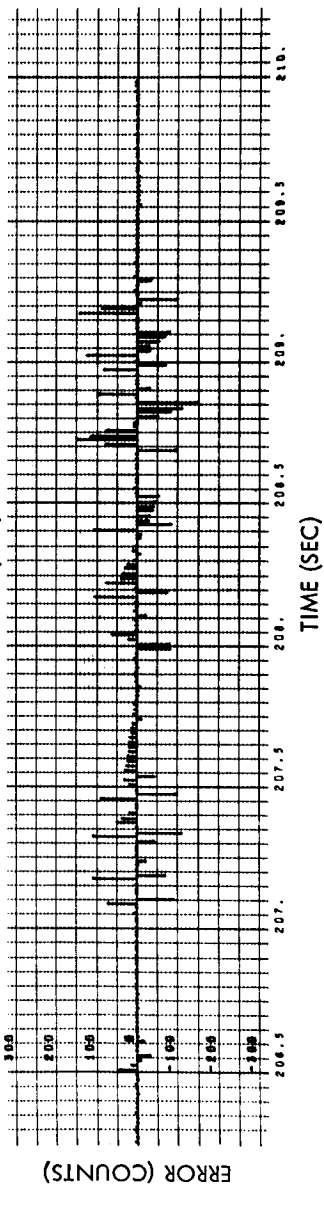
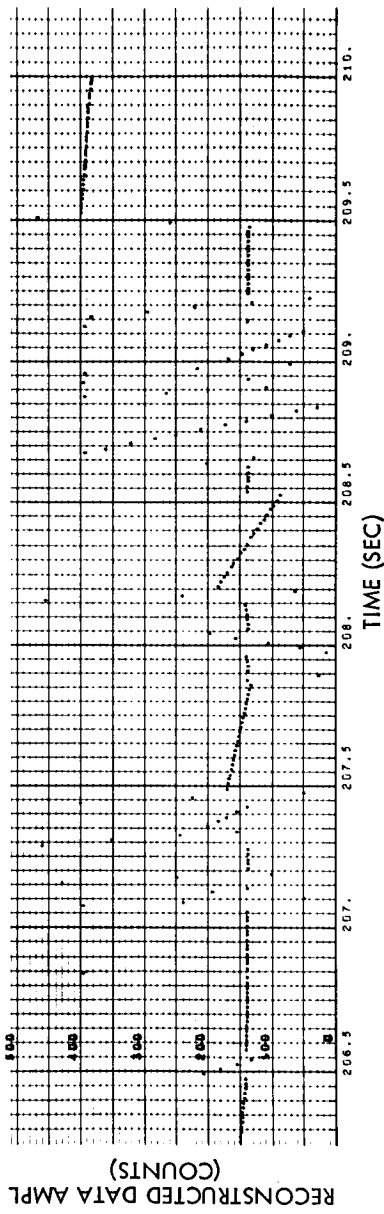
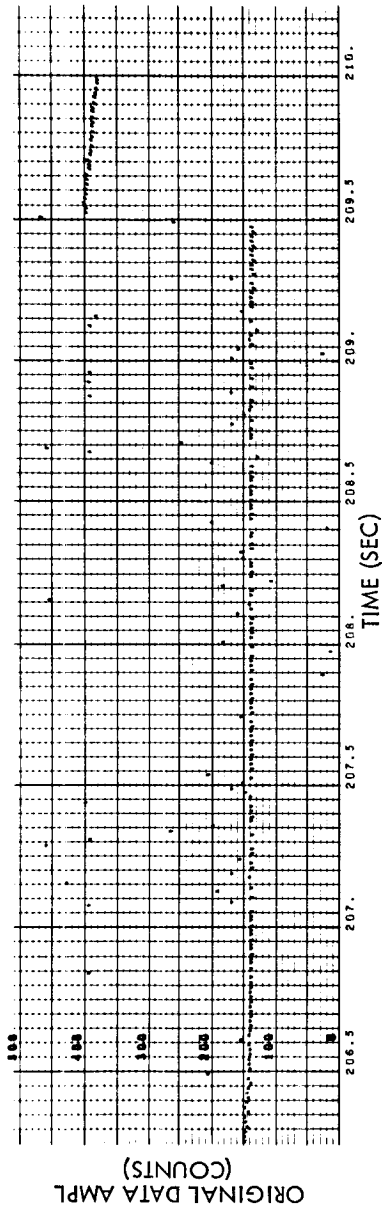


Fig. 4-28a (Cont'd) Sensor 9 Original Data, Reconstructed Data, and Error vs Time, Run S6-12

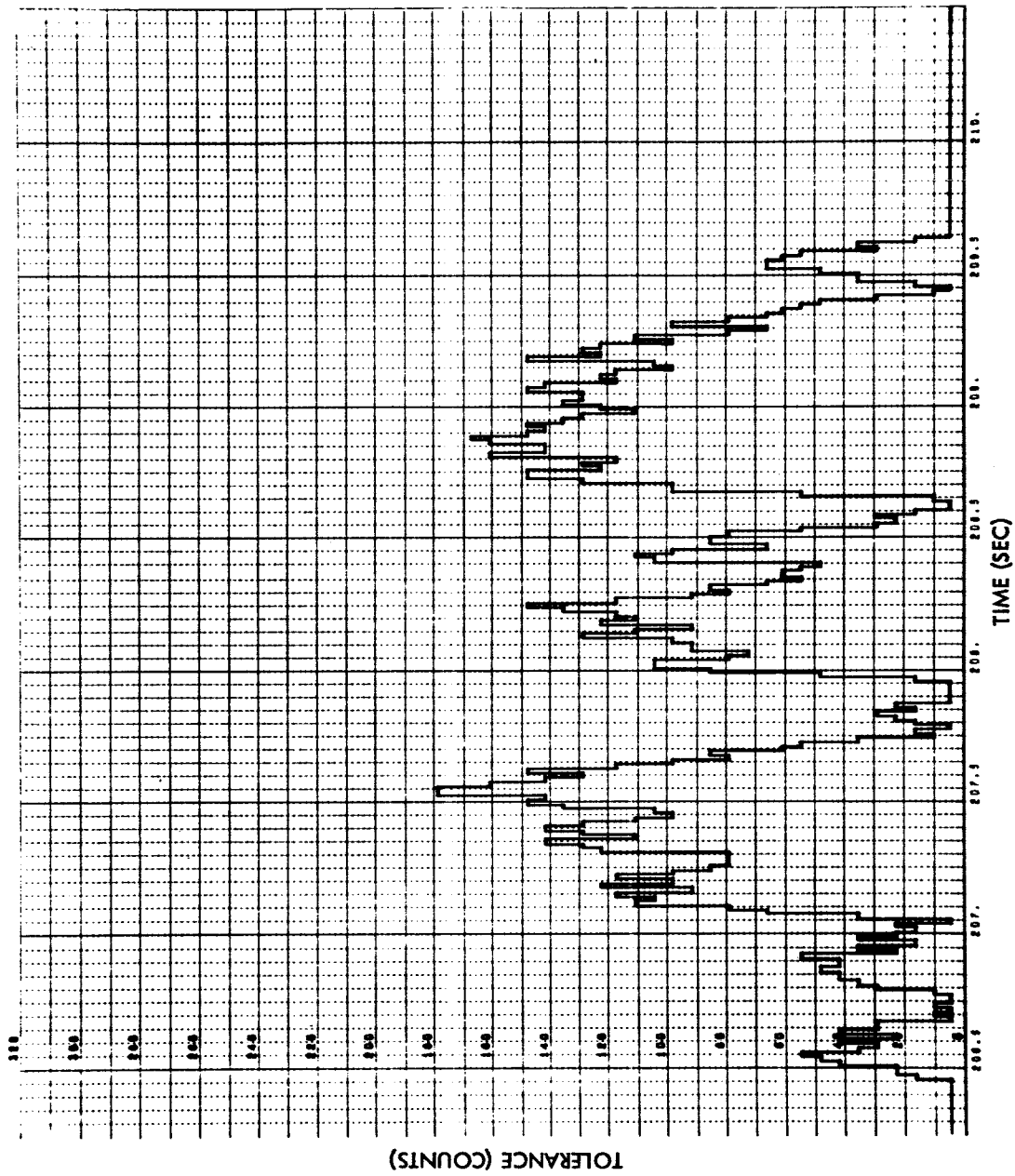


Fig. 4-28b (Cont'd) Sensor 9 Tolerance vs Time, Run S6 -12

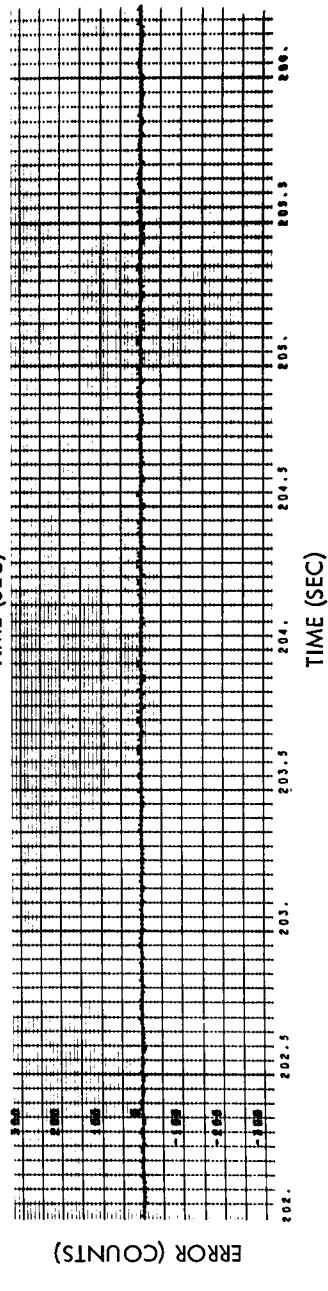
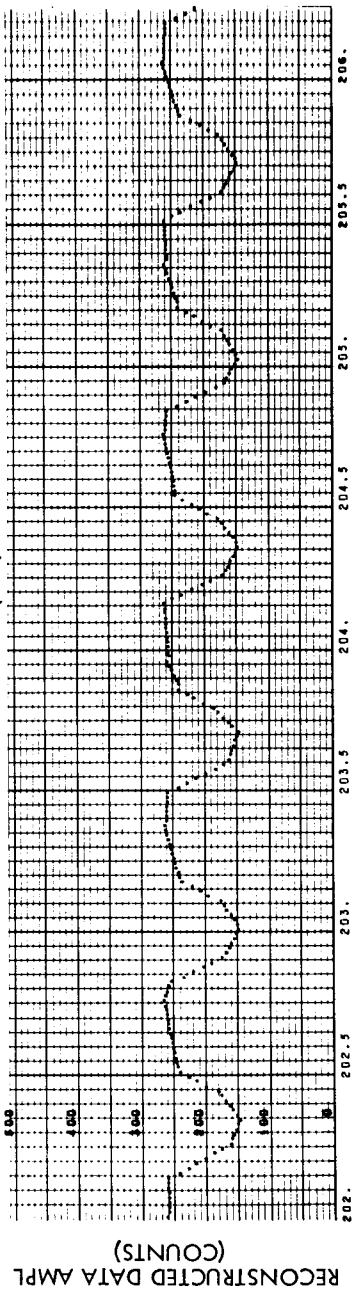
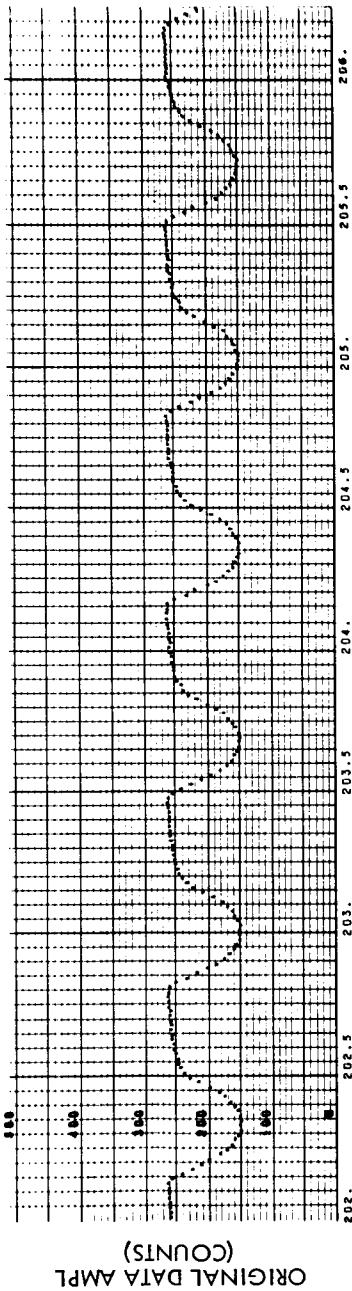


Fig. 4-29a Sensor 11 Original Data, Reconstructed Data, and Error vs Time, Run S6-12

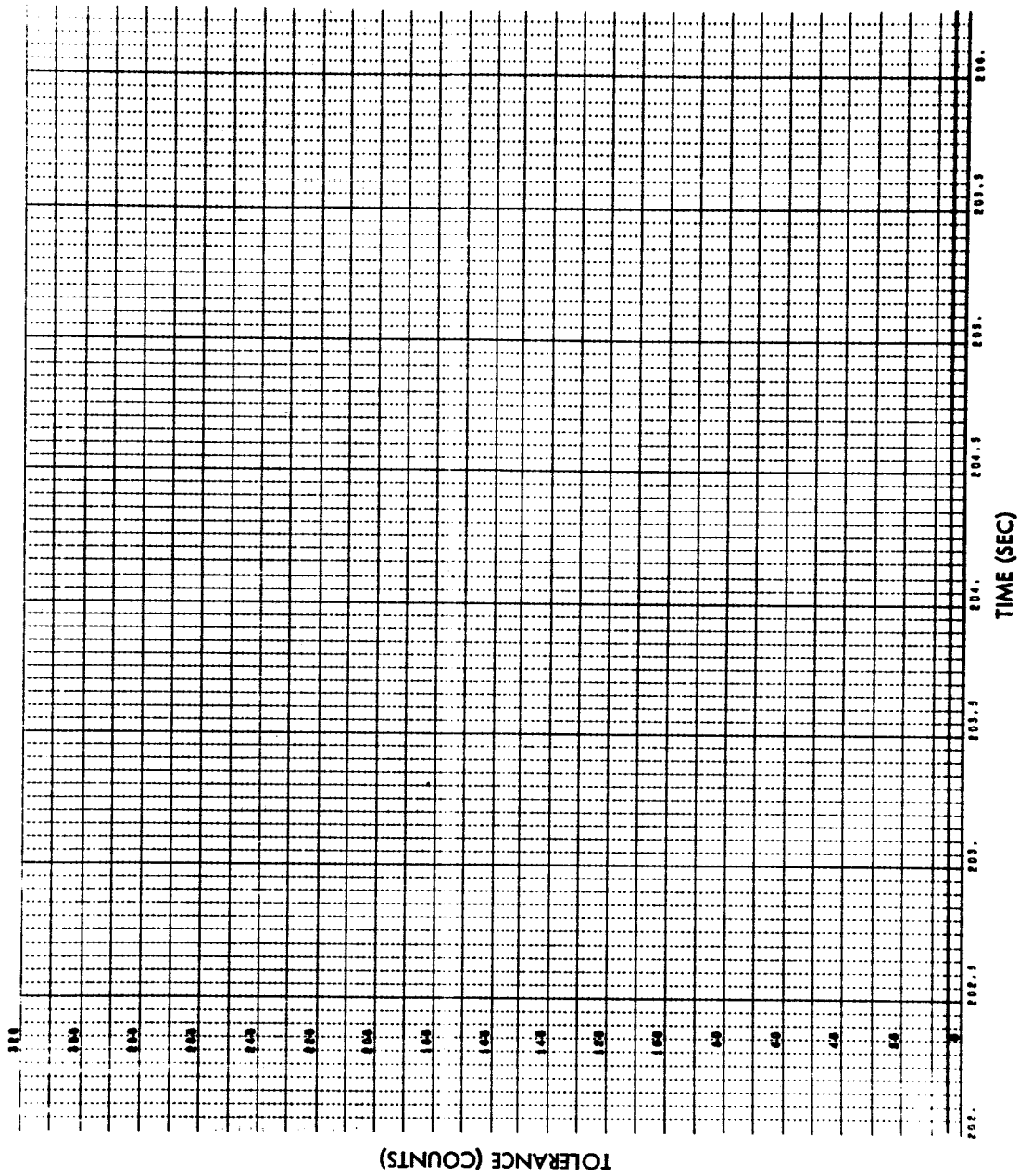


Fig. 4-29b Sensor 11 Tolerance vs Time, Run S6-12

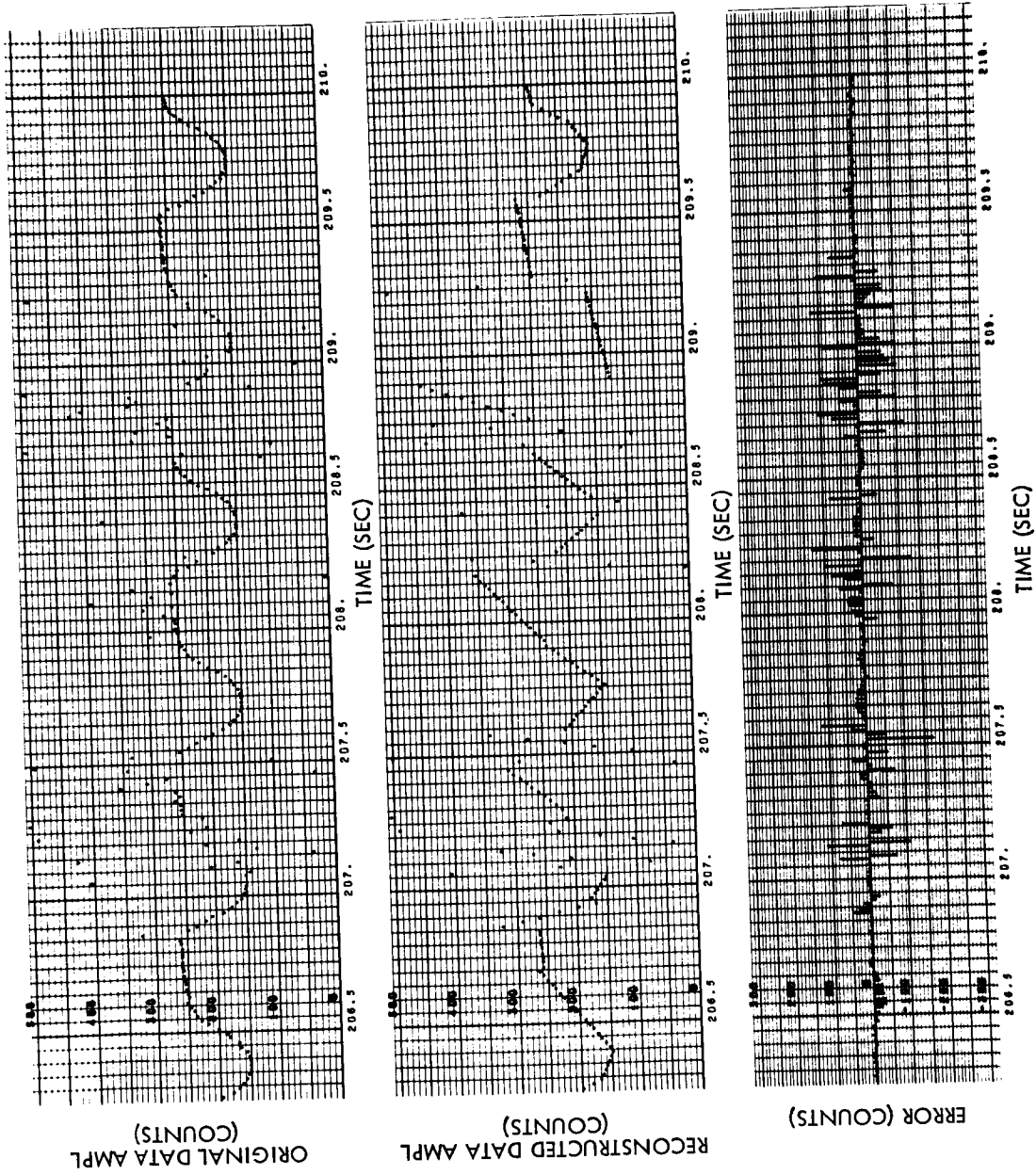


Fig. 4-29a (Cont'd) Sensor 11 Original Data, Reconstructed Data, and Error vs Time, Run S6-12

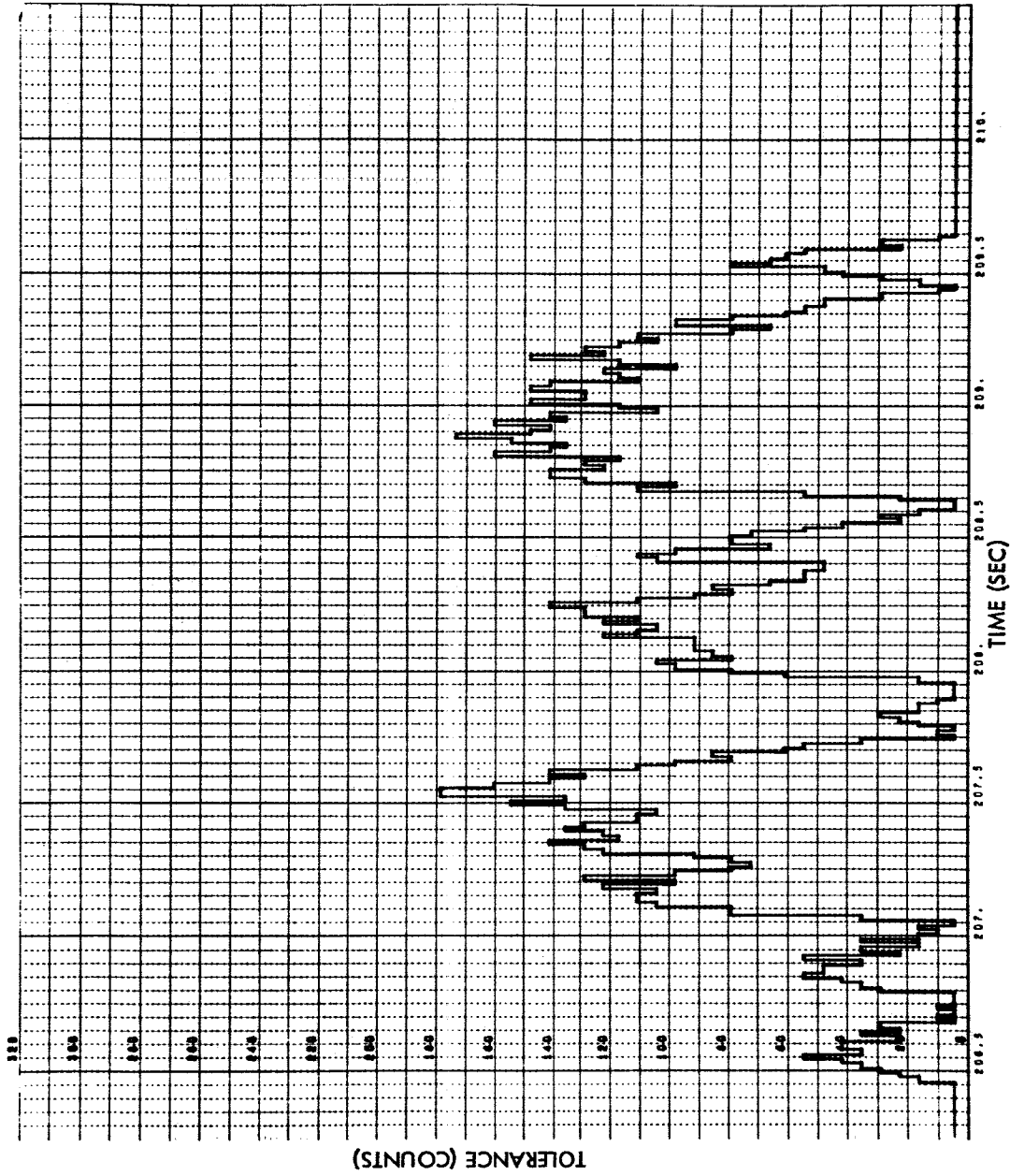


Fig. 4-29b (Cont'd) Sensor 11 Tolerance vs Time, Run S6-12

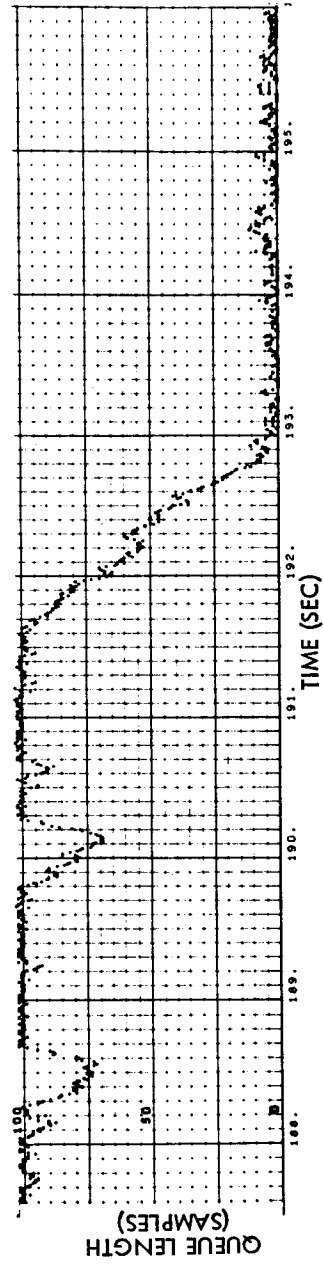
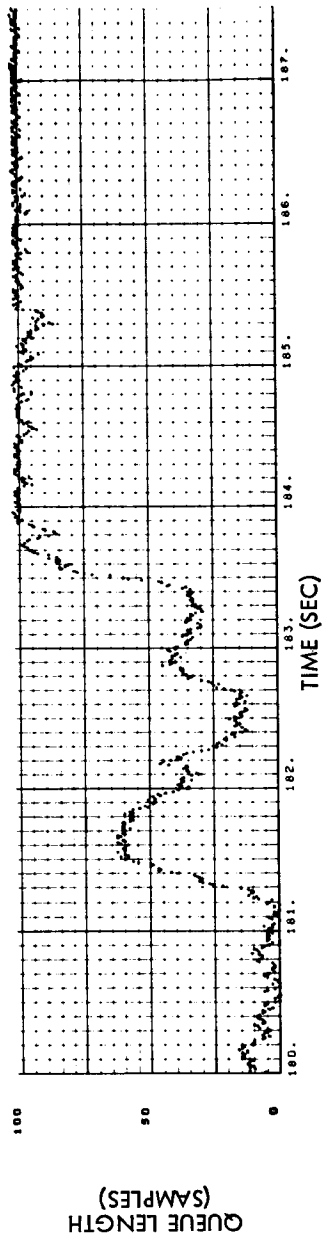


Fig. 4-30 Queue Length vs Time, Run S6-11

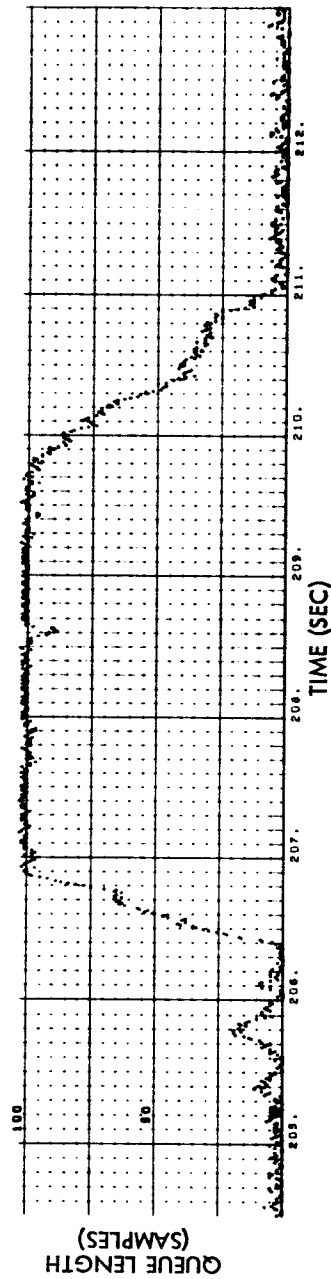
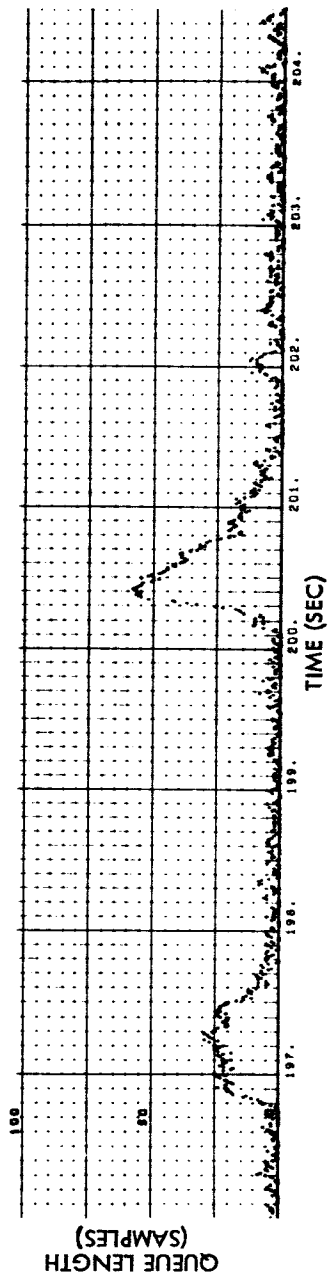


Fig. 4-30 (Cont'd) Queue Length vs Time, Run S6-11

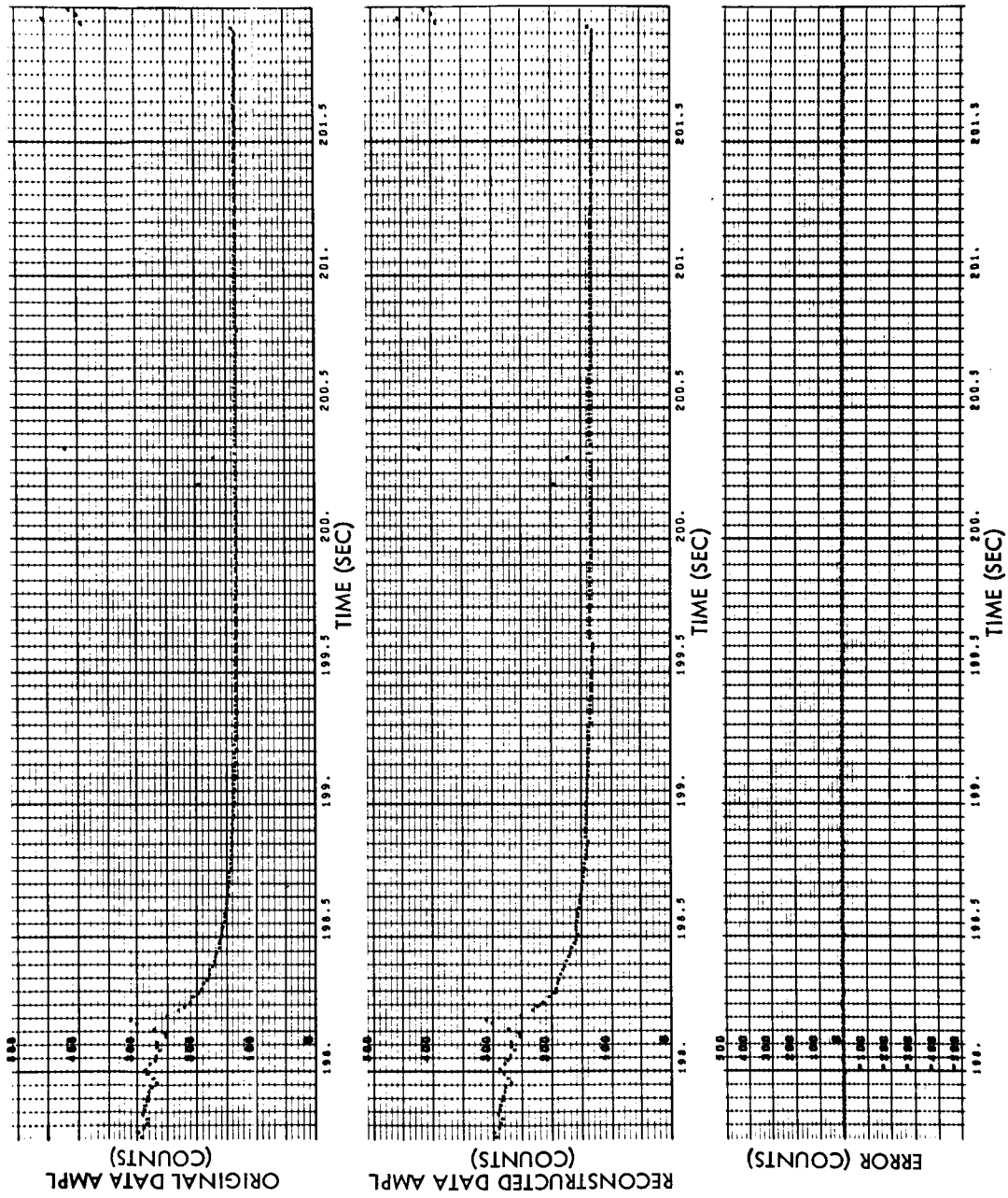


Fig. 4-31 Sensor 9 Original Data, Reconstructed Data, and Error vs Time, Run S6-11

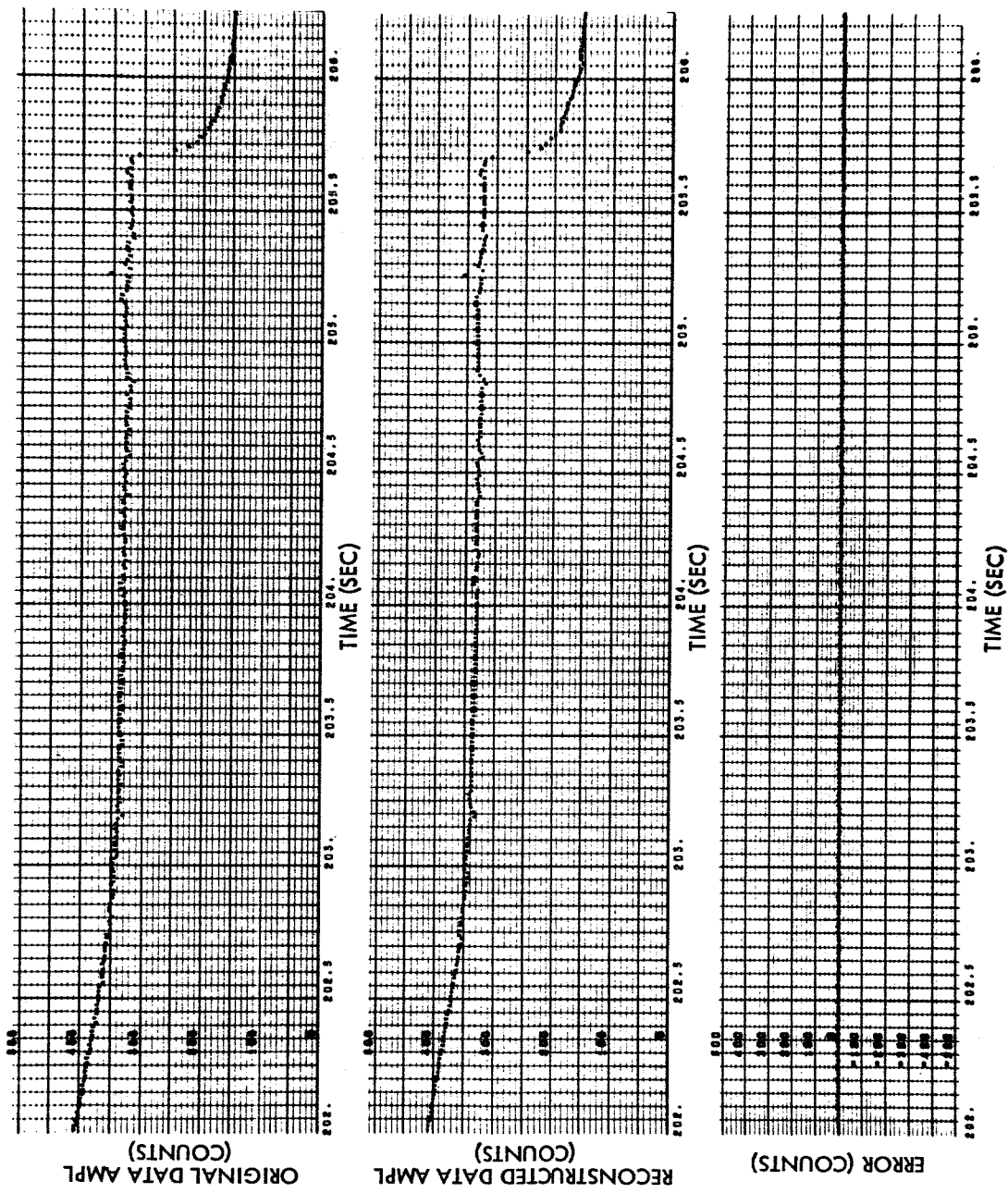


Fig. 4-31 (Cont'd) Sensor 9 Original Data, Reconstructed Data, and Error vs Time, Run S6-11

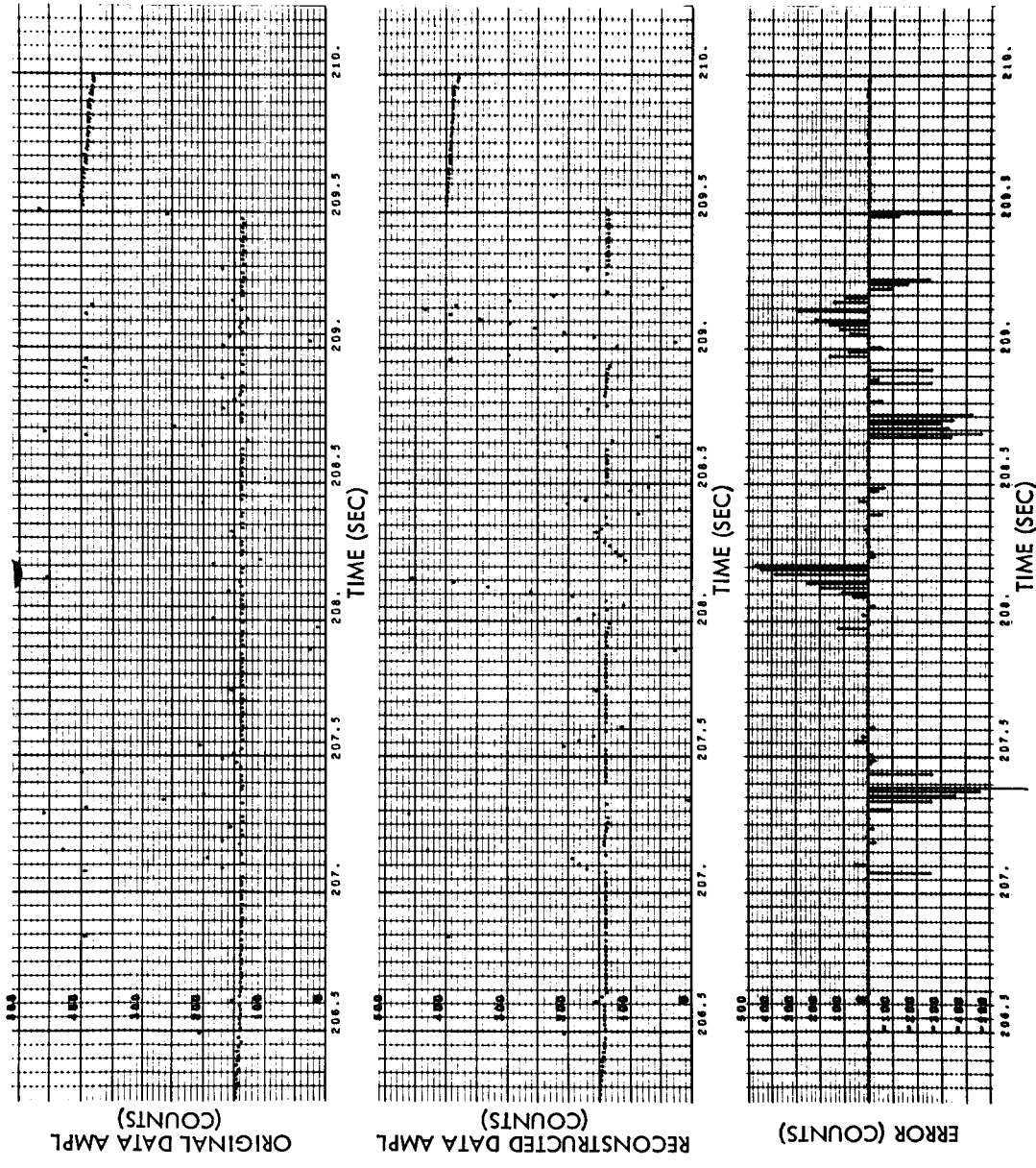


Fig. 4-31 (Cont'd) Sensor 9 Original Data, Reconstructed Data, and Error vs Time, S6-11

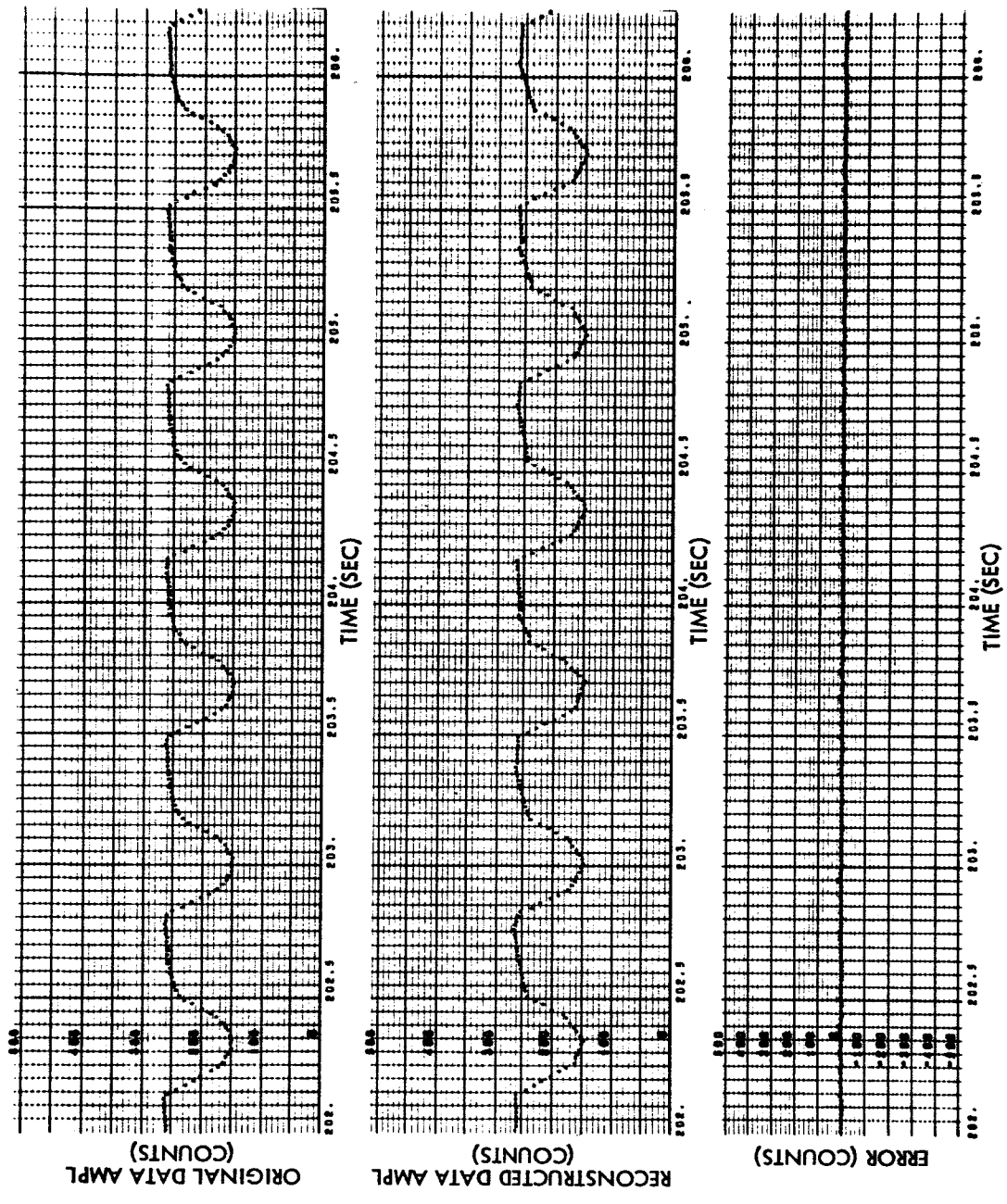


Fig. 4-32 Sensor 11 Original Data, Reconstructed Data, and Error vs Time, Run S6-11

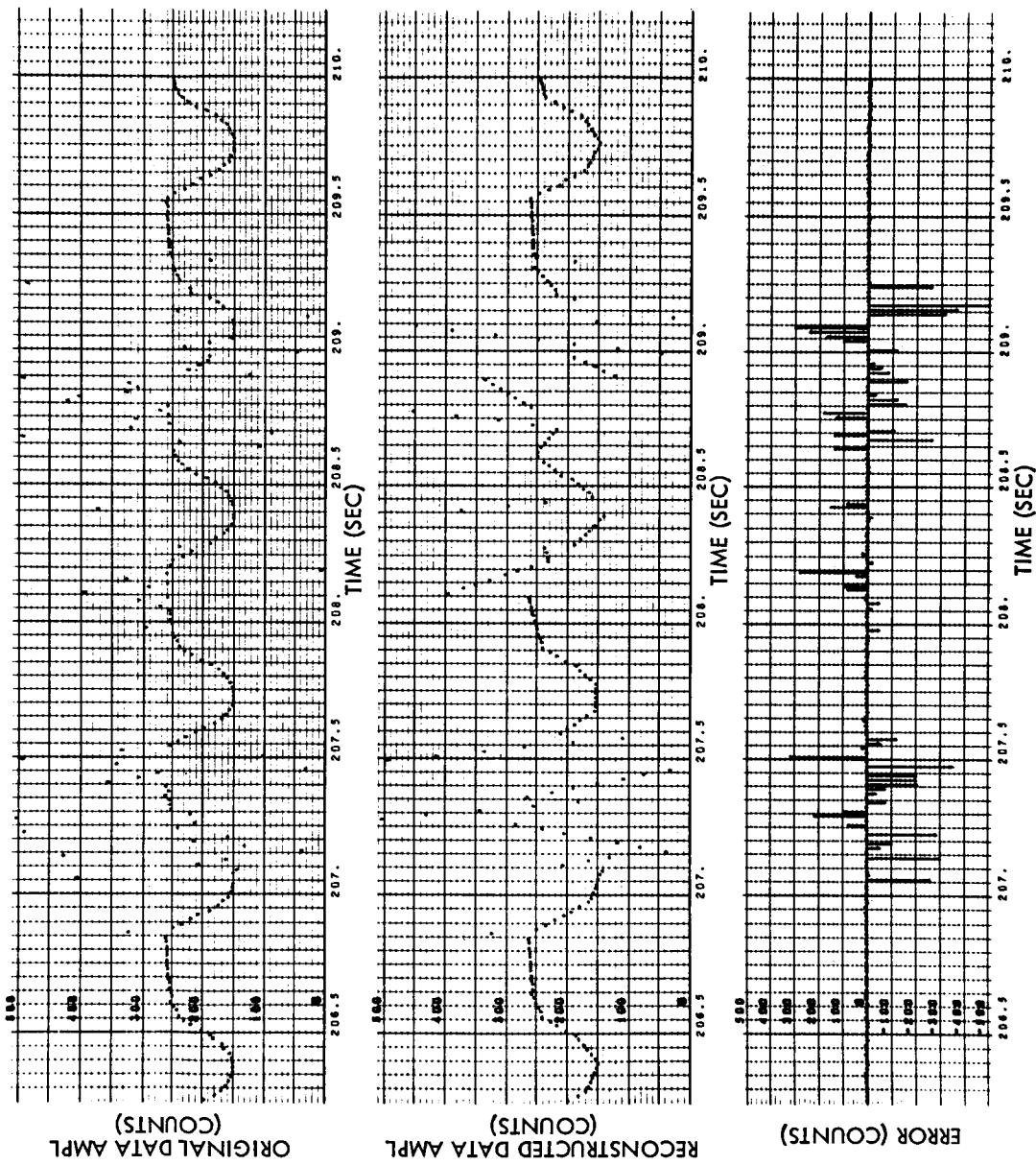


Fig. 4-32 (Cont'd) Sensor 11 Original Data, Reconstructed Data, and Error vs Time, Run S6-11

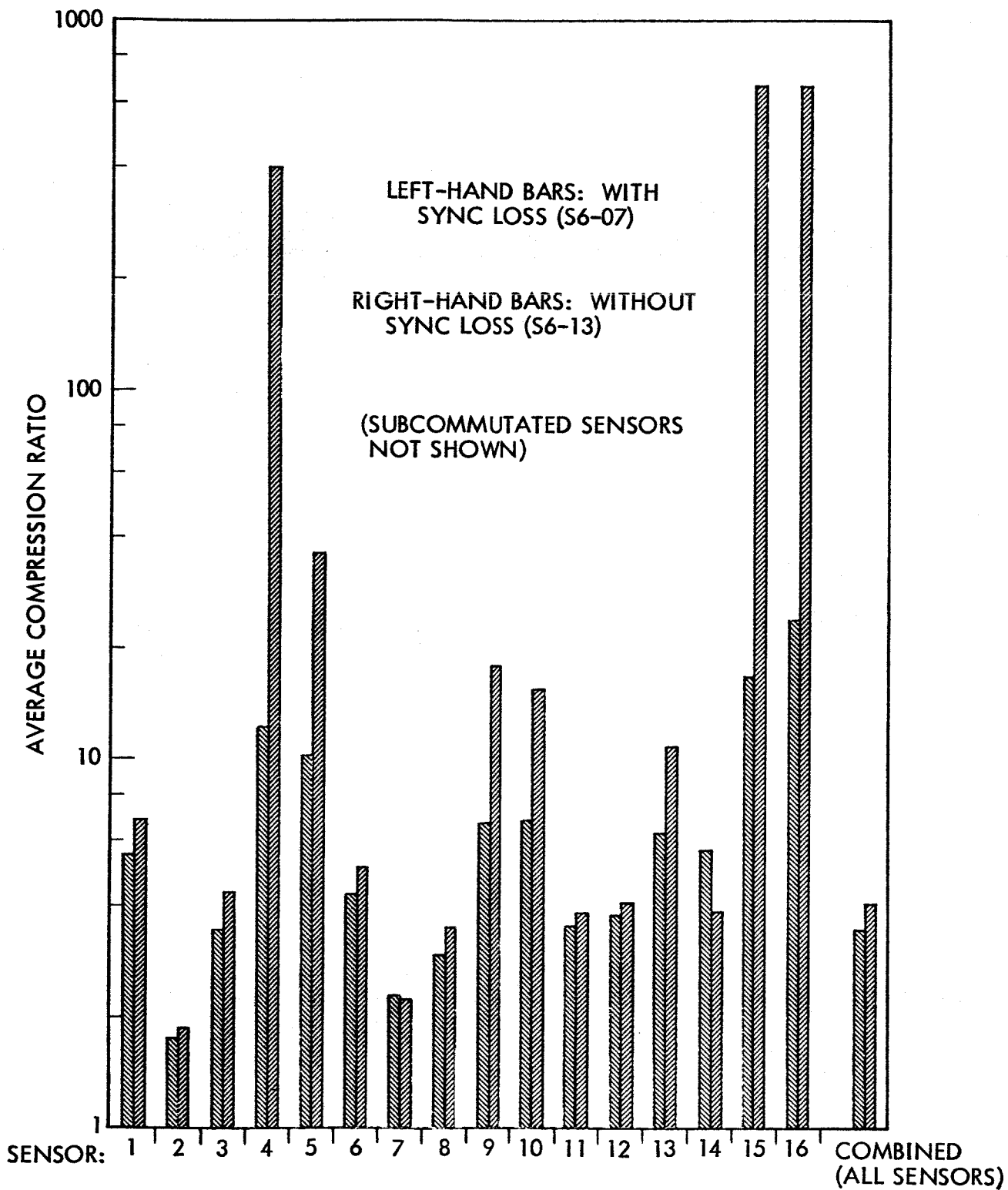


Figure 4-33 Comparison of Average Compression Ratios With and Without Sync Losses

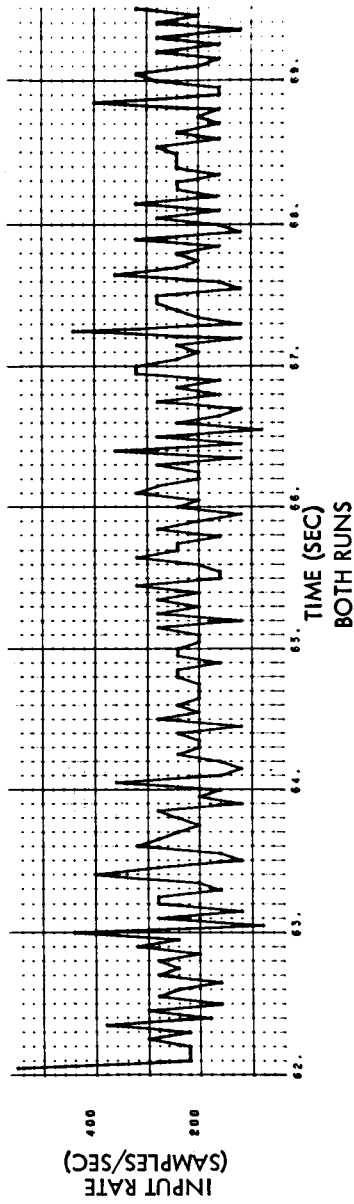
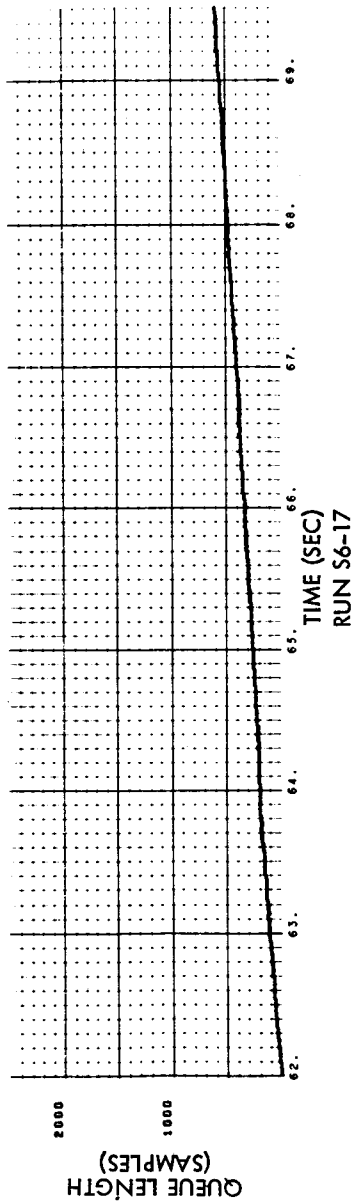
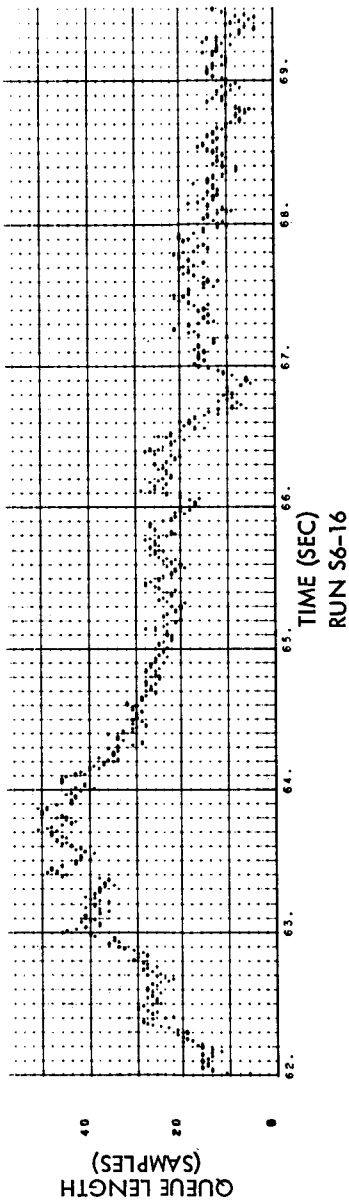
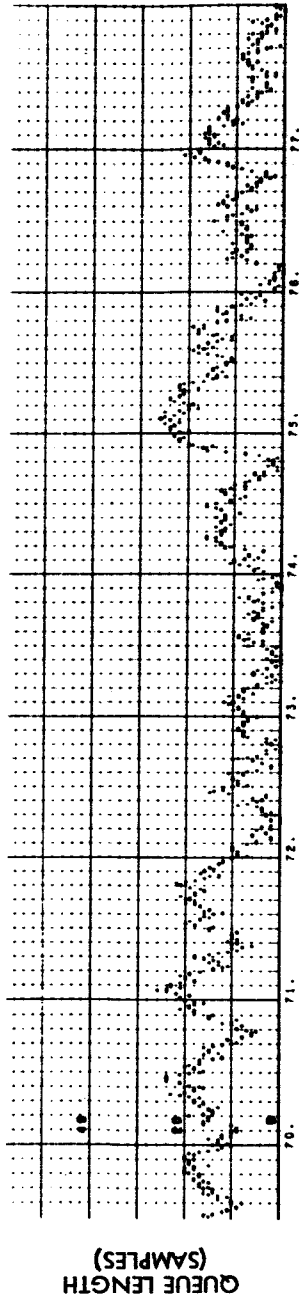
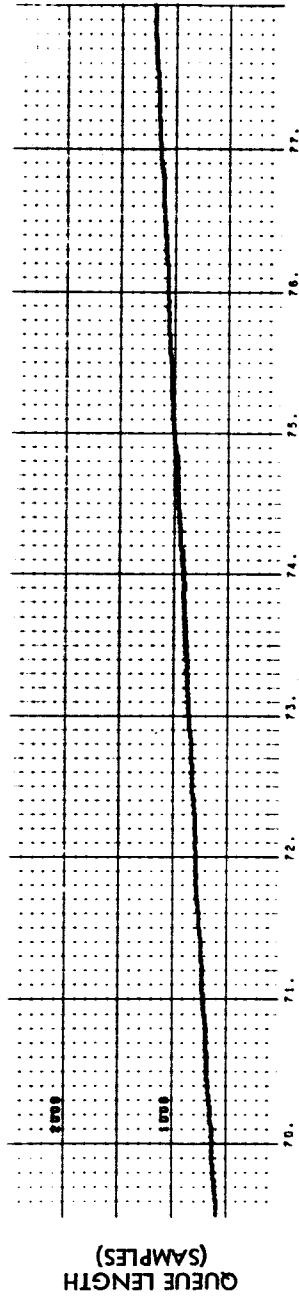


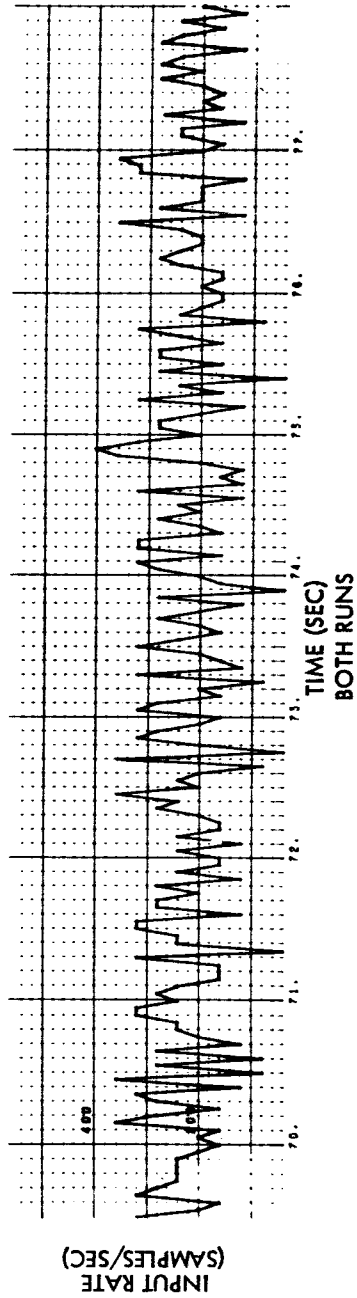
Fig. 4-34 Queue Length and Buffer Input Arrival Rate vs Time,
Runs S6-16 and S6-17



TIME (SEC)
RUN S6-16



TIME (SEC)
RUN S6-17



TIME (SEC)
BOTH RUNS

Fig. 4-34 (Cont'd) Queue Length and Buffer Input Arrival Rate vs Time, Runs S6-16 and S6-17

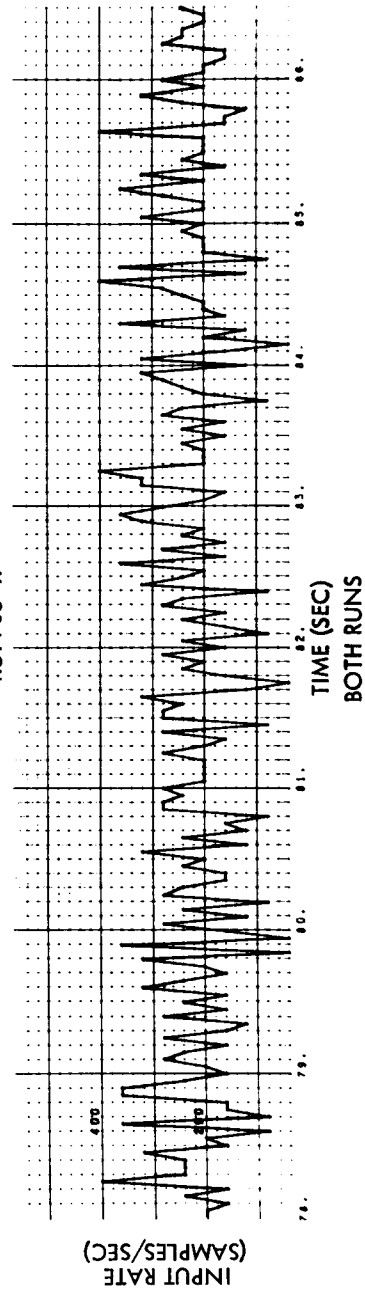
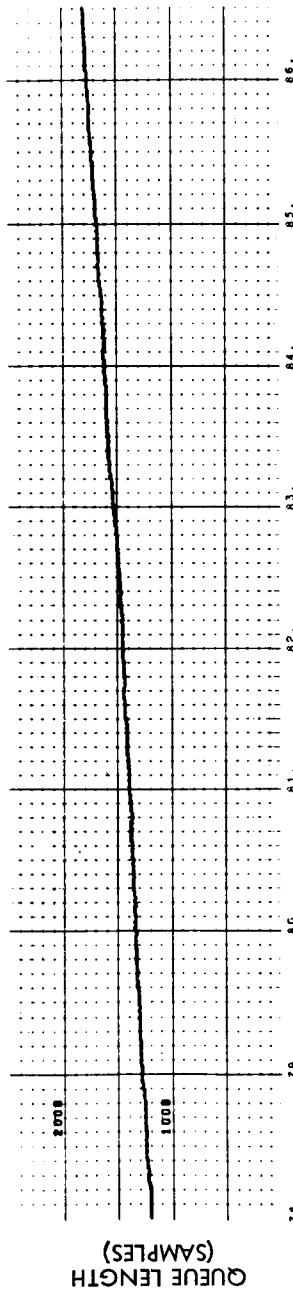
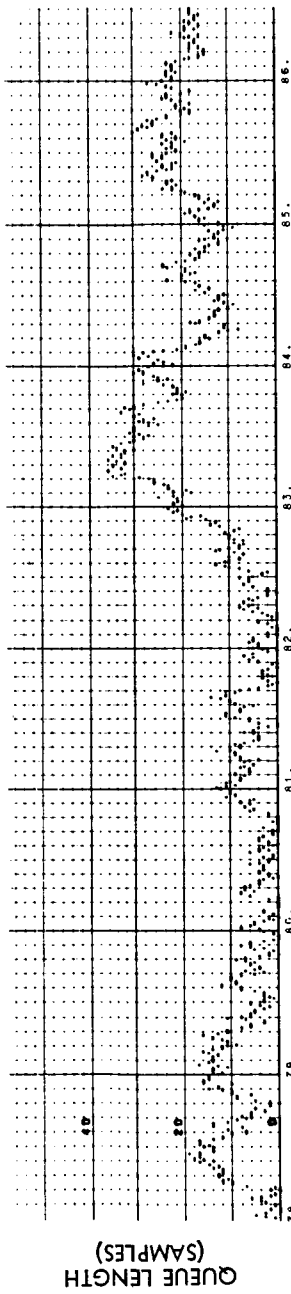
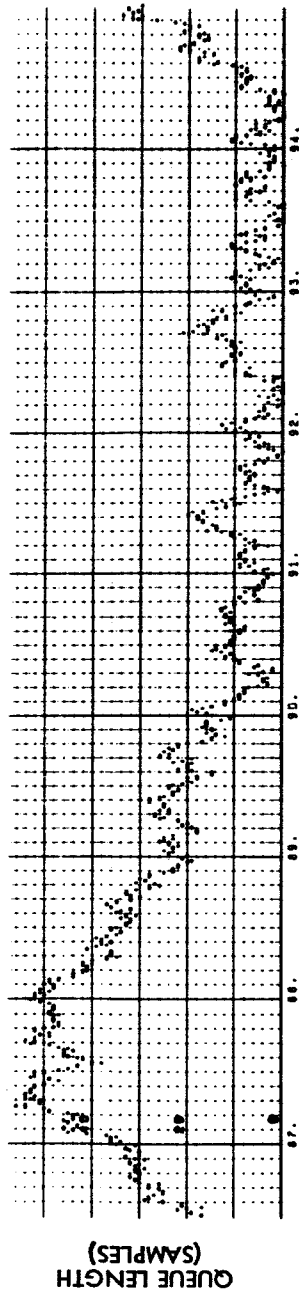
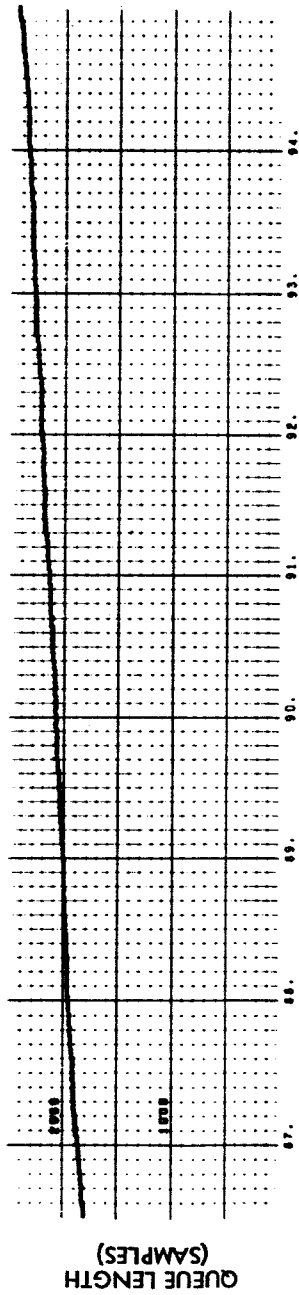


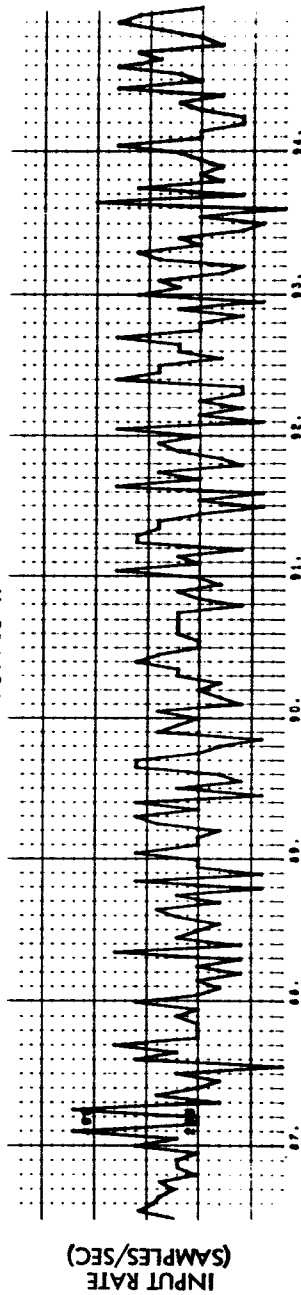
Fig. 4-34 (Cont'd) Queue Length and Buffer Input Arrival Rate vs Time, Runs S6-16 and S6-17



TIME (SEC)
RUN S6-16



TIME (SEC)
RUN S6-17



TIME (SEC)
BOTH RUNS

Fig. 4-34 (Cont'd) Queue Length and Buffer Input Arrival Rate vs Time, Runs S6-16 and S6-17

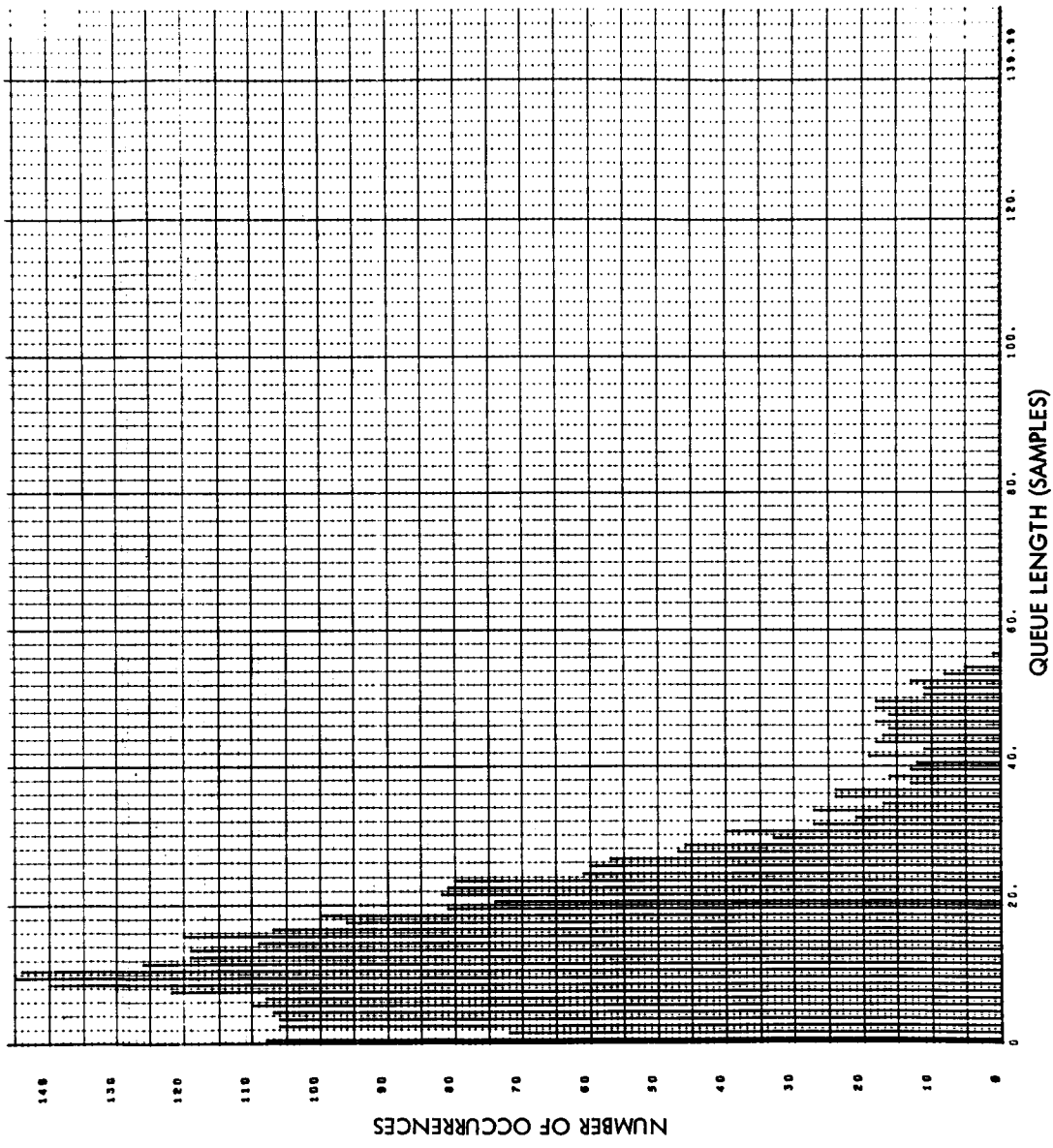


Fig. 4-35 Queue Length Histogram, Run S6-16

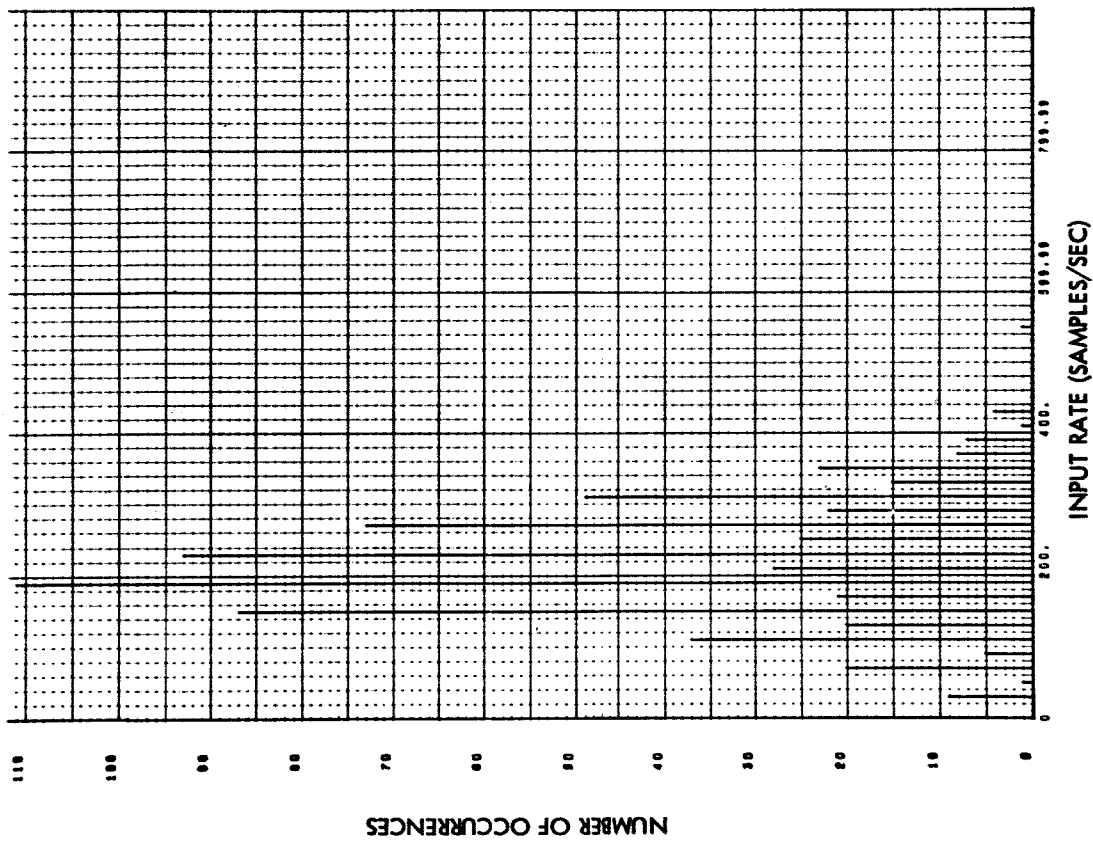


Fig. 4-36 Buffer Input Arrival Rate Histogram, Runs S6-14, S6-15, S6-16, and S6-17

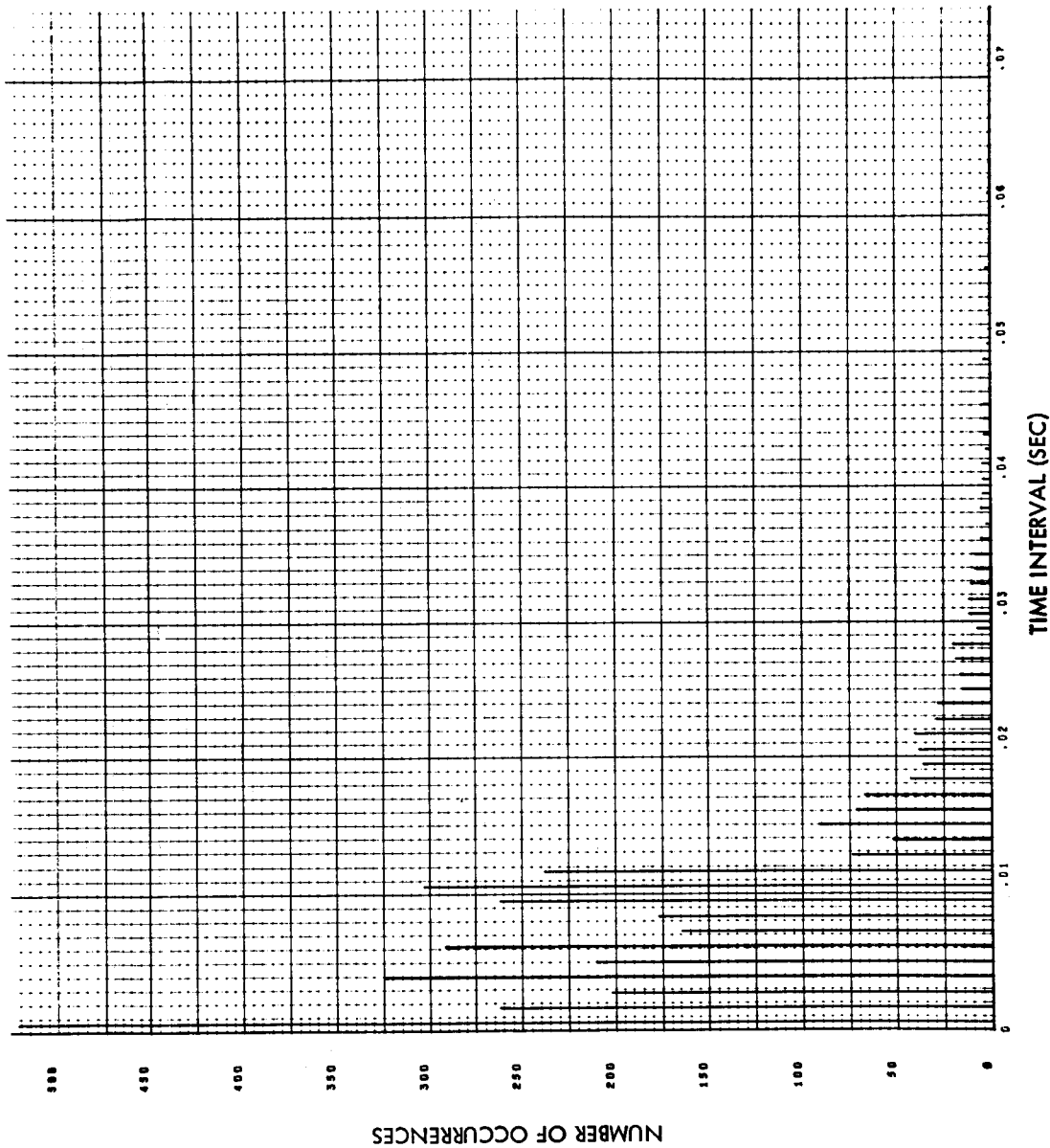


Fig. 4-37 Histogram of Time Intervals Between Buffer Input Arrivals, Runs S6-14, S6-15, S6-16, and S6-17

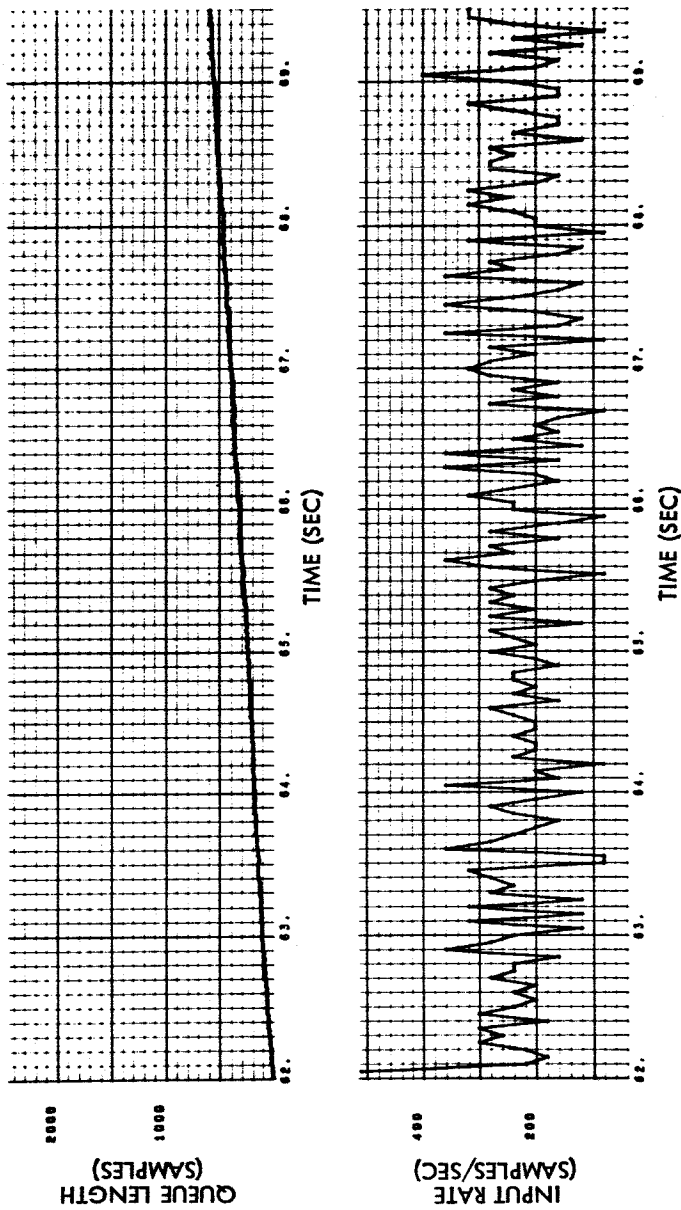


Fig. 4-38 Queue Length and Buffer Input Arrival Rate vs Time, Run S6-18

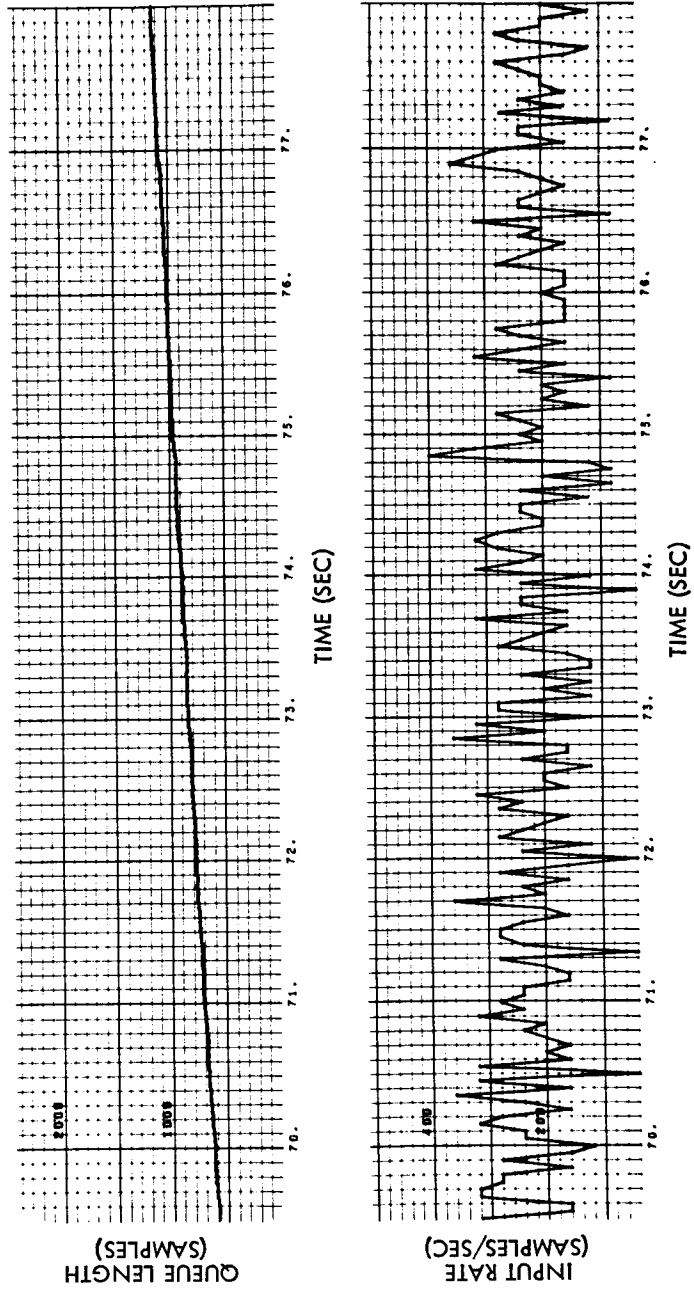


Fig. 4-38 (Cont'd) Queue Length and Buffer Input Arrival Rate vs Time, Run S6-18

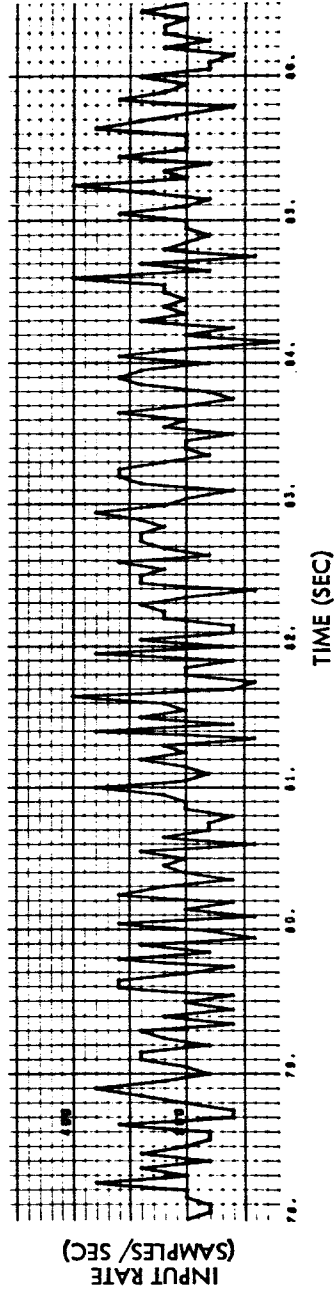
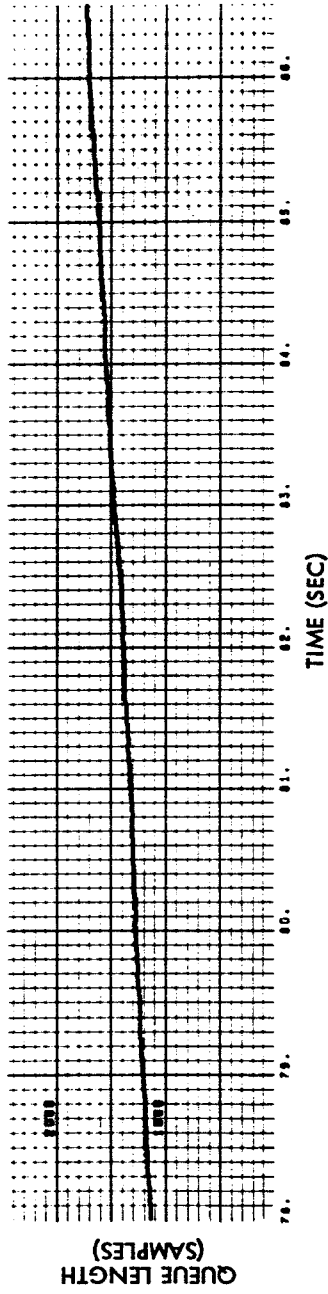


Fig. 4-38 (Cont'd) Queue Length and Buffer Input Arrival Rate vs Time, Run S6-18

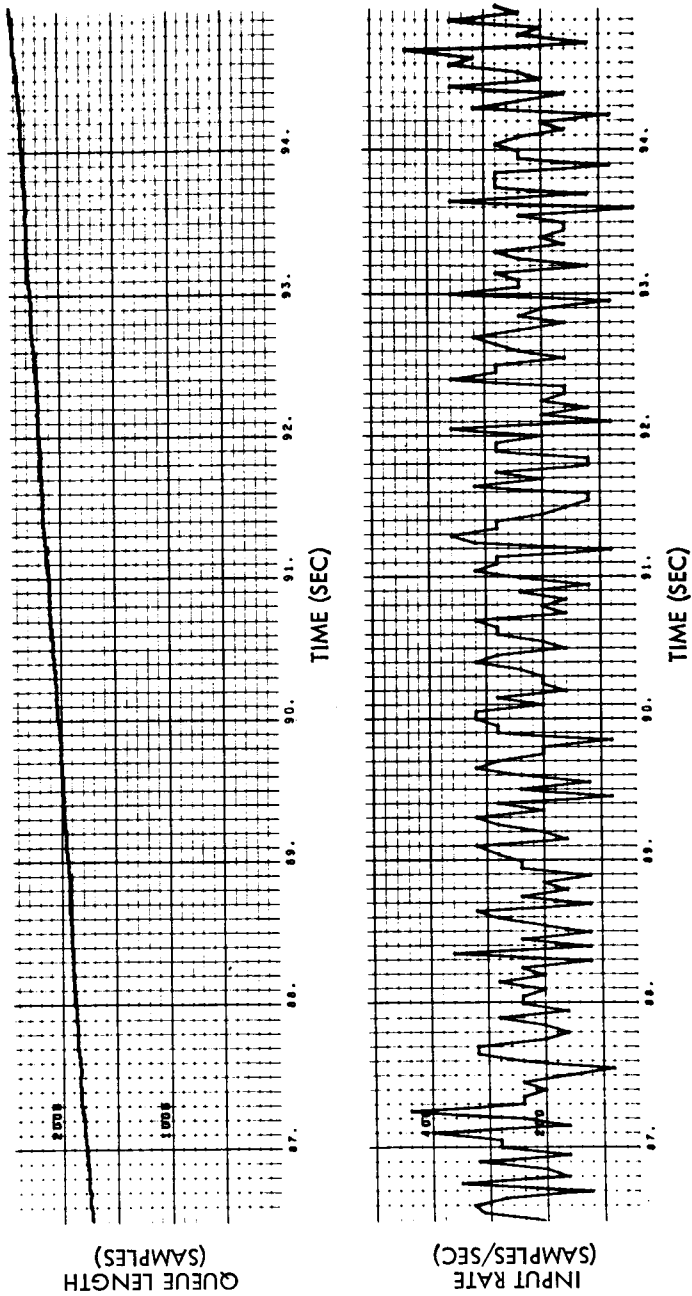


Fig. 4-38 (Cont'd) Queue Length and Buffer Input Arrival Rate vs Time, Run S6-18

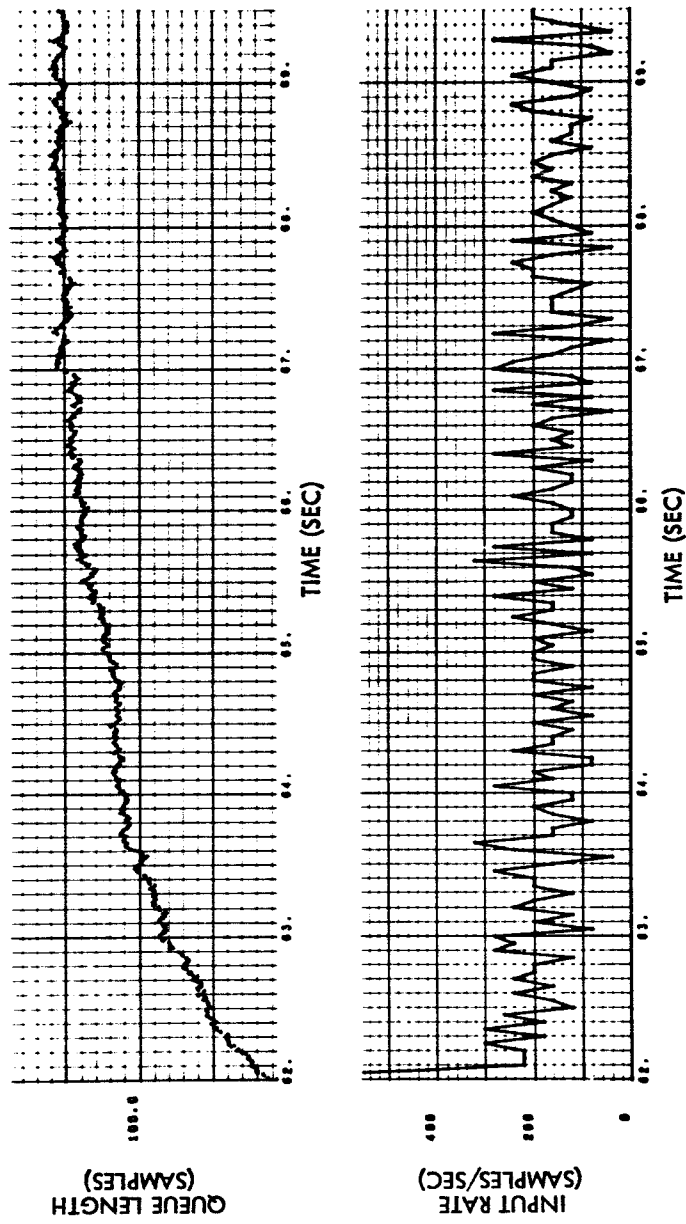


Fig. 4-39 Queue Length and Buffer Input Arrival Rate vs Time, Run S6-19

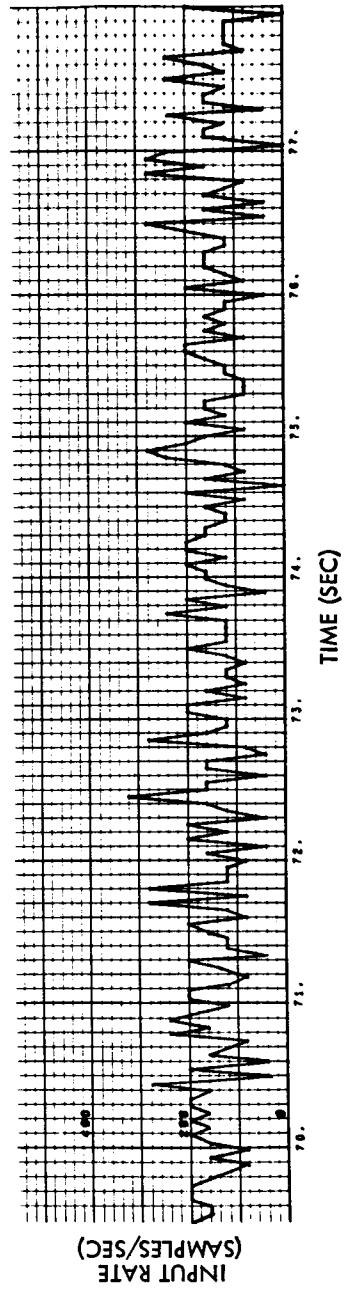
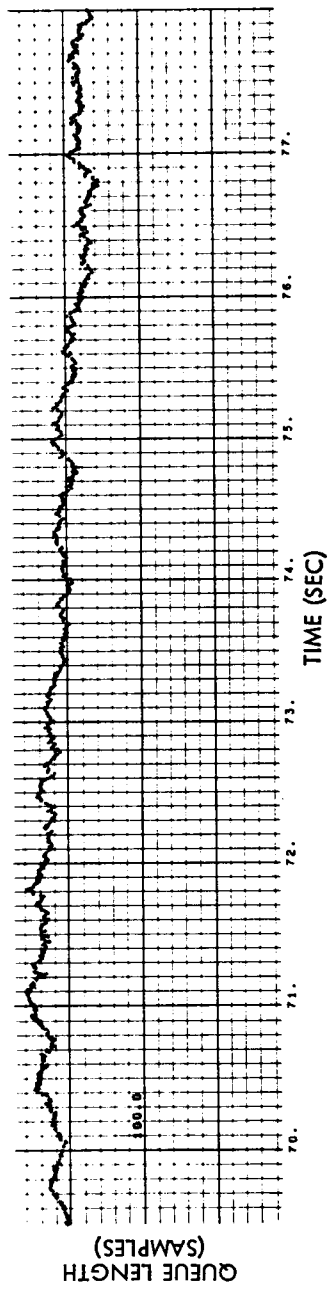


Fig. 4-39 (Cont'd) Queue Length and Buffer Input Arrival Rate vs Time, Run S6-19

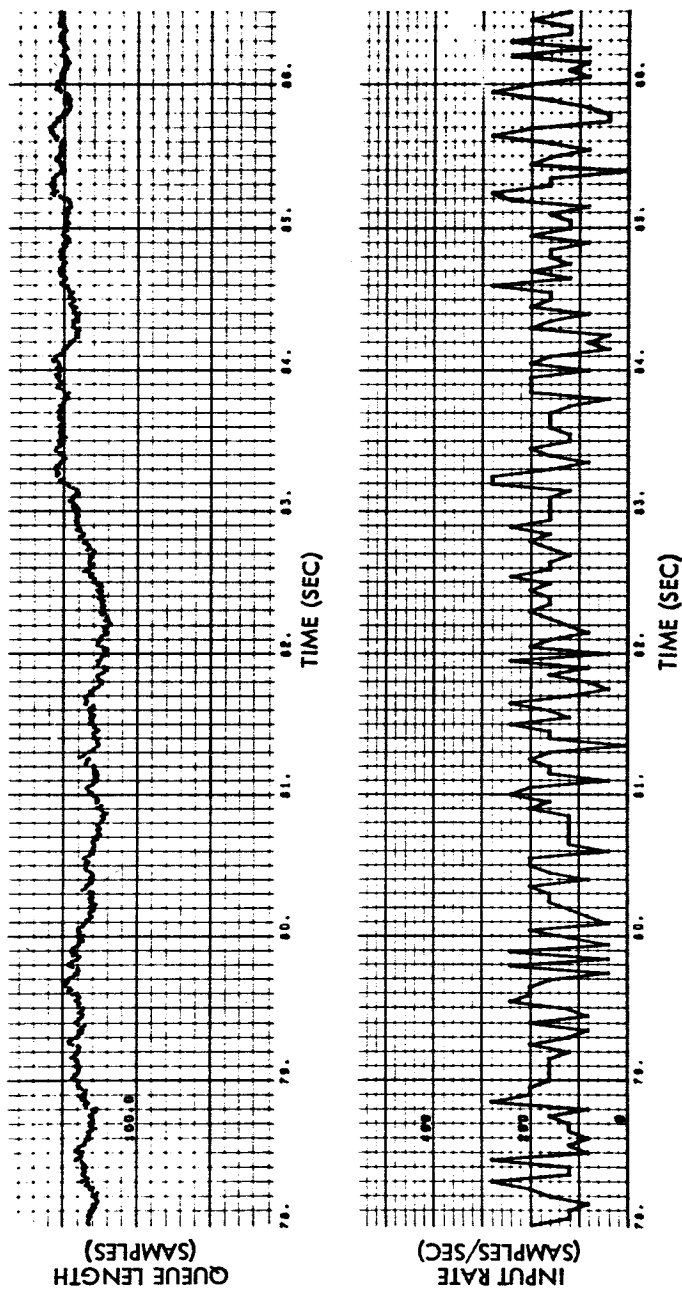


Fig. 4-39 (Cont'd) Queue Length and Buffer Input Arrival Rate vs Time, Run S6-19

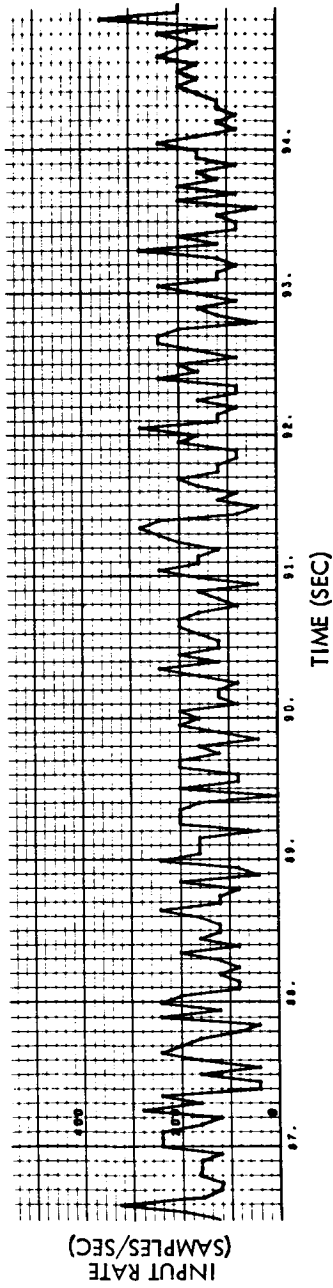
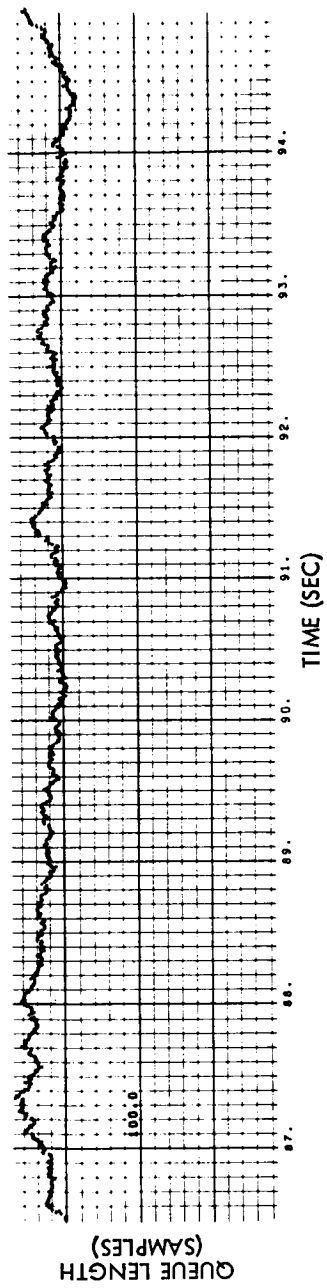


Fig. 4-39 (Cont'd) Queue Length and Buffer Input Arrival Rate vs Time, Run S6-19

(This page intentionally left blank .)

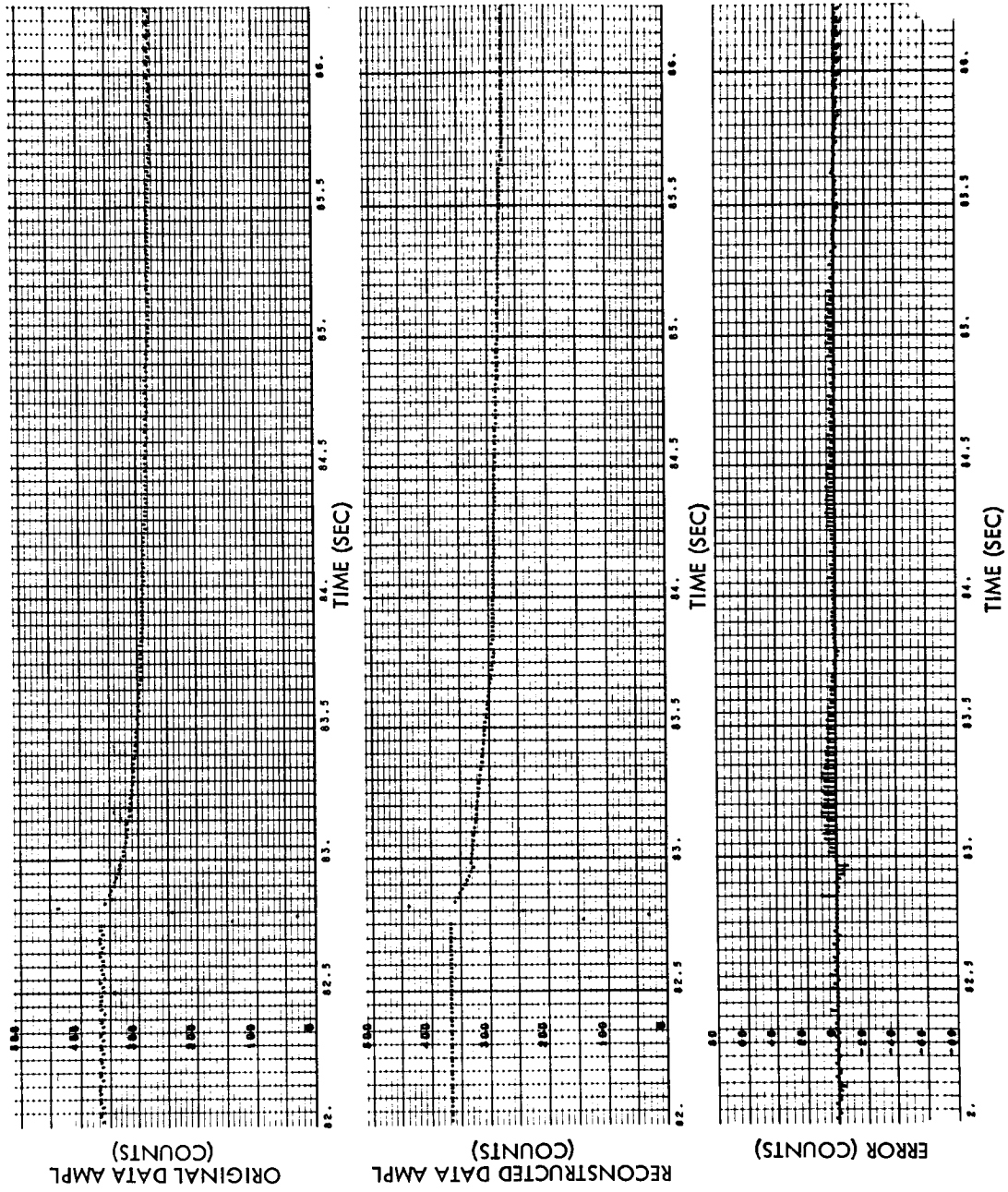


Fig. 4-40a Sensor 9 Original Data, Reconstructed Data, and Error vs Time, Run S6-18

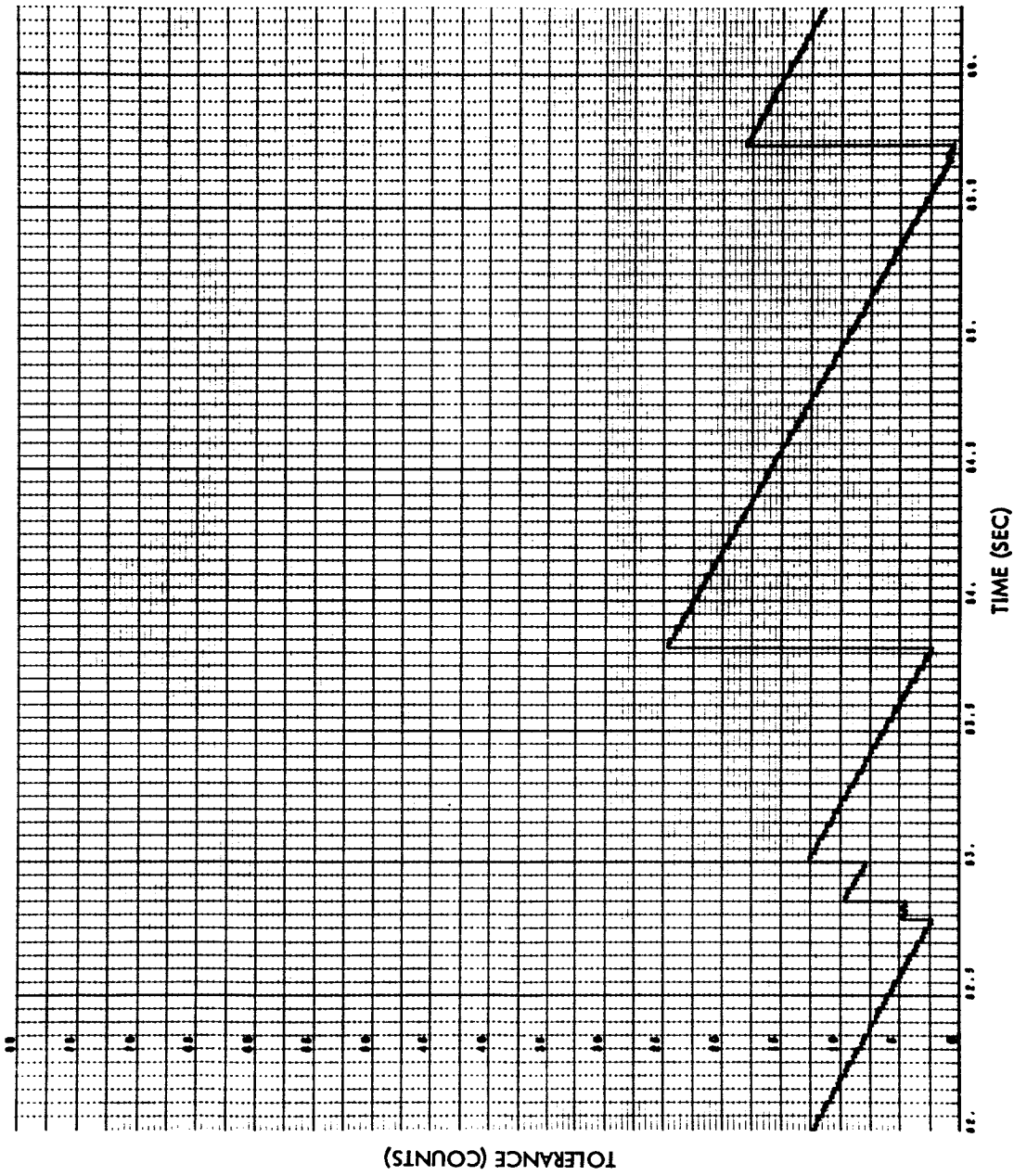


Fig. 4-40b Sensor 9 Tolerance vs Time, Run S6-18

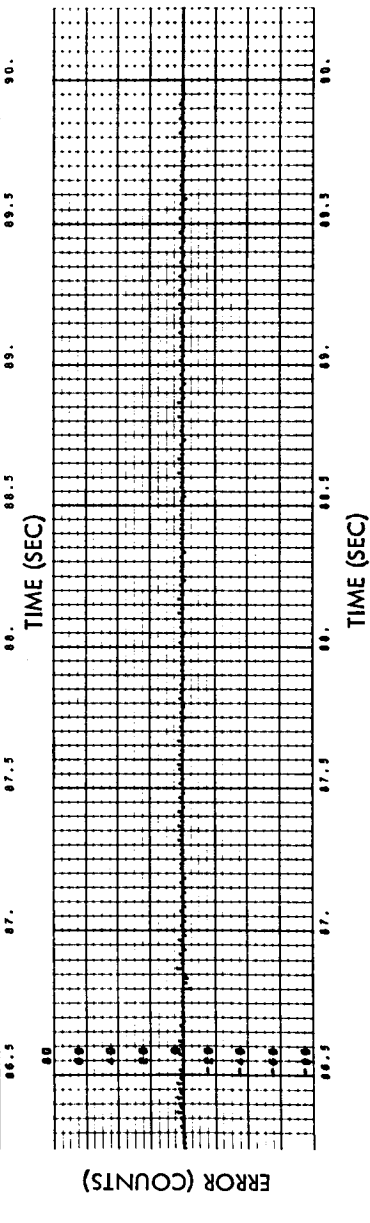
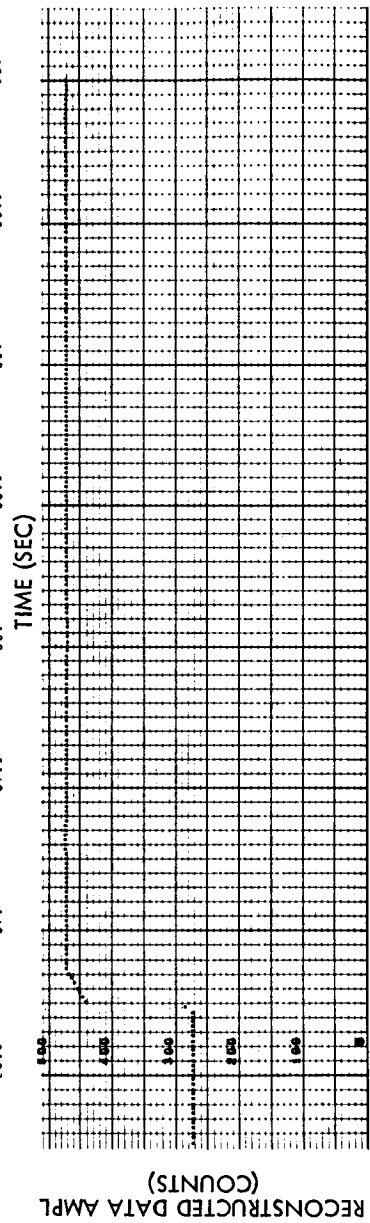
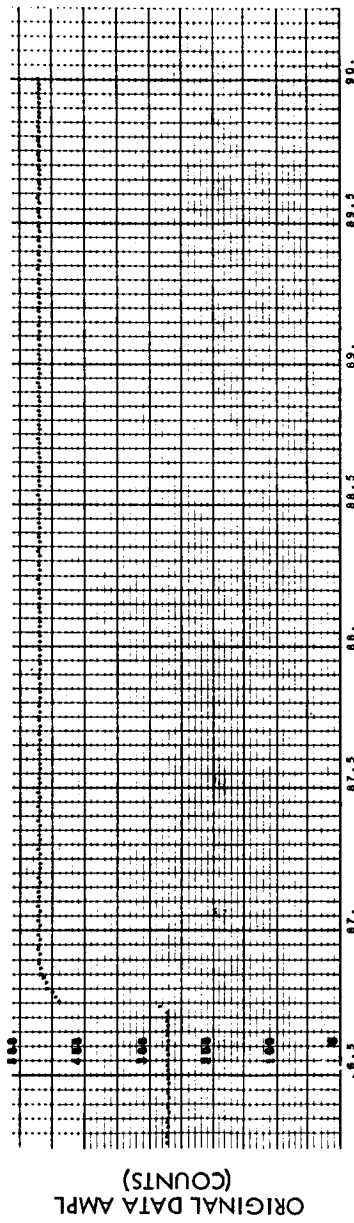


Fig. 4-40a (Cont'd) Sensor 9 Original Data, Reconstructed Data, and Error vs Time, Run S6-18

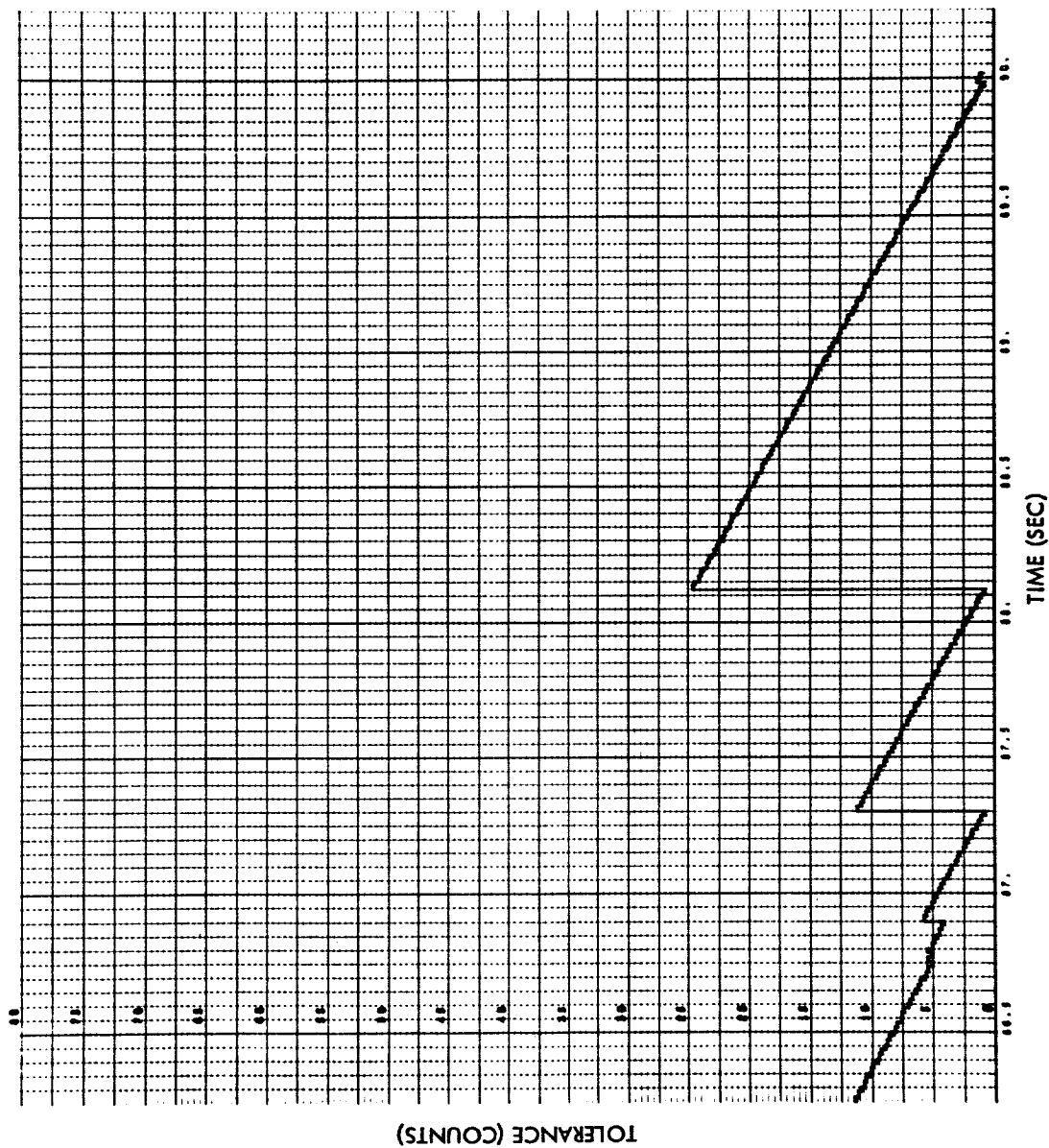


Fig. 4-40b (Cont'd) Sensor 9 Tolerance vs Time, Run S6-18

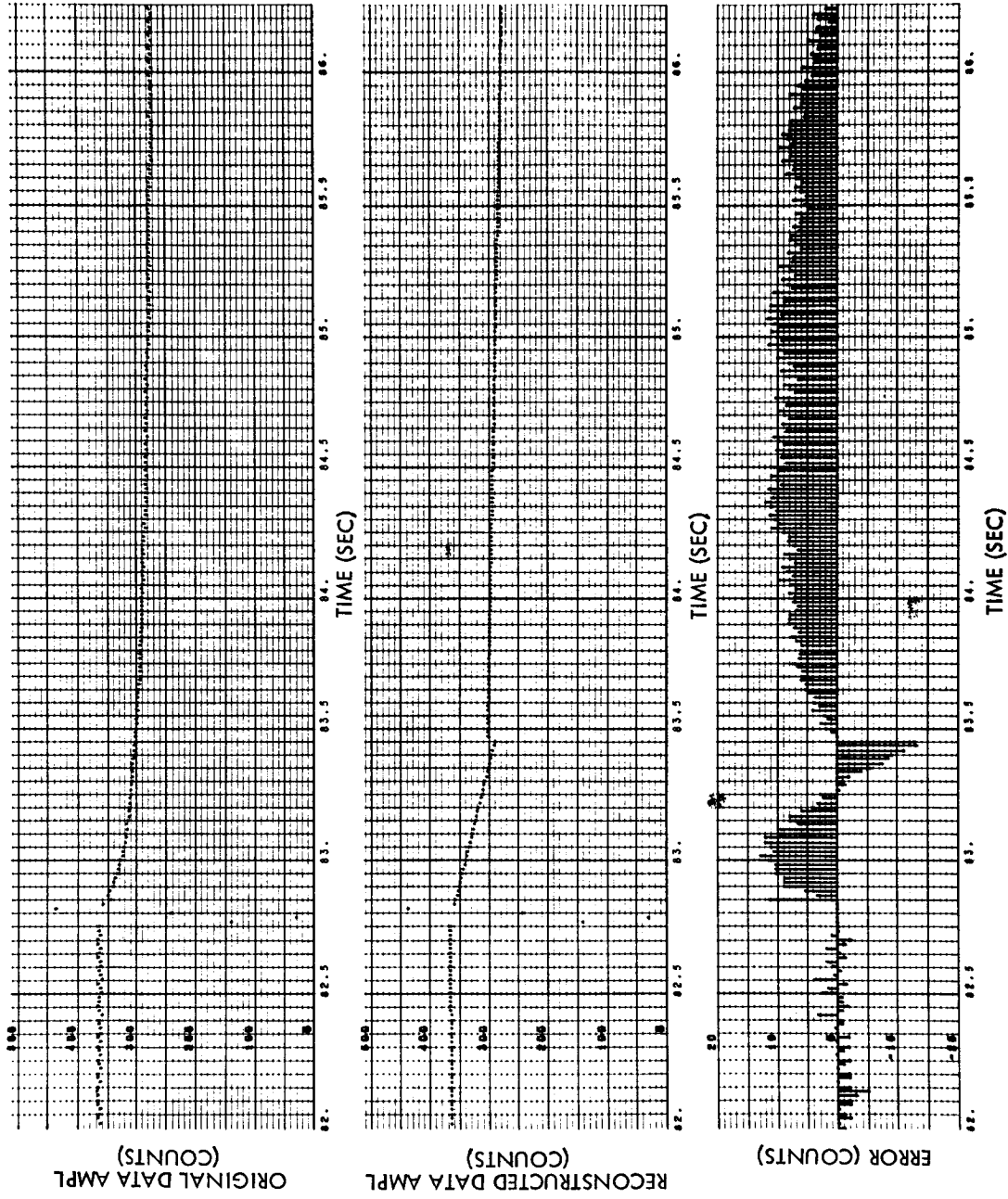


Fig. 4-41a Sensor 9 Original Data, Reconstructed Data, and Error vs Time, Run S6-19

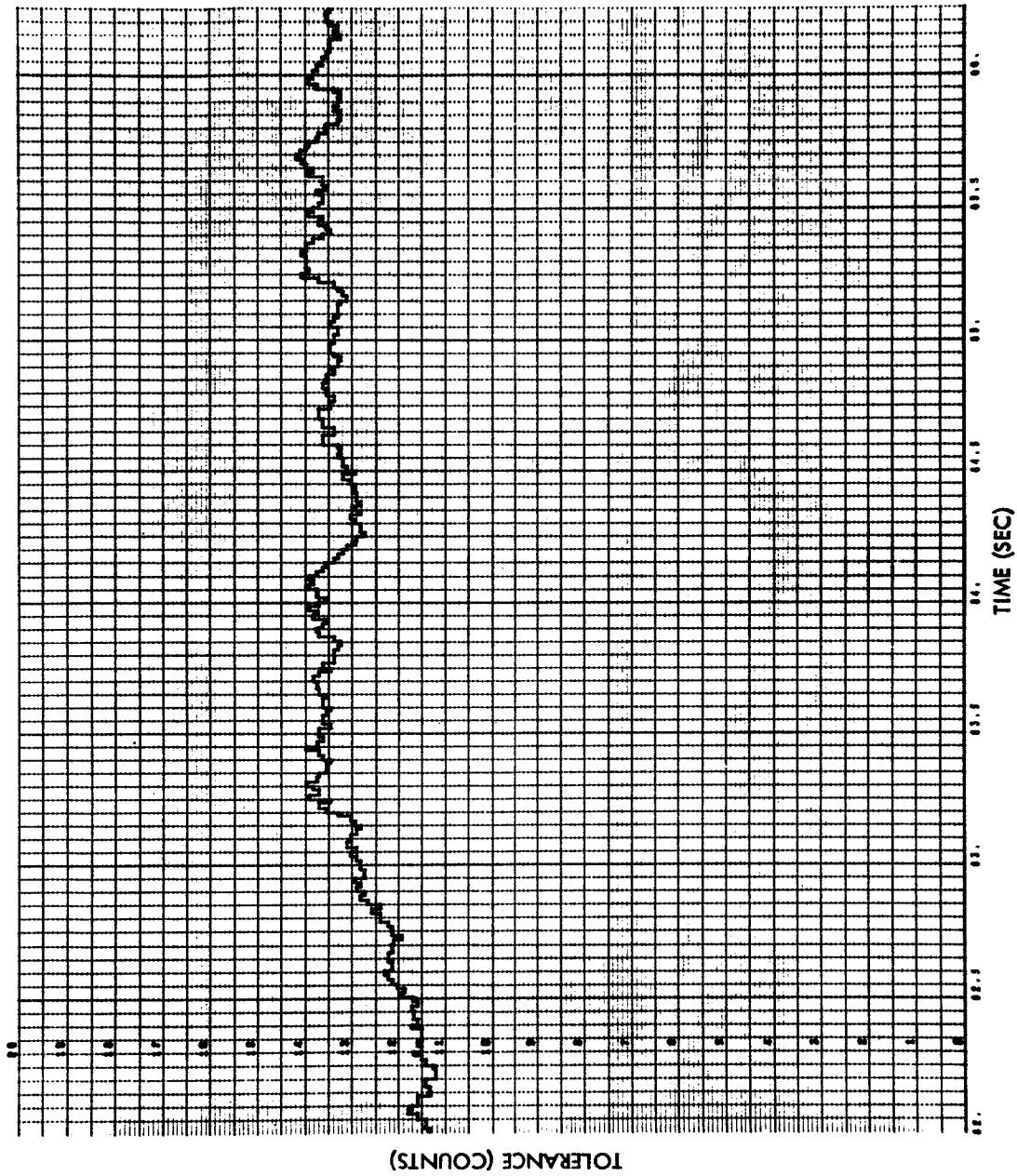


Fig. 4-41b Sensor 9 Tolerance vs Time, Run S6-19

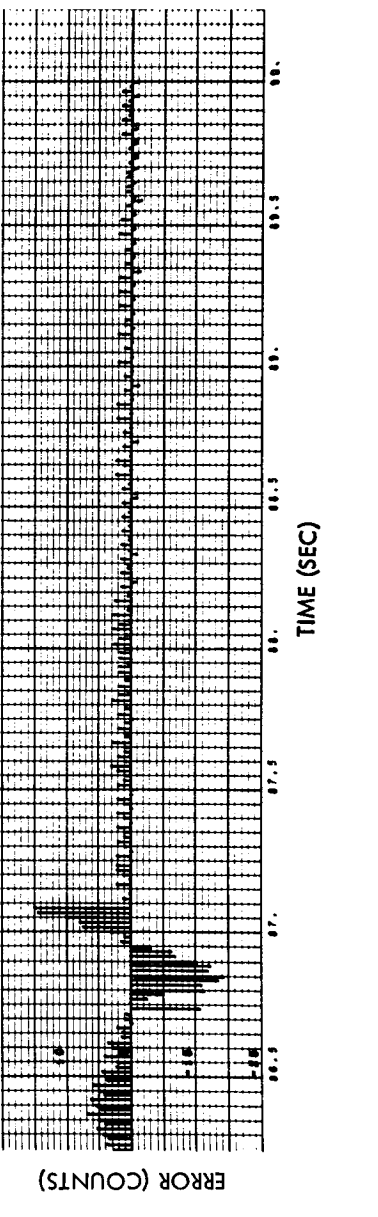
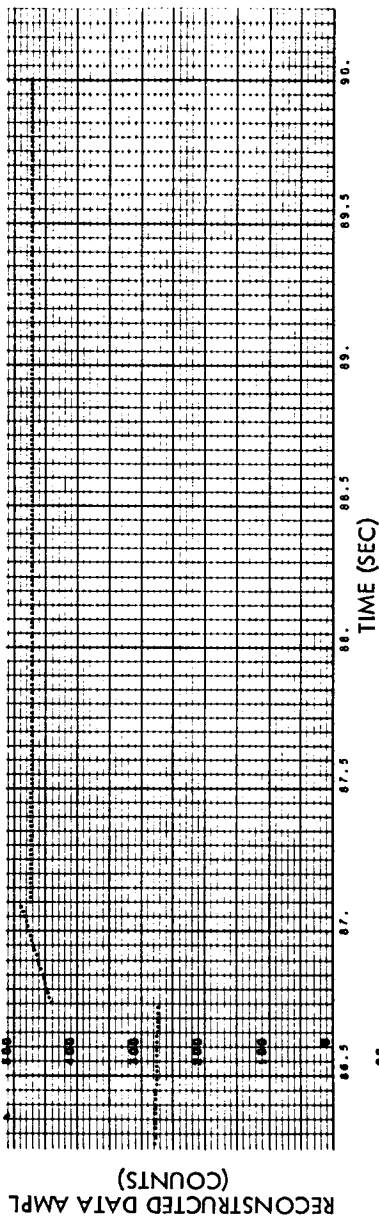
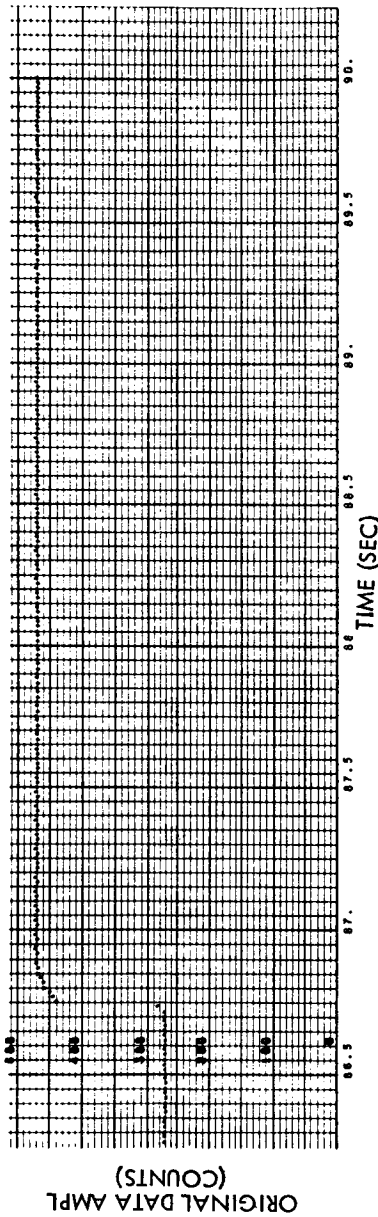


Fig. 4-41a (Cont'd) Sensor 9 Original Data, Reconstructed Data, and Error vs Time, Run S6-19

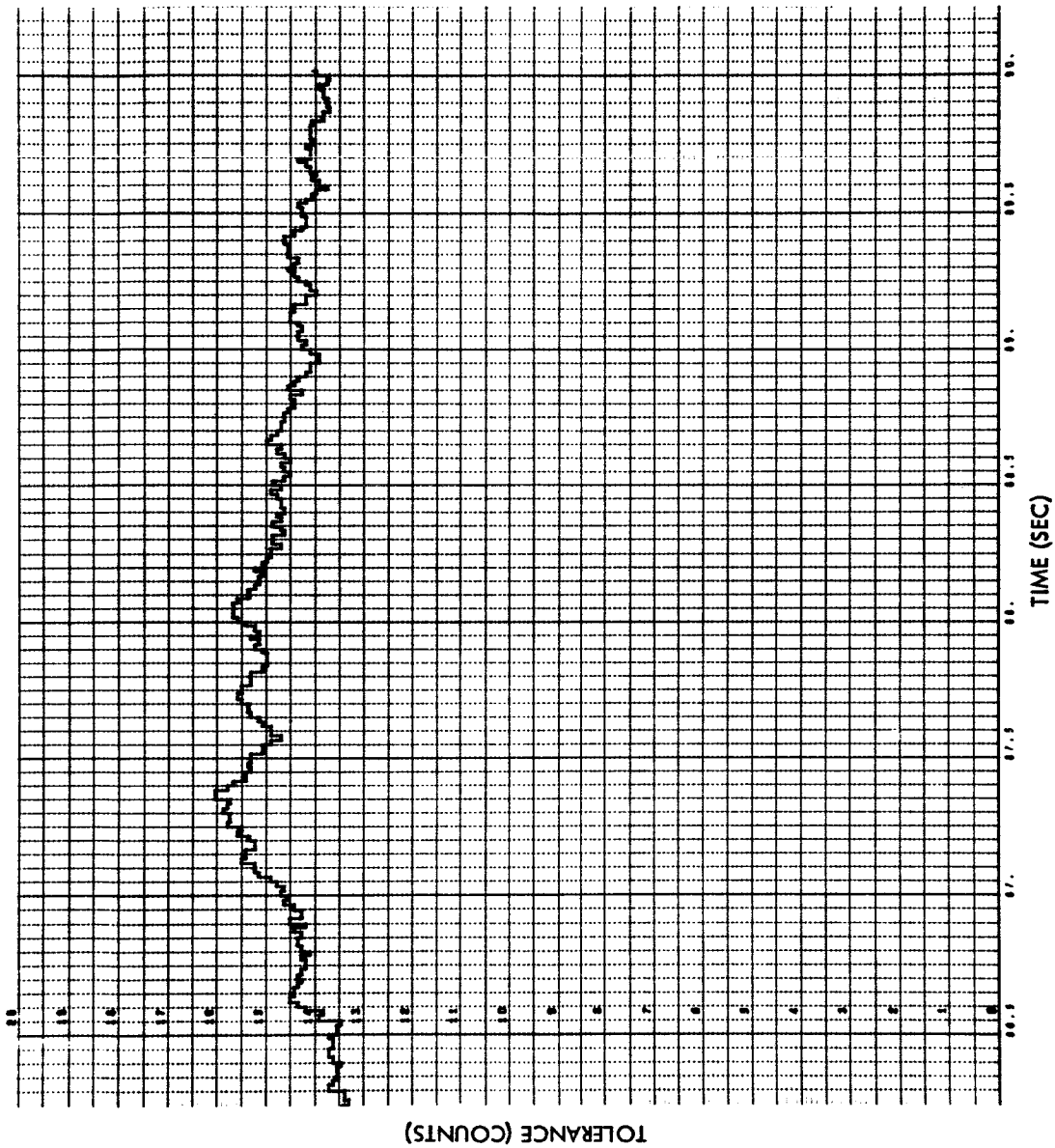


Fig. 4-41b (Cont'd) Sensor Tolerance vs Time, Run S6-19

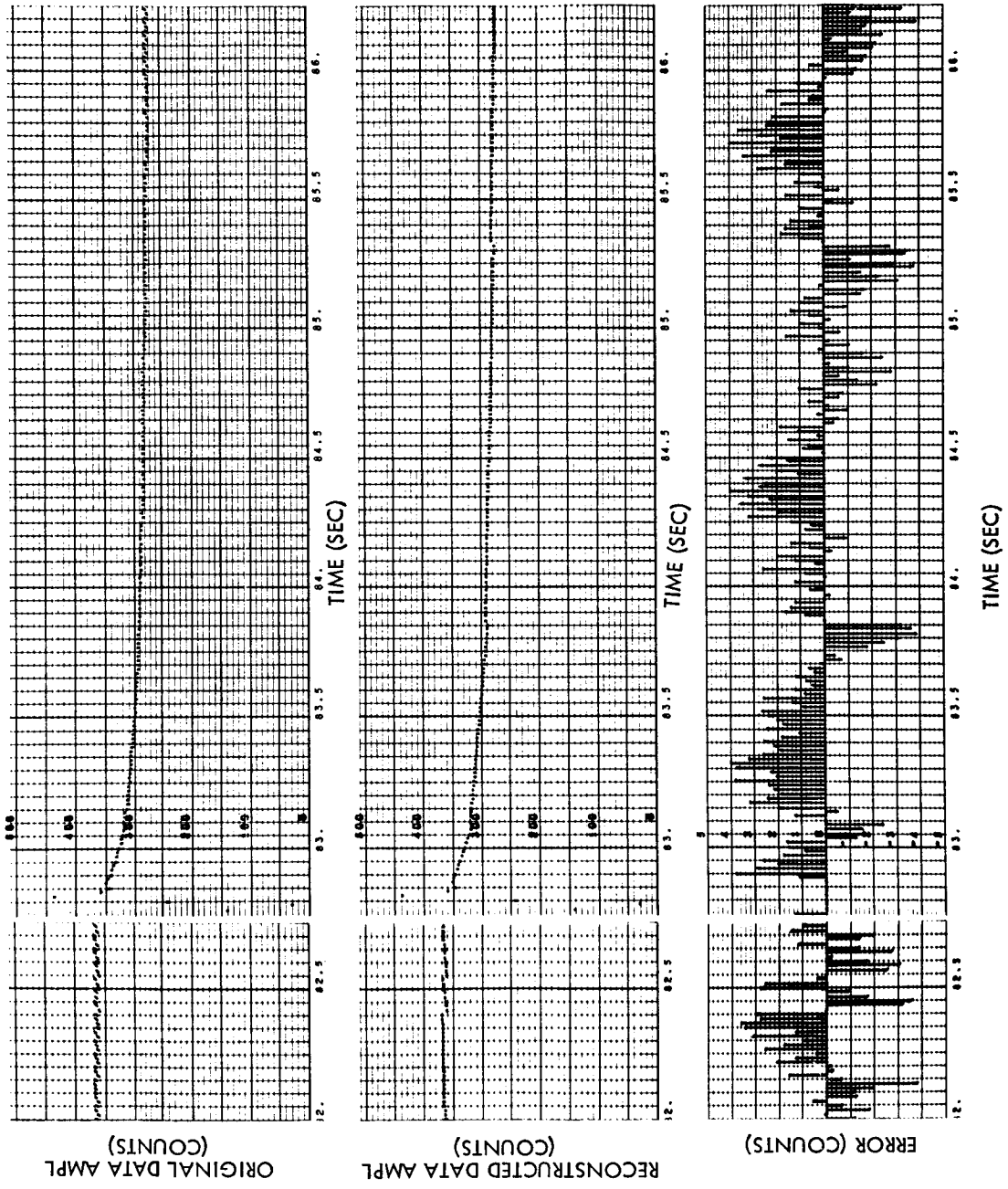


Fig. 4-42 Sensor 9 Original Data, Reconstructed Data, and Error vs Time, Run S6-07

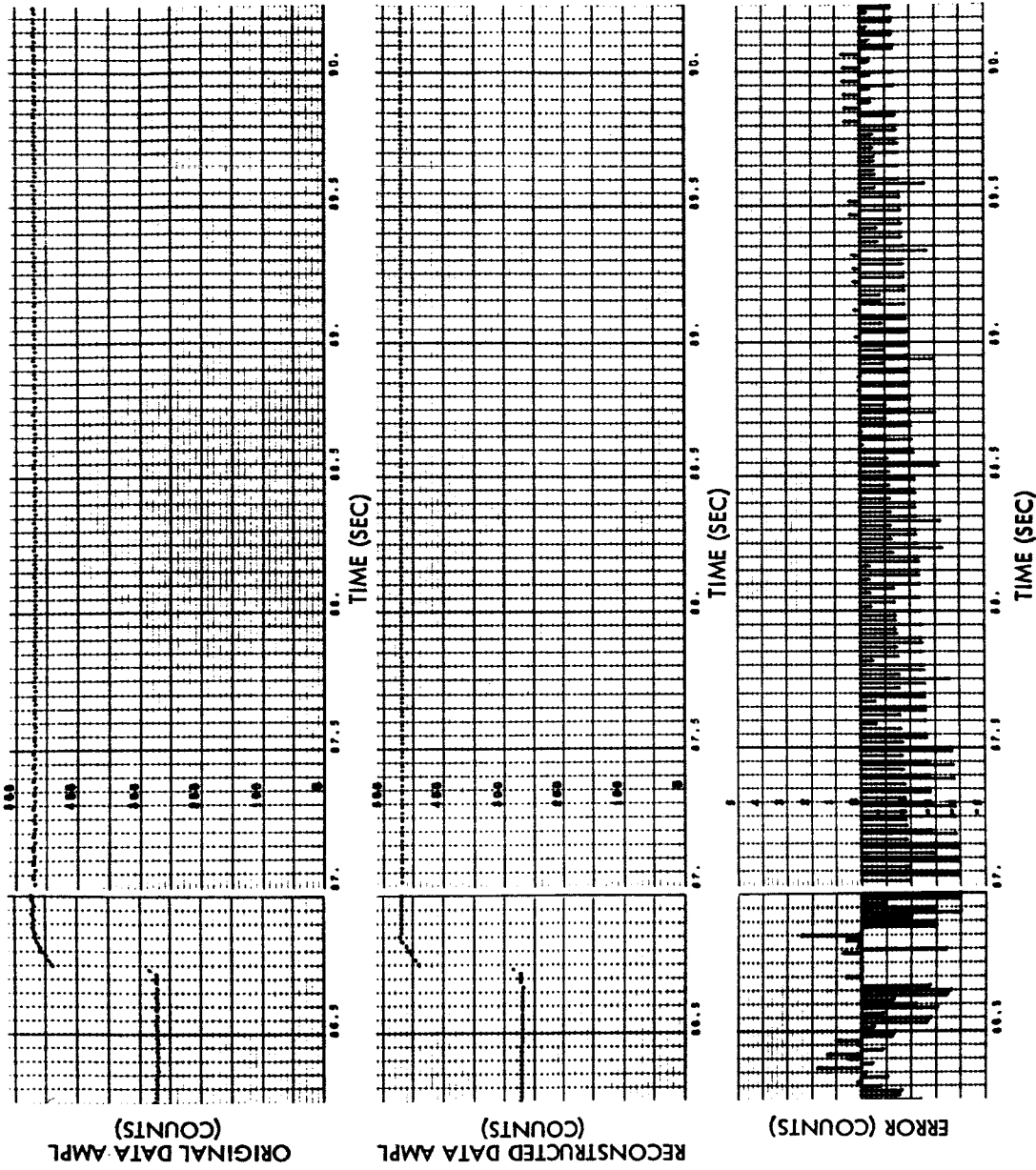


Fig. 4-42 (Cont'd) Sensor 9 Original Data, Reconstructed Data, and Error vs Time, Run S6-07

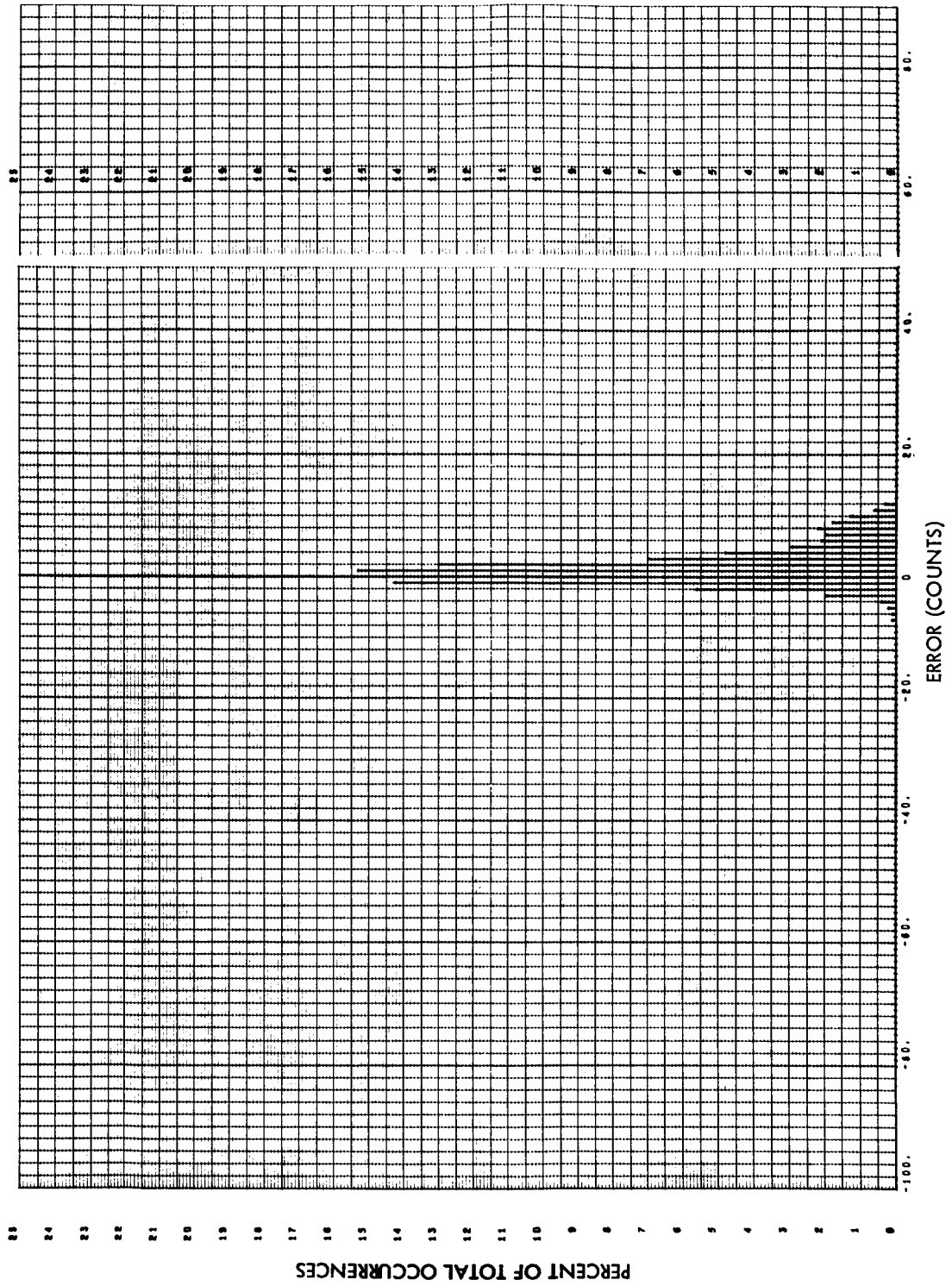


Fig. 4-43 Sensor 9 Error Histogram, Run S6-18

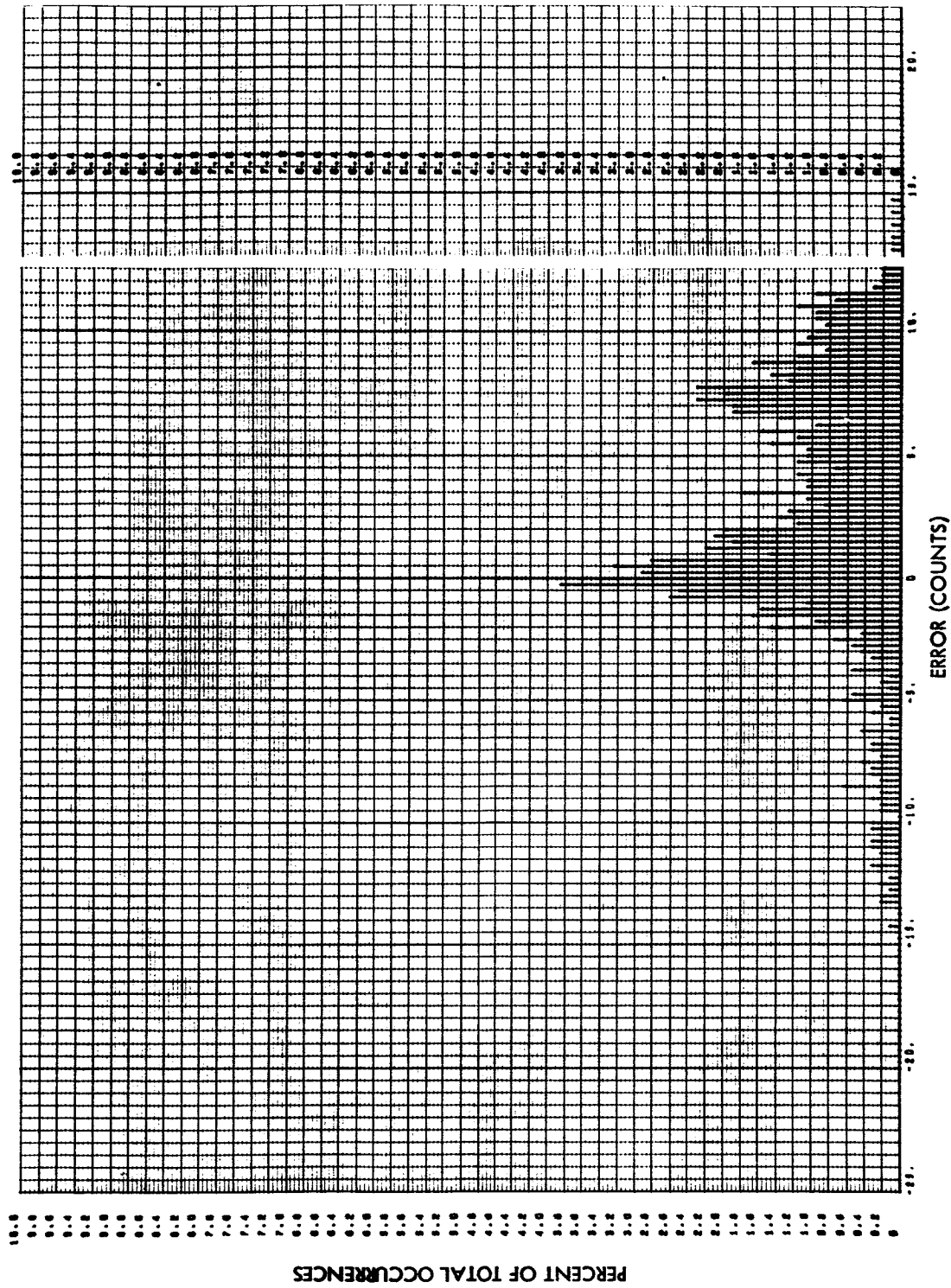


Fig. 4.44 Sensor 9 Error Histogram, Run S6-19

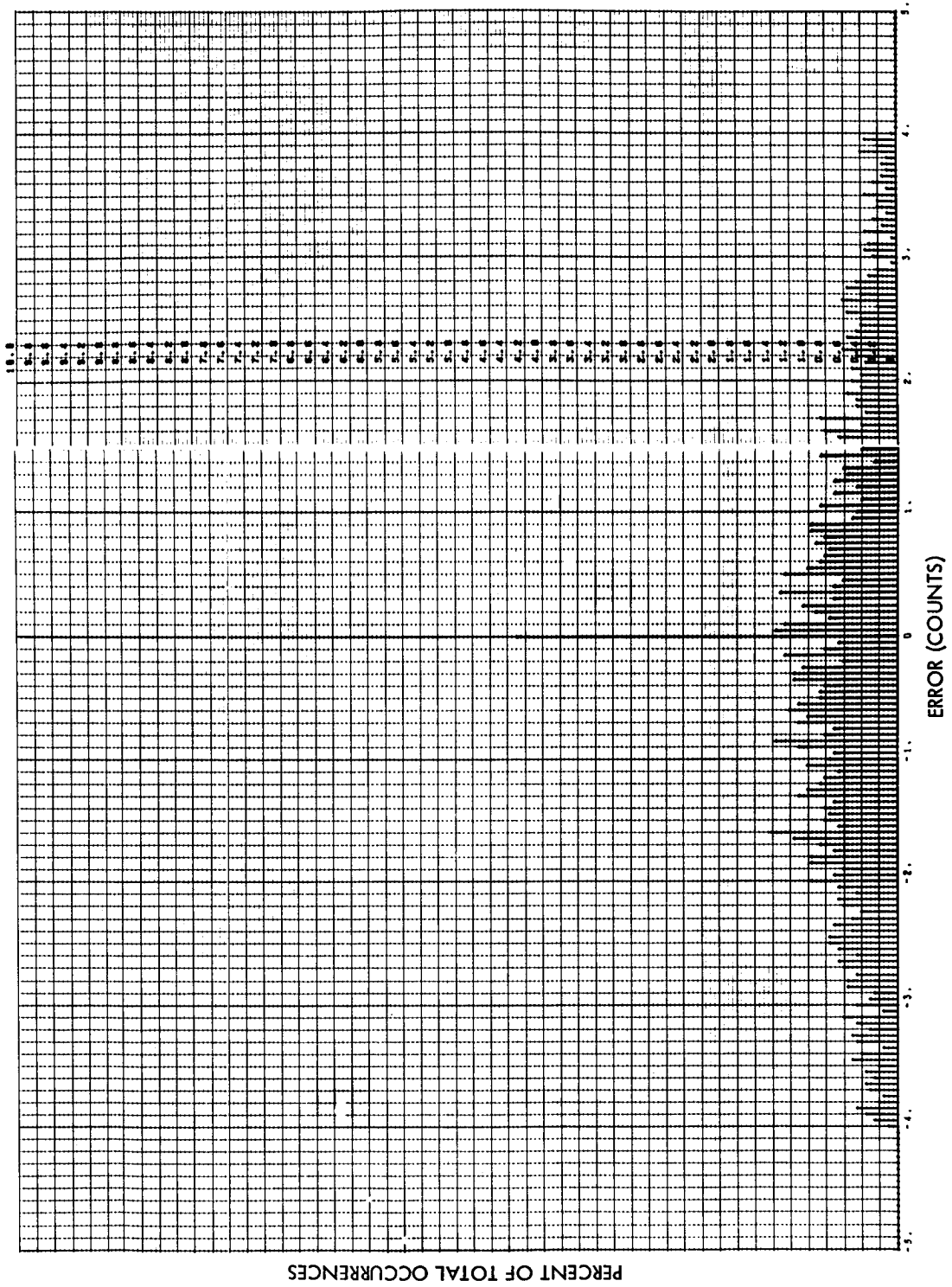


Fig. 4-45 Sensor 9 Error Histogram, Run S6-07

(This page intentionally left blank.)

4-165

LOCKHEED MISSILES & SPACE COMPANY

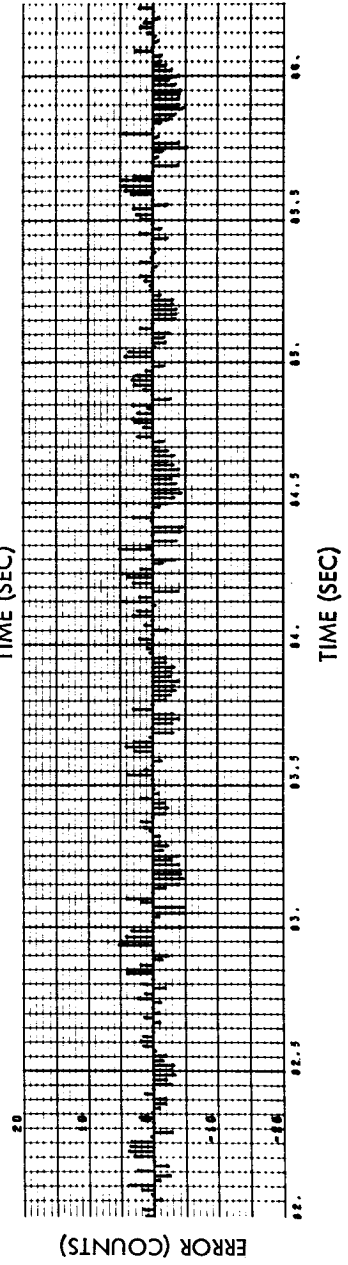
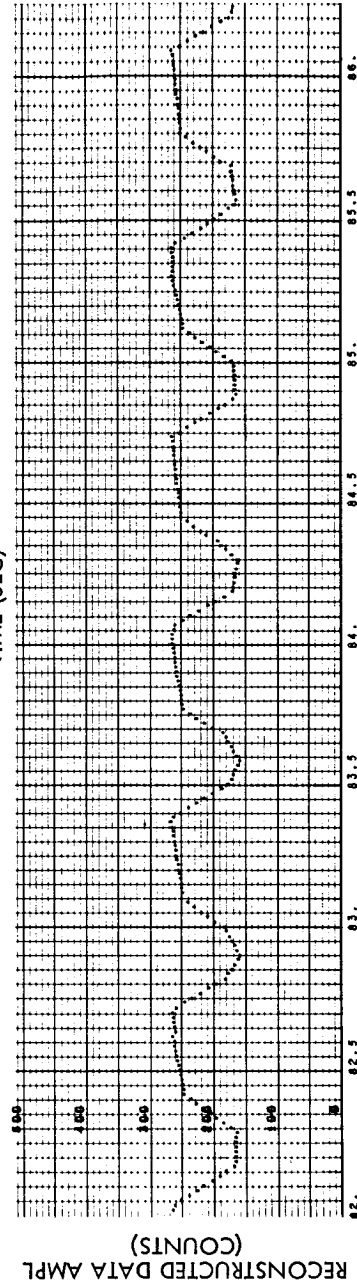
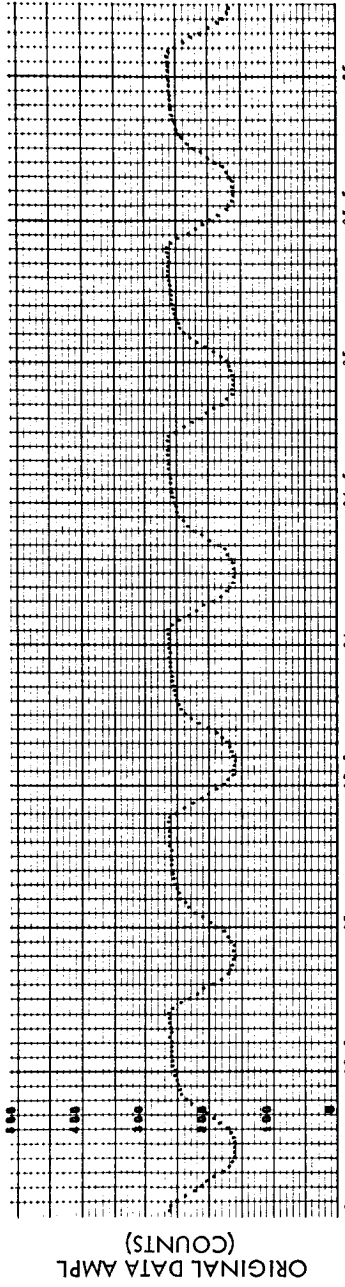


Fig. 4-46a Sensor 11 Original Data, Reconstructed Data, and Error vs Time, Run S6-18

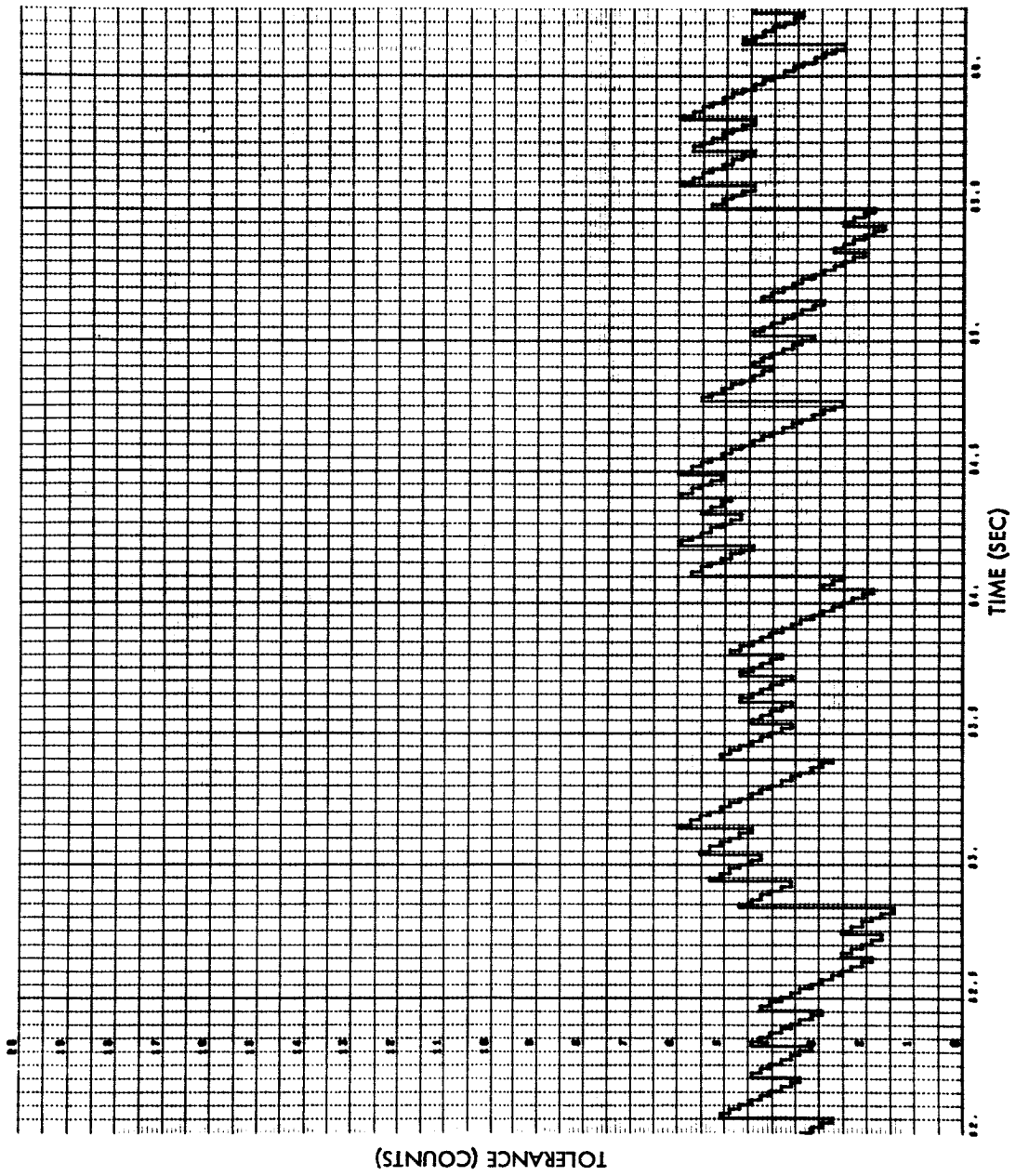


Fig. 4-46b Sensor 11 Tolerance vs Time, Run S6-18

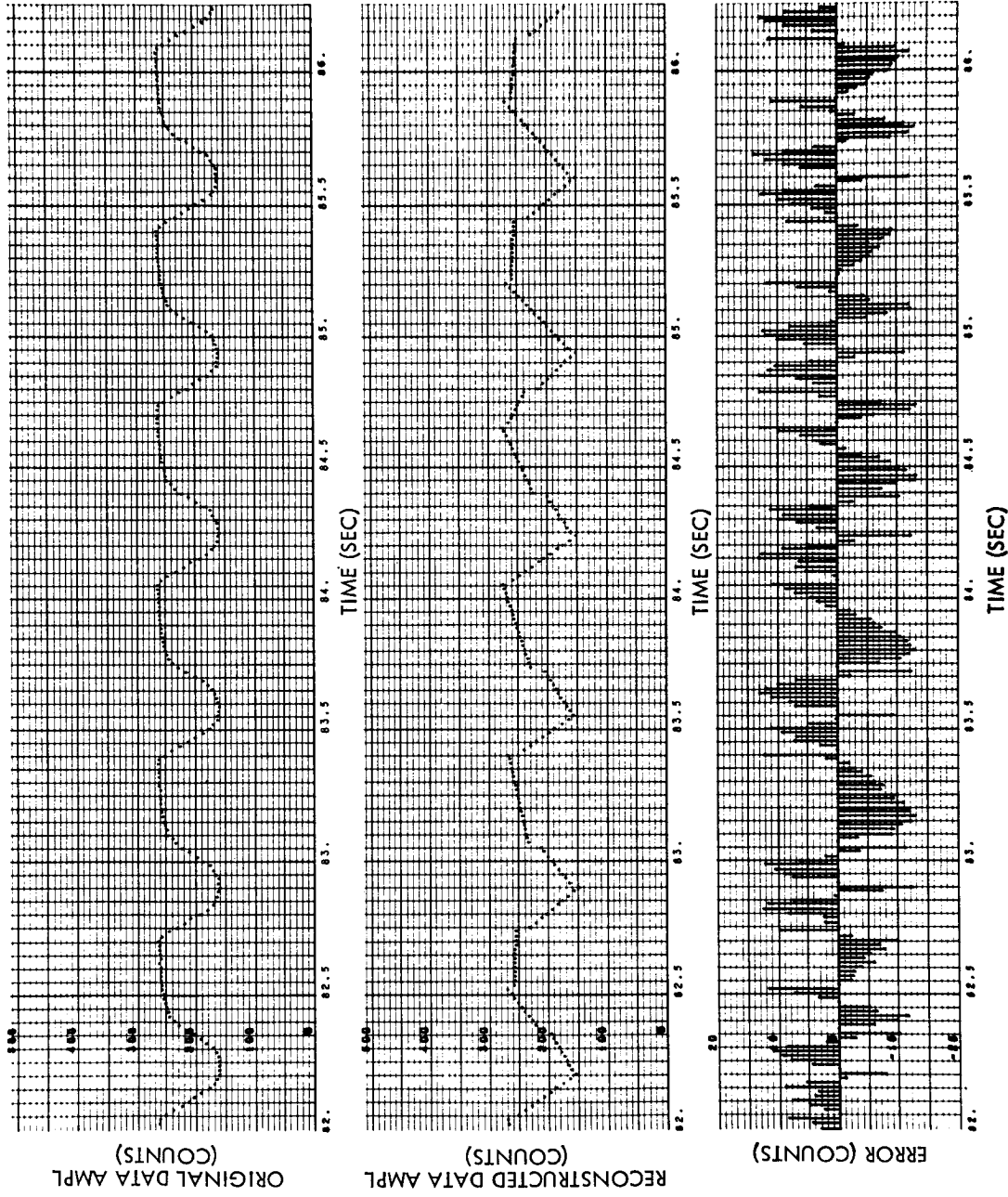


Fig. 4-47a Sensor 11 Original Data, Reconstructed Data, and Error vs Time, Run S6-19

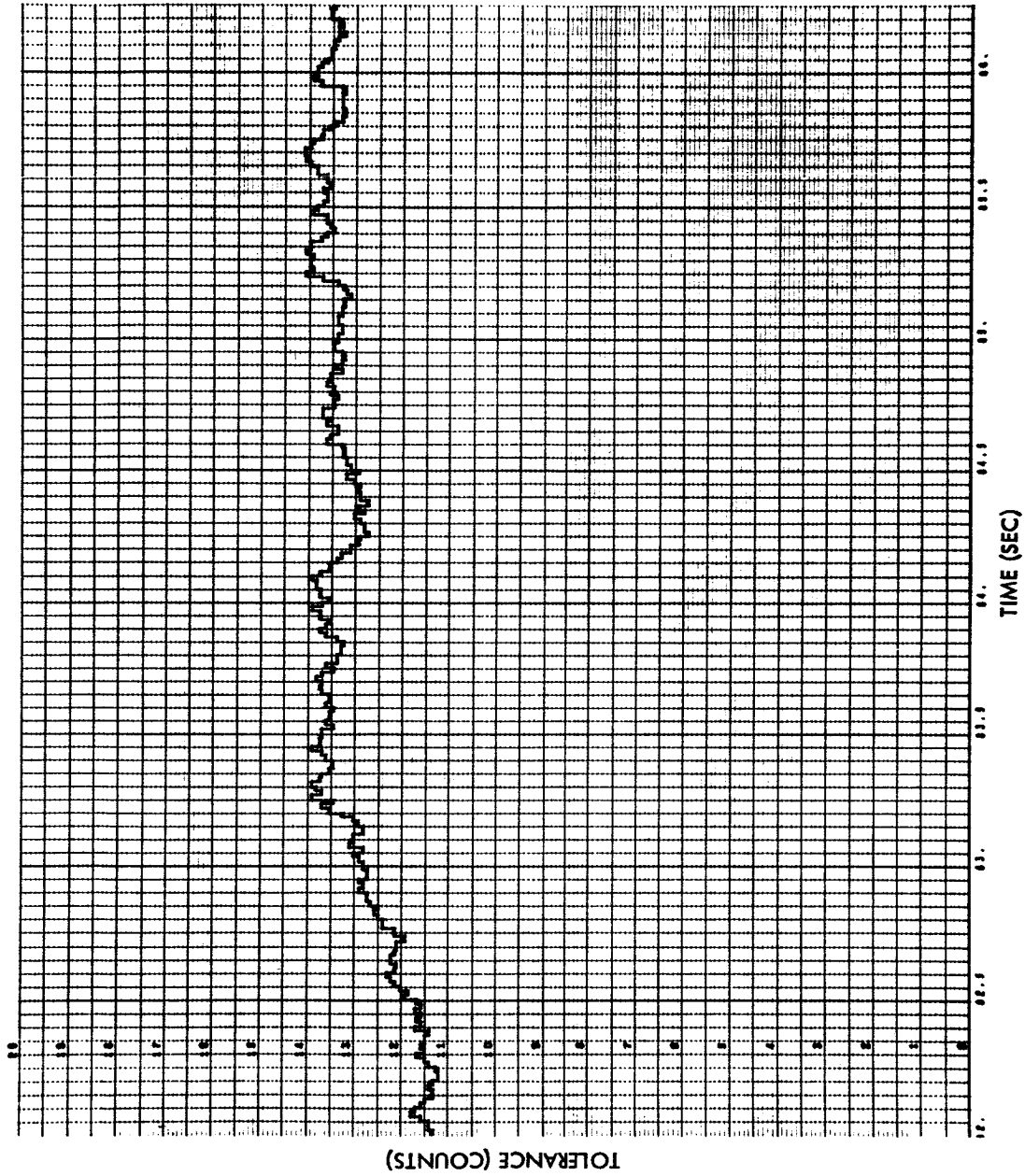


Fig. 4-47b Sensor 11 Tolerance vs Time, Run S6-19

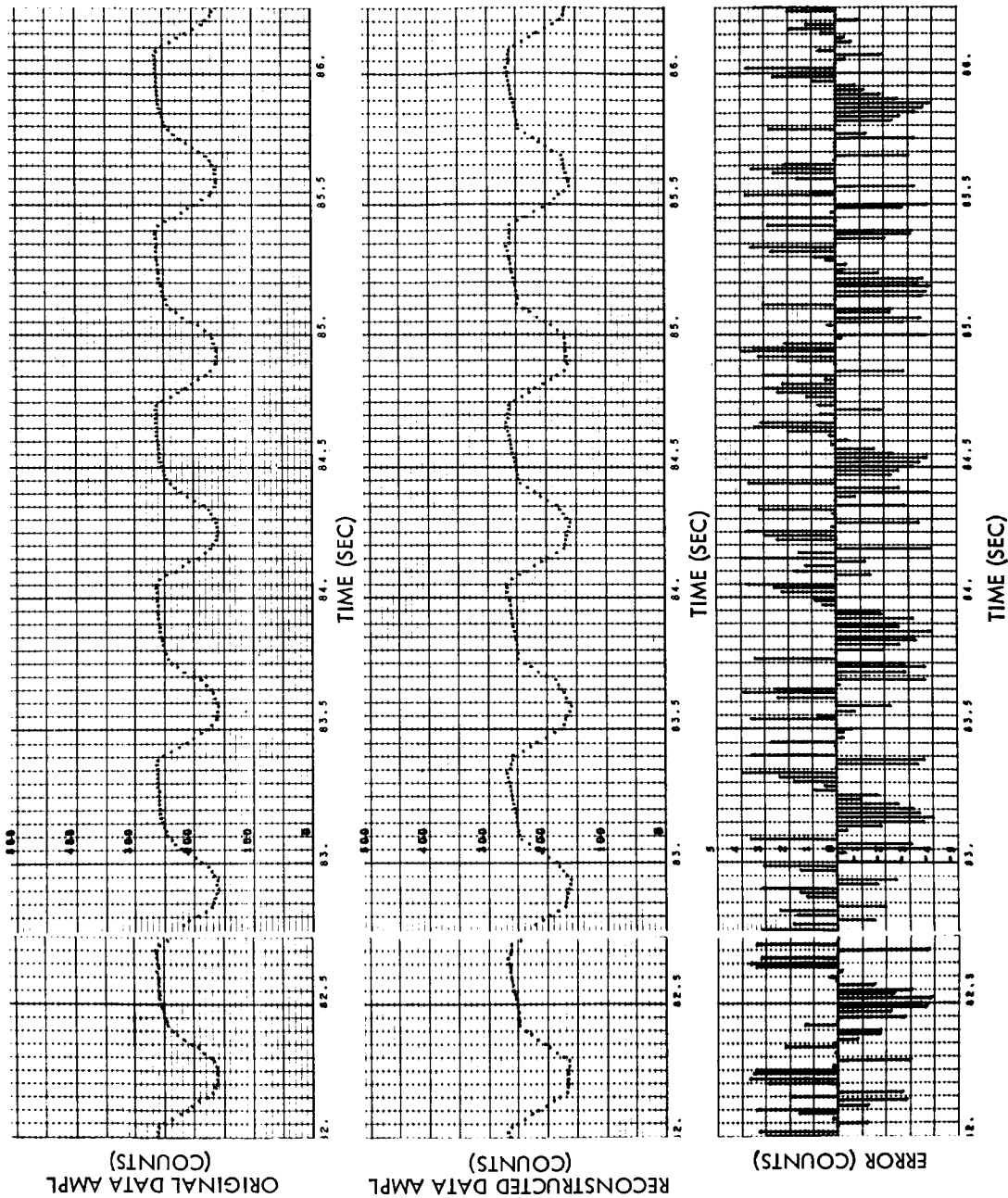


Fig. 4-48 Sensor 11 Original Data, Reconstructed Data, and Error vs Time, Run S6-07

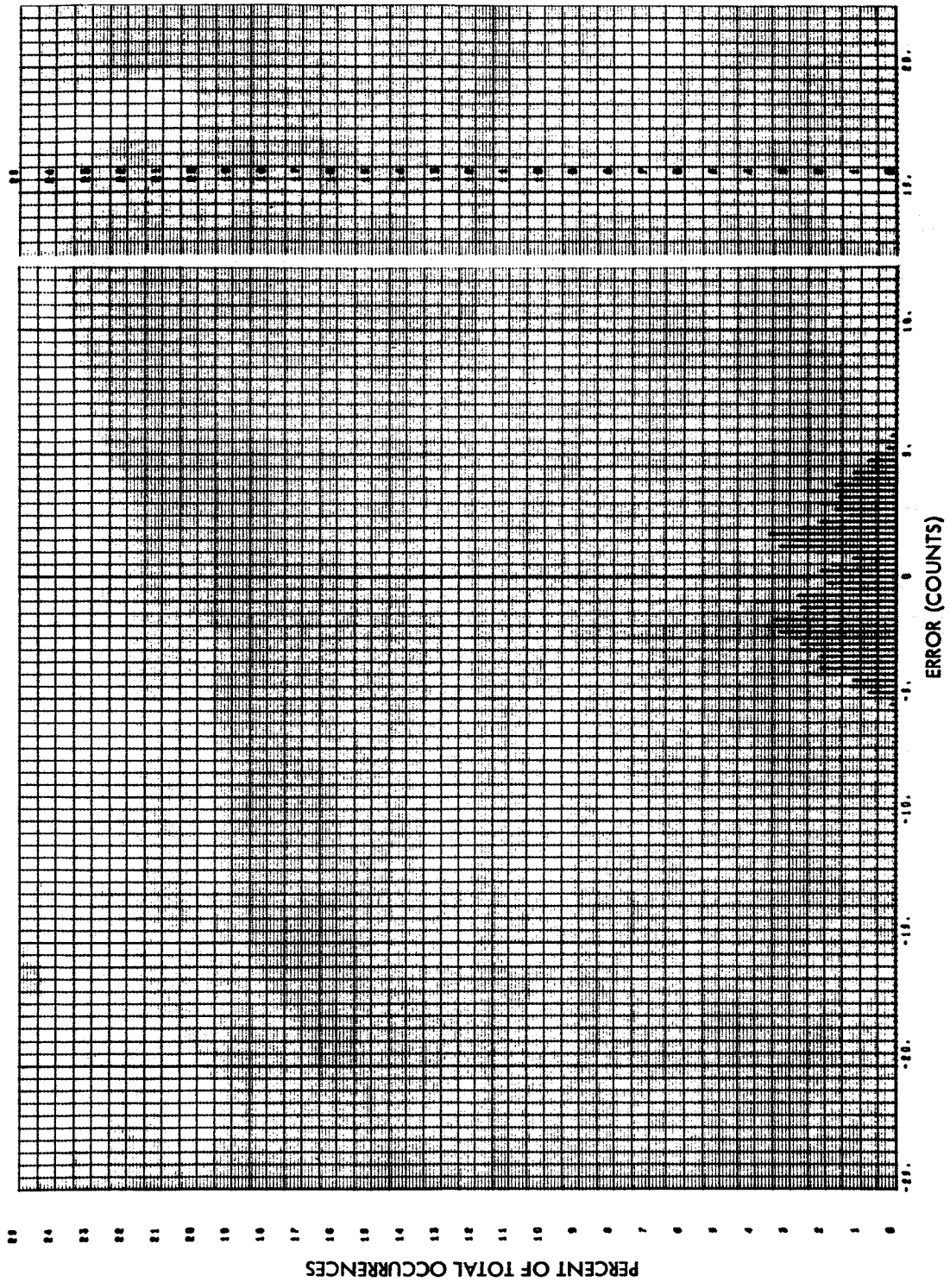


Fig. 4-49 Sensor 11 Histogram, Run S6-18

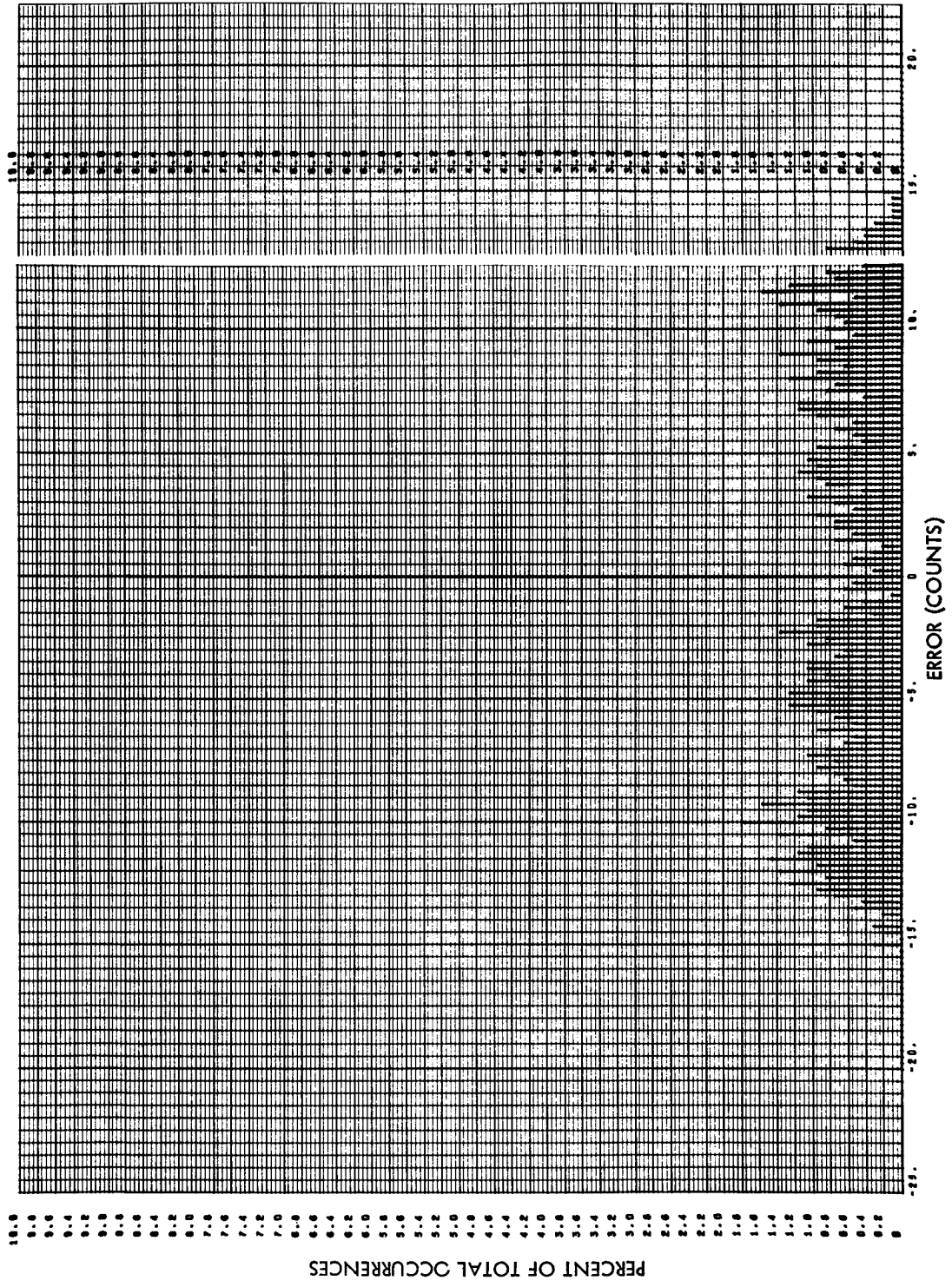


Fig. 4-50 Sensor 11 Error Histogram, Run S6-19

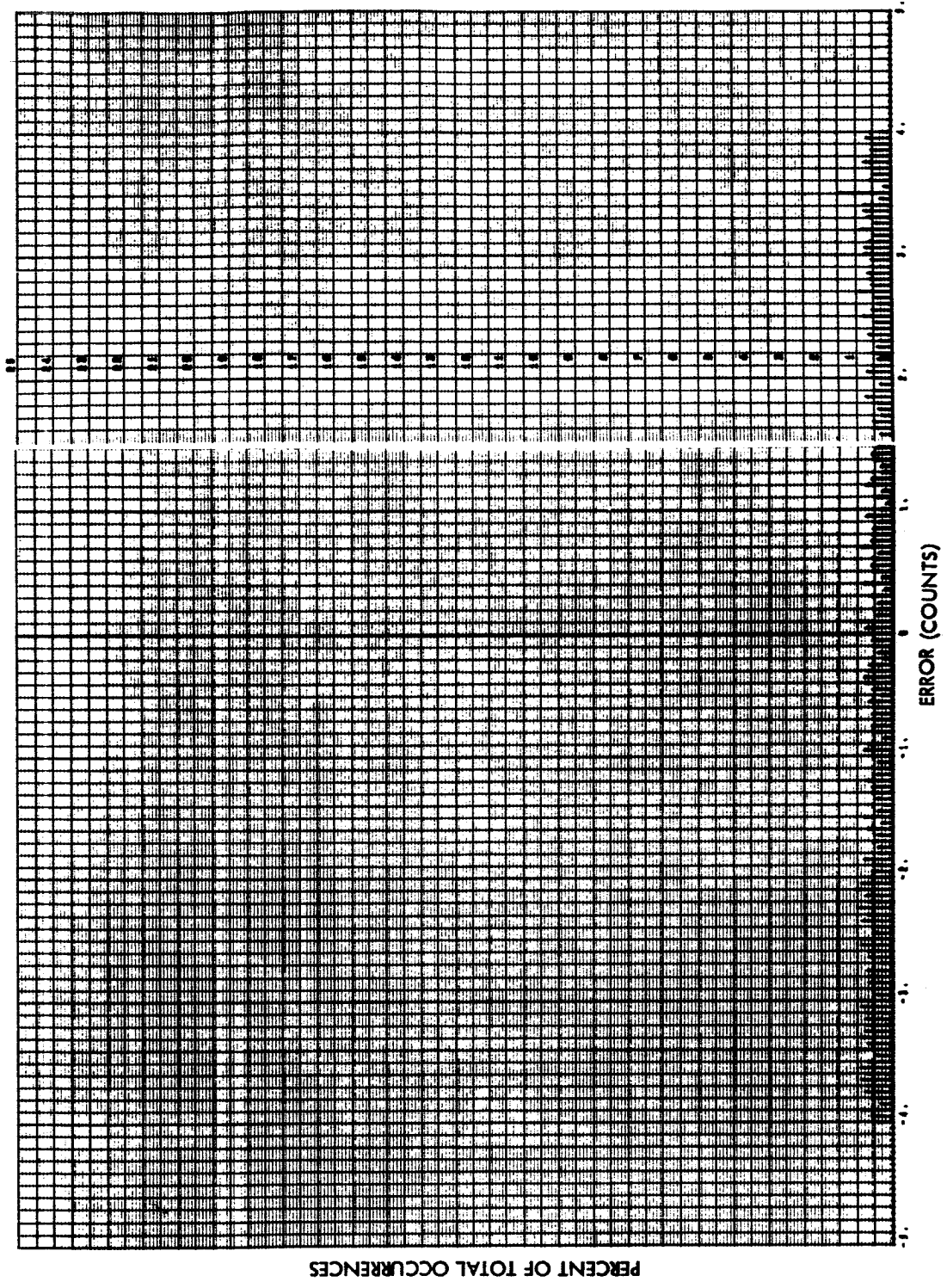


Fig. 4-51 Sensor 11 Error Histogram, Run S6-07

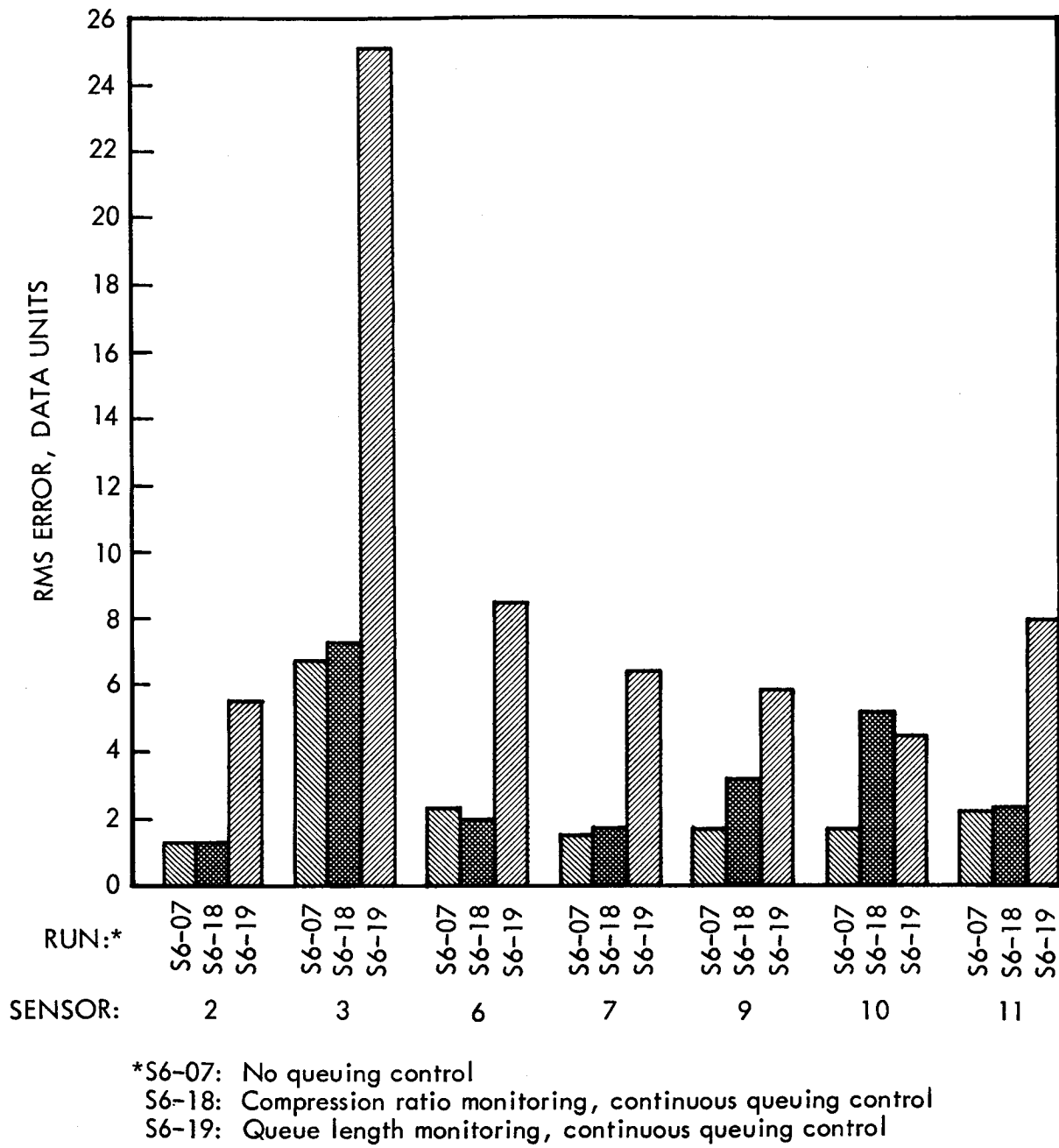


Figure 4-52 Comparative Rms Errors, Test Group 4

**Table 4-9
COMPRESSOR RUN SUMMARY**

Test Group	Time Segment, Sec	Run No.	Selector	$\bar{\rho}$	M	Queuing Control System	Remarks
1	92-148	S6-01	ZOI	-	-	NONE	No buffer simulation
		S6-02	FOIDIS	-	-	NONE	No buffer simulation
		S6-03	ZOI	0.95	261	NONE	
		S6-04	FOIDIS	0.96	273	NONE	
		S6-05	FOIDIS	0.90	288	NONE	
		S6-06	FOIDIS	1.10	236	NONE	
2	20-220	S6-07	FOIDIS	0.91	288	NONE	
3	180-215	S6-08	FOIDIS	0.97	288	CRC	$\beta_1 = -3, J_R = 3$ for all sensors
		S6-09	FOIDIS	1.01	288	CRC	$\beta_1 = -3, J_R = 11$ for all sensors
		S6-10	FOIDIS	0.98	288	QLC	Parameters chosen to correspond as closely as possible with S6-08
		S6-11	FOIDIS	*	288	See Remarks	QLC used to simulate sample loss caused by buffer overflow, without queuing control
		S6-12	FOIDIS	0.89	288	QLC	Control began at queue = 20; full-scale tolerance at queue = 100, for all sensors
4	62-95	S6-13	FOIDIS	-	-	NONE	No buffer simulation
		S6-14	FOIDIS	0.91	244	NONE	
		S6-15	FOIDIS	0.95	233	NONE	
		S6-16	FOIDIS	0.98	226	NONE	
		S6-17	FOIDIS	1.50	148	NONE	
		S6-18	FOIDIS	1.50	148	CRC	$\beta_1 = -3, J_R = 7$ for all sensors
		S6-19	FOIDIS	1.04	148	QLC	Control began at queue = 20; tolerance doubled at queue = 75, for all sensors

*The true value of $\bar{\rho}$ was not determined for Run S6-11.

Explanation of Symbols:

- $\bar{\rho}$ Ratio of average buffer sample readin rate to readout rate
- M Buffer readout rate in samples per sec
- ZOI Zero-order interpolator
- FOIDIS First order interpolator, disjoined
- CRC Compression ratio monitoring, continuous (linear) control
- QLC Queue length monitoring, continuous (linear) control
- β_1 Slope of queuing control curve
- J_R The number of most recent line segments, including current run, over which average run length is computed

Table 4-9 Compressor Run Summary

Section 5
CHANNEL AND TIME CODING

Section 5
CHANNEL AND TIME CODING

This section describes methods of channel identification and time base reconstruction for adaptive sampling, redundancy reduction and encoding. Channel identification is used to show which channel each non-redundant sample represents; time coding to re-establish the event time sequence. The coding selected to provide this must be considered in computing the overall bandwidth compression ratio.

An accurate, absolute time base is important when correlating data from a number of satellites, or even multiplexed data from the same satellite. Since the time resolution of a measurement is entirely dependent upon the sampling frequency of the multiplexer, redundancy reduction and encoding are able to achieve the same time resolution provided suitable time coding is included. In certain instances of adaptive sampling, time coding must be performed on an absolute or incremental time basis since the adaptive multiplexer may not have a basic frame rate. The following paragraphs discuss each category of time and channel coding independently since each has a unique solution.

When examining time-base reconstruction requirements it is important to note whether data is required in real time (delayed only by propagation effects), near real time (delayed for a few seconds by buffers, etc.), or hours to days after the actual event. In general, only those data required for closed loop command control have real-time requirements. Since real-time closed loop operation of a satellite is rarely used, most data can be transmitted using near real-time.

5.1 CHANNEL IDENTIFICATION

The method of coding to be used depends upon the model. With adaptive sampling and redundancy reduction, a channel identification code is required with each transmitted symbol. On the other hand, encoding models that produce an output symbol for each

input sample do not require special coding since, as in the case of conventional PCM, the order of symbols following a frame sync word identifies the channel number. However, synchronization will be difficult in those encoding models which employ variable word lengths. Word separation will also be difficult in these models unless end-of-word or comma codes are included. In the case of bit plane encoding, a single channel address is required to represent an entire block of encoded data from a given source, which results in less bandwidth required for channel identification.

5.2 RELATIVE TIME CODING

5.2.1 Adaptive Sampling

The two major forms of adaptive sampling discussed in Paragraph 2.3.2 are telemetry format variation by command-control from the ground station, and self-adaptive sampling. The first involves a constant speed multiplexer whose format is varied on command. Because the current format is known at all times at the ground station, relative timing is maintained as in the case of a conventional multiplexed telemetry system. The second category, self-adaptive sampling, however, is more involved.

Paragraph 2.3.2 described a number of different ways in which self-adaptive sampling could be implemented. Summarized, these are:

- Constant-speed multiplexer
 - a. Constant delay of each sensor waveform at multiplexer input.
 - b. Variable delay of each sensor waveform at multiplexer input.
- Variable speed multiplexer

Either a or b, as above.

If the multiplexer output rate and all delays at the multiplexer input are constant (therefore known a priori), the timing problem reduces to that of a conventional time-multiplexed telemetry system and relative timing between samples of the same sensor and among sensors can be determined at the receiver simply by monitoring the overall multiplexer sample rate.

However, if variable analog delays are employed at the input to the multiplexer, the timing problem becomes quite difficult. Data waveforms at the outputs of the variable delay networks are now distorted in the time dimension, and each resulting sample has a different delay associated with it. This delay would probably have to be transmitted along with each sample in order to reconstruct relative time.

If a variable-speed multiplexer is used, the original time reference is again destroyed, unless special steps are taken. One way to preserve this reference may be to transmit along with each sample the instantaneous speed of the multiplexer when the sample was taken. Another way may be to measure the buffer waiting time of each sample.

This discussion indicates that unless a constant speed multiplexer is used along with constant delays at the multiplexer input, the problem of relative time coding with self-adaptive sampling may be exceedingly difficult, and could very likely require implementation which exceeds the current state of the art.

5.2.2 Redundancy Reduction

The following discussion pertains to relative time coding required for redundancy reduction to reinstate the order of data samples in a time resolution equivalent to PCM telemetry.

Although one of the easiest methods for reinstating the order of reconstructed data samples is to include an absolute vehicle time identification with each significant sample transmitted, this method is not considered because of the resulting inefficient use of bandwidth.

It is possible to avoid transmitting time by taking advantage of the channel address which must accompany each significant data sample. The possible solutions are influenced to a certain degree by the organizational configuration of the multiplexer (number and variety of sampling rates). Four time resolution coding techniques were evaluated for the S-3 (Explorer XII), S-6 (Explorer XVII), and S-49 (OGO) satellite telemetry multiplexer formats.

5.2.2.1 Techniques. The techniques and the bit requirements associated with each are as follows:

a) Minor frame¹ identification (ID) in addition to one subframe ID² at the beginning of each minor frame. Bit requirements per transmitted word:

- Data magnitude, represented by \log_2 (no. of quanta between zero and full scale)
- Minor frame ID, represented by \log_2 (no. of minor frame channels)
- Subframe ID code indication, represented by 1 bit

In addition, a subframe ID word of equivalent length once each minor frame.

b) Absolute address with forced readout of redundant sample during an empty minor frame. (This technique will not establish exact time for cross-strapped sensors.) Bit requirements per transmitted word:

- Data magnitude, represented by \log_2 (no. of quanta between zero and full scale)
- Absolute address, represented by \log_2 (total no. of sensors)
- Indication of first word of a minor frame, represented by 1 bit

c) Minor frame ID with forced readout of redundant sample during an empty minor frame. Bit requirements per transmitted word:

- Data magnitude, represented by \log_2 (no. of quanta between zero and full scale)

¹ A minor frame is a group of consecutive telemetry words beginning with the frame sync pattern and ending with the last word before the next frame sync pattern.

² The subframe ID is the number of the minor frame relative to the subcommutation cycle.

- Minor frame ID, represented by \log_2 (no. of minor frame channels)
 - Indication of first word of a minor frame, represented by 1 bit
- d) Dual minor frame/ subframe ID. Bit requirements per transmitted word:
- Data magnitude, represented by \log_2 (no. of quanta between zero and full scale)
 - Minor frame ID, represented by \log_2 (no. of minor frame channels)
 - Subframe ID, represented by \log_2 (main frame³ length)

It is assumed in the evaluations which follow that empty main frames will be sufficiently rare that forced readouts which would be required to signify these frames need not be taken into account.

5.2.2.2 Evaluation. The subframe ID code indicator bit in (a) distinguishes between a data word and the subframe ID code. The subframe ID code requires the same number of bits as a data word so that the frame synchronization code will always be evenly spaced in time. Since in techniques (a), (b) and (c) a forced readout of either the subframe ID or a redundant sample will occur during an empty minor frame, the resulting bandwidth compression becomes asymptotic to a finite value with increasing sample compression ratios.

Figures 5-1, 5-2 and 5-3 show computed relationships between sample and bandwidth compression ratios for the four encoding techniques described in Paragraph 5.2.2.1. Figure 5-1 shows the relation between sample compression ratio and bandwidth compression ratio for the S-3 multiplexing format. It is seen that below sample compression ratios of 20, technique (c) results in the greatest bandwidth compression ratio. Technique (d) is more efficient for the higher ratios. The S-3 satellite has a 16-channel

³ A main frame is the smallest number of consecutive minor frames which constitutes a complete cycle of all the subcom channels.

minor frame and a single 16-channel subframe. In order to obtain a comparison among the four time resolution coding techniques for the multiplexing format of the S-3 satellite telemetry system, it was necessary to assume a data magnitude digital word length. (The S-3 telemetry system was actually pulse-frequency-modulated.) This word length was chosen to be eight bits.

Figure 5-2 shows the same conversion to bandwidth compression ratio for the S-6 satellite multiplexing format. Techniques (b) and (c) are equal in efficiency over the entire range of sample compression ratios shown, and are thus represented by one line in Figure 5-2. The S-6 minor frame has 45 channels and the three subframes have 16 channels each. The bandwidth conversion efficiency can be improved at the lower compression ratios by dividing the minor frame into a number of shorter higher-rate frames of equal length, thus requiring fewer bits for channel identification. This reorganization does not influence the total number of data channels being sampled or the sampling frequency of each input channel. The primed letters in Figure 5-2 denote the shorter minor frame. Note that (c)' is the most efficient for sample compression ratios below 15. In this case three short frames of 15 channels each were used, as shown in Figure 5-3.

Figure 5-4 shows the relationship between sample compression ratio and bandwidth compression ratio for the S-49 satellite multiplexing format. Technique (c) is consistently more efficient over the compression ratios shown. These examples show that the bandwidth compression is approximately equal to one-half of the sample compression ratio.

5.2.3 Encoding

Encoding models that produce an output symbol for each input sample do not have a relative time code requirement since this class of encoders provide time resolutions to within the accuracy of the PCM telemetry.

In the case of bit plane encoding, time codes are used to represent the number of sample periods (run length) between changes in binary state within a given "B" plane. See

Appendix III. It is seen that after the first sample in a block has been specified, the remaining contents in that block are represented by incremental time codes. If the encoding procedure fails to result in a fewer number of binary digits, the original sequence of binary digits in a plane is to be transmitted instead.

5.3 ABSOLUTE TIME CODING

5.3.1 Adaptive Sampling

Of the two major concepts of adaptive sampling discussed in Paragraphs 2.3.2 and 5.2.1, telemetry format variation by command control may be regarded, as far as absolute time coding is concerned, as a conventional time-multiplexed telemetry system. A self-adaptive system which uses a constant-speed multiplexer and constant delays at the multiplexer input would also determine absolute time in the same manner as a conventional system. The remaining self-adaptive system configurations discussed pose very difficult absolute as well as relative time coding problems, the solutions of which must be deferred to later studies.

5.3.2 Redundancy Reduction

In general, to relate the time of events within a vehicle to an absolute time base, the vehicle clock time must be merged with the multiplexer format, and the overall system time delays, including propagation delay, should be known. If an accurate clock, such as WWV, is monitored at the ground tracking station at least once during a minor frame and if the short term stability of the multiplexer is reasonably good, it is possible to correct for the time errors caused by vehicle clock instability to within the resolution of the sampled data.

When the data compression is employed, there is an additional system delay in the spaceborne equipment, caused by the operation of the buffer. This delay, of course, is variable because the queue length is variable. For near real time data presentation, however, all delays should remain relatively constant if time base errors are to be avoided. To compensate for the variable delay within the data compressor, a

complementary buffer delay at the ground station is required during data reconstruction so that the sum of the two buffer delays will always equal a constant, T. For this condition to be met,

$$(c_v)_t + (c_g)_{t+T} = K \quad (5-1)$$

where

$(c_v)_t$ is the fullness (queue length)
of the vehicle buffer at time t

$(c_g)_{t+T}$ is the fullness of the ground
buffer at time t+T

and K is a constant. For the overall time delay, T, to be minimum, K must be equal to C, the maximum capacity of the vehicle buffer. Under these conditions

$$T = \frac{C}{R_t}$$

where R_t is the transmission word rate. If the minimum delay requirement is to be satisfied, it is necessary that $(c_g)_{t+T}$ be maintained at the value indicated by Equation 5-1. To accomplish this, a periodic code word should be transmitted from the vehicle specifying the fullness of its buffer at time t. For initialization of the ground reconstruction buffer, (c_g) must have a fullness of $C - (c_v)_t$ at time t+T. The maximum capacity of the reconstruction buffer is also equal to C words under these conditions.

If the status of the buffer fullness is not transmitted, it is necessary for the ground reconstruction buffer to have a capacity of 2C words to guarantee that buffer overflow or buffer underflow at the ground station does not occur. To insure that underflow does not occur the reconstruction buffer is filled to a capacity of C words at initialization. Under these conditions the combined time delay of both buffers will be a constant between T and 2T seconds, depending on the fullness of the vehicle buffer at the time of initializing the reconstruction buffer. The actual buffer time delay could be determined, in due time, if the compressor were designed to indicate an empty buffer condition. However, there exists the danger that, if the transmission rate was selected to be less than the mean input rate to the buffer, the probability of an empty buffer would be extremely small.

5.3.3 Encoding

Since variable-length words require the use of a queuing buffer, absolute time coding requirements for statistical encoding systems which produce variable-length output code words for each input sample are identical to those of the redundancy reduction category of data compression. With bit plane encoding, it is necessary to include an absolute time code only once with each block of data, assuming a vehicle clock is available. If absolute time is not available, the problem of time coding is identical to redundancy reduction since a queuing buffer is again required.

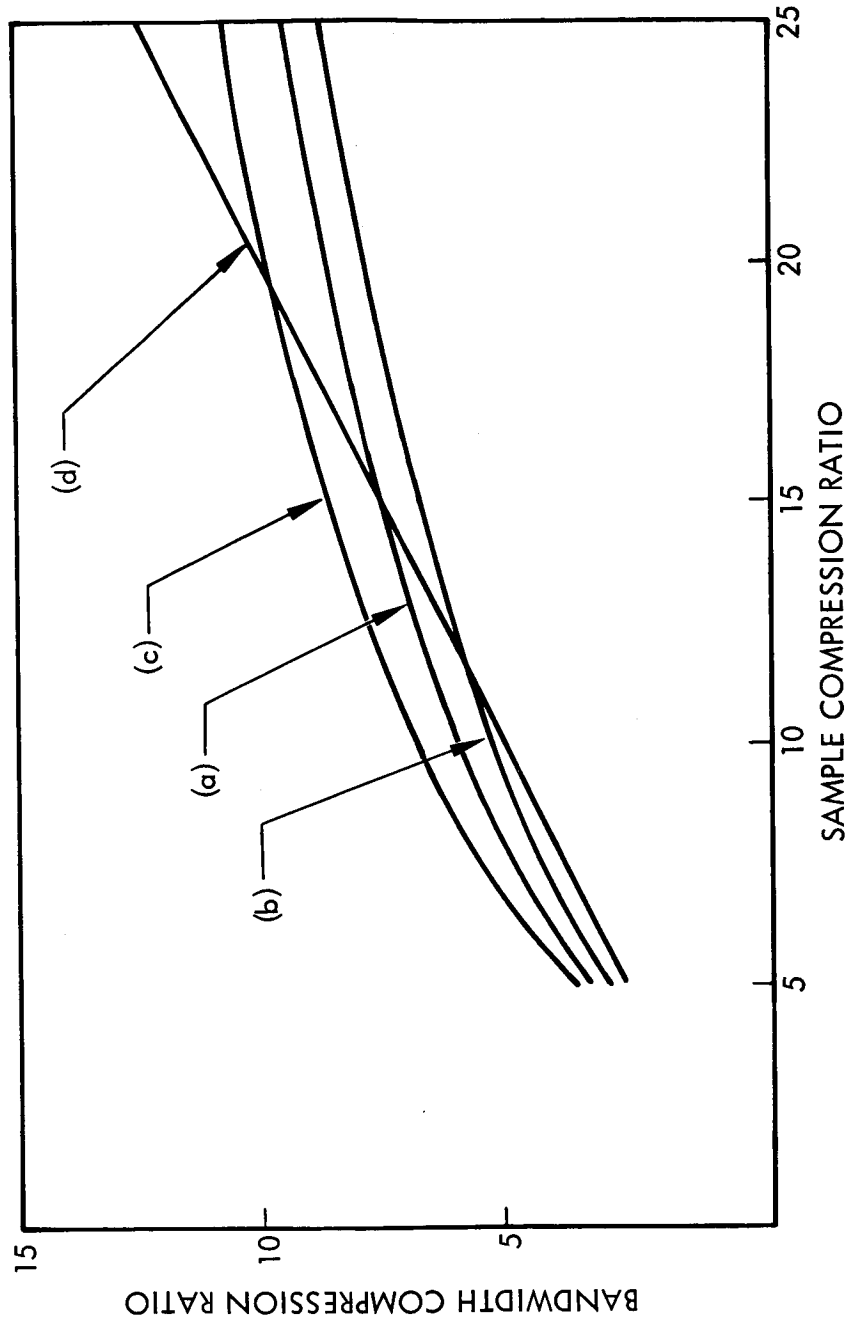


Fig. 5-1 Conversion Characteristics from Sample Compression Ratio to Bandwidth Compression Ratio for S-3 Satellite Telemetry Multiplexing Format

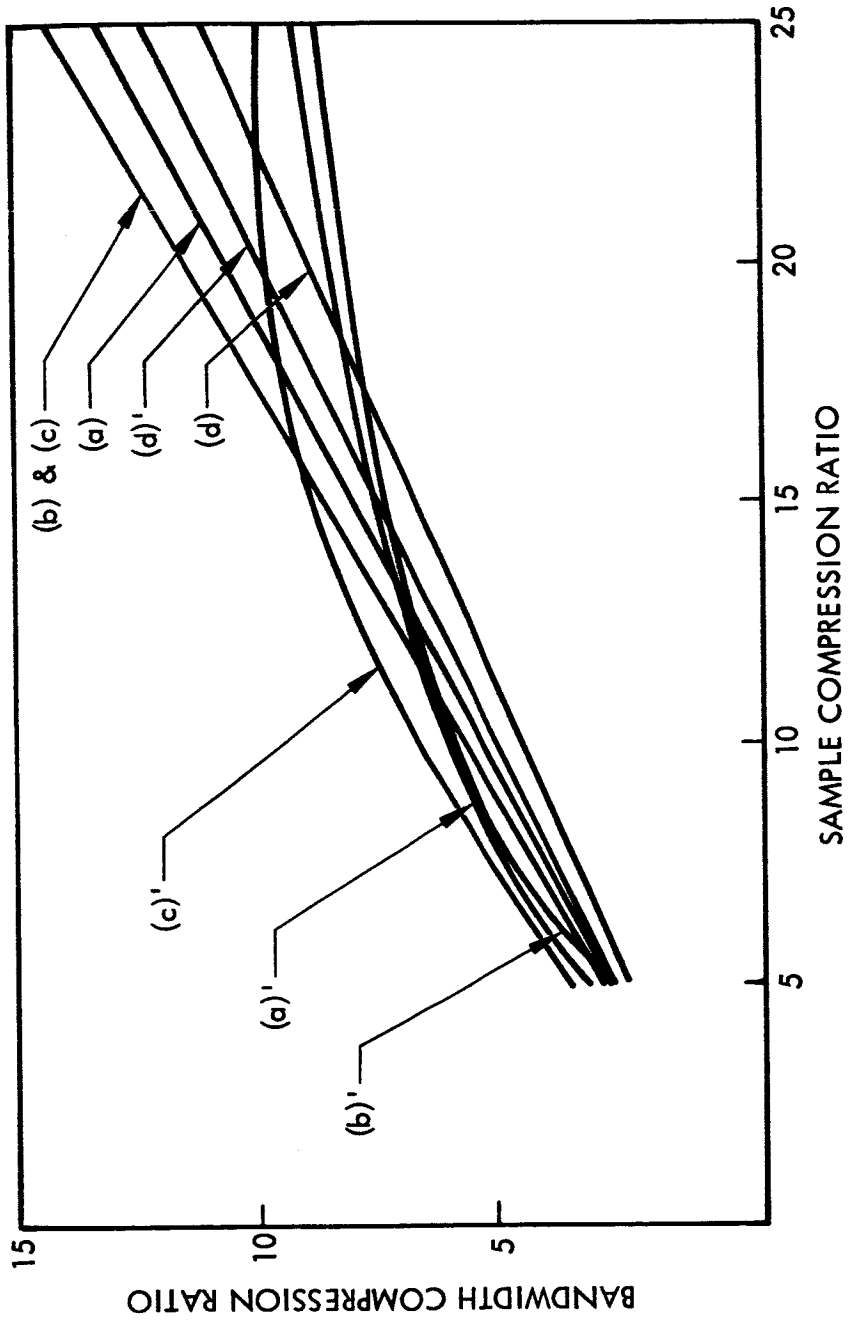


Fig. 5-2 Conversion Characteristics from Sample Compression Ratio to Bandwidth Compression Ratio for S-6 Satellite Telemetry Multiplexing Format

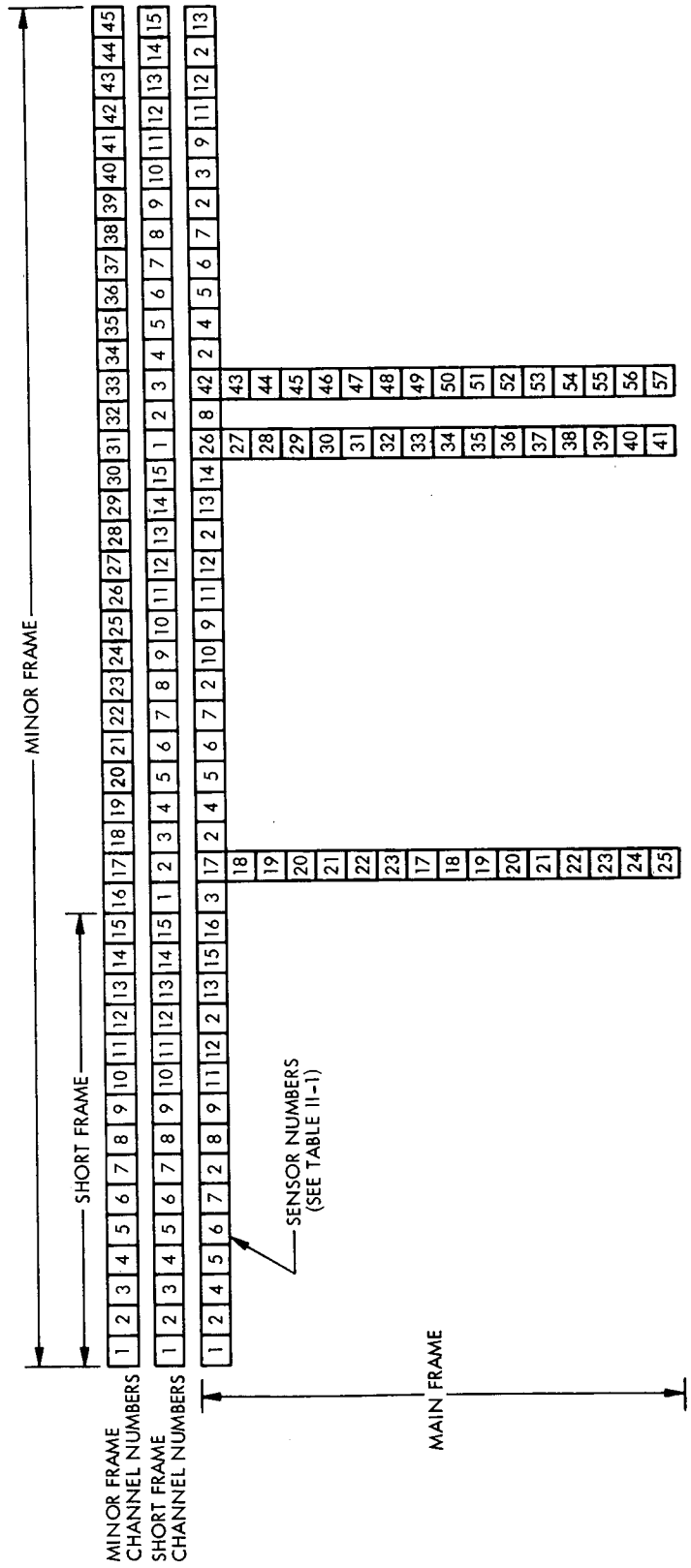


Fig. 5-3 S-6 Telemetry Frame Format, Showing Use of Short Frame in Time and Channel Coding

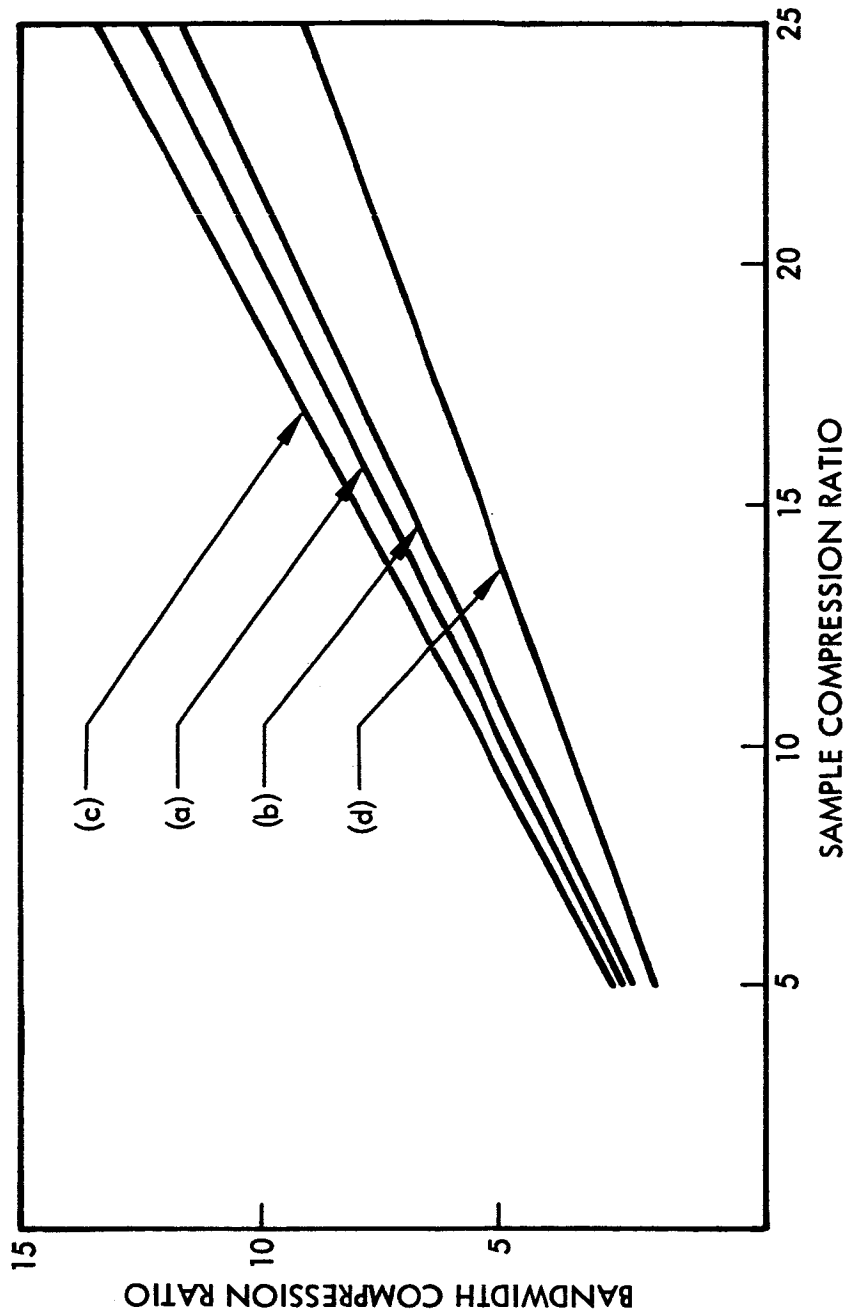


Fig. 5-4 Conversion Characteristics from Sample Compression Ratio to Bandwidth Compression Ratio for S-49 Satellite Telemetry Multiplexing Format

Section 6
FINAL ANALYSIS

Section 6 FINAL ANALYSIS

This section combines and analyzes the results presented in the previous sections of the report so that selections can be made of data compression methods and techniques that will most effectively reduce the bandwidth requirements of the S-6 satellite data without undue loss of data fidelity.

6.1 BANDWIDTH COMPRESSION RATIOS

First, the values of sample compression ratio presented in Sections 3 and 4 are converted to bandwidth compression ratios, using time resolution and address coding technique (c)' discussed in Section 5. This technique requires transmitting along with each data sample amplitude word, a word denoting the minor frame channel number. It was assumed that the minor frame could be divided into three short frames of 15 channels each, requiring four channel identification bits with each amplitude word. For the zero-order predictor (ZOP) and the zero-order interpolator (ZOI), each line segment can therefore be represented by nine data amplitude bits and four identification bits, a total of 13 bits per transmitted word. For the first-order disjointed interpolator (FOIDIS) and the first-order four-degree-of-freedom interpolator (FOI4DG), each line segment is assumed to be represented by two data amplitude words (18 bits), thus requiring a total of 22 bits in each transmitted word. For the first-order offset out of tolerance interpolator (FOIOOT), one offset indication bit is required along with the nine data amplitude bits for each line segment. Thus a total of 14 bits is required for this selector. Because of the relatively low compression ratios involved, no account is taken of forced readout requirements for empty short frames.

Using the above coding technique and word lengths, sample compression ratios presented in Table 3-2 are converted to bandwidth compression ratios for Sensors 9, 10 and 11. The results are shown in Table 6-1 for tolerances of two and four data units. The averages of the bandwidth compression ratios for the two tolerances are shown in

Table 6-1

BANDWIDTH COMPRESSION RATIOS
FROM SINGLE-SENSOR EXPERIMENTS (Section 3)

SENSOR	TOLERANCE, DATA UNITS	BANDWIDTH COMPRESSION RATIO					FOI4DG
		ZOP	ZOI	FOIDIS	FOIOT	FOI4DG	
9	2	1.81	3.52	3.62	3.66	4.00	
	4	3.92	5.99	5.54	5.82	6.30	
10	2	2.37	4.44	4.40	4.69	4.90	
	4	4.95	6.75	6.25	6.25	6.67	
11	2	1.89	4.15	4.70	4.89	5.54	
	4	4.38	5.45	6.20	6.58	7.13	

Figure 6-1, along with the average values of the three sensors. Figure 6-1 shows a superiority of the FOI4DG selector for all three sensors. The ZOI selector outperforms the FOIDIS and FOIOOT selectors for Sensors 9 and 10, but on the average is slightly inferior to these two selectors. For all three sensors, the ZOP selector is highly inferior to the other four.

The compression efficiency of bit plane encoding compared to those of the redundancy reduction selectors is shown in Figures 6-2 and 6-3. Note that with both Sensors 9 and 11, bit plane encoding surpasses the ZOI and FOIDIS selectors for tolerances of 0.5 and 1.5 data units. Further experimentation is necessary to determine the relative behaviors of the techniques for tolerances greater than 1.5. The positions and slopes of the curves for bit plane encoding suggest a possible reversal in relative performance at higher tolerances, but it should also be noted that more efficient coding techniques than the one selected in this study could increase the performance of bit plane encoding as a compression technique.

In order to compare the bandwidth compression ratios obtained during the single-sensor experiments (Section 3) with corresponding results of the multisensor experiments (Section 4), appropriate values of sample compression ratio presented in Table 4-7 were converted to bandwidth compression ratio. These values are shown in Table 6-2¹. The comparison can readily be made by observing (Figure 6-4) that the single-sensor measurements agree quite well with those of Run S6-07 for Sensors 9 and 10, but are much lower than the corresponding measurements from Run S6-13. This may be because the portions of the S-6 data used on Run S6-07 and the single-sensor run, though not identical intervals, contained about the same proportion of wild points caused by sync loss, while the data used on Run S6-13 were free of sync loss. On the other hand, the single-sensor run on Sensor 11 yielded a much higher bandwidth compression ratio than did Run S6-07 or S6-13. The reason for this is that the single-sensor run covered a portion of the Sensor 11 data that consisted mostly of calibration, resulting in a waveform which was primarily steady-state. This is in high contrast to the cyclic nature of the waveform generated by the measured phenomenon coupled with the effect of the spin of the vehicle.

¹For the case involving the combined compression ratio for all 57 sensors, the assigned tolerance for each sensor is given in Table 4-1. The tolerance was 4 data units on 80% of the data.

Table 6-2
**BANDWIDTH COMPRESSION RATIOS FROM
 MULTI-SENSOR EXPERIMENTS (SECTION 4)**

Sensor	S-6 Data Interval, Sec	Run	Sample Comp. Ratio*	Bandwidth Comp. Ratio
9	20-220	S6-07	13.44	5.50
	62-95	S6-13	35.70	14.60
10	20-220	S6-07	13.62	5.57
	62-95	S6-13	30.70	12.55
11	20-220	S6-07	7.02	2.87
	62-95	S6-13	7.64	3.13
Combined (57 sensors)	20-220	S6-07	6.88	2.82
	62-95	S6-13	8.12	3.32

Selector: FOIDIS

Tolerance: 4 data units

*The sample compression ratios shown in this table are twice the corresponding values presented in Table 4-7 (cf. paragraph 4.4.1, p. 4-6).

6.2 COMPRESSION MODELS AND DATA CLASSES

One of the purposes of this investigation was to determine which compression models are most effective on each of the five data classes discussed in Section 3. This subsection discusses the outcome of this work and some of the reasons why it is advantageous to consider single-model operation for all data on a given vehicle, rather than a multiple system with specific models tailored to each data class.

6.2.1 Model Applicability to Data Classes: Experimental Results

Bandwidth compression ratios obtained for the ZOI and FOIDIS selectors on each of four data classes (Class 4 was excluded) are shown in Table 6-3. The values were computed from the sample compression ratios in Table 3-3. Note that the compression effectiveness of the zero-order interpolator exceeds that of the first-order interpolator for Data Classes 1, 2 and 3, but that the situation is reversed for the Class 5 data specimen used in the test. Undoubtedly the first-order interpolator also would be more effective with Class 4 data, since these data consist of sawtooth waveforms.

Because of the step-wise constant and/or slowly-varying nature of the Class 1 and 2 data, it is not surprising that the zero-order interpolator may outperform the first-order interpolator for these two classes. It is interesting, however, that the ZOI selector also outperforms the FOIDIS selector on two examples of Class 3 (exponential transient) data. An intuitive comparison of the two selectors on such a waveform is difficult, but it is noted in observing Figures 3-3, p. 3-32 (Class 3, Example b: 79-87 sec.) and 3-3, pp. 3-35 and 3-36 (Class 3, Example c: 120 - 142 sec.) that a large proportion of these waveforms are tails of exponentials, which are essentially constant. Although the statistical sample used in these experiments is too small to draw any firm conclusions, it appears likely that the relative performance of the zero and first-order interpolators may depend on the particular exponential waveform in question.

By similar reasoning, since the waveforms contained in Class 5 consist of all those types which do not fall in Classes 1 through 4, it may be difficult to find a single compression model which performs best with Class 5 data.

Table 6-3
**BANDWIDTH COMPRESSION RATIOS VERSUS
 DATA CLASSES**

Data Class	Example	Sensor	Time Segment, Sec	Bandwidth Comp. Ratio	
				ZOI	FOIDIS
1	a	9	104-116.5	—	4.11
	b	10	87-120	3.52	1.81
2	a	11	104-120.5	3.39	2.30
3	a	9	116.5-133	—	2.33
	b	10	79-87	3.90	2.25
	c	10	120-142	3.85	1.81
5	a	11	130.5-136	1.92	2.63
Variance of bandwidth compression ratios				0.524	0.0833*

Note: Tolerance is 2 data units in all cases.

*Class 1, Example a and Class 3, Example a are not included in this figure.

6.2.2 Advantages of Single-Model Operation

When the problem of data waveform redundancy reduction is first considered, it is logical to surmise that additional system efficiency can be achieved by tailoring compression models to data classes. The difficulty with this approach, however, is that the telemetry data from one vehicle, and, indeed, data in a single multiplexer frame, usually contain waveforms from all five data classes. Paragraph 3.3.1.2 states that very few parameters (other than housekeeping parameters, which make up no more than 3/45 of all the S-6 data samples), appear to fall entirely in any one data class other than Class 5. Thus, to take advantage of any correlation that may exist between compression model and data class, it may be necessary not only to use more than one compression model to accommodate different sensors, but also to change models on single sensors during the course of the experiment.

Now, it is true that if the differences in bandwidth compression ratios between selectors for the various classes were sufficiently great, the increased equipment complexity required to implement such a multiple-model system might be warranted. However, the data obtained thus far (Table 6-3) indicate that such is not the case.

In light of the above, it should be considered an attribute for a compression model to exhibit a non-varying performance from one data class to the next, in addition to a high bandwidth compression ratio. This attribute is therefore included in the selector tradeoff analysis of Paragraph 6.4.

6.3 ADAPTIVE APERTURE AND FILTERING TECHNIQUES

There are two possible reasons for employing adaptive aperture and filtering techniques in a data compression system:

- To control the queue length in an attempt to curtail or eliminate buffer overflow
- To improve the fidelity of the reconstructed data and increase the compression ratio

Section 4 describes the investigation of adaptive aperture techniques for the purpose of buffer overflow curtailment, and Section 3 discusses the study of the effect of adaptive aperture and filtering techniques on data fidelity and compression ratio. This paragraph summarizes the findings of both these investigations.

6.3.1 Curtailment of Buffer Overflow

Paragraph 4.5.5 points out that, in the absence of wild data sample points, the arrival statistics of the S-6 satellite compressed data samples entering the buffer were found in the case of multisensor operation to be extremely stationary. This high degree of stability was shown by the extremely low maximum queue length of 56 samples during a simulated run consisting of 29,700 compressor input data samples, even when the ratio of average buffer input sample rate to output rate, $\bar{\rho}$, was set as high as 0.98.

Because of this stationarity it was concluded that a queuing control system would not be needed if it were useful to curtail only that buffer overflow caused by non-stationarity of the buffer input data sample rate. However, queuing control is also useful to prevent buffer overflow when the buffer sample readout rate is so low that $\bar{\rho}$, without the control, would exceed unity. It is shown in Section 4 that queuing control using queue length as the monitored parameter (rather than average compressed data run length) can most effectively cope with this situation. Thus, it is concluded that queue length monitoring should be used to curtail buffer overflow on a spaceborne data compressor (where noise is not a problem) when the telemetry data is similar to that of the S-6 satellite.

In a ground-based application (again considering S-6 satellite telemetry data) where wild points due to noise may exist, Section 4 concludes that queue length monitoring should be used to curtail buffer overflow during those data intervals when excessive wild points were not present. To cope with wild points that may exist, two approaches may be taken. Either (1) a buffer of reasonable capacity (100 to 200 samples) can be allowed to overflow during periods of excessive wild points (assuming the data during these intervals are of little use to the analyst anyway), or (2) methods can be devised to reject most wild points before the data enter the compressor. These methods can

be based on similar decision criteria that are currently used by data compression sample selectors.

It should be pointed out that in Section 4 the use of adaptive aperture techniques is considered solely with the intent of controlling the queue to curtail buffer overflow, and the above conclusions are based on this intent. They will of course be combined with the conclusions derived in Paragraph 6.3.2 regarding fidelity and compression ratio.

6.3.2 Improvement of Reconstructed Data Fidelity and Compression Efficiency

Section 3 reports the investigation of two general methods for the possible improvement of reconstructed data fidelity and compression efficiency. These are (1) precompression filtering and (2) adaptive aperture techniques. Precompression filtering can be either adaptive or nonadaptive; i. e., the effective bandwidth of the filter can be made to vary as a function of some parameter concerned with the compressed data (adaptive), or it can be fixed (nonadaptive).

6.3.2.1 Precompression Filtering. The following results were obtained from the nonadaptive filtering experiment discussed in Paragraph 3.4, regarding compression efficiency and reconstructed data fidelity:

Compression efficiency: In most instances average compression ratios were raised significantly for both the ZOI and FOIDS selectors when precompression filtering was used.

Reconstructed data fidelity: Rms errors in the reconstructed data, as compared to the original data, were much higher when precompression filtering was used. It is evident, however, that the increase was caused primarily by the presence of wild points in the data. It is conjectured that when large numbers of wild points are present in the data and filtering is involved, rms error may not be a valid gauge of data fidelity. A subjective inspection of the reconstructed data waveforms was inconclusive; but the

filtered, compressed, and reconstructed data appeared to be somewhat smoother than the unfiltered, compressed, and reconstructed data, for the same values of tolerance. (See Figures 3-7, p. 3-48, 3-21, p. 3-70 and 3-21, p. 3-72 for ZOI, and Figures 3-11, p. 3-54, 3-21, p. 3-71 and 3-21, p. 3-73 for FODIS).

Results from the adaptive filtering experiment discussed in Paragraph 3.5.2 can be summarized as follows:

Compression efficiency: For the three sensors examined, average compression ratios were raised by a fairly high margin, using the ZOI selector, over the ratios obtained with no precompression filtering.

Reconstructed data fidelity: As in the case of nonadaptive filtering, rms errors in the reconstructed data were much higher with adaptive precompression filtering. Again, however, this large increase was probably caused primarily by the presence of wild points in the original data. A subjective inspection of the reconstructed waveforms indicated that, in the absence of wild points, the filtered, compressed and reconstructed data appeared to be more representative of actual data trends and less susceptible to noise than the unfiltered, compressed and reconstructed data, for the same tolerance values.

It is not possible to compare nonadaptive with adaptive precompression filtering from the above results because of the different system configurations and techniques used in the two tests. (For example, samples were deleted prior to compressor input in the adaptive filtering experiment; they were not deleted in the case of nonadaptive filtering.) It can be concluded, however, that both adaptive and nonadaptive precompression filtering hold promise as means of both increasing compression efficiency and enhancing reconstructed data fidelity. A great deal of additional work is needed before their relative and absolute worth as accessories to sample selection techniques can be finally determined.

6.3.2.2 Adaptive Aperture Techniques. The adaptive aperture experiment discussed in Paragraph 3.5.1 monitored the following parameters:

- Short term compression ratio
- Present (line segment) run length
- Exponentially filtered present run length

Note that all three parameters were associated with current waveform activity, and not directly with queue length. The results of this experiment may be summarized as follows:

Compression efficiency: For the three sensors and two selectors examined, the average compression ratio was not significantly changed from the fixed-aperture cases.

Reconstructed data fidelity: Rms errors were slightly higher with the adaptive aperture techniques, than when fixed apertures were used. However, a subjective inspection of the reconstructed waveforms showed approximately equal fidelity between the fixed and adaptive aperture cases. Note, however, that while a subjective, visual inspection of two reconstructed data waveforms might reveal no difference in fidelity (because, for example, greater errors are associated with the more active portions of the data), the degradation of the specific information required from the waveform by the data analyst will, in the last analysis, determine relative data fidelity.

The general conclusion from the tests performed in this study is that adaptive aperture techniques which monitored parameters associated with current waveform activity did not appear to have an appreciable effect on either compression efficiency or overall data fidelity.

If the results of Sections 3 and 4 are combined, it is seen that an adaptive aperture control system which monitors queue length would be desirable for S-6 data in both

spaceborne and groundbased applications of data compression. The sole purpose of this control system would be the curtailment of buffer overflow. In addition, it may be desirable to include some form of precompression filtering (either adaptive or non-adaptive) in the S-6 data compression system to improve compression efficiency and reconstructed data fidelity. Further investigation is needed in this area before definite conclusions can be drawn.

6.4 COMPRESSION MODEL TRADE-OFF ANALYSIS

The following criteria were used in the trade-off analysis to select the most desirable data compression model among the six models examined:

- Bandwidth compression ratio
- Reconstructed data fidelity
- Sensitivity to data class
- Sensitivity to sensor noise
- Effectiveness with adaptive queuing control
- Complexity
- Sensitivity to noise in the compressed data transmission link
- Ease of reconstruction

Performance factors ranging between zero and one were derived for the six models according to each of the above criteria, using methods described in the following paragraphs. The maximum performance factor used was 0.95 to account for the possibility of higher performance by a new, currently unknown, model. For those criteria which could be evaluated from the experimental data, formulas were derived to determine the performance factors. A consideration was made of the relative importance of each criterion for the spaceborne, as well as the groundbased, application of data compression, and the performance factors were weighted accordingly. Finally, the weighted factors were added to obtain one figure of merit for each compression model in the spaceborne application, and another for the groundbased application.

6.4.1 Bandwidth Compression Ratio

The bandwidth compression ratio performance factor was determined for a given model, i , by finding the ratio of compression performance achieved by that model to the maximum performance of any of the models tested. The measure of performance in this instance is the sum of the four values of bandwidth compression ratio achieved for Sensors 9 and 11, with tolerances of 2 and 4 data units. Thus, the formula used to obtain the performance factor for bandwidth compression ratio is

$$f_p(\bar{N}_B)_i = \frac{0.95 \sum_{\text{Sens. 9, 11}} \left[\left(\bar{N}_B \right)_{K=2} + \left(\bar{N}_B \right)_{K=4} \right]_i}{\sum_{\text{Sens. 9, 11}} \left[\left(\bar{N}_B \right)_{K=2} + \left(\bar{N}_B \right)_{K=4} \right]_{\text{max}}} \quad (6.1)$$

where $f_p(\bar{N}_B)_i$ = bandwidth compression ratio performance factor for Model i

\bar{N}_B = bandwidth compression ratio

K = tolerance in data units

the denominator is the maximum sum obtained for the models tested

The values of \bar{N}_B were obtained from Figures 6-2 and 6-3. In the case of bit plane encoding, the straight-line curves in these figures were extended to include tolerances of 2 and 4 data units. (See Paragraph 6.1, p. 6-3, and Paragraph 6.4.9, p. 6-17 for comments regarding the validity of this extrapolation.)

6.4.2 Reconstructed Data Fidelity

This performance factor was evaluated for Compression Model i by finding the ratio of reconstructed data error for the model which achieved the minimum error of those tested, to reconstruction error for the i^{th} model. The measure of error used in this case is the sum of four measured values of rms error (normalized to the tolerance), for Sensors 9 and 11, with tolerances of 2 and 4 data units. Thus, the formula used to obtain the performance factor for reconstructed data fidelity is

$$f_p(F)_i = \frac{0.95 \sum_{\text{Sens. 9, 11}} \left[\left(\frac{E_R}{K} \right)_{K=2} + \left(\frac{E_R}{K} \right)_{K=4} \right]_{\min}}{\sum_{\text{Sens. 9, 11}} \left[\left(\frac{E_R}{K} \right)_{K=2} + \left(\frac{E_R}{K} \right)_{K=4} \right]_i} \quad (6.2)$$

where $f_p(F)_i$ = fidelity performance factor for Model i

E_R = rms error, in data units

K = tolerance, in data units

the numerator is the minimum sum obtained for the models tested

The values of E_R were obtained from Table 3-2. In the case of bit plane encoding the calculated values of E_R presented in Paragraph 3.3.2.1 were normalized to tolerances of 0.5 and 1.5 data units, rather than 2 and 4 as shown in Equation 6.2.

It should be emphasized that it is extremely difficult to find a suitable criterion of reconstructed data fidelity. A subjective inspection of the data waveform is not considered to be a valid method of fidelity determination in many cases where experimental data are involved, because an error which may be important to the data analyst might not be apparent to the eye. It is likely that a good case could be made simply for maximum allowable error as the criterion of reconstructed data fidelity. In this particular instance, because all the compression models tested operated with maximum error constraints, rms error is probably a more valid criterion than it would be if this restriction were not imposed. In the last analysis it is the experimenter who must decide whether or not a given compression model and tolerance produces acceptable reconstructed data.

6.4.3 Sensitivity to Data Class

The advantages of operating on all data classes with a single compression model were discussed in Paragraph 6.2.2. The method used in this study to determine relative sensitivity to data class was to calculate the variance of compression ratio obtained on the several classes of data by each compression model tested. The formula used to determine the performance factor for sensitivity to data class is

$$f_p(D)_i = \frac{0.95 \sigma^2_{\min}}{\sigma_i^2} \quad (6.3)$$

where $f_p(D)_i$ = data class sensitivity performance factor for Model i
 σ^2 = variance of bandwidth compression ratios among data classes
the numerator is the minimum variance obtained for the models tested

Since only two models (ZOI and FOIDIS) were tested on separate classes of data, performance factors for the remaining models had to be estimated. The values of σ^2 for the two models were obtained from Table 6-3, p. 6-6.

6.4.4 Sensitivity to Sensor Noise

In obtaining a formula for this performance factor, it was conjectured that the rate at which the compression ratio of a model decreases with decreasing tolerance is a valid indication of the sensitivity of that model to low-level sensor noise. This is based on the assumption that the effect of sensor noise on compression efficiency will generally increase as the tolerance decreases.

The formula used to determine the performance factor for sensitivity to sensor noise is

$$f_p(S)_i = \frac{0.95 \sum_{\text{Sens. 9, 11}} \left[\left(\bar{N}_B \right)_{K=4} - \left(\bar{N}_B \right)_{K=2} \right]_{\min}}{\sum_{\text{Sens. 9, 11}} \left[\left(\bar{N}_B \right)_{K=4} - \left(\bar{N}_B \right)_{K=2} \right]_i} \quad (6.4)$$

where $f_p(S)_i$ = sensor noise sensitivity performance factor for Model i
 \bar{N}_B = bandwidth compression ratio
K = tolerance, in data units
the numerator is the minimum sum obtained for the models tested

The values of \bar{N}_B were obtained in the manner described in Paragraph 6.4.1.

6.4.5 Effectiveness With Adaptive Queuing Control

As in the previous case, the performance factor selected for model effectiveness with adaptive queuing control is based on the rate of change of compression ratio with tolerance. It is logical to assume that if a given increase in tolerance produces a greater increase in compression ratio (i.e., a greater decrease in buffer input rate) for Model A than for Model B, then Model A should be more effective in operating with adaptive queuing control. Hence, the formula used to obtain the performance factor for effectiveness with adaptive queuing control is

$$f_p(A)_i = \frac{0.95 \sum_{\text{Sens. 9, 11}} \left[\left(\bar{N}_B \right)_{K=4} - \left(\bar{N}_B \right)_{K=2} \right]_i}{\sum_{\text{Sens. 9, 11}} \left[\left(\bar{N}_B \right)_{K=4} - \left(\bar{N}_B \right)_{K=2} \right]_{\text{max}}} \quad (6.5)$$

where $f_p(A)_i$ = adaptive queuing control effectiveness performance factor for Model i

\bar{N}_B = bandwidth compression ratio

K = tolerance, in data units

the denominator is the maximum sum obtained for the models tested

The values of \bar{N}_B were obtained in the manner described in Paragraph 6.4.1.

6.4.6 Complexity

Because an investigation of the relative complexity of the compression models was not included in this study, previous experience gained from other LMSC studies was drawn upon to estimate the performance factors for this criterion. As before, the maximum factor used was 0.95.

6.4.7 Sensitivity to Noise in the Compressed Data Transmission Link

As in the previous case, no work was done during the study on the relative sensitivity to noise in the transmission link; hence, all the performance factors for this criterion were estimated.

6.4.8 Ease of Reconstruction

Estimates of the performance factors for this criterion were derived primarily from the experience gained from other LMSC studies and from programming the reconstruction processes for various sample selectors.

6.4.9 Relative Compression Model Performance

The performance factors which were derived for the six compression models are shown on Table 6-4. Shown also are the weighting factors assigned to each performance criterion both for the spaceborne and for the groundbased application. The overall weighted performance factors, determined for each compression model by summing the products of the performance and weighting factors, are shown to the right of the table. These are also shown graphically in Figure 6-5.

The primary difference between the weighting factors assigned to the spaceborne and the groundbased applications is that complexity is considered a highly important factor in the design of a spaceborne compression system, while in the groundbased application it is not.

In observing Table 6-4, note that, while many of the performance factors for the five redundancy reduction models were derived from measurements, all the factors for bit plane encoding were either estimated or calculated. Three of these estimations were made by extrapolating the curves of measured bandwidth compression ratio for bit plane encoding, shown in Figures 6-2 and 6-3. The criteria involved in this extrapolation; namely (1) bandwidth compression ratio, (2) sensitivity to sensor noise, and (3) effectiveness with adaptive queuing control, account for 0.38 of the spaceborne weighting, and 0.46 of the weighting in the groundbased application. Additional experimental data would allow more credence to be placed on these performance factors.

In estimating the bit plane encoding performance factor for sensitivity to data class, it was argued that although bit plane encoding is primarily a zero-order technique, higher-order bit planes of the Gray code would be less disturbed by low-level data waveform

Table 6-4
COMPRESSION MODEL PERFORMANCE FACTORS

Weighting Factor	Spaceborne		Groundbased		Overall Weighted Performance Factor				
	0.30	0.14	0.10	0.05	0.25	0.10	0.03	0.03	
Performance Criterion	0.34	0.18	0.12	0.07	0.05	0.14	0.05		
Compression Model	Bandwidth Compression Ratio	Reconstructed Data Fidelity	Sensitivity to Data Class	Sensitivity to Sensor Noise	Effectiveness With Queuing Control	Complexity	Sensitivity to Link Noise	Ease of Reconstruction	Spaceborne
	ZOP	0.494	0.950	0.050**	0.555	0.950	0.950**	0.950**	0.661
	ZOI	0.790	0.693	0.135	0.678	0.778	0.850**	0.700**	0.691
	FODIS	0.830	0.675	0.850	0.748	0.706	0.700**	0.500**	0.769
	FOI00T	0.868	0.634	0.800**	0.664	0.795	0.700**	0.500**	0.764
	FOI4DG	0.950	0.674	0.950**	0.657	0.804	0.500**	0.500**	0.799
	Bit Plane Encoding	0.775**	0.322*	0.500**	0.950**	0.555**	0.600**	0.800**	0.636
									0.705
									0.724
									0.759
								0.758	
								0.746	
								0.632	

*Calculated value
 **Estimated value
 No asterisk indicates measured value

variations. Hence, its performance factor was estimated to be much higher than those of the zero-order redundancy reduction selectors.

In estimating the performance factors for sensitivity to link noise, the premise was taken that the higher the compression ratio attained by a model, the higher should be its sensitivity to transmission link noise, since a given transmitted sample would in this case represent a greater average number of missing samples in its corresponding line segment. In the case of bit plane encoding, however, it was estimated that a single bit error could, if the error occurred in a Class A bit plane, cause errors in all the remaining samples existing in the data group involved (see Appendix III). With the range of compression ratios found in this study, the number of samples in a data group would probably greatly exceed the number found in an average line segment produced by any of the redundancy reduction models tested. Hence, the performance factor was reduced in the case of bit plane encoding.

Figure 6-5 indicates that, in the groundbased application, the FOI4DG selector has the highest weighted performance factor, and in the spaceborne application the FOIDIS and FOIOOT selectors essentially share the maximum position (they differ by 0.001). Note, however, the relatively small spread in all the performance factors, especially in the spaceborne application. Two statements should be made about this small variation in overall performance.

(1) It is likely that one reason for the low performance spread stems from the fact that only those compression models which were considered to be among the best were originally chosen to be investigated in detail. It is logical that if the initial selection was made correctly the inclusion of many of the rejected models would cause a much greater spread in the bar graphs of Figure 6-5.

(2) Note that the maximum spread represents a difference of $\pm 11.4\%$. Time and budget severely limited the amount of telemetry data used and the number of computer runs performed during the study; hence experimental error could account for a large fraction of this percentage. This consideration, coupled with the number of values shown on Table 6-4 which were estimated rather than measured or calculated, suggests that the

confidence factor may be comparable to the spread. Hence, the relative performances shown in Figure 6-5 must be taken as preliminary; a great deal more study and experimentation must be done before this qualification can be removed. On the other hand, this tradeoff analysis and the results it has produced does represent an attempt to compare objectively the relative performance of the several compression models.

6.5 COMPRESSION RATIO ANALYSIS

The compression ratios achieved on the S-6 telemetry data were low compared to those achieved on other missile and satellite data. This outcome was not envisioned at the beginning of the study since satellite data had been found in the past to be generally more compressible than missile data. Figure 6-6 presents a summary of the bandwidth compression ratios obtained for Agena, Polaris, Saturn, Jupiter, TIROS Video and S-6 telemetry data. Conversion from sample compression ratios contained in References 137, 139, 154, 187, 219 and 244 to bandwidth compression ratio were made using the S-6 conversion factors presented earlier.

6.5.1 Signal Reduction

Table 4-7 shows the sample compression ratios obtained for each measurement in Runs S6-07 and S6-13. Submultiplexed Sensors 17 through 57 are of little concern in this analysis since the combined contribution of these sensors to the overall system compression ratio is $3/45$ the contribution of the remaining minor frame channels. Sensor number 2 has the greatest influence on overall compression ratio since it is cross-strapped to nine minor frame channels. Unfortunately Sensor 2 gave the lowest compression ratio of all minor frame sensors and accounted largely for the low system compression ratio. For example, if Sensor 2 had been eliminated the sample compression ratio would have increased from 4.06 to 6.0 for S6-13, assuming a minor frame length of 36 channels. Sensor 7 also contributed highly to the low compression ratio. If both Sensors 2 and 7 were eliminated, the sample compression ratio would increase to 7.1. Consequently, Sensors 2 and 7 caused a 42 percent reduction in compression ratio. These results indicate that further application of signal reduction prior to redundancy reduction would contribute significantly to improved system efficiency.

6.5.2 Wild Point Rejection

Throughout this report the impact of wild points on data compression was emphasized. It is reasonable to assume that the majority of wild points are caused from bit errors originating in the transmission link between the spacecraft and ground receiving station and loss of frame synchronization within the ground station. Therefore, the problem of wild points pertains only to ground application of data compression.

The influence of wild points on the performance of data compression is considered an important finding. It is apparent that ground data compression systems must include the provisions for rejecting wild points if reasonable compression ratios are to be achieved. Time and funds did not permit the means for rejecting wild points to be incorporated within the computer programs, but it is recommended that such processes be included in future studies.

6.5.3 Sensor Noise

Discussions with experimenters at the Goddard Space Flight Center disclosed that several of the sensors resulting in low compression ratios contained unwanted noise components. In fact, special filtering was used during data processing to reject these noise components prior to final computer analysis. Although the source was not isolated for each measurement, it was observed to be similar to the noise found on the Agena and Polaris vehicles.

Precompression filtering, as discussed in Section 3, was able to improve the compression efficiency as well as improve the apparent fidelity of the data during periods of little noise. Reference 244 has shown that precompression filtering not only improved compression ratios, but reduced the rms errors relative to the desired data components. The use of precompression filtering is believed to be an important and complementary process to redundancy reduction for the purpose of minimizing sensor and/or signal conditioner noise and for means of adaptive queuing control. The experiments conducted in Section 3 also emphasized the importance of wild point rejection prior to precompression filtering.

6.5.4 Asynchronization

During the course of the study it became apparent that many of the sensor waveforms were not being compressed satisfactorily, regardless of the compression model used. It was observed that many of the sensor waveforms for which low compression ratios were obtained were periodic in nature, and therefore highly redundant. If a method were used which could take advantage of this periodicity, it is believed that the overall compression efficiency would be measurably increased.

During discussions with the GSFC experimenters on the S-6 satellite, it was learned that the periodicity of many of the sensor waveforms was caused simply by the asynchronous rotation of the satellite vehicle relative to the frame rate of the telemetry multiplexer. A way to take advantage of the periodicity in these cases would be to synchronize the frame rate of the multiplexer to the spin rate of the vehicle, so that the spin period is an exact multiple of the minor frame period. Then each applicable sensor could be decommutated in such a manner that data samples on corresponding portions of the waveform cycle (roll position) would be compared by the selector. Because many natural phenomena are characteristically slowly-varying compared to the spin rate, even when the variation is caused by the lateral motion of the satellite itself, the shape and amplitude of the waveform cycles resulting from their measurement are not expected to change rapidly. It will be noted that six of the 12 minor frame analog sensors of the S-6 satellite data, viz., Sensors 4, 5, 6, 7, 11 and 12, normally exhibit a periodicity caused by satellite spin alone.

Should it be impossible to slave the frame rate of the multiplexer to the spin rate of the vehicle, it may be possible to achieve high compression ratios by treating each portion of the cyclic pattern as a submultiplexed channel. The asynchronous problem can be overcome by selecting subchannels in accordance with aspect angle of the vehicle relative to the frame position of the multiplexer. Either solution would not increase the number of multiplexer channels, but the number of reference channels in the data compressor would increase.

In many instances even the compression ratios obtained from digital sensors can be significantly improved. In the case of Sensor 8 of the S-6 data (aspect), for example, the technique of synchronizing the multiplexer to the vehicle rotation would result in a high compression efficiency, if appropriate decommutation and sample selection were employed.

6.5.5 Estimates of Future Compression Ratios

If the techniques of signal reduction, wild point rejection, precompression filtering and measurement synchronization were employed it is estimated that bandwidth compression ratios exceeding ten to one can be achieved for the S-6 class of telemetry data. Additional experiments utilizing these techniques are necessary to confirm this prediction. The application of advanced signal reduction processes will involve close coordination with the responsible experimenters and other GSFC personnel.

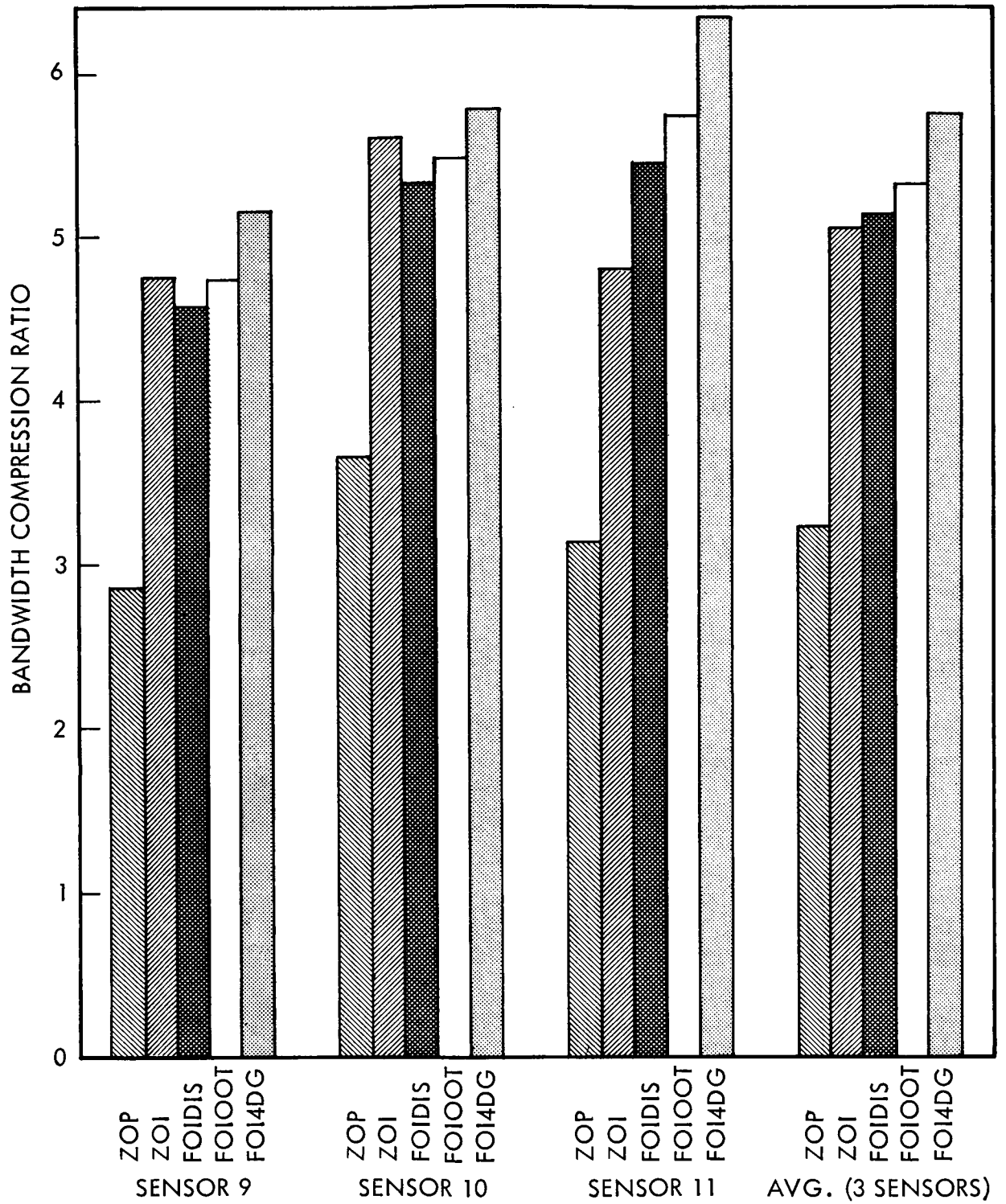


Figure 6-1 Comparative Bandwidth Compression Ratios, Averaged Between Tolerance Values of 2 and 4 Data Units

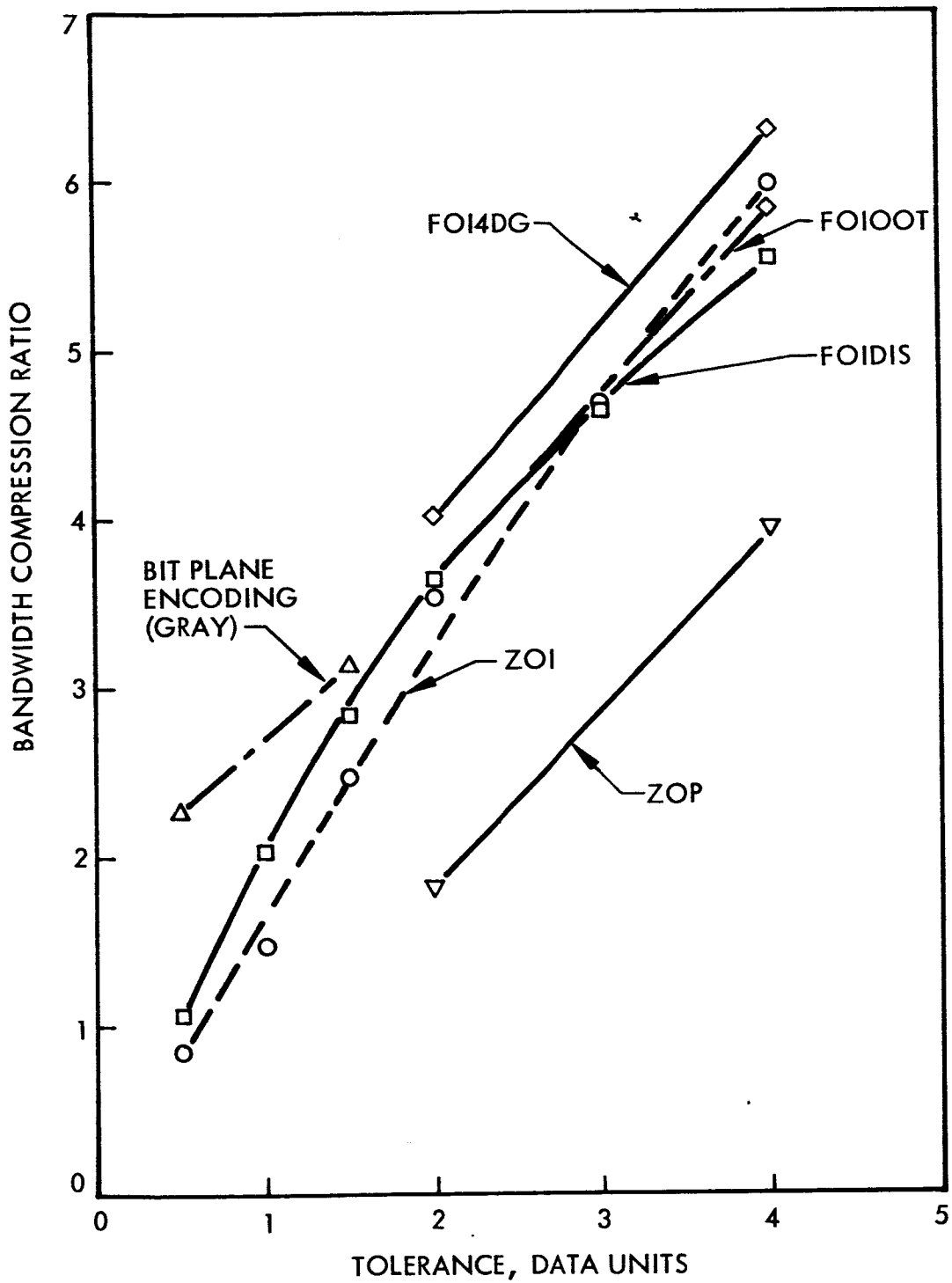


Fig. 6-2 Bandwidth Compression Efficiencies of Bit Plane Encoding and Redundancy Reduction Selectors, Sensor 9

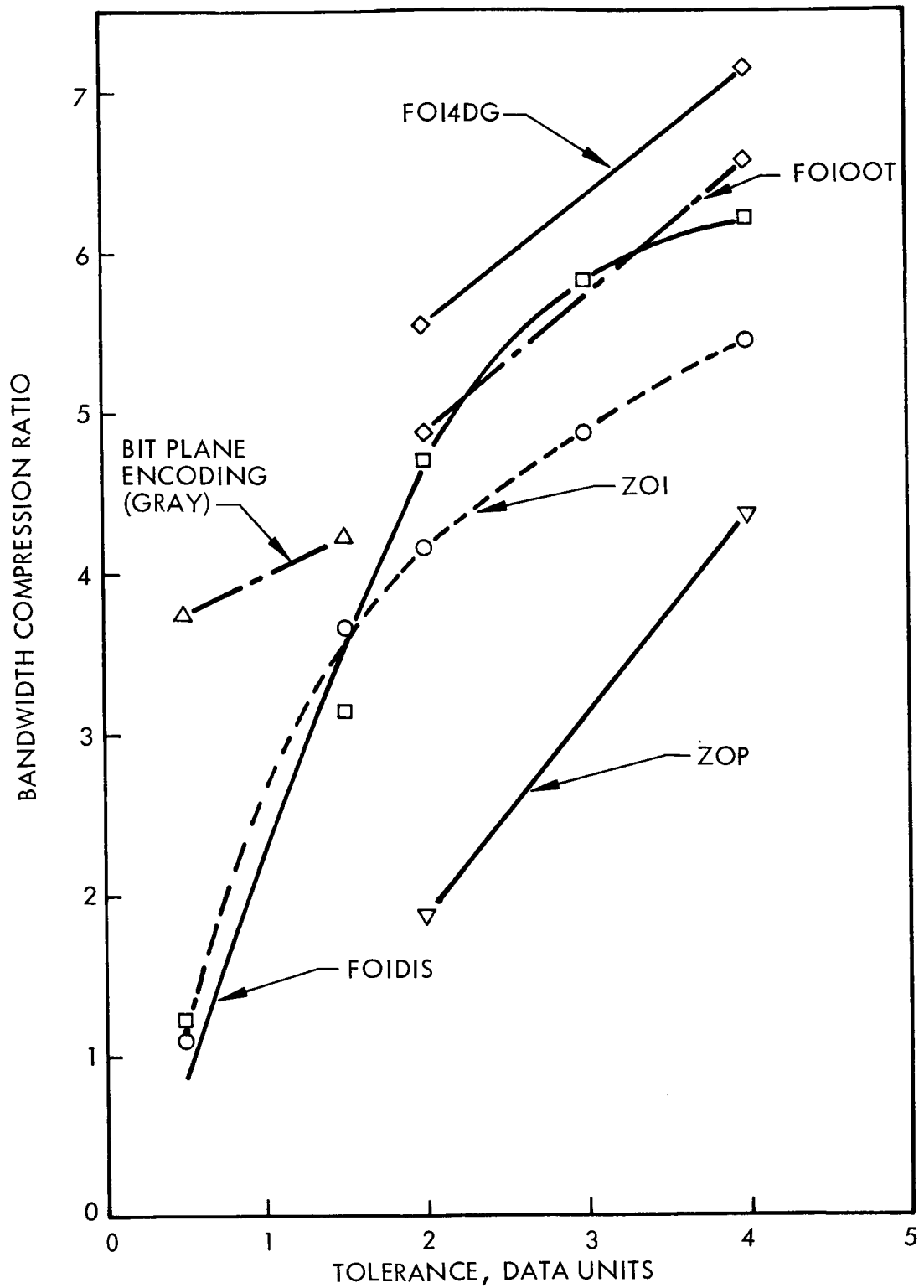


Fig. 6-3 Bandwidth Compression Efficiencies of Bit Plane Encoding and Redundancy Reduction Selectors, Sensor 11

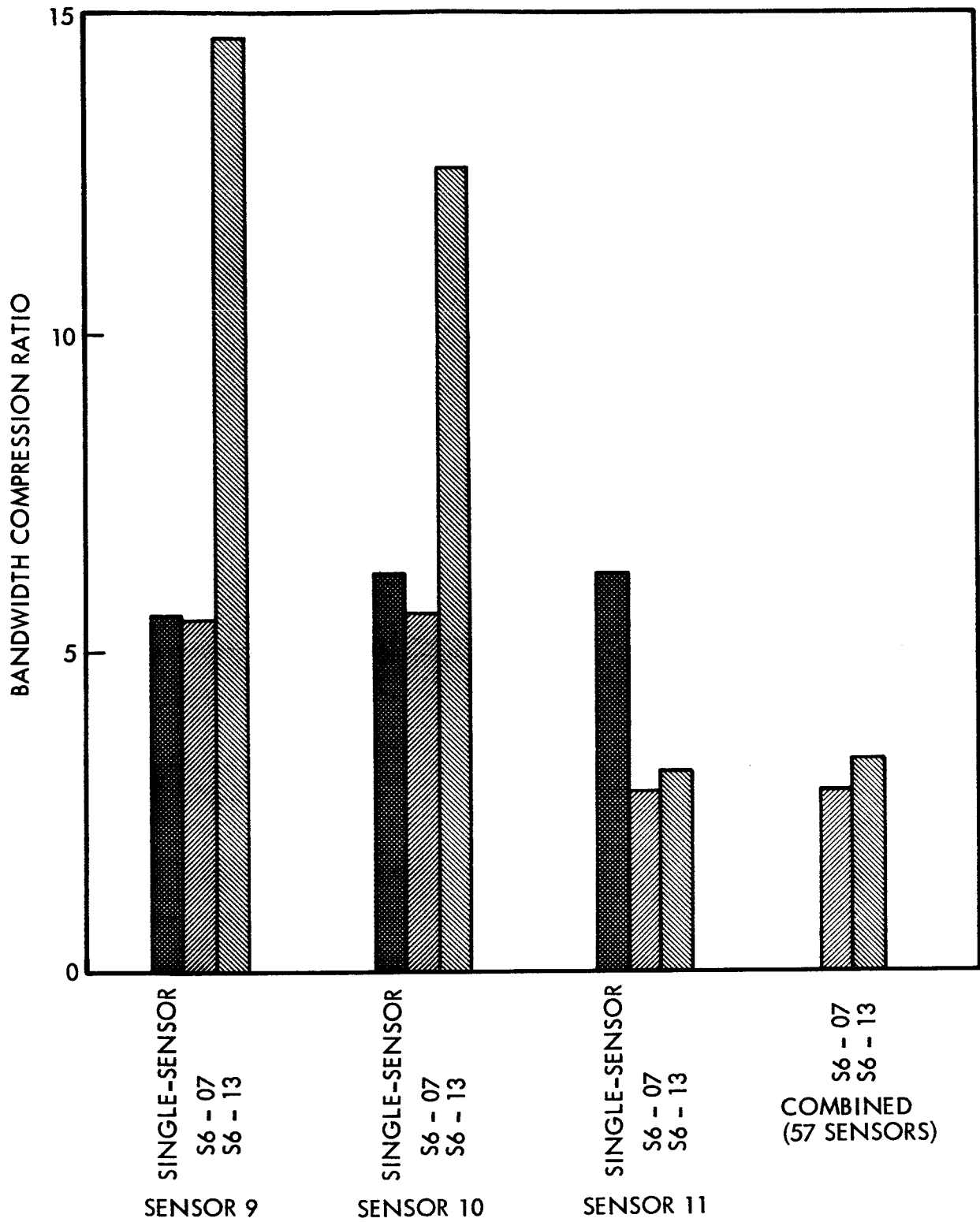


Fig. 6-4 Comparison of Bandwidth Compression Ratios, FOIDIS, Tolerance = 4 Data Units

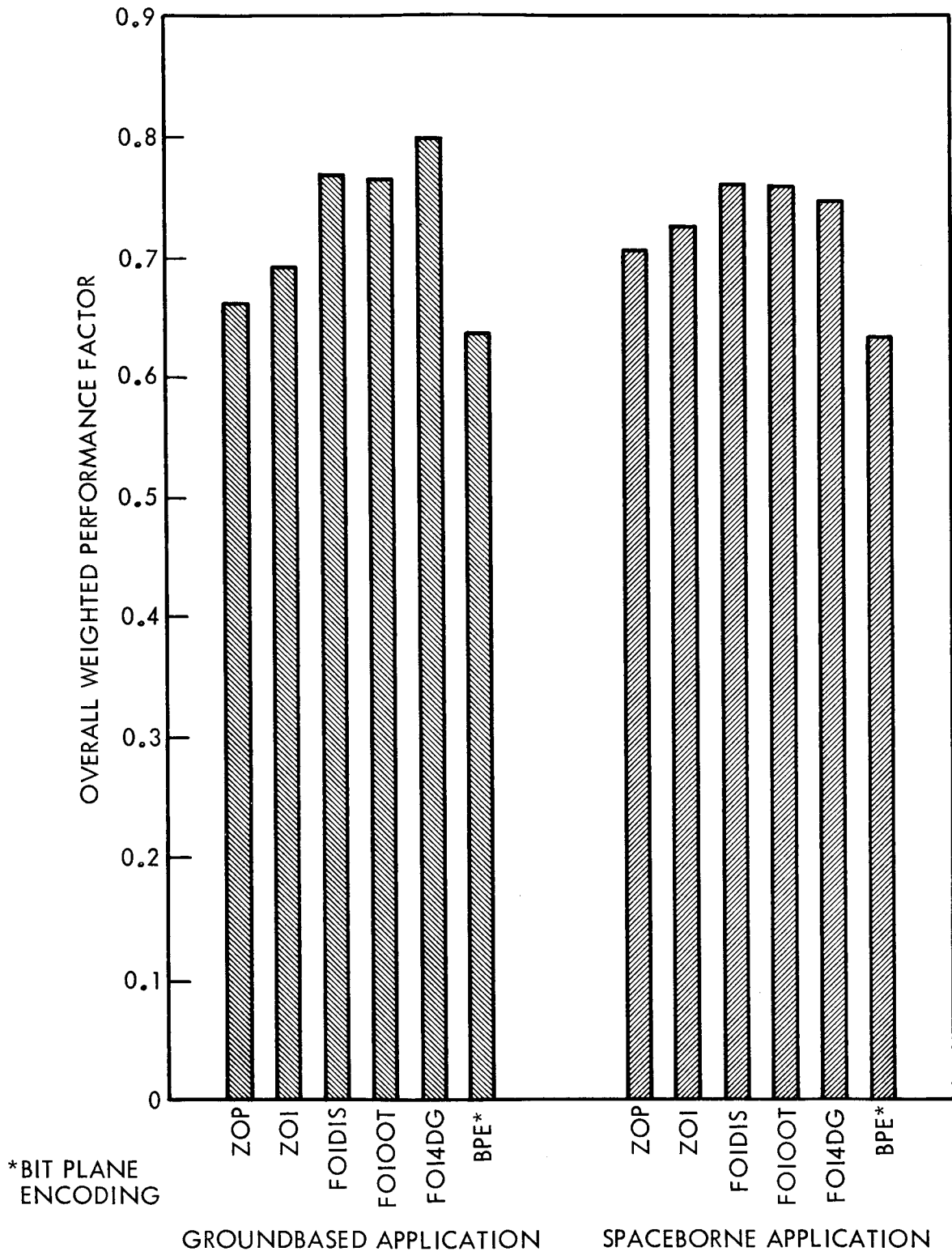


Fig. 6-5 Compression Model Performance Factors

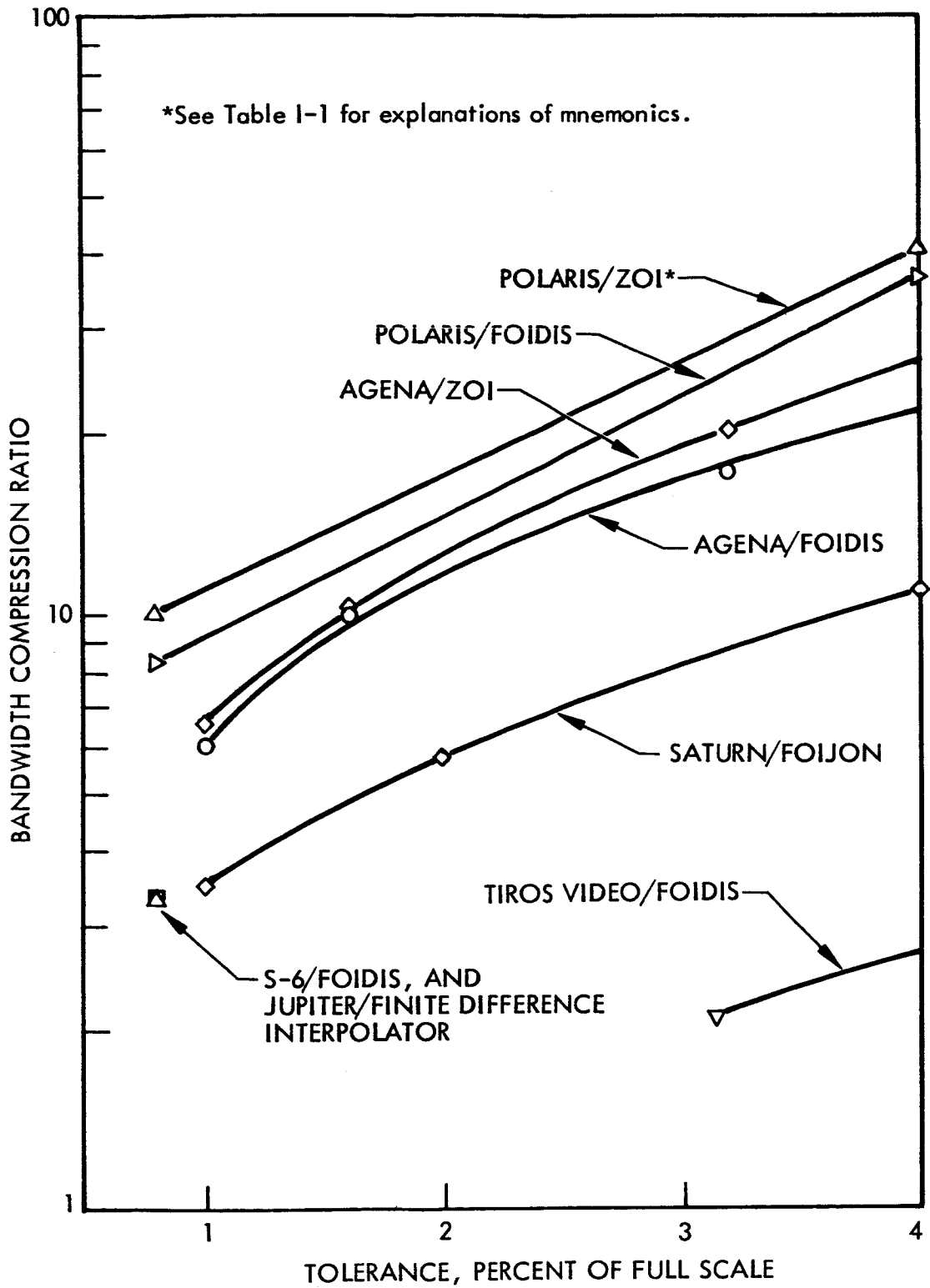


Figure 6-6 Summary of Bandwidth Compression Ratios for Other Telemetry Data

Section 7

CONCLUSIONS AND RECOMMENDATIONS

Section 7

CONCLUSIONS AND RECOMMENDATIONS

This section uses the results of the study to propose data compression models for use with telemetry data similar to that received from the S-6, Explorer XVII, satellite. It also discusses the conceptual designs of generalized future spaceborne and ground data compression systems, conjectures on the future state of the art of data compression, and presents recommendations for continued data compression study and analysis with special emphasis on problems associated with NASA satellite telemetry systems.

7.1 PROPOSED DATA COMPRESSION MODELS

Because of basic differences which exist between requirements for a spaceborne and a groundbased data compression system, a separate compression model will be proposed for each application. Note that these proposals are based on the results of this study, and are subject to possible future alterations as new experimental and theoretical data are compiled.

7.1.1 Spaceborne Application

The proposed spaceborne data compression model is shown in Figure 7-1. It is made up of the following major components:

7.1.1.1 Selector. Because Figure 6-5 shows a slight edge in performance of the FOIDIS over the other selectors, the FOIDIS is tentatively proposed for data similar to that of the S-6 in the spaceborne application.

7.1.1.2 Queuing Control System. The queuing control system proposed for use in the spaceborne compression model is a queue length monitoring system. The system should be capable of controlling sensors in groups and/or individually, so that a sensor priority system can be utilized by varying the "stiffness" of control among sensors.

The proposed buffer capacity lies between 100 and 200 sample amplitude words plus the associated bits required for channel identification. As pointed out in Paragraph 6.3.1, the sole use for the queuing control system would be to prevent buffer overflow in case a misjudgment is made in the projected overall compression ratio, resulting in a setting of buffer sample readout rate so low that the average buffer readin rate would exceed the output rate if there were no control.

Note that no precompression filtering (either adaptive or nonadaptive) is proposed at this time, because insufficient experimental data were obtained from this study to allow any conclusions to be drawn in this area.

7.1.1.3 Time and Channel Coding System. The proposed time and channel coding system provides a minor frame channel identification word along with each transmitted sample. In order to identify subcommutated sensors and to maintain time relationships this system must force a readout of a redundant sample word for each minor frame in which all samples are redundant. In this study it was estimated that by dividing the minor frame into three smaller frames of fifteen channels each, a saving in bandwidth compression ratio could be achieved with the S-6 data.

7.1.1.4 Data Reconstruction. Reconstruction of data samples compressed with the disjointed first-order interpolator (FOIDIS) can be accomplished first by dividing the difference in the transmitted data amplitude values at the ends of a given line segment by the number of sample intervals the segment contains, and then by successively incrementing (or decrementing) the initial value of the segment by the amount of the quotient, to obtain the intermediate amplitude values.

7.1.2 Groundbased Application

The proposed groundbased data compression model is shown in Figure 7-2. It consists of the following major components:

7.1.2.1 Selector. For the groundbased application, Figure 6-5 indicates that the FOI4DG selector holds a small edge in performance over the other selectors; hence, it is tentatively proposed for data similar to that of the S-6.

7.1.2.2 Queuing Control System. The queuing control system proposed for the groundbased application is the same as the one chosen for the spaceborne compressor; namely, a queue length monitoring system with the capability of controlling sensors in groups and/or individually. Because space, weight and power restrictions are usually not severe in the groundbased application the capacity of the buffer could be made greater than 200 words. However, with the proposed compressor model and the postulated telemetry data, no technical reason can be seen for making it larger than 200 words. As in the spaceborne case, the queuing control system would be included to prevent buffer overflow in case the buffer sample readout rate is set so low that the average buffer readin rate would exceed the output rate if there were no control.

In case data intervals containing frequent wild points are allowed to enter the data compressor, causing the buffer to overflow during these intervals, the data lost are considered to be of little value to data analyst. At the ends of these intervals the buffer will cease to be in an overflow condition, and the "good" data will not be lost.

7.1.2.3 Time and Channel Coding System. The proposed method of time and channel coding for this application is identical to that proposed for the spaceborne system, and discussed in Paragraph 7.1.1.3.

7.1.2.4 Data Reconstruction. Reconstruction of data samples compressed with the four-degree-of-freedom first-order interpolator (FOI4DG) is accomplished in precisely the same manner as in the case of the disjointed first-order interpolator. This method is described in Paragraph 7.1.1.4.

7.2 GROUND DATA COMPRESSION SYSTEM CONCEPT

Figure 7-3 shows a conceptual design of a data compression system for transmitting compressed data over conventional voice channels in real time. Note that the system

incorporates signal reduction and encoding as well as redundancy reduction. In order to increase the bandwidth compression ratios found for the S-6 data during this study to an effective value (i. e., above 10) it is necessary to include these additional techniques (see Paragraph 6. 5). The data compressor is shown as a special purpose, rather than a general purpose computer, because it must perform a limited number of repetitious functions rapidly.

A general purpose computer is included in the system to perform some of the more complicated signal reduction operations. The exact delegation of task assignments between the special purpose compressor and the general purpose computer requires additional study. The task assignments shown in Figure 7-3 are expected to be typical.

Channel identification of each sensor is assumed to be performed by the PCM decommutation station. In applications where a decom station does not exist, the decommutation function could be performed by the data compressor with little increase in equipment complexity. Greater buffer queuing control is expected for ground applications due to the greater bandwidth limitations of ground communication links ($\bar{\rho}$ is more apt to be greater than one).

7.3 FUTURE STATE OF THE ART

The possibility of including signal reduction, adaptive sampling, redundancy reduction and encoding techniques together in one system gives rise to some interesting adaptive telemetry system concepts. One such concept is shown in Figure 7-4.

Note that the data compression system is shown in Figure 7-4 as a special purpose computer. Although the organization of a data compressor is quite similar to the organization of a general purpose (GP) computer, as mentioned in Paragraph 7.2, a distinction is made in operational philosophy between the data compressor and GP computer, in that a data compressor is organized to perform a limited number of repetitious functions rapidly, whereas the GP computer is organized to perform many different types of operations at the sacrifice of speed or complexity. A data compressor thus appears to more closely fall into the category of a special purpose computer.

Because of the inherent flexibility of an adaptive telemetry system it would be relatively simple to include such features as:

- Command link reprogramming of sensor selection and sampling rates (multiplexer format)
- Command link reprogramming of signal reduction techniques
- Command link reprogramming of redundancy reduction selectors
- Command link reprogramming of transmission rate
- Combination of above to change mission objective
- Burst readout of compressed data for multi-satellite-to-satellite relay

It is contemplated that, in some cases, it will be advantageous to utilize special "black box" signal reduction devices. However, it is believed that a large percentage of the signal reduction operations can be performed by the data compressor. Advantage can be taken of the memory to achieve indirect addressing of the analog and digital gates, thus providing the means for modifying the multiplexing sequence. A hybrid analog-digital arithmetic unit is included so that the redundancy reduction and analog-to-digital conversion operations can be combined. It may be desirable to perform both analog and digital signal reduction operations. A single random access memory can be used for all operations including queuing and tape buffering.

Speaking in general on the future state of the art of data compression, it is anticipated that its future evolution will be primarily centered around signal reduction techniques. Due to the sophistication of present redundancy reduction techniques, it is believed that their further refinement will be slow. It is possible that new hardware developments will be able to overcome some of the mechanization problems of adaptive sampling discussed earlier. The concept of adaptive sampling may some day be extended to permit automatic assignment of all sampling rates based on measured channel activity. (No sampling rate assignments would be made by man.) Bit plane encoding was found during the study to be a very promising data compression technique. It is possible that in the future bit plane encoding will be used on data already compressed

with some method of redundancy reduction, resulting in higher overall compression efficiencies.

7.4 RECOMMENDATIONS FOR FUTURE WORK

The results of this study indicate a number of topics which warrant new or additional investigation.

7.4.1 Compression Model Analysis

It is recommended that additional data from Goddard satellites, such as data from the S-49 OGO satellite, be processed and analyzed along the guidelines established in the initial study. This processing should include the application of both adaptive and non-adaptive compression techniques on a single channel as well as on a multichannel basis. In addition, the effectiveness of both precompression and postcompression filtering techniques should be determined, especially when employing some form of pre-filtering wild point rejection.

7.4.2 New Compression Model Evaluation

Several compression models were not investigated in sufficient detail during the initial study, either because of the limited availability of funds, or because of the model having been developed late in the course of the study. It is recommended that the more promising of these models be evaluated by means of computer simulation using available Goddard satellite data. Several of the compression models which deserve study are:

- Exponential predictor
- Exponential interpolator
- Selection based on an adaptive reference pattern
- Selection based on data spectral properties
- Selection based on rms error
- Bit plane encoding (both raw and compressed data)
- Signal reduction techniques

- Synchronous demultiplexing, to cope with periodic waveform variations
- Precompression and postcompression filtering and/or wild point rejection in conjunction with above techniques

7.4.3 Channel Noise Simulation

Because of the fact that one given compressed data word contains information about many original data words, compressed data is more "fragile" than conventional PCM data. As a result of this "fragility", compressed data is more subject to catastrophic error due to channel noise than is conventional PCM data. It is recommended that a noisy binary transmission channel with an associated data reconstruction device be simulated, so that the effect of channel noise can be determined on the results obtained by using various compression models.

7.4.4 Mathematical Theory of Data Compression

In general, the art or practice of data compression has outstripped the development of the analogous theory of data compression. It is recommended that an effort be made to extend this theory of data compression, both to lend credence to the empirical results already obtained and to provide insight into data compression so as to facilitate new ideas and further development. This investigation might include the results of modern Wiener-Kalman prediction theory, and an attempt to develop an adequate mathematical model for nonstationary telemetry data.

7.4.5 Theoretical Buffer Queuing Control Analysis

Up to this time, buffer queuing control investigation as applied to data compression systems has been largely of an empirical nature, predicated on specific specimens of data and the judgment of the experimenter. In order to generalize the art of buffer queuing control into a science, and in order to seek optimum solutions to the problem of preventing buffer overflow it is recommended that a theoretical analysis of buffer queuing control be made.

7.4.6 Theoretical Transmission Error Analysis

In the case of conventional PCM transmission, the theory of errors due to channel noise has been well developed. It is recommended that this same theory be extended to the case of compressed data transmission. This theory would facilitate the selection of optimum compressed data transmission formats and encoding as well as other system design parameters.

7.4.7 Ground Data Compression System Analysis

It is recommended that an investigation be made of the modifications necessary to existing NASA ground stations, data processing facilities and ground-to-ground transmission links due to the addition of data compression. A large part of this investigation will center on the computer processing of compressed data, since it is desirable to be able to process compressed telemetry data with computers in either remote or central ground stations. It is necessary, therefore, that the investigation include a study of the feasibility of using NASA computer facilities to process compressed data. This feasibility study should involve a determination of comparative computer efficiencies and the impact of processing compressed data on existing data processing facilities, in both real time and non-real time applications.

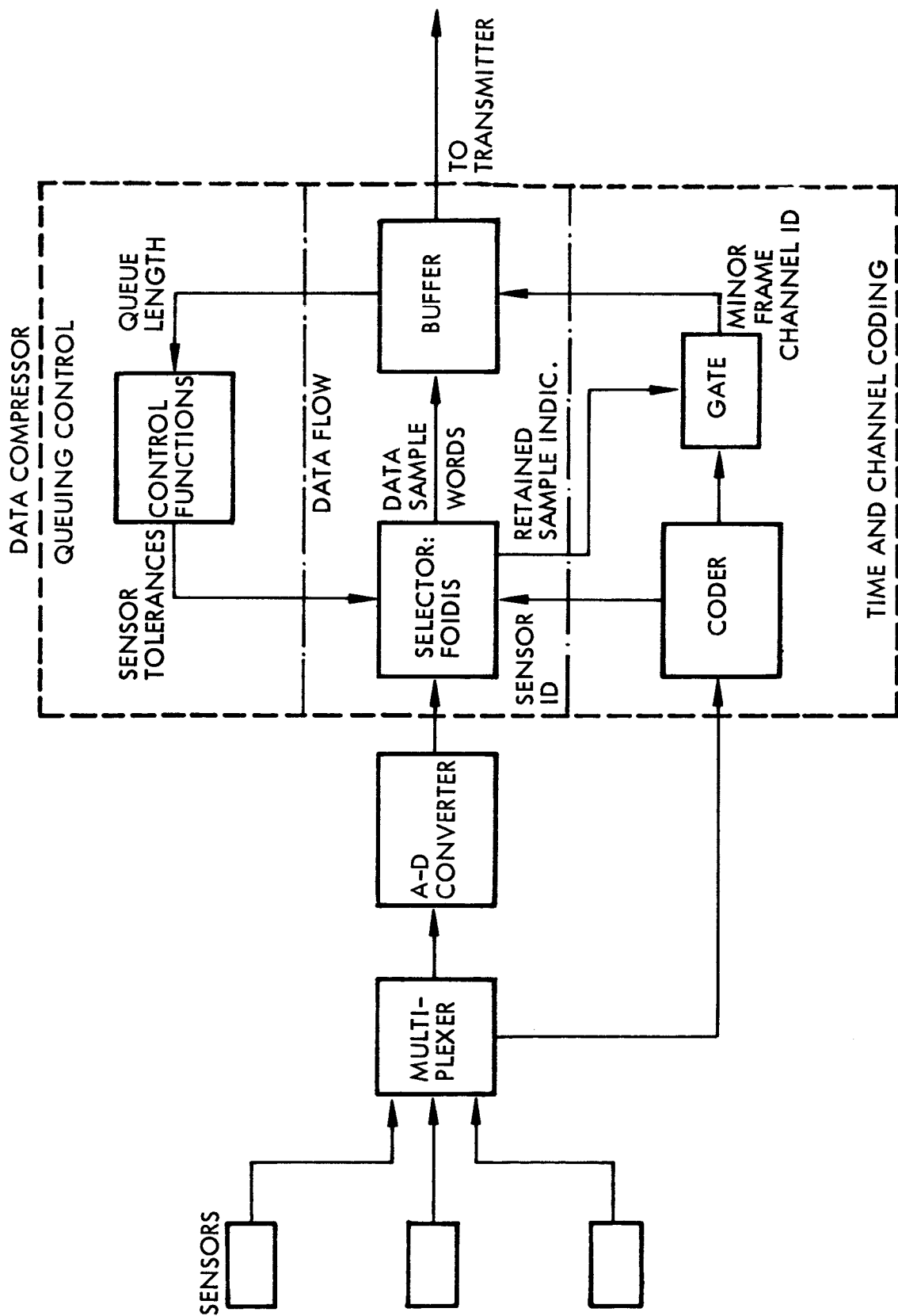


Figure 7-1 Proposed Spaceborne Data Compressor for S-6 Data

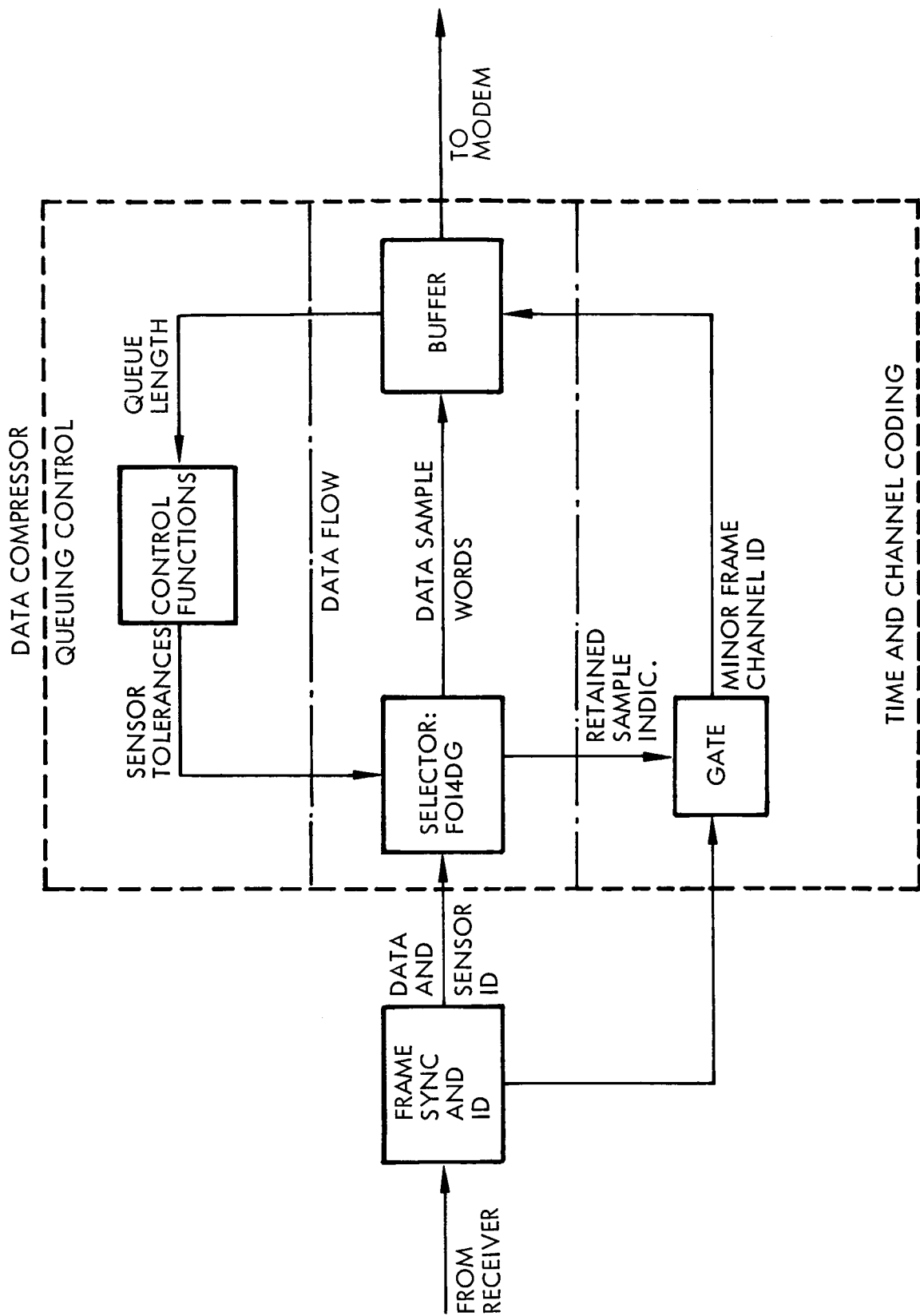


Figure 7-2 Proposed Groundbased Data Compressor for S-6 Data

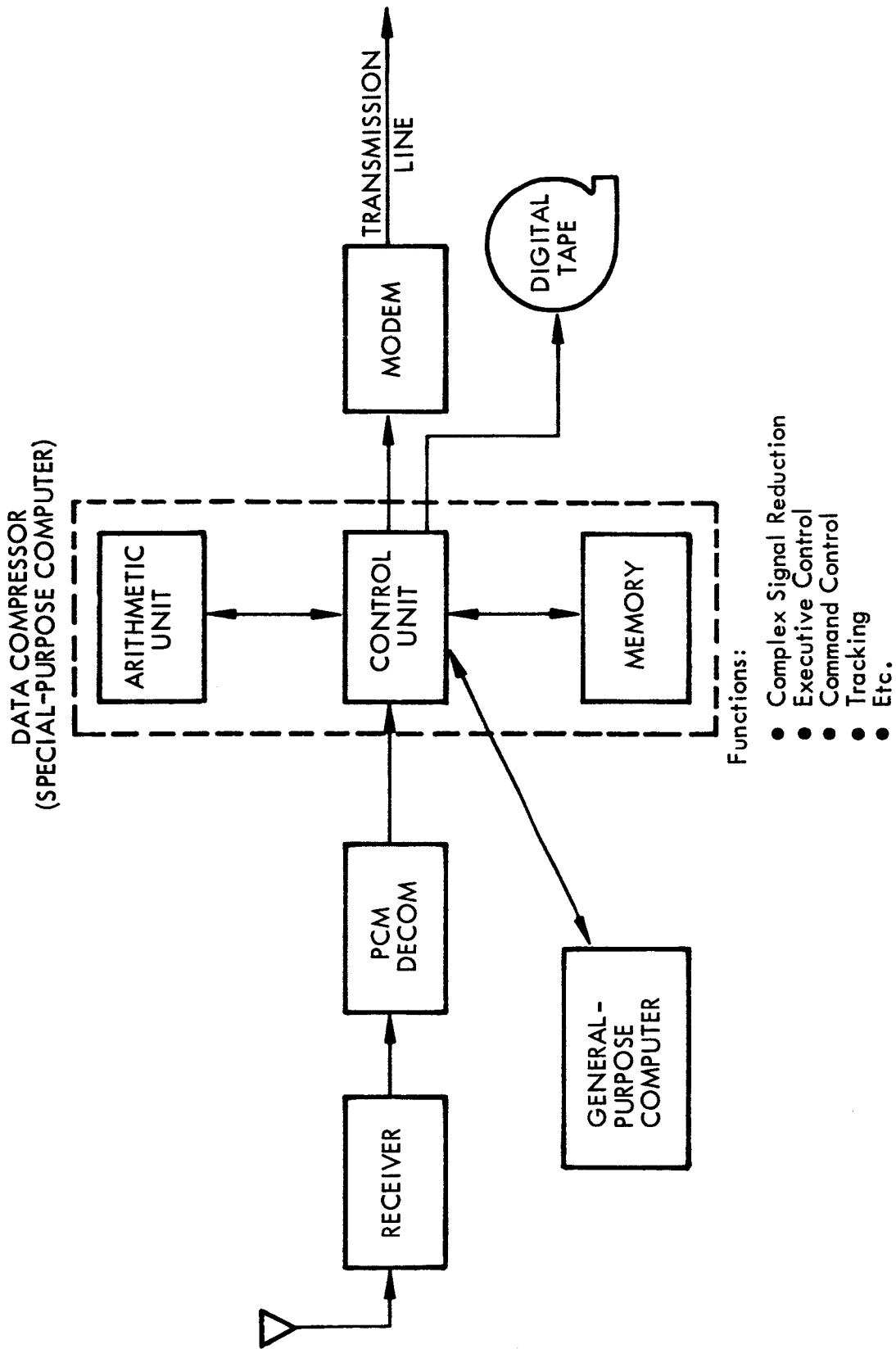


Fig. 7-3 Block Diagram, Generalized Ground Data Compression System

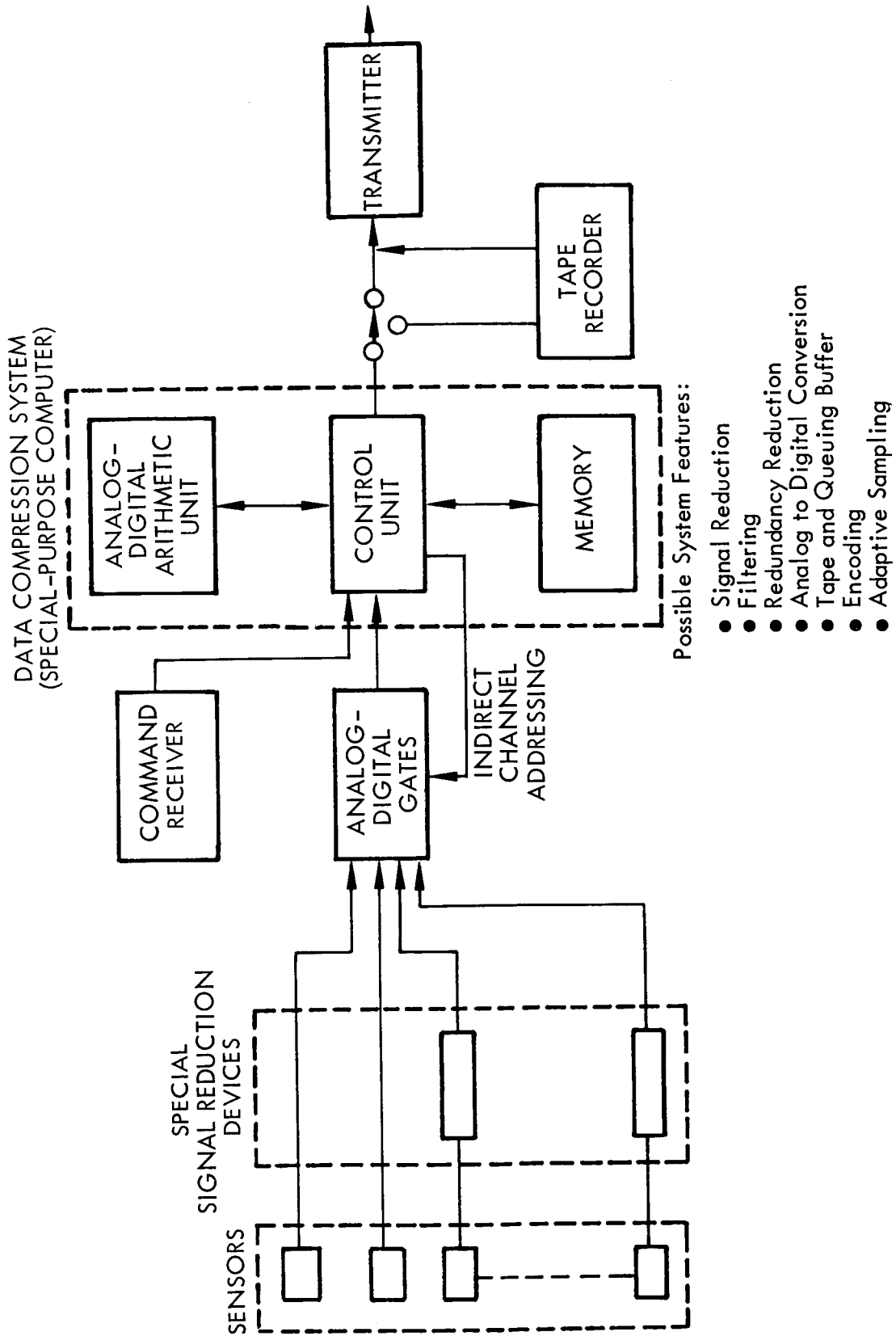


Fig. 7-4 Block Diagram, Future Adaptive Telemetry System

Section 8

NEW TECHNOLOGY

Section 8 NEW TECHNOLOGY

This section describes three new redundancy reduction concepts and techniques developed late in the study: adaptive reference pattern prediction and interpolation, sample selection based on short-term frequency components, and sample selection based on peak rms error. An exponential interpolator selector was also developed late in the study, but since the exponential pattern is included in the adaptive reference pattern selector, it is not discussed separately in this section.

8.1 ADAPTIVE REFERENCE PATTERN SELECTOR

A significant fraction of Goddard S-6 satellite data cannot be easily approximated by a series of either zero or first order polynomials. For this reason, predictors and interpolators using either zero or first order polynomial reference patterns, cannot effectively compress this fraction of the data. In an attempt to overcome this difficulty, a selector has been conceived that is capable of operating in either of two modes. In the initial mode, the selector is a zero order polynomial predictor (or interpolator). When an out-of-tolerance condition occurs, instead of beginning a new line segment in normal fashion, the selector changes to the second mode, chooses a stored reference pattern in a predetermined manner, and operates as a predictor (or interpolator) using this new pattern. These stored reference patterns might be high order polynomial or transcendental functions. When an out-of-tolerance condition occurs in this second mode, a data word is transmitted containing information about both modes. The selector then resets to the zero order mode and processing of a new line segment is initiated.

A tentative flow chart has been generated for this selector and preliminary FORTRAN coding has begun. It appears that this selector will be relatively difficult to implement with either a general purpose computer or special purpose hardware.

8.2 SHORT-TERM FREQUENCY COMPONENT SELECTOR

With this selector, a Fourier analysis is performed on a fixed number of data samples received from each sensor. This short-term frequency analysis is then used to decide whether or not the present data sample from that sensor is to be retained. The analyses are updated as new data samples are received. If a significant fraction of total short term data energy is present at relatively high frequencies the present sample is likely to be retained by the decision rule and, conversely, if a significant fraction of total short term data energy is present at relatively low frequencies, the present sample is likely to be deleted. The actual decision rule is somewhat arbitrary and should be chosen to correspond with the requirements of the user. This sample deletion technique tends to maintain the short term sampling rate of a given sensor in proportion with the short term information bandwidth of that sensor. The selector provides no peak error guarantee. Preliminary FORTRAN coding has begun on this selector.

8.3 PEAK RMS ERROR SELECTOR

In this version, data samples from a given sensor are deleted until some function of the rms error between original and reconstructed data exceeds the sensor threshold prescribed. When this occurs, the data sample is transmitted to reduce the rms error, or a function thereof, to an acceptable level below threshold. This selector therefore tends to maintain overall rms error between original and reconstructed data in the vicinity of some value chosen by the user. It provides no peak error guarantee.

Appendix I

CRITIQUE OF KNOWN MODELS

Appendix I CRITIQUE OF KNOWN MODELS

This Appendix describes the data compression models found during the literature search, obtained from the Lockheed Missiles & Space Company Independent Development program on data compression, and conceived during the study. Each discussion has two parts, (1) a description of the model and (2) a critique in terms of its compression efficiency, data fidelity, etc. A compression model listing is given in Table I-1.

I.1 SIGNAL REDUCTION

Signal reduction techniques are generally used in conjunction with other categories of data compression. Signal reduction techniques are usually selected on an individual channel basis since signal conversion requirements among signal sources usually vary. Due to the unusually large number of signal reduction techniques used for missile and spacecraft onboard processing, a summary of these techniques is not included. The large number of references found during the literature search represents only a small portion of the number of techniques which have been developed or used. References 2, 4, 7, 10, 14, 20, 24, 32, 34, 44, 49, 56, 57, 59, 62, 72, 86, 87, 91, 100, 105, 108, 127, 134, 155, 159, 167, 168, 192, 197, 209, 222, 230, 231, 232, 253 of Appendix V give detailed information.

I.2 ADAPTIVE SAMPLING

I.2.1 Model No. 1¹: Associative Data Compressor (Reference 50)

Description. The associative data compressor, which was designed for specific high-speed applications, identifies and reports the magnitude of data channels that are above a fixed or variable voltage threshold. This complex system, able to scan and compress

¹The model numbers are those listed in Table I-1.

Table I-1

COMPRESSION MODEL LISTING

Model No.	Discussed on Page:	Description	Lockheed FORTRAN Mnemonic	University of Alabama ¹ Mnemonic	Other Names
		ADAPTIVE SAMPLING			
1	I-1	Associative Data Compressor			
2	I-3	Adaptive (Format) Telemetry			
3	I-3	Transient Event Recorder			
4	I-4	Self-Adaptive Telemetry			
		REDUNDANCY REDUCTION			
		Predictors			
		Zero-Order Polynomial			
5	I-5	Simple Difference			
		Cumulative Difference			
6	I-5	Fixed Limit			
7	I-5	Floating Aperture	ZOP	ZFN	Simple Difference (Rad. Inc.)
8	I-7	Offset Limit			
		First-Order Polynomial			
9	I-8	Pred. based on two most recent out-of-tolerance samples			
10	I-9	Pred. based on last predicted sample and out-of-tolerance sample	FOP		
11	I-9	Same as Model 10, but transmit last predicted sample		FFA	
12	I-10	Pred. based on last redundant sample and out-of-tolerance sample		FFN	
13	I-10	Same as Model 12, but transmit last redundant sample		FFP	
14	I-11	Pred. based on adaptive slope			
15	I-13	Second-Order Polynomial	SOP		
16	I-14	Wiener			
17	I-14	Adaptive Nonlinear			
18	I-15	Exponential			
		Interpolators			
19	I-15	Finite Differences			
20	I-17	Least-Squares Polynomial			
		Zero-Order Polynomial			
21	I-17	Computed Sample Transmitted	ZOI	ZVA	
22	I-19	Last Redundant Sample Transmitted		ZVP	
		First-Order Polynomial			
		Computed Sample Transmitted			
23	I-19	Four Degrees of Freedom	FO4DG		
24	I-21	Joined Line Segment	FOLJON	FVA	
25	I-21	Disjoined Line Segment	FOIDS		
		Offset Out-of-Tolerance			
26	I-22	Last Slope	FOIOLS		
27	I-22	Out-of-Tolerance Direction	FOIOOT		
28	I-23	Last Data Sample Transmitted		FVP	Fan (Rad. Inc.) Linear Approx. (MIT)
29	I-23	Exponential	EI		
30	I-23	Adaptive Reference Pattern			
		ENCODING			
		Nonadaptive			
31	I-24	Delta Modulation			
32	I-25	Difference Modulation			
33	I-25	Probabilistic			
		Adaptive			
34	I-26	Adaptive Probabilistic			
35	I-26	Bit Plane			

¹Ref. 219

multi-channel data at a much higher rate than conventional digital systems, simultaneously tests each channel for significant samples once each frame period, and then sequentially scans only those sources that are above threshold. An associative logic is used to rapidly locate the addresses of the above threshold sensors, avoiding the need to sequentially scan every sensor.

Critique. This system is limited by the above-threshold reporting characteristic. If high speed were not a requirement, it is possible that other techniques described in this Appendix would be less complicated.

I.2.2 Model No. 2: Adaptive (Format) Telemetry (References 80, 226)

Description. This compression model was designed primarily for deep space probe applications. It uses a programmable vehicle-borne multiplexer to modify the sampling format and sampling frequency of the telemetry system upon request from the earth-to-spacecraft command link. This is a cooperative system requiring decision and command control action from an earth-based station.

Critique. This model was designed primarily for applications where command link communications can be continuously maintained. Usually only one acquisition with earth-orbiting satellites can be made per orbit with the limited number of ground stations currently available. As the number of satellites increase, the allowable acquisition time is expected to be reduced further because several satellites may be within range simultaneously and will therefore have to be serviced on a time shared basis. Onboard data storage and data management is therefore becoming increasingly important. This cooperative ground-link system is not the total answer because many scientific measurements cannot tolerate the aliasing errors resulting from the time delay.

I.2.3 Model No. 3: Transient Event Recorder (Reference 138)

Description. This model, which was designed for a specific application, is a unique ultra-high speed sampling technique for recording the response characteristics of a

transient. Single bursts of sequential samples are triggered by the start of transient events. Also, the sampling gates have memory to permit a delayed, reduced-rate readout of the data. This model could be regarded as a signal conditioner for a transient class of data.

Critique. Because this model was designed for a specific application, it does not represent a generalized solution to data compression.

I. 2. 4 Model No. 4: Self-Adaptive Telemetry (References 91, 163, 244)

Description. This model requires that each data source has its own analyzer for sampling frequency regulation. In the model described in Reference 163, a differentiator is used for each input channel to establish the respective sampling frequencies. The conflict of samples occurring simultaneously between channels is avoided by establishing a priority list prior to the flight. These priorities can be changed in a prearranged manner if a malfunction is detected in a given subsystem.

Critique. The priority solution proposed in Reference 163 may not be acceptable for some applications. The conflict of simultaneous sample arrival can be minimized if the delay elements have a variable delay characteristic for buffering. Providing variable analog delay units presents an interesting technical problem. As an alternate solution, the sample rate to the analog to digital converter could be made variable to conform with the sample demands of the adaptive multiplexer. The conflict of simultaneous data samples could then be resolved by including a queuing buffer following the analog to digital converter. This configuration rapidly approaches the organization of a redundancy reduction system with the one exception that many different analyzers are required. For this reason, self-adaptive telemetry as a general process is less attractive than other methods of compression. The following paragraphs show that channel selection based upon priority can be employed in conjunction with redundancy reduction.

I.3 REDUNDANCY REDUCTION

I.3.1 Predictors

I.3.1.1 Zero Order Polynomial. This model classifies a data sample as being redundant if the sample is within a specified tolerance from a stored reference sample. Thus, a prediction is made concerning the magnitude of one or more future samples based upon some past history. Since it is possible to mechanize this model many different ways, the following subsections describe all zero order predictor models found during the literature search.

I.3.1.1.1 Model No. 5: Simple Difference. (References 91, 104, 161, 184, 186, 187, 188, 241, 242, 243)

Description. This model performs a test to determine if the difference between consecutive samples of a given channel are within a predetermined threshold, i. e., the reference sample (predictor) is always the last sample. The threshold value is selected for each channel depending upon accuracy requirements specified by the experimenter. This model was used at LMSC in a hardware application that called for output data only when the derivative (simple difference) of the time function exceeded a predetermined limit.

Critique. This model can produce excessive errors for slowly varying data when the rate of change of the function is less than the selected threshold or tolerance value. Although the model is useful for certain applications, it does not represent an acceptable solution when absolute measurements are desired.

I.3.1.1.2 Cumulative Difference. Model No. 6: Fixed Limit (References 147, 176, 177); and Model No. 7: Floating Aperture, ZOP. (References 67, 91, 102, 120, 136, 139, 141, 147, 175, 176, 177)

Description. The errors associated with the simple difference model are avoided here by using the last transmitted sample (the last out-of-limit sample) as the reference

parameter. The ratio between the tolerance, K , (half-aperture) and the digital resolution of the analog to digital converter, Q , (quantization error) can appreciably effect the efficiency of this model. Reference 91 shows analytically that reducing the quantization error for a given K from $Q=K$ to $Q=K/8$ will result in a 40-percent increase in bandwidth compression ratio, even though more bits per transmitted word are required. This has been verified experimentally by JPL (Reference 109) where improvements in compression ratio in excess of 100-percent were achieved with Mariner II telemetry data. The term "fixed limit" has often been used for zero order predictors having a K/Q ratio of 1. The term "floating aperture" has been adopted for the condition that $K > Q$, and its functional operation is presented in Figure I-1. If y_0 was the last transmitted data sample, a prediction is made that subsequent data samples, $y_1, y_2 \dots y_{23}$ will be within K units of y_0 . As shown in Figure I-1, these samples are within the tolerance corridor denoted by y_t+K and y_t-K , and can be discarded as being redundant. Each sample falling on or outside of the corridor must be transmitted as a non-redundant or significant sample and is used as the new reference for subsequent predictions. The term "zero-order polynomial prediction" implies that the redundant portion of a time function will be approximated by a horizontal straight line. It should be noted that the zero order approximation does not necessarily apply when interpolating between a significant sample and its previous neighbor sample.

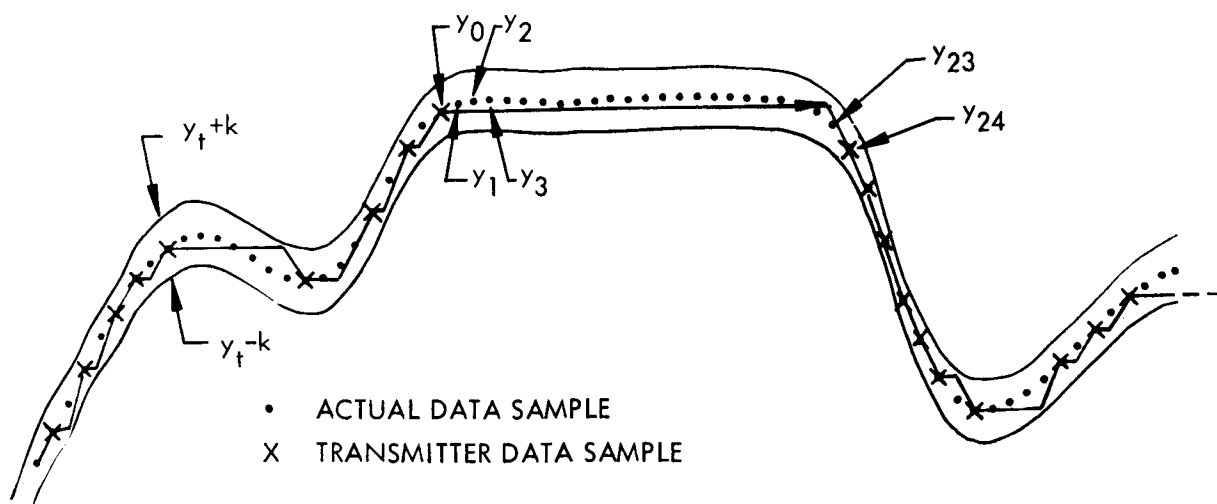


Fig. I-1 Cumulative Difference, Zero Order Predictor, Floating Aperture

Critique. The floating aperture model has proven to be highly effective for quasi-static data, and has attained operational status in several hardware designs. It is one of the simplest redundancy reduction models to mechanize and has achieved surprisingly high compression ratios for Agena (Reference 136) and Polaris (Reference 160) data. The technique has been found to be moderately sensitive to low level noise, however, and its compression efficiency falls off rapidly with increasing noise and data activity. The stair-step appearance of reconstructed data from this model has been objected to by some data analysts (Reference 160) where small tolerances have not been used. The compression efficiency of the fixed limit model has shown to be consistently lower than that of the floating-aperture model.

I. 3. 1. 1. 3 Model No. 8: Offset Limit. (References 139, 176, 177)

Description. This model is similar to the cumulative difference, floating aperture model except the tolerance limits are offset from the reference sample, i. e., the limits are not symmetrical about the reference sample. The direction of offset is based upon the sign of the error occurring during the last out-of-tolerance sample (the new reference sample). This model is equivalent in complexity to the cumulative difference floating aperture model (Model 7).

Critique. When the offset is made in the same direction as the out-of-tolerance sample, a decrease in compression efficiency on real data occurs (References 139 and 177). When the offset is made in the direction opposite from the out-of-tolerance sample some improvement in compression ratio on artificial data is noted for the smaller values of apertures. Whether or not an improvement in compression ratio would be achieved on real data using a reversed offset has never been determined. Its fidelity characteristics have not been determined.

I. 3. 1. 2 First Order Polynomial. The first order polynomial predictor takes advantage of the slope or first derivative of the time function to remove the more dynamic first order redundancy components. Like the zero order polynomial predictor, this model has many methods of mechanization. The differences in the various first-order selectors lie chiefly in (1) the data samples on which the prediction is based, (2) the particular samples transmitted, and (3) the method of reconstruction.

In the following paragraphs, the assumption is made that at time t a new data sample has just occurred, and a prediction is to be made on the value of the next sample, which is to occur at time $t+1$. In each first-order model, the predicted sample value, y'_{t+1} , is determined by adding an increment, Δy_t , to a quantity, y''_t , which represents the current sample, according to the expression

$$y'_{t+1} = y''_t + \Delta y_t$$

The quantity y''_t may be either the actual sample value or the value which was predicted for time t . An out-of-tolerance condition occurs whenever the absolute difference between the actual and predicted sample exceeds the tolerance. The variable, τ , will represent the number of sample periods between the two most recent out-of-tolerance samples.

I. 3. 1. 2. 1 Model No. 9: Prediction Based on Two Most Recent Out-of-Tolerance Sample Out-of-Tolerance Sample Transmitted. (Reference 91)

Description. If $y_{t-\tau}$ and y_t are the last two transmitted out-of-tolerance samples, then

$$\Delta y_t = \frac{y_t - y_{t-\tau}}{\tau}$$

therefore

$$y'_{t+1} = y_t + \Delta y_t$$

If y_{t+1} is redundant ($|y'_{t+1} - y_{t+1}| < K$), then the sample y_{t+2} is computed from the following equation:

$$\begin{aligned} y'_{t+2} &= y'_{t+1} + \Delta y_t \\ &= y_t + 2\Delta y_t \end{aligned}$$

The process is continued for subsequent samples. The data are reconstructed exactly as they were compressed: predictions are made at the receiver which are identical to those made at the data compressor, and all nontransmitted data samples are replaced by predicted values.

Critique. This model has been observed to provide better compression ratios than the zero order predictors on some active data specimens. However, the results that have been obtained from analyzing Agena data (relative to data classes) have been inconsistent. These investigations also showed that, on the average, the floating aperture zero order

predictor, Model 7, provided higher compression ratios. An analysis of these results has shown that this model, as well as other first order predictors, was extremely sensitive to low level noise components which were present on most Agena data. Mechanization of this model is considerably more complicated than the zero order predictor due to the requirement for a full divide in computing Δy_t .

I. 3. 1. 2. 2 Model No. 10: Prediction Based on Last Predicted Sample and Present Out-of-Tolerance Sample; Out-of-Tolerance Sample Transmitted, FOP. (References 139, 176, 177)

Description. If $y_{t-\tau}$ and y_t are the last two transmitted out-of-tolerance samples, then for the condition that $\tau > 1$,

$$\Delta y_t = y_t - y'_{t-1}$$

where y'_{t-1} is the predicted value for the preceding sample. Therefore

$$\begin{aligned} y'_{t+1} &= y_t + \Delta y_t \\ &= 2y_t - y'_{t-1} \end{aligned}$$

When $\tau=1$, the prediction is based both on actual samples. Therefore, in this case,

$$y'_{t+1} = 2y_t - y_{t-1}$$

The data are reconstructed exactly as the data were compressed: a straight line is connected between a transmitted sample and the predicted preceding sample. Subsequent redundant samples are generated by continuing the straight line prediction.

Critique. The performance characteristics of this model are similar to those of Model 9. Some differences have been noticed on selected data specimens, but these differences are not consistent. The complexity of the model is equivalent to that of Model 9.

I. 3. 1. 2. 3 Model No. 11: Prediction Based on Last Predicted Sample and Present Out-of-Tolerance Sample; Last Predicted Sample Transmitted. (Reference 219)

Description. The prediction process for this model is identical to that of Model 10; the difference between the two lies in the data samples which are transmitted and in the method of reconstruction. With Model 11 the last predicted sample is transmitted (except when two sequential out-of-tolerance samples occur, in which case the actual sample is transmitted), instead of the present out-of-tolerance sample. Reconstruction is achieved by connecting a straight line between transmitted samples.

Critique. This model is identical in performance to Model 10, since the lines used to connect transmitted samples during reconstruction are precisely the same lines on which the predicted samples lie. Since little difference in complexity can be seen between the two models, they are judged equal.

I. 3. 1. 2. 4 Model No. 12: Prediction Based on Last Redundant Sample and Present Out-of-Tolerance Sample; Out-of-Tolerance Sample Transmitted. (Reference 219)

Description. Let $y_{t-\tau}$ and y_t be the last two transmitted samples, then

$$\Delta y_t = y_t - y_{t-1}$$

It should be noted that y_{t-1} is the actual sample, and not the predicted value.

Therefore

$$\begin{aligned} y'_{t+1} &= y_t + \Delta y_t \\ &= 2y_t - y_{t-1} \end{aligned}$$

The data is reconstructed by connecting a straight line between $y_{t-\tau}$ and y_t .

Critique. Since different rules are used for reconstruction than for the removal of redundancy, the peak errors after reconstruction are no longer bounded by the tolerance value. Nevertheless, the University of Alabama analysis (Reference 219) has shown this model to provide slightly greater compression ratios for a given rms error than Models 10 and 11.

I. 3. 1. 2. 5 Model No. 13: Prediction Based on Last Redundant Sample and Present Out-of-Tolerance Sample; Last Redundant Sample Transmitted. (References 69, 177, 219)

Description. If y_t is an out-of-tolerance sample, then y_{t-1} is transmitted, and

$$\Delta y_t = y_t - y_{t-1}$$

therefore

$$\begin{aligned} y'_{t+1} &= y_t + \Delta y_t \\ &= 2y_t - y_{t-1} \end{aligned}$$

If $y_{t+\tau}$ is the next out-of-tolerance sample, then the data is reconstructed by connecting a straight line between y_{t-1} and $y_{t+\tau-1}$.

Critique. This model was classified by the University of Alabama (Reference 219) as being the most efficient first order predictor. In fact this model was the only first order predictor to produce higher compression ratios than the simpler zero order predictor with floating aperture, Model 7. Reference 177 found, however, that this model performed only slightly better than Model 10, using noise-generated synthetic telemetry data, and not as well as three zero-order predictors, Models 6, 7 and 8. Furthermore, the maximum allowable error is twice that of Model 10, for the same aperture. The overall value of this model is therefore highly questionable.

I. 3. 1. 2. 6 Model No. 14: Prediction Based on Adaptive Slope; Out-of-Tolerance Sample Transmitted. (References 139, 176)

Description. In this model modifications to the slope component are incorporated to minimize the sensitivity to low-level noise perturbations. The process may be described as follows:

If $|\epsilon| < K$,

$$y'_{t+1} = y'_t + \Delta y_\lambda \quad (I-1)$$

where

- ϵ = error or deviation between actual value and predicted value at time t , ie.,
- ϵ = $y_t - y'_t$
- K = one half the value of the floating aperture, which is centered around the predicted sample value

- y'_{t+1} = predicted sample value at time t+1
 y'_t = sample value which was predicted for time t
 Δy_λ = predicted increment in y, which was computed λ sample periods before t
 λ = number of sample periods between t and time of prior transmission
 $\lambda \geq 1$

When $|\epsilon| \geq K$, a new increment, Δy_o , is computed as follows:

$$\Delta y_o = \Delta y_\lambda + \frac{K \operatorname{sgn} \epsilon}{\lambda} + \frac{\epsilon - K \operatorname{sgn} \epsilon}{C} \quad (\text{I-2})$$

and

$$y'_{t+1} = y'_t + \Delta y_o$$

where

- y_t = transmitted sample value at time t
 Δy_o = new increment, computed at time t
 $C = \begin{cases} 2 & \text{if } \lambda > 1 \\ 1 & \text{if } \lambda = 1 \end{cases}$
 $\operatorname{sgn} \epsilon = \begin{cases} 1 & \text{if } \epsilon > 0 \\ -1 & \text{if } \epsilon < 0 \end{cases}$

One sample period later Δy_o becomes Δy_λ .

As shown by Eq. I-1, provided the actual sample value remains within tolerance, the prediction continues along the same slope line, and the process behaves exactly as Model 10. However, when the tolerance is exceeded, this slope is changed for the next prediction in the direction of the deviation in accordance with the last two terms of Eq. I-2. The amount of the change will vary inversely with the number of sample periods that have occurred since the previous transmission, with the effect of this inverse relationship decreasing as the magnitude of the deviation increases. Whenever two successive transmissions occur, C in Eq. I-2 becomes unity, and the next sample is again predicted in the same manner as Model 10.

The data are reconstructed exactly as they were compressed: predictions are made at the receiver which are identical to those made at the data compressor, and all non-transmitted data samples are replaced by predicted values.

Critique. Evaluation of this model at LMSC, using Agena telemetry data, showed a slight improvement over Model 10. However, this model did not produce average compression ratios as great as the floating aperture zero order predictor (Model 7).

I. 3. 1. 3 Model No. 15: Second Order Polynomial, SOP. (References 139, 177)

Description. If in the n^{th} order polynomial equation the value of n is set equal to 2, the prediction equation becomes

$$y'_{t+1} = y_t + \Delta y_t + \Delta^2 y_t$$

where y'_{t+1} = the predicted value at time $t+1$ and

$$\Delta y_t = y_t - y_{t-1}$$

$$\Delta^2 y_t = \Delta y_t - \Delta y_{t-1}$$

therefore

$$y'_{t+1} = 3y_t - 3y_{t-1} + y_{t-2}$$

The second order predictor thus makes a prediction based upon a constant rate of change of the slope and assumes that the change in slope between samples will remain constant. There are numerous ways to mechanize this basic model, as in the case of the zero and first order predictors.

Critique. This model has not received the attention that the zero and first order predictors have. This lack of attention can be attributed to the lack of success with the first order predictors. Limited experiments with second and third order predictors by LMSC's Independent Development Program have shown that the higher order predictors are even more sensitive to noise perturbations than first order predictors. (This work was not recorded.) Attempts to devise methods to overcome the noise sensitivity of the higher order predictors led to the interpolator concepts described later in this Appendix.

I.3.1.4 Model No. 16: Wiener. (References 53, 113, 154, 245)

Description. The Wiener predictor makes use of the known data autocorrelation function to assign weights to a given number of previous samples. The weighted average of this number of previous samples is then used as a prediction of the next data value. When the data value differs from the predicted value by more than the prescribed amount, the data value is transmitted. The data is reconstructed using an identical weighted average to replace the missing data values with predicted values. The peak error is not absolutely limited and only a probability of peak error is known.

Critique. The early work that was performed on the Wiener predictor in Reference 154 did not show promising results relative to the newer interpolator models. The technique has a major difficulty with nonstationary data (typical missile flight telemetry data) and for this reason, further investigation was discontinued.

I.3.1.5 Model No. 17: Adaptive Nonlinear. (Reference 9)

Description. The basic operations performed, to predict the data, begin with the examination of a specimen of data. This examination and an error criterion results in the selection of an operator to use in predicting data. This operator is as non-linear as necessary to fit the data. The current data samples are checked against the predictions using a programmed error criterion. The operator is changed as necessary according to changing data.

Critique. Information relating to the performance of this model was not available from the literature search. Preliminary comparisons of compression efficiency between this model and the interpolators on TIROS video data have indicated that interpolators provide higher compression efficiencies. The relative fidelity of reconstructed pictures between these techniques has not been established.

I.3.1.6 Model No. 18: Exponential.

Description. This model is postulated to handle a special class of data exhibiting exponential curves. The model uses exponential functions to extend the limits to the next data value. The prediction functions, in the case of the exponential predictor, are $(a+b^k)$, $a(1-b^{-k})$, or $a(1+b^{-k})$, where a and b are constants and k is an integral sampling index.

Critique. Flow diagram solutions to this model were devised during the study. However, time and funds did not permit software implementation of this model during the contract. Its relative performance is unknown at the writing of this report.

I.3.2 INTERPOLATORS

I.3.2.1 Model No. 19: Finite Differences. (References 184, 185, 186, 187, 188, 241, 242, 243)

Description. In this model, the first through the n^{th} order difference of consecutive data samples from a source are calculated. If an i^{th} order polynomial function is present in the data, the $i+1$ order difference will become zero at the $i+1$ sample of the polynomial and will remain zero until the polynomial trend changes. The model is adaptive in the sense that it can detect and represent any polynomial from a zero to $n-1$ order.

Let

$$\begin{aligned}\Delta y_t &= y_t - y_{t-1} \\ \Delta^2 y_t &= \Delta y_t - \Delta y_{t-1} \\ &= y_t - 2y_{t-1} + y_{t-2}\end{aligned}$$

and

$$\begin{aligned}\Delta^3 y_t &= \Delta^2 y_t - \Delta^2 y_{t-1} \\ &= y_t - 3y_{t-1} + 3y_{t-2} - y_{t-3} \text{ etc.}\end{aligned}$$

Then, for the example,

<u>t</u>	<u>y</u>	<u>Δy</u>	<u>$\Delta^2 y$</u>	<u>$\Delta^3 y$</u>	<u>$\Delta^4 y$</u>
0	0	-	-	-	-
1	4	4	-	-	-
2	6	2	-2	-	-
3	6	0	-2	0	-
4	4	-2	-2	0	0
5	0	-4	-2	0	0
6	-6	-6	-2	0	0
7	-13	-7	-1	1	1
8	-20	-7	0	1	0

a second order polynomial is present from $t = 0$ through $t = 6$, and the presence of the polynomial is detected by the $\Delta^3 y$ difference at $t = 3$, i. e., $\Delta^3 y = 0$. Samples y_0 , y_1 and y_2 are transmitted. At time $t = 7$, the second order polynomial terminated ($\Delta^3 y \neq 0$). At time $t = 8$, the presence of a third order polynomial was detected by the $\Delta^4 y$ difference term. The same procedure is used for data reconstruction using samples y_0 , y_1 , y_2 , and y_7 .

Critique. This model has difficulty producing high compression ratios since it is unlikely that a time function will exhibit exact polynomial behavior. Small noise perturbations, including quantization noise, affect this model and the higher order predictors in similar manners. Reference 187 describes computer simulation results of this model as applied to Jupiter and Saturn booster telemetry data. These results also

show that during reconstruction, both interpolation and prediction techniques are required. This model has extreme difficulty in controlling the peak errors, particularly during periods that predictor reconstruction is used. Attempts to overcome these problems led to the set of interpolators currently in use at LMSC.

I. 3. 2. 2 Model No. 20: Least Squares Polynomial. (Reference 137)

Description. This model, designed to confine peak errors and to minimize the variance of the error between the data and the approximation, uses the well known least squares polynomial fit technique to represent data samples (up through a seventh order polynomial). The algorithm was modified to include an additional test that would limit the peak errors between the polynomial interpolations and each data sample in the redundant set to a predetermined error value. This model has been used for several years to compress Agena subsystem data for both computer and manual analysis.

Critique. This model provides optimum sample compression efficiency with the following constraints.

- Polynomial approximation
- Minimum variance of error
- Peak error limitation

This model is the most complex of all models described in this Appendix and requires up to fifty computer words storage for each data channel. This complexity is expected to limit its application to special measurements requiring both peak and minimum variance error guarantees.

I. 3. 2. 3 Zero Order Polynomial

I. 3. 2. 3. 1 Model No. 21: Computed Sample Transmitted, ZOI. (References 51, 62, 91, 146, 148, 151, 153, 154, 158, 160, 219, 244)

Description. The functional operation of this version of the zero order interpolator is depicted in Figure I-2. This zero order interpolator is similar to the zero order

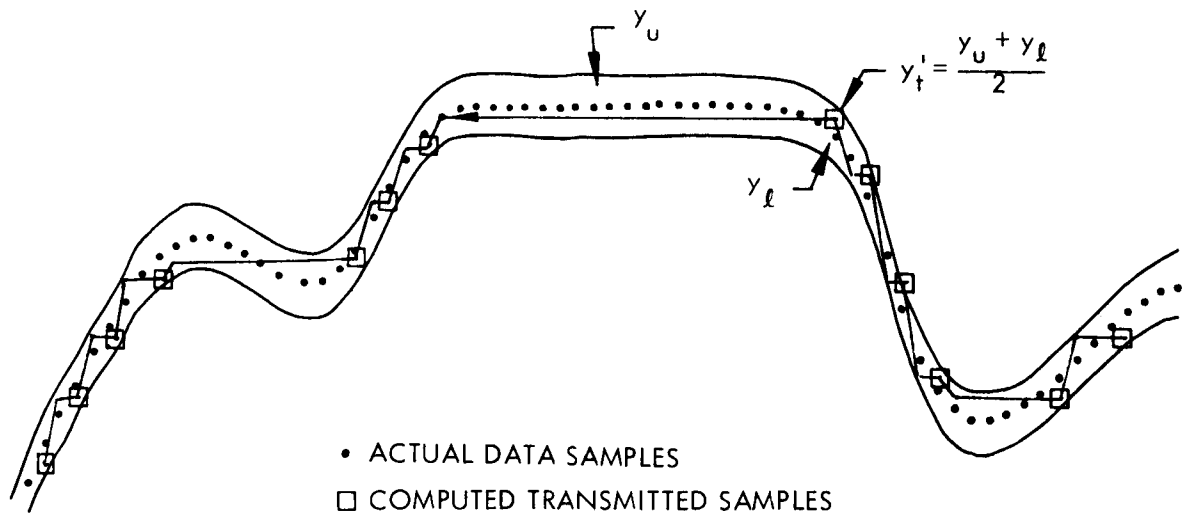


Fig. I-2 Zero Order Polynomial Interpolator,
Computed Sample Transmitted

predictor in the sense that points lying on a horizontal line are used to represent the largest set of consecutive data samples within a prescribed peak-error tolerance. The primary difference between the predictor and the interpolator is the reference sample selected to represent the redundant set. It is seen in Figure I-2 that the reference sample for the interpolator is determined at the end of the redundant set instead of with the first sample as in the case of the predictor. In this case, the reference sample y'_t used for the interpolator is computed as the average between the most positive sample, y_u , and most negative sample y_l in the redundant set.

Critique. This zero order interpolator is optimum in terms of sample compression efficiency, assuming a zero order polynomial approximation and a peak-error guarantee as mentioned in Paragraph I.3.2.2. (The least square polynomial interpolator described in that paragraph is the optimum redundancy reduction selector for a guaranteed minimum variance error criterion.) A graphical indication of the improved compression efficiency of this zero order interpolator over the zero order predictor can be seen by comparing Figures I-1 and I-2.

I.3.2.3.2 Model No. 22: Last Redundant Sample Transmitted. (Reference 219)

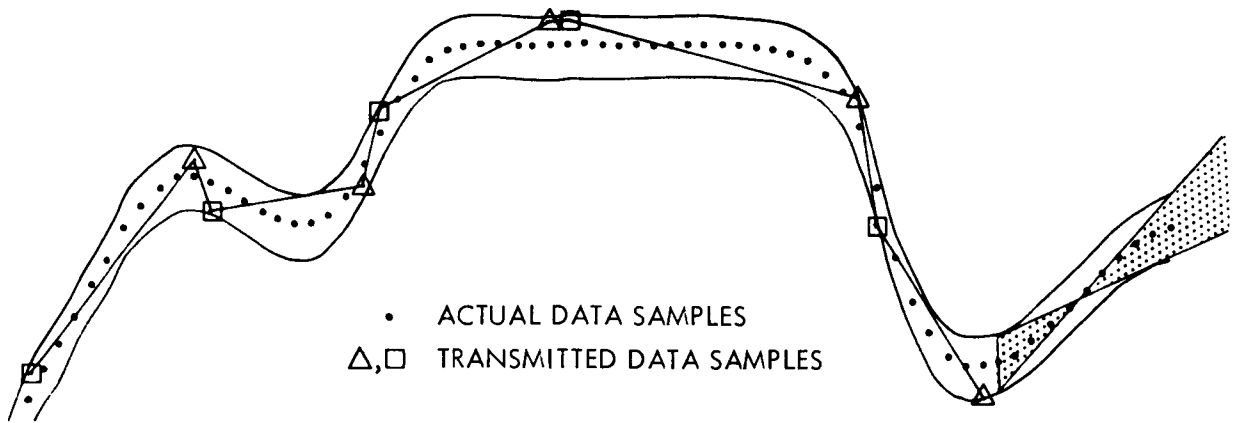
Description. This model operates in a manner similar to that of the selector described in Paragraph I.3.2.3.1. However, instead of transmitting the computed average of the most positive and most negative samples in the redundant set, it transmits the last redundant sample.

Critique. Because the last sample in the redundant set is transmitted instead of the computed average, the peak allowable error will be twice that of the computed-average method for the same compression efficiency. Thus the efficiency of this model will always be less than that of the previous model for the same maximum allowable error. The complexity of this model, however, would be slightly less than that of the previous model, because the average of two stored sample values would not have to be computed.

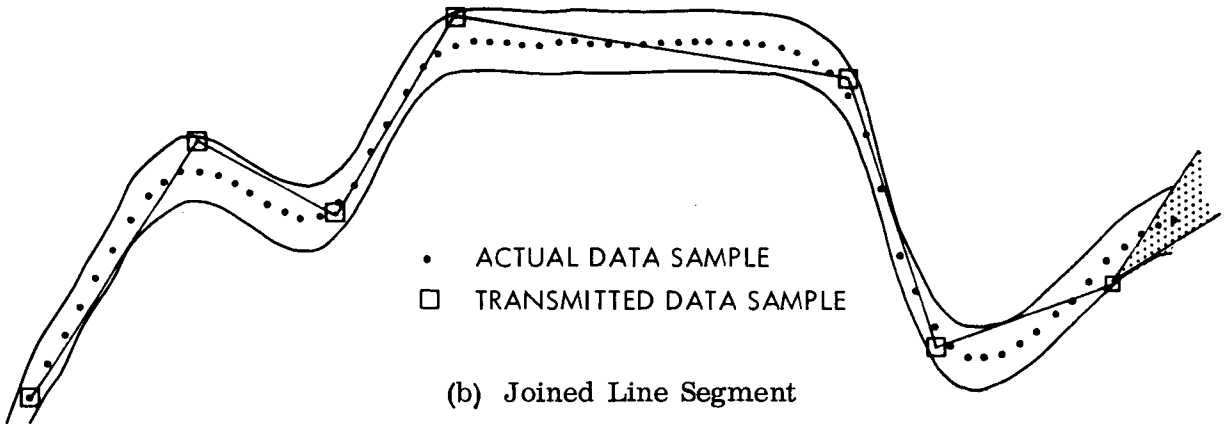
I.3.2.4 First Order Polynomial. As the name implies, the first order interpolator redundancy reduction compression technique approximates the data with a first order polynomial curve. The interpolator differs from the predictor by allowing all samples in a redundant set to influence the polynomial approximating the redundant samples.

I.3.2.4.1 Model No. 23: Four Degree of Freedom, FOI4DG. (References 91, 146, 153, 154, 160, 227, 244)

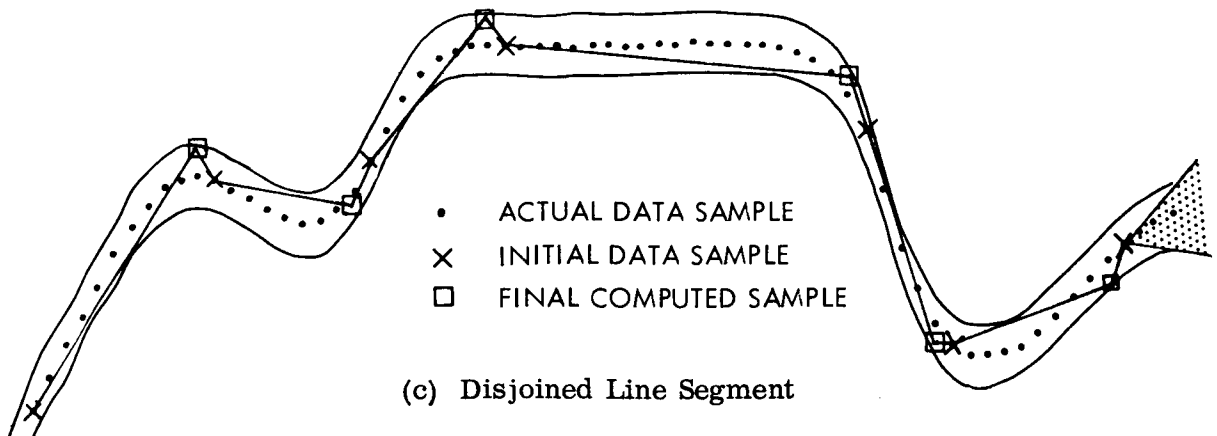
Description. This model matches the longest (first order) straight line to a set of redundant samples so that the most positive and most negative errors are within the prescribed tolerance and are equal in magnitude. Both ends of the straight line are unconstrained to allow an optimum fit to be made. The values of each end of the straight line are transmitted to permit reconstruction by interpolating between transmitted samples. The performance of this model is shown in Figure I-3a. Both the starting and end points of each line are computed values so that the length of each line is maximum for the assumed peak-error guarantee. It is seen that the end point of one line segment can be connected with a straight line to the beginning of the following line segment.



(a) Four Degrees of Freedom



(b) Joined Line Segment



(c) Disjoined Line Segment

Fig. I-3 First Order Interpolator Redundancy Reduction

Critique. This first order polynomial interpolator is designed to provide a maximum sample compression efficiency for the condition that the errors from approximation must be confined to a peak value. If peak errors are discarded in preference to other errors, then other models can be designed to produce higher compression ratios. Since this model is quite complex, prior to this study it was not expected to achieve recognition as a general solution to vehicle or ground compression applications. It is, however, less complicated and requires less memory than the least squares polynomial model (Model 20).

I. 3. 2. 4. 2 Model No. 24: Joined Line Segment, FOIJON. (References 91, 139, 146, 153, 154, 159, 160, 179, 219, 227, 244)

Description. This model is identical to the optimum, four degree of freedom interpolator except that the initial point of the line segment is anchored to the computed end point of the previous line. Thus, only the end point of each line segment is transmitted. The transmitted end point is computed so that the positive and negative peak errors are equal in magnitude and are within the prescribed tolerance. Reconstruction is accomplished by connecting all transmitted samples with a straight line. Figure I-3b illustrates the performance of the model.

Critique. Analysis of the joined line segment interpolator, (Reference 146), has shown that this model tends to oscillate and that the majority of other interpolators provide higher compression efficiencies. In fact, Reference 139 has shown that the zero order predictor provided greater compression ratios when subjected to Agena Telemetry data. The experiments conducted by Simpson, Reference 219, on Saturn data did not confirm this result. His results showed this model to be generally more efficient than the other models tested. It will be shown later in the report that an adaptive aperture tends to overcome the oscillation problem. This model is slightly more complicated to mechanize than a comparable first order predictor.

I. 3. 2. 4. 3 Model No. 25: Disjoined Line Segment, FOIDIS. (References 91, 139, 146, 153, 154, 159, 160, 179, 227, 244)

Description. This method gives a substantial improvement in sample-compression ratio by anchoring the starting point of the line segment to the actual out-of-tolerance data sample thus minimizing the tendency to oscillate. In fact, the improvement in sample-compression ratio will, under most conditions, more than compensate for the decrease in bandwidth-compression ratio caused by the requirement to code both ends of the line segment. The name "disjoined" line segment has been adopted for this configuration of the first-order interpolator. The operation of the disjoined line segment is presented in Figure I-3c.

Critique. The disjoined line segment has consistently produced high sample compression ratios. This model suffers when converting to bandwidth compression ratio because of the increased coding required to represent both ends of the line segment interpolator.

I. 3. 2. 4. 4 Offset Out-of-Tolerance. Model No. 26: Last Slope, FOIOLS; and Model No. 27: Out-of-Tolerance Direction, FOIOT. (References 139, 146, 153, 154, 159, 160, 179, 227, 244)

Description. The joined line segment model discussed in Paragraph I. 3. 2. 4. 2 has a definite tendency to oscillate resulting in low compression efficiency. This model offsets the initial point of the line segment to nearly eliminate this problem. The magnitude of offset is generally equal to the tolerance value. Two methods for determining the direction of offset have been used. These are:

- Offset based upon the sign of the last line segment slope
- Offset in the direction of the out-of-tolerance sample. This technique requires an additional bit to be transmitted denoting the direction of offset.

Critique. The offset out-of-tolerance model will generally provide higher bandwidth compression ratios than the other two degree of freedom interpolators (Reference 154). The offset in the direction of the out-of-tolerance sample has produced a larger bandwidth compression ratio than offsetting in a direction based upon the sign of the slope

of the last line segment even though one additional bit is required. The complexity of this model is equivalent to the other two degree of freedom interpolators.

I. 3. 2. 4. 5 Model No. 28: Last Data Sample Transmitted. (References 69, 70, 219)

Description. This model is also similar to the joined line segment interpolator except the last in-tolerance data sample is transmitted instead of a computed sample. This model was designed based on the assumption that it is better to terminate the end point of a line segment on an actual data sample rather than a computed value.

Critique. The evaluations conducted by the University of Alabama showed the joined line segment interpolator to achieve greater compression ratios for given rms error values than this model. Reference 158 also shows that the peak errors produced by this method cannot be controlled when adaptive aperture is used.

I. 3. 2. 5 Model No. 29: Exponential, EI.

Description. This model compresses a special class of data exhibiting exponential behavior. This model uses a zero order polynomial combined with an exponential term and is mechanized in a similar manner to the first order interpolator except the interpolated values follow an exponential curve instead of a straight line. The general functions which would be followed are $(a \pm b^k)$ or $a(1 \pm b^k)$ where a and b are constants and k is an integral sampling index.

Critique. This model was conceived so late in the study that its performance was not determined. It is reasonable to assume that the exponential interpolator will outperform the exponential predictor since noise perturbations can influence the exponential predictor in a manner similar to the polynomial predictor. It is anticipated that the exponential interpolator will be difficult to mechanize due to the additional exponential operations required.

I. 3. 2. 6 Model No. 30: Adaptive Reference Pattern.

Description. This model extends the exponential interpolator to include high order polynomials and transcendental functions. The model is adaptive in the sense that it can select the reference pattern that is likely to fit the data the closest.

Critique. Like the exponential interpolator, this model was developed late in the study and could not be evaluated. However, it would appear that this model would be even more difficult to mechanize than the exponential interpolator since it would include reference patterns other than exponential.

I. 4 ENCODING

Encoding can be used by itself as a data compression technique or it can be combined with the others. An encoding algorithm can be applied as a fixed rule based upon previous information, or it can be applied adaptively based upon measured statistics.

I. 4. 1 Nonadaptive

I. 4. 1. 1 Model No. 31: Delta Modulation. (References 28, 59, 98)

Description. This model integrates combinations of positive and negative pulses in a time-varying manner so that at any given time the sum of pulses closely approximates the magnitude of the signal. The positive and negative pulses represent a stream of zeros and ones which can be used to synthesize the signal. A transmitted pulse is a one if the synthesized integral is more negative than the input signal and the pulse is a zero if the integral is more positive than the input signal. The contribution of a zero or a one is chosen to represent the analog resolution of the data.

Critique. If aliasing errors are to be minimized, the sampling frequency of this model must be sufficiently high to allow a transient signal to be followed. This sampling frequency in turn determines the transmission bit rate since a one or a zero must be transmitted for each sample. This limitation places an upper bound on the compression ratio which can be achieved.

L. 4. 1. 2 Model No. 32: Difference Modulation. (References 59, 154)

Description. This model takes advantage of the high probability that the difference between two adjacent samples representing a channel will be small compared to full scale. Thus a shorter incremental code can be used to define the time history of a data channel. These differences can be summed to allow reconstruction.

Critique. Unless means are provided to rereference the data (re-establish the base line) a bit error in any difference code word will be reflected in the subsequent summation. Comparative evaluations of difference modulation techniques (Reference 59) have not produced encouraging results relative to other forms of data compression. However, combining difference modulation with first order interpolator models have resulted in higher overall bandwidth compression ratios (Reference 154).

L. 4. 1. 3 Model No. 33: Probabilistic. (References 33, 65, 190, 217, 237)

Description. If the amplitude probability density function of the waveform produced by a data source has a non-rectangular shape, and if it is known a priori, it is possible to code the digital words representing the data samples so that short words are assigned to data values that will most frequently occur, and longer words are assigned to values which rarely occur. In this manner a reduction in bandwidth can be achieved.

Critique. This method has been found to be moderately effective if the statistics of a source follow the assumed distribution. If the amplitude probability density function between sources are different, a stored conversion table for each source is required if reasonable efficiencies are to be achieved. Analysis of satellite telemetry data has shown that most measurements are highly correlated (Reference 139). As such, the probability of a long coded word followed by a long coded word is high. Thus, bunching of the input rate to the required queuing buffer can occur and cause a greater likelihood of buffer overflow and underflow. The variable message length characteristics of probabilistic encoding presents problems in maintaining word synchronization.

I. 4.2 Adaptive

I. 4.2.1 Model No. 34: Adaptive Probabilistic.

Description. This model is similar to the nonadaptive model discussed earlier, except that the encoder has the ability to measure new statistics as time passes. Consequently, if the data is nonstationary, new code assignments can be made based upon the most recent statistics. Information relative to all code assignments made by the encoder must be transmitted along with the coded messages to enable interpretation and reconstruction of data to be made at the receiving terminal.

Critique. Little is known about the relative merits of this model. Since adaptive probabilistic encoding was not considered as a data compression technique at the beginning of this study, the literature search did not disclose any references on this model.

I. 4.2.2 Model No. 35: Bit Plane. (References 59, 213, 225)

Description. Bit plane encoding is a technique for increasing the relative entropy of transmitted data bits. A bit plane may be defined as follows: given N-bit data words, the n^{th} bit plane consists of all those data bits corresponding to the coefficients of 2^{n-1} ($1 < n < N$). In its most general form, bit plane encoding requires that each of these N bit planes be coded as N independent, parallel binary data sources. Assuming a high interbit dependency within a given plane, recoding each bit plane with a more efficient code will result in a bandwidth (bit) reduction, or, increase in relative entropy.

Critique. Bit plane encoding has shown promise as being competitive to redundancy reduction data compression models for certain classes of data (Reference 214). On the other hand, Reference 58 has presented this solution as being less efficient than other data compression models when applied to television video data. Storage requirements and possible variable word length requirements of bit plane encoding are characteristics which must be considered in a detailed trade-off analysis.

Appendix II
S-6 SENSOR ASSIGNMENTS

Appendix II
S-6 SENSOR ASSIGNMENTS

The identification numbers which were assigned to the S-6 data sensors are shown in Table II-1. Also shown are corresponding channel numbers and sensor sample rates.

Table II-1
S-6 SENSOR DESIGNATIONS

SENSOR IDENT NO.	CHANNEL AND POSITION NO.	SENSOR NAME	NOMINAL SAMPLE RATE, SPS
1	1	Position and status	20
2	2, 7, 12, 18, 23 28, 34, 39, 44	Electron temp #1 output	180
3	16, 40	Electron temp #2 output	40
4	3, 19, 35	Bayard alpert gauge #1 DC	60
5	4, 20, 36	Bayard alpert gauge #1 AC	60
6	5, 21, 37	Bayard alpert gauge #2 DC	60
7	6, 22, 38	Bayard alpert gauge #2 AC	60
8	8, 32	Aspect	40
9	9, 25, 41	Mass spect #1 log amp output	60
10	24	Mass spect #1 elect biased output	20
11	10, 26, 42	Redhead gauge #1	60
12	11, 27, 43	Redhead gauge #2	60
13	13, 29, 45	Mass spect #2 log amp output	60
14	30	Mass spect #2 elect biased output	20
15	14	Zero-volt reference	20
16	15	Five-volt reference	20

Table II-1 (Cont'd)

SENSOR IDENT NO.	CHANNEL AND POSITION NO.	SENSOR NAME	NOMINAL SAMPLE RATE, SPS
17	17, pp 15, 6*	Ionization current/voltage	2.5
18	17, pp 0, 7	High-voltage monitor	2.5
19	17, pp 1, 8	Repeller monitor	2.5
20	17, pp 2, 9	Amplifier B+ monitor	2.5
21	17, pp 3, 10	Mass marker	2.5
22	17, pp 4, 11	Log amp temp	2.5
23	17, pp 5, 12	Electrometer temp	2.5
24	17, pp 13	Zero-volt reference	1.25
25	17, pp 14	Five-volt reference	1.25
26	31, pp 15	BA emission current #1	1.25
27	31, pp 0	BA emission current #2	1.25
28	31, pp 1	BA gauge temp #1	1.25
29	31, pp 2	BA gauge temp #2	1.25
30	31, pp 3	BA electrometer temp #1	1.25
31	31, pp 4	BA electrometer temp #2	1.25
32	31, pp 5	BA voltage bias #1	1.25
33	31, pp 6	BA voltage bias #2	1.25
34	31, pp 7	Sphere pressure	1.25
35	31, pp 8	Nutation damper squib monitor	1.25
36	31, pp 9	Experiment squib monitor	1.25
37	31, pp 10	Turn-on counter	1.25
38	31, pp 11	T/M voltage (+20.15v)	1.25
39	31, pp 12	9.3v battery monitor	1.25
40	31, pp 13	Five-volt reference	1.25
41	31, pp 14	Zero-volt reference	1.25

*Sensors 17 through 23 were erroneously thought to be cross-strapped as shown. Since only one minor frame channel in 45 was involved, the resulting abnormally-low compression ratios obtained for these sensors did not materially affect the overall outcome of the experiment.

Table II-1 (Cont'd)

SENSOR IDENT NO.	CHANNEL AND POSITION NO.	SENSOR NAME	NOMINAL SAMPLE RATE, SPS
42	33, pp 15	Zero-volt reference	1.25
43	33, pp 0	Five-volt reference	1.25
44	33, pp 1	BA card temp #1	1.25
45	33, pp 2	BA card temp #2	1.25
46	33, pp 3	BA ion trap filament monitor #1	1.25
47	33, pp 4	BA ion trap filament monitor #2	1.25
48	33, pp 5	6.2 v battery monitor	1.25
49	33, pp 6	-27.9 v battery monitor	1.25
50	33, pp 7	Thermistor #1 (lower MS boss)	1.25
51	33, pp 8	Thermistor #2 (skin, lower 45°)	1.25
52	33, pp 9	Thermistor #3 (ambient, top of RH)	1.25
53	33, pp 10	Thermistor #4 (skin, equator)	1.25
54	33, pp 11	+13.95 v monitor	1.25
55	33, pp 12	Thermistor #6 (upper MS boss)	1.25
56	33, pp 13	Thermistor #5 (skin, upper 45°)	1.25
57	33, pp 14	Spare	1.25

Appendix III

**BIT PLANE ENCODING AND
DATA ENTROPY CALCULATION**

Appendix III
BIT PLANE ENCODING AND DATA ENTROPY CALCULATION

This appendix describes the techniques used for encoding bit planes and calculating entropy, discusses reconstruction and gives error magnitudes.

III.1 BIT PLANE ENCODING

In each case, the data to be coded was divided into groups containing 128 words. Both binary and Gray coded data words were considered and, since the data range was 0 - 511, each data word consisted of 9 bits. (A straightforward, bit-by-bit transmission of such a data group requires $128 \times 9 = 1152$ bit s.)

To code the 9 bit planes in each data group, each bit plane was assigned a Class A, B, or C designation, following the convention of Schwartz¹. The Class C designations were made on an a priori basis so that resulting tolerances would coincide with the tolerances used with the polynomial interpolators. A coding algorithm was postulated, retaining Class B plane information by simple run length encoding, and Class A plane information by encoding of plane location and contents. This coding algorithm was not an optimum algorithm and certain improbable ambiguities might have occurred. It was a close enough approximation, however, to provide a meaningful comparison between bit plane coding and existing LMSC algorithms.

III.1.1 Coding Transmission Schedule

The coding transmission schedule was roughly as follows (all words contain 7 bits):

- Transmit special word (Class A Plane information follows)
- Transmit Class A Plane information (3 bits/location 1 bit/contents)

¹Schwartz, J., Data Processing in Scientific Space Probes, NASA Grant NSG-138-61, Sept 1963

- Transmit special word (Class B Plane information follows)
- Transmit special word (3 bits/ location of Class B Plane, 1/bit initial value)
- Transmit changes in Class B Plane (7 bits/ change)
- Transmit special words and changes in Class B Plane as necessary to transmit all Class B Planes
- Transmit special word (bit-by-bit transmission of Class B Plane information follows, count of changes ≥ 21)
- Transmit special word (3 bits/ location of Class B Plane, 1 bit/ i nitial value)
- Transmit Class B Plane bit-by-bit (19 7-bit words)
- Repeat last three steps as necessary to transmit all Class B Planes requiring bit-by-bit transmission

III. 1. 2 Coding Scheme

III. 1. 2. 1 Format. The coding format is shown in the following illustration.

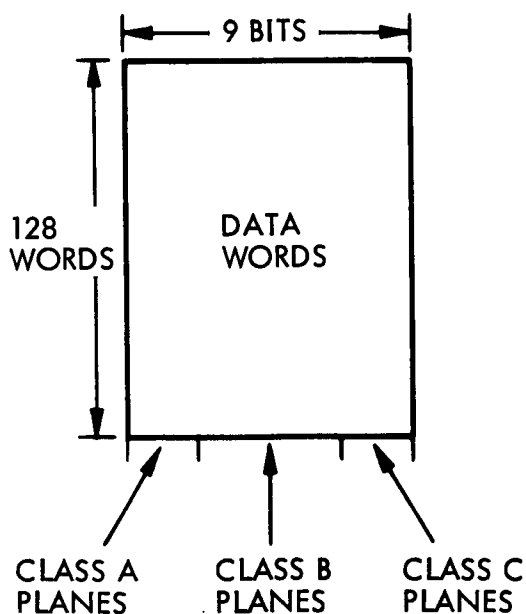


Fig. III-1 Coding Format

III. 1. 2. 2 Code Words and Groups. The code words and code word groups are listed and described in the following table.

Table III-1
CODE WORDS AND CODE WORD GROUPS

CASE	WORDS AND GROUPS							DEFINITION
(a)	0	0	0	0	0	0	0	Class A Plane information follows
(b)	1	1	1	1	1	1	1	Class B Plane information follows (also separates Class B plane information)
(c)	0	0	0	0	0	0	0	Bit-by-bit transmission follows
	0	0	0	0	0	0	0	
(d)	e_{1a}	e_{1b}	e_{1c}	c_1	e_{2a}	e_{2b}	e_{2c}	$e_{ia} e_{ib} e_{ic}$ locate the i^{th} A Plane c_i describes the contents of the A Plane
	c_2	e_{3a}	e_{3b}	e_{3c}	c_3	e_{3a}	e_{3b}	
	e_{3c}	c_4	e_{4a}	e_{4b}	e_{4c}	etc.		
(e)	a_i	0	0	0	e_{ia}	e_{ib}	e_{ic}	a_i describes contents of first bit in the B Plane located by $e_{ia} e_{ib} e_{ic}$
(f)	b_{ij1}	b_{ij2}	b_{ij3}	b_{ij4}	b_{ij5}	b_{ij6}	b_{ij7}	These bits describe the location of the j^{th} change in the i^{th} bit plane. (Class B)
(g)	c_{i1}	c_{i2}	The contents of the i^{th} bit plane when transmitted bit-by-bit (Class B)
	c_{i8}	
	.	c_{i128}	0	0	0	0	0	

III. 1.2.3 Bit-by-Bit Transmission. Bit-by-bit transmission is initiated when the count of changes for a given Class B Plane equals or exceeds 21. This is shown by

Run Length Coding (No. of Bits)	Bit-by-Bit Transmission (No. of Bits)	Count of Changes
$(19 + 1) \times 7$	$(2 + 19) \times 7$	19
$(20 + 1) \times 7$	$(2 + 19) \times 7$	20
$(21 + 1) \times 7$	$(2 + 19) \times 7$	21
No. of changes	2 special words	
Special word	No. of words to send 128 bits	

III. 1.2.4 Typical Code Group Sequence. A typical sequence of code groups might be as follows: (The letters refer to the convention used in Table III-1.)

a d b e f b e f f f - - - f b e f f f - - - f
 b e f f f - - - f c e g a d b e f f b e f f
 - - - f c e g c e g etc.

This sequence may be interpreted as follows:

First block of 128 data words	}	3 Class A Planes
		5 Class B Planes, one of which has been transmitted bit-by-bit
Second block of 128 data words	}	4 Class A Planes
		4 Class B Planes, two of which have been transmitted bit-by-bit

Note: In each case it was assumed a priori there was 1 Class C Plane.

III.2 ENTROPY CALCULATIONS

Entropy is a measure of average information per data source symbol. In the case of a binary data source alphabet, the units of entropy are bits/binit (binit = binary digit). To calculate entropy it is first necessary to postulate a probabilistic data source model. After data statistics associated with this model are measured, data entropy is calculated. It should be noted that this data entropy is meaningful only in the context of the chosen data source model. Data entropy may be used to calculate an upper bound on attainable bit compression ratios. Again, this upper bound is meaningful only in the context of the data source model.

III.2.1 Data Source Model

In this study, a Markov data source model was postulated for each data bit plane. This approach is a reasonable approximation to reality and is mathematically tractable. In the case of a zero order and first order Markov source model, the following expressions for the entropy of the k^{th} bit plane were used²:

Zero Order	First Order
$H_k^0 = - \sum_{i=0}^1 P_k(i) \log_2 (P_k(i))$	$H_k^1 = - \sum_{i=0}^1 \sum_{j=0}^1 P_k(i,j) \log_2 (P_k(i j))$

where $P_k(i)$ is the probability of an i ($i=0, 1$) in the k^{th} bit plane and $P_k(i, j)$ and $P_k(i|j)$ are similar joint and conditional probabilities referring to the k^{th} bit plane.

These bit plane entropies were then averaged over the Class A and Class B bit planes as follows (assuming N Class A and B planes):

Zero Order	First Order
$H_{\text{avg}}^0 = \frac{1}{N} \sum_{k \in A, B \text{ Planes}} H_k^0$	$H_{\text{avg}}^1 = \frac{1}{N} \sum_{k \in A, B \text{ Planes}} H_k^1$

² Abramson, Information Theory and Coding, McGraw-Hill, 1963

Using these average entropies, the upper bounds on obtainable compression ratios, consistent with the zero and first order Markov source models, were calculated as follows:

$$N_{\max}^0 = (1/H_{\text{avg}}^0) \cdot (\text{no. of bit planes} / \text{no. of A, B Planes})$$

$$N_{\max}^1 = (1/H_{\text{avg}}^1) \cdot (\text{no. of bit planes} / \text{no. of A, B Planes})$$

These upper bounds ignore any existing inter-plane information.

III.3 RECONSTRUCTION CONSIDERATIONS AND ERROR CALCULATIONS

III.3.1 Reconstruction

Errors in bit plane encoded data words due to nontransmission of Class C planes vary in magnitude, but always have the same sign. For example, if the least significant bit of each data word were removed, which would correspond to one Class C plane, the error would either be +1 or 0, depending on the original value of the bit. Assuming each value would be equally likely, a positive average error of 1/2 data unit would result. In a like manner, two Class C planes result in a positive average error of 1-1/2 data units. In reconstructing bit plane encoded data, one can take advantage of a priori knowledge of this non-zero average error by adding this known average error to every bit plane encoded data word that is received. This achieves three objectives:

- The peak error (tolerance) is reduced by a factor of 2 over bit plane encoding without addition of the average error to reconstructed data
- The overall average error approaches zero
- The absolute rms error for a given number of Class C planes is reduced.

III.3.2 Errors

The rms errors due to nontransmission of Class C planes can be calculated as follows. The possible error magnitudes are -1/2 and 1/2 in the case of one Class C plane and

$-3/2$, $-1/2$, $1/2$ and $3/2$ in the case of two Class C planes. It is assumed that these error magnitudes have the same probability of occurring in both cases. This is equivalent to assuming that there is no organization in the Class C planes being considered, and that in these planes zeros and ones are equally possible.

- For one Class C plane, the rms error is $\left[1/2 (-1/2)^2 + 1/2 (1/2)^2 \right]^{1/2} = 0.5$.

- For two Class C planes, the rms error is

$$\left[1/4 (-3/2)^2 + 1/4 (-1/2)^2 + 1/4 (1/2)^2 + 1/4 (3/2)^2 \right]^{1/2} = 1.12$$

For both one and two Class C planes the average error is zero.

Appendix IV

**SIMULATED MULTISENSOR
DATA COMPRESSOR**

Appendix IV
SIMULATED MULTISENSOR
DATA COMPRESSOR

Four programs were used; three to simulate the multisensor data compressor system used in the buffer queuing control study described in Appendix I. 4, and one to unpack and decommutate the original GSFC data tape to put the S-6 data into a form compatible with the data compression study programs. The programs, shown in Figure IV-1, are as follows:

- Unpacking and decommutation (DECOM)
- Compression, buffer simulation, and queuing control (COMPRESS)
- Data reconstruction (RECON)
- Deviation limit plot (K-PLOT).

IV.1 DECOM

The DECOM program accepts the original GSFC digital data tape and assigns a specific sensor number and time value to each data sample. Its output consists of two tapes: (1) a TAD tape whose data samples are in the same multiplexed time sequence as the original tape, but are accompanied by sensor identification and time words, and (2) a T-3 tape in which all the data samples from a given sensor are sorted and grouped on one portion of the tape. A time word accompanies each data sample word.

IV.2 COMPRESS

The COMPRESS program is the heart of the simulated data compression system. This program accepts the telemetry data in the TAD format and employing the sample selector assigned for the run, compresses the data from each sensor individually. It also simulates buffer readin and readout¹, as well as queuing control.

¹The buffer readout rate and buffer capacity are assigned as input control variables.

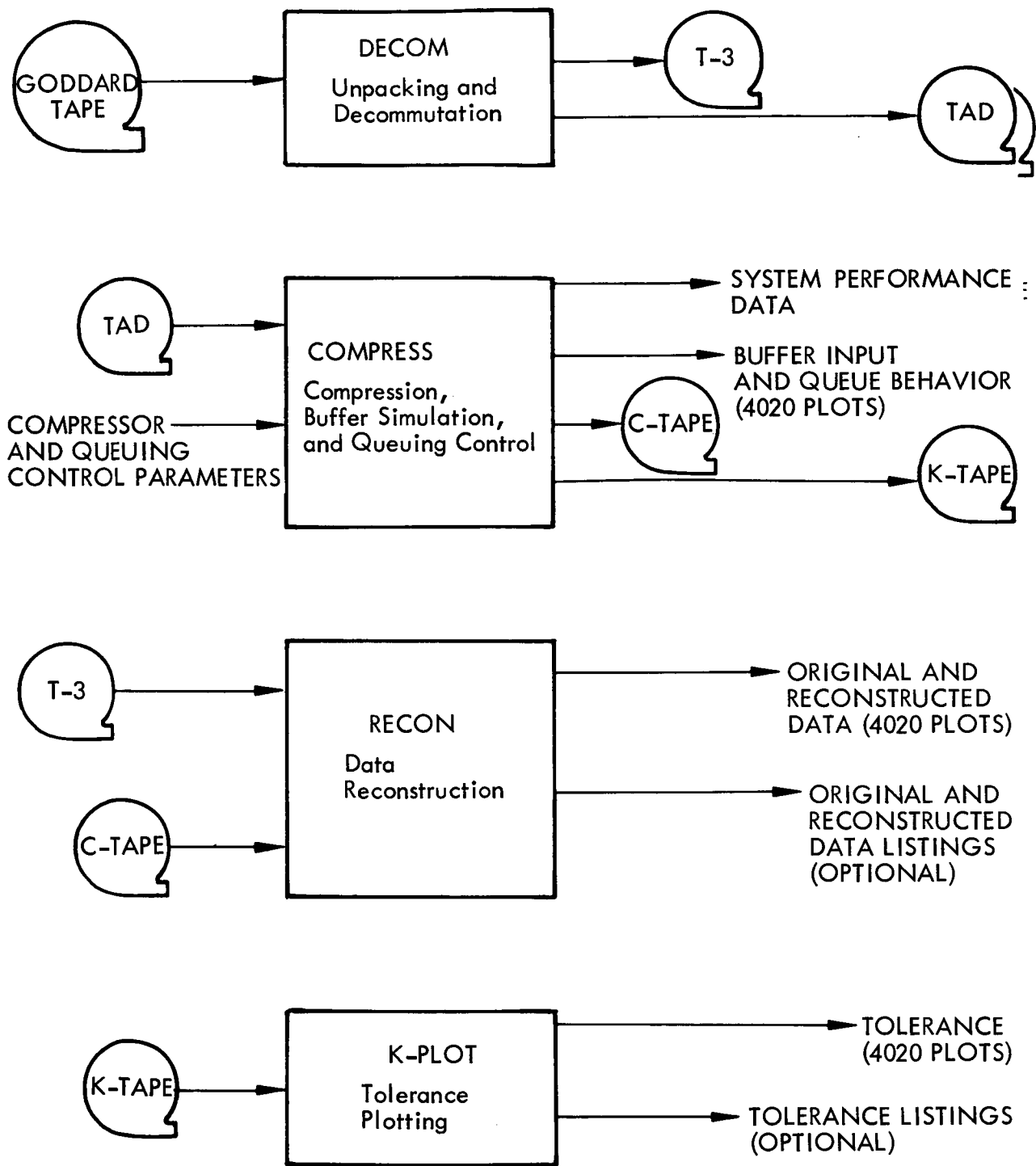


Fig. IV-1 Generalized Simulation Program Block Diagram

In addition to system performance output data and SC 4020 plots showing buffer input and queue behavior, the COMPRESS program writes a C-TAPE containing the transmitted (compressed) data sample values, and a K-TAPE containing time records of the tolerances as they are varied by the queuing control system.

IV.3 RECON

The RECON program reconstructs the data from selected sensors using the C-TAPE and plots the reconstructed waveform on an SC 4020 plot. It also plots the original waveform from the T-3 tape and compares the reconstructed waveform to the original.

IV.4 K-PLOT

The K-PLOT program takes values of tolerance from the K-TAPE for selected sensors and plots a time record of tolerance for each sensor. Four sample selectors were programmed to operate with the simulated data compression system², a zero order predictor (ZOP), a first order predictor (FOP), a zero order interpolator (ZOI), and a first order interpolator, disjoined (FOIDIS). These selectors were programmed as subroutines; any one of the four subroutines can be used on any given computer run.

IV.5 QUEUING CONTROL SUBROUTINES

The six queuing control subroutines all employ aperture width as the controlled parameter. The six subroutines are:

- Compression ratio monitoring, continuous control
- Compression ratio monitoring, step control
- Queue length monitoring, continuous control
- Queue length monitoring, step control
- Combination monitoring, continuous control
- Combination monitoring, step control

² The reader is referred to Appendix I for detailed explanations of the sample selectors.

The first two control systems monitor the average run length of a given fixed number of most recent line segments for each data sensor³ and control the width of the aperture associated with that sensor. The difference between the two systems lies in the shapes of the control curves, which are shown in Figure IV-2. As shown in the figure, one system employs continuous, straight-line control, and the other step control. An individual control curve is assigned to each sensor.

The second pair of control systems monitor queue length, and control the width of the aperture associated with each sensor, according to a control curve individually assigned to the sensor. Typical control curves are shown in Figure IV-3. As in the first pair of control systems, one system employs continuous, straight-line control, and the other uses step control.

The third pair of control systems uses a combination of average run length and queue length to control the aperture of each individual sensor. The control curves are similar to those shown in Figures IV-2 and IV-3, except that in this case a variation of either the average run length or queue length can alter the tolerance value. As with the previous pairs of systems, one is continuously controlled on a straight-line basis, and the other is step-controlled.

Any one of these subroutines may be used with the simulated data compression system, or no queuing control may be employed, as desired.

IV.6 COMPRESSOR SIMULATION OUTPUT

To aid in the analysis of system performance, the following output data are available from each compressor simulation run:

- Combined compression ratio (total number of samples processed divided by the total number of samples sent to the buffer -- all sensors) averaged over a computer run on one data specimen

³This number, designated J_{Ri} for sensor i , is assigned as an input control variable.

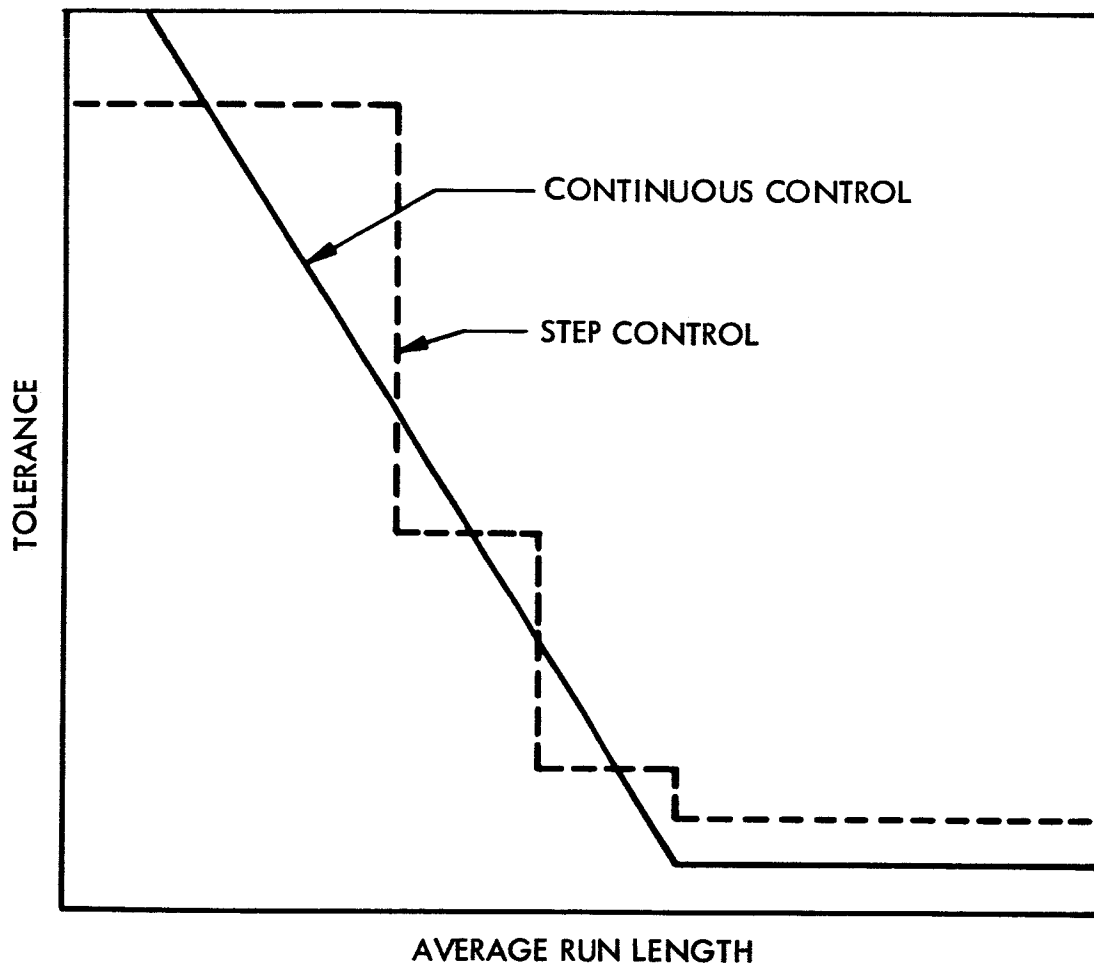


Fig. IV-2 Typical Control Curves for Compression Ratio Monitoring Queuing Control System

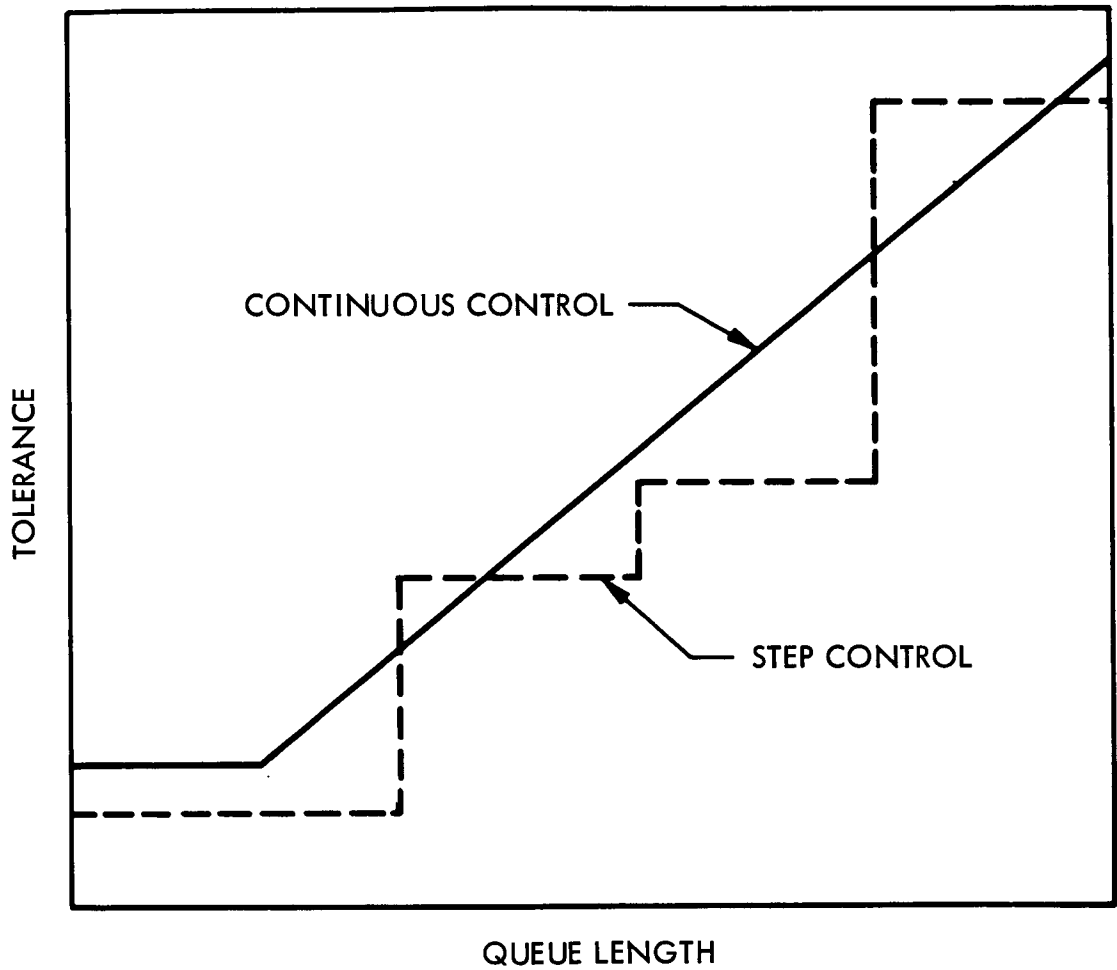


Fig. IV-3 Typical Control Curves for Queue Length Monitoring Queuing Control System

- Combined removal factor (total number of samples removed divided by the number of samples processed -- all sensors) averaged over a computer run on one data specimen
- Total number of samples removed (all sensors)
- Total number of samples processed (all sensors)
- Compression ratio averaged over a computer run on one data specimen, for each sensor
- Removal factor averaged over a computer run on one data specimen, for each sensor
- Total number of samples removed, for each sensor
- Total number of samples processed, for each sensor
- Total number of data samples lost by buffer overflow (this will always be zero when the buffer capacity is set to ∞)
- Queue length versus time (4020 plot)
- Buffer input arrival rate versus time (4020 plot)
- Samples lost by overflow versus time (4020 plot)
- Queue length histogram (4020 plot)
- Buffer input arrival rate histogram (4020 plot)
- Histogram of time intervals between buffer input arrivals (4020 plot)
- Reconstructed data versus time (4020 plot)
- Original data versus time (4020 plot)
- Error versus time (4020 plot)
- Error histogram (4020 plot)
- RMS error

- Tolerance versus time (4020 plot)
- Tolerance histogram (4020 plot)

Appendix V
BIBLIOGRAPHY

Appendix V
BIBLIOGRAPHY

A search of international literature on data compression was made to uncover new data compression models. More than 250 of the references found are contained in this Appendix including references on signal reduction, adaptive sampling, redundancy reduction and encoding. This list represents only a small percentage of the total number of articles written since general rather than specific solutions to data compression were being sought.

1. Abdullaev, Granovskii, Nabiev, and Feider (USSR), "Pulse Code Telemetry Transmitter," Instrum. Constr. (G.B.), Oct 1962
2. Abel and Stine, "Techniques for Narrow Band Telemetry of Nonrecurrent Data," (Paper presented at National Telemetering Conference, May 1963)
3. Aerospace Information Division, Washington, D. C., "Computation of Abstracts on Russian Transmitting Satellite Propagation Studies," Feb 1964
4. PRD Electronics, Inc., Speech Bandwidth Compression System - Scanning Filter, by Albanese and Wand, 34L 0911 FR, Sept 1961.
5. Anderson, "Quadrature Subcarrier Technique of Transmission of Two Independent PCM Channels," (paper presented at National Telemetering Conference, May 1963)
6. Redstone Arsenal, Improved Utilization of Telemetry Capacity, by Asquit, ANC/RA RG TR63 17, June 1963
7. ASTIA, Scientific Satellites Bibliography, ASTIA A-290-800, Dec 1962
8. Baghdady, Communication System Theory, McGraw Hill, 1961
9. Balakrishnan (UCLA), "An Adaptive Nonlinear Data Predictor," (paper presented at National Telemetering Conference, 1962)
10. Bolt, Beranek and Newman, Inc., Study of a Speech Compression System, by Ball, Colaruotolo, Kryter, AD-274466, Jan 1962
11. Balchan (Poland), "Some Aspects of Telemetry Quality" Arch. Automat. Telemekh., (Poland) Vol. 7, 1962

12. Bailey, Johnson, Lawson and Luck (General Electric), "Computer Operational Systems Engineering for an Orbiting Satellite and its Command and Telemetry Data Acquisition Systems," paper presented at Intl. Conf. on Aerospace Technology, Apr 1964, and IEEE Transactions on Aerospace, Apr 1964
13. Barker, Low Power, Low Speed Data Storage and Processing Techniques, X63-12970, Aug 1962
14. Baron, Monahan, and Piccirilli, "A Data Conditioning System for Mariner Spacecraft," (paper presented at 1962 National Symposium on Space Electronics and Telemetry, Miami, Florida, Oct 1962
15. Lincoln Lab of MIT, Interim Report on Development of an Integral: On-Board RF Communication System for the Apollo Spacecraft, by Barry, MIT-LL-AP-11 Jul 1962
16. White Sands Missile Range, Telemetry Data Analysis Techniques Study, by Barto, AO-288908, 15 Apr 1962
17. Army Ballistic Missile Agency, Redstone Arsenal, A Digital Computer Procedure for Least-Squares Polynominal Approximation, by Beard, RE-TR-61-3, Jun 1961
18. Beckman Systems Division, Telemetry Data Compression, BR-514, Jun 1962
19. Beddoes, "A Two-Channel Method of Compressing the Bandwidth of Television Signals," Proc. Instn. Elect. Engrs. (G. B.), Feb 1963
20. Radio Corporation of America, Study of Speech Compression Systems, by Belar, Sobrino, Rogers, AD 284-811, Jul 1962 and AD-406-365, Oct 1962
21. Belsadski, Rosner, (Roumania) "Improvement of the Signal to Noise Ratio on Broadcasting Transmission Channels by Compression-Expansion Techniques," Telecomunicatii, Sept - Oct 1960
22. General Electric Co., "An Adaptive Data Sampling System," by Berkowitz, N64-16164, National Space Electron Symposium, 1964
23. Billings, "A Coder for Halving the Bandwidth of Signals," Proc. Instn. Elect. Engrs., Mar 1958
24. International Business Machines, "Message Compression," IRE Transactions on Space Electronics and Telemetry, by Blasbalg and Van Blerkom, Vol. SET-8, No. 3, Sept 1962
25. Borkum, "Smoothing - Predicting Sampled Data," Electronics Industr., Sept 1963

26. International Business Machines, "Discrete Queuing Problem with Variable Service Times," by Bondreau and Griffin, IBM J Res. & Dev., Oct 1962
27. California Institute of Technology, Jet Propulsion Laboratory, "Some Considerations in Establishing the Feasibility of Data Compression in Unmanned Spacecraft," by Bourke and Jewell, (paper presented at Symposium on Unmanned Exploration of Solar System, Denver, Feb 1965)
28. Bowers, "Delta Modulation for Cheap and Simple Telemetering," IRE Trans. on Space Electronics and Telemetry, Vol. SET-5, pp. 205-209, Dec 1959
29. Boyce (General Dynamics), "Information Content of Space Vehicle Data Sources," (paper presented at International Space Electronics Symposium, Oct 1964)
30. Lockheed Missiles and Space Company, Telemetry Data - Characteristics and Processing Tabulation, by Boysen and Nakata, LMSC BO 78-911, Vol. I & II, Jan 1964
31. Brothman, Gomery, Halpern and Miller (Transitel International Corporation), "Multi-Threshold Digital Data Transmission Systems," Intl. Tlm. Conference Proceedings, London, Sept 1963
32. Lockheed Missiles and Space Company, Eigenfunctions and Data Compressors, by Brown, LMSC Technical Note, Nov 1964
33. Butayev (USSR), The Effectiveness of Optimum Coding of Primary Meter Scale in Pulse Code Telemetering, AD-412-239, 1963
34. National Aeronautics and Space Administration, MSFC, The Use of Filtering and Smoothing Functions in the Analysis of Atmospheric Data, by Camp and Laufman, X63- 12914, Jun 1962
35. Campanella, Coulter and Irons, "Influence of Transmission Error on Formant Coded Compressed Speech Signals," J. Audio Eng. Soc., Apr 1962
36. Chang, "Adaptive Information Processing," (paper presented at Western Electronic Show and Convention (WESCON), Los Angeles, Aug 1962)
37. Bell Laboratories, "Command and Telemetry Systems," by Chapman, Critchlow and Mann, Bell Sup. Tech J., Jul 1963
38. Cherry, "The Bandwidth Compression of Television and Facsimile," J. Televis Soc. (G. B.), AM - Jun 1962
39. Childers, "Sampling Rate and Aliasing in Time Division Telemetry Systems," IRE Trans. on Space Electron & TLM, Dec 1962

40. Christie, "General Purpose PCM Telemetry Processor Handles Present and Future Mission," IEEE International Conv. Record, 1963
41. Goddard Space Flight Center, Telemetry Data Processing for the Eccentric Orbiting Geophysical Observatory Satellite, by Coates, Creveling, Habib, Mahoney, and Stout, N64 11812
42. Redstone Arsenal, Improved Utilization of Telemetry Capacity, by Cobb and Baxter, AD 285440, Jun 1962
43. Westinghouse Corporation, Adaptive Data Management Techniques, by Cole, AD 351-447, May 1964
44. Coleman, "Signal Processing for Space Vehicle Experiment," Fifth National Symposium on Space TLM, Electronics, Sept 1960
45. Melpar Incorporated, A Digitized Speech Compression System, by Coulter, Early and Irons, AD 266 959, Sept 1961
46. Das, "Bandwidth Compression of Speech, Sampling in the Frequency Domain," Electronics Technol. (GB), Aug 1961
47. David, Schroeder and Logan, "Voice-Excited Vocoders for Practical Speech Bandwidth Reduction," IRE Trans. Inform. Theory, Sept 1962
48. Davidson (Princeton University), "A Theory of Adaptive Compression," (paper presented at Nat. Electronics Conf. , Chicago, Oct 1964)
49. Dolder, "The Orbiting Solar Observatory," Proc. of 3rd Int. Space Sci. Symposium, May 1962
50. Drapkin and Pentz, "An Associative Data Compressor," (paper presented at IEEE International Convention, Mar 1965)
51. Drapkin and Specht, "Biomedical Data Compression," (paper presented at National Telemetry Conference, Apr 1965)
52. Lockheed Missiles and Space Company, Reconnaissance Photo Experiment, by Drapkin and Weber, LMSC 5-65-65-1, Feb 1965
53. Drenick, "A Non-linear Prediction Theory," Trans. IRE Information Theory 4, 1954
54. Dresser and Dunlop, "An Analog On-Line Data Reduction System for Engine Testing," (paper presented at National Telemetry Conference, Denver, Colorado, 1959)

55. Dynatronics Company, Adaptive Techniques for Long Range Transmission of Pulse Code Modulation Telemetry Data, AD 288076, Aug 1962
56. -----, 1964 Rept. to Wright-Field on Data Compression
57. California Institute of Technology, Jet Propulsion Laboratory, Systematic Statistics Used for Data Compression in Space Telemetry, by Eisenberger and Posner, N64-13279, Oct 1963
58. Electro-Mechanical Research, Inc., PCM Summary Engineering Report for X-20, AD 432 627, 1963
59. Electro-Mechanical Research Inc., Video Data Modulation Study, Final Report, Jul 1964
60. Elias (MIT), Predictive Coding, Parts I & II, Harvard University Press, May 1950
61. Ellersick (IBM), "Data Compactors for Space Vehicles," National Telemetering Conference Proc., 1961
62. Evans (Republic Aviation), "Solar Observatory Spacecraft - AOSO," Am. Inst. of Aeronautics and Astronautics, Jul 1964
63. Farley (UCLA) Establishment of a Space Physics Laboratory to Develop Instrumentation for Space Research, NASA CR-58043, Apr 1963
64. Franklin, Bibby and Page (Canada), "Electronic and System Design of the Canadian Ionospheric Satellite," IEEE Int. Conv. Record, 1963
65. Ford Instrument Company, Division of Sperry-Rand Corp., Fourth Technical Note Special Facsimile Techniques, RADC-TN-59-332, Sept 1959
66. Frost and King (ABMA), "SS-FM A Frequency Division Telemetry System with High Data Capability," (paper presented at National Symposium on Space Electronics and Telemetry, Sept 1959)
67. Furstenu (Lockheed), "PCM Telemetry and Data Compression Applied to Real Time Flight Evaluation," (paper presented at AIAA/ AFLC/ ASD Support for Manned Flight Conference, Apr 1965)
68. Gardenhire (Radiation, Inc.), "Use of Digital Data Systems," (paper presented at National Telemetering Conference, May 1963)
69. -----, "Redundancy Reduction, The Key to Adaptive Telemetry," (paper presented at National Telemetering Conference, 1964)
70. -----, "Data Compaction of Rocket Booster PCM Telemetry Data," (paper presented at 2nd Space Congress, Apr 1965)

71. Pan American Aviation, Interim Report on Data Compaction, by Germond, Tech. Staff Memo No. 16, Jul 1964
72. Germond (Pan American Aviation), "Compression of Bioastronautical Data," (paper presented at National Telemetering Conference, 1965)
73. Gicca (Raytheon Corporation), "Optimizing Space Television Transmission," (paper presented at Intl. TLM Conference, London, Sept 1963)
74. Glenn and Land, "Data Compaction and High Speed Circuitry," (paper presented at IRE East Coast Conference on Aerospace & Navigation, Oct 1962)
75. Bell Laboratories, "Television by PCM," by Goodall, Bell Sys. Tech J., Jan 1951
76. Godwin, "Unified Approach to Data Processing," British Interplanetary Soc. J., Sept - Oct 1963
77. Gol'shtein and Iudin (USSR), "Methods of Calculation and Synthesis for Automatic Sampled - Data Systems," Automatikai Telemekhanika, Dec 1963
78. California Institute of Technology, Jet Propulsion Laboratory, A Fokker-Planck Equation Arising in Data Compression, by Goldstein, Posner, Rumsey and Viterbi, Space Programs Summary, No. 37-19, Vol. IV, 28 Feb 1963, pp. 172-178
79. Goltfried (STL), "Adaptive Telemetry Format Control," (paper presented at National Telemetering Conference, 1962)
80. Gruenberg, "Data Processing and Information Transmission for Space," Proceedings of the IRE, May 1962
81. Haagen (Ohio State University), Video Bandwidth Compression, AD 273-671, Feb 1962
82. Hancock and Schwartzlander (Purdue Univ.), "On The Usefulness of Signal Design Techniques in Adaptive Telemetry Links," (paper presented at Int. TLM Conf., London, Sept 1963)
83. Bell Laboratories, Experiments with Linear Prediction in Television, by Harrison, Bell Syst. Tech. Journ. 31 764-783, 1952
84. Hauptschein and Sommer (New York University), "Getting the Most Out of Aerospace Telemetry," Electronics, 27 Sept 1965
85. Lockheed Missiles and Space Company, An Automatic System for Real-Time Reduction of Telemetry Data, by Healy and McFarland, LMSC TR 3-35-62-3, May 1962

86. Himmelberg and Barrier (North American), "Signal Conditioning for the Apollo Manned Spacecraft," (paper presented at National Telemetry Conference, Jun 1964)
87. Hoberg, Finkel and Carr (Tele Dynamics), "DAEMON, An Advanced System for Data Management in Manned Space Vehicle," (paper presented at National Telemetry Conference, 1962)
88. Lockheed Missiles and Space Company, "Digital Data Compression," by Hochman, Space/ Aeronautics, Jun 1962
89. Hochman, (Lockheed), "Digital Systems and Space Communications," (paper presented at Third International Congress of Aero Sciences, Aug 1962)
90. -----, Space-Borne Digital Systems for Data Bandwidth Compression, Stanford University Press, 1963
91. Hochman and Weber, "Adaptive Telemetry - Data Compression," Aerospace Telemetry, Volume II by Stiltz, to be released
92. Holahan, "Distance, Digits, Data," Aerospace - Electronics, Nov 1962
93. Lockheed Missiles and Space Company, Advanced Telemetry System with Adaptive Capability, by Horton, LMSC 657-617, 30 Jul 1963
94. Hulme and Schomburg (Lockheed), "A Data Bandwidth Compressor for Space Vehicle Telemetry," (paper presented at National Telemetry Conference, Washington, D. C. , May 1962)
95. Hutton (ASTIA), ASTIA Report Bibliography on Speech Compression, AD 288-850, Nov 1962
96. IBM Guidance Center, ASDR/ MDS Sampled Data Reduction and Digital Storage for Saturn, Report No. 61-928-39, Nov 1961
97. Il'yin (USSR), A Method of Time-Compression and Expansion of Continuously Passing Information, AD 265-722, Oct 1961
98. Inose, Yasuda and Murakami (University of Tokyo), "A Telemetry System by Delta-Sigma Code Modulation," (paper presented at Int. Symp. on Space Technology, Japan, Aug 1962)
99. Jaenke and Lotze, "Analysis of Systematic Errors of Smoothing Processes," Proc. of AF Sci. & Eng. Symp., Oct 1962
100. Jet Propulsion Laboratory, Transmission of Statistical Information, Research Summary No. 36-12, Vol. I, 2 Jan 1962, p. 76

101. -----, Information Processing, Space Programs Summary No. 37-15, Vol. IV, 30 Jun 1962, p. 46
102. -----, Data Compression at Low Data Rates, Space Programs Summary No. 37-16, Vol. IV, 31 Aug 1962, p. 54
103. -----, Data Compression of Television Pictures and Automatic Landing Site Selection, Space Programs Summary No. 37-16, Vol. IV, 31 Aug 1962, p. 56
104. -----, Data Compression by First Differences, Space Programs Summary No. 37-16, Vol. IV, 31 Aug 1962, p. 57
105. -----, Telemetry With a Small Number of Quantization-Levels, Space Programs Summary No. 37-17, Vol. IV, 30 Oct 1962, p. 66
106. -----, Information Processing, Space Programs Summary No. 37-17, Vol. IV, 30 Oct 1962, p. 74
107. -----, On the Determination of Quantization-Levels in a Data Sampling System, Space Programs Summary No. 37-18, Vol. IV, 31 Dec 1962, p. 180
108. -----, Sequential Goodness-of-Fit Tests Using Quantiles, Space Programs Summary No. 37-19, Vol. IV, 28 Feb 1963, p. 169
109. -----, A Method to Increase the Data Compression Ratio in a Zero Order System, by J. L. Pierce, TM 3341-65-2, Jan 1965
110. John (Germany), "Selective Telemetry," Arch. Tech. Messen (Ger), Jul 1963
111. Kailath, Adaptive Matched Filters, Doctoral Thesis at MIT, Rand Corp. , Calif. Math Optimization Tech. , Apr 1963
112. Kalatozishvili and Slovinskii (USSR), "Application of a Binary-Decimal Code with Digital Display in a Pulse Code Telemetering System," Instrum. Constr. (G. B.), Sept 1963
113. Kalman, "A New Approach to Linear Filtering and Prediction Problems," ASME Transactions, Series D, Vol. 82-83, Mar 1960
114. Katkovnik and Poluektov (USSR), "Selection of Programs and Sampling Periods in Digital Control Systems," Automatikai Telemekhanika, Apr 1963
115. Key and Sailor (Lockheed), "Stored Program Approach to Multi-Link PCM Decommuation," (paper presented at National Telemetering Conference, May 1963)
116. King, (NASA), "SS-FM Telemetry System," (paper presented at National Telemetering Conference, May 1961)

117. Kitsopoulos and Kretzmer, "Computer Simulation of Television Coding Scheme," Proc. of IRE, Jun 1961
118. Kock, "Speech Communication Systems," Proc. Inst. Radio Engrs., May 1962
119. Kodis, "Telemetry Buffer Storage for Space Vehicles," Data Systems Eng., Oct 1963
120. Kortman (Lockheed), "Data Compression and Adaptive Telemetry," (paper presented at Western Electronic Show and Convention, WESCON, 1965)
121. Kotov (USSR), "Carrying Capacity of Transmission System with Automatic Interrogation of Erroneous Combinations in the Transmission of Binary Signals," Elektrosviaz, Feb 1964
122. Krassner, "Introduction to Space Communication Systems," McGraw-Hill, 1964
123. Kretzmer, "Statistics of Television Signals," Bell Sys. Tech. Journal, Jul 1952
124. Kryter and Ball, "An Evaluation of Speech Compression Techniques," AD 402-604, Feb 1963
125. Lincoln Lab, MIT, "The Orthomatch Data Transmission System," by Kuhn, AD 602 130, Feb 1964
126. Kulya (USSR), "Application of Laguerre Functions to Parametric Coding of Speech Signals," Telecomm. Radio Eng., Jul 1962
127. Kushner, "Data Processing for Goddard Experiment," (paper presented at National Symposium on Space Electronics and TLM, 1962)
128. Lanin (USSR), "Selection of the Number of Quantization Domains in Analog Discrete Converters," Automatika Telemekhamika, Apr 1963
129. Lauler, "A High-Speed Pulse Code Modulation (PCM) Processor," (paper presented at ISA National Convention, Sept 1963)
130. -----, "A System-Oriented PCM Ground Station Incorporating Data Compression," (paper presented at National Space Electronics Symposium, Oct 1963)
131. Lewis (IBM), "Primary Processor and Data Storage Equipment for the Orbiting Astronomical Observatory," IEEE Trans. on Electronic Computers, Dec 1963
132. Lieberman, "Adaptive Digital Communication For a Slowly Varying Channel," IEEE Trans. Commun. Electronics, Mar 1963

133. Link and Eatough, "Experimental Optimization and Evaluation of Telemetry Systems," IRE Trans. on Space Electronics & TLM, Sept 1962
134. Lincoln Labs, paper on Signal Conditioning by F. W. Sarles
135. Lockheed Missiles and Space Company, Analysis and Design of a Data Compressor, LMSC - A030575, Nov 1961
136. -----, Effectiveness of Data Compression in Space Communication Systems, LMSC 3-70-62-5, Aug 1962
137. -----, Flight Data Processing and Analysis Techniques, LMSC 657789, Oct 1963
138. -----, Report on Feasibility Studies of a Transient Event Recorder, 15 Feb 1963
139. -----, Techniques and Application of Data Compression, LMSC 8-51-63-2, Jun 1963
140. -----, Program 461 Telemetry Aliasing Error Analysis, LMSC A324768 - AD-409887, 10 Jun 1963
141. -----, Advanced Telemetry System with Adaptive Capability, LMSC 657617, Jul 1963
142. -----, Feasibility Study of Telemetry Data Compression, LMSC 453-58-12, Jul 1963
143. -----, 698BK Electronic Systems Analysis - Adaptability and Bandwidth Conservation, Interim Report 454 (58-12), Jul 1963
144. -----, Data Compression Engineering Analysis, LMSC 5-10-63-35, Oct 1963
145. -----, Interim Report - Program 461 Preliminary Data Compression Study, LMSC B086186 (Secret), 16 Dec 1963
146. -----, Independent Development - Advanced Data Compression Study, Quarterly Report: January - March 1964, LMSC 659165
147. -----, Effectiveness of Data Compression in Flight Data Processing, LMSC 658800, Feb 1964
148. -----, STARS Technical Report Program Summary, LMSC 6-62-64-4, Apr 1964
149. -----, Engineering Plan for SCF Remote Station Telemetry Data Compression, LMSC A661531, May 1964
150. -----, Program 461 Data Compression Study Interim Report, LMSC B107292 (Secret), 15 Jun 1964
151. -----, Evaluation Report on Strain Gage Data Compression, LMSC 6-65-65-16, Jun 1965

152. ----, Data Compression Study, LMSC A659257, May 1964
153. ----, Biomedical Data Compression, LMSC 5-44-64-9, Nov 1964
154. ----, Summary - Advanced Data Compression - 1964, LMSC 6-62-65-1,
Jan 1965
155. ----, Adaptive and Non-Adaptive Precompression Filtering, LMSC 664229,
Feb 1965
156. ----, Investigation of Post-Reception Telemetry Data Compression,
LMSC A014221, Nov 1962
157. ----, Applicability of Error Detecting or Correcting Codes to Communications
Systems with Data Compression, LMSC 5-65-65-2, Jun 1965
158. ----, Preliminary Implementation Study of Advanced Compression Algorithms,
Interim Report, LMSC 8-39-65-1, Jul 1965
159. ----, Program 461 Data Compressor Breadboard Test Results, LMSC B108570
(Secret), 19 Aug 1964
160. ----, Data Compression for Polaris, LMSC 895376, Aug 1964
161. Lohse and Nelson (Lockheed), "Telemetry Data Reduction for Space Vehicles,"
(paper presented at Intl. Conf. on Aerospace Electro-Technology, Apr 1964)
162. Lorens, "Recovery of Randomly Sampled Time Sequence," IRE Trans. Commun.
Syst. (USA), Jun 1962
163. Lowy, "A Self Adaptor Telemetering System," Proc. of National Telemetering
Conference, 1961
164. Lozovoy, "Regarding the Computation of the Characteristics of Compression in
Systems with Pulse-Code Modulation," Elektrosvyaz (USSR), Telecommunica-
tions (USA), 1961
165. NASA, The NASA Program for Particles and Fields Research in Space, by
Ludwig, NASA TN D-1173, Apr 1962
166. ----, Spacecraft Information Systems, by Ludwig, NASA TN D-1348, Oct 1962
167. Ludwig and McDonald, "Cosmic Ray Experiments for Explorer XII," Proc. of
3rd Int. Science Symposium, May 1962
168. Ludwig and Porreca, "Signal Conditioning for Satellite Borne Cosmic Ray Ex-
periments," Proc. of Nat. TLM Conf., May 1961
169. Mallett, Perkins and Knapp (England), "Telemetry Data Processing Equipment,"
(paper presented at International Telemetering Conference, London, Sept 1963)

170. MacRae and Marquand, "Error Detection and Correction Without Bandspreading," International Space Electronics Symposium, Oct 1964
171. Marko, "The Efficient Utilization of A Telegraphy Channel for the Transmission of Information," Nachrichtentech, Z. (NTZ), Sept 1962
172. Massey (Lockheed), "Advanced Telemetry System with Adaptive Capability," NASA CR-56803, 20 Mar 1964
173. ----, "An Experimental Telemetry Data Compressor," (paper presented at National Telemetering Conference, 1965)
174. McFarland, "Auto-Drape - A Real Time Telemetry Reduction System," (paper presented at Institute of Radio Engineers, National Symposium on Space Electronics and Telemetry, Miami Beach, Florida, 2-4 Oct 1962)
175. Medlin (Lockheed), "Buffer Length Requirements for a Telemetry Data Compressor," (paper presented at National Telemetering Conference, Washington, D. C. , May 1962)
176. -----, "The Comparative Effectiveness of Several Telemetry Data Compression Techniques," (paper presented at International Telemetering Conference, Sept 1963)
177. -----, "Sampled Data Prediction for Telemetry Bandwidth Compression," (paper presented at Western Electronics Show and Conference (WESCON), Aug 1964)
178. Mitriaev, "Transmission of Telemetry Data By Means of Group Codes," Radio Eng. and Electronic Physics, Jun 1963
179. Morrison, Hogan, and Pentz (Lockheed), "Application of Data Compression to Flight Data Processing," (paper presented at Western Electronics Show and Conference (WESCON), Aug 1964)
180. Mueller (STL), Practical Aspects of Data Processing and Encoding for Space Communications, NASA CR-55017 and paper presented at Intl. TLM Conf. , London, Sept 1963
181. Noroberg, "Physical Measurements and Data Processing," Proc. Intl. Meteorological Satellite Workshop, NASA N62-11230, Washington, D. C. , Nov 1961
182. North American Aviation, Telemetering Systems for the Life Sciences - A Survey, SID 63-284, 15 Mar 1963

183. Bell Laboratories, "Efficient Coding," by Oliver, Bell System Technical Journal, Jul 1952
184. Packard Bell Electronics, Dyna Soar Communications and Telemetry, PBE 3106, Aug 1960
185. -----, Test Data Analysis Study, PBE 6458, Nov 1960
186. Packard Bell Computer Corp., The Concept of Adaptive Bandwidth Compression, PBC-10642, Nov 1961
187. -----, Redundancy Data Analysis Study, PBC-4121, Mar 1962
188. -----, Data Compression Study for Apollo PCM Telemetry, PBC-10762, Sept 1962
189. Parin, Bayevski and Eazenko, "Problems of Biological Telemetry," Problems of Space Biology, Nov 1963
190. Perry and Paulsen (Packard Bell), "A Digital Data Compression Technique," (paper presented at Sixth National Communications Symposium, Oct 1960)
191. Poole, "Telemetry Sampling Phenomena," Electronic Eng. (GB), May 1964
192. Posner (JPL), "The Use of Quantiles for Space Telemetry Data Compression," National TLM Conference Proc., Jun 1964
193. Powers, "Some Relations Between Television Picture Redundancy and Bandwidth Requirements," Trans. AIEE, Vol. 76, 1957
194. Radiation, Inc., "Redundancy Reduction Device," AD 600-766, May 1964
195. Raga (EMR), "A Unified Approach to Digital Television Compression," (paper presented at National Telemetry Conference, 1965)
196. Ratz, "Telemetry Bandwidth Compression Using Airborne Spectrum Analyzers," Proc. Inst. Radio Engineers, Apr 1960
197. Ratz and Salberta (Gulton Inc.), "The Development of Airborne Spectrum Analyzers for Telemetry Bandwidth Compression," (paper presented at National Telemetry Conference, May 1963)
198. Rechtin, "Communication Techniques for Space Exploration," IRE Trans. on Space Elec., Sept 1959
199. Riblet and Randolph (Applied Physics Lab), "Satellite Telemetry and Data Processing," (paper presented at Int. TLM Conf., London, Sept 1963)
200. Rich, "Tchebycheff Approximation in a Compact Metric Space," Bulletin American Mathematical Society, 1962

201. Rutman (USSR), Synthesis of Sampled-Data Control Systems by Means of Pulse-Shape Correction, NASA TT F-8547, Feb 1963
202. Rybashov (USSR), Determination of the Required Frequency of Periodic Measurements of a Continuous Signal, AD 412-242, 1963
203. Sampson (STL), "Maximum Utilization of Narrow-Band Data Links for Interplanetary Communications," IRE Proceedings, Apr 1960
204. Sanders, "Recent Advances in Telemetry," (paper presented at International Space Electronics Symposium, Oct 1964)
205. Schaphorst (Philco), "Automatic Video Data Analysis," AD 284237, Mar 1962
206. Schmidt, Galvin, Rasche, Roberge and Sarles, "Data Processing of MIT Gamma-Ray Telescope Aboard OSO-C," (paper presented at International Space Electronics Symposium, Oct 1964)
207. Schomburg (Lockheed), "Computer Simulation of a Data Compressor for Aerospace Telemetry Systems," (paper presented at Institute of Radio Engineers, National Symposium on Space Electronics and Telemetry, Miami Beach, Florida, 2-4 Oct 1962)
208. -----, "The Effectiveness of Data Compression in Space Telemetry," (paper presented at NAECON Convention, 1963)
209. Schuster (Sandia), "An Airborne Vibration Analysis System," Nat. TLM Conf. Proc., Albuquerque, May 1963
210. Schroeder, "Correlation Techniques for Speech Bandwidth Compression," J. Audio Eng. Soc., Apr 1962
211. Schwab (Applied Development Corporation), "Data Compression," IRE WESCON Convention Record, 1960
212. Schwarz, Information Transmission, Modulation and Noise, McGraw-Hill, 1959
213. Schwartz (Armour Res.), "An Adaptive Information Transmission System Employing Minimum Redundancy Word Codes," ASD TDR 62-265, Apr 1962
214. Schwartz (Yale University), Data Processing in Scientific Space Probes, NASA CR-55401, Sept 1963
215. Schwartz (New York University), "Application of Communications Theory," Aerospace-Electronics, Nov 1962
216. Seyler, "The Coding of Visual Signals to Reduce Channel - Capacity Requirements," Proc. Instn. Elect. Engrs. (G. B.), Jul 1962

217. Bell Laboratories, "A Mathematical Theory of Communications," by Shannon, Bell System Tech. J., Oct 1948
218. Simpson, Griffin and James, Compressibility of Saturn S-1 PCM Data, Technical Report #1, Systems Engineering Group, University of Alabama, Jun 1963
219. Simpson, Griffin, James and Bjorn, A Study of Redundancy Removal for Saturn Telemetry Data, Tech. Rept. #5, Systems Engineering Group, University of Alabama, Nov 1964
220. Simpson, "Buffer Control in Data Compression Systems for Non-Stationary Data," (paper presented at National Telemetering Conference, 1964)
221. Simpson, Griffin, Hassell and Brown, A Queuing Problem Encountered in an Adaptive Telemetry Data Compression System, Technical Report #4, University of Alabama, Aug 1964
222. Slaymaker, "Bandwidth Compression by Means of Vocoders," IRE Trans. Audio, Jan - Feb 1960
223. Smith, Speech Compression Studies, AD 291-740, Sept 1962
224. Autonetics, Future of On-Board Computers for Space Vehicles, by Smith, AD 417 402, Jun 1963
225. NASA-Goddard, A Bit-Saving Encoding Scheme for a Set of Monotonic Numbers, by Snively, to be published, 1965
226. Sommer and Harris (N. Y. University), "Some Recent Advances in Adaptive Digital Space Telemetry Systems," (paper presented at National Telemetering Conference, 1962)
227. Specht and Drapkin (Lockheed), "Biomedical Data Compression," (paper presented at National Telemetering Conference, 1965)
228. Stewart (General Dynamics), Format Vocoder Speech Compression System, AD 276-654, Mar 1962
229. Stroup (NASA) and Ingram (Grumman), "The NASA Orbiting Astronautical Observatory," (paper presented at Intl. Symp. on Space Technology, Tokyo, Aug 1962)
230. Sturkie (North American), "The Apollo Pre-Modulation Processor," (paper presented at National Telemetering Conference, Jun 1964)
231. Systems Laboratories, Feasibility of Employing Bandwidth Compression Techniques for Acquisition of Dynamic Data, CMCC 121.69, Jan 1960

232. Thompson, "Logic Modules for Signal Conditioning in Space Radiation Experiments," (paper presented at Natl. TLM Conference, May 1961)
233. Tooley and Sarrafian, "A Programmable Spacecraft Data Handling System," (paper presented at International Space Electronics Symposium, Oct 1964)
234. NASA-Goddard, "A Medium Data Rate Digital Telemetry System," by Townsend, Feinberg and Lesko, NASA TN D 23 15, Jun 1964
235. Uglow and Crow, "Tomorrow's Telemetry," Space/Aeronautics, Sept 1963
236. Van Valck (Stelma Inc.), Development of PCM Data Buffers, AD 435-083, Jan 1964
237. Vasil'yev and Shastova (USSR), Statistical Coding in Telemechanics, AD 412-241, 1963
238. Vernov (USSR), "The ELEKTRON Space System," RAE-TRANS-1062: JPRS-23810 Apr 1964
239. Viterbi, "System Design Criteria for Space Television," J. Brit. Instn. Radio Engineers, Sept 1959
240. ----, "Classification and Evaluation of Coherent Synchronous Sampler Data Telemetry Systems," IRE Trans. on Space Electronics, Mar 1962
241. Packard Bell Electronics Corp., Technical Notes for Adaptive Bandwidth Compression, Internal Report, by Weber, 15 Sept 1960
242. ----, The Concept of Adaptive Bandwidth Compression, PB-10642, Nov 1961
243. Weber and Wynhoff (Packard Bell), "The Concept of Self-Adaptive Data Compression," Institute of Radio Engineers, (paper presented at National Symposium on Space Electronics and Telemetry, Miami Beach, Florida, 2-4 Oct 1962)
244. Weber (Lockheed), "A Synopsis on Data Compression," (paper presented at National Telemetering Conference, 1965)
245. Wiener, Extrapolation, Interpolation and Smoothing of Stationary Time Series, Wiley, 1949
246. Weiss, "Compression and Coding," IRE Transactions on Information Theory, Vol. IT-8, No. 8, Apr 1962
247. White, "Consideration on Design of PFM Telemetry Encoders," (paper presented at National Telemetering Conference, May 1962)
248. White, Thornwall, "Electronics for Satellite Gamma-Ray Spectrometer," (paper presented at Natl. Symposium on Space Elec., Oct 1962)

- 249. White, "Theoretical Aspects of Asynchronous Multiplexing," Proc. IRE., 38, 1950, pp 270-275
- 250. Wholey, "The Coding of Pictorial Data," IRE Trans. on Info. Theory, Apr 1961
- 251. Williard and Ratner, "A Universal PCM Data Collection System," Proc of National TLM Conf., May 1960
- 252. Winkler, "Pictorial Transmission with HIDM," IEEE Convention Record, 1965
- 253. Yeagley and Godwin (Martin Company), "Pre-Transmission Analysis, A Cure for Telemetry's Growing Pains," (paper presented at National Telemetry Conference, 1960)
- 254. Yen, "On Non-Uniform Sampling of Bandwidth - Limited Signals," IRE Trans. on CKT. Theory, Dec 1956
- 255. Lockheed Missiles and Space Company, Investigations of Applications of General Purpose Computers to Space Systems Communications/ Control Systems, LMSC TR 3-72-62-1, Dec 1962
- 256. ----, Data Compression Study, by Yocke, LMSC A659257, 6 May 1964
- 257. Young, "Ambiguities in Telemetry Sampling," Electronic Engineering, May 1963
- 258. Zukerman and Ross, "Some Coding Concepts to Conserve Bandwidth," (paper presented at National Telemetry Conference, Denver, Colorado, 1959)

Appendix VI

GLOSSARY

Section 1
INTRODUCTION